



HAL
open science

Asterisk-Shaped Arenes and Heteroarenes Incorporating Sulfur, Oxygen and Nitrogen: Synthesis, Structures, Photophysics, Dynamic and Supramolecular Covalent Chemistry.

Sapna Gahlot

► **To cite this version:**

Sapna Gahlot. Asterisk-Shaped Arenes and Heteroarenes Incorporating Sulfur, Oxygen and Nitrogen: Synthesis, Structures, Photophysics, Dynamic and Supramolecular Covalent Chemistry.. Organic chemistry. Aix-Marseille Université, 2022. English. NNT: . tel-03589656

HAL Id: tel-03589656

<https://amu.hal.science/tel-03589656>

Submitted on 25 Feb 2022

HAL is a multi-disciplinary open access archive for the deposit and dissemination of scientific research documents, whether they are published or not. The documents may come from teaching and research institutions in France or abroad, or from public or private research centers.

L'archive ouverte pluridisciplinaire **HAL**, est destinée au dépôt et à la diffusion de documents scientifiques de niveau recherche, publiés ou non, émanant des établissements d'enseignement et de recherche français ou étrangers, des laboratoires publics ou privés.

THÈSE DE DOCTORAT

Soutenue à Aix-Marseille Université

Sapna GAHLOT

Titre de la thèse: Arènes et Hétéroarènes Sulfurés, Oxygénés et Azotés sous Forme d'Astérisques: Synthèse, Structures, Photophysique, Chimie Covalente Dynamique et Supramoléculaire.

Discipline

Chimie

Spécialité

Chimie organique et matériaux organiques

École doctorale

ECOLE DOCTORALE 250-SCIENCES CHIMIQUES

Laboratoire/Partenaires de recherche

UMR CNRS 7325 CINaM (Centre Interdisciplinaire de Nanoscience de Marseille)

- Composition du jury:
- Dr. Jeanne CRASSOUS
- Université de Rennes (Rapporteur)
- Dr. Jean-François NIERENGARTEN,
- Université de Strasbourg (Rapporteur)
- Dr. Didier GIGMES
- Aix-Marseille Université (Examineur)
- Dr. Sylvia PIETRI
- Aix-Marseille Université (Examinatrice, Présidente du jury)
- Dr. Laure GUY (Examineur externe)
- École Normale Supérieure de Lyon
- Pr. Peter GOEKJIAN (Examineur externe)
- Université of Lyon
- Pr. Marc GINGRAS (Directeur de thèse)
- Aix-Marseille Université

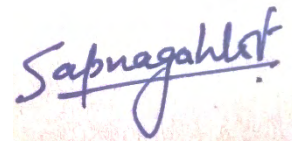
Affidavit

I, undersigned, Sapna GAHLOT, hereby declare that the work presented in this manuscript is my own work, carried out under the scientific direction of Prof. Marc GINGRAS, in accordance with the principles of honesty, integrity and responsibility inherent to the research mission. The research work and the writing of this manuscript have been carried out in compliance with both the French national charter for Research Integrity and the Aix-Marseille Université charter on the fight against plagiarism.

This work has not been submitted previously either in this country or in another country in the same or in a similar version to any other examination body, excepted for the submission of some manuscripts for publication to scientific journals.

Lieu: Marseille, France ,

Date: 28 mars 2022

A handwritten signature in blue ink that reads "Sapnagahlot". The signature is written in a cursive style with a horizontal line underlining the name.

Liste de publications et participation aux conférences

1) Liste des publications¹ réalisées dans le cadre du projet de thèse :

1) "The Sulfur Dance" Around Arenes and Heteroarenes - Dynamic Covalent Nucleophilic Aromatic Substitutions.

Auteurs (en ordre): Sapna Gahlot, Jean-Louis Schmitt,* Marco Villa, Myriam Roy, Ceroni, Jean-Marie Lehn,* Marc Gingras*

Journal: article complet soumis à *Angewandte Chemie International Edition* le 16 janvier 2022.

2) Persulfurated Benzene-Cored Asterisks with π -Extended ThioNaphthyl Arms: Synthesis, Structural, Photophysical and Covalent Dynamic Properties.

Auteurs (en ordre): Sapna Gahlot, Jean-Louis Schmitt,* Marco Villa, Myriam Roy, Ceroni, Jean-Marie Lehn,* Marc Gingras*

Auteurs (en ordre): Sapna Gahlot, Alessandro Gradone, Myriam Roy, Michel Giorgi, Simone Conti, Paola Ceroni, Marco Villa* and Marc Gingras*

Journal: article complet soumis à *Chemistry, A European Journal* le 28 janvier 2022.

3) A Novel Route to Functionalized Pyrenes in the K-Region: Synthesis, Structural, Computational and Photophysical Properties.

Auteurs (en ordre): Sapna Gahlot, Marco Villa, Anouk Siri, Didier Siri*, Paola Ceroni,* Marc Gingras*

Journal: article complet en rédaction vers une soumission à *Chemistry, A European Journal* ou autre journal en 2022.

4) Sulfurated and Oxygenated Polycyanated Arenes: Synthesis, Structures, Photophysical and Covalent Dynamic Properties.

Auteurs: Sapna Gahlot, Jean-Louis Schmitt, Myriam Roy, Michel Giorgi, Marco Villa, Paola Ceroni,* Jean-Marie Lehn* and Marc Gingras*

Journal: article complet en rédaction vers une soumission à *Chemistry, A European Journal* ou autre journal en 2022.

2) Participation aux conférences² et écoles d'été au cours de la période de thèse :

¹ Cette liste comprend les articles publiés, les articles soumis à publication et les articles en préparation ainsi que les livres, chapitres de livre et/ou toutes formes de valorisation des résultats des travaux propres à la discipline du projet de thèse. La référence aux publications doit suivre les règles standards de bibliographie et doit être conforme à la charte des publications d'AMU.

² Le terme « conférence » est générique. Il désigne à la fois « conférence », « congrès », « workshop », « colloques », « rencontres nationales et/ou internationales » ... etc.

Communications orales

1) Titre: Chiral Enantiomerically Stable 3D-Nanographenes Embedding Helicenes Units
Auteurs: Sapna Gahlot, Veronika Bereznaia, Myriam Roy, Nicolas Vanthuyne, Marco Villa, Jean-Valère Naubron, Jean Rodriguez, Yoann Coquerel* and Marc Gingras* (20 min) Congrès: International Congress on Heteroatom Chemistry, 30 June-5 July 2019 Prague, Czech Republic.

Communications par affiches

1) Titre: Multichromophoric Highly Luminescent Polysulfurated Pyrenes as Efficient Light-Harvesting Antenna and Their Metal Coordination
Auteurs: Andrea Fermi, Marco Villa, Giacomo Bergamini, Myriam Roy, Sapna Gahlot, Paola Ceroni, Marc Gingras
Congrès: International Congress on Heteroatom Chemistry, 30 June-5 July 2019 Prague, Czech Republic.

2) Titre: Chiral Enantiomerically Stable 3D-Nanographenes Embedding Helicenes Units.
Auteurs: Sapna Gahlot, Veronika Bereznaia, Myriam Roy, Nicolas Vanthuyne, Marco Villa, Jean-Valère Naubron, Jean Rodriguez, Yoann Coquerel and Marc Gingras
Congrès: International Congress on Heteroatom Chemistry, 30 June-5 July 2019 Prague, Czech Republic.

RESUME (Français)

Le contenu de cette thèse porte sur les astérisques moléculaires fonctionnalisés, ramifiés et polysulfurés, polyoxygénés ou polycyanés incorporant soit un noyau benzénique, un noyau pyridine, ou un noyau pyrène. Les principaux objectifs sont de rapporter la synthèse et les propriétés structurales, photophysiques, supramoléculaires et covalentes dynamiques des architectures moléculaires nouvellement créées, afin de développer d'autres utilisations et applications de celles-ci dans un futur proche, vers l'électronique moléculaire, l'imagerie, les sciences des matériaux et de la vie, en général. Ce travail aborde également la relation entre la topologie (chaines, rubans, torsades, etc.) et les propriétés optoélectroniques afin d'ouvrir une nouvelle direction et des perspectives futures en science des matériaux et en chimie polyaromatique. Elle interroge également certains principes et mécanismes fondamentaux en chimie organique, notamment la réversibilité d'un mécanisme principal et historique en chimie organique : la substitution nucléophile aromatique, connue depuis 1854. Dans un premier temps, la thèse porte sur de

Indiquer si vous avez fait une présentation orale ou sous forme de poster.

nouvelles approches synthétiques pour fonctionnaliser le pyrène dans sa région K, ce qui a été négligé malgré l'importance historique des pyrènes dans les capteurs optoélectroniques, les matériaux et les sciences biologiques. Elle se poursuit par la synthèse de divers astérisques moléculaires soufrés, oxygénés et cyanés à noyau benzénique ou pyridinique, à la recherche d'un nouveau domaine de la chimie covalente dynamique (DCC) avec les arènes et les hétéroarènes, en mettant en œuvre et en promouvant des substitutions nucléophiles aromatiques réversibles pour la DCC, tout en développant des matériaux intelligents entièrement organiques hautement phosphorescents via un phénomène de phosphorescence induite par la rigidité (RIP). Ainsi, nous rapportons la « danse du soufre » autour des arènes et des hétéroarènes à partir d'un échange réversible de composants soufrés autour d'un template aromatique, un nouveau processus en chimie aromatique. Afin d'étudier les réactions S_NAr réversibles, plusieurs conditions de réaction, effets de substituants, méthodes analytiques et séparatives étaient nécessaires pour analyser la bibliothèque de composés créés par DCC. Dans cette direction, nous avons également analysé l'importance des astérisques sulfurés et oxygénés avec un système π étendus autour d'un noyau benzénique, en incorporant des bras phényle, biphényle, naphtyle ou hétéroaromatiques, à la recherche de propriétés photophysiques exaltées ou de coordination de cations métalliques vers des applications en chimie supramoléculaire. Cette thèse couvre donc des larges domaines de la chimie aromatique, mécanismes réactionnels de base, photophysique et chimie covalente dynamique et supramoléculaire, vers les sciences de matériaux et de la vie.

RESUME (Anglais)

The content of this thesis focusses on functionalized and branched polysulfurated, polyoxygenated or polycyanated molecular asterisks incorporating either a benzene, a pyridine or a pyrene core. The main objectives are to report the synthesis and the structural, photophysical, supramolecular and covalent dynamic properties of the newly created molecular architectures, in order to develop further uses and applications of them in a near future, toward molecular electronics, imaging, materials and life sciences in general. This work also tackles the relation between topology and optoelectronic properties for opening a new direction and future perspectives in materials science and polyaromatic chemistry. It also questions some fundamental

principles and mechanisms in organic chemistry, notably the reversibility of a main and historical mechanism in organic chemistry: the nucleophilic aromatic substitution, which is known since 1854. At first, the thesis covers new synthetic approaches to functionalize pyrene in its K-region, which has been neglected in spite of the historical importance of pyrenes in optoelectronic sensing, materials and biological sciences. It is followed by the synthesis of various sulfurated, oxygenated and cyanated molecular asterisks with a benzene or pyridine core, in search for a new field in dynamic covalent chemistry (DCC) with arenes and heteroarenes, by implementing and promoting reversible nucleophilic aromatic substitutions in DCC, while at the same time developing all-organic highly phosphorescent smart materials via a rigidity-induced phosphorescence (RIP) phenomena. Thus, we report the "Sulfur Dance" around arenes and heteroarenes from a reversible exchange of sulfur components around an aromatic template, a new process in aromatic chemistry. In order to study reversible S_NAr reactions, several reaction conditions, substituent effects, analytical and separative methods were necessary in DCC for analyzing the created library of compounds. In that direction, we also analyzed the importance of π -extended sulfurated and oxygenated asterisks with a benzene core, incorporating phenyl, biphenyl, naphthyl or heteroaromatic arms, in search for some exalted photophysical properties or metal cations bindings of uses in supramolecular chemistry. Therefore, this thesis covers broad areas of aromatic chemistry, basic reaction mechanisms, photophysics and dynamic covalent and supramolecular chemistry, towards materials and life sciences.

ACKNOWLEDGEMENTS

I thank my doctoral supervisor, Prof. Marc GINGRAS, for his help during the last three years and his advice whenever I went wrong in my work. Also, I thank him for his help in writing the manuscripts, reports and guidance for the presentations. I thank Dr. Myriam Roy (Sorbonne Université, Paris, France), who helped me to analyze and to report my data, in a systematic writing of my results from the very first year. I thank Marco Villa and Prof. Paola Ceroni for making some photophysical measurements on my compounds. I want to thank Prof. Jean-Marie Lehn and his group for collaborating on the work on Dynamic Covalent Chemistry (DCC), for his guidance, and especially for numerous LC-HRMS analyses made by Dr. Jean-Louis Schmitt and his colleagues at ISIS, Strasbourg University. I want to thank Dr. Michel Giorgi (Aix-Marseille Université, FSCM, Spectropole, Marseille France), who recorded and analyzed many single-crystal X-Ray diffraction data of my compounds and Dr. Frédéric Brunel for advices and NMR data. I also thank master-1 and Licence-3 students Alexis Agostini and Richard Sfeir (AMU) to briefly initiate a couple of reactions in chapter-5. I appreciated the help from Yashraj Kapadiya, as a Master 2 student trained at CINAM.

I would like to thank all the members of my doctoral jury and committee thesis: special thanks to Pr. Peter Goekjian because of him I was able to start my journey in France from Lyon. I thank Dr. Didier Gigmes, Dr. Sylvia Piétri, Dr. Arnaud Haudrechy, Pr. Corinne Moustrou, Dr. Didier Tonneau, Dr. Jeanne Crassous, Dr. Jean-François Nierengarten, Dr. Laure Guy, for accepting to be part of my three-year research activities at CINAM.

Finally, I would like to thank the Agence Nationale de la Recherche (ANR) in France (program PRC) for the grant ANR-20-CE07-0031 Acronym: "SulfurDance". I also acknowledge the financial support from the Excellence Initiative of Aix-Marseille University – A*Midex, a French "Investissements d'Avenir" programme for my doctoral contract.

I would also like to thank my mother (Kavita Devi), who helped me throughout my life and especially in the past three years. I want to thank my grandmaternal mother and father, Late Smt. Kartari Devi and Jai Parkash Godara were always there to help and

take the initiative for my education. Thanks to Amita Devi, Rajesh Gahlot, Kavita Devi, Rakesh Gahlot, my brothers Sameer Gahlot, and Nikhil Gahlot for always being there.

I would like to thank Anshil Chaudhary (my friend) and Sweta Gahlot (my sister), Kunal Kumar for their constant mental support from day one.

All of my family (Reena Kumari, Sandeep Godara, Bharati Godara). And all my siblings (Prateek Gahlot, Priyanshi Godara, Vansaj Godara, Anaya Jhakad).

I want to thank my friends from Marseille Nouara Messab, Sreebash Denath, and his wife, Simmi Chakraborty, who helped me mentally. Pavlo Perkhun, Johnathan Phelipot, Quantain, Yatzil Avalos, Dinesh Dhumal, Sanjay Febvre, would not be the same without them.

I would like to thank my close friends (Vibha Chaudhary, Shruti Upadhyay, Shefali Sharma, Shikha Dagar, Navroz Kaur, Arshiya Chawla) who helped me mentally during covid-19 lock down.

Table of Contents

CHAPTER 1: Introduction	1-68
1.0 Arenes and heteroarenes with star-shaped topology	2-7
1.1 Benzene-cored asterisks	7-18
1.1.1 Polysulfurated benzene-cored asterisks	
1.1.2 Polyoxygenated benzene-cored asterisks	
1.1.3 Sulfurated, oxygenated and cyanated benzene-cored asterisks	
1.2 Sulfurated pyrene-cored asterisks	18-23
1.3 Photophysical properties of the asterisks	23-35
1.3.1 Basic concepts in photophysics	
1.3.2 Aggregation-Induced Emission (AIE)	
1.3.3 Aggregation-Caused Quenching (ACQ)	
1.3.4 Rigidity-Induced Phosphorescence (RIP) from persulfurated benzene-cored asterisks	
1.3.5 Fluorescence of polysulfurated pyrene-cored asterisks	
1.4 Reactivity of arenes - nucleophilic aromatic substitutions	35-48
1.4.1 History	
1.4.2 Nucleophilic aromatic substitution mechanisms	
1.4.2.1 S_NAr , Nucleophilic aromatic substitution (Addition-Elimination)	
1.4.2.2 S_N1 (with diazonium salts)	
1.4.2.3 $E1cb$ -AdN Benzyne	
1.4.2.4 $S_{RN}1$ Free radical	
1.4.2.5 ANRORC (addition of nucleophile, ring opening, ring closure in a nucleophilic reaction)	
1.4.2.6 S_NArH - Vicarious nucleophilic substitution	
1.4.2.7 cS_NAr - Concerted S_NAr reaction	
1.5 Dynamic Covalent Chemistry and reversible S_NAr	45-58
1.5.1 What is Dynamic Covalent Chemistry?	
1.5.2 Reversible reactions in DCC	
1.5.2.1 Reversible imine formation and exchanges	
1.5.2.2 Reversible exchange with quaternary ammonium salts by S_N2 and S_N2' mechanisms.	
1.5.2.3 Reversible Diels-Alder reactions	
1.5.2.4 Reversible olefin metathesis and exchange	
1.5.2.5 Reversible disulfide formation and exchange	
1.5.3 Reversible nucleophilic aromatic substitutions in DCC	
1.6 General objectives of the thesis work	58-59
CHAPTER 2: Functionalization of Pyrene In The K-Region: Synthesis, Structural, And Photophysical Studies	69-103
2.0 Introduction	69

2.1 Objectives	70
2.2 Results and discussion	70-83
2.2.1 Functionalization of pyrene at positions 1,3,6,8 (non K-region)	
2.2.2 Functionalization of pyrene at positions 4,5,9,10 (K-region)	
2.2.3 Functionalization of pyrene at positions 1,6; 1,8 and 2,7 (non K-region)	
2.3 Ring-closing via benzylic-type couplings	79-83
2.4 New route to functionalized pyrenes in the K-region via benzylic-type ring Closures	83-88
2.4.1 Preliminary results and model studies on phenanthrene	
2.3.2 Long route to 4,5,9,10-tetrabromo pyrene	
2.3.3 Short and optimized route to 4,5,9,10-tetrabromo pyrene	
2.5 Sulfurated pyrenyl derivatives from 4,5,9,10-tetrabromo pyrene	89-93
2.6 Cyanated pyrenyl derivatives from 4,5,9,10-tetrabromo pyrene	93-94
2.7 Photophysical studies on sulfurated pyrenes in the K-region.	94-97
2.8 Conclusion	97-98

CHAPTER 3: Synthesis of Polysulfurated Benzene-Cored Asterisks With Arylthio or Heteroarylthio Arms **104-118**

3.0 Introduction	104
3.1 General synthetic scheme	104-106
3.2 Synthesis of hexathiosubstituted benzene-cored asterisks	106-110
3.3 Synthesis of tetrathiosubstituted benzene-cored asterisks	110-113
3.4 Synthesis of trithiosubstituted benzene-cored asterisks	113-114
3.5 Persulfurated benzene-cored asterisks with heteroaryl arms: "the heteroasterisks"	114-117
3.5.1 Literature on polysulfurated benzene-cored "heteroasterisks"	
3.5.2 Synthesis of the "heteroasterisks"	
3.6 Conclusion	117

CHAPTER 4: Dicyanated, Sulfurated And Oxygenated Benzene-Cored Asterisks - Structural, Supramolecular And Photophysical Properties **119-136**

4.0 Introduction and objectives	119-120
4.1 Literature search and precedent work	120-123
4.2 Results and discussion	124-131
4.2.1 Dicyanated and tetrasulfurated benzene-cored asterisks	
4.2.2 Dicyanated and tetraoxygenated benzene-cored asterisks	
4.2.3 Dicyanated poly(biphenylthio) benzene-cored asterisks with π -extended systems	
4.3 Photophysical studies	131-135
4.4 Conclusion	135

CHAPTER 5: Persulfurated Benzene-Cored Asterisks With π-Extended Thio-Naphthyl Arms: Synthesis, Structural, Photophysical And Covalent Dynamic Properties	137-151
5.0 Introduction	137-138
5.1 Objectives	139
5.2 Results and discussion	140-142
5.2.1 Synthesis	
5.2.2 Mechanistic observation	
5.3 Sulfur exchange components (the "sulfur dance")	142-146
5.4 Structural and supramolecular studies by sc-XRD	146-148
5.5 Conclusion	148-149
CHAPTER 6: "The Sulfur And Oxygen Dance" Around Arenes And Heteroarenes - Dynamic Covalent Nucleophilic Aromatic Substitution	152-193
6.1 Introduction - Dynamic Covalent Chemistry (DCC)	153-154
6.2 Scope of reversible processes and reactions in DCC	154-157
6.3 Methods to verify the reversibility of a chemical process.	157-158
6.4 Summary of general applications relevant to DCC	158-160
6.5 Survey of reversible nucleophilic aromatic substitutions in the literature	160-167
6.6 Thesis work on DCC with polysulfurated benzene-cored asterisks	169
6.7 Manuscript submitted for publication entitled: "The Sulfur Dance" Around Arenes and Heteroarenes - Dynamic Covalent Nucleophilic Aromatic Substitution"	169-182
6.7.1 Introduction	169-172
6.7.2 Results and Discussion	171-172
6.7.3 Sulfur component exchanges	173-177
6.7.3.1 Hexasulfurated asterisks	
6.7.3.2 Pentasulfurated asterisks.	
6.7.3.3 Tetrasulfurated asterisks.	
6.7.3.4 Pentasulfurated pyridine-cored asterisk.	
6.7.4 Mechanistic considerations	177-179
6.7.5 Synthetic applications.	179
6.7.6 Demonstration of reversibility in S_NAr .	180-182
6.7.7 Conclusion	182-183
6.8 Additional data to the submitted article: reversible S_NAr on tetra-, hexasulfurated and 1,2-dicyano-tetrasulfurated/tetraoxygenated benzene with different phenyl thiolates	187-193
CHAPTER 7: Experimental Part of the Thesis	194-436

CHAPTER 1

INTRODUCTION

- 1.0 Arenes and heteroarenes with star-shaped topology
- 1.1 Benzene-cored asterisks
 - 1.1.1 Polysulfurated benzene-cored asterisks
 - 1.1.2 Polyoxygenated benzene-cored asterisks
 - 1.1.3 Sulfurated, oxygenated and cyanated benzene-cored asterisks
- 1.2 Sulfurated pyrene-cored asterisks
- 1.3 Photophysical properties of the asterisks
 - 1.3.1 Basic concepts in photophysics
 - 1.3.2 Aggregation-Induced Emission (AIE)
 - 1.3.3 Aggregation-Caused Quenching (ACQ)
 - 1.3.4 Rigidity-Induced Phosphorescence (RIP) from persulfurated benzene-cored asterisks
 - 1.3.5 Fluorescence of polysulfurated pyrene-cored asterisks
- 1.4 Reactivity of arenes - nucleophilic aromatic substitutions
 - 1.4.1 History
 - 1.4.2 Nucleophilic aromatic substitution mechanisms
 - 1.4.2.1 S_NAr , Nucleophilic aromatic substitution reaction (Addition-Elimination)
 - 1.4.2.2 S_N1 (with diazonium salts)
 - 1.4.2.3 $E1cb$ -AdN Benzyne
 - 1.4.2.4 $S_{RN}1$ Free radical
 - 1.4.2.5 ANRORC (addition of nucleophile, ring opening, ring closure in a nucleophilic reaction)
 - 1.4.2.6 S_NArH - Vicarious nucleophilic substitution
 - 1.4.2.7 cS_NAr - Concerted S_NAr reaction
- 1.5 Dynamic Covalent Chemistry and reversible S_NAr
 - 1.5.1 What is Dynamic Covalent Chemistry?
 - 1.5.2 Reversible reactions in DCC
 - 1.5.2.1 Reversible imine formation and exchanges
 - 1.5.2.2 Reversible exchange with quaternary ammonium salts by S_N2 and S_N2' mechanisms.
 - 1.5.2.3 Reversible Diels-Alder reactions
 - 1.5.2.4 Reversible olefin metathesis and exchange
 - 1.5.2.5 Reversible disulfide formation and exchange
 - 1.5.3 Reversible nucleophilic aromatic substitutions in DCC
- 1.6 General objectives of the thesis work

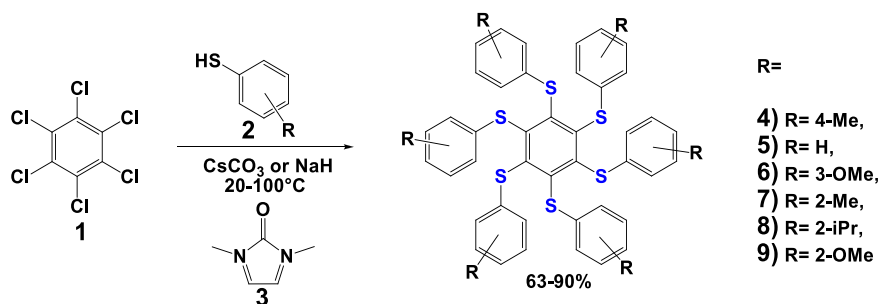
1.0 Arenes and heteroarenes with star-shaped topology

Arenes can be broadly defined as molecular species containing hybridized sp^2 carbon atoms and hydrogens atoms in their chemical structure, while generating a π -system with an aromatic character due to some electronic delocalization. They are also members of a chemical family named Polycyclic Aromatic Hydrocarbons (PAH). Heteroarenes are similarly described, but they incorporate at least one heteroatom in a π -system. Benzene is thus one of the smallest arenes. It is the parent compound and the basic unit of higher PAH and arenes. An electronic delocalization in its π -system provides an extra thermodynamic stabilization of the molecule, which is commonly known as resonance energy, as a main feature describing aromaticity. Many electronic, thermodynamic, photochemical, structural and chemical reactivity studies have been carried out over the years on benzene derivatives and arenes since the early days of aromatic chemistry. However, not only arenes (such as benzene, naphthalene, pyrene) but also heterocyclic aromatic compounds are of significant importance in organic chemistry and in heteroaromatic chemistry. Many heterocyclic aromatic compounds (such as pyridine, thiophene, furan, pyrrole, etc.) are also parent compounds of higher heteroarenes in the field of polycyclic heteroaromatic chemistry. Thus, arenes and heteroarenes could have various properties due to their molecular diversity, but also due to the aromatic character of some rings with sp^2 - hybridized carbon atoms and sp^2 -hybridized heteroatoms. This electronic contribution could thus come from some substituents and/or heteroatoms interacting with such π systems. In many cases, arenes and heteroarenes are thus rather planar with 2D dimension, even if some family of arenes could be distorted, such as carbohelicenes.

Regarding deviation of planarity, another feature is the characteristic 3D star-shaped topology of the molecules. It often confers them a greater solubility with different solvation and 3D features, leading to different supramolecular interactions. Branching effects can be important for modulating supramolecular interactions and self-assemblies. This is regularly found in dendrimer chemistry, for instance.

In this work, it is of special interest to explore the role of sulfur and oxygen atoms surrounding an aromatic or heteroaromatic core and also the star shaped molecular topology. Sulfur and oxygen atoms have an impact on the molecular conformation and on the supramolecular properties, while also contributing to

covalently-assemble the asterisk molecules in a peculiar (star-shaped) topology and conformation. They could also be used for coordinating metal ions. These heteroatoms, their multiplicity and their electronic contributions within aromatic cycles or at the periphery of an aromatic core should have a strong importance in the modulation of optical, electronic and supramolecular properties in the solid state or in solution. As a proof of concept, sulfur atoms surrounding an aromatic core are known to strongly stabilize negatively charged species. [1] Some studies were also achieved on their aromatic character as it is related to reactivity. [2-9] [10] Heteroatoms such as sulfur or oxygen are different from carbon or hydrogen atoms in their electronegativity and covalent radius. Incorporating heteroatoms such as sulfur/oxygen or sulfur/oxygen-containing groups to a benzene or a pyrene core can greatly change the core's photophysical or redox properties. [1] A recent example is related to the discovery of one of the most phosphorescent crystals known to date with a near 100% quantum yield of efficiency (Scheme 1 - compound 4).[11] The photophysical mode of emission is related to a rigidity-induced phosphorescence (RIP) as a relatively rare phenomena in the field of aggregation-induced emission (most phenomena involve fluorescence), which will be demonstrated in the next part of this chapter. Lastly, this family of asterisk compounds has been lately used in the development of novel cations and anions sensing devices using RIP and exalted phosphorescence. [12]



Scheme 1: Hexakis(p-tolylthio)benzene (1) is one of the most phosphorescent solid or crystal known to date ($\Phi \sim 100\%$). A new family of highly phosphorescent crystals has been discovered in 2013. [13]

Their attractive features are based on rich supramolecular interactions and optical-electronic properties, which could be modulated from the coordination of divalent sulfur atoms to thiophilic metallic species, from some cation- π interactions and from some π -complexes. Additionally, polysulfuration often enhances some electronic, photophysical and biophysical properties, leading to phosphorescence,

fluorescence, several redox states, metal ion coordination ability, aggregation or crystallization- induced phosphorescence or fluorescence emission (AIE or CIE). We are thus interested in studying their electronic, photophysical properties by introducing substituents around a benzene or a pyrene core with sulfur or oxygenated ligands (Figure 1).

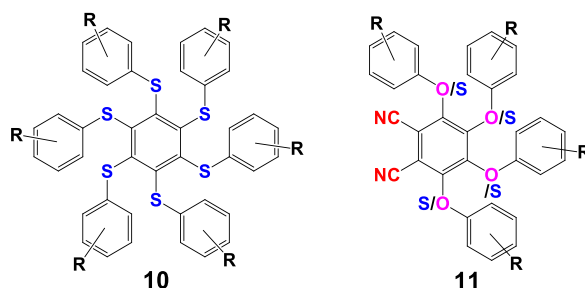


Figure 1: New persulfurated, cyanated or oxygenated aromatic compounds of interest.

Further, we would like to study the reversibility of nucleophilic aromatic substitutions of these persulfurated asterisks and other congeners in the frame of Dynamic Covalent Chemistry (discussed in detail in section 1.5 and chapter 6), after the discovery of some sulfur exchange reactions.

Besides benzene, we previously found that pyrene's properties could also be strongly influenced by functionalization with sulfur substituents for making pyrene-type asterisks. Pyrene is a common peri-fused polycyclic aromatic hydrocarbon, [14] with a highly symmetrical point group (D_{2h}). [15] It is considered aromatic in its behavior, despite having 16 π -electrons a number which does not following the Huckle's rule of aromaticity ($4n+2$ π -electrons). [16] There are multiple issues regarding regioselectivity and purification of substituted pyrenes. An electrophilic substitution preferentially occurs at positions **1**-,**3**-,**6**- and **8** of pyrene, due to the electronic density and nucleophilic characteristic at these positions at the so-called non K-region of pyrene. [17-19] As a consequence, most electrophilic substitutions are reported at these postions in the literature for making most pyrene derivatives. In spite of a large number of reactions and functionalizations of pyrene, a major challenge remains a quick functionalization of the so-called K-region of pyrene (Figure 2). Thus, we are interested in the functionalization of pyrene at positions 4,5,9,10, which are less common and less easy in synthesis.

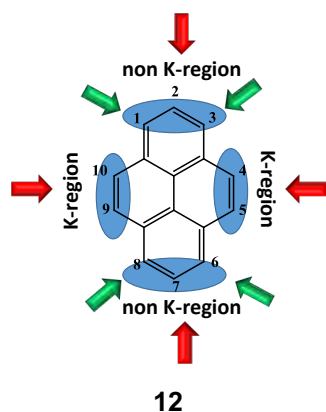
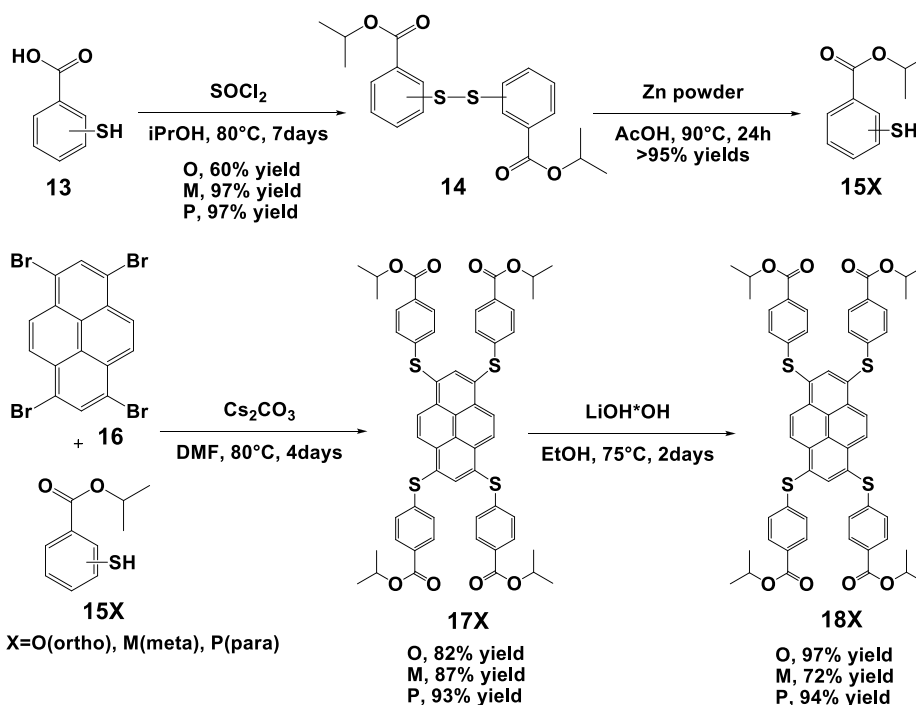


Figure 2: green arrow represents common functionalization sites on pyrene whereas red arrow represents uncommon functionalization sites on pyrene (12).

In basic pyrene chemistry, a selected and recent example is shown in scheme 2. A regioselective bromination of pyrene in warm nitrobenzene provided 1,3,6,8-tetrabromopyrene in a high yield. It was followed by a sulfuration by S_NAr for incorporating new “solubility enhancers” at the non K-region (solubilizing groups with reactive or activating functions).



Scheme 2: Water-soluble polysulfurated pyrene-based chromophores as dual mode sensors of metal ions. Recent example of highly emissive (tetracarboxylated tetra(phenylthio)pyrenes decorated with four peripheral and regioisomeric carboxylic acid groups at ortho (1O), meta (1M) or para (1P) positions). [20]

Electrophilic sulfonation proceeds in a similar regioselectivity on pyrene. These sulfurations are now common. Nevertheless, sulfurated pyrene derivatives, especially those with a thioether linkage (or sulfide) still remain underexploited. Similar reactions

and functionalizations are even more scarce at the K-region of pyrene, in spite of real opportunities. This is the reason, we focussed in the functionalization of the K-region as an added-value toward unusual pyrene-based building blocks for making various objects, such as large wires, ribbons, torsades, rings and helices. At first, we propose some efficient syntheses, functionalization and characterization of pyrene derivatives, having in mind to make oligomers and higher pyrene-based architectures.

Along these lines, scheme 2 presents recent examples of polysulfurated and tetracarboxylated pyrene-cored asterisks, which were synthesized via direct aromatic nucleophilic substitution reactions of thiolates on 1,3,6,8-tetrabromopyrene (16), giving four peripheral (17X) and regioisomeric carboxylic acid groups at ortho (1O), meta (1M), and para (1P) positions of a benzene ring. The carboxylic acids can chelate with divalent metal ions for generating a supramolecular object or assembly in water, with a substantial change in the photophysical properties. Photophysical measurements of carboxylated asterisks are achieved in neutral or basic aqueous solution (1M, 17) with metal ions. Several metal ions were tested and found to reduce emission quantum yields, with a controlled formation of 3-D nanoscopic objects in a dual-mode sensing. Adding EDTA (ethylenediaminetetraacetic acid) can disassemble the nanoobject by a competitive coordination to metal ions, leaving the pyrene-cored asterisks restoring the fluorescence of pyrene. It thus opened new avenues for heavy metal ion sensing. [20]

Other common derivatizations of pyrene can be done via metal-catalyzed cross-coupling reactions such as Suzuki-Miyaura cross-couplings. [19] It is also common to use a Stille coupling involving organostannanes for making pyrene-thiophene derivatives, as an example. Heck-Miyosaki coupling reactions [22], Wittig reactions involving a triphenyl phosphonium ylide [23] were also used. A Sonogashira coupling with terminal alkynes is a valuable method for the synthesis of conjugated acetylenic systems to pyrene. All of the above-mentioned methods allow the design of pyrene derivatives of interest in molecular electronics and in devices, such as OLEDs.

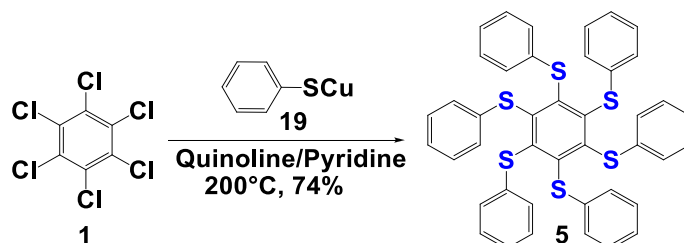
The positions at **4,5,9,10** of the pyrene ring are very interesting for preparing new extended aromatic systems at the K-region toward more complex pyrene-based structures. It is worth noting that professor Klaus Müllen and his group in Germany made several assays to prepare pyrene-4,5-diones and pyrene-4,5,9,10-tetraones directly from pyrene. [24-25] An indirect method is to transform pyrene into

hydrogenated pyrene in the non K-region and to functionalize the resulting key synthon by electrophilic substitution in the K-region. [26-27] It will be described in Chapter 2.

1.1 Benzene-Cored Asterisks

1.1.1 Polysulfurated Benzene-cored Asterisks

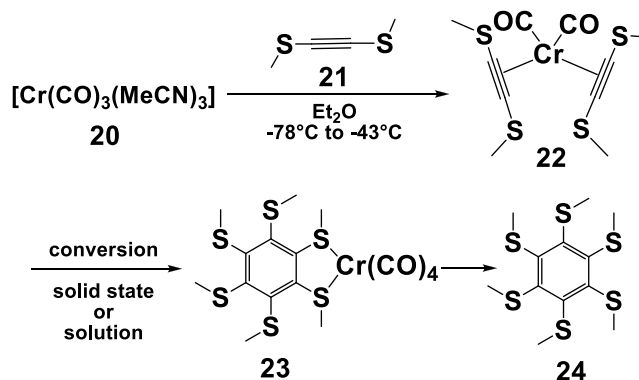
The direct or indirect incorporation of the functional group carrying sulfur, oxygen, or nitrogen on a benzene, pyridine, or pyrene ring may considerably impact its reactivity, physical properties, and biological activities. The formation of C-X (X=S, N, O) or C-C bonds is valuable, and complex molecular entities can be fabricated by linking small fragments of organic molecules or moieties. Direct functionalization of C-X (Cl, Br, F, I) bonds for C-X (X=S, N, O) bond formation is an atom and step efficient alternative to cross-coupling reactions. The benefits of direct functionalization have been overshadowed before, because of early harsh conditions and the right combinations of catalysts and other reaction parameters to take care of. [28-30]



Scheme 3: first synthesis of hexakis(phenylthio)benzene (5) [35]

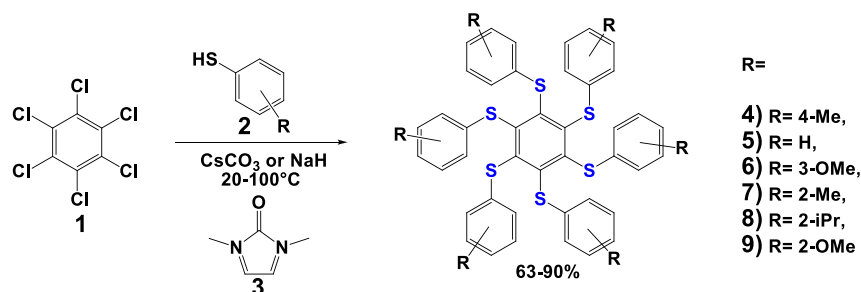
Among some early examples, when hexachlorobenzene was treated with mercaptides in pyridine in 1956, the reaction was quick, but no persulfurated product was obtained. [31-32] Three years later, the same reaction in ethanol reported only tetra and disubstituted products and not fully substituted hexa-substituted products. [33] After 13 years, a Canadian team published their work on the reactivity of perfluoroaromatic compounds towards thiolates in ethylene glycol/ pyridine and obtained similar results. [34] In 1957, the first report of hexakis(phenylthio)benzene (5) came from a reaction of hexachlorobenzene (1) with phenylthiocuprate (20) in a quinoline/pyridine mixture at ~200°C (Scheme 3). [35] It was among the first Ar-S bond created from thiocuprates. Later on, an appropriate polar aprotic solvent was

found for such reactions at reduced temperatures (e.g. DMF, HMPA, DMI). [36-40] Many researchers are now utilizing these reaction conditions for making persulfurated arenes.



Scheme 5: trimerization of bis(thiomethyl) acetylene and generation of hexakis(methylthio)benzene [41]

In 1975, a trimerization with a chromium complex provided hexakis(methylthio)benzene (Scheme 4). [41] Maiolo et al. reported a one-pot synthesis of mercaptobenzenes starting from easily available polychlorobenzenes. [42-43] It provided a direct sulfuration of a perhalobenzene.

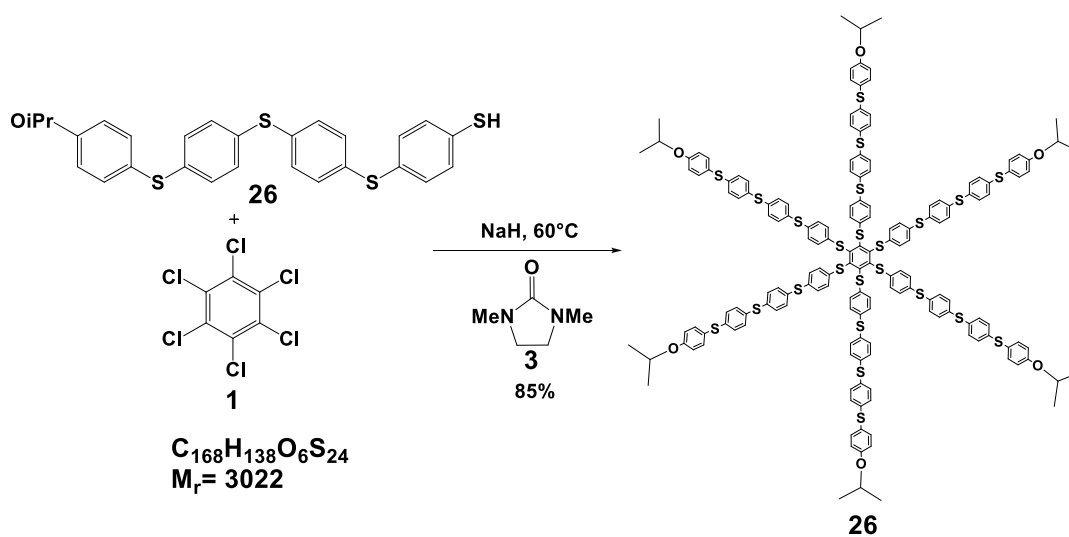


Scheme 5: one-pot synthesis of several persulfurated asterisks [1]

In 2014, Gingras and co-workers published their results on the persulfurated benzene-cored asterisks (4-9) by simply treating hexachlorobenzene (1) with the corresponding thiols at 20-100°C in DMI with a base such as cesium carbonate or sodium hydride (scheme 5). The created molecular asterisks were evaluated for their photophysical properties in the solid state. [1]

In 1998, Gingras and his group took persulfurated arene chemistry to the next level by synthesizing elongated molecular asterisks with a benzene core (scheme 6). They were synthesized as functionalized asterisks via the MacNicol method using DMI

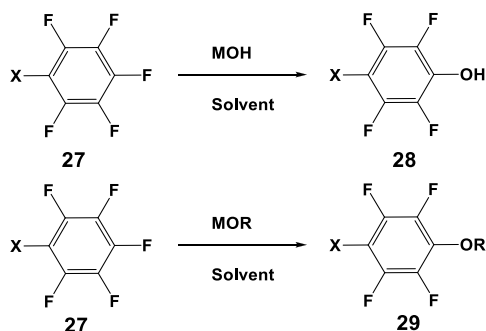
as a solvent. [44] It set the pace to other syntheses of complex asterisks with potent applications in asymmetric catalysis, as phosphorescent metal ion sensors, or as glycodendrimers for studying lectin-carbohydrate interactions.



Scheme 6: synthesis of fourth generation molecular asterisk with a benzene core. [44]

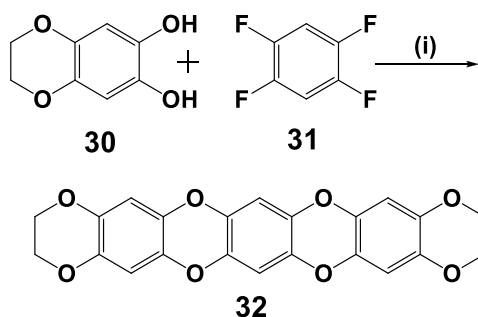
1.1.2 Polyoxygenated Benzene-Cored Asterisks

There is significantly less literature data on peroxygenated arenes, and this area is underexploited. Aromatic halides without activating group do not react so easily with phenols or alcohols in the presence of a base. [45] Harsh conditions are required with a strong heating. Peroxygenated arenes can mainly be synthesized by treating hexachloro-, hexafluoro-, or hexabromobenzene with the desired phenols at very high temperatures, and other parameters need to be optimized according to the reaction. The simplest pentafluorophenol was synthesized by refluxing hexafluorobenzene with potassium hydroxide in pyridine (scheme 7), an effective solvent for the reaction. In 1956, several reactions with hexachlorobenzene were reported. It was found that pyridine as a solvent provides better results than other solvents because of its catalytic effect due to pyridine. When making pentafluorophenol, tetrafluorodihydroxybenzene was also formed. As pentafluorophenol is deprotonated, it reacts with difficulty by $\text{S}_{\text{N}}\text{Ar}$ due to an increase of electronic density on the benzene core. [32, 46] Disubstituted products were also obtained via a reaction of hexafluorobenzene with phenolate anions.



Scheme 7: reaction of hexafluorobenzene with hydroxide or alkoxides (28-29). [45]

In 1994, more complex compounds such as linear benzodioxins were synthesized as donors for making cation radical salts, as candidates for electrolytes in field-effect transistors (scheme 8). The dioxins are more soluble than the corresponding all carbon acenes. Also, O is a lighter element; it has a good charge carrier mobility because of regular π -stacking. Furthermore, the design and π -system properties (such as solubility, crystallinity, intramolecular π -overlap, etc.) can be modified. [47]



Scheme 8: reagents and conditions (i) NaH, NMP, 205C, 81%. [47]

Peroxygenated hexasubstituted asterisks (33-34) were synthesized with a benzene core in 1987 for studying their supramolecular interactions by demonstrating H-bonding for making clathrate structures (cage-like structures) after some structural studies by X-ray diffraction (figure 3). The central benzene ring does not change its planarity, but the ether oxygen atoms were slightly displaced from the outer plane of the benzene core. [48]

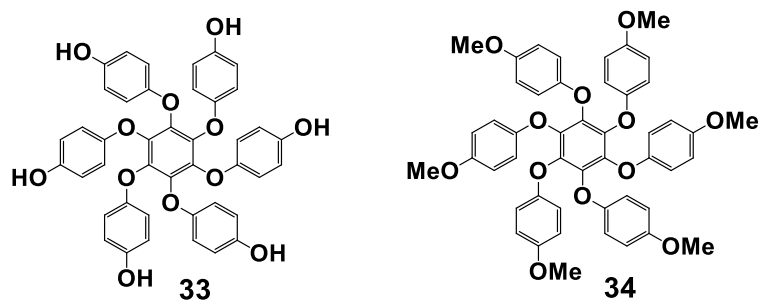
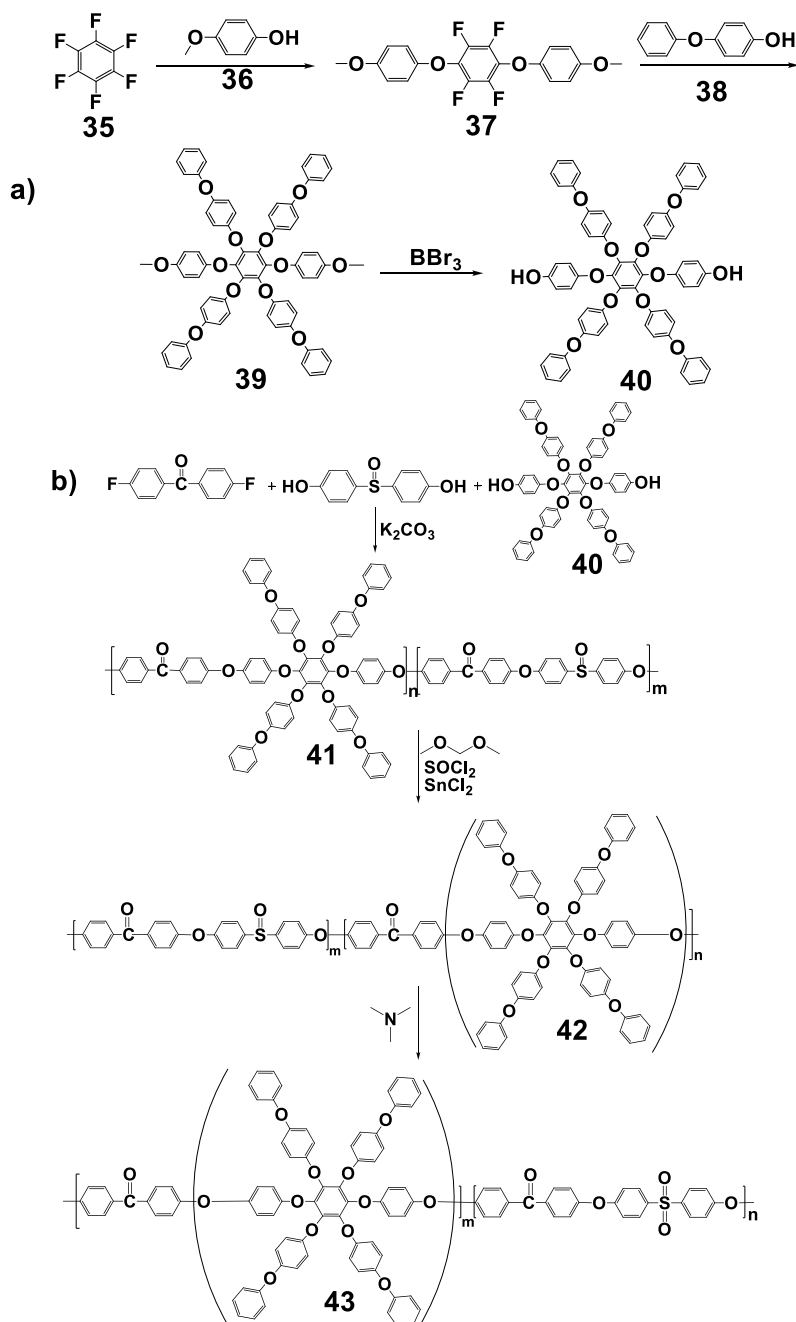


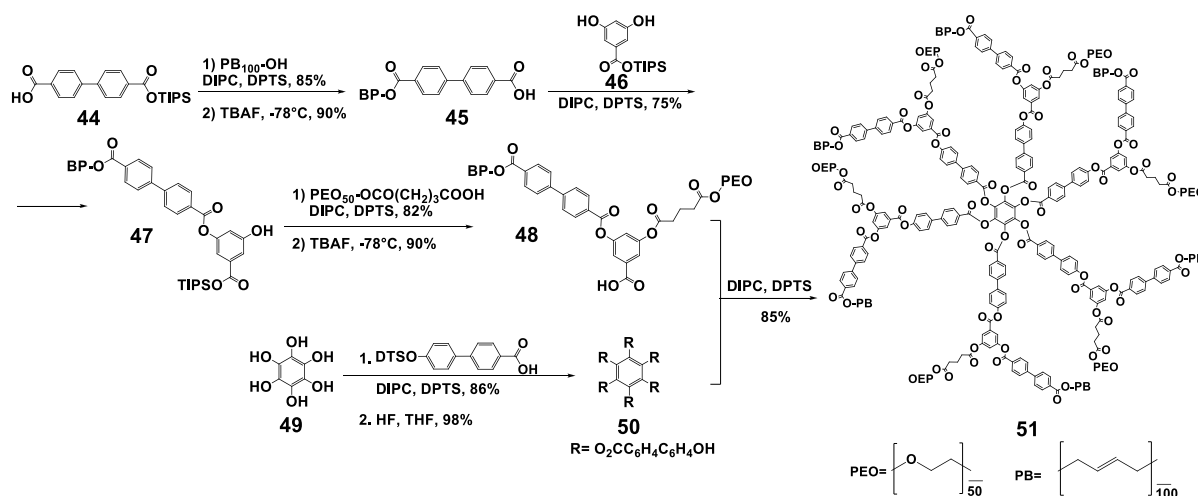
Figure 3: Peroxygenated benzene-cored asterisks synthesized by MacNicol in 1987. [48]



Scheme 9: a) synthesis of bisphenol monomer with 10 electron rich phenyl group; b) Bisphenol monomer polymerized to yield PAEKs, CMPAEKs and QAPAESs (41-43). [49]

In 2004, a new bisphenol derivative with ten electron-rich phenyl groups was synthesized. Monomers, polymers were synthesized and functionalized for high-performance anion exchange membranes. [49]

In 2006, more challenging branched structures were synthesized, as some dendrimers. Well-defined, highly branched peroxygenated molecules are still limited. They used a modular stepwise method instead of a direct approach. [50] The star-shaped molecule consists of 12 hydrophilic and hydrophobic arms with a benzene core (scheme 10). [51]

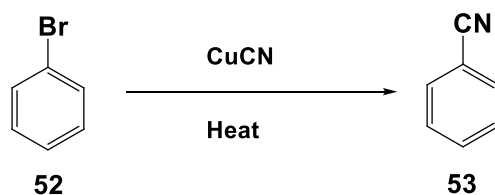


Scheme 10: Star-like amphiphiles with a peroxygenated benzene core. (reprinted with permission of [51])

Recently a Chinese team synthesized perchalcogenated arenes, including peroxygenated asterisk, to study their photophysical properties, as they can emit brightly in the solid-state. [52]

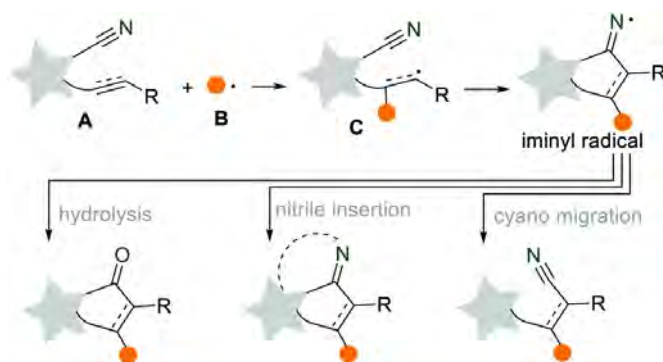
1.1.3 Sulfurated, oxygenated and cyanated benzene-cored asterisks

A cyano function is an activating group for S_NAr reactions when positioned on a benzene ring due to electronegative nitrogen atom, which pulls electron density towards it, making the ring electron-deficient. Hence, it acts as an activating group toward S_NAr and as a deactivating one for S_EAr reactions. Arylated nitriles can be prepared by classical synthetic routes using the Sandmeyer [53] or Rosenmund-von Braun reactions (scheme 11), [54] but both require toxic CuCN reagent and harsh conditions (strong heating).



Scheme 11: Rosenmund–von Braun reaction [54]

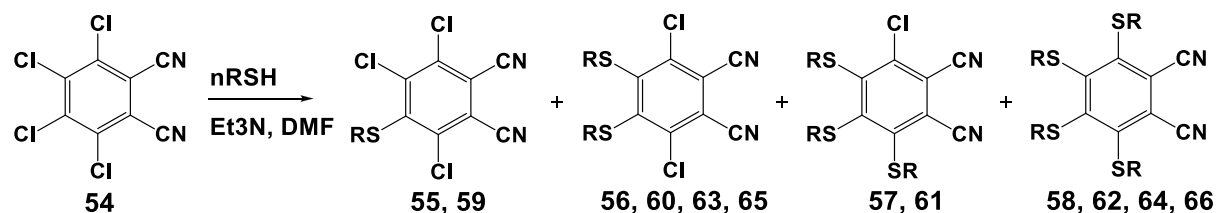
In spite of toxicity, it is one of the common reactions to prepare benzonitrile in the laboratory, with toxic CuCN in DMSO while heating. Cyanated benzene derivatives are interesting because the cyano group changes the redox and the photophysical properties of the polysulfurated or polyoxygenated benzene core, and offers interesting mechanistic studies for organic reactions. A recent study showed that cyanated benzene derivatives could undergo radical cascade reactions when irradiated by light. The cyano group is thus an important and easily available function for preparing various functional groups in organic chemistry such as amines, acids, ketones, etc.. Recent applications of the cyano group as a radical acceptor can lead to different interesting heterocycles and carbocycles. [55] This publication showed the transformation of iminyl radicals into N-heterocycles via nitrile insertion, and remote cyano migration can be seen from scheme 12.



Scheme 12: The cyano function as a radical acceptor in cascade reactions. [55] Reprinted with permission from Organic Chemistry Frontiers. [55]

Several methods were developed for the cyanation of arenes [56] as they have many applications in dyes and pigments, catalysis, photo- and electrocatalysis, heat resistant polymers, lasers and optical filters. [57-68] However, there is a very limited number of publications in the literature on persulfurated or on peroxygenated cyanated benzene derivatives. In 2007, a Russian publication indicates the synthesis of poly[phenyl(alkyl)sulfanyl]-substituted phthalonitriles and some phthalocyanines. By

reacting tetrachlorophthalonitrile with the corresponding thiols at different ratios with triethylamine as a base in DMF at room temperature, a series of cyanated aryl sulfides were formed (scheme 13). Interestingly, they observed the first replacement of the fourth chlorine atom and then chlorine at the fifth position. They also tried 1:1; 1:3 ratios of (**54**)/thiol and found that on using a 1:1 ratio gives three products: one is the starting compound-I, and the others are the mono and disubstituted sulfides.



55-58, R=Ph; **59-62**, R= tBu; **63, 64**, R= nBu; **65, 66**, R= n-C₁₀H₂₁

Scheme 13 : synthesis of different polysulfurated dicyanated benzene-cored asterisks. [67]

It was notable that each thiol gave only one monosubstituted and one disubstituted product. The reaction was regioselective. While using a 1:2 ratio (compound-54 and thiols), only the disubstituted products (56, 60, 63, 65) are formed in high yields with traces of mono and trisubstituted products. For the 1:3 ratio (di-, tri-, and tetra- products were formed), whereas for the 1:4 ratio, only tetrasubstituted products were observed (58, 62, 64, 66). A sc-X-ray diffraction structure determination was obtained from the monocrystal of compound 56 (Figure 4). Reactions with ratio (compound-I and thiols) 1:2 and 1:4 gave results in high yield for 4,5-bis[phenyl(alkyl)sulfanyl]-3,6-dichlorophthalonitriles and tetrakis[phenyl(alkyl)sulfanyl]-phthalonitriles which absorb in red and near-IR region of electronic spectra. [69]

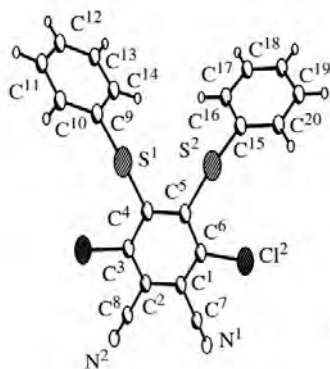
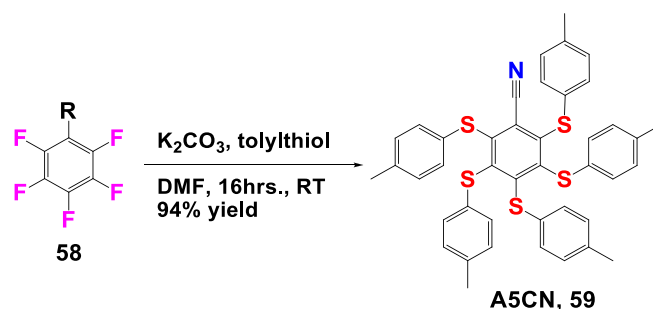


Figure 4 : sc-XRD of 3,6-dichloro-4,5-bis(phenylsulfanyl)phthalonitrile (57). [69]

In 2012, three pentasulfurated asterisks were published, out of which one is the pentasulfurated cyanated asterisk (A5CN), from a work previously done by doctoral students Raymond Noel and Marco Villa from the Gingras's laboratory (scheme 14). The cyano function is an electron-withdrawing group that pulls out the electron density of benzene, making it electron deficient, and strongly polarizes the central benzene ring, mainly responsible for the emissive properties. [70]



Scheme 14: synthesis of a pentasulfurated cyanated asterisk (59). [70]

In the crystal packing (figure 5), this asterisk showed one intramolecular interaction in orange color (between C(14)-H(14)) with a C-S distance of 3.4 Å, a C-H---S single bond 120.5° and two intermolecular interactions in green color (between S(4)-C(29)) of 3.4 Å and C-H---S angle of 136°) between the cyano group and an aromatic carbon atom is belonging to a toluene ring of a symmetry-related molecule on the other hand (shown in light blue in Figure 4) with N(1) ...C(21) distance of 3.02 Å and C-H...N angle of 136°.

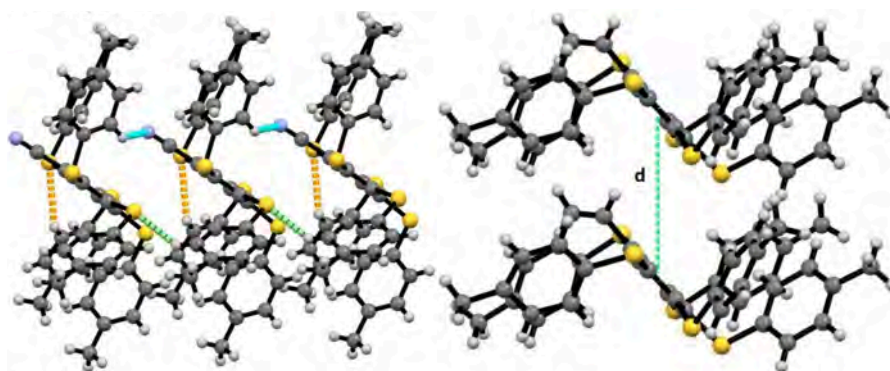
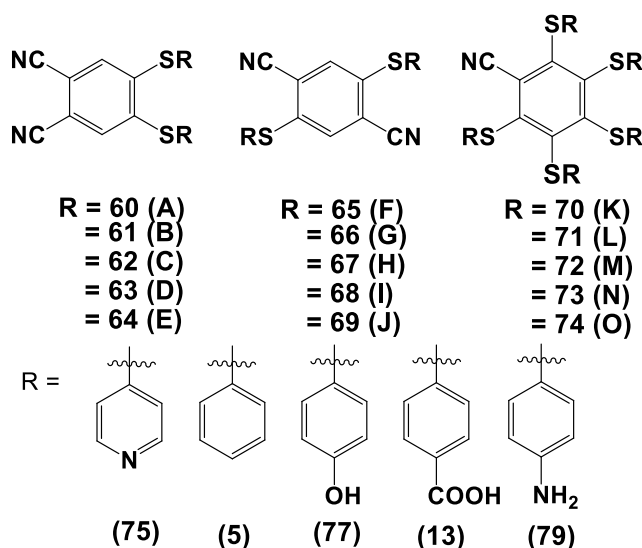


Figure 5: a) H-bonding network in A5CN asterisk (59) with one intra (orange lines) and 2 intermolecular interactions (green and blue lines); b) Interplanar distance between the central benzene ring (reprinted with permission). [70]

The interplanar distance between the central benzene ring can be seen from scheme-14b, which is 5.9 Å and positioned in an edge-to-face manner. Most importantly, this asterisk emits in both solid and in solution states. It is strongly phosphorescent, with an orange color. The blue shift in the emission from room temperature to 77K (in fluid solution) is a typical example of rigidochromic effect that suggests that electronic transition has a charge transfer involving sulfur. In the solid-state, a red shift was observed compared to 77K in a matrix, a phosphorescence band was observed, and the corresponding lifetimes were affected by dioxygen concentration. Moreover, the orange phosphorescence is not so common, thus it can have potential applications in bioimaging since orange light can have higher tissue penetration compared to a green light, from the previously reported hexakis(phenylthio)benzene (5). [11]

In 2017, a novel series of tetrasubstituted aromatic thioethers with a benzene core were synthesized (Scheme 15). Out of 15 different compounds, three ortho compounds (60, 61, 62) were synthesized before in the literature but never investigated for their fluorescence properties. [71]

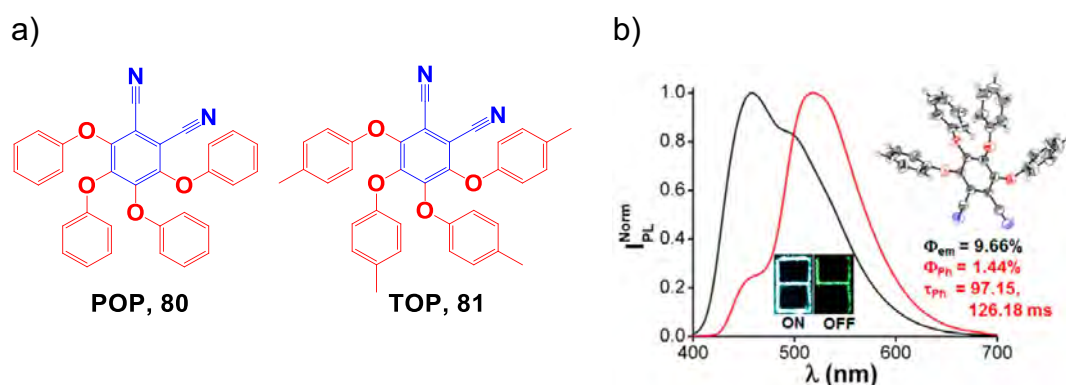


Scheme 15: synthesis and photophysical studies of some cyanated and sulfureted benzene derivatives

These asterisks cover the full visible region from blue to orange-red light. Electron withdrawing groups reveals a blue shift, whereas electron-donating groups reveal a redshift in the spectrum. The aggregated size (40 to 300 nm) and the dispersion were studied via DLS and TEM. Metal ion complexation was not achieved with these asterisks, but it could be interesting. All compounds were AIE active. [72]

Recently in 2018, some cyano groups were introduced on tetrasubstituted peroxygenated benzene-cored asterisks and the bioluminescence was studied. Two asterisks (scheme 15, POP & TOP) were synthesized with two different aromatic alcohols (phenol and cresol) with phenyl (POP) and tolyl (TOP) substituents via some aromatic nucleophilic substitution reactions at room temperature. The studies were done for both in amorphous powder and crystal forms after some X-ray studies. , it was found that inter and intramolecular interactions in POP ($1p(O)\cdots\pi$, $\pi(C=C)\cdots\pi(C\equiv N)$, H-bonding and C-H $\cdots\pi$ interactions from head to tail) and in TOP ($\pi(C=C)\cdots\pi(C\equiv N)$, H-bonding) leads to rigidity and suppress the non-radiative pathway, in POP this indicates more non-covalent interactions reinforce intersystem crossing that leads to green afterglow phosphorescence or p-RTP (persistent room-temperature phosphorescence) can be seen from scheme 16b.

For studying the AIE effect, studies were done in a THF-H₂O mixture, a bathochromic shift from 400 to 462nm was found with a decrease in intensity on the increase in the concentration of water up to 50% (v/v) to THF solution in POP. Also, increasing H₂O content (90% v/v) increases intensity by 3.5 fold, with a red shift results from restricted rotations of the phenoxy groups due to aggregation. For TOP, a bathochromic shift was observed with an increased in solvent polarity caused by the charge-transfer character in an excited state. Hypochromic shift observed with an increase in water content (70%, v/v) causes aggregation.



Scheme 16: a) POP and TOP; b) sc-XRD structure of POP and photophysical studies, number 8 pattern (UV ON) with POP and afterglow 4 pattern (UV OFF) when UV lamp 365nm was switched off (reprinted with permission of the Journal of Physical Chemistry Letters). [73]

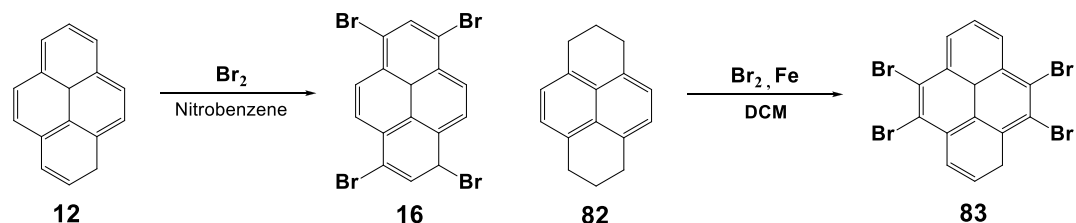
POP shows RTP at 520nm (12.6ms) for phosphorescence studies with λ excitation = 365 nm and a broad peak 415-470 nm (97.2 ms), extended lifetime confirms p-RTP observed with naked eyes in the powder form. In crystal form, similar features were observed along with relatively long green afterglow (λ emission = 415-470nm, 197.8 ms; λ emission = 520 nm, 253.2 ms) former band completely quenched at ~415-470 nm. Compared to the behavior with AIE in THF-H₂O, the peak at 457nm in powder and crystal originates from the same species (exciplex) present in the solvent mixture. Confirms origin of 520 nm peak from inhomogeneity of aggregates in powder. In TOP, lack of p-RTP due to molecular arrangements that activate non-radiative pathways. [73]

1.2 Sulfurated pyrene-cored asterisks

Pyrene is the smallest peri-fused polycyclic aromatic hydrocarbon, as discussed in section 1 in details [16], which offers an extended π -system. Due to its attractive electronic and optoelectronic properties, it can be used as a building block for many organic molecules which have applications in OLEDs (organic light-emitting diode), OFETs (organic field-effect transistors) and OPVs (organic photovoltaics). [74-75] Due to its supramolecular properties, it is capable of π -stacking and CH- π interactions which, in water, can be reinforced by hydrophobic effect. [76-77] This has been much exploited in the non-covalent functionalization of extended planar π -system such as carbon nanotubes [78-81] and graphene. [82-83] It can also be helpful in the biological system for binding nucleic acids. [76-85]

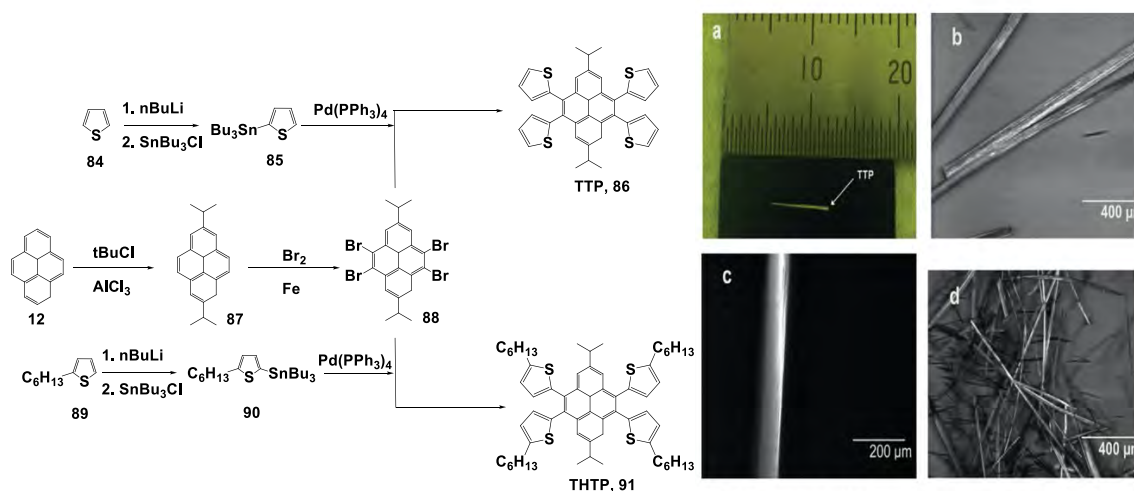
Electrophilic substitution preferably takes place at 1,3,6,8 position on pyrene as these are the most electron-rich centers and most reactive [78] whereas substitutions at positions 4,6,9,10 are not so common and easy. Most of the pyrene derivatives are mono-substituted [16], here we will present tetrasubstituted pyrene derivatives, more precisely, tetrasulfurated pyrene derivatives. As previously reported in 1987, bromination of pyrene takes place in gram scale at the positions 1,3,6,8 by treating it with bromine in nitrobenzene at high temperature in a yield of 90% (scheme 17, left). [86] The route to the synthesis of 4,5,9,10-tetrabromopyrene (83) via halogenation of 1,2,3,6,7,8-hexahydropyrene (82) in DCM is shown below (scheme 17, right). [87] Several indirect methods were discussed to provide a range of 4,5,9,10-substituted pyrenes, which is a real challenge to prepare them directly in one step. This difficulty encourages the development of new synthetic routes and the design of new pyrenic

systems which could be exploited due to their optical, electronic and structural properties, as novel building blocks in materials science. [75]



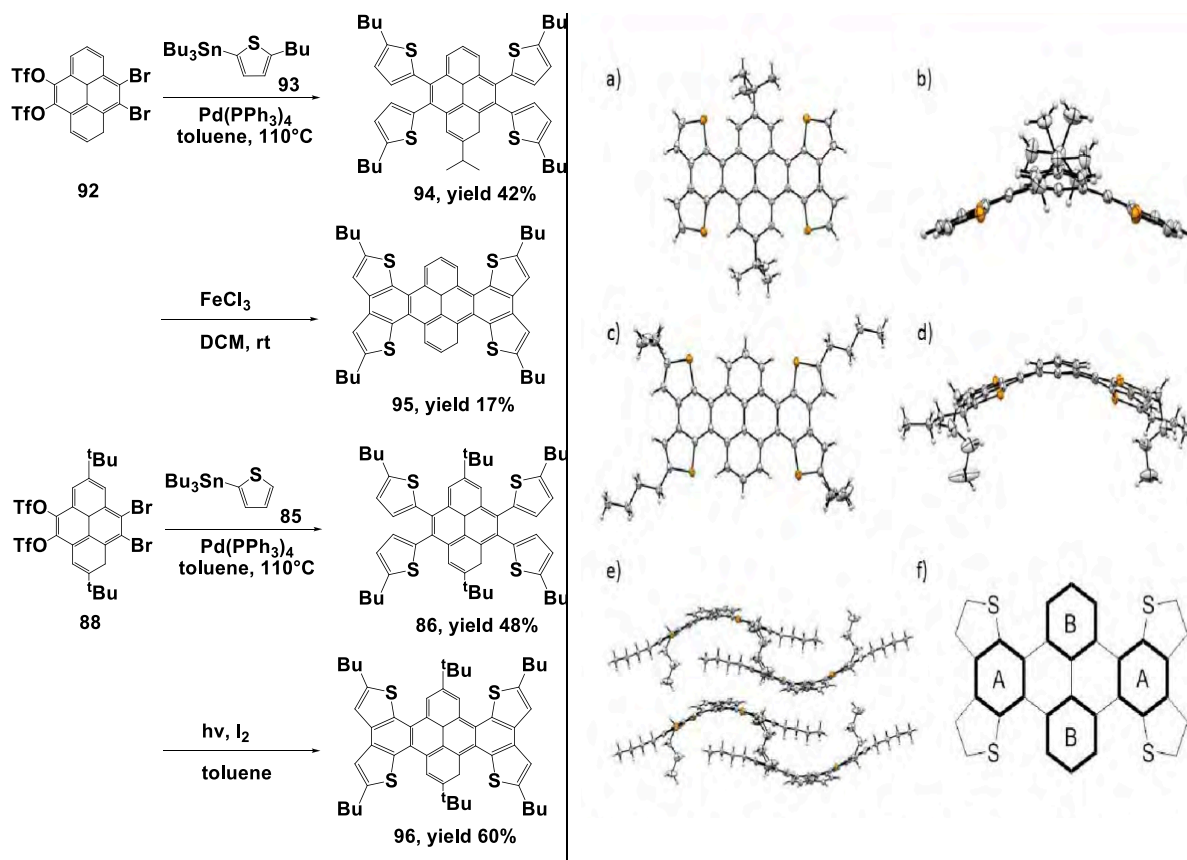
Scheme 17. Left: synthesis of 1,3,6,8-tetrabromopyrene (16) [86]. **Right:** synthesis of 4,5,9,10 tetrabromopyrene (83). [87]

The uses of 4,5,9,10-tetrabromopyrene (83) and such pyrene functionalization in the K-region are still underexploited but a few articles mentioned it. In 2011, the synthesis of a novel pyrene derivative with four substitutions at positions 4,5,9,10 with a thienyl group was undertaken from another indirect method using a Friedel-craft alkylation with a sterically congested tertiary halide. It was followed by a regioselective tetrabromination at positions 4,5,9,10, followed by Stille couplings to incorporate the thienyl groups. The optical and electrochemical properties were studied, as well as the morphology of the solid. The UV-vis spectra indicated a small redshift for THTP compared to TTP (scheme 18) owing to the electron-donating effect of the hexyl chains of the thienyl groups, to provide a good solubility and some Van der Waal interactions between the alkyl chains. Extended π - π stacking makes it easy to grow large microwires, which can be seen from the picture given in scheme 18 (right side). [88]



Scheme 18. Left: synthetic procedure of TTP and THTP. **Right:** camera picture of TTP micro-wire (a), optical micrographs of TTP micro-wires (b, c) and (d)THTP micro-wires (reprinted with permission from Molecular Crystals and Liquid Crystals). [88]

Müllen and his group published their work (scheme 19) showing pyrene substitutions at positions 4,5,9,10. Thienylations at positions 4,5,9,10 via Stille couplings produced hexaaryl[a,c,f,g,j,l,o,p]tetracene via cyclodehydrogenation. Low yield was observed for 95 (17%) due to side reactions at the beta position of the thienyl groups. Compound 94 was polymerized with iron chloride. However, iron can cause a side polymerization reaction at the alpha-thienyl free position for 10, thus an oxidative photocyclodehydrogenation with iodine was successfully applied. X-ray diffraction studies were performed on both crystals of 95 and 96. They both exhibit a saddle conformation, as shown in scheme 19. [74]

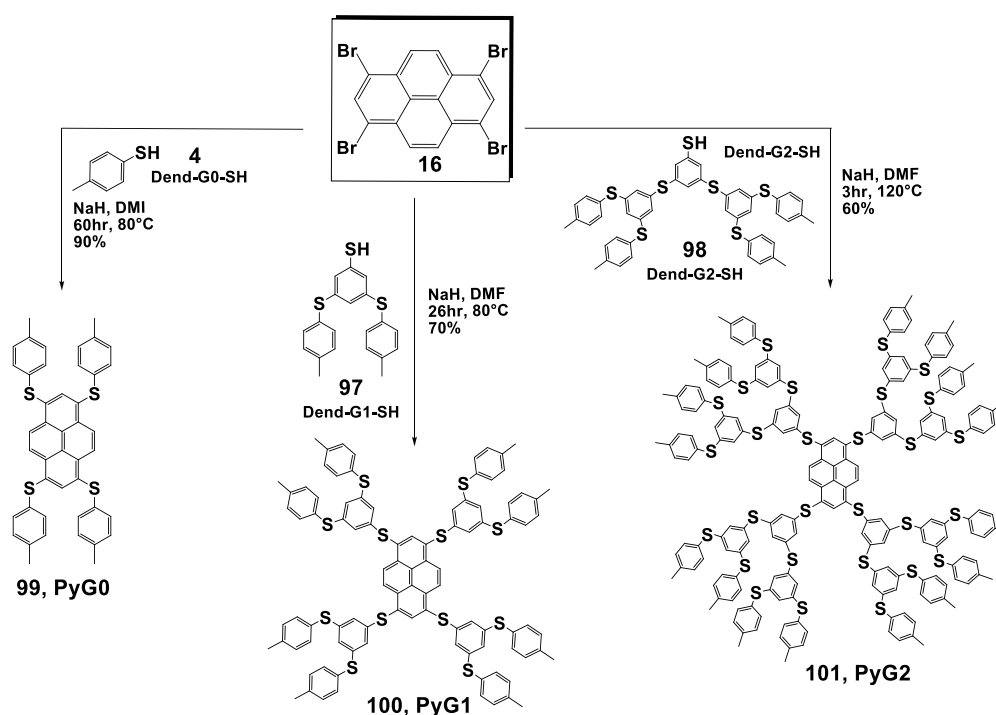


Scheme 19: Left: 4,5,9,10-Tetrathienylation and Subsequent Oxidative Cyclodehydrogenation to Hexaaryl[a,c,f,g,j,l,o,p]tetracenes 95 and 96. Right: X-ray structure of 95 and 96. Two of four n-butyl side chains are disordered. For clarity, only the majority component is shown. (a) 96 front view; (b) 96 side view; (c) 1 front view; (d) 95 side view; (e) crystal packing of 95; (f) illustration of planar benzene rings A and B; used for calculation of curving angles (reprinted with permission).

As for 1,3,6,8-tetrabromopyrene (16), previous work were established from its C-arylations and C-alkynylations. However, the sulfuration of pyrene at these positions

were mainly limited to sulfonations. In 2008, the synthesis of a new series of polysulfurated pyrene-cored dendrimers (given below) was produced from 1,3,6,8-tetrabromopyrene by the group of Pr. Marc Gingras (scheme 20). By increasing the dendritic generation number, a dendron localized absorption band at ~260 nm increases strongly in intensity and becomes red-shifted. These are stable redox switches that possess reversible redox states, electrochromic and luminescent properties, even in the presence of air. [89]

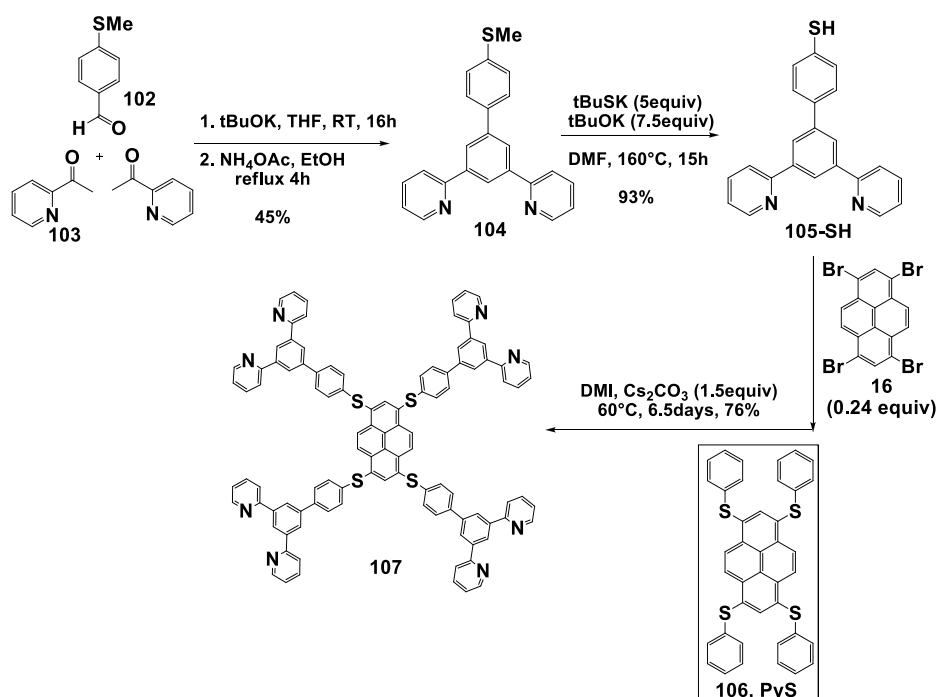
In 2014, the investigations of their electrochemical, photophysical, and electrochemically generated chemiluminescence (ECL) were achieved with some collaborators in Bologna. [90] For this family of dendrimers, it was found that the redox properties were dependent on the generation number, and it was easier to oxidize and to reduce the higher dendritic generations.



Scheme 20: synthesis of electro- and chemically responsive sulfurated pyrene-cored dendrimers. [90]

The 1,3,6,8-tetrabrominated pyrene core (16) was chosen because of its synthetic access and its geometry for making star-shaped structures. Its enhanced photophysical and electrochemical properties were established after sulfuration (i.e. sulfur effects on the properties). Further work was achieved in 2014 with a multichromophoric system, with four appended terpyridine units to pyrene, which

collects light from the peripheral units and funnels the energy to the pyrene core, as shown in scheme 21. Photophysical studies were done by chelating 104 and 107 with different metal ions (Zn^{2+} , Fe^{2+} , Nd^{3+}). It was observed that for compound 104, a redshift of lowest energy for free ligand was observed. The bands appearance in the visible region at 575 nm due to metal-to-ligand transfer was observed with Fe^{2+} in DCM, and complete quenching at 390 nm was observed. Whereas for compound 107, there is a decrease of the emission band of the tetra(thio)pyrene, indicating that the complexation of the metal by the external terpyridine quenches the luminescence of the core. By exciting at the isosbestic point at 410 nm, the emission band at 460 nm decreases upon additions of Fe^{2+} , reaching a complete quenching at two equivalents of metal ions. The results prove the formation of metal complexes in a ratio of 1:2 of ligand 107 to metal ions. Because four terpyridine moieties are present in each molecule, the stoichiometry of terpy to a metal ion is 2:1, as for the model compound 104. The geometry suggests the formation of oligomeric structures built on $[\text{M}(\text{tpy})_2]^{n+}$ interactions. The dimensions of the nanoparticles were studied via DLS and AFM. [91]



Scheme 21: synthesis of a new multichromophoric tetra(phenylthio)pyrene (107) core appended with four terpyridine units, as a highly luminescent polysulfurated pyrene derivative for sensing metal ions. (reprinted with permission from Chem. Eur. J.) [91]

These preliminary results set the departure for a new research area in the heterofunctionalization of pyrenes which is still in its infancy state, especially for

sulfuration (besides sulfonation of pyrene which is known). This is thus a clear demonstration of preliminary results encouraging the development of sulfurated pyrenes toward organic materials, but also for biological sciences and (bio)sensing devices. Thus the regioselective sulfuration of pyrene is still underexploited in pyrene chemistry. Sulfonation has been one of the preferred methods in the history of pyrene. Rare monothioarylations at positions 1 and tetrathioalkylations at positions 1,3,6,8 for making organic conductors are known. However, other sulfurated pyrene derivatives could be sought by simply using nucleophilic aromatic substitutions from pyrenyl bromides or fluorides with nucleophilic sulfur sources. Cu- or Pd-catalyzed reactions of pyrenyl iodides or bromides with aryl- or alkylthiolates are also possible but almost non-existent. Sulfur substituents would drastically change the redox properties, solubility, and conformational issues and promote molecular diversity by oxidizing a sulfur linkage to a sulfoxide or a sulfone. Sterically demanding *t*-BuS groups are attractive because of their dual use as solubilizing groups and a protecting group for thiols. They could also direct halogenations in pyrenes. They could be cleaved and *in situ* acylated without disclosing oxidizable sulfhydryl functions in air. *t*-BuS groups can be introduced via standard Pd-catalyzed Ar-S coupling methods. [92-93]

1.3 Photophysical properties of the asterisks

1.3.1 Basic concept in photophysics

As shown in figure 6, when molecule (A) absorbs suitable energy from irradiation, the electrons get excited and jump to a suitable excited state (A^*), but when the electrons come back to their ground state (to their original energized state), it will emit the extra energy absorbed. This energy can be emitted in a photoreaction, non-radiative decay (degradation of heat), or radiative decay (luminescence). [94-95]

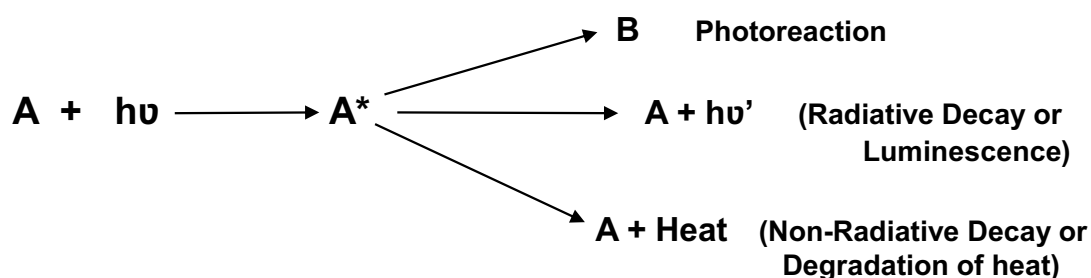


Figure 6: Possible pathways for an excited molecule to relax.

We can better understand these terms with the help of a Jablonski energy diagram (figure 7). [96]:

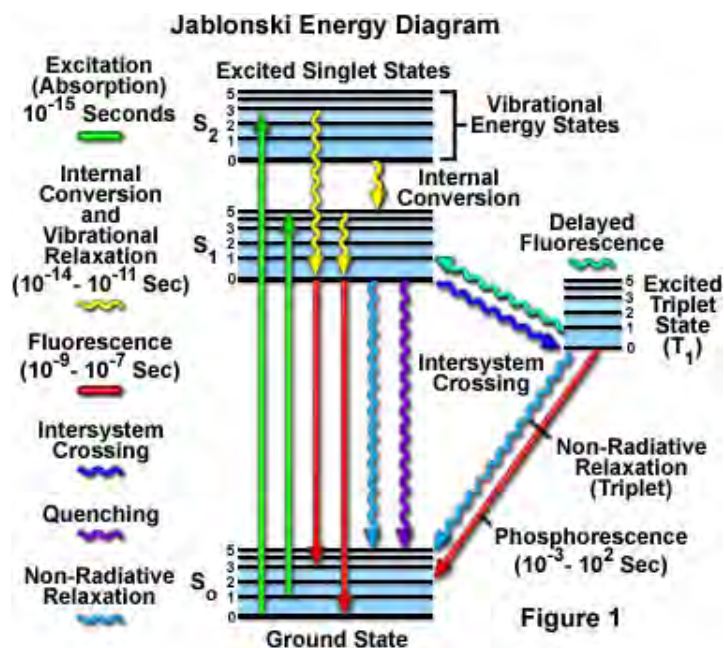


Figure 7: Jablonski energy diagram (reprinted with permission Molecular Expressions website). [96]

All these events take place over a range of time given above. The straight arrows represent the radiative decays, spontaneous emission, and a quantum mechanical system (a molecule, an atom, or subatomic particle) that emits light when it relaxes back to a lower energy state or ground state. If an electron suffers vibrational relaxation and then relaxes to its ground state, it is known as **fluorescence**. This transition occurs from singlet (S_1) excited state to ground state (S_0). If an electron jumps to an excited triplet state (T_1 , also known as intersystem crossing) and then relaxes back to the ground state (S_0) is known as **phosphorescence**. This phenomenon is slower than fluorescence (S_1 to S_0) and occurs from (T_1 to S_0). Internal conversion from S_1 to S_0 , the lowest-energy (or ground) state, is much slower, allowing time for the molecule to either emit a photon (fluorescence). Whereas, for non-radiative decays, the excess of energy of the excited state A^* is dissipated as heat by collision with the solvent molecules or by specific vibration or rotation of molecules. [94-96]

1.3.2 Aggregation-Induced Emission (AIE)

As the name suggests, it is emission of light due to aggregation caused by restriction of intramolecular motions (rotations or vibrations). A typical example of molecule for AIE is tetraphenylethene (TPE). Such luminogens with an AIE property are referred as AIEgens. In figure 8, the rotation of four phenyl rings linked to central ethene core represents one major intramolecular motion. In dilute solution, the intramolecular rotations are free and electron can relax back to its ground state via non-radiative decay. In contrast, when the solution is highly concentrated, it forms aggregates and blocks non radiative pathway and opens radiative decay pathway for relaxation. The intramolecular rotations are restricted, meaning the path for an excited electron to come to its ground state is blocked, and hence it emits light in AIE. This phenomena is possible in a rigidity state, in aggregate or in solid state.



Figure 8: AIE phenomenon in TPE (tetraphenylethene); (reprinted with permission). [97]

From figure 9, we can see another example of AIE, where aggregation-induced emission is due to restricted rotations. However, in another example with THBA (10,10',11,11'-tetrahydro-5,5'-bidibenzo[a,d][7]annulenyliene), the aggregation-induced emission is due to restricted vibrations of two phenyl rings connected by bendable double bond. There is no single bond rotation in this molecule, and it is non-coplanar in an anti-conformation. The flexibility allows phenyl rings to vibrate in solution for non radiative decay. [97]

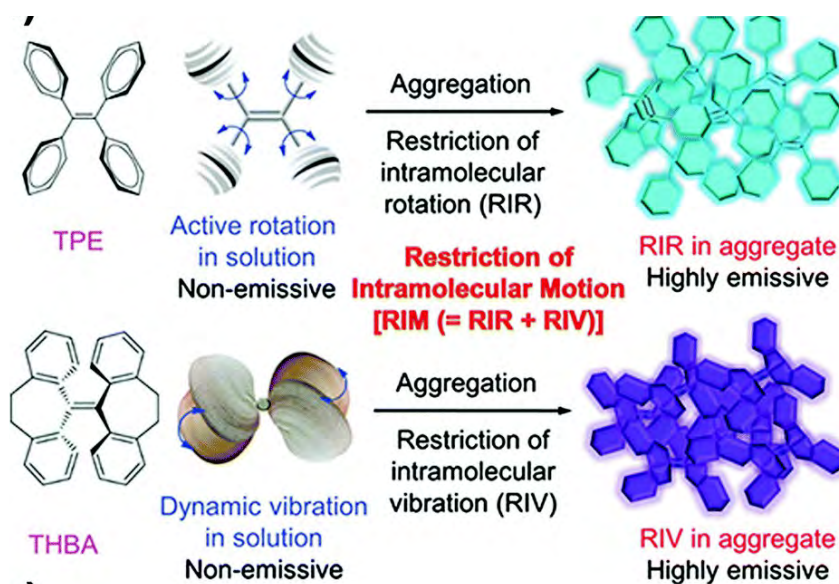


Figure 9: Tetraphenylethene (TPE) with unrestricted rotation and in aggregate form with restricted intramolecular rotations (RIR); 10,10',11,11'-tetrahydro-5,5'-bidibenzo[a,d][7]annulenyliene (THBA) with unrestricted vibrations and in aggregate form with restricted vibrations (RIV). (Reprinted with permission Acta Polymerica Sinica). [97]

1.3.3 Aggregation-Caused Quenching (ACQ)

Aggregation-caused emission (ACE) occurs when a molecule can emit light, but its emission is quenched in the aggregated state. Aggregate refers to an ensemble or a cluster of molecules. When emission from a luminophore in solution is quenched with an increase of its concentration, it is known as concentration quenching (CQ), a common phenomenon with aromatic hydrocarbons and their derivatives. In a highly concentrated solution, a weak emission can occur through the aggregation of luminophores. [97-102] The chromophores usually exhibit high fluorescence in dilute solutions, yet luminescence is quenched at high concentrations or in the aggregate state, by aggregation-caused quenching. [103] A typical example of ACQ comes from fluorescein (figure 10). It is soluble in water but insoluble in organic solvents. In water (flask 0 with no acetone), it emits bright green fluorescence, but as the acetone is added to the flask, the ACQ effect dominates and quenches the fluorescence due to its poor miscibility in acetone. The solute self-assembles via π - π stacking. Fluorescein powder does not emit light in the solid-state.



Figure 10: ACQ in fluorescein ($15\mu\text{M}$) in water/acetone mixture with different fractions of acetone (f_a). (Reprinted with permission). [97]

ACQ is opposite to that of AIE. As we can see from Figure 11, the emission weakened with the addition of water in ACQ, whereas the emission intensified with the addition of water in AIE.

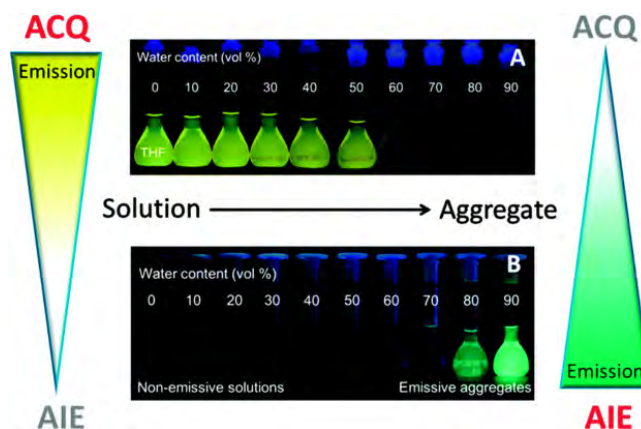


Figure 11: difference in AIE (Aggregation-Induced Emission) and ACQ (Aggregation- Caused Quenching). (Reprinted with permission). [97]

1.3.4 Rigidity-Induced Phosphorescence (RIP) from persulfurated benzene-cored asterisks

When the intramolecular rotations/vibrations are restricted because of aggregation of the molecules in concentrated solution, it is known as AIE (Aggregation-Induced Emission) when the luminescence intensity increases. The intramolecular rotations/vibrations are restricted due to matrix solidification and the molecule relaxes via a radiative pathway known as RIP (Rigidity-Induced Phosphorescence). Usually, organic molecules at room temperature have their phosphorescence quenched by dioxygen due to a long lifetime of the triplet excited state, but this limitation is overcome by molecules having ability to aggregate.

There are many examples of phosphorescent materials based on complexes with heavy metals; it increases the efficiency for populating the triplet excited states leading to phosphorescence. The hexathiobenzene core with six tolyl groups exhibits excellent phosphorescence properties as a powder or in dichloromethane:methanol (1:1, v/v) at 77K due to restricted intramolecular rotations of C-S bond, and reduced conformational mobility of the tolylthio substituents (Figure 12). It slows down the non radiative decay compared to radiative decay from lowest excited state (triplet state). It is not phosphorescent in fluid form. The emission was recorded over a range of temperatures and an increase in the intensity (30 times more) is accompanied by a blue shift of emission maximum at 555-515 nm at 115 K. [11]



Figure 12: highly phosphorescent persulfurated benzene-cored asterisk (4), hexakis(4-methyl-1-phenylthio)benzene) in solid state at 77K. (Reprinted with permission). [29]

In figure 13, 1,2,3,4,5,6-hexakis ((4-([2,2':6',2''-terpyridin]-4'-yl) phenyl)-thio) benzene asterisk (108) incorporates of 6 terpyridine units, each one have three nitrogen atoms which help in the coordination to a metal ion. The asterisk itself is luminescent in the solid-state (as a powder), but not in a fluid solution. The synthesis was achieved with hexachlorobenzene, cesium carbonate, and the corresponding thiol (tpy-SH: terpyridine thiol) in DMI at 60°C in a yield of 97%. The model compound used to compare the data was hexakis (4-methyl-1-phenylthio)benzene).

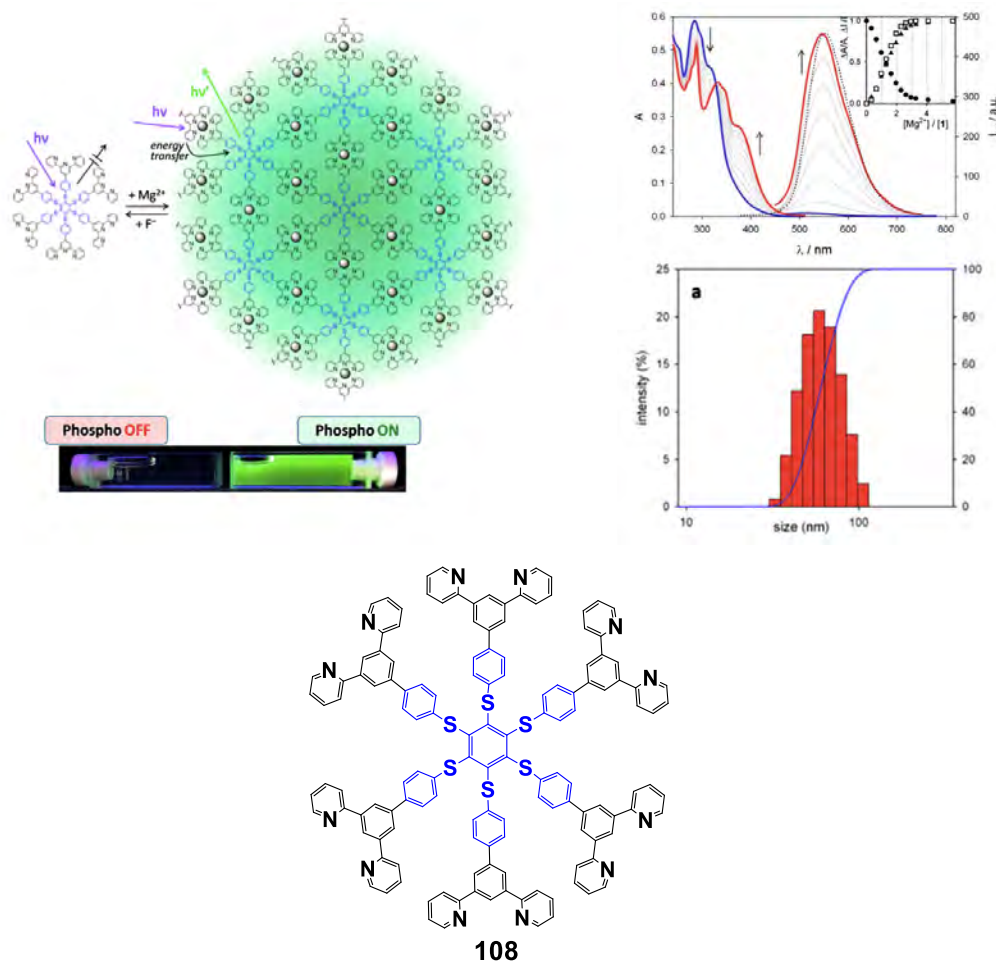
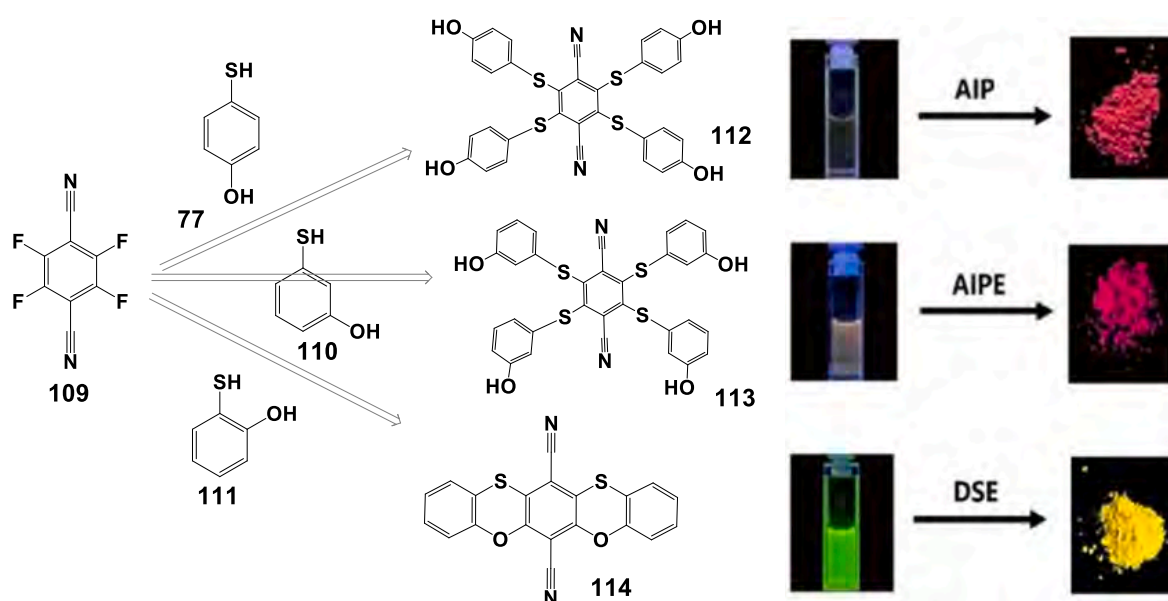


Figure 13: Metal coordination to a terpyridine ligand and spectral changes of absorption and emission upon titration of Mg^{2+} ions to a THF solution. Absorption (left) and phosphorescence spectra (right) of a 3.3×10^{-6} M solution of terpyridine asterisk (**108**) in air-equilibrated THF solution; Size distribution by DLS. (Reprinted with permission). [12]

The long lifetime of this Tpy asterisk molecule (**108**) suggested that this radiative deactivation is phosphorescence. In an air equilibrated solution in THF, changes in absorption and emission spectra were observed after addition of Mg^{2+} ions (Figure 13). A red-shift at 380 nm was observed with an isosbestic point at 326 nm. On exciting at this wavelength, new phosphorescence appears at 545 nm. Both emission and absorption intensities reach a plateau at 3 eq. of Mg^{2+} ions per Tpy asterisk molecule (**108**). The final emission for (**108**) (red line) and in solid form (dotted line) were superimposed and similar lifetimes were found, which suggested that it is a typical phosphorescence of 4-methyl-1-phenylthio)benzene. Also, from DLS studies, it was observed that the size of aggregates reaches a plateau at the end of the titration (3.5 eq. of metal ions per (**108**)) with an average diameter of 60 nm. However, the phosphorescence turned on after adding Mg^{2+} because of the formation of

supramolecular polymers, which restrict intramolecular rotations of the chromophore in the asterisk (108). This supramolecular system can be disabled by adding fluoride ions; by complexation with the Mg^{2+} ions. [12] Similar studies were recently achieved in 2019 by same group with hexakis(4-carboxylic-1-phenylthio)benzene asterisk with a selective Pb^{2+} complexation, and disassembly was shown with EDTA. [107]

In 2020, Feng et al. modified 2,3,5,6-tetrafluorobenzene-1,4-dinitrile (TFBD) with three mercaptophenols. They designed and synthesized three persulfurated molecules with para or meta to ortho substituents (scheme 22), among which para-compound (p-THPT: with para substituents) had typical AIP properties, meta-compound (m-THPT) had aggregate-induced phosphorescence enhancement (AIP) properties. BOPDC was a luminescent agent that could emit light in both liquid and aggregated states. [104, 106] Dual state emission (DSE) is defined as molecular entities capable of intensely fluorescing both in solution and in the solid-state. [104]



Scheme 22: Three classes of luminogens, from RIP (rigidity-induced emission) to DSE (dual-state emission). (Reprinted with permission). [104]

Synthesis, sc-X-ray structure determination, and phosphorescence of pentasulfurated and cyanated benzene cored asterisk (A5CN, 59) were previously presented in section 1.1.3, Scheme 14. However, a comparison of photophysical studies with these three asterisks was not made (Figure 14). The emission spectra (figure 15) were recorded both in solution (dichloromethane/ methanol;1:1 (v/v)) and in a rigid matrix.

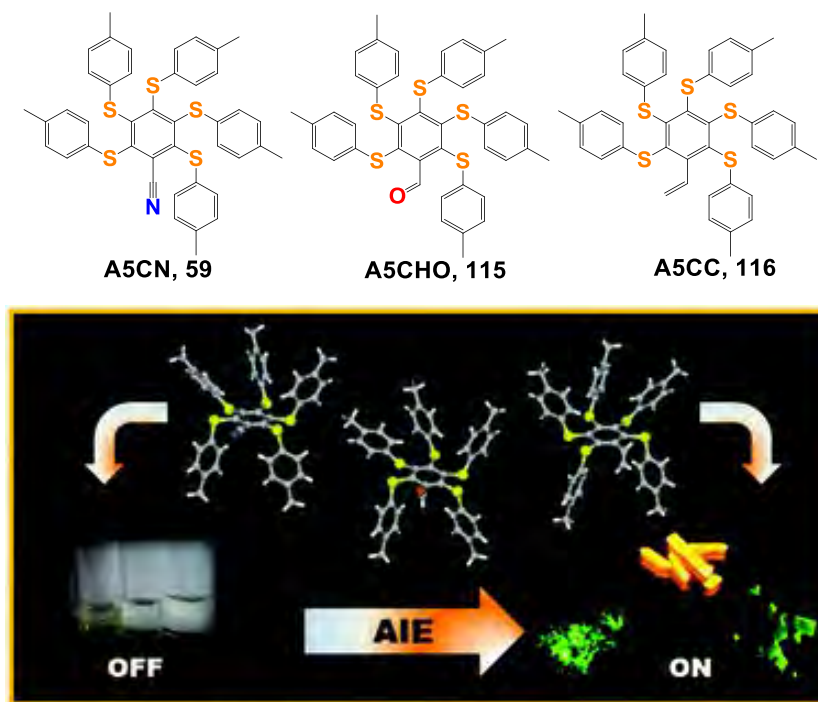


Figure 14: Pentasulfurated benzene-cored asterisks and luminescence studies. (Reprinted with permission). [70]

In solution, two absorption bands were recorded for all three asterisks at 250 and 340 nm. The low energy absorption band, slightly red-shifted with a tail up to 460 nm, is for A5CN.

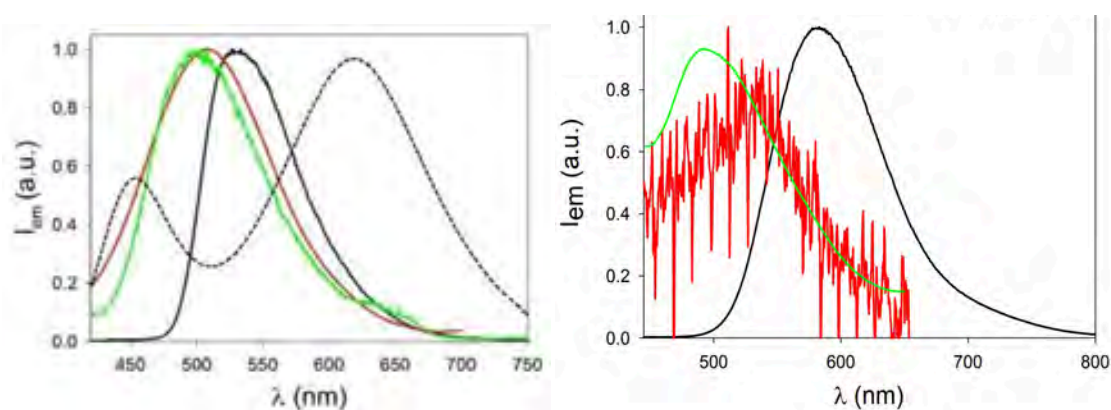


Figure 15: a) luminescence spectra in $\text{CH}_2\text{Cl}_2:\text{MeOH}$ (1:1 v/v) at 77 K of A5CN (black line), A5CHO (red line), A5CC (green line) and A5CN at room temperature (black dashed line). $\lambda_{\text{ex}} = 350\text{nm}$. Luminescence spectra at 77 K were recorded in time-gated mode (delay time = 0.05 ms); b) Luminescence spectra of A5CN (black line), A5CHO (red line), A5CC (green line) in the solid state at room temperature, recorded in time-gated mode (delay time = 0.05 ms), $\lambda_{\text{ex}} = 360\text{nm}$. [70]

In fluid solution, only A5CN displays luminescence with two bands at 448nm (high energy band of fluorescence with lifetime 0.2ns, not sensitive to dioxygen) and 616nm (due to phosphorescence with lifetime 0.34 μ s (in the presence of dioxygen) and 0.20 μ s (in the absence of dioxygen) with quantum yield 0.02 in an air-equilibrated solution. In a rigid matrix, all three display phosphorescence, progressive blue was observed for A5CN (530nm), A5CHO (508nm), and A5CC (498nm), a lifetime in ms suggested it is phosphorescence. The strong blue shift for A5CN from room temperature to 77K, is an example of a rigidochromic effect, whereas the solid show a phosphorescence band, red-shifted compared to the matrix at 77K with a lifetime in μ s. Emission of the other two asterisks was negligible and very low for A5CC and A5CHO in the solid state. The intense orange phosphorescence of A5CN makes it important in bioimaging, as orange light can largely penetrate tissues. [70]

1.3.5 Fluorescence of polysulfurated pyrene-cored asterisks

Pyrene exhibits very different behavior in aggregate or in solution. ACQ is harmful to some practical applications, as it is often observed in pyrene chemistry. It absorbs and emits in near-UV region whereas there is search for optoelectronic device emitting in the visible region. Studies have been done to overcome these limitations by introducing suitable bulky substituents on pyrene at different positions, which enhances the fluorescence efficiency by AIE effect. [108] The structure of the pyrene crystal is composed of partially-overlapping card-packed dimeric units in which the pyrene molecules of each pair are separated by a distance of 3.53 Å (figure-16a).

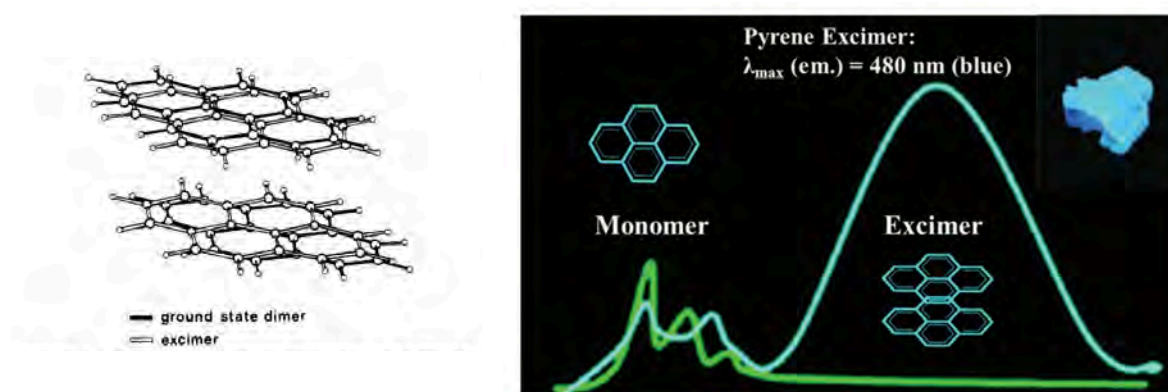


Figure 16: a) calculated equilibrium geometries of ground state and excimer in pyrene crystal [19] ; b) packing mode of pyrene and excimer fluorescence. (Reprinted with permission). [111]

Pyrene monomer emission is normally observed in the 380 to 400 nm range. When a pyrene molecule in the crystal absorbs light, two parallel molecules will tend to move toward one another and toward more complete overlap. These movements are resisted by the environment. As a result an excimer in the crystal may not attain the geometry it would do in solution. As a result, a red-shifted and broad emission band of the excimer in the range of 450–500 nm could be observed with strong fluorescence, much different from the weak emission of the single pyrene molecule in the UV region. Thus, the strong π – π stacking with the pairwise alignment can also be beneficial to the enhancement of fluorescence in the aggregated state. [109] Similar to this packing mode, more emissive excimers have been reported, and the emission spectra can extend to the red or even far-red region, showing the potentially application in biology field as fluorescent probes. [111-115] From benzene to pyrene, the enlarged sizes of the aromatic rings favor the coplanar packing mode with the shortest distance between the molecular centers, mainly due to the dispersion attraction of the adjacent molecules. Normally, this strong π – π stacking can quench the fluorescence in the aggregated state, but the formed pyrene excimer exhibits the opposite effect, indicating the importance of the alignment in the aggregated state. [110]

In 2008, Gingras and his co-workers synthesized a novel class of polysulfurated dendrimers via some aromatic nucleophilic substitutions of 1,3,6,8-tetrabromo pyrene, exhibiting interesting photophysical and redox properties, due to the sulfur effects of the substituents, as seen in scheme 20. [90]

From figure 17 (i), it was observed that the peak at 435nm was attributed to the pyrene core of polysulfurated dendrimers, and the intensity increases with the generation number of the dendrimers from (PG0) to (PG2). The emission spectra were recorded from figure 17b(ii) in cyclohexane, DCM, and dichloromethane/ chloroform (1:1). In cyclohexane (a non-polar solvent), a strong red-shifted fluorescence band was observed for all the dendrimers in comparison to pyrene with slight changes in energies. However, in a highly polar solvent (DCM, 17(ii)b) strong fluorescence band was observed, but lifetimes for PG0 and PG1 were lower than that of PG2 suggested deactivation pathways for PG0 and PG1. The intensity for PG2 is higher due to the shielding effect of dendrons. In a rigid matrix at 77K (dichloromethane/ chloroform

(1:1)), a fluorescence band is shifted by 15nm compared to the solution spectrum; no evidence of phosphorescence was observed. [90]

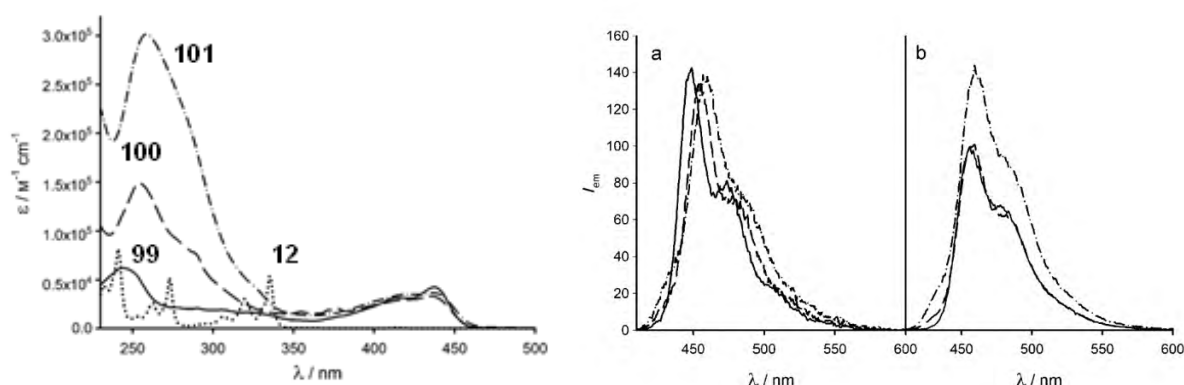


Figure 17: i) Absorption spectra for pyrene (12), PG0 (99), PG1 (100), PG2 (101) in DCM at 293K; ii) Emission spectra for pyrene (12), PG0 (99), PG1 (100), PG2 (101) in a) Cyclohexane at 293K and b) Dichloromethane at 293K

Table 1: photophysical data of the polysulfurated dendrimers

Solvent Compounds	Absorption dichloromethane		cyclohexane		Emission dichloromethane			$E_{1/2}$ [V] (vs. SCE) dichloromethane		
	λ_{max} [nm] ^[a]	ϵ [$\text{M}^{-1} \text{cm}^{-1}$]	λ_{max} [nm]	τ [ns]	Φ_{em}	λ_{max} [nm]	τ [ns]	Φ_{em}	I	II
pyrene	335	54000	370	650	0.65	375	277	0.61	1.30	–
PyG0	435	39000	448	2.5	0.60	457	1.4	0.33	0.85	1.19
PyG1	435	34000	452	2.5	0.60	457	1.6	0.35	1.10	1.28
PyG2	435	36000	457	2.6	0.60	460	2.4	0.55	1.09	1.35

[a] Lowest energy band.

Electrochemical studies found that the dendrimers undergo reversible chemical and electrochemical one-electron oxidation with the formation of deep blue colored radical cation, and the second reversible one-electron oxidation was observed at more positive potential values. [89]

In 2020, a recent work was also published from the groups of Prs. Gingras and Ceroni, as shown in figure 18. The synthesis of the pyrene-based acids was achieved by starting with 1,3,6,8-tetrabromopyrene, and transforming it to the corresponding isopropyl mercaptobenzoates. Esters 2O (ortho), 2P (para), 2M (meta) were then hydrolyzed to their corresponding acids 1O (ortho), 1P (para), 1M (meta). Absorption and emission spectra were recorded in THF for all the regioisomers of esters and acids, and all carboxylic acids were studied under basic aqueous solutions. It was found that in THF, the fluorescence emission (blue-green) and the quantum yield were

similar, but in a basic aqueous solution (pH=8), the acids were deprotonated. Becoming more soluble, the fluorescence was less intense, but still high for 1M (meta isomer) due to less efficient deactivation of excited state by a supposed proton transfer. Metal complexation was studied with various metal ions. In addition to quenching the fluorescence of the pyrene core, the emission quantum yield was reduced to almost zero. It can also control the formation of 3D nanoscopic objects as a dual mode sensor (figure 18). [20]

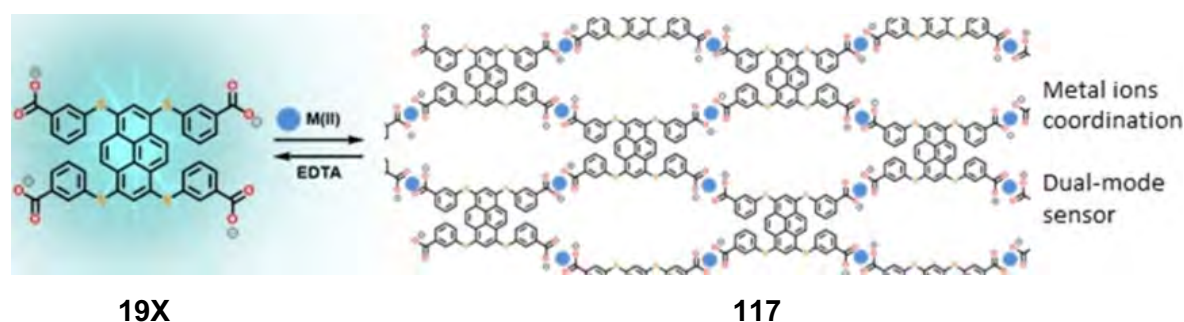


Figure 18: Highly emissive water-soluble polysulfurated pyrene based chromophore as DMS showing reversible formation of supramolecular polymer upon addition of M(II) and can be disassemble by adding EDTA. (Reprinted with permission from ChemPlusChem). [20]

1.4 Reactivity of arenes - nucleophilic aromatic substitutions

1.4.1 History

Nucleophilic substitution reactions on aromatic compounds are known since 1854. [116] They were further explored in the 1950's, when several laboratories started to work on the mechanisms independently in physical chemistry. [116], [45, 117] There are mainly three general types of aromatic reactions, they can be electrophilic, radical, or nucleophilic depending on the substrate and conditions used. When a bond is broken and a bond is formed by replacing a substituent by another one in an aromatic ring, the process is called an aromatic substitution. If a reagent is negatively charged or possess a lone pair of electrons and donates both electrons in a bond formation, it is called a nucleophilic aromatic substitution reaction. When a reagent is a free radical and donates one electron to the newly formed bond, it is known as free radical substitution. If a reagent contributes zero electron to the new bond formed, it is known as an electrophilic substitution reaction (ex. Friedel-crafts reactions, nitration, halogenation, etc.). [45, 118] Electrophilic aromatic substitution reactions [119] are

common and facilitated with an electron-rich benzene ring or with polycyclic arenes. Electron-rich or electron-donating substituents favor such processes. However, nucleophilic aromatic substitution reactions are facilitated on benzene or on electron-deficient heteroaromatic systems, i.e. when the aromatic system is electron-poor, usually incorporating electron-withdrawing groups (i.e. $-\text{NO}_2$, $-\text{Cl}$, $-\text{F}$, $-\text{CN}$, $-\text{CF}_3$). In this way, the electron density decreases and a nucleophile with a high electronic density can easily add to an electron-deficient carbon site where is connected a leaving group, as described by the classical $\text{S}_{\text{N}}\text{Ar}$ mechanism. [118] However, other type of nucleophilic aromatic mechanisms are known, as it will be described later in this section. We will focus more on nucleophilic aromatic substitution reactions in the coming chapters, especially for sulfuration and in dynamic covalent chemistry (DCC).

1.4.2 Nucleophilic aromatic substitutions mechanisms

When a nucleophile replaces a leaving group in an aromatic system at a sp^2 hybridized carbon of a ring, it is known as a nucleophilic aromatic substitution. This area shows a broad conceptual framework over many years of research work, and an in-depth knowledge is needed to understand the kinetics and the stepwise mechanism. The nucleophilic aromatic substitutions can be further divided into many types :

1. $\text{S}_{\text{N}}\text{Ar}$ - Nucleophilic aromatic substitution reaction (Addition-Elimination)
2. $\text{S}_{\text{N}}1$ commonly observed with diazonium salts
3. E1cb-AdN Benzyne
4. $\text{S}_{\text{RN}}1$ Free radical
5. ANRORC (addition of nucleophile, ring opening, ring closure in a nucleophilic reaction)
6. $\text{S}_{\text{N}}\text{ArH}$ - Vicarious Nucleophilic Aromatic Substitution
7. $\text{cS}_{\text{N}}\text{Ar}$ - Concerted $\text{S}_{\text{N}}\text{Ar}$ reaction

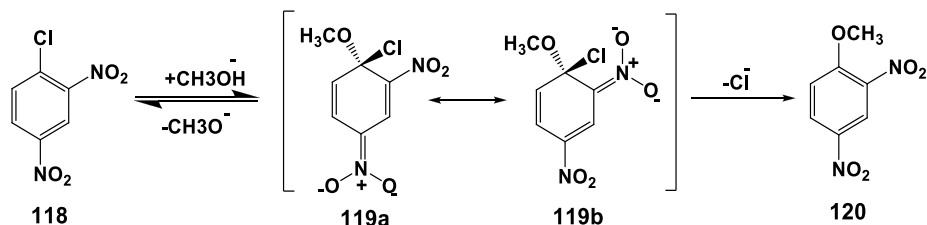
We can further divide these substitution reaction mechanisms in 1, nucleophilic aromatic substitution reaction ($\text{S}_{\text{N}}\text{Ar}$, Addition-Elimination) by two principal mechanisms by which a nucleophilic substitution can occur in aromatic compounds:

1) Addition-Elimination (AE) mechanism: favored when suitably oriented activating groups are present;

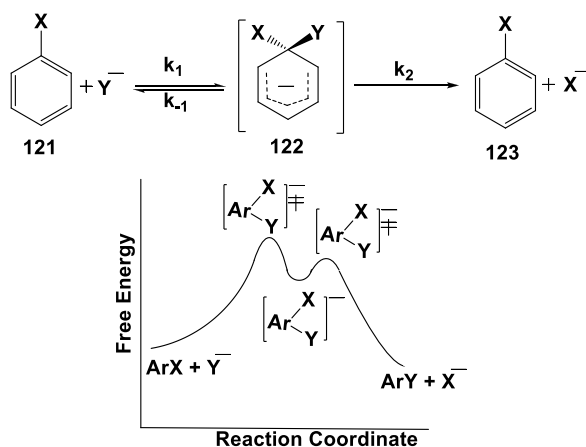
2) Elimination-Addition (EA) mechanism: it occurs in the presence of strong bases, which generally also act as nucleophiles

1.4.2.1. S_NAr - Nucleophilic Aromatic Substitution (Addition-Elimination)

Nucleophilic aromatic substitutions usually occur by an addition-elimination mechanism when suitable electron-withdrawing substituents are placed at para or ortho positions to a leaving group in the substrate. The most suitable reaction of this type is shown in scheme 23. A nucleophile (OMe) adding above the plane of the ring forming resonance stabilized Meisenheimer intermediate (119a-119b) in which orbital hybridization changes from sp² (planar) to sp³ (tetrahedral) at the carbon site. Spectroscopic methods allowed observation of the Meisenheimer intermediate like 119. In the second step, chloride ion will eliminate to give the product. The rate depends on several important parameters such as: activating groups, nature of leaving groups and nature of nucleophile, among many parameters. One should notice that the second step is always described as an irreversible step. A large part of this thesis will demonstrate an equilibrated process in many reactions of potent uses in DCC.

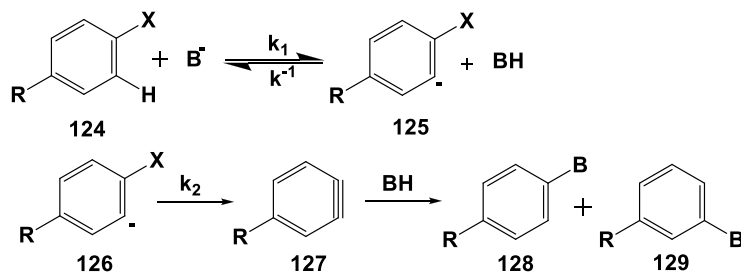


Scheme 23: reaction showing the intermediate Meisenheimer complex in brackets.



Scheme 24: free energy profile for reactions, where the first step is rate-determining step the reaction follows second order kinetics.

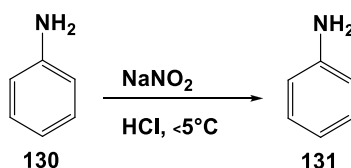
The second general type of mechanism is an elimination-addition nucleophilic substitution or aryne mechanism (scheme 25). It requires a strong base and only occurs when a hydrogen atom is adjacent to the leaving group. The new substitution is found not only in positions occupied initially by leaving the group, but also in positions ortho to this site, also called a "cine substitution". [120-122]



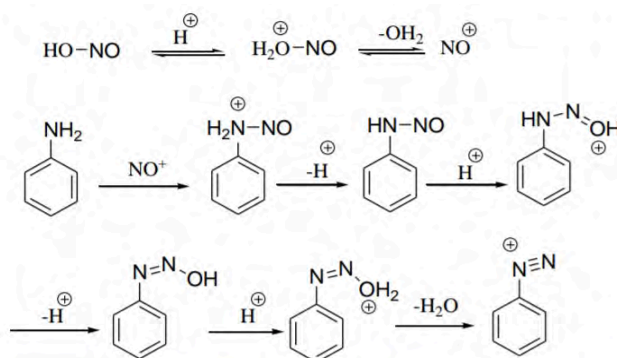
Scheme 25: an example of an addition-elimination reaction or aryne mechanism requires a strong base and occurs when hydrogen is adjacent to the leaving group.

1.4.2.2 S_N1 (with diazonium salts)

Diazonium salts are organic compounds with molecular structure RN₂⁺ X⁻ where R= alkyl or aryl group and X= halogen, hydrogen sulfate, etc. These salts are ionic and frequently used in organic synthesis as an essential intermediate. Diazonium salts of primary aliphatic amines are highly unstable even at low temperatures. As soon as they are formed, they can liberate nitrogen, forming a carbocation. The carbocation can further undergo substitution or elimination. This is why primary aliphatic amines have not such importance. Scheme 26 indicates a common formation of a diazonium salt.

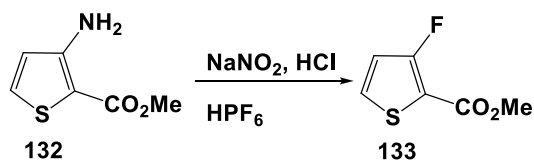


Mechanism:

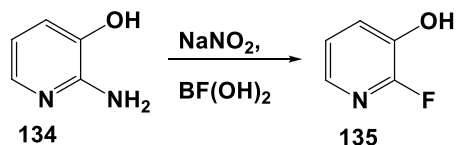


Scheme 26: preparation of diazonium salts

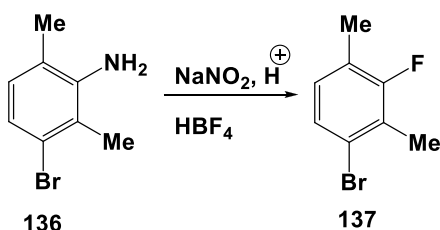
In contrast to alkyl diazonium salts, arene diazonium salts are more stable, but can be dangerously unstable under certain conditions. A few examples of S_N1 with diazonium salts are shown in scheme 27:



A. Kiryanov, A. Seed, P. Sampson, *Tetrahedron Lett.* **2001**, *42*, 8797



F. Dolle, L. Dolei, H. Valette, F. Hinnen, F. Vaufrey, H. Guenther, O. Fuseasu, C. Coulon, M. Buttalender, C. Corouzel, *J. Med. Chem.* **1999**, *42*, 2251



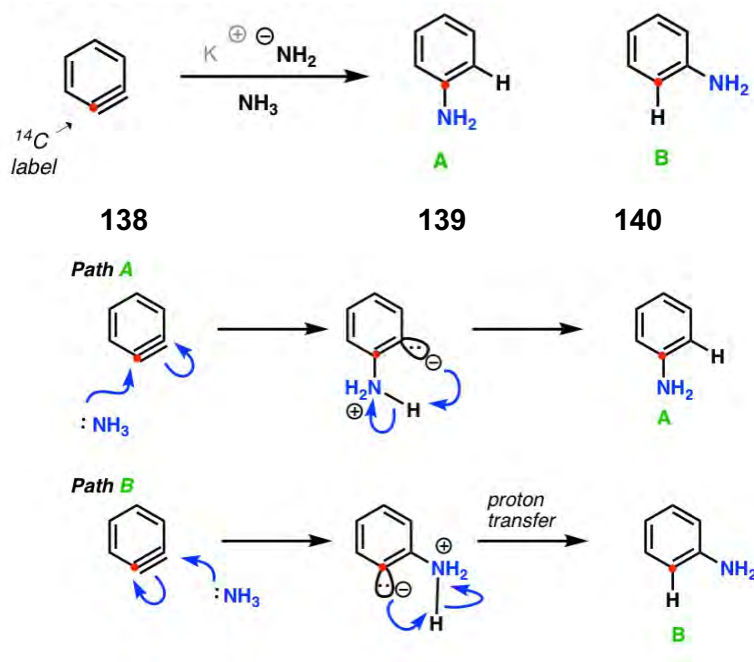
H. Hart, J. F. Janssen, *J. Org. Chem.*, **1970**, *35*, 3637

Scheme 27: examples of S_N1 mechanisms with diazonium salts.

They can undergo S_N1 (Ar), dissociative unimolecular nucleophilic aromatic substitution in a few cases, while a majority of their reactions occur by $S_{RN}1$. S_N2 mechanisms on diazonium salts seems geometrically impossible, however Peter Burrai and Heinrich Zollinger reported S_N2 mechanism on heterolytic arylations in 2,2,2-trifluoroethanol), [125] while S_N1 occurs with difficulty. [122-124]

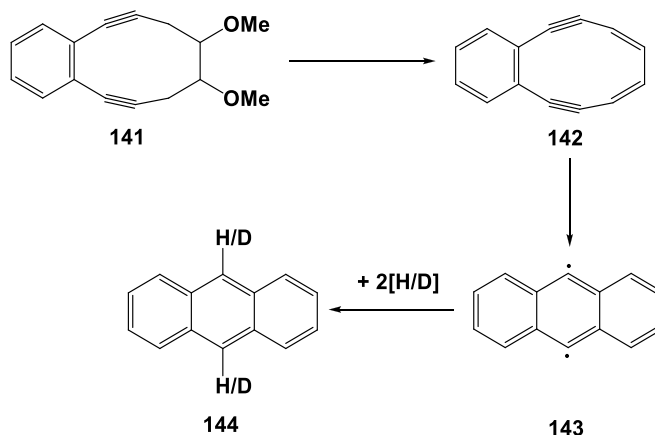
1.4.2.3 E1cb-AdN Benzynes

A benzyne intermediate is very unstable and a highly reactive species. In 1953, John D. Roberts and coworkers from MIT labelled chlorobenzene with radioactive isotope ^{14}C instead of ^{12}C to see if the substitution would happen at the labelled carbon or not. Reaction conditions were with a strong base (KNH_2) at low temperature (-30°C). They found 50% substitution at the labelled carbon, and 50% substitution at the adjacent carbon. Thus, the nucleophile can attack either side of a triple bond, showing equal mixture of products A or B (given below in scheme 28). [126-127]



Scheme 28: A nucleophile can add on either side of the triple bond of the aryne, showing equal mixture of products A or B. (Reprinted with permission)

Some classical experiments from Jones and Bergman were published in 1972 for para-aryne substitution. In scheme 29, is an example of the existence of p-aryne obtained by Masamune et al. in 1971. [126, 128].

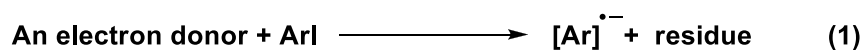


Scheme 29: example of an aryne intermediate in the so-called Bergman's cyclization. [126, 128]

1.4.2.4. S_{RN}1 Free radical mechanism

S_{RN}1 stands for substitution, RN for radical nucleophilic, and 1 for unimolecular. This mechanism was first reported reaction of this type was in 1966. This type of substitution reactions occurs with aromatic/aliphatic compounds that do not react or react slowly through polar nucleophilic mechanisms. This is an important synthetic method for inactivated aromatic and heteroaromatic substrates. [116, 129] Unimolecular refers to molecularity of the reaction, as for S_N1, except that unimolecular fission occurs in a radical anion instead of a neutral molecule. Evidence from Kornblum and Russell studies from chloro, iodo, and bromo benzene derivatives with KNH₂, in liquid ammonia showed evidence of electron transfer radical mechanism for nucleophilic substitution at a saturated carbon. In addition, with aryne / benzyne intermediates, they succeeded in trapping radicals with the help of a spin-trapping agents such as 2-methyl-2-nitrosopropane and tetraphenyl hydrazine.

A hypothesis as to the character of the radical mechanism



"Ar" stands for the 5- or 6-pseudocumyl moiety

Scheme 30: proposed S_{RN}1 mechanism.

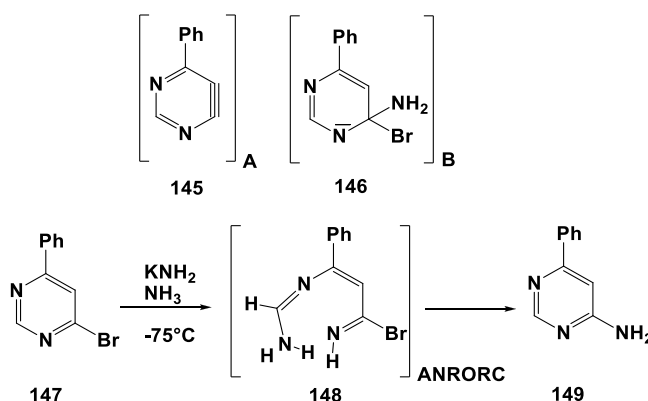
The mechanism in scheme 30 is supported by the fact that a non-rearranged substitution product, which cannot be the aryne pathway, is stimulated by the addition of potassium metal to the reactions of an iodo aryl system with KNH₂, in liquid ammonia. Also, they concluded that step 1 and step 2 in scheme 30 should occur far more readily with iodide than with chloride and bromide. [45, 117]

1.4.2.5 ANRORC (addition of nucleophile, ring-opening, ring closure in nucleophilic reaction)

This is a special type of substitution reaction [130] which is very important in medicinal chemistry, [131] because it is mainly used in heterocyclic aromatic systems. This

reaction does not include aryne intermediate or Meisenheimer complex formation. It was ruled out by doing some experiments by labelling with deuterium. When 3- or 4-halopyridine (halogen = chloro, bromo, iodo) was treated with potassium amide at -33°C , in all mixtures were observed only 3- and 4-aminopyridine and not 2-aminopyridine with a ratio of 1:2 (ratio independent of nature and position of halogen substituent). This indicates the formation of 3,4-pyridyne intermediate which was confirmed by trapping the intermediate by cycloaddition. Similar results were observed by treating 3-chloro and 3-bromopyridine with lithium piperidine/ piperidine in boiling ether, which indicates the formation of a 3,4-pyridyne intermediate. These reactions proceed via $\text{S}_{\text{N}}(\text{EA})$ steps which include elimination of hydrogen and addition of a nucleophile. A 2,3-pyridyne intermediate was not observed. However, there is evidence of 2,3-pyridyne in the amination of 3-halopyridine N-oxide, and the 2-substituted product was formed. This type of reaction can occur if the heterocyclic compound is able to undergo a reaction with a nucleophile (considerable π -electron deficiency), a heteroatom in the reagent needs to carry one hydrogen atom and the reagent contains the same heteroatom present in the heterocyclic ring. In summary, this type of reaction can be seen in triazines, tetrazines, pyridazines, phthalazines, and pyrazines. The Zincke reaction is an example of $\text{S}_{\text{N}}(\text{ANRORC})$. [130, 132]

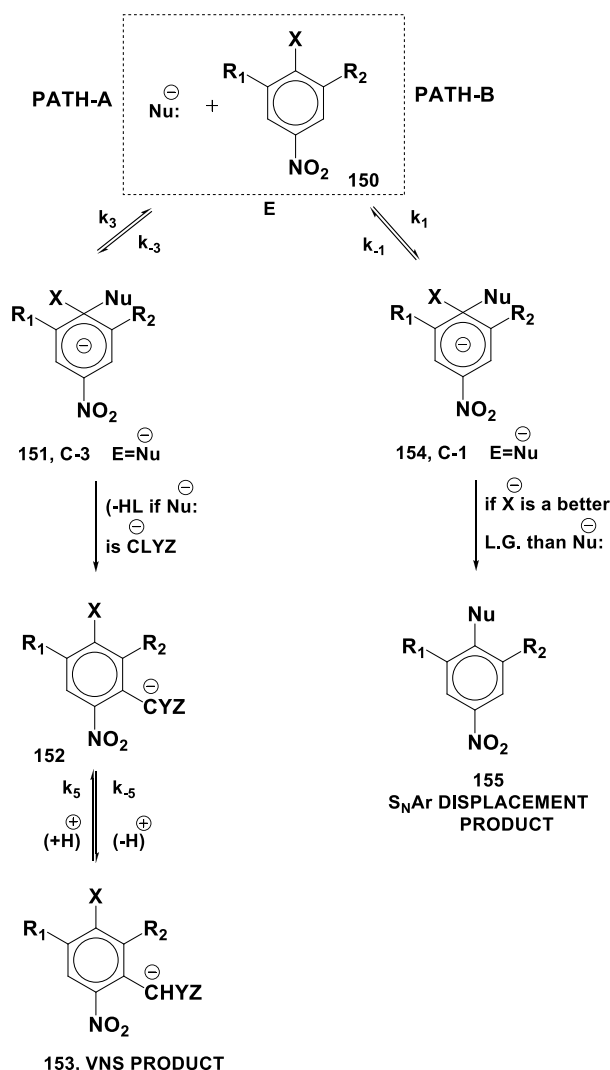
In scheme 31, an example of $\text{S}_{\text{N}}(\text{ANRORC})$ reaction is shown. A widely studied process involves a metal amide as a nucleophile (such as sodium amide) reacting with substituted pyrimidines (4-phenyl-6-aminopyrimidine), forming product 2 (4-phenyl-6-aminopyridine), which excludes the formation of intermediate A and B. It was confirmed by several isotope labelling experiments, which were conclusive for a ring-opening and a ring-closing mechanism. [133-135]



Scheme 31: example of a reaction involving a $\text{S}_{\text{N}}(\text{ANRORC})$ mechanism.

1.4.2.6 S_NArH - Vicarious nucleophilic aromatic substitution

When a nucleophile adds to an aromatic sp² carbon atom of a benzene or an aromatic substrate, and a hydrogen atom leaves instead of a halogen (X=Cl, Br, I) or another leaving group, the mechanism is known as a vicarious nucleophilic substitution. To make it feasible, the benzene or the aromatic ring needs to be electrophilic by incorporating one or more electron-deficient substituents, such as a nitro group (scheme 32). [136]



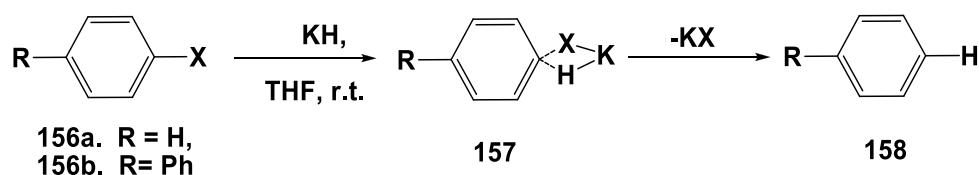
Scheme 32: example of vicarious nucleophilic substitution with a benzene ring substituted with a nitro function.

This kind of reaction can typically be seen in nitro arenes. Nucleophilic substitution can occur at ortho or para position, reversing the selectivity for meta position usually observed with such compounds under electrophilic substitution. [137] For example, in

the reaction given above, a hydrogen atom ortho to the nitro group is replaced with a nucleophile, a so-called vicarious substitution. The formation of a Meisenheimer-type complex (or σ -complex) as an intermediate is observed, and the leaving group is a hydrogen atom. As a second reaction, if the nucleophile adds to the para position to the nitro group, at the ipso position of the leaving group X (other than a hydrogen atom), a sigma adduct or a Meisenheimer complex is formed. This sigma adduct is converted into the product by rearomatization. It then proceeds via a S_NAr reaction. [136-137]

1.4.2.7 cS_NAr - concerted S_NAr reaction

In general, the accepted mechanism for S_NAr reactions involves a two-step addition and elimination. The formation of discrete Meisenheimer complex as an intermediate requires an anionic adduct to be more thermodynamically stable than a transition state for a concerted pathway, and to possess sufficient kinetic stability to have a significant lifetime before elimination. [138] In 1980, Pierre et al. studied the reaction of aryl halides with KH in THF-d₈ and showed hydrogen substitutions from KH, and no benzyne mechanism is involved since no evolution of hydrogen was formed. The order of reactivity was $ArI > ArBr > ArCl > ArF$, which is the reverse order often found in classical S_NAr reactions. The reaction proceeds without any activating groups on the ring; hence they proposed a four-centered transition state (scheme 33); detailed mechanisms were not studied at that time due to the limitation of appropriate techniques. [118, 139]

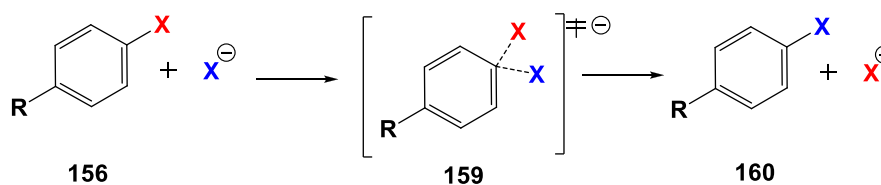


Scheme 33: proposed concerted S_NAr mechanism by Pierre et al [118]

Then in 1985, Fry and Pienta achieved some mechanistic studies with hammett correlations on arenesulfonate groups displaced by halide anions in dodecyltributylphosphonium salts, using a range of substituents. [118-140] William et

al. also reported many publications with concerted mechanisms on substituted 1,3,5-triazines. [141-144]

Computational studies were made in the gas phase by Glukhovtsev et al., and it was found that exchange of substituents (scheme 34) with halide ($X = \text{Cl}, \text{Br}, \text{I}$) proceeds via Meisenheimer complex, and no intermediate was found. A Meisenheimer intermediate was observed for all three second-row nucleophiles with substituents as different as NH_2 and NO_2 (for both NH_2^- and F^- as nucleophiles) and substituents $-\text{H}$ and NO_2^- with OH^- as the nucleophile. For the third- and fourth-row nucleophiles, concerted mechanisms were calculated in several instances. In general, a concerted mechanism was predicted for more electron-rich aromatic systems.

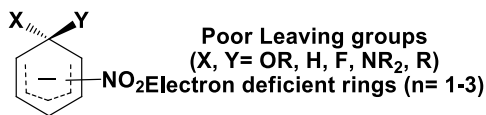


Scheme 34: computational investigations by varying the substituents and nucleophiles. [118]

A stepwise mechanism with a Meisenheimer intermediate would become more favorable as electron-withdrawing groups are attached to the aromatic ring. [118] In recent studies, the concerted mechanism was shown via $^{12}\text{C}/^{13}\text{C}$ kinetic isotopic effect or isotopic labeling of ^{19}F . In scheme 35, are presented three examples to understand the concerted mechanism. Nitro groups strongly stabilize complex-A in the first reaction, and poor leaving groups (fluoride and methoxide) and related reactions undergo stepwise mechanisms. [146] Complex-B, weakly stabilized by a nitrogen-containing heterocycle and an ester with a good leaving group (Br), which favors a concerted mechanism. The third complex-C, strongly stabilized by electron-withdrawing substituents, but destabilized by an excellent leaving group (chloride), is a borderline reaction. Therefore, if the Meisenheimer complex (MC) is highly stabilized, it will proceed stepwise. If the MC is less stable, a concerted reaction will occur, whereas the MC is highly stabilized, but the elimination of the leaving group is fast, it represents a borderline situation. [145] PhenoFluor chemistry is different from conventional reaction mechanisms for aromatic fluorination chemistry.

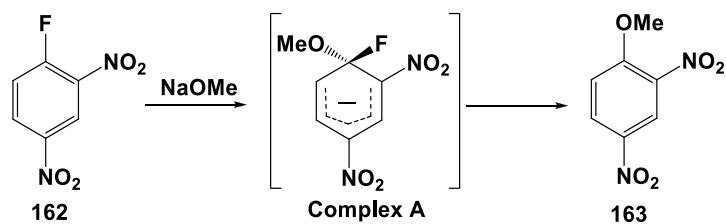
Deoxyfluorination was done on an electron-rich phenol with PhenoFluoro (deoxyfluorination reagent), as shown in scheme 36.

a Previously studied Meisenheimer complexes

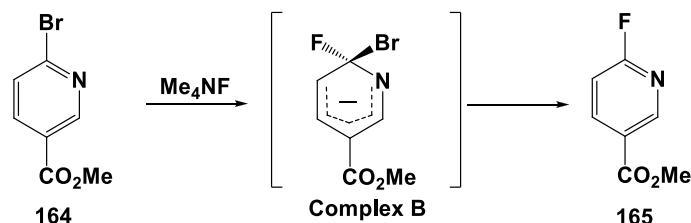


b This study

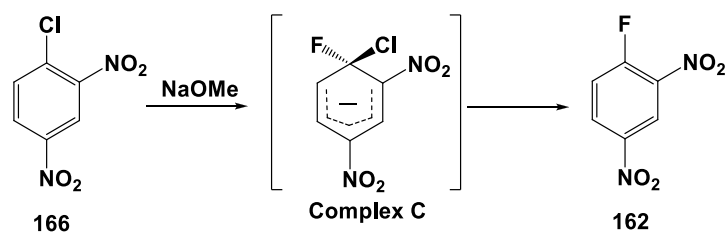
Reaction A (stepwise)



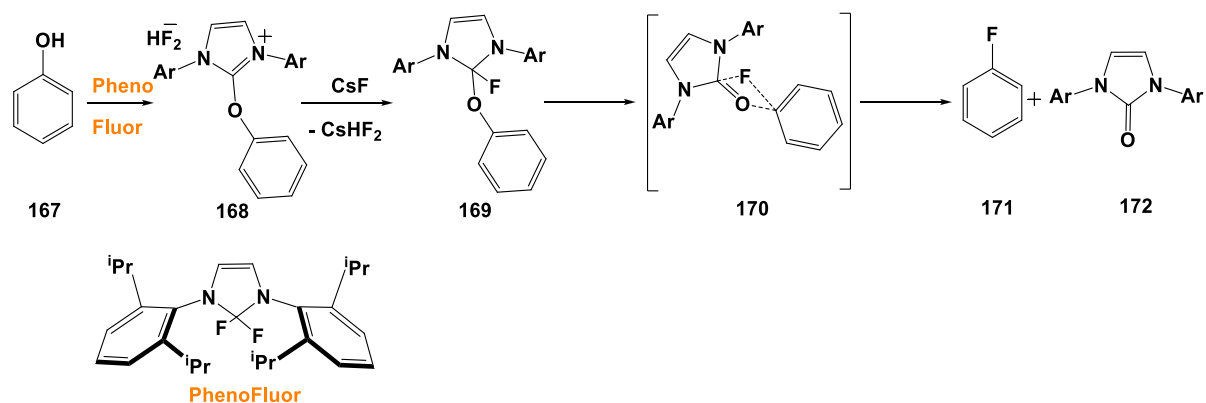
Reaction B (concerted)

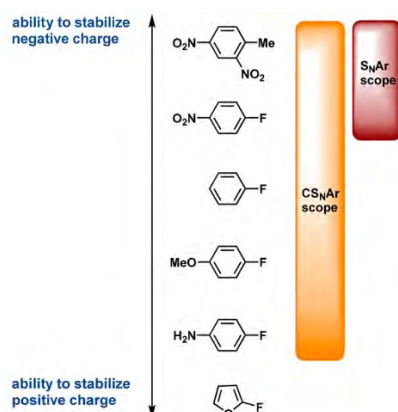


Reaction C (borderline)



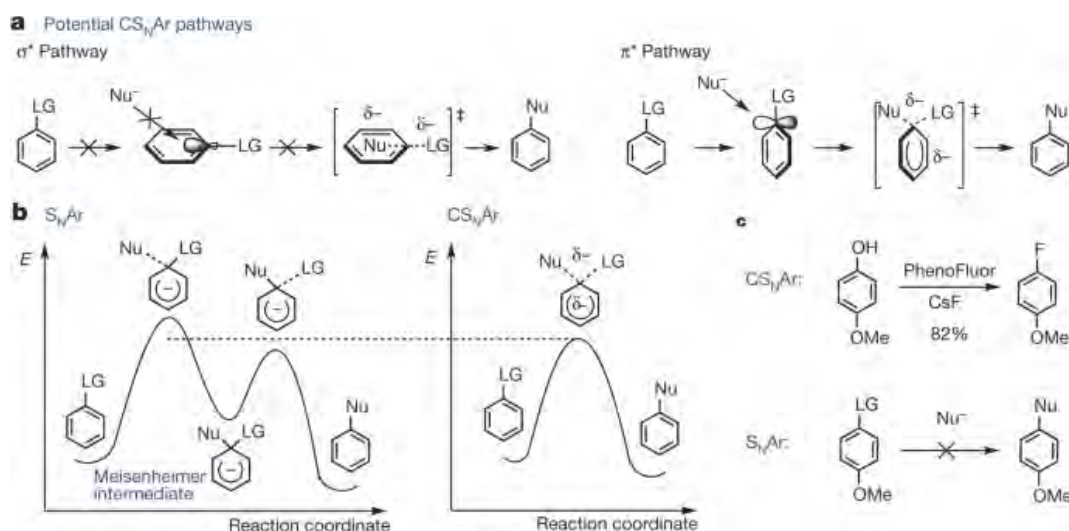
Scheme 35: scope of study with Meisenheimer complexes, which spans a range of stabilities. [145]





Scheme 36: deoxyfluorination of phenol proceeds via cS_NAr . (Reprinted with permission) [148]

This reaction proceeds via a concerted pathway in which nucleophilic attack and leaving group loss happens simultaneously. Three steps are involved independently in this reaction—the condensation of phenol and PhenoFluor to form compound (169), a tetrahedral adduct (170), and a nucleophilic displacement. No intermediate was formed as the tetrahedral intermediate is converted to the product (171) and urea (172). [148]



Scheme 37: comparison of orbital interactions and energy profiles in S_NAr and cS_NAr [147]

A wide range of nucleophiles favors S_NAr reactivity. During S_NAr (scheme 37), the addition of the nucleophile at the carbon atom bearing a leaving group leads to a negatively charged intermediate known as the Meisenheimer complex (MC). Only arenes with electron-withdrawing groups can sufficiently stabilize the resulting build-

up of negative charge during MC formation, limiting the scope of S_NAr reactions. Most common S_NAr substrates contain π -acceptors in ortho / para positions. cS_NAr is not limited to poor electron arenes because it does not involve a MC, and addition of the nucleophile and leaving group loss happens simultaneously, as shown above for the deoxyfluorination reaction for which S_NAr is favored over a stepwise displacement. [147]

1.5 Dynamic Covalent Chemistry (DCC) and reversible S_NAr

1.5.1 What is dynamic covalent chemistry (DCC)?

DCC is concerned with the covalent assembly of chemical structures when occurring under thermodynamic or kinetic control, using reversible reactions involving covalent bonds formation and dissociation. It allows the coexistence of different chemical species (in a chemical library), among which some of them can be selected with desired properties. It is a synthetic strategy that chemists employ to make selective complex assemblies, from reversible reactions and discrete molecular building blocks, with dynamic and adaptative properties to their environment, with errors and corrections processes (self-corrections). [149]

Dynamic systems in DCC are collections of discrete molecular components that can reversibly assemble and disassemble. Systems may include multiple interacting species leading to competing reaction in an inherent reversibility. It includes fast exchange of molecular components under thermodynamic or kinetic control and offers the ability to make extended networks. Despite a growing interest in the dynamic covalent chemistry field, the organic synthesis of materials has primarily been confined to imine condensation, boronic ester condensation, disulfide exchange, olefin metathesis, and alkyne metathesis. However, nucleophilic aromatic substitution reactions between thiols and thioarenes or heteroarenes involving labile and reversible bonds have been underexploited in spite of a large number of reactions since the early days of aromatic chemistry in the mid 19th century. [150] This thesis will report some work in that direction as a major contribution.

Not to be confused with dynamic combinatorial chemistry, DCC concerns only reversible covalent bonding. In contrast, in constitutional dynamic chemistry (CDC), all possible combinations of compounds are generated through reversible connection processes, both covalent and non-covalent bondings. [149]

Dynamic covalent chemistry is a part of Constitutional Dynamic Chemistry (CDC). A chemical entity undergoes a continuous change in its constitution by dissociating various components and reconstructing the same entity or different ones.

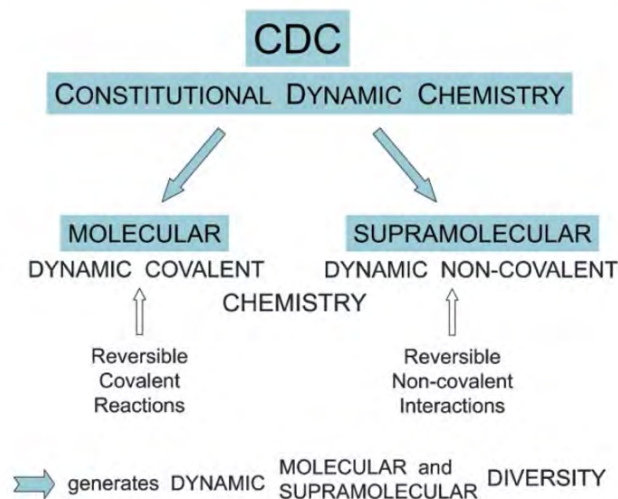


Figure 19: general view on Constitutional Dynamic Chemistry (CDC), Dynamic Covalent Chemistry and Supramolecular Chemistry according to Pr. Jean-Marie Lehn. (Reprinted with permission).

Molecular dynamic chemistry comes under constitutional chemistry, which refers to reversible covalent bonds, whereas dynamic supramolecular chemistry refers to reversible non-covalent bonds. We will discuss more on molecular dynamic covalent chemistry in the coming chapters. [149]

1.5.2 Reversible reactions in DCC

Reversible reactions involve covalent, non-covalent, and coordinate bonds. The reversible exchange reactions should have these three features:

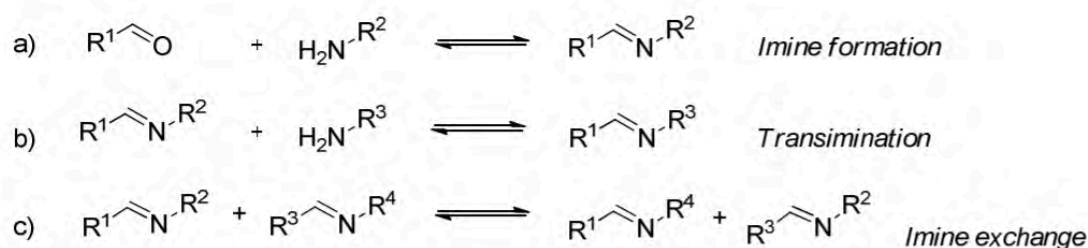
1. The timescale of the exchange reaction should be short so that equilibration and selection occur essentially simultaneously.
2. They need to operate under mild experimental conditions (e.g., temperature, pressure, concentration, solvent, pH, catalyst).
3. The solubility of all building blocks and library components is required. If any insoluble material is present, it can act as a thermodynamic sink or slow the reaction rate (kinetic trap).

The non-covalent interactions typically reach equilibrium rapidly, whereas the covalent reactions proceed more slowly and often require a catalyst to fulfill the requirement for lability listed above. [151] Some examples of DCC using covalent exchange reactions are discussed below, as some selected examples.

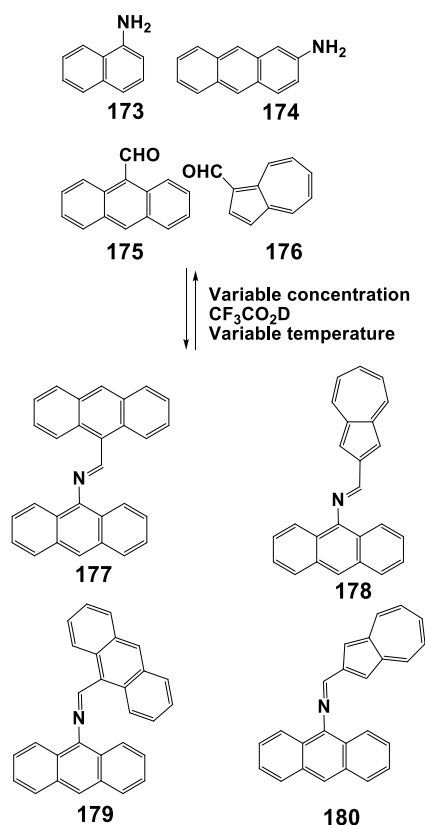
1.5.2.1 Reversible imine formation and exchanges

Preparation of imines or Schiff's bases (C=N functional group) [152] is simple; amine and aldehyde are dissolved in benzene and heated under reduced pressure until the elimination of water is complete or by addition of a drying agent to remove water which is formed (scheme 38). [153] Imine formation is a reversible reaction; it can be hydrolyzed back to the corresponding 1° amine under acidic conditions. [154] Their reversibility was also studied in 1992, in template-directed synthesis, which showed the enhancement in thermodynamic control. [155] In 1999, the thermodynamic nature of imine bonds was used to synthesize rotaxanes (these are mechanically interlocked molecular systems consisting dumbbell-shaped molecule, which is threaded through a macrocycle). [156]

In 2006, Lehn and his group published their work explaining the constitutional behavior of a dynamic library of imines on changing temperature and acidity.



Scheme 38 : Imine formation and exchanges [151]



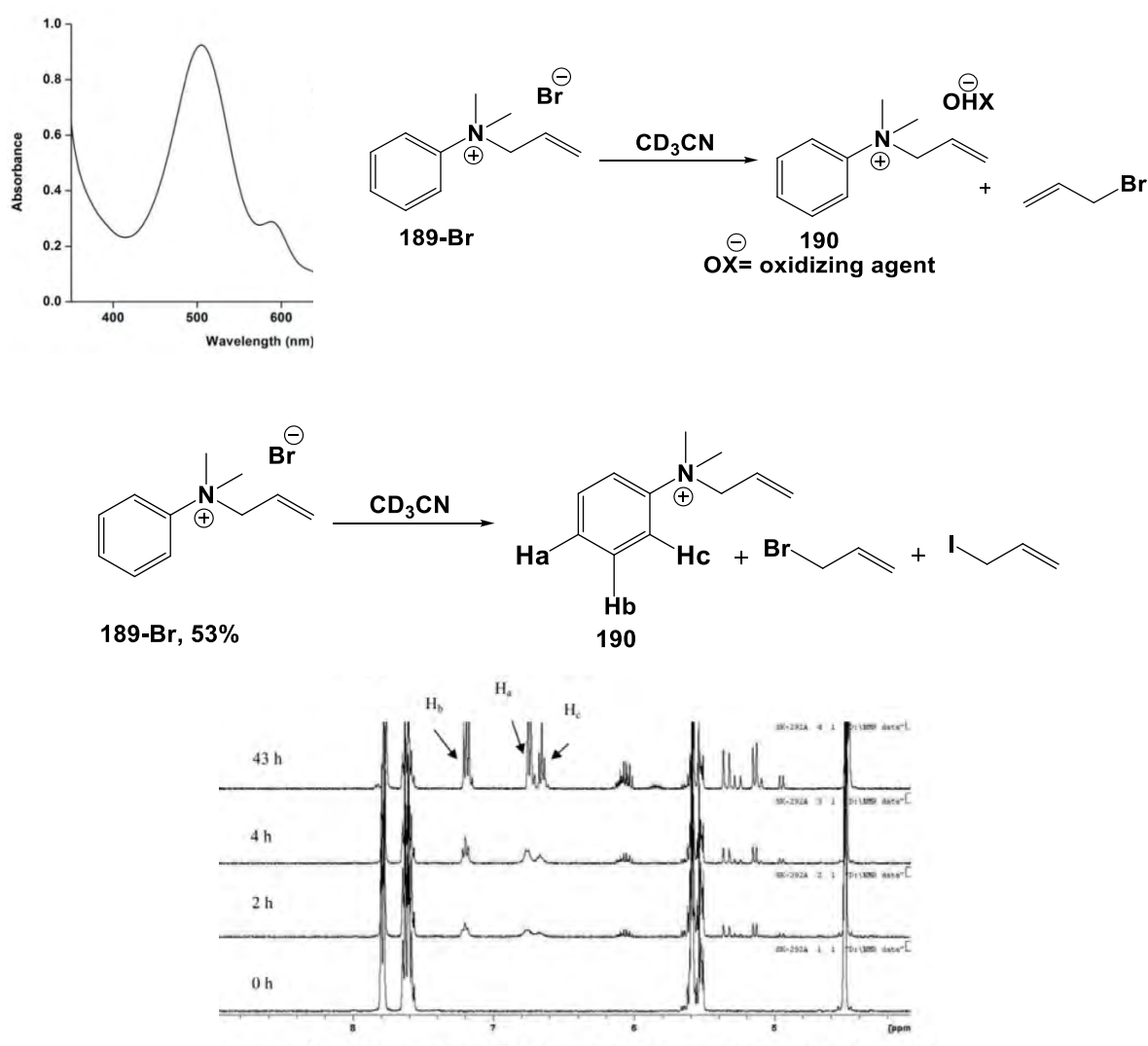
Scheme 39: Dynamic Library of four components 173-176 and four constituents 177-180, concentration used 5.12×10^{-2} M for each component. [157]

A dynamic set of aromatic amines was produced from a stoichiometric mixture of 1-naphthylamine (173), 2-aminoanthracene (2), 9-anthracene carboxaldehyde (3), and 1-azulenecarbox-aldehyde (4) (scheme 39). [157] When an amine reacts with an imine to undergo a reversible exchange, it is known as a transamination (schemes 38 and 39).

Moreover, an imine can exchange its amine component (and simultaneously its carbonyl compound component) for that of another imine, the so-called imine/imine exchange reaction (schemes 38 and 39), via either nucleophilic catalysis, [158] hydrolysis/re-combination being an obvious example of such a pathway, [159] or by a direct metathesis involving a single, cyclic intermediate/transition state. In 2014, an amine-imine exchange reaction with aromatic-aromatic and aromatic-aliphatic amines at ambient temperature in an organic solvent under non-acidic conditions was reported. It showed an imine metathesis catalyzed by the substoichiometric amount of amines in the absence of proton or metal catalysis. [160]

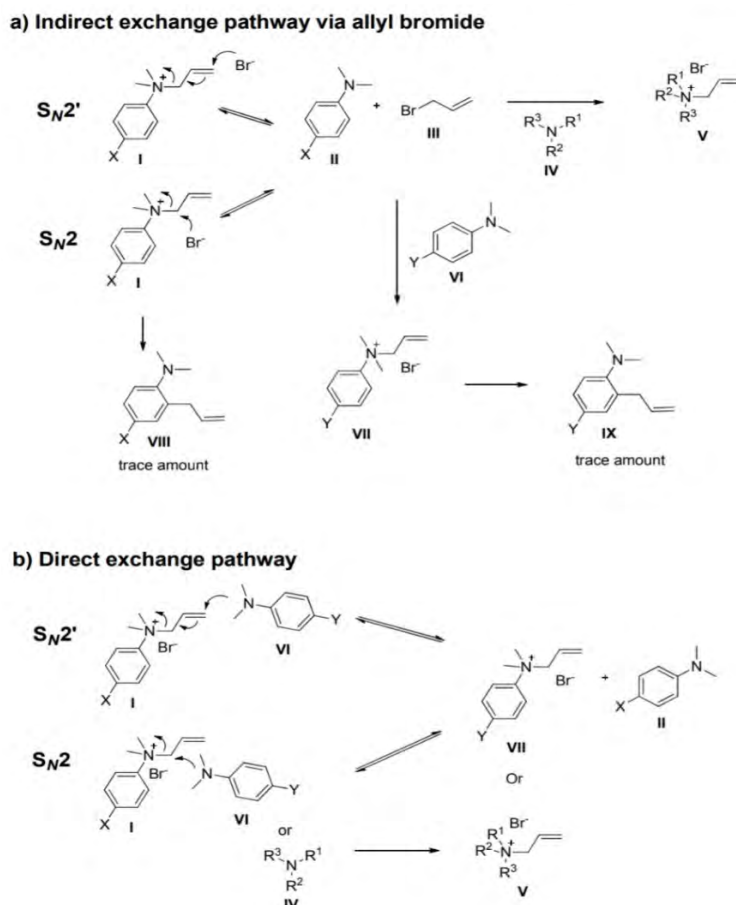
1.5.2.2 Reversible exchange with quaternary ammonium salts by S_N2 and S_N2' mechanisms.

In 2015, a thesis from Pr. Jean-Marie Lehn's student showed a generation of dynamic covalent library based on nucleophilic substitutions involving an exchange of an amine component of quaternary ammonium salts based on S_N2 and S_N2' mechanisms.



Scheme 40: a) absorption spectra showing the presence of an intermediate (radical cation) of dimethylamine (at $\lambda_{\max}=505$ nm in acetonitrile 5 mM) in visible region; b) progress of product distribution after 43h via ¹H-NMR, in presence of iodine at 60°C in deuterated-acetonitrile (CD₃CN). [151]

Iodide anion was used as a catalyst for these exchange reactions. Microwave was used for the pyridine and pyridinium salts derivatives; some were ionic liquids. All exchange progress was monitored and demonstrated by ¹H-NMR, and different dynamic combinational libraries were determined by NMR signal integration.



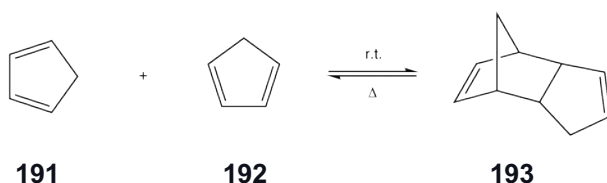
Scheme 41 : possible pathways for exchange of the amine moiety between N-allyl-N,N-dimethylanilinium bromide and an aliphatic or aromatic tertiary amine via a S_N2' mechanism. [151]

In scheme 40, the product distribution at equilibrium is attained after 43 h, in the dissociation of 1a-Br in the presence of iodide anion, and the evidence for radical cation was observed via absorption spectra. The results obtained indicated that exchanges occurred via direct or indirect pathways given in scheme 40. Together, the results indicate that the exchange reactions may occur by the indirect pathway, via the intermediate formation of allyl bromide/halide and the direct pathway (scheme 41), by the addition of the free amine at the γ carbon of the allyl group. The presence of catalytic iodide anions may be expected to favor the indirect pathway via the formation of allyl iodide. [151]

1.5.2.3 Reversible Diels-Alder reactions

The reaction between a diene and a dienophile is known as Diels-Alder reaction, which is sometimes reversible. The equilibrium usually lies by far toward the Diels-Alder

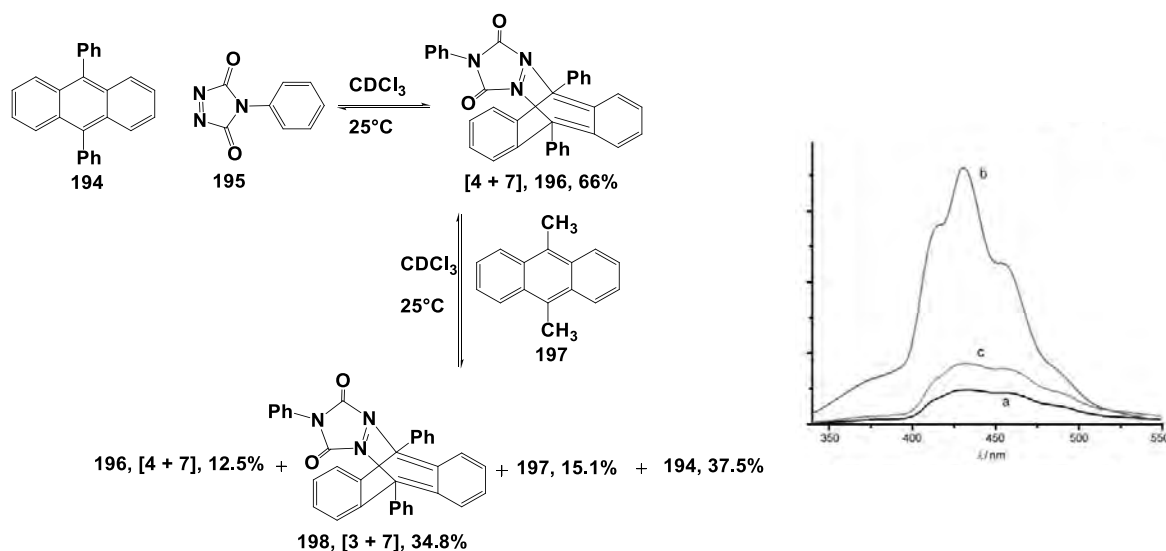
adduct at a lower temperature and, at a higher temperature, toward the diene and the dienophile (scheme 42). [161]



Scheme 42: reversible Diels-Alder reaction. [161]

In 2009, professor Lehn and his group published some Diels-Alder reactions between 9,10-dimethylantracene and cyanated dienophiles, reversible at room temperature for exploring new (opto)dynamic covalent systems. [162] Later in 2011, some reversible Diels-Alder reactions at room temperature with many anthracene derivatives (dienes), and triazolinedione based dienophiles were published.

The diene component exchange experiment was conducted by reacting 194 and 195 (scheme 43a) at room temperature. To the equilibrating mixture of 4+7 (196), diene 197 is added and the component exchanges are observed by ^1H NMR. The addition of one equivalent of 197 favored the reaction in the forward direction (towards 3+7 adduct (198)), which was formed in a superior amount to that of 4+7 adduct (196) formed initially before the addition of 197.



Scheme 43: a) Diene component-exchange experiment between 197 and 194 by the addition of 197 to an equilibrating mixture of 4+7(196); b) Temperature effect on the fluorescence spectra of a 5 mm solution of 197 in CHCl_3 with and without the addition of dienophile 195 at

25 and 50°C. Fluorescence spectrum of a) 197 at 25°C, b) [3+7] (198) at 25°C, and c) [3+7] (198) at 50°C. Excitation at 300 nm [162]

A mixture of products was generated, as shown in scheme 43a. The absorption spectra (scheme 43b) were recorded to study the temperature effect on the solution of diene 197, with and without the addition of dienophile 195. Increasing the temperature leads to fluorescence quenching, whereas decreasing the temperature renders the system fluorescent. [164] The above example represents an optodynamic device. [163]

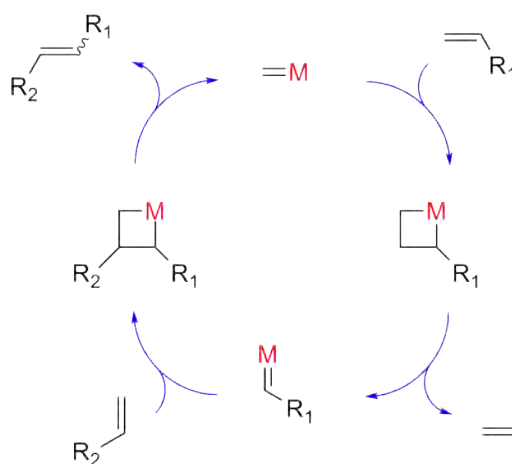
1.5.2.4 Reversible olefin metathesis and exchange

Metathesis is a well-known Ru-catalyzed reaction, which includes reversible a series of [2+2] cycloadditions and retro [2+2] cycloadditions (scheme 44a). [164] The given mechanism below in scheme 44 indicates that it goes through a catalytic cycle involving metallocyclobutane intermediates, which can lead to new products (scheme 44b). [165-167] This mechanism was confirmed by the synthesis of homogeneous complexes containing a nucleophilic carbenic function and the formation of a metallacyclobutane by reaction with an olefin. [168-169]



Scheme 44a: General Reaction for the olefin metathesis reaction [166-167]

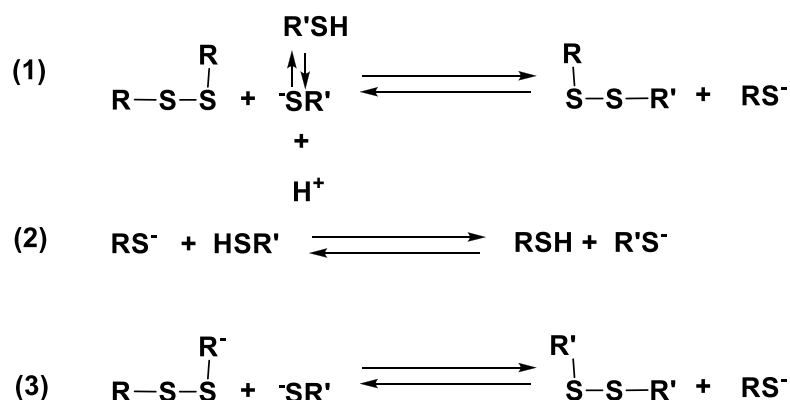
Mechanism:



Scheme 44b: mechanism for the olefin metathesis reaction [166-167]

1.5.2.5 Reversible disulfide formation and exchange

In 1951, a preliminary study to exchange sulfur between thiosulfate and sulfite was reported. It was observed that monosulfide does not exchange even in extreme conditions. Exchange with higher polysulfides is complicated as they can undergo side reactions or be oxidized to disulfide, but the exchange was fast and free of side reactions with disulfide. [170] Similar to the reduction of disulfide in nature, the reversible nature of disulfides in the presence of an excess of mercaptan (thiol) is important for DCC. It can be an anionic exchange or displacement reaction of mercaptide with disulfide. If R-S-S-R is the disulfide to be reduced and R'-SH is the mercaptan in excess, the reaction will proceed as shown in Scheme 45. It is a rapid with a reversible proton exchange. However, when $[R'S] \gg [RS^-]$, the equilibrium will shift in the forward direction. [171-173]

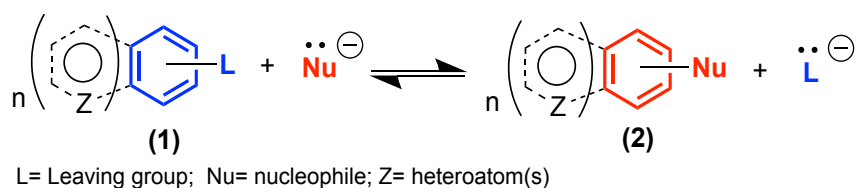


Scheme 45: mechanism of reversible sulfur exchange reactions in disulfides. [171]

1.5.3 Reversible nucleophilic aromatic substitutions in DCC

Nucleophilic aromatic substitutions are among the most frequently used reactions in organic chemistry. Such exchanges of chemical components may occur by different mechanisms, as we stated before (S_NAr , [74] $S_{RN}1$, [175] cS_NAr , [176] S_NArH [177]). We will use the denomination S_NAr for representing these different mechanistic possibilities of nucleophilic aromatic substitutions. Even if their reversibility was shown

in rare cases, [6] it was overlooked in spite of a great number of S_NAr reactions reported since 1854.[7] It is conceptually of much interest in aromatic chemistry and in Dynamic Covalent Chemistry (DCC), beside a number of reversible reactions studied, with imines, esters, disulfides, dithioacetals, hemiacetals, metathesis, S_N2 , and Diels-Alder reactions. Reversible S_NAr reactions could present a wide scope, involving several types of nucleophiles, leaving groups and aromatic or heteroaromatic substrates, without the need for metal catalysis, as schematically depicted in scheme 45.



Scheme 45: schematic representation of the reversibility in nucleophilic aromatic substitutions.

To put this concept into practice, and because persulfuration mechanisms and sulfur component in exchanges by S_NAr have rarely been investigated, [150] it is the purpose of this thesis to investigate these fundamental concept and to apply them in the frame of DCC. When it is combined to rigidity-induced phosphorescence (RIP) and redox properties, the colorful molecular asterisks can be considered as ideal building blocks for DCC toward innovative materials, in line with multifunctional devices in the fields of nanoscience, imaging, supramolecular, materials and life sciences.

As a general example of DCC in this thesis, a hexakis(phenylthio)benzene asterisk undergoes simultaneous chemical, supramolecular, topological, and optical changes after a triggering event (figure 20). If this event is caused by a thiolate anion, we observed reversible nucleophilic aromatic substitutions by DCC, a process which we called the "Sulfur Danse" around an aromatic ring. Thus, a library of luminophores can be produced, depending on the sulfur exchange components conditions, including concentration, temperature, solvent, presence of ions, etc.. More importantly, we put forward S_NAr reactions, and their reversibility of in the frame of dynamic covalent chemistry.

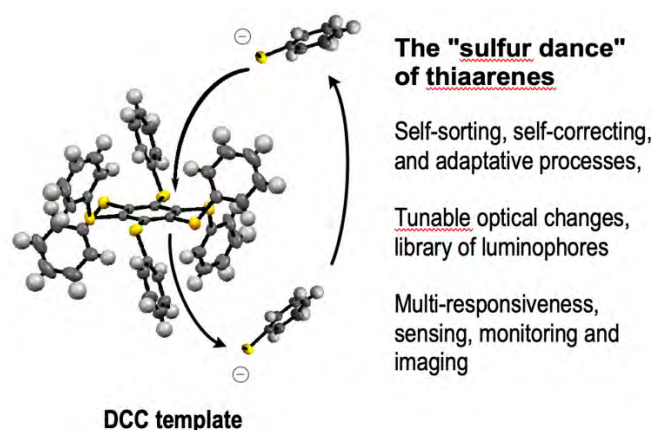


Figure 20: Example of a persulfurated benzene ring undergoing reversible nucleophilic aromatic substitutions with a thiolate anion in DCC.

Up to now, no one has questioned the synthesis, the kinetics, and the mechanisms of formation and sulfur exchanges of these asterisks, excepted in one report from MIT on the use of DCC. However, in a limited scope with 1,2-benzenedithiol. [150] Because the persulfuration mechanism and ligands exchanges have rarely been investigated (one report), [150] when it is combined to rigidity-induced phosphorescence (RIP) and redox properties, the colorful molecular asterisks can be considered as ideal building blocks for innovative (bio)materials in DCC, in line with multifunctional devices in the fields of nanoscience, imaging, supramolecular, materials and life sciences, typical applications are found in several DCC reviews. [174] Interestingly, the industry was more advanced in some applicative areas without noticing these unique properties. From 1963-67, biocidal properties of hexakis(arylthio)benzenes were reported, [175] and a patent on "Hexakis Thioethers" claims new herbicides, insecticides, anti-oxidant additives to lubricating oils, intermediates in dyestuffs, and biologically active materials. [176-177] One should also note that some asterisks are non toxic according to preliminary MTT assays with tetrazolium salts.

1.6 General objectives of the thesis work

This thesis focusses on functionalized and branched polysulfurated, polyoxygenated or polycyanated molecular asterisks incorporating either a benzene, a pyridine or a pyrene core. The main objectives are to report the synthesis and the structural, photophysical, supramolecular and covalent dynamic properties of the newly created molecular architectures, in order to further develop their uses and applications in a

near future, toward molecular electronics, imaging, materials and life sciences. Importantly, it also questions some fundamental principles and mechanisms in organic chemistry, notably the reversibility of a main and historical mechanism in organic chemistry: the nucleophilic aromatic substitution, which is known since 1854.

At first, the thesis covers new synthetic approaches to functionalize pyrene in its K-region, which has been neglected in spite of the historical importance of pyrenes in optoelectronic sensing, in materials and in biological sciences. It is followed by the synthesis of various sulfurated, oxygenated and cyanated molecular asterisks with a benzene or a pyridine core, in search for a new field in dynamic covalent chemistry (DCC) with arenes and heteroarenes, by implementing and promoting reversible nucleophilic aromatic substitutions in DCC, while at the same time developing all-organic highly phosphorescent smart materials via a rigidity-induced phosphorescence (RIP) phenomena. The "Sulfur Dance" around arenes and heteroarenes from a reversible exchange of sulfur components around an aromatic template, is a newly discovered process in aromatic chemistry. In order to study reversible S_NAr reactions, several reaction conditions, substituent effects, analytical and separative methods were necessary in DCC for analyzing the created libraries of compounds. In that direction, we also analyzed the importance of π -extended sulfurated and oxygenated asterisks with a benzene core, incorporating phenyl, biphenyl, naphthyl or heteroaromatic arms, in search for some exalted photophysical properties or metal cations bindings toward future molecular assemblies in supramolecular chemistry. Therefore, this thesis covers broad areas of aromatic chemistry, basic reaction mechanisms, photophysics and dynamic covalent and supramolecular chemistry, towards materials and life sciences.

References in Chapter 1

1. A. Fermi, G. Bergamini, R. Peresutti, E. Marchi, M. Roy, P. Ceroni, M. Gingras, *Dyes & Pigments*, **2014**, *11*, 113-122.
2. a) L. Gajda, T. Kupka, M. A. Broda, M. Leszczyńska, K. M. Ejsmont, *Magn. Reson Chem.* **2018**, *56*, 265–275; b) A. W. Hofmann, *Proc. Royal Soc.* **1856**, *8*, 1-3.
3. A. J. Rocke, *Angew. Chem. int. Ed.*, **2014**, *54*, 46-50.
4. F. A. Kekulé, *Bull. Soc. Chim.*, **1865**, *3*, 98-110.

5. F. A. Kekulé, *Ann. Chem. Pharmacie*, **1872**, 162, 77-124.
6. F. A. Kekulé, *Ann. Chem. Pharmacie*, **1866**, 137, 129-196.
7. P. v. R. Schleyer, C. Maerker, A. Dransfeld, H. Jiao, N. J. R. v. E. Hommes, *J. Am. Chem. Soc.*, **1996**, 118, 6317-6318.
8. P. v. R. Schleyer, H. Jiao, *Pure Appl. Chem.*, **1996**, 68, 209-218.
9. S. Gabaly, G.M. Youssif, A.M. Bayoumy, H. Ezzat, H. Elhaes, A. Refaat and M. A. Ibrahim, *Egypt. J. Chem.*, **2019**, 62, 1-11.
10. Z. Liu, K. Ouyang, N. Yang, *Org. Biomol. Chem.*, **2018**, 16, 988–992.
11. G. Bergamini, A. Fermi, C. Botta, U. Giovanella, S. Di Motta, F. Negri, R. Peresutti, M. Gingras, P. Ceroni, *J. Mater. Chem.*, **2013**, 1, 2717-2724.
12. A. Fermi, G. Bergamini, M. Roy, M. Gingras, P. Ceroni, *J. Am. Chem. Soc.*, **2014**, 136, 6395–6400.
13. J. I. Wu, M. A. Dobrowolski, M. K. Cyrański, B. L. Merner, G. J. Bodwell, Y. Mo and P.v.R. Schleyer, *Mol. Phys.*, **2009**, 107, 1177-1186.
14. M. Hammonds, A. Pathak, P. J. Sarre, *Phys. Chem.* **2009**, 11, 4458-4464.
15. M. Randić, *Chem. Rev.* **2003**, 103, 3449-3606.
16. T. M. F. Duarte, K. Müllen, *Chem. Rev.* **2011**, 111, 7260–7314.
17. L. Altschuler, E. Berliner, *J. Am. Chem. Soc.*, **1966**, 88, 5837-5845.
18. M. J. S. Dewar, R. D. Dennington, *J. Am. Chem. Soc.*, **1989**, 111, 3804-3808.
19. R. A. Hites, W J. Simonsick Jr. in *Calculated Molecular Properties of Polycyclic Aromatic Hydrocarbons*, Elsevier, New York, **1987**, pp. 272
20. M. Villa, M. Roy, G. Bergamini, P. Ceroni, M. Gingras, *Chem. Plus. Chem.* **2020**, 85, 1481–1486.
21. J. A. Mikroyannidis, L. Fenenko, C. Adachi, *J. Phys. Chem.*, **2006**, 110, 20317-20326.
22. H. Okamoto, T. Arai, H. Sakuragi, K. Tokumaru, *Bull. Chem. Soc. Jpn.* **1990**, 63, 2881-2890.
23. F. Liu, C. Tang, Q. Chen, S. Z. Li, H. B. Wu, L. H. Xie, B. Peng, W. Wei, Y. Cao, W. Huang, *Org. Electron.* **2009**, 10, 256- 265.
24. A. C. Benniston, A. Harriman, D. J. Lawrie, S. A Rostron, *Eur. J. Org. Chem.*, **2004**, 10, 2272-2276.
25. H. HO, R. G. Harvey, *Tetrahedron Lett.* **1974**, 1491-1494.
26. J. M. C. Solvas, J. D. Howgego, A. P. Davis, *Org. Biomol. Chem.* **2014**, 12, 212-232.

27. J. K. Stille, E. L. Mainen, *Macromolecules*, **1968**, *1*, 36-42.
28. M. R. Yadav, R. K. Rit, M. Shankar, A. K. Sahoo, *Asian J. Org. Chem.* **2015**, *4*, 846-864.
29. E. Bellamy, O. Bayh, C. Hoarau, F. Trécourt, G. Q. Guiner, F. Marsais, *Chem. Commun.*, **2010**, *46*, 7043-7045.
30. S. T. Gadge, P. Gautam, B. M. Bhanage, *Chem. Rec.*, **2016**, *16*, 835-856
31. M. Gingras, J.M. Raimundo, and Y. M. Chabre, *Angew. Chem. Int. Ed.*, **2006**, *45*, 1686-1712.
32. A. L. Rocklin, *J. Org. Chem.*, **1956**, *21*, 1478-1480.
33. M. Kulka, *J. Org. Chem.*, **1959**, *24*, 235-237.
34. a) K. R. Langille, M. E. Peach, *J. Fluorine Chem.*, **1972**, *1*, 407-414; b) M. E. Peach, A. M. Smith, *J. Fluorine Chem.*, **1974**, *4*, 341-344; c) M. E. Peach, A. M. Smith, *J. Fluorine Chem.*, **1974**, *4*, 399-408.
35. a) R. Adams, A. Ferretti, *J. Am. Chem. Soc.*, **1959**, *81*, 4927-4931; b) R. Adams, W. Reifschneider, M. D. Nair, *Croat. Chem. Acta.*, **1957**, *29*, 277-285.
36. L. P. Robota, B. F. Malichenko, *J. Org. Chem. (USSR)*, **1976**, *11*, 233.
37. B. C. Musial, M. E. Peach, *Phosphorus, Sulfur Silicon, Relat. Elem.*, **1977**, *3*, 41-42.
38. a) D. D. MacNicol, D. R. Wilson, *J. Chem. Soc. Chem. Commun.* **1976**, 494-495; b) D. D. MacNicol, A. D. U. Hardy, D. R. Wilson, *Nature*, **1977**, *266*, 611-612; c) D. D. MacNicol, D. R. Wilson, *Chem. Ind.*, **1977**, 84-85.
39. a) A. D. U. Hardy, D. D. MacNicol, D. R. Wilson, *J. Chem. Soc. Perkin Trans*, **1979**, *2*, 1011-1019.
40. a) J. R. Beck, J. A. Yahner, *J. Org. Chem.* **1978**, *43*, 2048-2052; b) M. E. Peach, E. S. Rayner, *J. Fluorine Chem.*, **1979**, *13*, 447-454.
41. J. A. Connor, G. A. Hudson, *J. Organomet. Chem.* **1975**, *97*, C43-C45.
42. A. M. Richter, V. Engels, N. Beye, E. Fanghanel, *Z. Chem.* **1989**, *29*, 444-445.
43. F. Maiolo, L. Testaferri, M. Tiecco, M. Tingoli, *J. Org. Chem.*, **1981**, *46*, 3070-3073.
44. M. Gingras, A. Pinchart, C. Dallaire, *Angew. Chem. Int. Ed.* **1998**, *37*, *22*, 3149-3151.
45. J. F. Bunnett, R. E. Zahler, *Chem. Rev.* **1951**, *49*, 273-412.
46. L. A. Wall, W.J. Pummer, J. E. Fearn, J. M. Antonucci, *Phys Chem.* **1963**, *67A*, 481-497.

47. J. Hellberg, E. Dahlstedt, M. E. Pelcman, *Tetrahedron*, **2004**, *60*, 8899-8912.
48. D. D. MacNicol, P. R. Mallinson, A. Murphy, C. D. Robertson, *J. Inclusion Phenom.* **1987**, *5*, 233–239.
49. L. Xionga , Y. F. Hua , Z. G. Zhenga , Z. L. Xieb, D. Y. Chena, *Chin. J. Polymer Science*, **2020**, *38*, 278–287.
50. R. Matmour, R. Francis, R. S. Duran, Y. Gnanou, *Macromolecules* **2005**, *38*, 7754-7767.
51. E. R. Zubarev, J. Xu, J. D. Gibson, A. Sayyad, *Org. Lett.*, **2006**, *8*, 1367-1370.
52. T. Weng, G. Baryshnikov, C. Deng, X. Li, B. Wu, H. Wu, H. Ågren, Q. Zou, T. Zeng, L. Zhu, *Small*, **2020**, *16*, 1906475.
53. a) T. Sandmeyer, *B. Dtsch. Chem. Ges.* **1884**, *17*, 1633- 1635; b) T. Sandmeyer, *Chem. Ber.* **1884**, *17*, 2650-2653; c) T. Sandmeyer, *Chem. Ber.* **1885**, *18*, 1492-1496; d) T. Sandmeyer, *Chem. Ber.* **1885**, *18*, 1946-1948.
54. K. W. Rosenmund, E. Struck, *Chem. Ber.* **1919**, *2*, 1749-1756.
55. K. Suna, Q. Y. Lva, Y. W. Lind, B. Yua, W. M. He, *Org. Chem. Front.*, **2021**, *8*, 445-465.
56. G. Yan, Y. Zhang, J. Wang, *Adv. Synth. Catal.* **2017**, *359*, 4068-4105.
57. P. Gregory, *J. Porphyrins Phthalocyanines*, **2000**, *4*, 432-437.
58. H. Ecker, Y. Kiesel, *Angew. Chem., Int. Ed. Engl.*, **1991**, *20*, 473-475.
59. N. Kobayashi, K. Sudo, and T. Osa, *Bull. Chem. Soc. Jpn.*, **1990**, *63*, 317.
60. A. Goux, F. Bedioui, L. Robbiola, M. Pontie, *Electroanalysis*, **2003**, *15*, 969-974.
61. S. Shahrokhian, A. Hamzehloei, A. Thaghani, S.R. Mousavi, *Electroanalysis*, **2004**, *16*, 915-921.
62. K. Wael, P. Westbroek, E. Temmerman, *Electroanalysis*, **2005**, *17*, 263-268.
63. P. Zhang, H. Wang, X. Yan, J. Wang, J. Shi, and D. Yan, *Adv. Mater.*, **2005**, *17*, 1191-1193.
64. Molecular Semiconductors. Photoelectrical Properties and Solar Cells, (J. Simon, J.-J. Andre, Edrs), Springer-Verlag, Berlin, **1985**.
65. B. N. Achar, G. M. Fohlen, J. A. Parker, *J. Polym. Sci.: Polym. Chem.*, **1982**, *20*, 2773-2780.
66. B. N. Achar, G. M. Fohlen, J.A. Parker, *J. Appl. Polym. Sci.*, **1984**, *29*, 353-359.
67. M. K Casstevens, M. Samoc, J. Pflieger, P. N. Prasad, *J. Chem. Phys.*, **1990**, *92*, 2019-2024.

68. K. D. Schiebaum, R. Zhou, S. Knecht, R. Dieing, M. Hanack, W. Göpel, *Sensors Actuators, B: Chem.*, **1995**, *24*, 69-71.
69. K. A. Volkov, G. V. Avramenko, V. M. Negrimovsky, *Russ. J. Gen. Chem.*, **2007**, *77*, 1108–1116.
70. M. Villa, S. D'Agostino, P. Sabatino, R. Noel, J. Busto, M. Roy, M. Gingras, P. Ceroni, *New J. Chem.*, **2020**, *44*, 3249-3254.
71. a) M. J. Plater, A. Jeremiah, G. Bourhill, *J. Chem. Soc., Perkin Trans.*, **2002**, *1*, 91-96; b) J. B. Pereira, E. F. A. Carvalho, M. A. F. Faustino, R. Fernandes, M. G. P. M. S. Neves, J. A. S. Cavaleiro, N. C. M. Gomes, Â. Cunha, A. Almeida, J. P. C. Tomé, *Photochem. Photobiol*, **2012**, *88*, 537-547; c) M. Mayukh, C.-W. Lu, E. Hernandez, D. V. McGrath, *Chem. Eur. J.*, **2011**, *17*, 8472-8478.
72. S. Riebe, C. Vallet, F. van der Vight, D. G. Abradelo, C. Wölper, P. D. Cristian, A. Strassert, G. Jansen, S. Knauer, J. Voskuhl, *Chem. Eur. J.*, **2017**, *55*, 13660-13668.
73. H. Bhatia, I. Bhattacharjee, D. Ray, *J. Phys. Chem. Lett.*, **2018**, *9*, 3808–3813.
74. L. Zophel, V. Enkelmann, R. Rieger, K. Müllen, *Org. Lett.*, **2011**, *13*, 4506-4509.
75. J. M. Casas-Solvas, J. D. Howgego, A. P. Davis, *Org. Biomol. Chem.*, **2014**, *12*, 212–232
76. J. C. Wu, Y. Zou, C. Y. Li, W. Sicking, I. Piantanida, T. Yi and C. Schmuck, *J. Am. Chem. Soc.*, **2012**, *134*, 1958–1961
77. M. Printz and C. Richert, *Chem. Eur. J.*, **2009**, *15*, 3390– 3402
78. D. Tasis, N. Tagmatarchis, A. Bianco, M. Prato, *Chem. Rev.*, **2006**, *106*, 1105–1136.
79. N. Karousis, N. Tagmatarchis, D. Tasis, *Chem. Rev.*, **2010**, *110*, 5366–5397.
80. A. Le Goff, K. Gorgy, M. Holzinger, R. Haddad, M. Zimmerman, S. Cosnier, *Chem. Eur. J.*, **2011**, *17*, 10216–10221.
81. a) Y. Chen, B. Zhu, Y. Han, Z. Bo, *J. Mater. Chem.*, **2012**, *22*, 4927–4931; b) Y. Xu, H. Bai, G. Lu, C. Li, S. Shi, *J. Am. Chem. Soc.*, **2008**, *130*, 5856–5857.
82. V. K. Kodali, J. Scrimgeour, S. Kim, J. H. Hankinson, K. M. Carroll, W. A. de Heer, C. Berger, J. E. Curtis, *Langmuir*, **2011**, *27*, 863–865.
83. J. A. Mann, J. Rodríguez-López, H. D. Abruña, W. R. Dichtel, *J. Am. Chem. Soc.*, **2011**, *133*, 17614–17617.
84. M. Endo, H. Sugiyama, *ChemBioChem*, **2009**, *10*, 2420– 2443.
85. I. V. Astakhova, V. A. Korshun, J. Wengel, *Chem. Eur. J.*, **2008**, *14*, 11010–1102

86. W. Sotoyama, H. Sato, M. Kinoshita, T. Takahashi, *Sym. Dig. Tech. I Pap.*, **2003**, 34, 1, 1294-129.
87. Z. H. Wu, Z. T. Huang, R. X. Guo, C. L. Sun, L. C. Chen, B. Sun, Z. S. Shi, X. Shao, H. Li, H. L. Zhang, *Angew. Chem. Int. Ed.*, **2017**, 56, 13031-13035.
88. Z. Duan, D. Hoshino, Z. Yang, H. Yano, H. Ueki, Y. Liu, H. Ohuchi, Y. Takayanagi, G. Zhao, And Y. Nishioka, *Mol. Cryst. Liq. Cryst.*, **2011**, 538, 199–207.
89. G. Valenti, A. Fiorani, S. D. Motta, G. Bergamini, M. Gingras, P. Ceroni, F. Negri, F. Paolucci, M. Marcaccio, *Chem. Eur. J.*, **2014**, 20, 1-13.
90. M. Gingras, V. Placide, J. M. Raimundo, G. Bergamini, P. Ceroni, V. Balzani, *Chem. Eur. J.*, **2008**, 14, 10357-10363.
91. A. Fermi, P. Ceroni, M. Roy, M. Gingras, G. Bergamini, *Chem. Eur. J.*, **2014**, 20, 1–9.
92. S. Goretta, C. Tasciotti, S. Mathieu, M. Smet, W. Maes, Y. M. Chabre, W. Dehaen, R. Giasson, J. M. Raimundo, C. R. Henry, C. Barth, M. Gingras *Org. Lett.*, **2009**, 11, 3846-3849.
93. T. Okauchi, K. Kuramoto, M. Kitamura, *Synlett*, **2010**, 19, 2891–2894.
94. B. P. Fleming Krueger, R. Graham and J. Longworth, *Encyclopedia Britannica*, **2018**, <https://www.britannica.com/science/photochemical-reaction>.
95. H. B. Laurent, J.-P. Desvergne *Molecular Gels*, Springer, **2006**, 363-429.
96. I. D. Johnson, M. W. Davidson, <http://images.app.hoo.gl/UMpUg14cHFG9aEvz6>
97. X. Zhang, *Acta Polym. Sin.*, **2020**, 51, 1.
98. H. Staudinger, *Ber. Dtsch. Chem. Ges. (A and B)* **1920**, 53, 1073-1077.
99. K. Miyagi, Y. Teramoto, *J. Mater. Chem.*, **2018**, 6, 1370-1376.
100. Z. Ma, M. Teng, Z. Wang, S. Yang, X. Jia, *Angew. Chem. Int. Ed.*, **2013**, 52, 12268-12272.
101. R. Mülhaupt, *Angew. Chem. Int. Ed.*, **2004**, 43, 1054-1063.
102. K. K. Neena, P. Sudhakar, K. Dipak, P. Thilagar, *Chem. Commun.*, **2017**, 53, 3641-3644.
103. L. Qianqian, L. Zhen, *Adv. Sci.*, **2017**, 4, 1600484.
104. Y. Xing, Y. Wang, L. Zhou, L. Zhu, *Dyes & Pigments*, **2021**, 186, 109032.
105. A. Lizbeth, R. Cortés, A. N. Huerta, B. R. Molina, *Matter*, **2021**, 4, 2622-2624.
106. W. Xi, J. Yu, M. Wei, Q. Qiu, P. Xu, Z. Qian, *Chem. Eur. J.*, **2020**, 26, 3733–3737.

107. M. Villa, M. Roy, G. Bergamini, M. Gingras, P. Ceroni, *Dalton Trans.*, **2019**, 48, 3815-3818.
108. Md. M. Islam, Z. Hu, Q. Wang, C. Redshaw, X. Feng, *Mater. Chem. Front.*, **2019**, 3, 762-781.
109. F. M. Winnik, *Chem. Rev.*, **1993**, 93, 587-414.
110. Q. Li, Z. Li, *Adv. Sci.*, **2017**, 4, 1600484.
111. F. Zheng, S. Guo, F. Zeng, J. Li, S. Wu, *Anal. Chem.*, **2014**, 86, 9873-9879.
112. S. Lohar, D. A. Safin, A. Sengupta, A. Chattopadhyay, J. S. Matalobos, M. G. Babashkina, Koen Robeyns, M. P. Mitoraj, P. Kubisiak, Y. Garciab, D. Das, *Chem. Commun.*, **2015**, 51, 8536-8539.
113. S. Nagatoishi, T. Nojima, B. Juskowiak, S. Takenaka, *Angew. Chem. Int. Ed.*, **2005**, 44, 5067-5198.
114. H. S. Jung, M. Park, D. Y. Han, E. Kim, C. Lee, S. Ham, J. S. Kim, *Org. Lett.*, **2009**, 11, 3378-3381.
115. J. Chen, D. Liao, Y. Wang, H. Zhou, W. Li, C. Yu, *Org. Lett.* 2013, 15, 2132-2135.
116. J. F. Bunnett, *Q. Rev. Chem. Soc.*, **1958**, 12, 1-16
117. J. F. Bunnett, R. E. Zahler, *Chem. Rev.* **1951**, 49, 273-412.
118. S. Rohrbach, A. J. Smith, J. H. Pang, D. L. Poole, T. Tuttle, S. Chiba, J. A. Murphy, *Angew. Chem. Int. Ed.* **2019**, 58, 6368-6388.
119. M. B. Smyth, in March's Advanced Organic Chemistry: Reactions, Mechanisms and Structure, 7th ed., *Wiley, Hoboken*, **2013**, Chap. 11, pp. 569-641, e-book ISBN: 9781118472217.
120. Nucleophilic Aromatic Substitution - The Addition-Elimination Mechanism" *LibreTexts*. NPTEL – Chemistry – Principles of Organic Synthesis
121. Addition-Elimination Mechanism (**2020**), <https://chem.libretexts.org/@go/page/16576>
122. <https://digital.library.adelaide.edu.au/dspace/bitstream/2440/20115/2/02whole.pdf>
123. F. Mo, G. Dong, Y. Zhanga, J. Wang, *Org. Biomol. Chem.*, **2013**, 11, 1582-1593
124. https://en.wikipedia.org/wiki/Diazonium_compound
125. P. Burri, H. Loewenschuss, H. Zollinger, G. K. Zwolinski, *Helv. Chim. Acta*, **1973**, 56, 2204-2216.

126. a) N. Darby, C. U. Kim, J. A. Salan, K. W. Shelton, S. Takada, S. Masamune, *J. Chem. Soc. Chem. Commun.*, **1971**, 1516-1517; b) S. Masamune, N. Darby, *Acc. Chem. Res.*, **1972**, *5*, 272-281.
127. H. H. Wenk, M. Winkler, W. Sander, *Angew. Chem. Int. Ed.* **2003**, *42*, 502-528.
128. a) R. R. Jones, R. G. Bergman, *J. Am. Chem. Soc.*, **1972**, *94*, 660-661; b) R. G. Bergman, *Acc. Chem. Res.*, **1973**, *6*, 25.
129. a) J. Williamson and Scrugham, *Annalen*, **1854**, *7*; b) *ibid*, *Compt. Rend.*, **1854**, *39*, 852; c) *ibid*, *Annalen*, **1854**, *92*, 316; d) *Pisani*, *Compt. Rend.*, **1854**, *39*, 852.
130. H. C. Van der Plas, *Acc. Chem. Res.*, **1978**, *11*, 462-468.
131. S. D. Roughley, A. M. Jordan, *J. Med. Chem.* **2011**, *54*, 3451-3479.
132. H. V. Plas, A. Katritzky, *Adv. Heterocycl. Chem.*, **1999**, *74*, 9-86.
133. K. Breuker, H. C. van der Plas, *J. Org. Chem.*, **1979**, *44*, 4679-4680.
134. S. Kunugi, T. Okubo, N. Ise, *J. Am. Chem. Soc.* **1976**, *98*, 8, 2282-2287.
135. E. N. Marvell, G. Caple, I. Shahidi, *J. Am. Chem. Soc.* **1970**, *92*, 5641-5645.
136. M. Makosza, *Russ. Chem. Rev.*, **1989**, *58*, 747-757.
137. E. Buncel, J. M. Dust, F. Terrier, *Chem. Rev.*, **1995**, *95*, 7, 2261-2280.
138. E. E. Kwan, Y. Zeng, H. A. Besser, E. N. Jacobsen, *Nat. Chem.* **2018**, *10*, 917-923.
139. J. Miller, *Aust. J. Chem.*, **1956**, *9*, 61-73.
140. S. E. Fry, N. J. Pienta, *J. Am. Chem. Soc.*, **1985**, *107*, 6399-6400.
141. A. Hunter, M. Renfrew, J. A. Taylor, J. M. J. Whitmore, A. Williams, *J. Chem. Soc. Perkin Trans. 2*, **1993**, 1703-1704.
142. A. Hunter, M. Renfrew, D. Rettura, J. A. Taylor, J. M. J. Whitmore, A. Williams, *J. Am. Chem. Soc.*, **1995**, *117*, 5484-5491.
143. J. Shakes, C. Raymond, D. Rettura, A. Williams, *J. Chem. Soc. Perkin Trans. 2*, **1996**, 1553-1557.
144. N. R. Cullum, D. Rettura, J. M. J. Whitmore, A. Williams, *J. Chem. Soc. Perkin Trans. 2* **1996**, 1559-1563.
145. J. Persson, S. Axelsson, O. Matsson, *J. Am. Chem. Soc.*, **1996**, *118*, 20-23.
146. C. Neuman, J. Hooker, T. Ritter, *Nature*, **2016**, *534*, 369-373.
147. N. Constanze Neumann and T. Ritter, *Acc. Chem. Res.* **2017**, *50*, 11, 2822-2833.
148. H. Beyzavi, D. Mandal, M. G. Strebl, C. N. Neumann, E. M. D'Amato, J. Chen, J. M. Hooker, T. Ritter, *ACS Central Science*, **2017** *3*, 944-948.

149. J.-M. Lehn, *Chem. Soc. Rev.*, **2007**, 36, 151–160.
150. W. J. Ong, T. M. Swager, *Nat. Chem.*, **2018**, 10, 1023–1030.
151. S. Kulchat, doctoral thesis, "Dynamic covalent chemistry of C=N, C=C and quaternary ammonium constituents." Université de Strasbourg, **2015**.
152. R. B. Moffett, W. M. Hoehn, *J. Am. Chem. Soc.*, **1947**, 69, 1792-1794.
153. M. Freifelder, *J. Org. Chem.*, **1966**, 31, 3875-3877.
154. Nucleophilic Addition of Amines- Imine and Enamine Formation. **2021**, <https://chem.libretexts.org/@go/page/36388>
155. J. T. Goodwin, D. G. Lynn, *J. Am. Chem. Soc.*, **1992**, 114, 9197-9198
156. S. J. Rowan, J. F. Stoddart, *Org. Lett.*, **1999**, 1, 1913-1916.
157. N. Giuseppone, J.-M. Lehn, *Chem. Eur. J.*, **2006**, 12, 1715-1722.
158. M. Ciaccia, S. Pilati, R. Cacciapaglia, L. Mandolini, S. D. Stefano, *Org. Biomol. Chem.*, **2014**, 12, 3282–3287.
159. N. Wilhelms, S. Kulchat, J.-M. Lehn, *Helv. Chim. Acta*, **2012**, 95, 2635-2651.
160. M. C. Thompson, D. H. Busch, *J. Am. Chem. Soc.*, **1962**, 84, 1762-1763.
161. Retro Diels-Alder Reaction, **2020**, <https://chem.libretexts.org/@go/page/42549>
162. N. Roy, J.-M. Lehn, *Chem. Asian J.*, **2011**, 6, 2419-2425.
163. P. Reutenauer, P. J. Boul, J.- M. Lehn, *Eur. J. Org. Chem.*, **2009**, 1691-1697.
164. D. J. Nelson, S. Manzini, A. César, U. Blanco, S. P. Nolan, *Chem. Commun.*, **2014**, 50, 10355-10375.
165. F. Lefebvre, Y. Bouhoute, K. C. Szeto, N. Merle, A. Mallmann, R. Gauvin, M. Taoufik, Intech, Chapt. 3, **2018**; <http://dx.doi.org/10.5772/intechopen.69320>
166. Olefin Metathesis by Group VI (Mo, W) Metal Compounds - https://www.researchgate.net/figure/Mechanism-of-the-olefin-metathesis-reaction_fig3_323001561
167. https://commons.wikimedia.org/wiki/File:Metathesis_mechanism_jypx3.png
168. C. P. Casey, T. J. Burkhardt, *J. Am. Chem. Soc.*, **1973**, 95, 5833-5834.
169. R. R. Schrock, *J. Am. Chem. Soc.*, **1974**, 96, 6796-6797.
170. A. Fava, A. Iliceto, E. Camer, *J. Am. Chem. Soc.*, **1957**, 79, 833-838
171. M. Calvin, report-<https://www.osti.gov/servlets/purl/4414774/>
172. D. P. Ames, J. E. Willard, *J. Am. Chem. Soc.* **1951**, 73,164-172.
173. P. Massini, M. Calvin, *Experientia*, **1952**, 8, 445.
174. a) A. Herrmann, *Chem. Soc. Rev.* **2014**, 43, 1899-1933; b) Y. Jin, Q. Wang, P. Taynton, W. Zhang, *Acc. Chem. Res.* **2014**, 47, 1575-1586; c) Y.Jin, C. Yu, R.J.

- Denman, W. Zhang, *Chem. Soc. Rev.*, **2013**, 42, 6634-6654; d) F. B. L. Cougnon, J. K. M. Sanders, *Acc. Chem. Res.* **2012**, 45, 2211-2221; e) J.-M. Lehn, *Chem. Soc. Rev.*, **2007**, 36, 151-160.
175. a) W. Reifschneider (Dow Chemicals Co.), US 3,100,802, 1963 [Chem. Abstr. 1964, 60,2951]; b) W. Reifschneider (Dow chemicals Co.), US 3,206,467, [Chem. Abstr. **1965**, 63,98005].
176. W. Reifschneider (Dow Chemicals Co.), US 3,311,664, [Chem. Abstr. **1967**, 67,402893].
177. J. D. Spivack (Ciba-Geigy AG), DE 2819882, [Chem. Abstr. **1978**, 90,88309 z].

CHAPTER 2

FUNCTIONALIZATION OF PYRENE IN THE K-REGION: SYNTHESIS, STRUCTURAL AND PHOTOPHYSICAL STUDIES

- 2.0 Introduction
- 2.1 Objectives
- 2.2 Results and discussion
 - 2.2.1 Functionalization of pyrene at positions 1,3,6,8 (non K-region)
 - 2.2.2 Functionalization of pyrene at positions 4,5,9,10 (K-region)
 - 2.2.3 Functionalization of pyrene at positions 1,6; 1,8 and 2,7 (non K-region)
- 2.3 Ring-closure via benzylic-type couplings
- 2.4 New routes to functionalized pyrenes in the K-region via benzylic-type ring closures
 - 2.4.1 Preliminary results and model studies on phenanthrene
 - 2.4.2 Long route to 4,5,9,10-tetrabromo pyrene
 - 2.4.3 Short and optimized route to 4,5,9,10-tetrabromo pyrene
- 2.5 Sulfurated pyrenyl derivatives from 4,5,9,10-tetrabromo pyrene
- 2.6 Cyanated pyrenyl derivatives from 4,5,9,10-tetrabromo pyrene
- 2.7 Photophysical studies on sulfurated pyrenes in the K-region.
- 2.8 Conclusion

2.0 Introduction

Pyrene derivatives have attracted much attention in the last few years due to their blue emissive properties and long fluorescence lifetime, which are influenced by the molecular environment. Pyrene is one of the most important basic units in materials chemistry and in the history of chemistry. Unfortunately, derivatization of the monomeric pyrene unit is still poorly developed, especially with sulfur and fluorine, but also in its K-region. The synthesis of pyrenic oligomers, polymers, and other complex architectures is thus limited by the usual functionalizations of pyrene at specific positions, mostly in the non K-region. It could be highly valuable to functionalize pyrene at different positions with different substituents, and to compare the photophysical and redox properties with pyrene itself. More precisely, the polysulfuration of pyrene could strongly modulate its REDOX and photophysical properties, as well as complex pyrene-based architectures. All these derivatives could find some applications as (bio)sensors, electroluminescent materials, in organic light-emitting diode (OLEDs) and in organic electronics in general.

2.1 Objectives

Several objectives are sought in this work, which could be listed below:

1. To explore novel and short routes to functionalize pyrene in its K-region,
2. To make new derivatives of pyrene functionalized in its K-region, especially the sulfurated or heterofunctionalized ones, as novel building blocks of uses in materials and biological sciences.
3. To study the photophysical, electronic, and structural properties of these derivatives by NMR, HRMS, X-ray diffraction, and calculations,
4. To use pyrene as a universal building block for the design of novel π -conjugation and architectures with various topologies, such as chains and ribbons.
5. To gradually increase the complexity of the pyrenic systems from monomers to dimers, to oligomers, and to polymers for studying their photophysical, electronic, and structural properties (coupling mode, photophysics, redox, structural studies by NMR, MS, X-ray diffraction, and calculations).

2.2 Results and discussion

The regioselective functionalization of pyrene is very challenging. As a consequence, most derivatives are coming from the non K-region functionalization of pyrene. For instance, an electrophilic substitution preferentially occurs at positions 1-,3-,6- and 8 of pyrene, but larger electrophiles prefer to react at positions 2 and 7 for steric reasons.

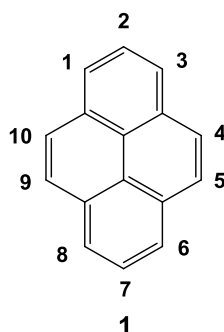


Figure 1: Pyrene (1) structure and numbering of positions for functionalization.

As a consequence, most electrophilic substitutions are reported at these positions in the literature for making most pyrene derivatives. In spite of a large number of reactions and functionalizations of pyrene, a major challenge remains a quick functionalization of the so-called K-region of pyrene (Figure 1). Thus, we are more interested in the functionalization of pyrenes at positions 4, 5, 9,10, which are less common and less easy in synthesis.

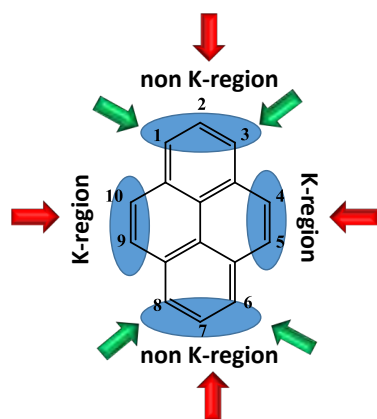
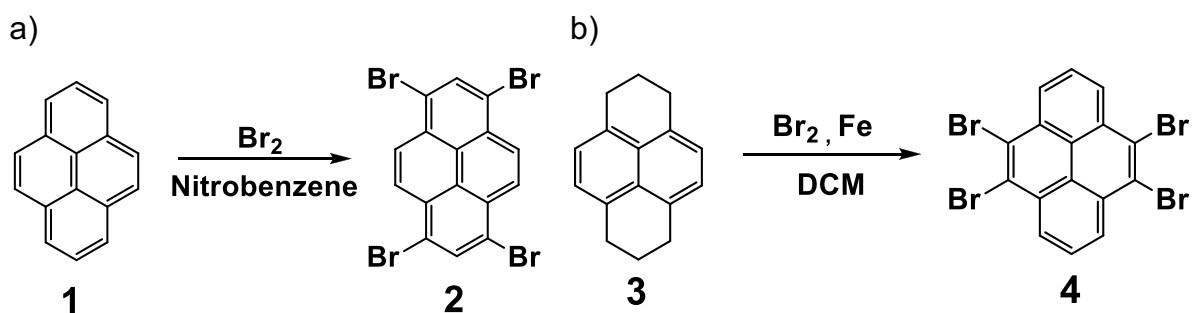


Figure 2: green arrow represents common functionalization sites on pyrene in the non K-region, whereas red arrows represent uncommon functionalization sites on pyrene in the K-region.

2.2.1 Functionalization of pyrene at positions 1,3,6,8 (non K-region)

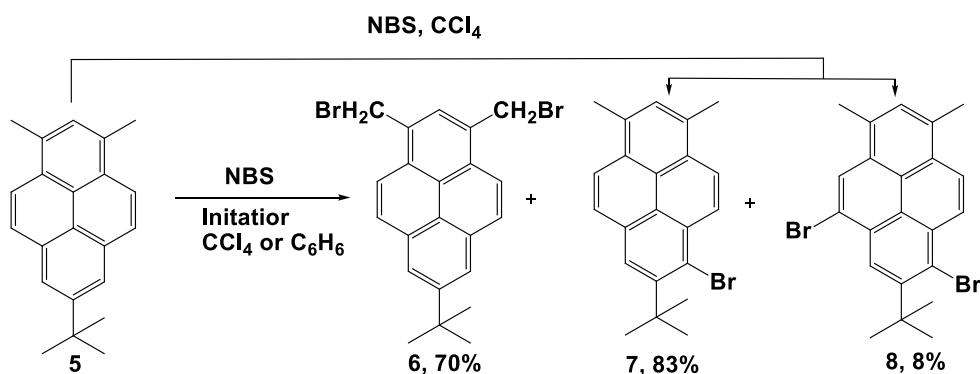
As already discussed in the main introduction (chapter 1, section 1.3, scheme 1), electrophilic substitutions at pyrene usually occur at positions 1,3,6,8. In this way, the bromination of pyrene could provide 1-bromo-pyrene, 1,6-dibromopyrene, 1,8-dibromopyrene and 1,3,6-tribromopyrene and 1,3,6,8-tetrabromo pyrene depending on the molar ratio of bromine and pyrene. 1,3,6,8-tetrabromo pyrene (**2**) is known and easy to synthesize by treating pyrene (**1**) with bromine in warm nitrobenzene. It thus became an important building block to synthesize star-shaped pyrenic structures. An alternative indirect method to make a similar compound, but in the K-region, is by treating tetrahydropyrene (**3**) with N-bromosuccinimide and a radical initiator in carbon tetrachloride or benzene to provide 4,5,9,10-tetrabromo pyrene (**4**) (scheme 1). [1] Only two reactions have been reported so far to make this compound (discussed in section 2.2.2); another one is to synthesize 4,5,9,10-tetrabromo pyrene by treating 4,5,9,10-tetrahydropyrene (**4**) with bromine and iron in dichloromethane. [2]



Scheme 1: a) Synthesis of 1,3,6,8-tetrabromopyrene (**2**) [3], b) Synthesis of 4,5,9,10-tetrabromopyrene (**4**). [2]

Substitutions at the 1,3,6,8 positions (non K-region) is comparatively easy (energy is lower by 8.8 Kcal/mol from calculations) [4] in comparison to the 4,5,9,10 positions (K-region). For the first series, the substitution order is 1 > 8 > 6 > 3. [5] Simple bromination

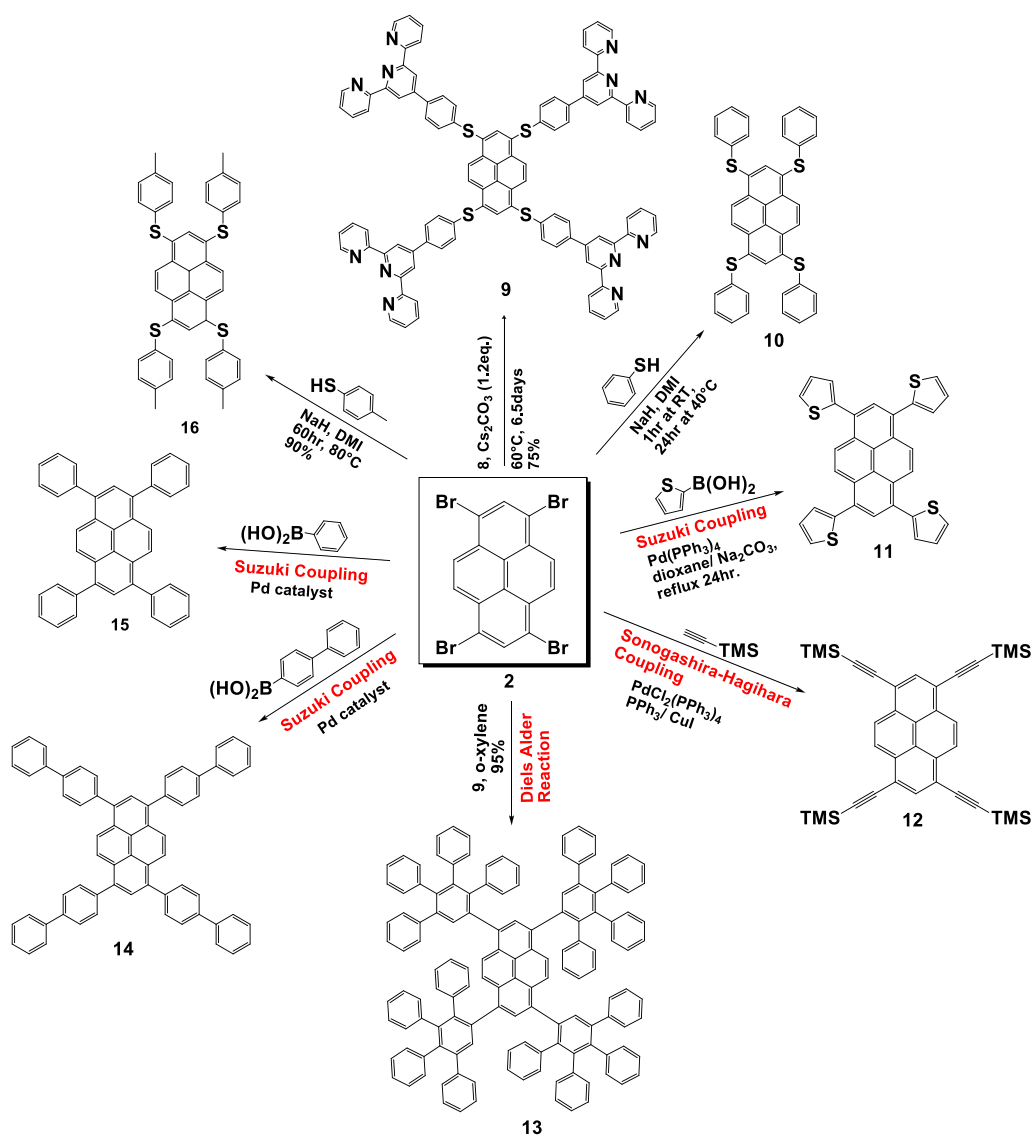
of pyrene in nitrobenzene gives a mixture of four products with 1,3,6,8-tetrabromopyrene and other mono, di, tri substituted products at the 1,3,6,8 positions, and not 4,5,9,10-tetrabromo pyrene or derivatives in the k-region. [5] Another example of bromination with NBS with is presented in scheme 2, but several by-products are formed. [6]



Scheme 2: Bromination at 1,3,4,6 using N-bromosuccinimide with benzoyl peroxide as an initiator. [1, 6]

In Section 2.2.2 (scheme 7), we can see that positions 2,7 of pyrene are already substituted with *t*-butyl groups, and treating this compound with 1.1 mol-equiv, and 2.2 mol-equiv of bromine with iron powder provides brominated pyrenic compounds at position 1 for (1.1 mol-equiv.), and 1,6; 1,8-dibrominated pyrenes (2.2 mol-equiv.).

1,3,6,8-Tetrabromo pyrene is an important building block to synthesize polysulfurated derivatives, as shown in schemes 3, 4 and 5. Compound **9** can be prepared from nucleophilic aromatic substitutions on (**2**) using 4 mol-eq. of terpyridine thiol (figure 3) in a 76% yield. The tetrakis(phenylthio)pyrene core is appended with four terpyridine units as a multichromophoric system. The addition of metals ions can switch the direction of the intramolecular energy transfer of the excited state and control the formation of three-dimensional nanoscopic objects in a dual function. [7] Compounds **10** and **16** were also synthesized by S_NAr reactions using sodium hydride as a base in a polar solvent (DMI or DMF). In addition, sulfurated dendrimers were also synthesized with a pyrene core (scheme 4). [8-9]



Scheme 3: reactions with key intermediate 1,3,6,8-tetrabromo pyrene (**2**) [7-12]

Suzuki couplings with different boronic acids and palladium catalysts provide various Ar-C compounds such as compounds **11**, **14** and **15**. Tetrasubstituted compounds **14** and **15** avoid aggregation between pyrenes and can be useful as light-emitting diodes. [10-11]

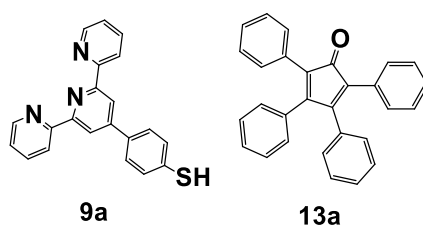
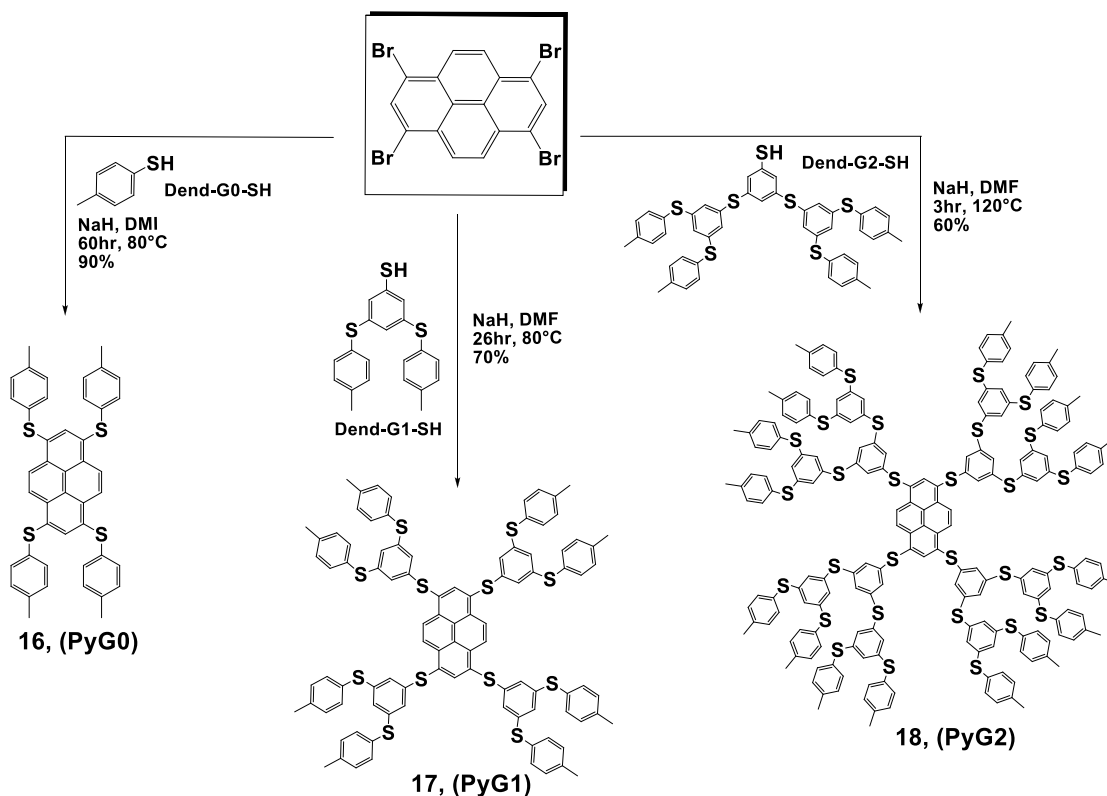


Figure 3: structures of **1a** and **5a** required to synthesize **1** and **5** (see scheme 3).

Compound 13 is a first-generation dendrimer synthesized from Diels-Alder cycloadditions from a tetraalkynated pyrene and tetraphenylcyclopentadienone (figure 3, scheme 3). To synthesize 12, a Sonogashira-Mirozoki coupling was done. Deprotection of the TMS-protected 12 with potassium carbonate in MeOH provides the corresponding tetraalkynated pyrene, ready for the cycloadditions. [12]

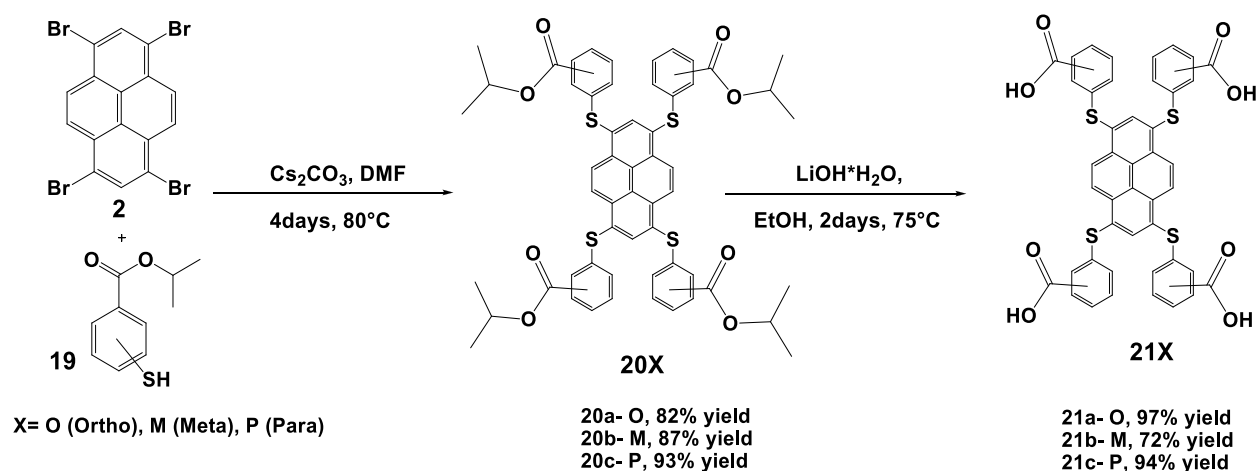


Scheme 4: three generations of polysulfurated 1,3,6,8-tetrasubstituted pyrene-cored asterisks. [9]

Three generations of polysulfurated dendrimers were synthesized by Gingras and his group in 2008 by simply treating 1,3,6,8-tetrabromo pyrene (2), (1.0 mol-eq) with the corresponding thiols (4.5 mol-eq) at 80°C for 3 to 60 hours (scheme 4). The photophysical properties were discussed in detail in chapter 1 (section 1.3, Scheme 23).

In 2020, another published work from our laboratory reported water-soluble pyrene asterisks with carboxylic acid functions at the periphery of the pyrene core. [9] Their synthesis are described in scheme 5. The properties of the carboxylic acid give water solubility, and provide complexations with metal ions. Compounds 20X= PyO, PyM, PyP were synthesized by a nucleophilic aromatic substitution in good yields with the desired thiolate isomers and 1,3,6,8-tetrabromopyrene (2) in DMF with Cs₂CO₃ as a base at 80°C. The saponification of the ester with LiOH·H₂O in ethanol at 75°C was

achieved to deprotect the acid functions. The preparation of the corresponding ortho, meta, and para benzenethiols was already described. [13]



Scheme 5: water-soluble pyrene-cored asterisks with peripheral carboxylic acid functions. [13]

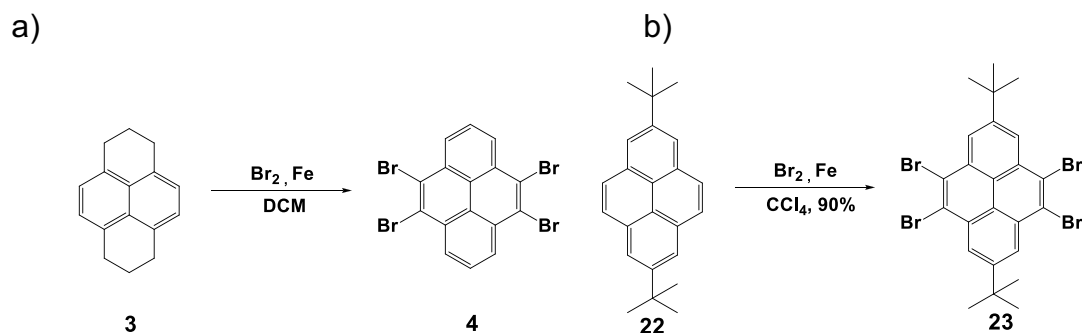
The pyrene-cored asterisk 21X with carboxylic acid units (scheme 5) is a water-soluble organic chromophore that could selectively complex divalent metal ion, like Pb(II). At the same time, the fluorescence of the core is quenched. This system could be used as a fluorescent ON-OFF sensor for metal ions in a dual mode (fluorescence variation and aggregation to make particles).

2.2.2 Functionalization of pyrene at positions 4,5,9,10 (K-region)

This section reports the synthesis of 4,5,9,10-tetrabromo pyrene (4) and its derivatives from some indirect methods. This compound can not be obtained in a direct bromination of pyrene, as for 1,3,6,8-tetrabromo pyrene (2) which is directly formed by electrophilic aromatic substitutions. Only a few reports exist in the literature for making 4,5,9,10-tetrabromo pyrene (4) and its derivatives and the latter could serve for making new chains, ribbons and polymers.

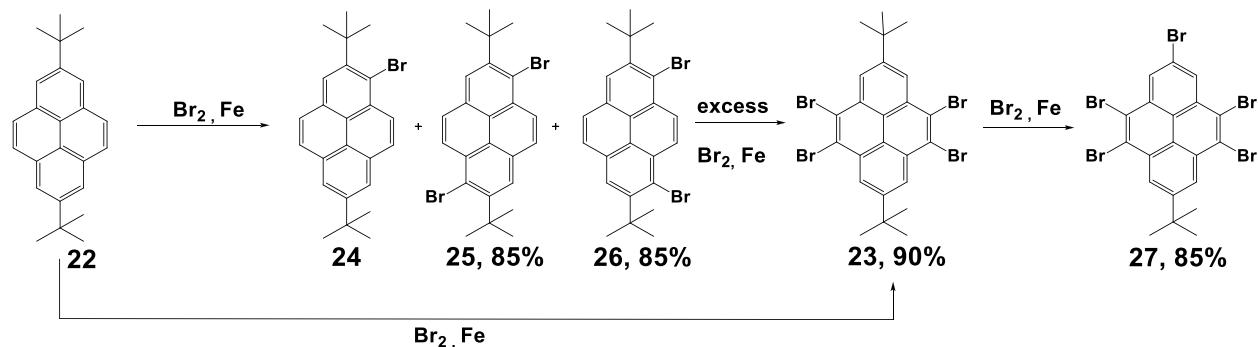
As indicated in scheme 6a, 4,5,9,10-tetrabromo pyrene (4) can be synthesized for the 4,5,9,10-tetrahydropyrene (3) by bromination in the presence of iron in DCM. [3] Another derivatives can be made by a direct tetrabromination of a 2,7-disubstituted t-butyl derivative of pyrene (22) with 6 mol-eq. of bromine and iron. The t-butyl groups are necessary to sterically inhibit some electrophilic substitutions at positions 1,3,6,8. Thus, the K-region becomes accessible by default for electrophilic substitutions by

bromine to give 4,5,9,10-tetrabromo-2,7-ditert-butylpyrene (23) (scheme 6b). However, this example is restricted to bulky substituents and not general enough.



Scheme 6: a) synthesis of 4,5,9,10 tetrabromopyrene (4) [3]; b) synthesis of 4,5,9,10-tetrabromo-2,7-ditert-butylpyrene (23) [14]

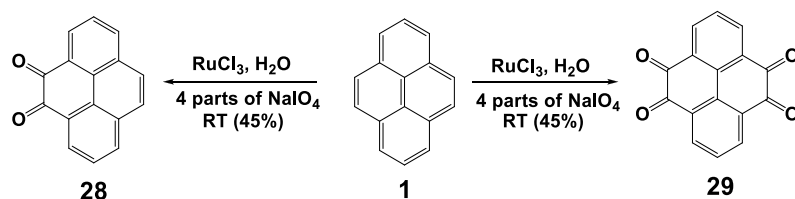
This reaction was analyzed in detail. If the positions 2,7 of pyrene is already substituted with t-butyl groups, the addition of 1.1 mol-equiv and 2.2 mol-equiv of bromine with iron powder provides 1-bromo- (24), and 1,6; 1,8-dibromosubstituted derivatives (25, 26) (scheme 7). With an excess of bromine (6.0 mol-equiv) a tetrabromo-2,7-ditert-butylpyrene is obtained (24), and further reaction prolongation provides the 2-tert-butyl-4,5,7,9,10-pentabromopyrene derivative (28). [1, 15]



Scheme 7: synthetic routes to mono-, di-, tetra- and pentabrominated pyrenes derivatives incorporating t-butyl groups. [1, 15]

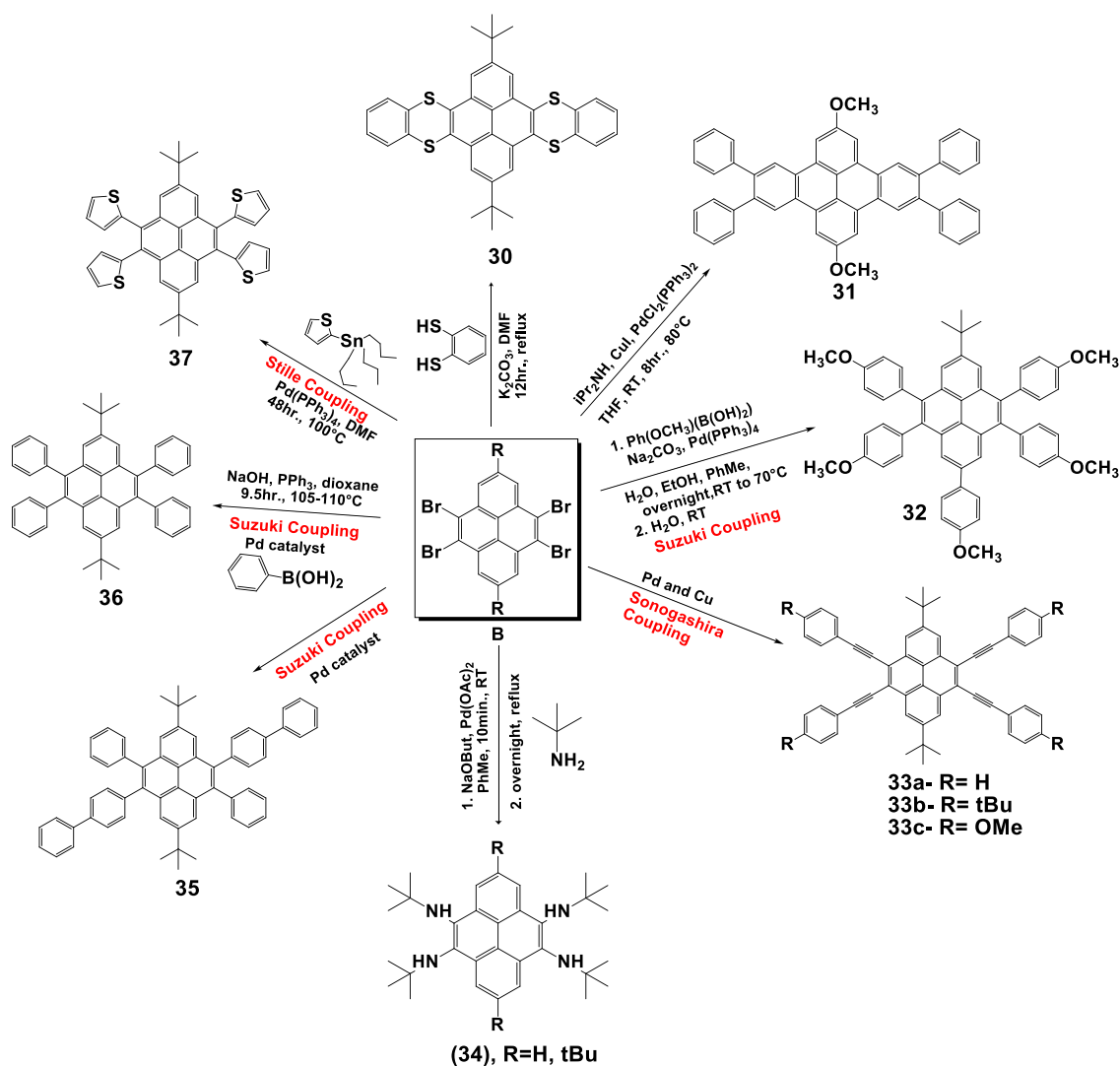
The third possible way to substitute pyrene at positions 4,5,9,10 is from a tetraone of pyrene (scheme 8). By condensation of tetraone, for instance with a diamine, it is possible to extend the pyrene conjugation. Several methods were tried before to directly oxidize pyrene for producing its 4,5,9,10-tetraone (29) or 4,5-dione (28). The dione was prepared by using osmium tetroxide, which is highly toxic. [5] To avoid a multistep pathway, ruthenium (III) chloride (RuCl_3), with sodium periodate (NaIO_4) in dichloromethane, water, and acetonitrile was used to selectively prepare the

4,5,9,10-tetraone (29) and the 4,5-dione (28) of pyrene, depending on temperature and the amount of oxidant used. However, the yields are modest. [16]



Scheme 8 : one-step synthesis of pyrene-4,5-dione (28) and pyrene-4,5,9,10-tetraone (29). [16]

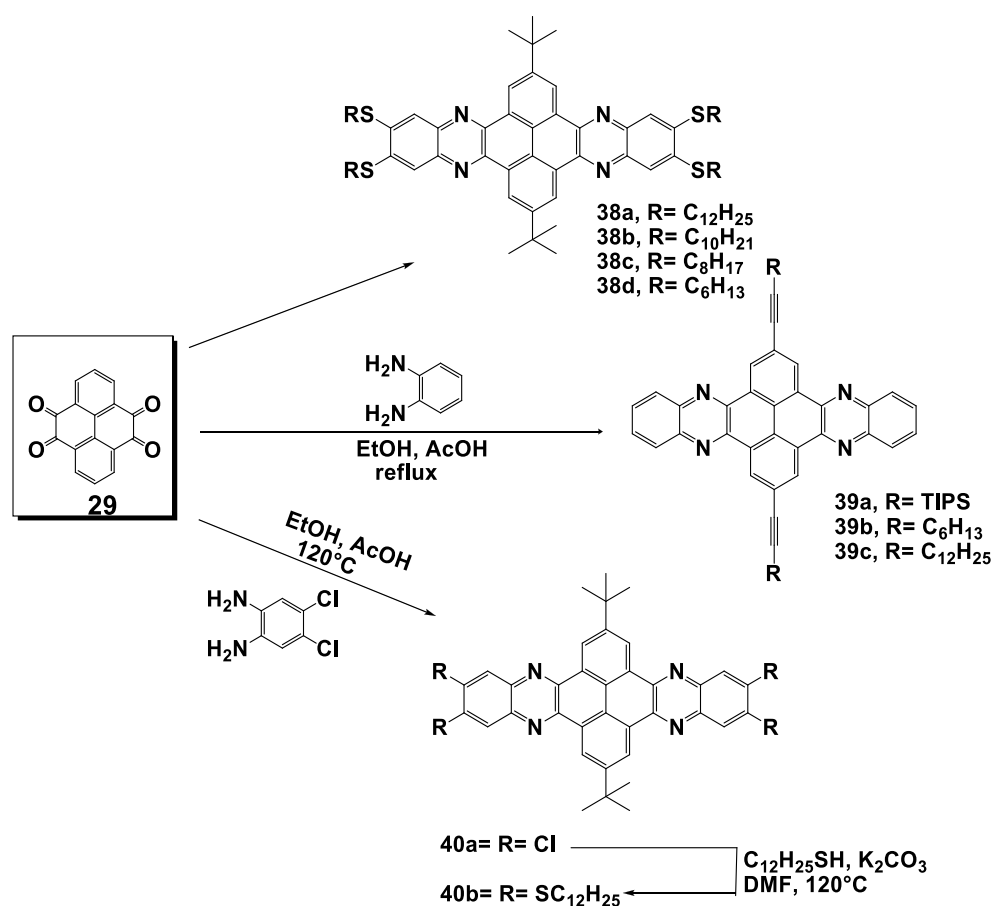
In Scheme 9, some derivatives of pyrene were synthesized via different methods such as Suzuki-Miyaura couplings (compounds 32, 33, 34), [15, 17-18] Sonogashira-Mirozoki couplings (compound 33a-c), using tert-butyl groups as positional protective groups. [19] Compounds 30 and 37 are examples of polysulfurated pyrene derivatives.



Scheme 9: pyrene derivatives from 4,5,9,10-tetrabromo pyrene and 2,4,5,9,10-pentabromo pyrene [15, 17-22]

Compound 37 was synthesized via Stille couplings, [20] whereas compound 30 was formed via some nucleophilic aromatic substitutions. [21] Compound 31 was patented in 2012. Apart from the heterofunctionalization with sulfur, pyrene is also substituted by a nitrogen atom such as in compound 35. [22]

A few examples of heteroaromatic pyrene derivatives from pyrene-4,5,9,10-tetraone (29) are given in scheme 10. They were used in some applications in molecular electronics, as *p*-type and *n*-type organic semiconductors. [11] Compounds 38a to 38d, 39a to 39c, and 40a were synthesized by condensation of compound 29 with a diamine (scheme 10). The simple route for the preparation of azaacenes is the cyclocondensation of the diketone and a diamine. Following this route, there are many pyrene-fused azaacenes prepared. The solution-processable pyrene-based organic semiconductor compound 40b was also synthesized. The molecular orientation and packing mode in the thin film were also studied by using various techniques. [26-27]



Scheme 10 : derivatization of the tetraone of pyrene (29) with ortho-diamino benzenic reagents.

The synthesis of tetraazahexacene compounds 39a to 39c was achieved by cyclo condensation with an *o*-phenylenediamine and pyrene 4,5,9,10-tetraone (29). These reactions were carried out in refluxing conditions with EtOH/AcOH and purified by filtration. The solubilities of these compounds depend on the type of substituents and size of the π -system. The TIPS substituted "hexacene" is more soluble than others, it may be due to this bulky group which inhibit π - π stacking by steric hindrance. [24-25]

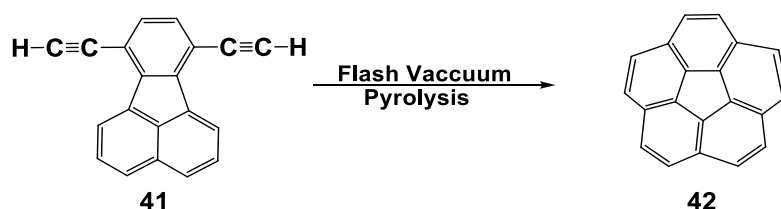
2.2.3 Functionalization of pyrene at positions 1,6; 1,8 and 2,7

Bromination of pyrene could give both 1,6 and 1,8-dibromopyrene. However, these are extremely difficult to separate, as their solubility is similar in many solvents. Many fractional crystallizations in toluene can succeed. Couplings reactions can be performed at these positions. [1-16] Substitutions at the position 2 and 7 is not possible via electrophilic substitutions, it needs an indirect route. To overcome these difficulties, two main approaches have been employed: (a) the reduction of pyrene to 4,5,9,10-tetrahydropyrene followed by electrophilic substitution and subsequent rearomatization and (b) the use of cine substitution via a 1,2-dehydropyrene intermediate to convert 1-bromopyrene to a mixture of 1- and 2-aminopyrene, separation of the amines, and conversion to the halide. However, these are multistep and low-yielding processes, which increase the difficulty in obtaining the 2,7-substituted pyrenes. Several indirect routes were thus developed such as a modified bromination developed by Harvey et al. and a one-step synthesis was reported to obtain pyrene-2,7-bis(boronate)ester in very good yields using an iridium-based catalyst. [28] In conclusion, functionalization at positions 2,7 of pyrene still remain a challenge. Reactivity at positions 1,6 and 1,8 is good but a mixture of regioisomers could be troublesome, due to moderate regioselectivity.

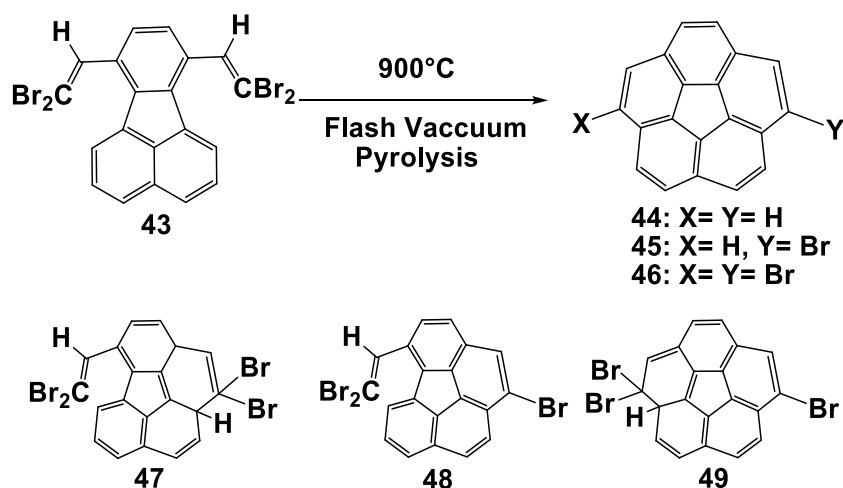
2.3 Ring-closure via benzylic-type couplings

In 1966 Barth and Lawton synthesized corannulene 9, [29] and later in 1991, the procedure was simplified by heating compound 41 at high temperature to cyclize it into

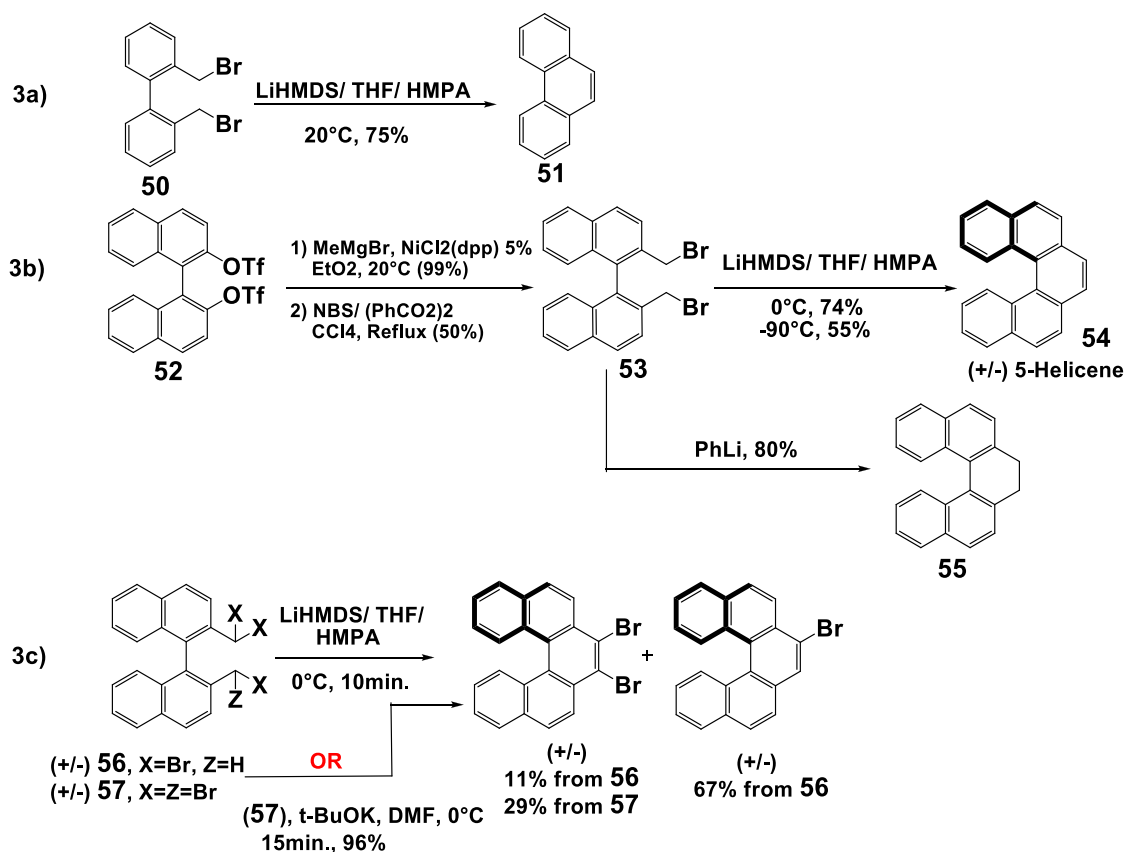
corannulene 42 (scheme 11). [30] In 1992, different substituted corannulenes were synthesized via a similar method (flash vacuum pyrolysis) by heating at 900°C (scheme 12). Compounds 44, 45, and 46 were purified by column chromatography. It is stated that “the initial formation of 46 can reasonably be explained by an electrocyclic ring closure of 43 to give the pentacyclic intermediate 49, which should spontaneously aromatize to 41 by loss of HBr. Repetition of these steps on the other side of the molecule would lead via 42 to 1,6-dibromocorannulene (46). An alternative mechanism involving cyclization reactions of vinyl radicals, generated by homolysis of C-Br bonds, can also be envisaged; however, no direct evidence is presently available on the mechanisms of these transformations. [31]



Scheme 11: synthesis of corannulene by flash vacuum pyrolysis. [29]



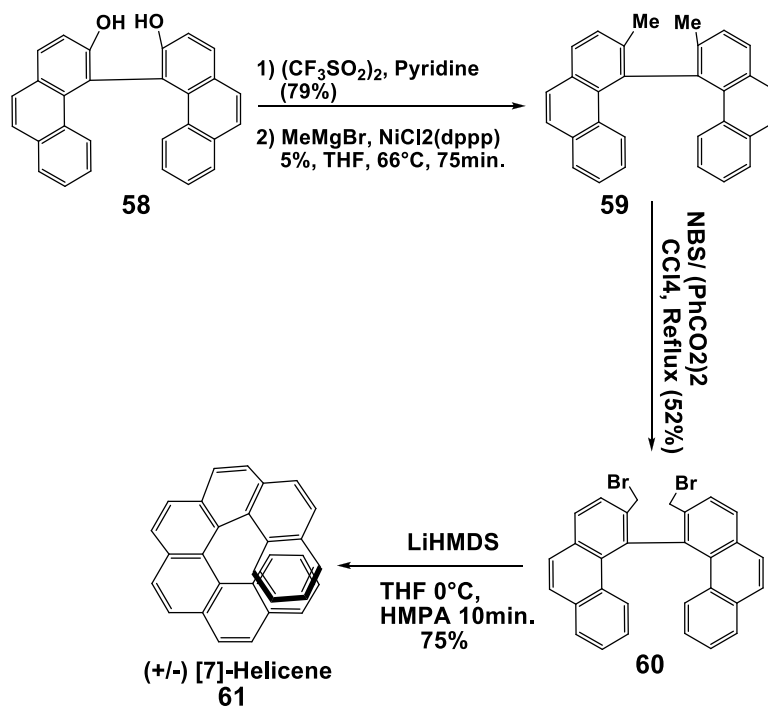
Scheme 12 : synthesis of substituted corannulenes (44-46) from 7,10-bis(2,2-dibromovinyl)-fluoranthene (43). [31]



Scheme 13 : a) synthesis of phenanthrene; b) synthesis of [5]-helicene and carbohelicenes (51) via benzylic-type couplings; [34-35] c) carbenoid couplings of propargyl bromide reported for cyclic enediynes. [35-36, 39]

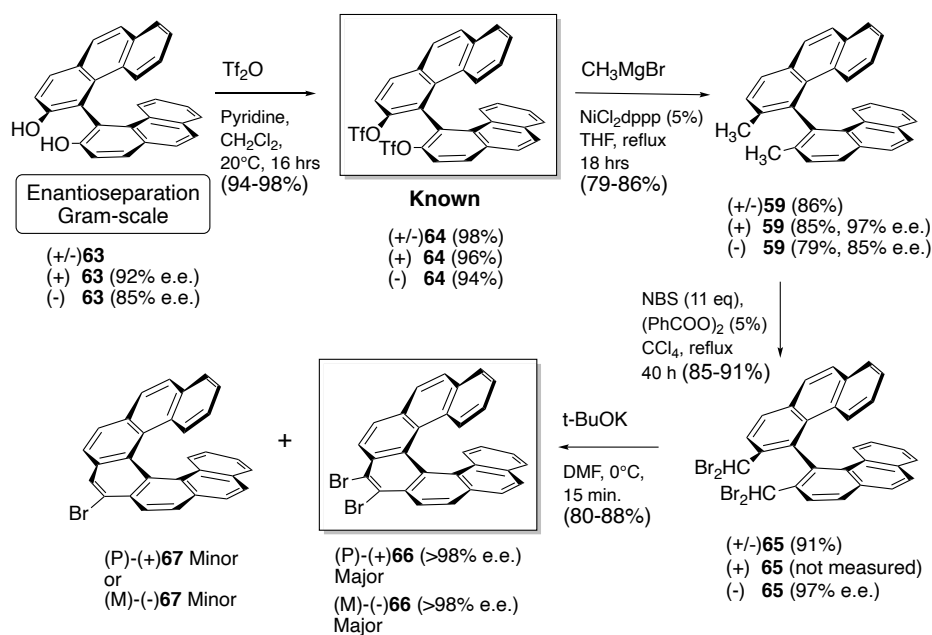
[7]helicene (57) was photosynthesized by Martin and coworkers in 1967 but a large-scale preparation is difficult due to high dilution conditions to prevent photodimerization of the alkenes as substrates. [32] Because it is easy to prepare some functionalized binaphthyl derivatives, it was thought that this family of compounds could serve as synthons, in the synthesis of helicenes via a benzylic-type coupling as a ring-closure method. In 1998, our group was inspired by the method of Jones for making propargyl couplings toward enediynes, with LiHMDS as a base. [33] A benzylic-type coupling was successfully tested with a bis(bromomethyl)-biphenyl (50) for making 75% of phenanthrene (51), starting from compound 53 in scheme 13a. Thus, a two-step synthesis of [5]helicene (54) from commercially available (52) via benzylic-type couplings of the corresponding benzylic bromide (53) is shown in scheme 13b. Also, a short synthetic route is presented to make partly saturated [5]helicene (55) in a 80% yield. [35] It was inspired from the formation of tetrabenzophenanthrene from the Kharasch's method (KNH₂ in liq. NH₃). [37] [7]helicene (61) was also prepared via similar method as shown in scheme 14, starting

from 3-phenanthrol and oxidative dimerization leading to compound 58 which is a racemic mixture (77% yield). Converting the bis-phenanthrol to the bis-triflate (79% yield) is achieved by the Snieckus' method with MeMgBr and NiCl₂(dppp) as a catalyst in THF to provide compound (59) in a 78% yield. Bromination with NBS was achieved from a Wohl-Ziegler dibromination to afford (60) in a 52% yield. [35-36]



Scheme 14 : synthesis of rac-[7]helicene (61) via benzylic-type couplings. [35]

Benzylic-type couplings were used to produce non-racemic helicenes (scheme 15). This is a short, efficient and scalable asymmetric route to functionalized [7]helicenes. Several bases and solvents were tried to optimize the formation of (+/-)-9,10-dibromo-[7]helicene from this benzylic coupling, as shown in scheme 15. The base LiHMDS is only useful in HMPA, and K₂CO₃ did not promoted the cyclization in DMF. *t*-BuOK in DMF was efficient and chosen after all tested bases. At -35°C the rate of cyclization is too slow, whereas it works better at 0-3°C. Solvents such as THF, dioxane or DCM were tried and did not provide good results with *t*-BuOK. A fast addition of *t*-BuOK to compound (65) produced the best results. A hypothetical mechanism is also reported in this work. This kind of easy and scalable synthesis for making enantiopure 9,10-dibromo-[7]helicene is rare in literature.

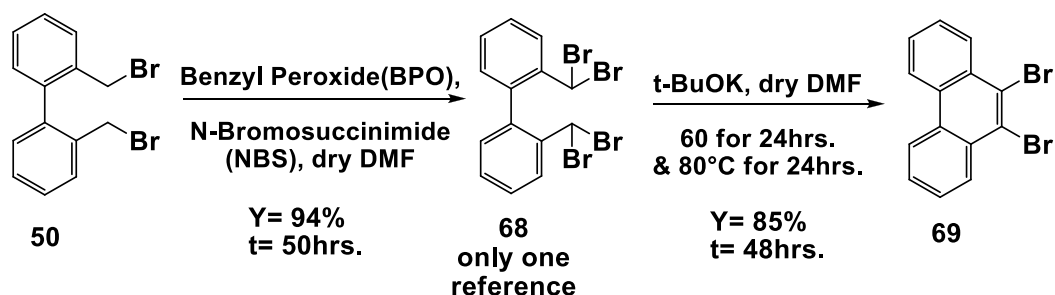


Scheme 15 : Non-racemic and racemic syntheses of brominated [7]helicenes via benzylic-type couplings. [39]

2.4 New routes to functionalized pyrenes in the K-region by benzylic-type ring-closing

2.4.1 Preliminary results and model studies on phenanthrene

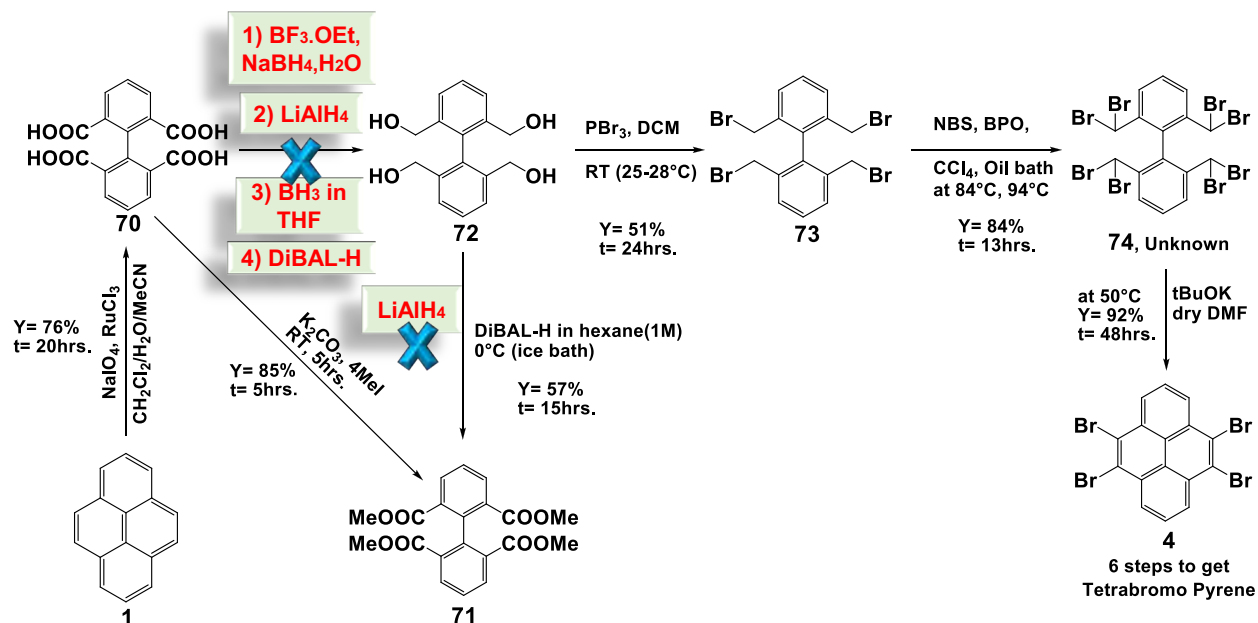
Preliminary reactions with 2,2'-bis(bromomethyl)-1,1'-biphenyl (**50**) were achieved prior to prepare 4,5,9,10-tetrabromo pyrene (scheme 16). Only one reference is known so far to prepare compound (**68**) from 2,2'-dimethyl-1,1'-biphenyl and not from compound (**50**) (2,2'-bis(bromomethyl)-1,1'-biphenyl). [40] A radical bromination with an excess of N-bromosuccinimide was achieved on (**50**) with a radical initiator (5 mol% of benzoyl peroxide) to provide 94% yield of (**68**). This method was used to brominate 2,2'-bis(bromomethyl)-1,1'-naphthalene to prepare pentahelicene in our laboratory in a 96% yield. [36] Furthermore, 2,2'-bis(dibromomethyl)-1,1'-biphenyl (**68**) was treated with a strong base such as potassium tert-butoxide (t-BuOK) to close the ring in DMF. As the benzylic dibromomethine function (ArCHBr₂) is more acidic than a bromomethylene one (ArCH₂Br), a weaker base than NaNH₂ or LiHMDS is thus effective. [36]



Scheme 16: model reaction on ring-closing on 2,2'-bis(bromomethyl)-1,1'-biphenyl (68) to 5,6-dibromophenanthrene (69).

2.4.2 Long route to 4,5,9,10-tetrabromo pyrene

As a first study to functionalize pyrene in the K-region at positions 4,5,9,10, we searched for new routes via 4,5,9,10-tetrabromo pyrene as shown in scheme 17. Each step is discussed below.

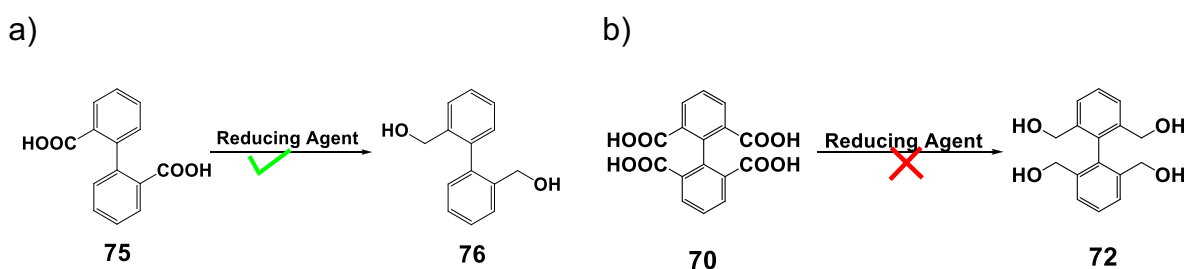


Scheme 17: synthesis of key intermediate 4,5,9,10-tetrabromo pyrene (4) in 6 steps.

We first investigated the Ru-oxidative cleavage of pyrene in the K-region. These central double bonds of pyrene are more reactive, and the Ru-catalyst selectively cleaves these bonds at positions 4,5, and 9,10 on pyrene. Ruthenium changes its oxidation state from +8 to +6, and sodium periodate (co-oxidant) regenerates the catalyst in a mixture of DCM/water/acetonitrile. The tetraacid (70) was separated from the tetraone (29, minor product) by refluxing the mixture twice in DCM and filtration, as the tetraone is more soluble in DCM than the tetraacid. When the reaction time was increased from 16 to 20 hours, the yield was increased from 50% to 76% (Experimental

Section chapter-2, Table 3). The tetraacid (70) was thus prepared in a 76% yield as a major product, whereas the tetraone (29) was formed as a minor product in a 8% yield. [16, 41-42]

We tried to reduce the tetraacid (70) to tetraalcohol (72), but all four reactions tried with different reagents failed. First, sodium borohydride with lewis acidic boron trifluoride etherate was used, and did not work. The reduction of 2,2-biphenyldimethanoic acid (75) afforded the diol (76) in a 90% yield, [43] but surprisingly we did not succeed with tetraacid (70). The second and third reagent was lithium aluminium hydride (LAH), which reduces many functional groups, and diisobutylaluminium hydride (DiBAL-H), but all conditions failed. [44-45] In addition to these three reagents, borane also did not work. [46] The reduction works on the 1,1'-biphenyl-2,2'-diacid (75) shown in scheme 18. [47]

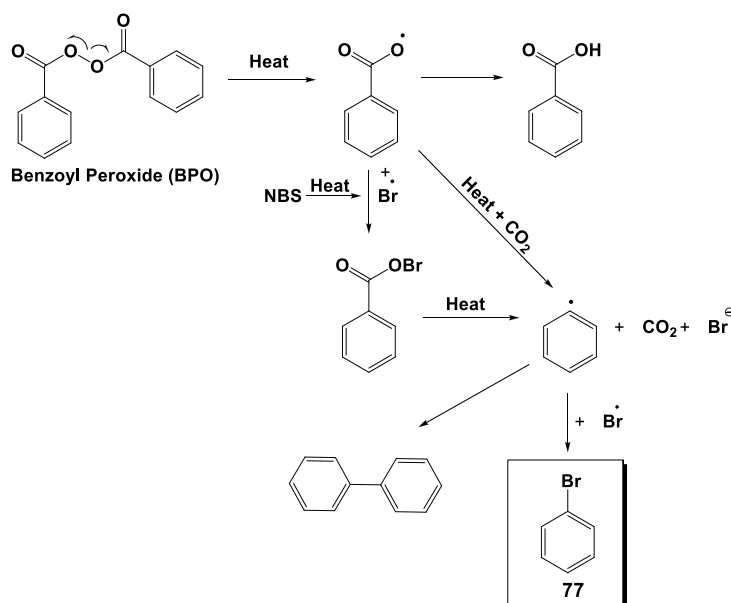


Scheme 18: a) reduction of 1,1'-biphenyl-2,2'-diacid (75) with borane; b) failure to reduce the tetraacid with diborane (70).

After several attempts had been made (Experimental Section, Table-19), we decided to change the route to the facilitated reduction of the tetraester (71). Esterification was achieved using iodomethane (10 mol-eq.) and potassium carbonate (3 mol-eq.) at 80°C. Three reactions were performed (Experimental Section, Table-4) and the yield was improved from 42% to 85%. [48-49] Finally, the tetraester ([1,1'-biphenyl]-2,2',6,6'-tetramethyl ester) (71) was successfully reduced to the tetraalcohol (2,2',6,6'-tetrakis(hydroxymethyl)-1,1'-biphenyl) (72) with DIBAL-H in hexane (1M) at ~0°C in an ice bath when stirred for 15 hours (Experimental Section, Table-5). The yield was low, 57%, in spite of adding DiBALH in excess over time. From thin layer chromatography, three spots were observed, which indicated some side-products. The tetraalcohol (72) may also have remained as a complex with aluminum. [33, 50] It is to be noted that LiAlH₄ did not work on the tetraester (Experimental Section, Table 20). The tetraalcohol (72) was treated with an excess of phosphorus tribromide in DCM at

room temperature for 24 hours to get the 2,2',6,6'-tetrakis(bromomethyl)-1,1'-biphenyl (73) in 51% yield. Six reactions were performed (Experimental Section, Table-6). The reaction worked better at room temperature (51% yield) compared to 50-55°C (15% yield). [51] One reaction was tried with triphenylphosphine dibromide, but the yield was poor (11% yield). [52]

2,2',6,6'-Tetrakis(dibromomethyl)-1,1'-biphenyl (74) was synthesized in good yield (>85%) by reacting the tetrabromide (73) with N-bromosuccinimide (NBS), and benzoyl peroxide (BPO) as a radical initiator in carbon tetrachloride for several days at 84-94°C. Several small additions of NBS and BPO were made until the starting material was fully consumed (Experimental Section, Table-7). In the crude, ¹H NMR indicated the presence of bromobenzene as NBS and BPO were added in important amount (scheme 19). Bromobenzene (B.P.=156°C) was removed under vacuum and slight heating. No other side product was observed by NMR and TLC. [36, 53] Compound (74) is unknown in the literature and the sc-X-ray structure determination is available in the next section (Fig. 5).



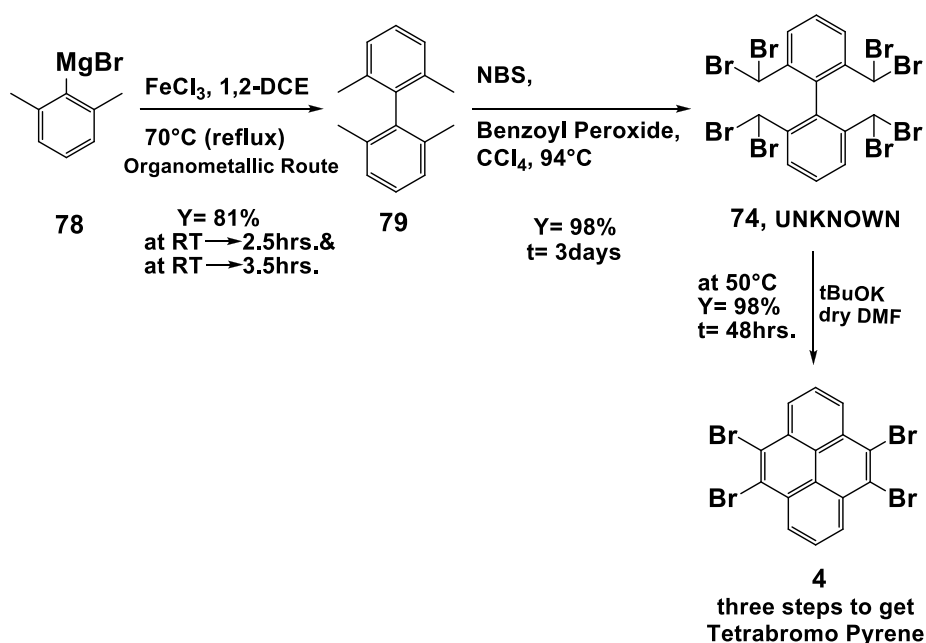
Scheme 19: hypothetical mechanism for the formation of bromobenzene from the NBS reaction with compound (74).

The key intermediate 4,5,9,10-tetrabromo pyrene (4) was finally prepared by two ring-closing reactions of the octabromide (74) on both sides by using potassium tert-butoxide (t-BuOK) as a base, as in the synthesis of model product (69). The reaction was optimized by running four reactions from room temperature to 80°C, and it was found that a temperature at 50°C for 24 hours gave the best results (Experimental Section, Table-8). [36] In conclusion, the synthesis of 4,5,9,10-

tetrabromo pyrene (4) was achieved in six steps, which is a large number of steps to be of practical utility.

2.4.3 Short and optimized route to 4,5,9,10-tetrabromopyrene

Having demonstrated that 4,5,9,10-tetrabromo pyrene could be formed in six steps, and after validation of the two ring-closing benzylic-type couplings to make a pyrene unit, we optimized the chemical sequence to this important synthon. At first, we tried to make and use 2,2',6,6'-tetramethyl-1,1'-biphenyl (79) and to make the octabromide (74) in one step, as we did previously in helicene chemistry.



Scheme 20: synthesis of key intermediate 4,5,9,10-tetrabromopyrene via a short route (3 steps).

2,2',6,6'-tetramethyl-1,1'-biphenyl (79) was synthesized via a known organometallic route by oxidative coupling of the commercially available (2,6-dimethylphenyl)magnesium bromide (78). The latter was treated with iron trichloride (FeCl_3) in 1,2-dichloroethane and the reaction conditions were optimized (scheme 20). The best results were (Experimental Section, Table-9) when the reaction mixture was stirred for 2.5 hours at room temperature and 3.5 hours at 70°C to provide 81% yield of (79). [53-56] Further, the octabromide (74) was synthesized in a 98% yield from (79) via radical bromination by similar conditions as before for making the model tetrabromide (68) (NBS and BPO) in carbon tetrachloride at 94°C . The NBS and BPO were added several times to complete the reaction, and it was monitored by ^1H NMR

and thin layer chromatography (Experimental Section, Table 10). [36, 53] This unusual octabromide was characterized by ^1H , ^{13}C NMR but all assays to obtain HRMS with various techniques of ionisation failed up to now. Fortunately, this compound could be nicely crystallized (figure 5) and the sc-XRD studies confirmed the chemical structure, as can be seen below in Figure 4.

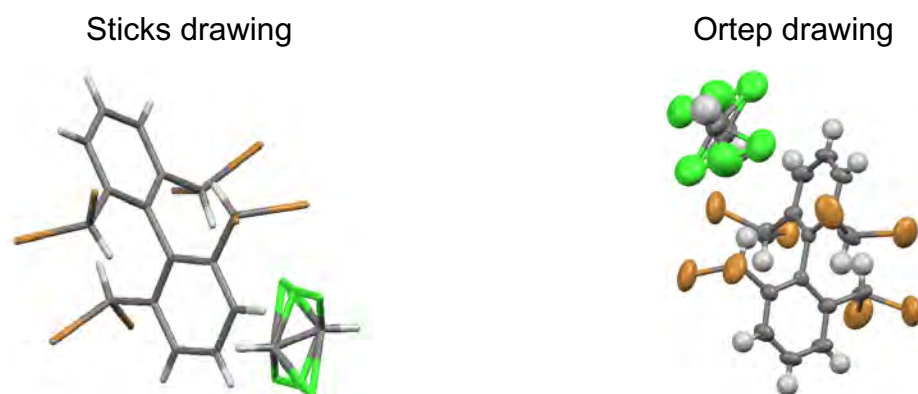


Figure 4: sc-XRD structure determination of 2,2',6,6'-tetrakis(dibromomethyl)-1,1'-biphenyl (**74**).

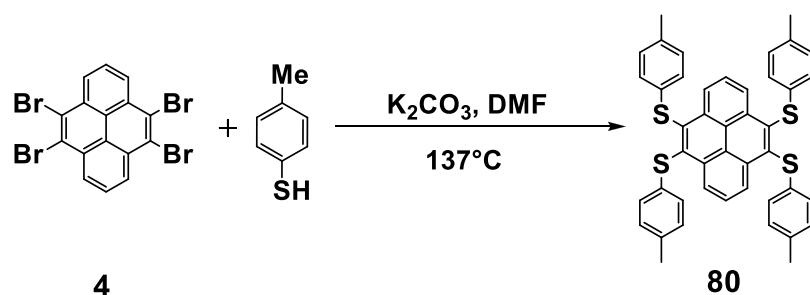


Figure 5: pictures of colorless crystals of 2,2',6,6'-tetrakis(dibromomethyl)-1,1'-biphenyl (**74**), formed after a slow evaporation in CDCl_3 .

Having in hands the octabromide 2,2',6,6'-tetrakis(dibromomethyl)-1,1'-biphenyl (**74**), two ring-closing reactions produces 4,5,9,10-tetrabromo pyrene (**4**) in a 92% yield, after optimisation of the conditions. As discussed in the long route synthesis of (**4**) in the previous section, a strong base such as *t*-BuOK in DMF produces (**4**) (Experimental Section, Table 11). This optimized synthetic sequence requires only 3 steps, whereas the longer route requires 6 steps. [36] As a consequence, this novel synthetic route to functionalized pyrene in the K-region is important. The 4,5,9,10-tetrabromo pyrene (**4**) synthon is now easily available in good yield and with optimized procedures, toward further derivatives of pyrenes at these 4,5,9,10 positions, but also at the non K-region.

2.5 Sulfurated pyrenyl derivatives from 4,5,9,10-tetrabromo pyrene

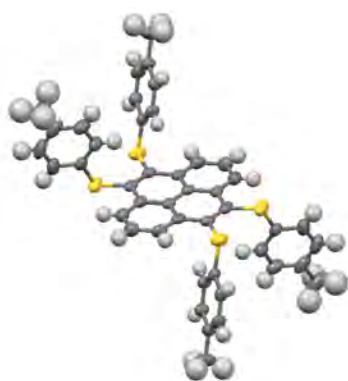
The sulfuration of 4,5,9,10-tetrabromo pyrene (**4**) is the first step to study the production of a new family of pyrene derivatives in the K-region. Thus, 4,5,9,10-tetrakis(4-methyl-phenylthio) pyrene (**80**) was synthesized by four nucleophilic aromatic substitutions of the bromine atoms on a 90 mg scale from 4,5,9,10-tetrabromo pyrene (**4**) and 4 mol-eq. of 4-methylbenzenethiol with dry potassium carbonate as a base in DMF at 137°C (5 days) to provide a 99% yield of the expected product (**80**), as shown in scheme 21. No reference in the literature is found for (**80**). The characterization of (**80**) was achieved by ^1H , ^{13}C NMR, HRMS and sc-XRD studies determined the structure (figure 6) from the crystalline needles in Figure 7.



Scheme 21: synthesis of 4,5,9,10-tetrakis (4-methyl-phenylthio) pyrene (**80**) from 4,5,9,10-tetrabromo pyrene (**4**).

No reference is found for compounds **81** and **82**. Two reactions were performed on tetrabromo pyrene (**4**) with 4-methoxybenzenethiol at high temperature (100°C) and at moderate temperature (65°C, scheme 22). At 65°C, the main product is 4,5,9,10-

a) Balls & sticks drawing



b) Sticks drawing



Figure 6 : sc-XRD structure determination of 4,5,9,10-tetrakis(4-methyl-phenylthio)pyrene (**80**); a) Ortep drawing; b) sticks drawing.

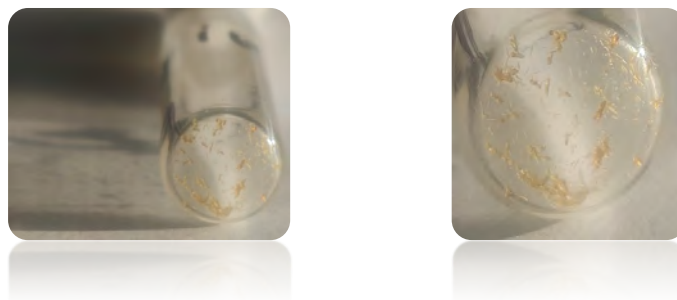
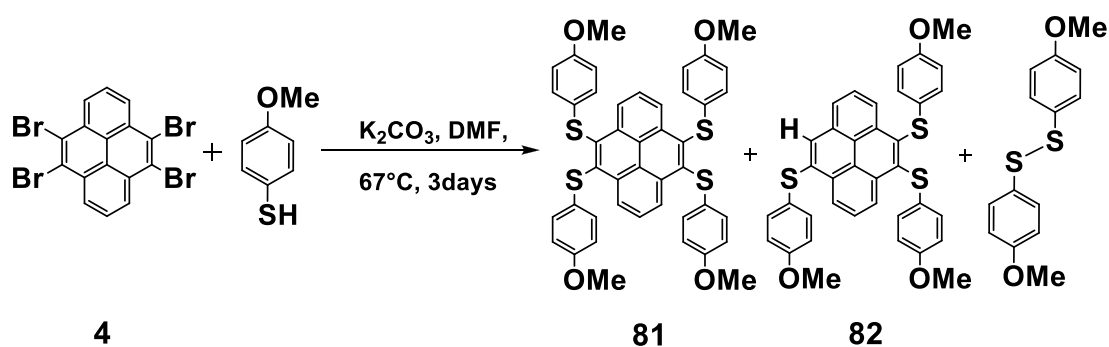


Figure 7: pictures of crystalline needles of 4,5,9,10-tetrakis(4-methyl-phenylthio)pyrene (80) in a test tube, obtained after a slow evaporation of toluene.

tetrakis(*p*-methoxy-phenylthio)pyrene (81) in a 60% yield, and a minor component 4,5,9-tris(*p*-methoxy-phenylthio)pyrene (82) as a by-product in a >60% yield, when using 5 mol.-eq. of 4-methoxybenzenethiol. Both compounds were separated and purified by column chromatography (tol/cyclohex, 80/20 v/v). At high temperature (100°C for 2 days), (81) was recovered from a column in trace amount.

From these results, some electron transfer reactions probably competes with the S_NAr reactions, as evidenced by the formation of (82). This electron transfer could come from the electron-rich *p*-methoxy-phenylthiolate anion. This electron transfer probably generates a radical anion of a pyrene derivative. The latter releases a neutral radical and an anion. Then, the pyrenyl radical abstracts a hydrogen atom in the medium to produce (82). Overall, a hydrogenative debromination occurs. One should note different reactivity with *p*-methylbenzenethiol (99 % yield of product), even at 137°C.



Scheme 22: synthesis of 4,5,9,10-tetrakis(*p*-methoxy-phenylthio)pyrene (81) and 4,5,9-tris(*p*-methoxy-phenylthio)pyrene (82) from 4,5,9,10-tetrabromo pyrene (4).

Crystalline 4,5,9,10-tetrakis(*p*-methoxy-phenylthio)pyrene (81) was formed after a slow evaporation of toluene (see bright yellow crystals in figure 8).

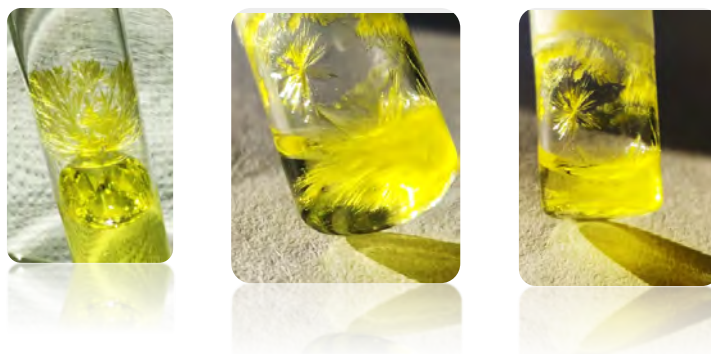
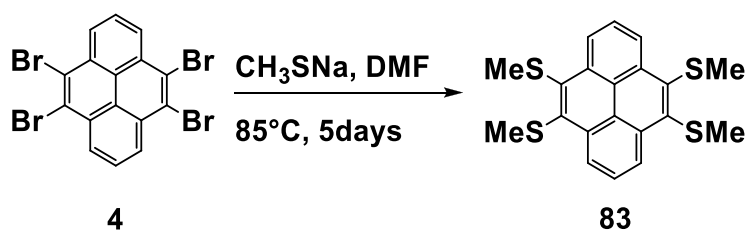


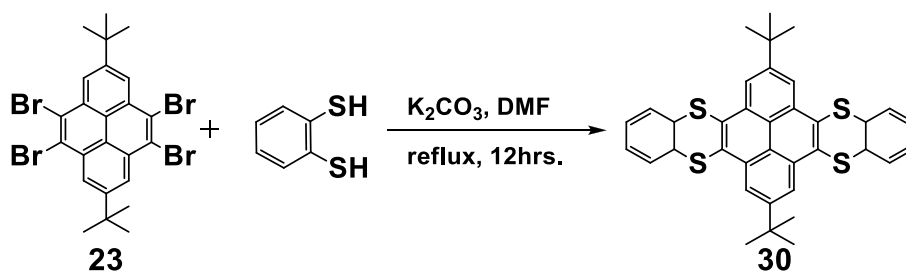
Figure 8: yellow crystalline needles of 4,5,9,10-tetrakis(*p*-methoxy-phenylthio)pyrene (81) in a test tube, after a slow evaporation of toluene.

After investigating the reactions of thiophenol derivatives with 4,5,9,10-tetrabromo pyrene (4) in the presence of dry potassium carbonate in DMF, it was necessary to test thioalkylations, and as a basic reference in photophysical studies. Thus, 4,5,9,10-tetrakis(methylthio)pyrene (83) was synthesized from an excess of commercial sodium methanethiolate and 4,5,9,10-tetrabromo pyrene (4) in DMF under an inert atmosphere of argon. Compound (83) was isolated from a column chromatography (tol/cyclohex, 50/50, v/v) and characterized by ^1H , ^{13}C NMR (HRMS in progress).



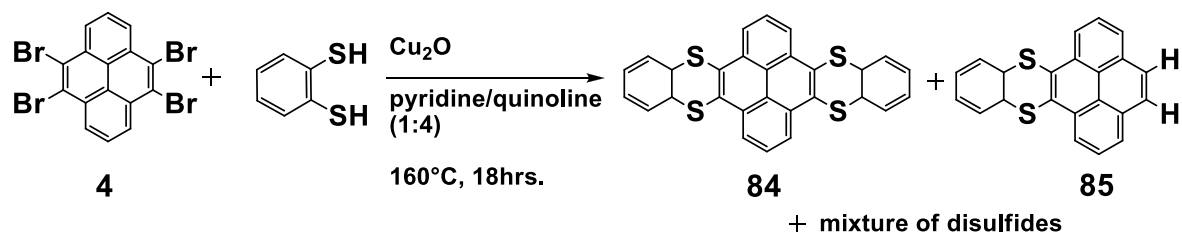
Scheme 23: synthesis of 4,5,9,10-tetrakis(methylthio)pyrene (83) from 4,5,9,10-tetrabromo pyrene (4).

Functionalization of 4,5,9,10-tetrabromo pyrene (4) was sought with 1,2-benzenedithiol (2 mol-eq.). Prior to run this reaction, a literature search indicated one reference known in 2020 for a similar expected product, as shown in scheme 24. In this work, two fused central thianthrene units are embedded in a pyrene structure incorporating *t*-butyl substituents at positions 2 and 7 (compound 30). This type of structure corresponds to a kind of thianthrene ribbon. By reacting it with $\text{NO}[\text{Al}(\text{ORF})_4]$ ($\text{ORF} = \text{OC}(\text{CF}_3)_3$), it resulted in a radical cation salt and diradical dication salt. Both were recrystallized and sc-XRD studies were achieved. [61]



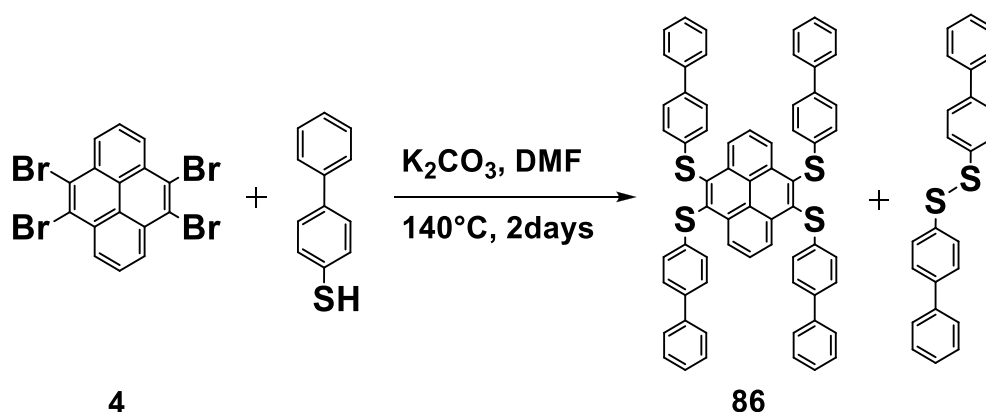
Scheme 24: synthesis of compound 30 known in the literature. [61]

A reaction was run with 4,5,9,10-tetrabromo pyrene (4) and 1,2-benzenedithiol (2 mol-eq.) by using potassium carbonate in DMF and refluxing the mixture for several hours. Another reaction was tested in our laboratory (scheme 25) with 1,2-benzenedithiol, 4,5,9,10-tetrabromo pyrene, copper oxide in pyridine and quinoline (1:4 v/v) at 160°C for 18 hours. The crude was purified by column chromatography. However, the results of this reaction are still under investigation.

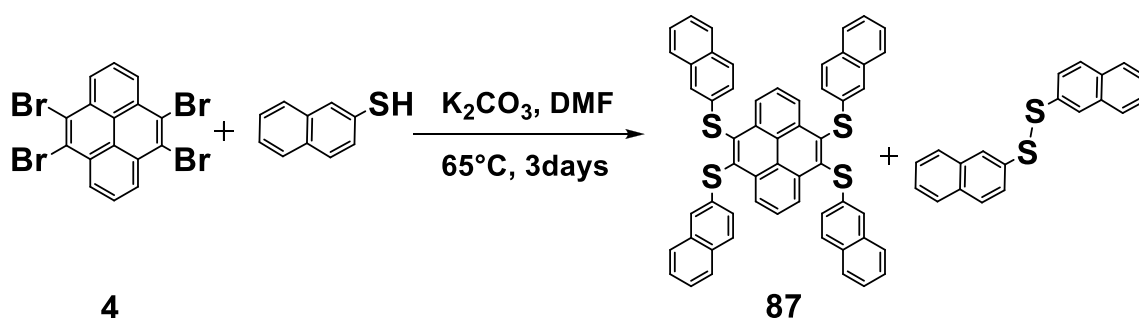


Scheme 25: attempted synthesis of compound 84 using copper oxide in pyridine and quinoline (1:4 v/v) at 160°C.

An attempt was made to synthesize π -extended tetrasulfurated pyrene derivatives in the K-region by reacting 4-biphenylthiol (4.4 mol.-eq.) and 4,5,9,10-tetrabromo pyrene (4) at 140°C for 2 days in order to get compound 29. The yellow crude was triturated with water/acetone (2/1 v/v) and filtered to afford a bright yellow solid, insoluble in CDCl_3 . The compound is being analyzed and characterized.



Scheme 26: synthesis of 4,5,9,10-tetra(4-biphenylthio) pyrene (86) from 4,5,9,10-tetrabromo pyrene (4) (in progress).

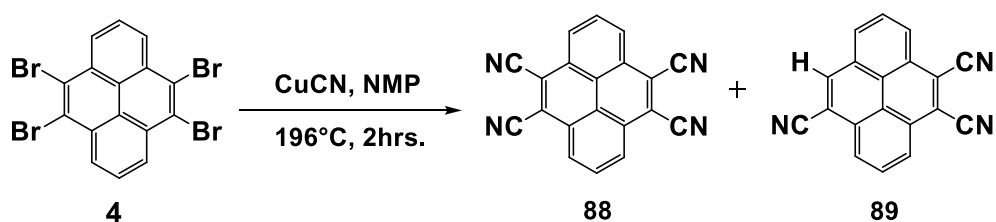


Scheme 27: attempted synthesis of 4,5,9,10-tetrakis(2-naphthylthio) pyrene (87) from 4,5,9,10-tetrabromopyrene (4) (in progress).

Compound 87 is unknown and we tried to recrystallize it in ortho-dichlorobenzene. Due to its insolubility in $CDCl_3$ it was not possible to record 1H or ^{13}C NMR in $CDCl_3$. Before concluding, more data will be required (in progress).

2.6 Cyanated pyrenyl derivatives from 4,5,9,10-tetrabromopyrene

We tried to derivatize compound (4) by using $CuCN$ for making the tetracyanide compound (88) as shown in scheme 28. Only three references are present in literature so far, out of which one is a patent. [3, 57]. However, no characterization data are found in the literature. In addition, compound 89 is not published. This reaction is an example of Rosenmund–von Braun synthesis where an aryl halide (4) reacts with cuprous cyanide to provide a cyanated arene (88). [58]



Scheme 28: synthesis of 4,5,9,10-tetracyanopyrene (88) and 4,5,9-tricyanopyrene (89) from 4,5,9,10-tetrabromopyrene.

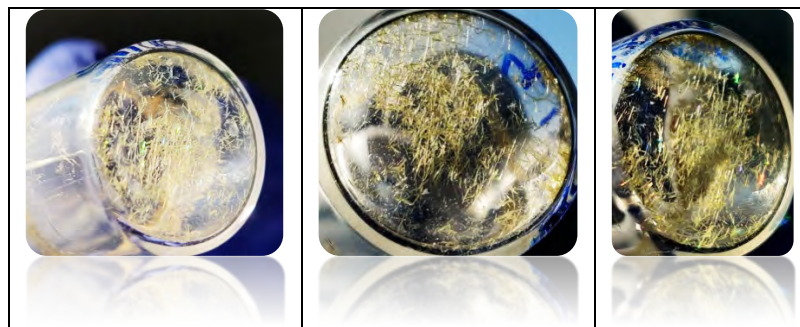
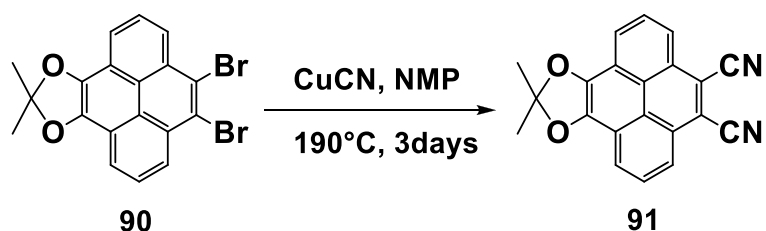


Figure 9 : Needle-shaped crystals of compound 88 (4,5,9,10-tetracyanopyrene) in DCM.



Scheme 29 : example of cyanation in the K-region of pyrene. [4]

As shown in scheme 29, we found an example related to the functionalization of the K-region of pyrene by two cyano groups, by using the Sandmeyer reaction. [59] The pyrene derivative 9,10-dihydroxyacetoneid-pyrene-4,5-dicarbonitrile (91) was synthesized from 9,10-dibromopyrene-4,5-diolacetonide (90) using copper (I) cyanide in NMP (N-methylpyrrolidone).

2.7 Photophysical studies on pyrenes sulfurated in the K-region.

The photophysical characterization of 4,5,9,10-tetra(4-methylphenylthio) pyrene (80) (**PyB**) was achieved by the group of Pr. Paola Ceroni from the chemistry department of the University of Bologna. Other asterisks are being analyzed.

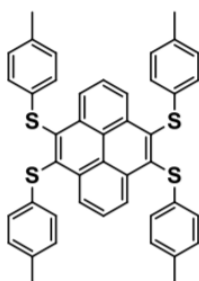


Figure 10: structure of 4,5,9,10-tetra(4-methylphenylthio) pyrene (**PyB**) (80).

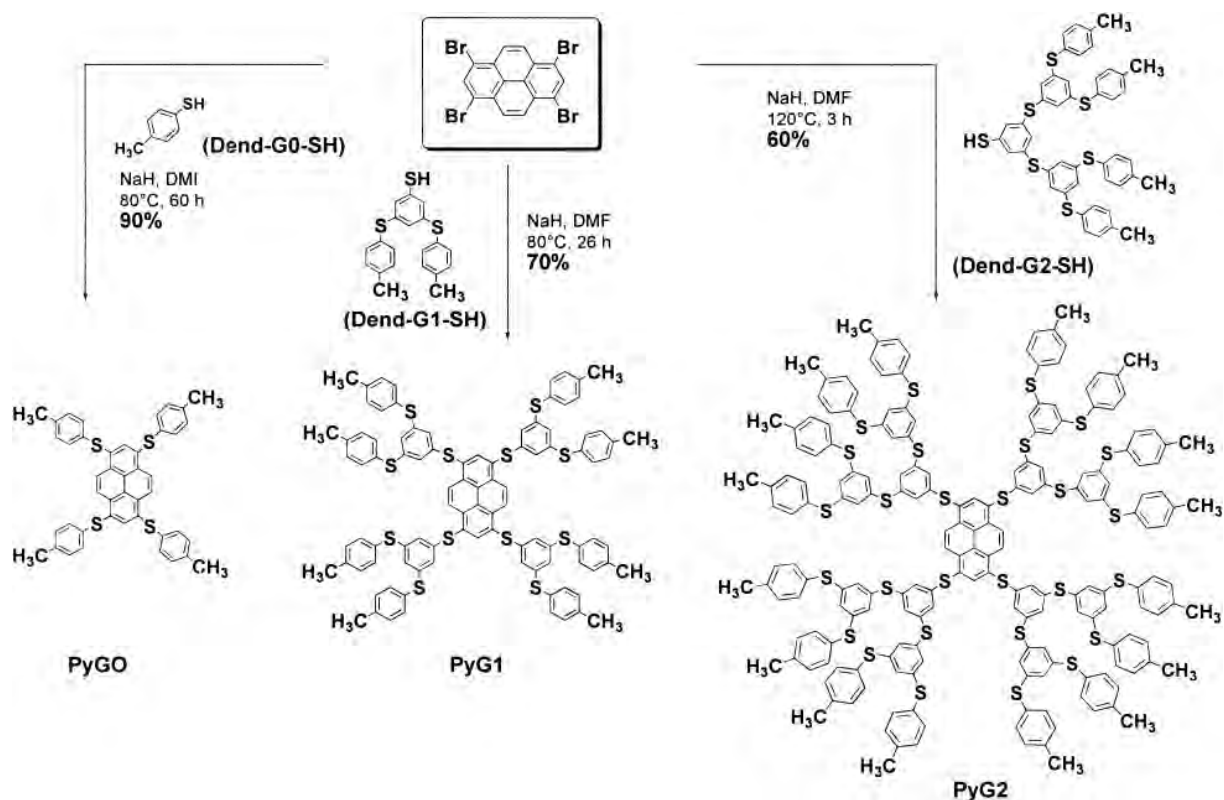


Figure 11 : synthesis of polysulfurated pyrene dendrimers used for comparison with 4,5,9,10-tetra(4-methylphenylthio) pyrene (**PyB**) (80) for a photophysical characterization in DCM.

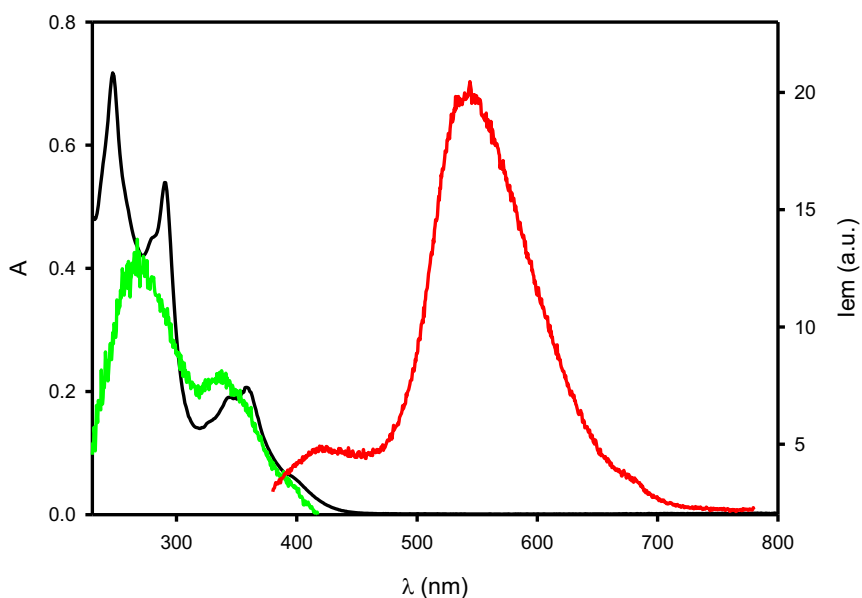


Figure 12: absorption (black line), fluorescence (red line) and excitation spectra (green line) of **PyB** in DCM. λ_{exc} = 340 nm for excitation spectrum and λ_{em} = 540 nm for emission spectrum.

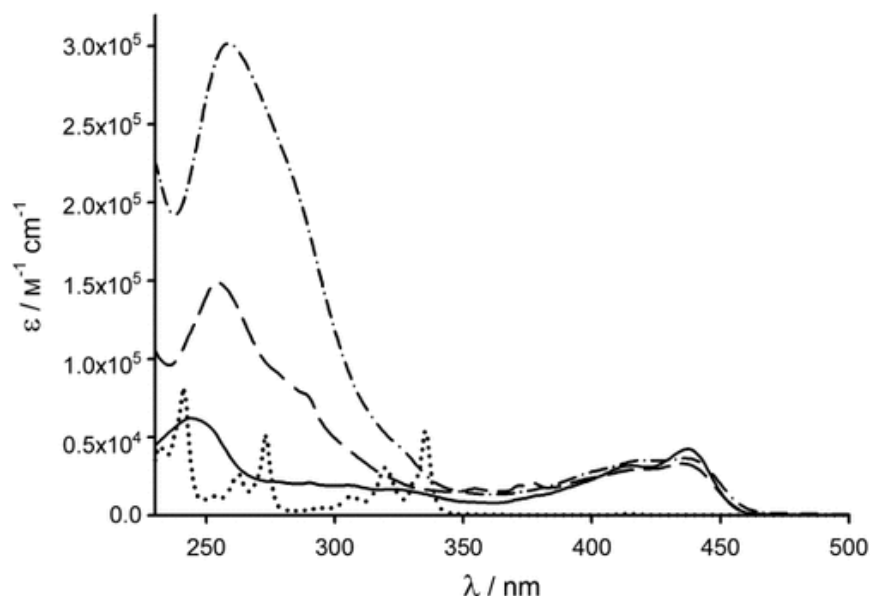


Figure 13 : absorption spectra of PyG0 (solid line), PyG1 (dashed line), and PyG2 (dashed-dotted line) in DCM solution at 293 K. For comparison purposes the spectrum of pyrene (dotted line) is also shown.

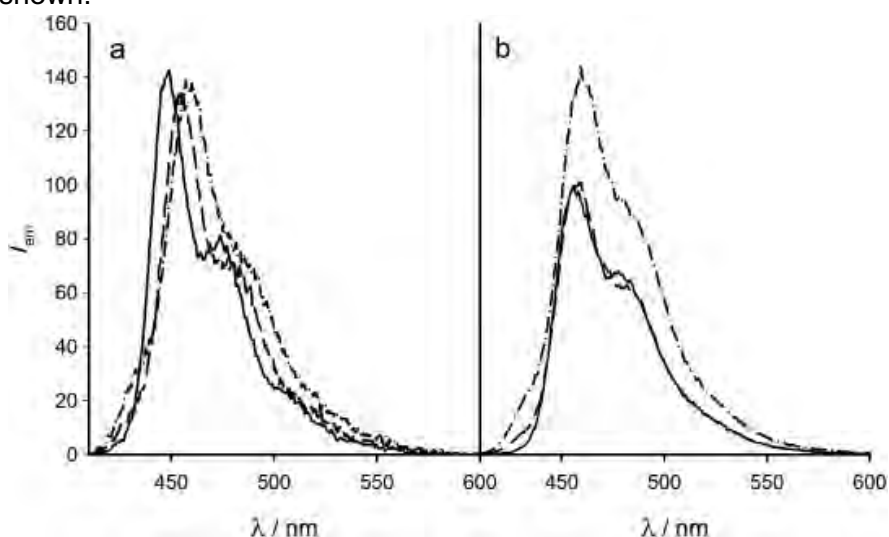


Figure 14 : Emission spectra in cyclohexane (a) and in DCM (b) solution at 293 K of **PyG0** (solid line), **PyG1** (dashed line), and **PyG2** (dashed-dotted line). $\lambda_{ex} = 390$ nm.

The absorption spectrum of **PyB** is significantly different, compared to the **PyGx** series, the band at lower energy is blueshifted, to a value similar to the pristine pyrene. The emission of **PyB** in solution (DCM) is also different from the **PyGx** series and pyrene, the emission is redshifted with a maximum at 540 nm, the lifetime is longer (8.6 ns), but the emission quantum yield of **PyB** is **very significantly lower** at 0.1%, compared to 30-60% for **PyGx**, for the other pyrene derivatives. The emission in the

solid state is almost absent for **PyB** and no emission in solid was recorded for the **PyGx** series.

Compounds	$\lambda_{\max \text{ abs}}$ (nm)	$\lambda_{\max \text{ em}}$ (nm)	Φ_{em} (%)	τ (ns)
Pyrene	335	375	61	277
PyG0	435	457	33	1.4
PyG1	435	457	35	1.6
PyG2	435	460	55	2.4
PyB	360	540	0.1	8.6

Table 1 : photophysical properties of the investigated compounds **PyB**, **PyG0**, **PyG1**, **PyG2**.

2.8 Conclusion

4,5,9,10-Tetrabromopyrene (**4**) was synthesized via a synthetic route in 6 steps. A novel key intermediate 2,2',6,6'-tetrakis(dibromomethyl)-1,1'-biphenyl (**74**) was generated for applying the benzylic-type couplings (two ring-closing reactions) toward 4,5,9,10-tetrabromopyrene (**4**) in an excellent yield. The synthetic sequence was then shorten to a 3-step synthesis. The octabromide intermediate (**74**) was unambiguously characterized by a sc-XRD structure determination. The sulfuration and cyanation of 4,5,9,10-tetrabromopyrene (**4**) were achieved by S_NAr and by using the Rosenmund–von Braun reaction. Thus, 4,5,9,10-tetra(4-methylphenylthio) pyrene (**80**) and 4,5,9,10-tetra(4-methoxyphenylthio) pyrene (**81**) were synthesized from 4,5,9,10-tetrabromopyrene (**4**) by simple nucleophilic aromatic substitutions in 99% yield for (**80**), and > 60% yield for (**81**). In the last case, a side-product results from a radical reaction. A sc-XRD structure determination was provided for (**80**). A methylthiolation of pyrene in the K-region (compound **83**) was also effective with MeSNa. The Rosenmund–von Braun reaction furnished a tetracyanated pyrene (**88**) and a tricyanated pyrene (**89**). Other sulfurations were tried with 4-biphenylthiol, 1,2-benzenedithiol, 2-naphthylthiol and the analyses are in progress.

Preliminary photophysical studies on **PyB** (**80**) were achieved. The absorption and emission spectra were compared to the polysulfurated pyrene dendrimers functionalized at positions 1,3,6,8 (non K-region). The emission for **PyB** was redshifted to 540nm as compared to the other dendrimers (435nm) but the emission quantum yield is low (0.1%). Thus, sulfuration in the K-region provides pyrenyl sulfides with poor

luminescence, compared to pyrenyl sulfides from the non K-region (at positions 1,3,6,8).

References for Chapter-2

1. X. Feng, J. Y. Hu, C. Redshaw, T. Yamato, *Chem. Eur. J.* **2016**, *22*, 1-20.
2. W. Sotoyama, H. Sato, M. Kinoshita, T. Takahashi, SID 03 Dig. **2003**, 1294.
3. Z. H. Wu, Z. T. Huang, R. X. Guo, C. L. Sun, L. C. Chen, B. Sun, Z. F. Shi, X. Shao, H. Li, H. L. Zhang, *Angew. Chem. Int. Ed.*, **2017**, *56*, 13031-13035.
4. a) M. J. J. Dewar, R. D. Dennington II, *J. Am. Chem. Soc.*, **1989**, *111*, 3804-3808;
b) H. Cerfontain, K. Laali, H. J. A. Lambrechts, *Recl. Trav. Chim. Pays-Bas*, **1983**, *102*, 210-214.
5. H. Vollmann, M. Becker, M. Correl, H. Streeck, J. Liebigs, *Ann. Chem.*, **1937**, *531*, 1-159.
6. J.-Y. Hu, A. Paudel, T. Yamato, *J. Chem. Res.*, **2008**, 308-311.
7. A. Fermi, P. Ceroni, M. Roy, M. Gingras, G. Bergamini, *Chem. Eur. J.* **2014**, *20*, 1-9.
8. G. Heywang, F. Jonas, *Eur. Pat. Appl.*, **1989**, no. EP0339419A3.
9. M. Gingras, V. Placide, J. M. Raimundo, G. Bergamini, P. Ceroni, V. Balzani, *Chem. Eur. J.*, **2008**, *14*, 10357-10363.
10. W. Sotoyama, Sato, M. Kinoshita, T. Takahashi, SID 03 Dig., **2003**, 1294.
11. T. M. F.-Duarte, K. Müllen, *Chem. Rev.* **2011**, *111*, 7260–7314
12. A. Hayer, de V. Halleux, A. Kohler, A. El-Garouhy, E. W. Meijer, J. Barbera, J. Tant, J. Levin, M. Lehmann, J. Gierschner, J. Cornil, Y. H. Geerts, *J. Phys. Chem. B*, **2006**, *110*, 7653.
13. M. Villa, M. Roy, G. Bergamini, P. Ceroni, M. Gingras, *Chem. Plus. Chem.*, **2020**, *85*, 1481–1486.
14. T. Yamato, M. Fujimoto, A. Miyazawa, K. Matsuo, *J. Chem. Soc. Perkin Trans.* **1997**, *1*, 1201-1207.
15. J.-Y. Hu, X.-L. Ni, X. Feng, M. Era, M. R. J. Elsegood, S. J. Teatd, T. Yamato, *Org. Biomol. Chem.*, **2012**, *10*, 2255-2262.
16. J. Hu, D. Zhang, F. W. Harris, *J. Org. Chem.* **2005**, *70*, 707-708.
17. J. B. Shaik, V Ramkumar, B. Varghese, S. Sankararaman, *Beilstein J. Org. Chem.*, **2013**, *9*, 698–704

18. Patent: Organic electroluminescent device having host-guest light-emitting layer composed of highly oriented planar molecules and its manufacturing method, By Yonekuta, Yasunori et al, PCT Int. Appl., 2012141273, 18 Oct **2012**
19. J. Y. Hu, M. Era, M. R. J Elsegood, T. Yamato, *Eur. J. Org. Chem.*, **2010**, 72-79.
20. Z. Duan, D. Hoshino, Z. Yang, H. Yano, H. Ueki, Y. Liu, H. Ohuchi, Y. Takayanagi, G. Zhao, Y. Nishioka, *Mol. Cryst. Liq. Cryst.*, **2011**, 538, 199-207.
21. S. Tang, L. Zhang, H. Ruan, Y. Zhao, and X. Wang, *J. Am. Chem. Soc.*, **2020**, *142*, 7340-7344.
22. Tetracene derivative field effect transistor material and its preparation, By Tian, Bo et al, patent from Faming Zhuanli Shenqing, 102659752, 12 Sep **2012**
23. S. Gonell, N. Poyatos, E. Peris, *Chem. Eur. J.* **2014**, *20*, 9716-9724.
24. Doctoral thesis. Design, synthesis and properties of pyrene-fused azaacenes and their applications in organic electronics <https://www.researchgate.net/publication/279845879>.
25. M. S. Bhosale R, S. Choudhary, A. Mateo-Alonso, *Org. Lett.*, **2012**, *14*, 4170-4173.
26. B. R. Kaafarani, L. A. Lucas, B. Wex, G. E. Jabbour, *Tetrahedron Lett.*, **2007**, *48*, 5995-5998.
27. L. A. Lucas, D. M. DeLongchamp, L. J. Richter, R. J. Kline, D. A. Fischer, B. R. Kaafarani, G. E. Jabbour, *Chem. Mat.*, **2008**, *20*, 5743-5749.
28. D. N. Coventry, A. S. Batsanov, A. E. Goeta, J. A. K Howard, T. B. Marder, R. N. Perutz, *Chem. Commun.*, **2005**, 2172-2174.
29. a) W. E. Barth, Ph.D. Thesis, University of Michigan, 1966; b) W. E Barth: R. G. Lawton, *J. Am. Chem. Soc.* **1966**, *88*, 380-381; c) W. E. Barth; R. G. Lawton, *J. Am. Chem. Soc.* **1971**, *93*, 1730-1745.
30. L. T. Scott, M. M. Hashemi, D. T. Meyer, and H. B. Warren, *J. Am. Chem. Soc.*, **1991**, *113*, 7082-7084.
31. L. T. Scott, M. M. Hashemi, and M. S. Bratcher, *J. Am. Chem. Soc.*, **1992**, *114*, 1921-1923.
32. a) R. Weitzentik, A. M. Klingler, **1918**, *39*, 315-323; b) J. W. Cook, *J. Chem. Soc.* **1933**, 1592-1597.
33. R. S Huber, G. B. Jones, *Tetrahedron*, **1994**, *35*, 2655-2658.
34. F. Dubois, M. Gingras, *Tetrahedron Lett.*, **1998**, *39*, 5039-504
35. M. Gingras, F. Dubois, *Tetrahedron Lett.*, **1999**, *40*, 1309-1312

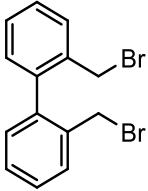
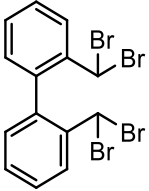
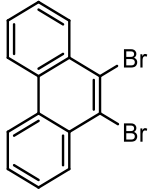
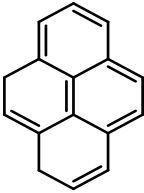
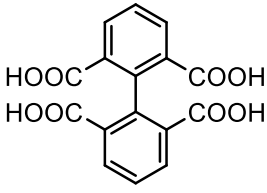
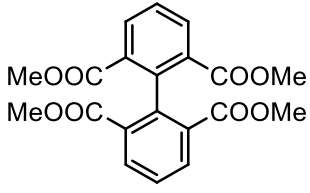
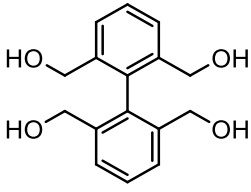
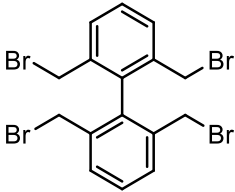
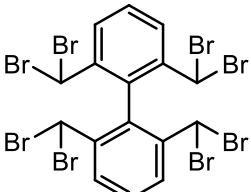
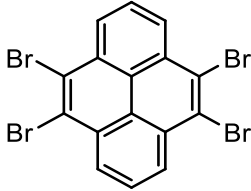
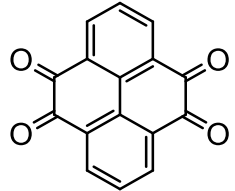
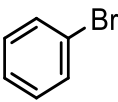
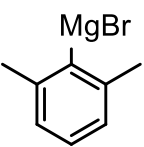
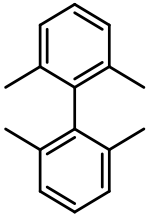
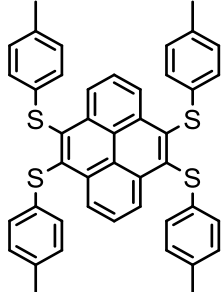
36. S. Goretta, C. Tasciotti, S. Mathieu, M. Smet, W. Maes, Y. M. Chabre, W. Dehaen, R. Giasson, J.M. Raimundo, C. R. Henry, C. Barth, M. Gingras, *Org. Lett.*, **2009**, *11*, 3846-3849.
37. M.S. Kharash, W. Nudenberg, E.K. Fields, *J. Am. Chem. Soc.*, **1944**, *66*, 1276-1279.
38. a) R.S. Huber, G.B. Jones, *Tetrahedron Lett.*, **1994**, 2655-2658; b) S. Borman, *Chem. & Eng. News*, **1995**, Aug. 28.
39. V. Terrasson, M. Roy, S. Moutard, M. P. Lafontaine, G. Pepe, G. Felix, M. Gingras *RSC Adv.*, **2014**, *4*, 32412.
40. M. Mansø , L. Fernandez, Z. Wang, K. M. Poulsen, M. B. Nielsen, *Molecules*, **2020**, *25*, 322.
41. K. E. Pryor, G. W. Shipps Jr, D. A. Skyler, J. Rebek Jr, *Tetrahedron*, **1998**, *54*, 4107-4124.
42. K. Sakayori, Y. Shibasaki, M. Ueda, *J. Polym. Sci., Part A: Polym. Chem.*, **2006**, *44*, 6385-6393.
43. W. Han, S. Qin, X. Shu, Q. Wu, B. Xu, R. Li, X. Zheng, H. Chen, *RSC Adv.*, **2016**, *6*, 53012-53016
44. Y.H. Lia, L. P. Lua, *IUCrData* *1*, **2016**, no. 8 x161274, <http://dx.doi.org/10.1107/S2414314616012748>
45. A. E. G. Miller, J. W. Biss, L. H. Schwartzman, *J. Org. Chem.*, **1959**, *24*, 627-630.
46. N. M. Yoon, C. S. Pak, H. C. Brown., S. Krishnamurthy, P. S. Thomas , *J. Org. Chem.*, **1973**, *38*, 2786-2792.
47. D. Vonlanthen, J. Rotzler, M. Neuburger, M. Mayor, *Eur. J. Org. Chem.*, **2010**, 120-133.
48. S. Dana, D. Chowdhury, A. Mandal, F. A. S. Chipem, M. Baidya, *ACS Catal.*, **2018**, *8*, 10173-10179.
49. S. Gundala, C. L. Fagan, E. G. Delany, S. J. Connon, *Synlett* , **2013**; *24*, 1225-1228
50. S. Yu, X. Zhang, Y. Yan, C. Cai, L. Dai, X. Zhang, *Chemistry*, **2010**, *16*, 4938-4943.
51. M. Gingras, C. Collet, *Synlett*, **2005**, 2337-2341.
52. T. J. Seiders, E. L. Elliott, G. H. Grube, J. S. Siegel, *J. Am. Chem. Soc.*, **1999**, *121*, 7804-7813.

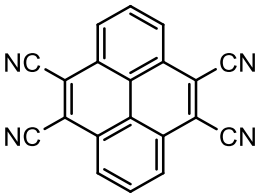
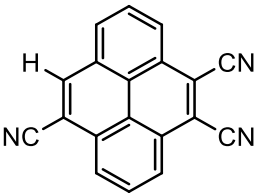
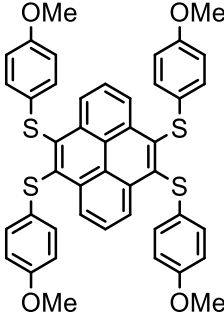
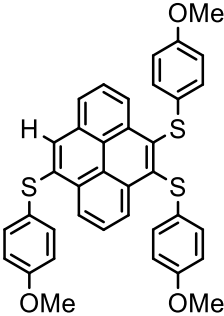
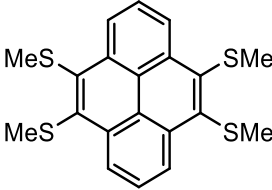
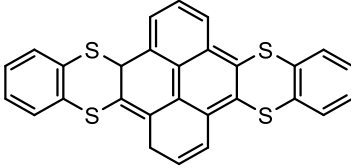
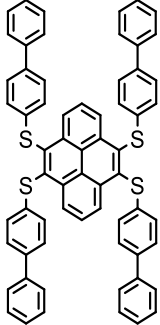
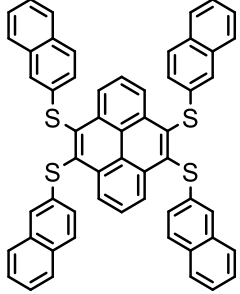
53. S. Seth, G. Savitha, J. N. Moorthy, *Inorg Chem.*, **2015**, *54*, 6829-6835.
54. C. Chen, P. Li, Z. Hu, H. Wang, H. Zhu, X. Hu, Y. Wang, H. Lv, X. Zhang, *Org. Chem. Front.*, **2014**, *1*, 947-951.
55. D. D. Lu, X. X. He, and F. S. Liu, *J. Org. Chem.*, **2017**, *82*, 10898-10911.
56. S. Ostrowska, S. Rogalski, J. Lorkowski, J. Walkowiak, C. Pietraszuk, *Synlett*, **2018**, *29*, 1735-1740.
57. D. Zhao, Q. Wu, Z. Cai, T. Zheng, W. Chen, J. Lu, and L. Yu, *Chem. Mater.* **2016**, *28*, 1139-1146.
58. E. C. Joseph; A. D. Clinton; H. C. George, *Org. Synth.*, **1948**, *28*, 34.
59. L. Zöphel, V. Enkelmann, K. Müllen, *Org. Lett.* **2013**, *15*, 804-807.
60. R. Zhang, L. H. Xu, H. Che, Z. H. Qin, Y. Zhao, Z. H. Ni, *Chem. Res. Chin. Univ.*, **2015**, *31*, 224-227.
61. S. Tang, L. Zhang, H. Ruan, Y. Zhao, X. Wang, *J. Am. Chem. Soc.* **2020**, *142*, 7340-7344.

List of compounds in chapter-2: 50, 68, 69, 70, 71, 72, 73, 74, 4, 29, 79, 80, 88, 81, 83, 93, 94, 84, 86, 87

Side products: 29, 77, 89, 82

Commercially available: 1, 78, 92

		
50	68	69
		
1	70	71
		
72	73	74
		
4	29	78
		
78	79	80

		
88	89	81
		
82	83	84
		
86	87	

CHAPTER 3

SYNTHESIS OF POLYSULFURATED BENZENE-CORED ASTERISKS WITH ARYLTHIO OR HETEROARYLTHIO ARMS

- 3.0 Introduction
- 3.1 General synthetic scheme
- 3.2 Synthesis of hexathiosubstituted benzene-cored asterisks
- 3.3 Synthesis of tetrathiosubstituted benzene-cored asterisks
- 3.4 Synthesis of trithiosubstituted benzene-cored asterisks
- 3.5 Persulfurated benzene-cored asterisks with heteroaryl arms: "the heteroasterisks"
 - 3.5.1 Literature on polysulfurated benzene-cored "heteroasterisks"
 - 3.5.2 Synthesis of the "heteroasterisks"
- 3.6 Conclusion

3.0 Introduction

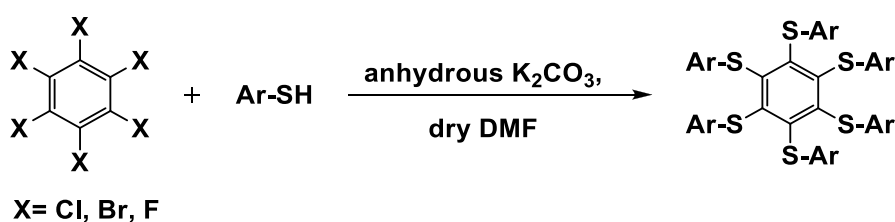
Polysulfurated arenes and heteroarenes are still underexploited, even though some parent compounds are known since the early days of organic chemistry. Of a special attention, reports on persulfurated arenes and heteroarenes are much less common in the literature, but have become recently popular after some recent discoveries of their exalted properties (photophysical, electrochemical, REDOX, and supramolecular ones) caused by a multiplicity of sulfur atoms or arylthio groups surrounding an aromatic core. Along these lines and such research theme being involved for many years in the group of professor Gingras, we decided to further explore some star-shaped arenes in order to optimize and to delineate their properties and features. Thus, a series of polysulfurated arenes were under study in this thesis. It comprises hexathio-, tetrathio- and trithiosubstituted benzene- or pyridine-cored asterisks. The arms can include heteroarylthio or arylthio substituents. Also, a new series of π -extended, polysulfurated benzene-cored asterisks were synthesized from biphenylene and triphenylene thiols, in search for their photophysical, structural, electrochemical, REDOX, covalent dynamic and supramolecular chemistry. The series of compounds with naphthylthio arms will be in a separate chapter. Dynamic covalent chemistry with these entities will be further detailed in chapter 6. Many of these compounds are characterized by NMR (^1H , ^{13}C , ^{19}F), single-crystal-X-ray diffraction data, LC-MS (ESI), LC-HRMS, HRMS and elemental analysis. In this chapter, the

synthetic processes will be discussed. These polysulfurated arenes are usually easy to synthesize and to obtain on a multiple-gram scale from cheap and readily available commercial starting substrates.

The main objectives in this chapter are to report the synthesis of novel chemical arene and heteroarene entities incorporating many sulfur atoms, and to characterize well these compounds in search for some exalted or extraordinary properties (photophysical, structural, electrochemical, REDOX, covalent dynamic and supramolecular properties) in which sulfur has a major effect in these properties. A special attention has been paid to the asterisks with heteroaromatic arms in view of future modulations of properties by metal ions binding and the related coordination chemistry of uses in supramolecular or dynamic covalent chemistry.

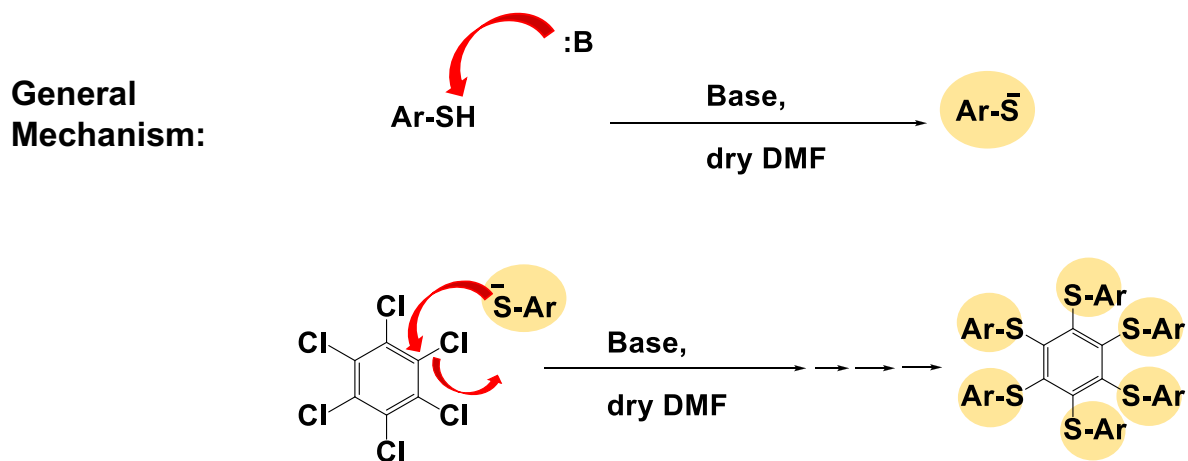
3.1 General synthetic scheme

Below is a general mechanism for making these asterisks with a benzene core (scheme 1). In the first step, the base will abstract a proton to make more nucleophilic species, such as thiolates (instead of a thiol). In the second step, many nucleophilic thiolates can substitute the chlorine atoms bound to the benzene core, which is electron deficient, as it has six chlorine atoms on the benzene ring to start with (scheme 2).



Scheme 1: a general reaction scheme for generating the benzen-cored asterisks.

These persulfurated asterisks are considered as some DCC templates (chapter 6) with exalted optoelectronic properties, including phosphorescence in solid or aggregated state.



Scheme 2: A schematic representation of the mechanism where the nucleophilic aromatic substitutions are repeated six times.

3.2 Synthesis of hexathiosubstituted benzene-cored asterisks

The procedure envisaged to obtain the benzene-cored asterisks was influenced from the known procedures in literature. [1] Most often, we chose potassium carbonate because of its practicality, cost and efficiency in these reactions, along with a polar solvent such as DMF, instead of costly and high boiling point DMI (1,3-dimethyl-2-imidazolidinone). The latter is difficult to remove by vacuum or by aqueous dissolution. Previously, several molecular asterisks were synthesized in our laboratory with different functional groups like: R= Me, iPr, OMe, CN, Br, F, CF₃, CHO, CO₂iPr in ortho, meta or para positions. This work evaluates the reactivity of the perhalogenated benzenes (X = Cl, F) and has improved the reaction conditions to increase the yields and to facilitate the purification of these compounds. It is worth noting that C₆Cl₆ has been used in the 60's as a commercial biocide. Today, it is a toxic waste, carcinogenic in animals, coming from the partial chlorination of benzene, thus a relatively cheap reagent to recycle. From Marco Villa's thesis at CINaM, it was observed that di-, tetra-, and hexathio asterisks were consistently obtained depending on the ratio of thiol/C₆F₆ or thiol/C₆Cl₆, but never mono-, tri- and pentasubstituted asterisks, as it was also reported elsewhere. Hence, the desired molecular asterisks (1 to 4) were synthesized (figure 1) by simply reacting hexachlorobenzene, potassium carbonate, and the corresponding thiols in DMF for a given time and temperature, under an inert atmosphere of argon (oxygen-free conditions). The purifications are easy, most often by precipitation of the product after addition of EtOH and H₂O, followed by a trituration. The by-products such as disulfides, salts, and other partially substituted asterisks were

removed in the mother liquor, and the collected solid was often pure, to afford excellent yields of asterisks (>90%).

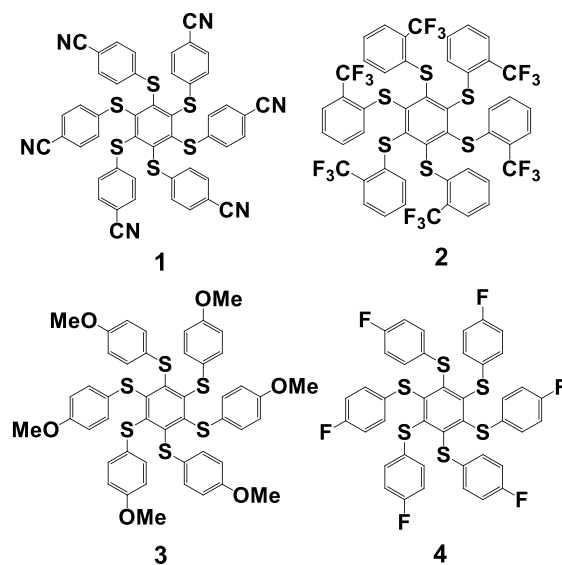
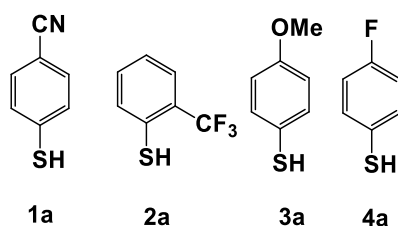
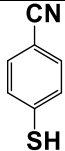
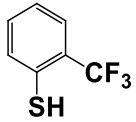
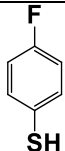
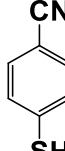
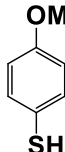


Figure 1: persulfurated benzene-cored asterisks (1-4) synthesized and characterized.



Asterisks (1), (2) and (4) are unknown, whereas asterisk (3) was first synthesized in 2004 (see Table 1). [2] Compound (1) was generated via some nucleophilic aromatic substitutions of hexachlorobenzene with 4-cyanobenzenethiol in the presence of potassium carbonate in DMF at 40°C for 16 hours to give 92% yield of (1). The workup is simply achieved by trituration in water and ethanol at room temperature, and the pure compound was filtered, collected and dried. Hexakis(2-trifluoromethylphenylthio) benzene (2) was synthesized by the same method using 2-(trifluoromethyl)benzenethiol, hexachlorobenzene, dry potassium carbonate in DMF at 60°C for 68 hours to provide (2) in a 90% yield.

Table 1: synthesis of various asterisks and reaction parameters

Reaction Number	C ₆ Cl ₆ (mg, mmol, eq.)	Thiol (mg/ g, mmol, eq.)	K ₂ CO ₃ (mg/ g, mmol, eq.)	Solvent (dry DMF) (mL)	Time	Temp. (°C)	Yield (%)
R-201 Asterisk-1	394.7, 1.386, 1.0	 (1.501g, 11.100, 8.0)	(1.535g, 11.111, 8.0)	10.0	48hrs.	40°C	99
R-122 Asterisk-2	355.3, 1.247, 1.0	 (1.5mL, 2.025g, 11.365, 9.0)	(1.557g, 11.268, 9.0)	16.0	5days	60°C	97
R-146 Asterisk-4	447.0, 1.57, 1.00	 (1.50mL, 1.804g, 14.08, 9.0)	1.945g, 14.07, 8.96	6.0	3days	27°C	95
R-26 Competition between two thiols Asterisk-3	44.99, 0.158, 1.0	 (109 mg, 0.806, 5.0)  (0.1mL, 114 mg, 0.813, 5.0)	225.4, 1.626, 10.0	0.5	6days	27°C	90

The sc-XRD structure determination is given in figure 2. In 2004, hexakis (4-methoxyphenylthio) benzene (**3**) was synthesized using hexafluorobenzene and *p*-

methoxybenzenethiol with sodium hydride in DMI at 0°C, and then to 20°C for 6 hours, to provide **(3)** in 95% yield. [2] A competition between 4-methoxybenzenethiol (electron-rich thiol) and 4-mercaptobenzonitrile (electron-poor thiol) mainly afforded **(4)**. The yield is estimated because small aliquots were taken out to check the reaction progress (see experimental section of chapter 6).

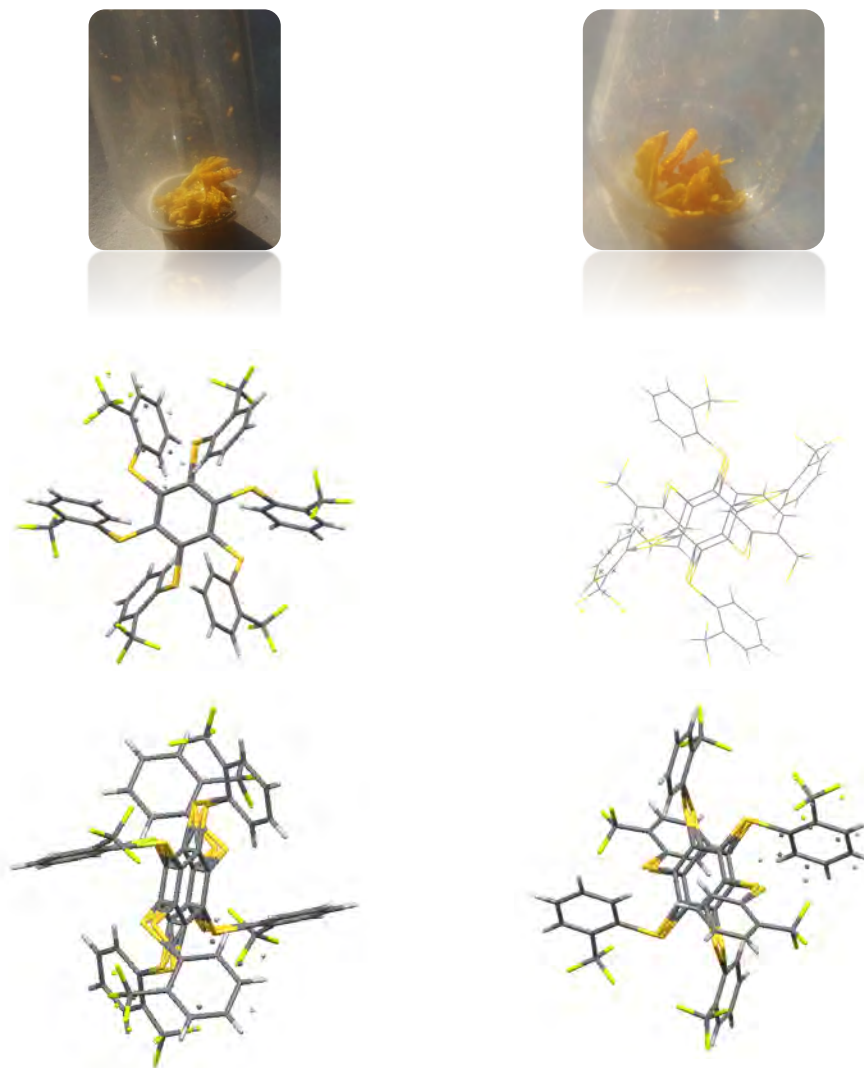
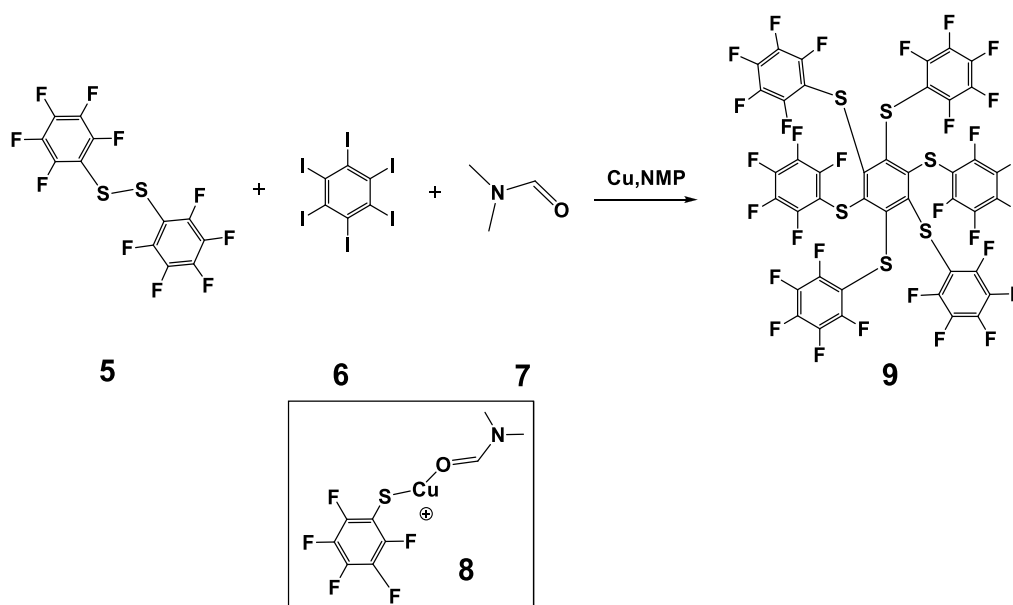


Figure 2: sticks model of **(2)** from a sc-XRD structure determination of hexakis(2-trifluoromethylphenylthio) benzene **(2)** and its yellow crystals.

In 2008 and 2012, our group synthesized **(3)** as a building block for making a multivalent PyBox asterisk, as a multisite catalyst in the presence of a rhodium salt. Metal-catalysis with a persulfurated aromatic ligand was demonstrated for the first time in a model reaction: the Rh-enantioselective hydrosilylation of acetophenone. The interesting features were the reactivity and the enantioselective behavior while varying

the metal content. [3-4] During our studies in DCC (chapter 6), asterisks (**3**) was synthesized by making competition between two thiols such as 4-cyanobenzenethiol (4,5 mol-eq.) and 4-methoxybenzenethiol (4,5 mol-eq.) with hexachlorobenzene (1,0 mol-eq.) and potassium carbonate (excess) in DMF at 20°C for six days, to provide (**3**) in a 90% yield. Asterisk (**4**) was synthesized by using 4-fluorobenzenethiol under similar conditions, at 27°C for 3 days to afford the *p*-fluorinated asterisk (**4**) in a 95% yield. Interestingly, the perfluorinated asterisk (**5**) is known in the literature, after reacting commercial pentafluorobenzenethiol with hexaiodobenzene (scheme 3). [5]



Scheme 3: Synthesis of fluorinated asterisk (**5**)

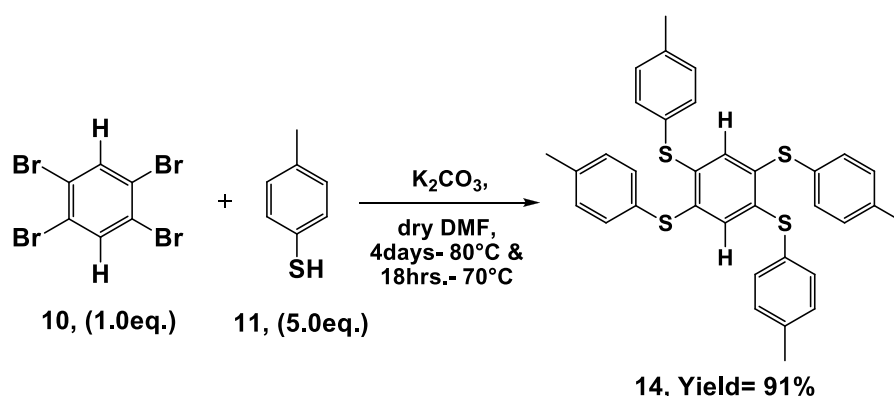
3.3 Synthesis of tetrathiosubstituted benzene-cored asterisks

In our laboratory, several pentathiosubstituted benzene-cored asterisks were previously synthesized in order to evaluate their photophysical and structural properties in the solid state. We also needed these compounds as substrates for DCC studies in chapter 6. The next step was to prepare the tetrathiosubstituted benzene-cored asterisks in order to furnish more compounds to the library of sulfurated arenes for evaluating the sulfur effects, in relation to the multiplicity of sulfur atoms around the benzene core. As shown in figure 3, the tetrathiosubstituted asterisks (**14**) [6] and (**15**) [7-9] are known in literature. Both asterisks were synthesized (Schemes 4 and 5) by

using the corresponding thiols: 4-methylbenzene thiol (11) for asterisk (**14**) and thiophenol (12) for asterisk (**15**).

By reacting 1,2,4,5-tetrabromobenzene (10) with an excess of thiocresol (11) (5.0 mol-eq.) with potassium carbonate in DMF at 80°C for 4 days and then at 70°C for 18 hours, it afforded 91% yield of (**14**) on a several-gram scale after purification. Asterisk (**14**) was recrystallized in toluene and a sc-XRD structure determination of the asterisk was done (figure 3). The preferred conformation shows all C-S-C bonds almost in the same plane (periplanar) as for central benzene core, which is unusual for poly(phenylthio) benzenes. A possible explanation comes from two cohesive pairs of π -complexes from the *p*-tolylthio arms. Otherwise, without π -complex of two arms, the preferred conformation is usually an alternating pattern of the arms above and below the plane of the central benzene core.

Similarly, asterisk (**15**) was prepared from 1,2,4,5-tetrafluorobenzene (12), dry potassium carbonate in DMF, and the mixture was stirred at 80°C for 4 days and at 116°C for 18 hours to afford a 99% yield of (**15**), as shown in scheme 5. The asterisk (**15**) was recrystallized in *n*-butanol and sc-XRD studies were achieved (figure 4). The preferred conformation presents three C-S-C bonds of the phenylthio arms periplanar to the central benzene core, and one C-S-C bond above this plane. Two adjacent 1,3-phenylthio arms act a pair of cohesive π -complexe, whereas the two others in the 4,6 positions adopt an almost orthogonal position.



Scheme 4: synthesis of of asterisk (**14**) (1,2,4,5-tetra(4-methyl-phenylthio) benzene).

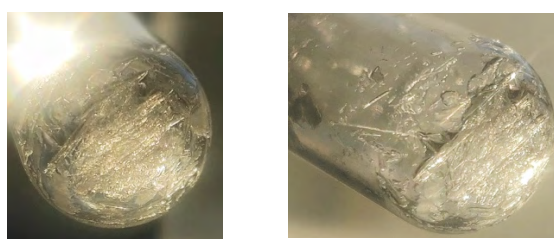
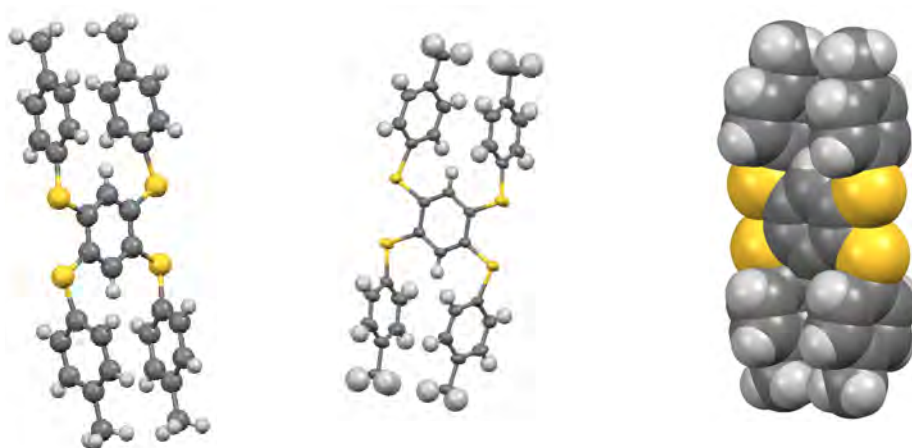
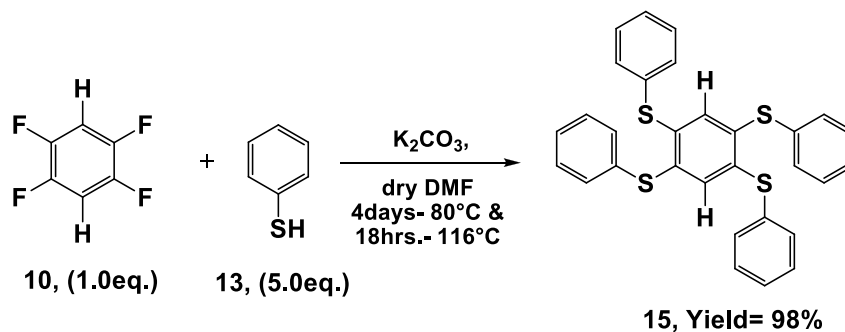


Figure 3: sc-XRD structure determination of **(14)** (1,2,4,5-tetra(4-methyl-phenylthio) benzene) and its colorless crystals.



Scheme 5: synthesis of asterisk **(15)** (1,3,4,5-tetra(phenylthio)benzene).

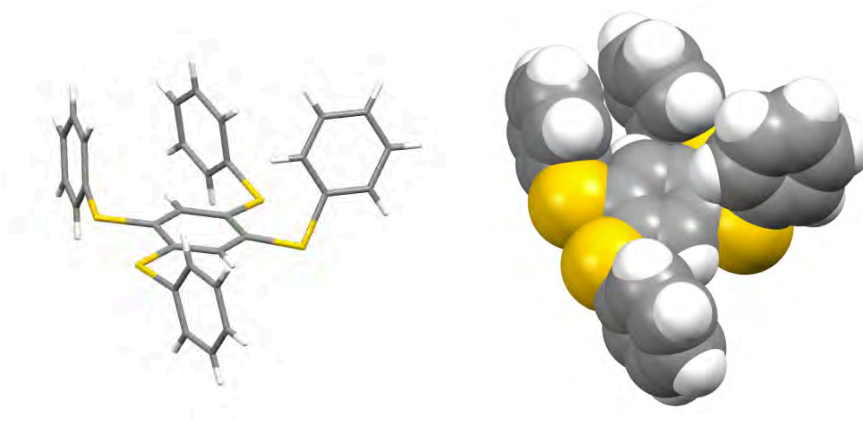
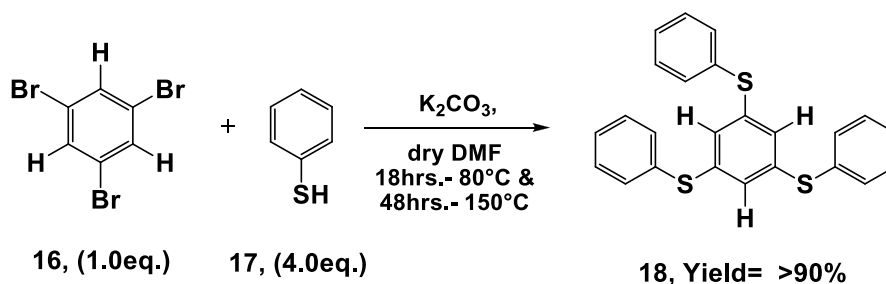




Figure 4: sc-XRD structure determination of asterisk (**15**) (1,3,4,5-tetra(phenylthio)benzene) and its colorless crystals.

3.4 Synthesis of trithiosubstituted benzene-cored asterisk (**18**)

One of the simplest polysulfurated arene is compound (**18**) (1,3,5-tri(phenylthio)benzene) which is needed to complete the series for polysulfurated benzene-cored asterisks of uses in DCC (chapter 6), as shown in scheme 6.



Scheme 6: synthesis of trisubstituted benzene-cored asterisk (**18**) (1,3,5-tri(phenylthio)benzene).

The photophysical properties of (**18**) are not exceptional due to the low multiplicity of sulfur atoms, which renders this compound as a regular one, without significant sulfur effects on the properties.

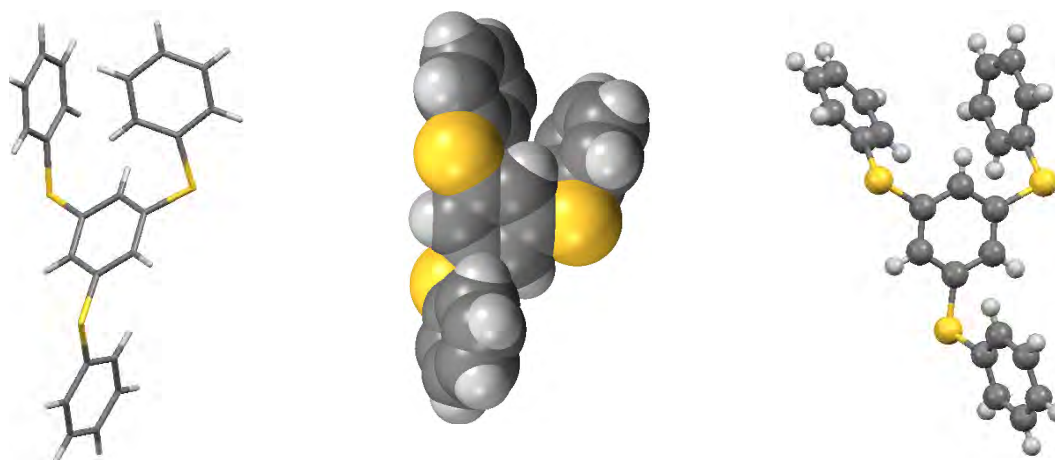


Figure 5: sc-XRD structure determination of 1,3,5-tri(phenylthio)benzene (**18**)

This trisubstituted asterisk (**18**) was synthesized under similar conditions as for the hexathio- and tetrathiosubstituted asterisks (scheme 6). Some characterization data from literature were also taken into account and matches with our data. [10-12] Figure 5 shows the sc-XRD structure determination of asterisk (**18**) where the preferred conformation indicates two phenylthio groups above (a) and one below (b) the plane of the central benzene core in a (a a,b) pattern.

3.5 Persulfurated benzene-cored asterisks with heteroaryl arms: "the heteroasterisks"

Persulfurated benzene-cored asterisks comprising some heteroaromatic arms are extremely rare in the literature, besides the terpyridine (TPY) structure which we previously described Section 1.3, Scheme 24, Chapter 1. These novel star-shaped structures can incorporate many sulfur, oxygen or nitrogen atoms together in a single asterisk. Because of these heteroatoms and their multiplicity, one can easily imagine some studies of their coordination with metal cations as supramolecular sensors, supramolecular assemblies, and to perform S_NAr reactions for components exchange in DCC (chapter 6). Additionally, we survey their photophysical properties, which could be modulated by metal ions. As a consequence, we also synthesized five novel "heteroasterisks". All of them are structurally characterized by usual NMR and mass spectrometric methods.

3.5.1 Literature on the polysulfurated benzene-cored "heteroasterisks"

As mentioned, there is a literature precedent on heteroasterisks incorporating terpyridine units at the periphery of a persulfurated benzene-cored asterisk, as already described in this thesis, section 1.3, scheme 24, chapter 1. Besides this study, no relevant academic publications could be found.

In 2014, our group previously reported a work on a heteroatomic asterisk where six terpyridine units were incorporated to a hexathiosubstituted asterisk, as a multivalent ligand. Also, its metal coordination and phosphorescence upon Mg^{2+} complexation in THF were reported. The luminescence can be turned on by adding Mg^{2+} or switched off by disassembling the supramolecular structure upon fluoride addition, which sequesters Mg^{2+} ions to prevent rigidity-induced phosphorescence. The coupling of the arms incorporating a thiol function was achieved in DMI with

cesium carbonate as a base at 60°C to afford 97% yield of the TPY-based structure. [1]

Knowing that many heteroaromatic ligands are used in supramolecular chemistry, we could also find some inspirations for building up the new heteroasterisks. For instance, in 2007 prof. Jean-Marie Lehn and his group published this work while explaining all the terms related from supramolecular chemistry to dynamic constitutional chemistry with many data. He showed the coordination of a tritopic ligand strand, which can form a dynamic library of circular helicites (figure 6) by simply adding Fe^{2+} (d6, transition metal), which can coordinate octahedrally, and can form different shapes or it can self-organize itself depending on its counterions, such as sulphate or chloride anion. [12-13]

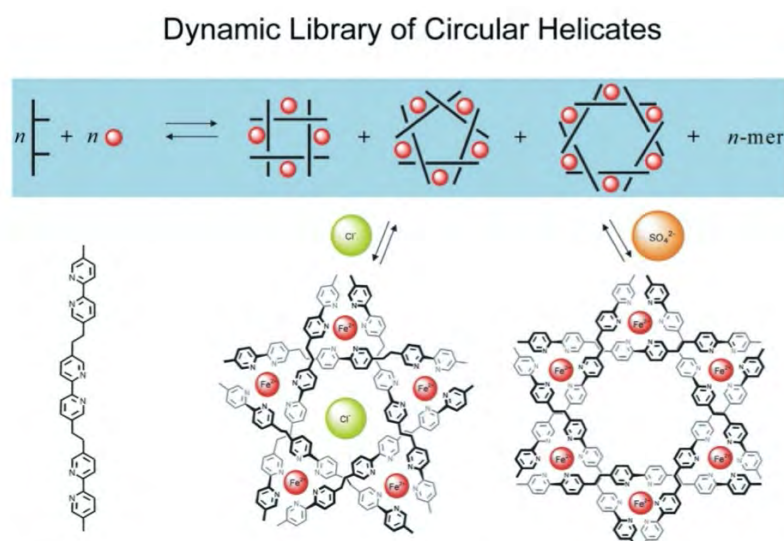


Figure 6: Dynamic (virtual) library of circular helicites generated from a tritopic ligand strand and octahedrally-coordinating metal ions, expressing different constituents depending on the counter ion present (chloride or sulfate anion). (Reprinted with permission). [12-13]

3.5.2 Synthesis of the "heteroasterisks"

All four heteroaroasterisks (19-22) are unknown and were synthesized via a similar method as discussed before for other persulfurated benzene-cored asterisks. Detailed syntheses are given in the experimental section. All these asterisks are not very soluble in many organic solvents, but can be partially soluble in DMF, o-xylene and DMSO. None of them had been recrystallized so far after many trials in order to do sc-XRD studies. They can also be used for some metal ions complexation studies or to

study reversible S_NAr in dynamic covalent chemistry, in the presence or absence of metal ions.

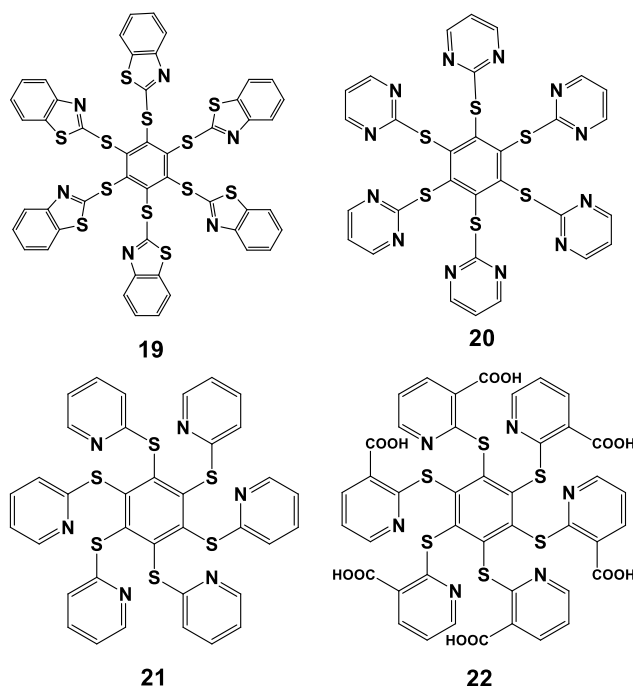


Figure 7: Heteroasterisks with a benzene-core (19-22) synthesized and characterized.

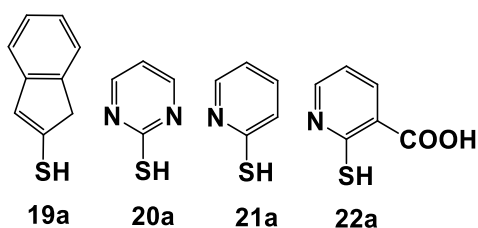
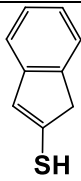
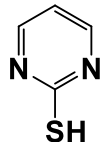
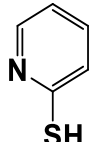
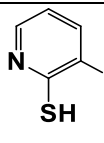


Table 2: synthesis of various heteroasterisks and reaction parameters

Reaction Number	C6Cl6 (mg, g./mmol, eq.)	Thiol (mg/ g, mmol, eq.)	K ₂ CO ₃ (mg/ g, mmol, eq.)	Solvent (dry DMF mL)	Time	Temp (°C)	Yield (%)
R-96 (Asterisk-19)	(0.200g, 0.702, 1.00)	 SH (1.00g, 5.979, 8.5)	(1.163g, 8.415, 12.0)	15.0	5days	60°C	84

R-97 (Asterisk-20)	2.00g, 7.023, 1.0	 (7.015g, 62.547, 9.0)	(11.629g, 84.143, 12.0)	44.0	12day s	60°C	97
R-125 (Asterisk-21)	213.4mg, 0.749, 1.0	 (500.3mg, 4.500, 6.0)	621.8mg, 4.499, 6.0	3.0	6days	60°C	86
R-26 (Asterisk-22)	305.9mg, 1.074, 1.0	 (1000.3mg, 6.463, 6.0)	890.9mg, 6.446, 6.0	10.0	8days	60°C	86

3.6 Conclusion

Eleven asterisks were synthesized in good yields, seven are unknown and four asterisks (19-22) incorporate heteroarylthio arms. The latter can be used for future metal ion complexation studies and to investigate reversible S_NAr in DCC, in the presence or absence of metal ions. Two tetrathiosubstituted asterisks (14 and 15) and a trithiosubstituted (18) asterisk were recrystallized and *sc*-XRD studies were achieved. The preferred conformation in the solid state is discussed. All asterisks, excepted the heteroarylthio ones, have been used as substrates for evaluating reversible nucleophilic aromatic substitution reactions (chapter 6), notably to test the importance of the number of phenylthio groups for the dynamics of S_NAr reversibility in the frame of DCC.

References of chapter 3

1. A. Fermi, G. Bergamini, R. Peresutti, E. Marchi, M. Roy, P. Ceroni, M. Gingras, *Dyes & Pigments*, **2014**, 110, 113-122.
2. J. N. Lowe, D. A. Fulton, S. H. Chiu, A. M. Elizarov, S. J. R. Cantrill, J. F. Stoddart, *J. Org. Chem.*, **2004**, 69, 4390-4402.
3. C. Aubert, C. Dallaire, M. Gingras, *Tetrahedron Letters*, **2008**, 49, 5355–5358.

4. C. Aubert, C. Dallaire, G. Pèpe, E. Levillain, G. Félix, M. Gingras, *Eur. J. Org. Chem.*, **2012**, *31*, 6145-6154.
5. N. V. Kondratenko, A. A. Kolomeytsev, V. I. Popov, L. M. Yagupolskii, *Synthesis*, **1985**; *6/7*, 667-669.
6. M. Arisawa, T. Suzuki, T. Ishikawa, M. Yamaguchi, *J. Am. Chem. Soc.*, **2008**, *130*, 12214–12215
7. P.H. Lee, Y. Park, S. Park, E. Lee, S. Kim, *J. Org. Chem.*, **2011**, *76*, 3, 760–765
8. S. Dhibar, A. Dey, R. Jana, A. Chatterjee, G. K. Das, P. P. Ray, B. Dey, *Dalton Trans.*, **2019**, *48*, 17388-17394.
9. S. D. Pastor, E. T. Hessell, *J. Org. Chem.*, **1985**, *50*, 4812-4815.
10. P. H. Lee, Y. Park, S. Park, E. Lee and S. Kim, *J. Org. Chem.*, **2011**, *76*, 760–765
11. S. Dhibar, A. Dey, R. Jana, A. Chatterjee, G. K. Das, P. P. Ray, B. Dey, *Dalton Trans.*, **2019**, *48*, 17388-17394
12. J.-M. Lehn, *Chem. Soc. Rev.*, **2007**, *36*, 151–160.
13. a) B. Hasenknopf, J.-M. Lehn, B. O. Kneisel, G. Baum, D. Fenske, *Angew. Chem. Int. Ed. Engl.*, **1996**, *35*, 1838-1840; b) B. Hasenknopf, J.-M. Lehn, N. Boumediene, A. Dupont-Gervais, A. Van Dorselaer, D. Fenske, *J. Am. Chem. Soc.*, **1997**, *119*, 10956-10962.

CHAPTER 4

DICYANATED, SULFURATED AND OXYGENATED BENZENE-CORED ASTERISKS - STRUCTURAL, SUPRAMOLECULAR AND PHOTOPHYSICAL PROPERTIES

- 4.0 Introduction and objectives
- 4.1 Literature search and precedent work
- 4.2 Results and discussion
 - 4.2.1 Dicyanated and tetrasulfurated benzene-cored asterisks
 - 4.2.2 Dicyanated and tetraoxygenated benzene-cored asterisks
 - 4.2.3 Dicyanated poly(biphenylthio) benzene-cored asterisks
with π -extended systems
- 4.3 Photophysical studies
- 4.4 Conclusion

4.0 Introduction and objectives

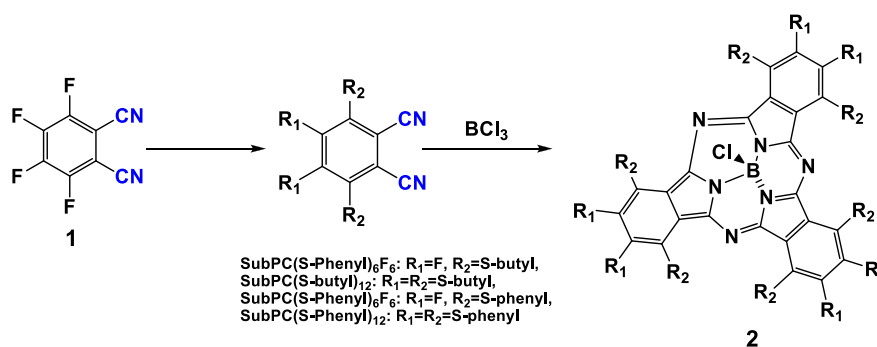
The search for new luminophores and AIEgens with exalted properties is important for developing optical and electronic materials, as well as for (bio)sensing. In that direction, we report here a study for making novel luminophores, hopefully with RIP or AIE phenomena. In a general way, the cyano groups have been excellent for promoting luminescence, as can be stated in several publications on arenes, including arenes with distorted π -systems such as in helicenes. The electron-withdrawing effect of a cyano function (mesomeric and inductive acceptor effects) offers the possibility to create a dipole moment in molecules, and possibly makes use of the electronic push-pull effect, with optical non-linear effects. In addition, the cyano groups could serve for weak metal ions complexation (e.g. with Ag^+ ions) or for making phthalocyanine derivatives. Another major issue is that many sulfur and oxygen exchange reactions occur around these molecules, which could allow their uses for developing reversible nucleophilic aromatic substitutions in the frame of DCC (Dynamic Covalent Chemistry). For all these reasons, it seems interesting to follow this path toward the search for optimized structures incorporating cyano groups with either oxygen or sulfur atoms (or both) to fine-tune the properties. We will thus report the synthesis of six novel cyanated aromatic arenes in good yields, along with an investigation on their luminescence properties with the help of the photophysicists from the University of

Bologna. **All photophysical studies were performed by the Italian research group of professor Paola Ceroni**, and we are very thankful for these studies reported here.

In summary, some nucleophilic reactions occur at room temperature and the photophysical measurements were performed in DCM and in DMF, showing quantum yields from 0.35-12.9%, whereas in the solid-state the quantum yield reaches up to 41%, indicating that they are good phosphorescent emitters with yellow-green and yellow-orange emission and few microsecond lifetimes. Single-crystal-X-ray diffraction studies were achieved on a monocrystal of (3). Overall, these data indicate that some applications could be foreseen in biology [1], as sensors [2], as metal-organic frameworks [3], as photosensitizers [4], in supramolecular and dynamic covalent chemistry.

4.1 Literature search and precedent work

In 2002, the synthesis of six types of non-anisotropic subphthalocyanine (2) inducers incorporating either fluoro, thiophenyl, and thiobutyl groups are represented in scheme 1. They were made from substrate (1). [5]



Scheme 1: synthesis of non-anisotropic subphthalocyanine inducers introduced with a fluoro group, a thiophenyl group, and a thiobutyl group [5]

The first reaction to make a per- or polysulfurated dicyanated asterisks was reported in 2007, starting from the commercially available (1) tetrafluorophthalonitrile. Thirteen compounds were synthesized with different substituents such as: phenyl, *t*-Bu, *n*-Bu, or *n*-C₁₀H₂₁. Out of these thirteen compounds, two of them were of interest as shown below: compounds (3) and (4). The sc-XRD structure determination is given for compound (4), and the reported yields are between 20-40% for all the compounds

with different substituents. Photophysical and metal ions complexation studies were reported. Also, they commented on the regioselectivity of nucleophilic aromatic substitutions on tetrachlorophthalonitrile, the chlorine atom in position 4 is replaced first and then follow the chlorine atom at the fifth position. [6] In short, the first two positions to react are para to the cyano groups.

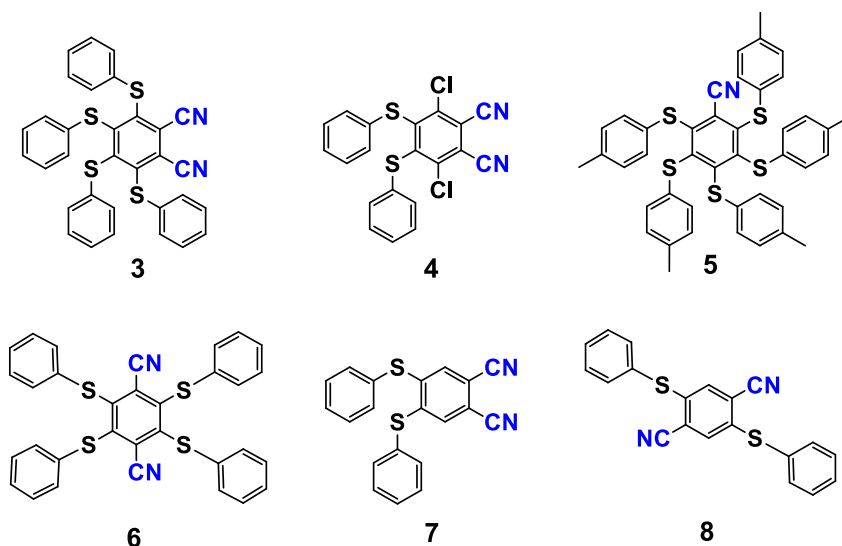


Figure 1 : a) synthesis of asterisk (3) and (5); b) compound (4) is from reference [6]; c) AIE active luminophores (6), (7) and (8). [7]

In 2017, fifteen novel compounds were synthesized, such as compounds (6), (7), and (8). The range of colors covers the full visible spectrum. A sc-XRD structure determination is given for compound (6). [7] The ortho-substituted compounds show an absorption between 320-350 nm, whereas para-substituted ones absorb between 365-406 nm. Compounds (7) and (8) exhibit a light emission between 430 and 530 nm, whereas compound (6) exhibits a long lifetime (4950 ns), reminiscent of phosphorescence. The lifetime was increased with a conjugated system, they can be excellent visible light absorbing materials due to their chemical stability and high extinction coefficients. [8]

Compound (9) was used as a ligand to prepare a photosensitizer (A3B type zinc phthalocyanine) with quantum yields of 5.5, 4.0, and 2.3%. [8]

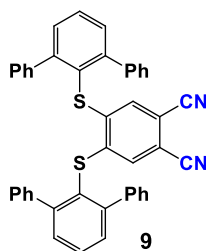
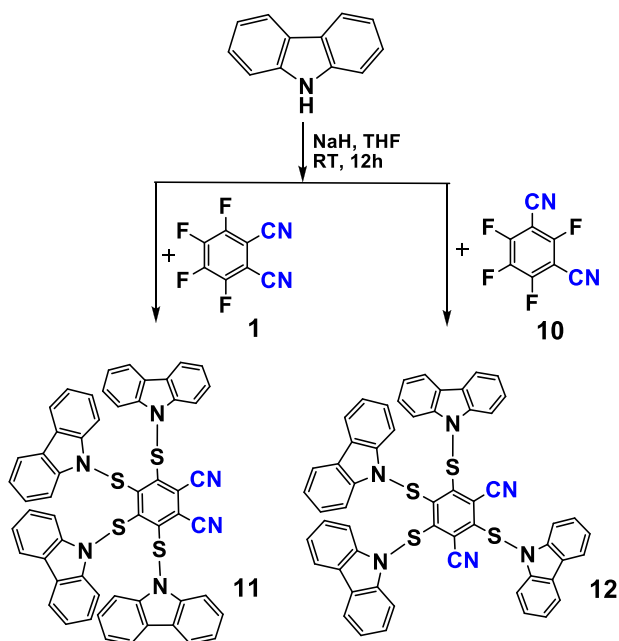


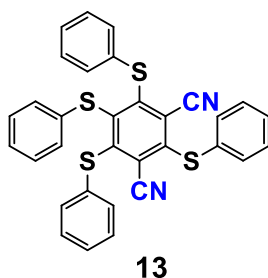
Figure 2 : compound (9) is used as a ligand. [8]

Some organic photocatalysts such as compound (11) and (12) were synthesized in 2019 via some aromatic nucleophilic substitution reactions. The latter do not use expensive metals (Ru or Ir). They are low cost, tunable, scalable, and good alternatives to metal-containing photocatalysts, due to their valuable photoredox activities (scheme 2). [9]



Scheme 2: carbazoyl 1,2-dicyanobenzene-based organic photoredox catalysts (11) and (12). [9]

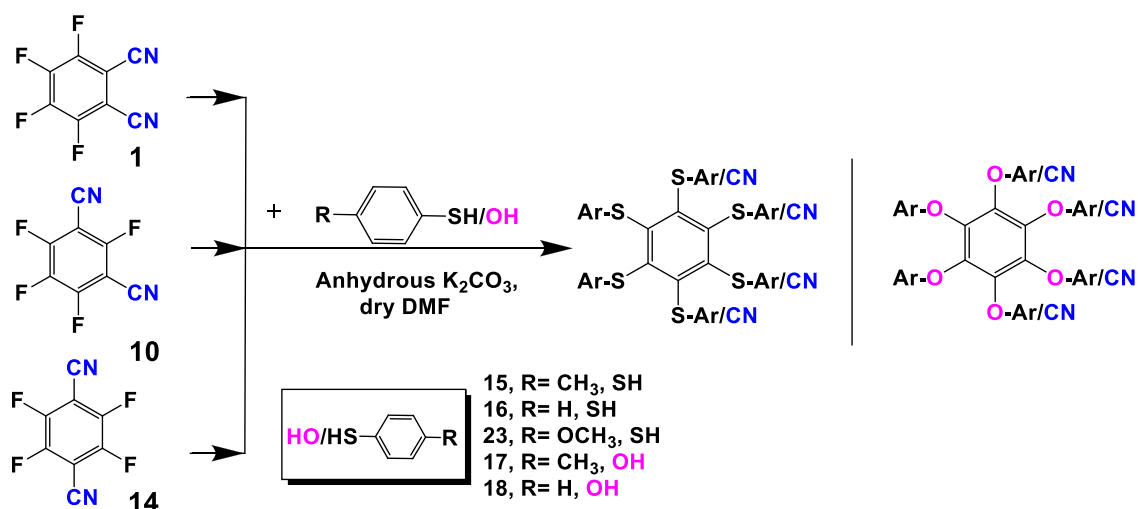
Compound (5) (2,3,4,5,6-pentafluorobenzonitrile) was synthesized in our laboratory and published in 2020. [9] It displayed a bright-green phosphorescence in the solid state at room temperature, while not being luminescent in solution. Its crystal structure and optical properties (already discussed in chapter 1) were reported. [10] Compound (13) is unknown, and so far, no data has been found.



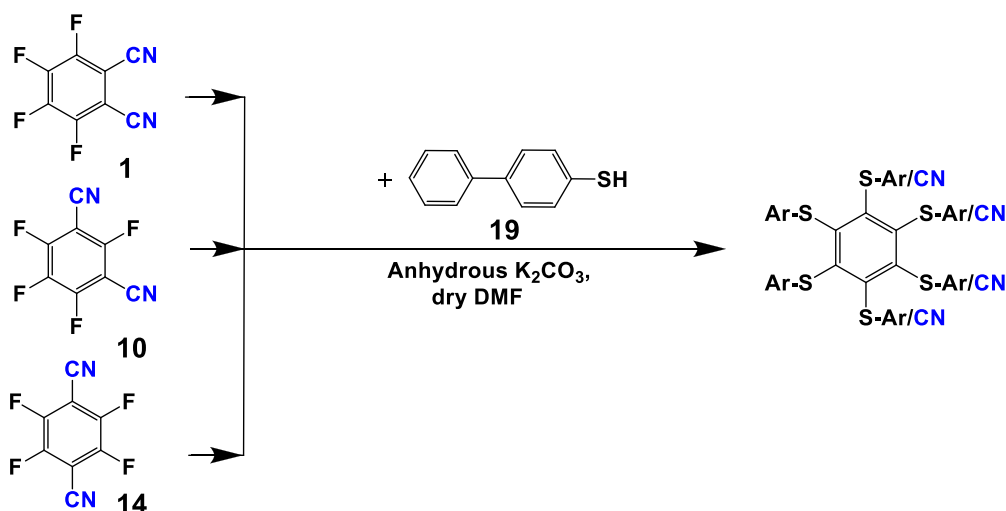
4.2 Results and discussion

Taking into account the work above, rare data have been reported on cyanated sulfurated and oxygenated benzene-cored asterisks. As a consequence, we investigated further this area by first synthesizing isomeric dicyanated tetrasulfurated and dicyanated tetraoxygenated benzene-cored asterisks. A photophysical study was undertaken on many of these compounds by the group of Pr.. Paola Ceroni from the University of Bologna. [11]

Scheme 3 represents the general synthetic method leading to dicyanated, polysulfurated (compounds 3, 20, 21, 22) and polyoxygenated (compounds 26, 27) benzene-cored asterisks. The fluorinated and dicyanated aromatic substrates were used because of their reactivity, and because they are commercially available. In general, the fluorine group helps for activating the nucleophilic addition step, which is here the rate-determining step in the S_NAr mechanism (if it is the case here, as no mechanism is rigorously established). Two electron-withdrawing cyano groups on the benzene core reduce its electron density, and further facilitate the addition of a thiolate or an alkoxyde anions at the ipso position of the fluorine atom.



Scheme 3: general scheme for the synthesis of tetrasulfurated or tetraoxygenated 1,2; 1,3 and 1,4-dicyano benzene-cored asterisks (3, 20, 21, 22, 26, 27).



Scheme 4: general scheme for the synthesis of tetrasulfurated or tetraoxygenated 1,2; 1,3; 1,4-dicyano benzene-cored asterisks (28, 29, 30) with π -extended 4-biphenylthio arms.

Similarly, π -extended systems can also be synthesized by reacting the same fluorinated substrates (28, 29, 30) with 4-biphenylthiol in dry DMF, in the presence of a base, such as anhydrous potassium carbonate (scheme 4).

4.2.1 Dicyanated and tetrasulfurated benzene-cored asterisks

As shown in figure 3, four dicyanated and tetrasulfurated benzene-cored asterisks were synthesized for future studies, out of which asterisk (3) (3,4,5,6-tetrakis(phenylthio)phthalonitrile) with two cyano groups at positions 1- and 2- and four phenyl groups at positions 3, 4, 5 and 6 of a benzene ring is already known. [11] However, no sc-X-ray diffraction data were reported in the literature to get some information about the crystalline structure and the molecular conformation in the solid state. Thus, we did sc-XRD studies on (3) (figure 4). The other three asterisks (20, 21, 22) are unknown in the literature. In order to synthesize asterisk (3), tetrafluorophthalonitrile (1) was treated with thiophenol (16) (5,0 mol-eq.), dry potassium carbonate (5,0 mol-eq.) in DMF at 50°C for 18 hours. After a work-up, the crude was purified by column chromatography over silica gel to yield asterisk (3) in a 60% yield. Prolongation of reaction time and an increase in temperature can lead to several side products, making it difficult to remove.

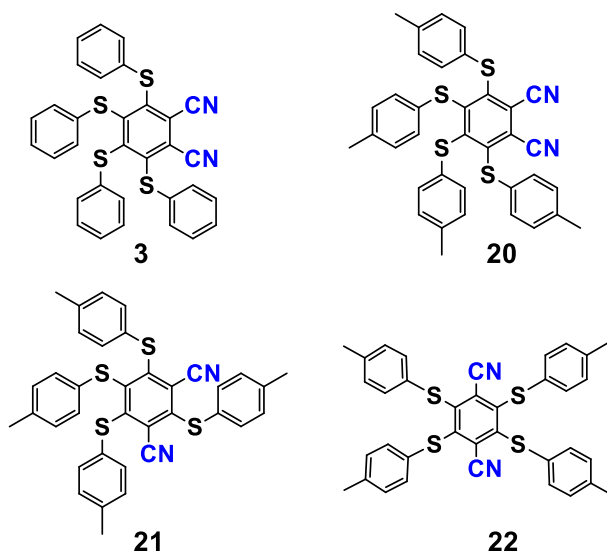
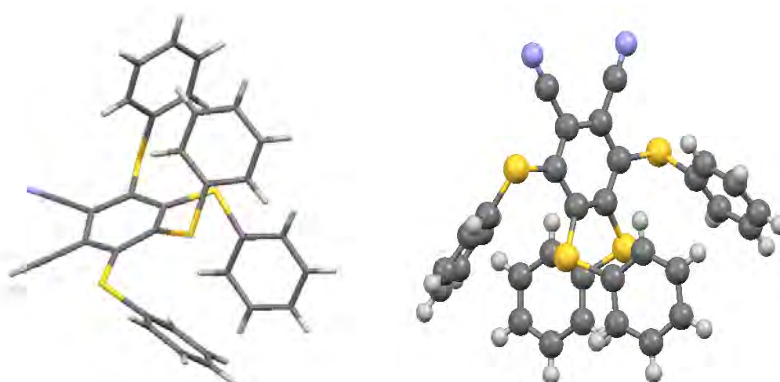


Figure 3: Dicyanated and tetrasulfurated benzene-cored asterisks (3, 20, 21, 22)

3,4,5,6-tetrakis (*p*-tolylthio) phthalonitrile (20), 2,4,5,6-tetrakis (*p*-tolylthio) isophthalonitrile (21) and 2,3,5,6-tetrakis (*p*-tolylthio) teraphthalonitrile (22) were simply synthesized by treating the corresponding tetrahalophthalonitriles (compounds 1, 10, 14) and thiol (15) with dry potassium carbonate in DMF by heating at 60°C for several hours. The workup and purification were easier for asterisks (20) and (22), by simply triturating them in ethanol and water (50:50, v/v). A yellow solid precipitates out to yield 95% of asterisk (20) (sc-X-ray structure determination shown in figure 5), and 90% yield of asterisk (22). Asterisk (21) needed a purification by column chromatography over silica gel, and the yield was only 47%, maybe because of prolonged reaction time and a high reaction temperature leading to several side products. The reaction conditions could be further improved for optimizing the yield and the procedure.



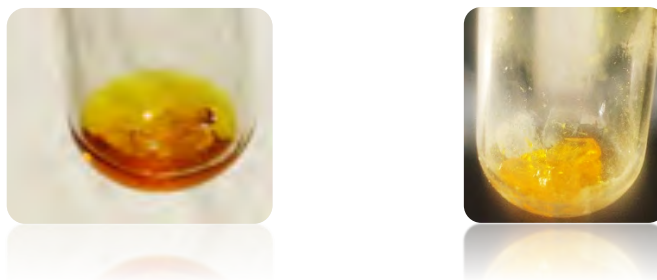


Figure 4: sc-XRD structure determination and bright yellow crystals of 3,4,5,6-tetrakis (phenylthio) phthalonitrile (3).

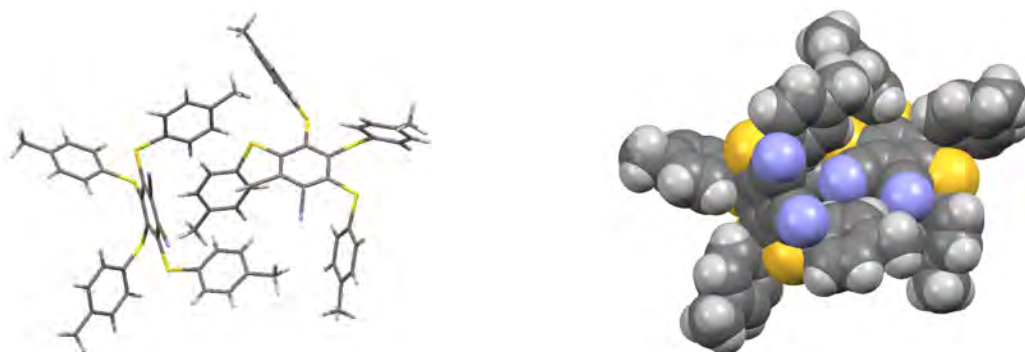
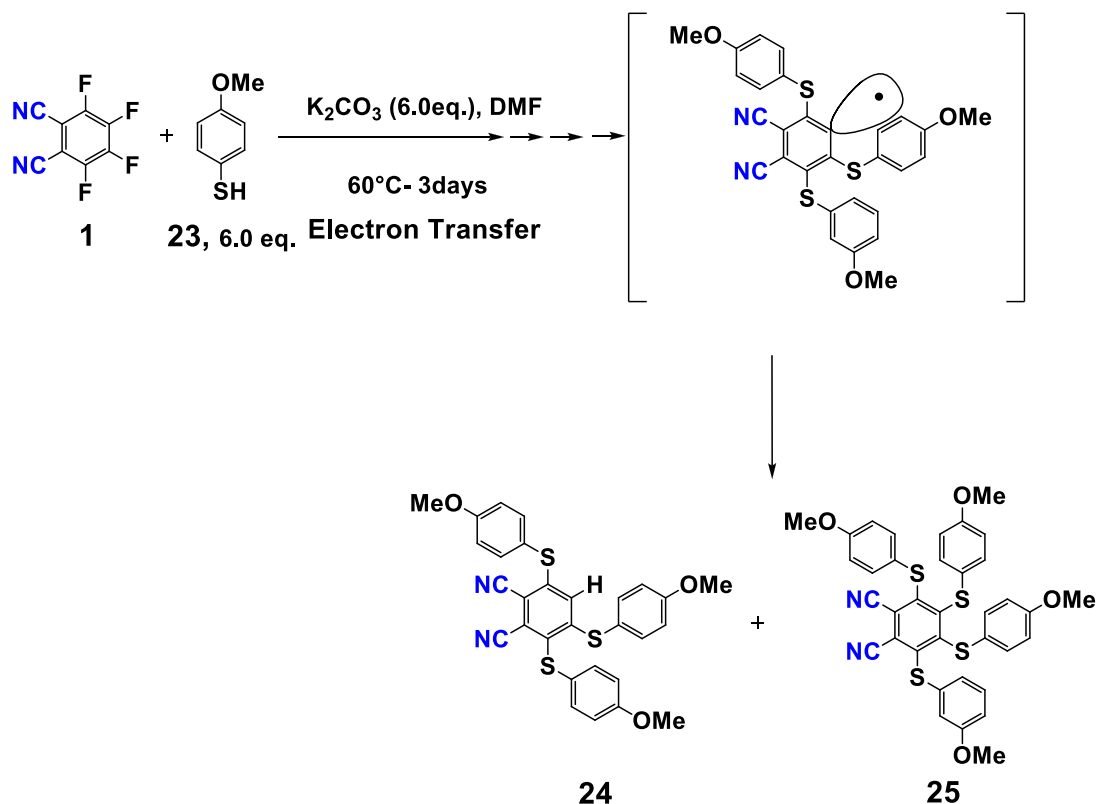


Figure 5: sc-XRD structure of 3,4,5,6-tetrakis(p-tolylthio) phthalonitrile. (20).



Scheme 5: suggested radical mechanism for generating 3,5,6-tris[(4-methoxyphenylthio)-1,2-benzenedicarbonitrile (24) during the synthesis of 2,4,5,6-tetrakis [(4-methoxyphenylthio)] phthalonitrile) (25, >40%).

A reaction was tried to make an dicyanated and tetrasulfurated asterisk (25) where a push-pull effect and a strong molecular dipole moment could be generated from the two strong electron-withdrawing cyano groups on one side of the molecule, and four electron-donor sulfurated substituents on the opposite side (scheme 6). As mentioned, it is for exploring this effect on the photophysical properties. Compound (25) was thus obtained in a >40% yield, but with another side product having a C-H bond at the benzene core (24). A most probable work hypothesis for explaining this result is an electron transfer from the electron-rich *p*-methoxyphenylthiolate anion to the electron-poor dicyanated benzene ring at some stage of the reaction (scheme 5). In this way, a radical anion is formed and a C-F or a C-S bond could be cleaved for generating a neutral radical and an anion (F^- or ArS^-). The radical could then abstract a hydrogen atom in the medium for making (24). There is no reference found in the literature for (24) and (25). When the sulfuration was run as usual, but with 4-methoxybenzenethiol (23) (6.0 mol-eq.), two major yellow spots were seen on TLC (acetone/cyclohex: 30/70 v/v). After purification by column chromatography over silica gel, the first spot corresponded to *p*-methoxybenzene disulfide in the first fractions, and in the fractions corresponding to the second more polar spot, some crystals were formed in the test tubes (as seen in figure 6).

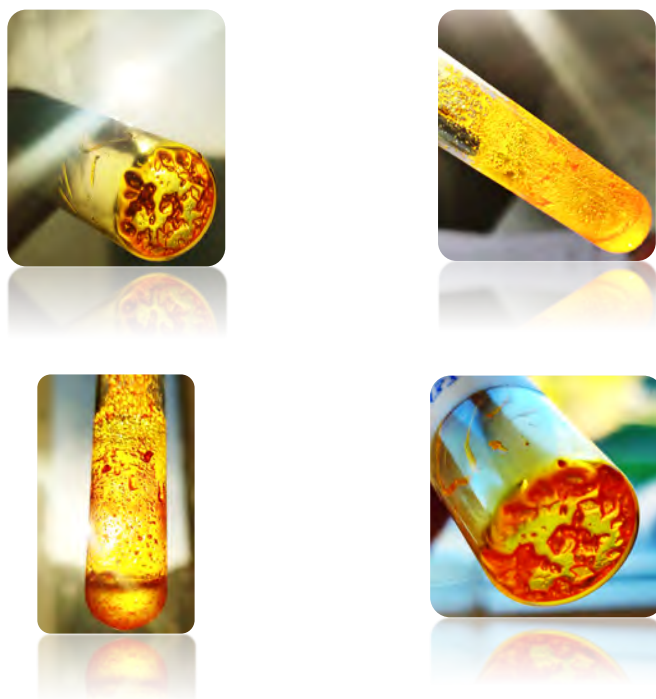


Figure 6: Orange crystals of 3,5,6-tris[(4-methoxy-phenylthio)]-1,2-benzenedicarbonitrile (24).

The sc-X-ray diffraction data were recorded from a monocrystal of asterisk (24) (figure 7). The conformation presented the 4-methoxyphenylthio groups at positions 3 and 5 upward (above the plane of the central benzene core) and the 4-methoxyphenylthio groups at position 6 downward (below that plane), probably for avoidance of some intramolecular steric hindrance between some sulfurated substituents. A second column chromatography was performed to separate (24) and (25). Compound (25) crystallized in a tube after a slow evaporation of a solution of DCM / cyclohexane (80/20 v/v), as seen figure 8. Sc-X-ray diffraction of (25) is not available yet.

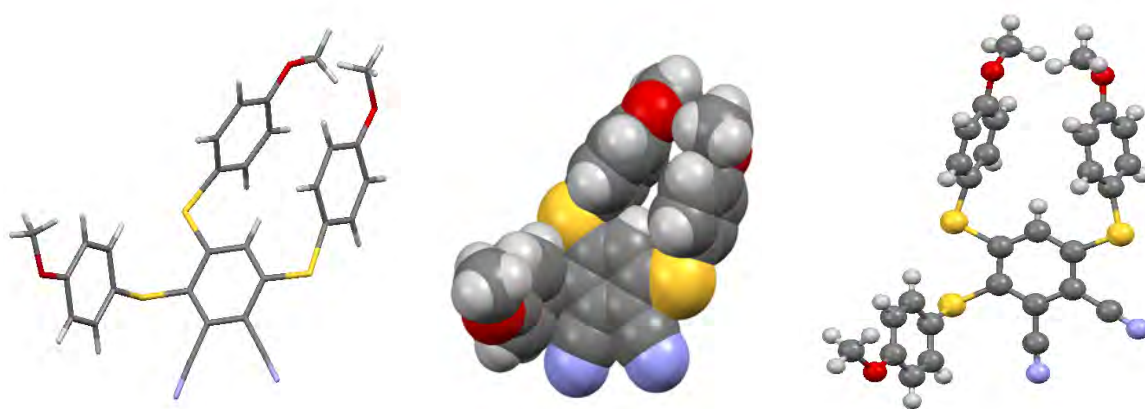


Figure 7: sc-XRD structure determination of 3,5,6-tris[4-methoxyphenylthio]-1,2-benzenedicarbonitrile (24).

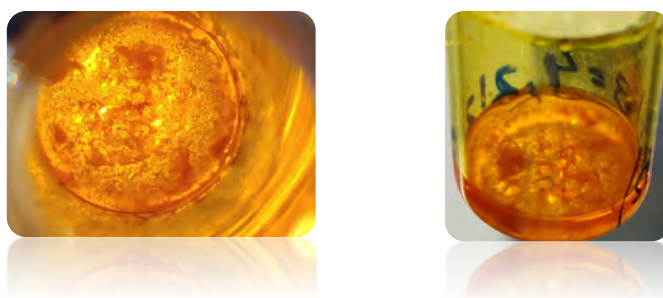


Figure 8: pictures of 2,4,5,6-tetrakis(*p*-methoxyphenylthio)phthalonitrile (25) as some crystals in a tube.

4.2.2 Dicyanated tetraoxygenated benzene-cored asterisks

Two polyoxygenated asterisks were prepared in excellent yields: 3,4,5,6-tetrakis(phenyloxy) phthalonitrile (26) and 3,4,5,6-tetrakis(4-methyl-phenoxy)

phthalonitrile (27), as shown in figure 9. Asterisks (6) was synthesized by treating (11) with *p*-cresol (17) and potassium carbonate in DMF at room temperature for 2 days to yield 95% of (27). Similarly, asterisk (26) was synthesized from phenols (11 and 18) and potassium carbonate in DMF at 60°C for 18 hours to yield 99.8% of (26). These two polyoxygenated asterisks were used to check the reversibility and sulfur/oxygen substituents exchanges in dynamic covalent chemistry (chapter 6). These two asterisks are already known, but the yields were not reported in the literature.

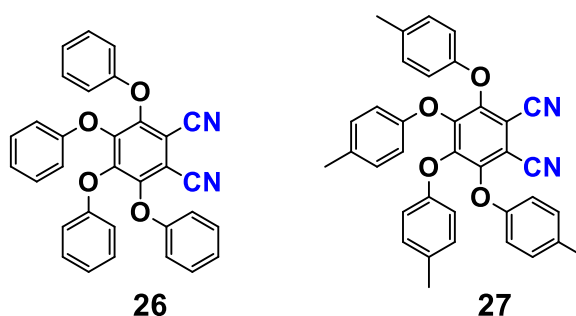


Figure 9: chemical structures of 3,4,5,6-tetrakis(phenyloxy) phthalonitrile (26) and 3,4,5,6-tetrakis(4-methyl-phenoxy) phthalonitrile (27).

These two dicyanated and polyoxygenated asterisks (figure 9) were found to exhibit fluorescence and persistent room temperature green phosphorescence (p-RTGP) in amorphous powders and in crystalline states. Both show AIE (aggregation-induced emission) in a THF-water solution. Sc-X-ray diffraction studies were reported after recrystallizing these asterisks in dichloromethane. [12]

4.2.3 Dicyanated poly(4-biphenylthio) benzene-cored asterisks with π -extended systems

All asterisks from (28 to 31) are unknown in the literature (figure 10). π -Extended asterisks (28) and (29) with four 4-biphenylthio substituents were synthesized from a similar method as for other small asterisks (such as 20-22). Asterisks (28-31) were obtained, by heating at 60°C for several hours, the corresponding tetrafluoro-dicyano benzene (11), (10), (14) with 4-biphenylthiol (19) (4.2 mol-eq. for asterisk (28) and (29); and 9.0 mol-eq for asterisk (31)) and with potassium carbonate in DMF. The purification was easy for asterisk (29) (70% yield) and asterisk (31) (82% yield) by simply triturating the crude solid with ethanol and water (50:50, v/v). As for asterisk

(30), the mixture with ethanol and water was triturated at 50°C for 18 hours with a vigorous stirring to get a red-orange solid after filtration and drying. Asterisk (28) was purified by column chromatography to afford a 72% yield of solid.

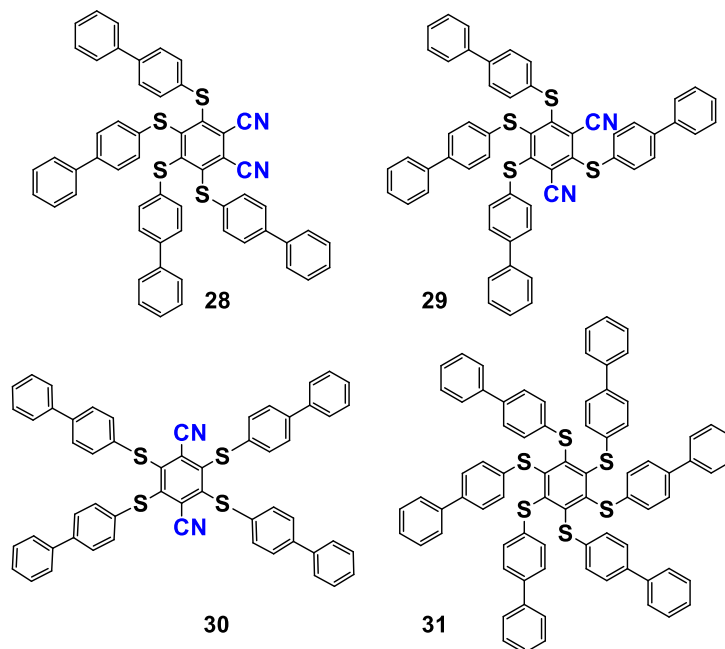


Figure 10: newly synthesized dicyano tetrakis(4-biphenylthio) benzene-cored asterisks (**28-30**) and hexakis(4-biphenylthio) benzene (**31**) with π -extended systems.

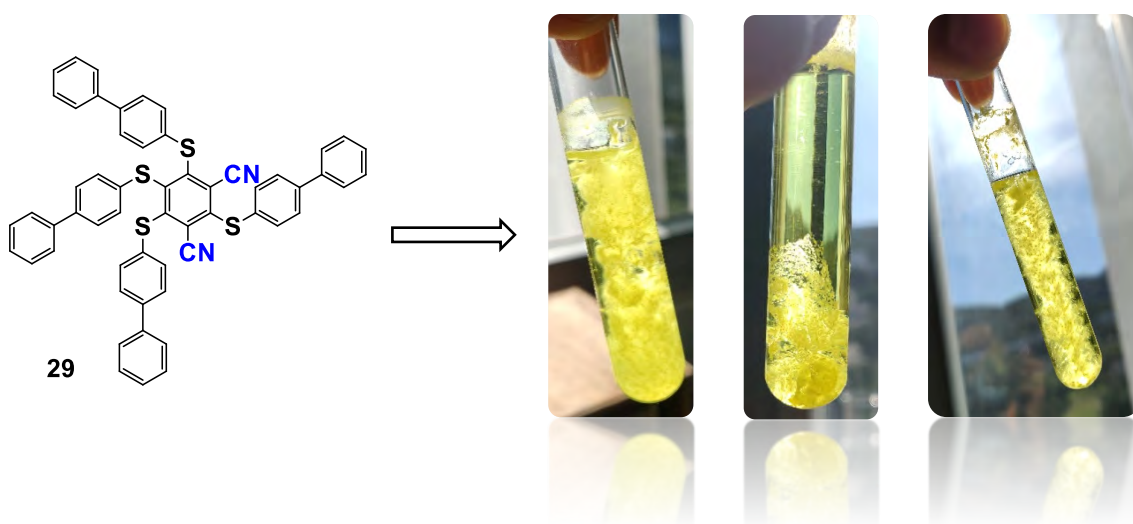


Figure 11: picture of asterisk 29 in a solvent (DCM/MeOH) and formation of helical coiled sheets by self-assembly.

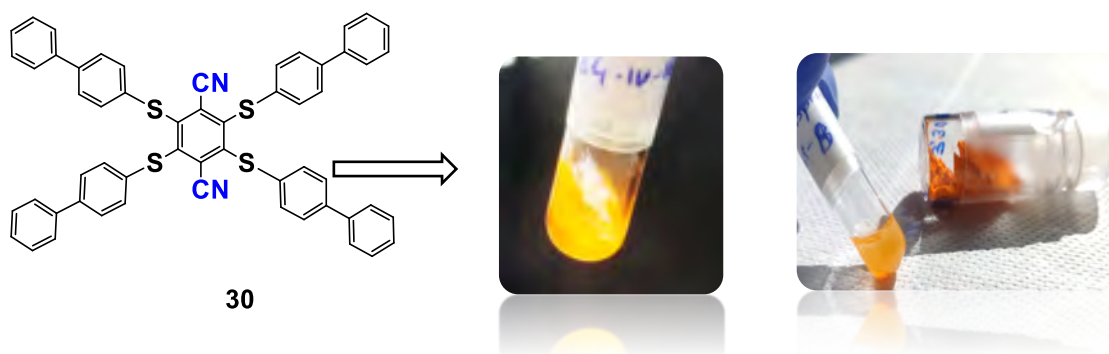


Figure 12: Highly luminescent asterisks (30) as bright yellow-orange solid (right).

All four asterisks (28 to 31) are luminescent. Asterisks (28) and (29) are yellow-orange but asterisk (29) shows some yellow helical coiled sheets by self-assembly in the tube (figure 11), whereas asterisk (30) is highly luminescent and bright orange in solution (figure 12). However, it is not much soluble in many organic solvents, but soluble in DMF, 1,2-dichlorobenzene and DMSO on heating.

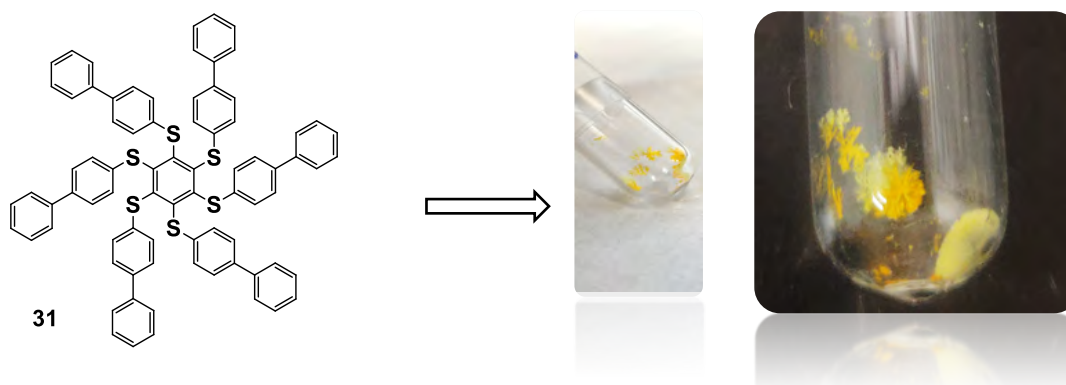


Figure 13: Recrystallized asterisk 31 with two different colors (yellow and orange), a solvatochromic effect.

Hexakis (4-biphenylthio)benzene (31) is a π -extended asterisk which recrystallizes in two different colors. Yellow and orange small crystals in DCM were obtained by slow evaporation of the solvent at room temperature. This compound seems solvatochromic (figure 13).

4.3 Photophysical studies (from the University of Bologna)

All compounds indicated in figure 14 were studied in DMF or in DCM **at the "G. Ciamician" chemistry department at the University of Bologna, under the**

supervision of professor Paola Ceroni and her colleagues. The absorption spectra of the compounds in DCM show several bands, the main one is peaked at 250 nm for the phenylthio asterisks and at 280 nm for the 4-biphenylthio asterisks (figure 15). The second one is observed at 330 nm for the phenylthio asterisks and redshifted by 20 nm for the 4-biphenylthio asterisks. In DMF, this series of compounds shows similar absorption spectra: PCNB is well soluble, only in a DMF solution (figure 15).

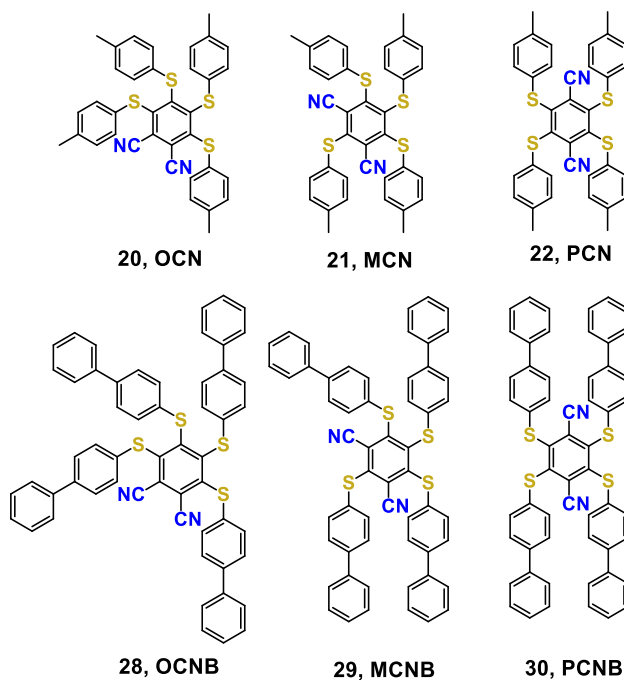


Figure 14 : chemical structures of the dicyanated asterisks under photophysical study.

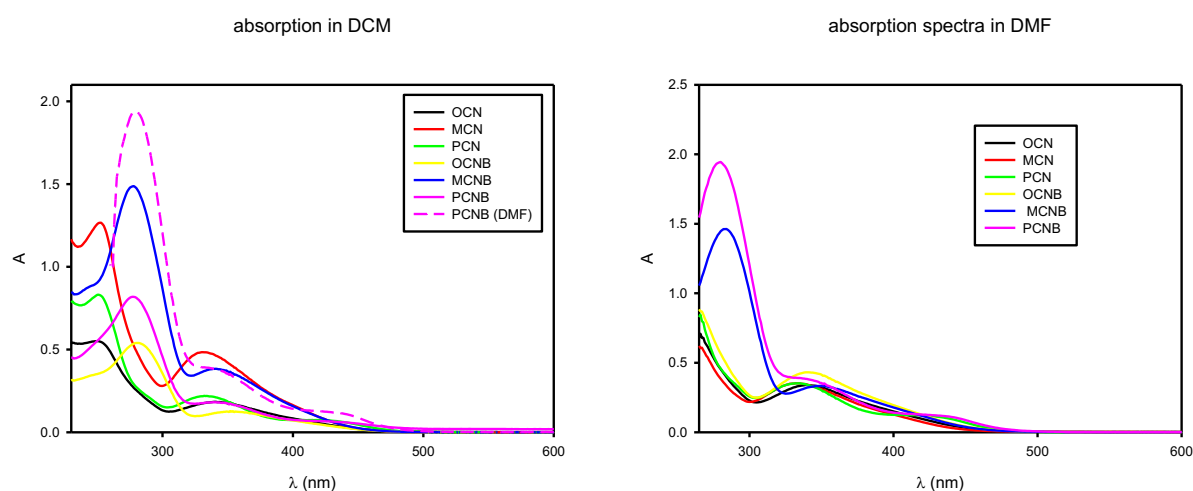


Figure 15: absorption spectra in DCM solution (left) and DMF solution (right) of **OCN** (black), **MCN** (red), **PCN** (green), **OCNB** (yellow), **MCNB** (blue), **PCNB** (purple).

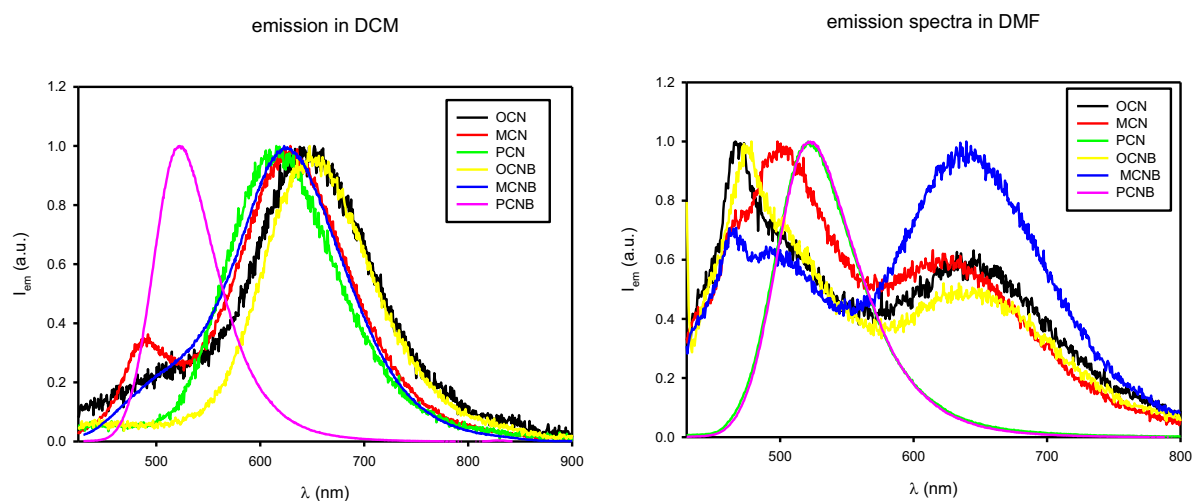


Figure 16 : Emission spectra in DCM solution (left) and DMF solution (right) of **OCN** (black), **MCN** (red), **PCN** (green), **OCNB** (yellow), **MCNB** (blue), **PCNB** (purple). $\lambda_{exc}=350$ nm

These compounds have different emission spectra as shown in figure 16. In DCM a weak emission is observed at 650 nm for all the compounds but for **PCNB**, it is observed an intense emission at 523 nm, due to scattering of this solution. As a consequence, the photophysical properties were recorded in DMF. In a DMF solution, **PCNB** is fully soluble and the same emission at 523 nm is observed with an emission quantum yield of 12.9% and a lifetime of 7 ns (figure 16). In a degassed solution, the emission quantum yield is slightly increased from 12.9% to 13.8%: this difference is within the experimental error and it demonstrates that this emission is a fluorescence. **PCNB** also shows a singlet oxygen production with a quantum yield of 32%. In DMF solution, also **PCN** shows a similar emission as **PCNB** with a lower emission quantum yield (4.3%) but a similar lifetime (6.9 ns). All the other compounds have a weak emission (emission quantum yield <1%) and a biexponential lifetime with a picosecond component and 5 or 25 ns components.

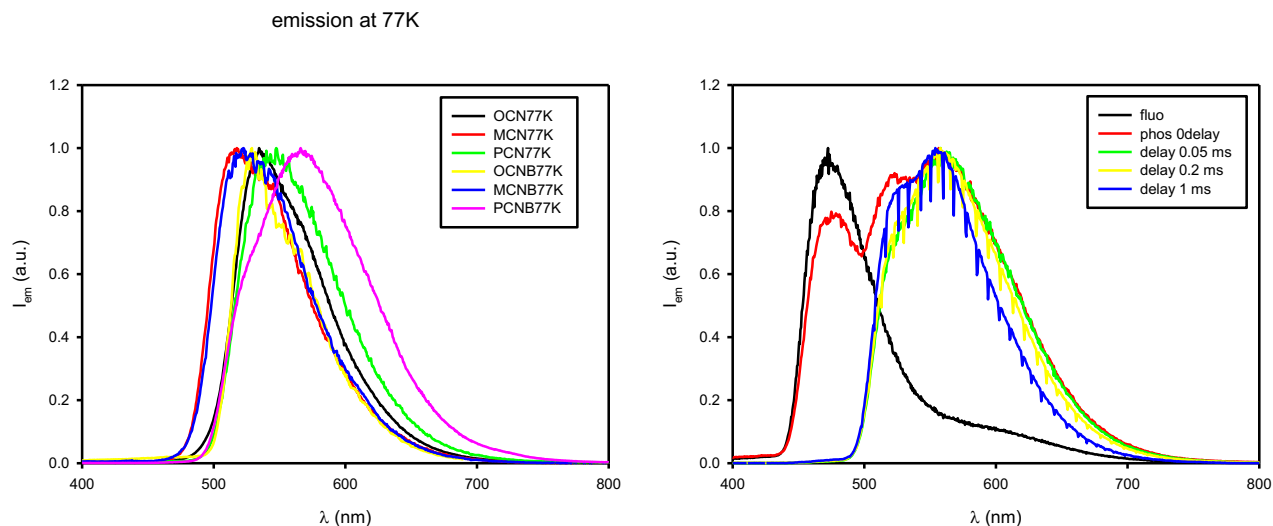


Figure 17: Emission spectra in DCM/MeOH 1:1 rigid matrix at 77K (left) of **OCN** (black), **MCN** (red), **PCN** (green), **OCNB** (yellow), **MCNB** (blue), **PCNB** (purple) and emission spectra at 77K at different delay of **PCNB**. $\lambda_{exc}=350$ nm, delay 0.05 ms **OCNB** (yellow), **MCNB** (blue), **PCNB** (purple).

The emission spectra of this series of compounds in a rigid matrix at 77 K (DCM/MeOH 1:1) is similar to the known hexakis(phenylthio)benzene asterisks with a green emission and a millisecond lifetime (figure 17). Differences were observed for **PCNB** where it is possible to observe a first emission with short lifetime at 480 nm and a second emission with longer lifetime at 550 nm (4 ms).

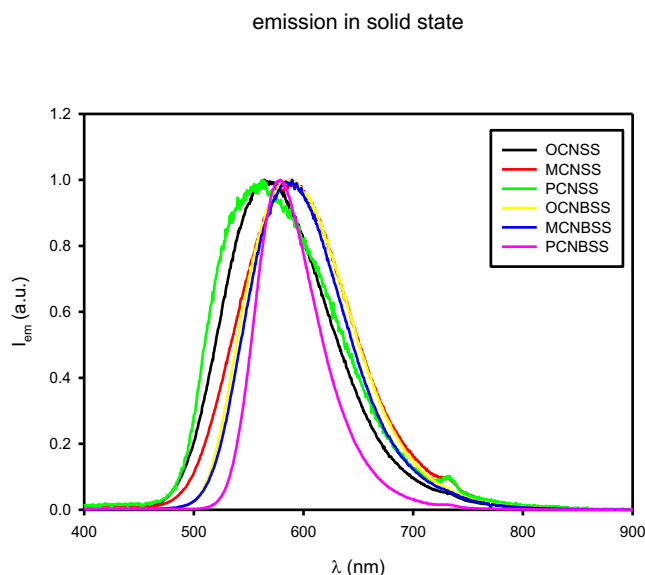


Figure 18: Emission spectra in solid state of **OCN** (black), **MCN** (red), **PCN** (green),

All these compounds are good phosphorescent emitters in the solid state with a yellow-orange emission and a microsecond lifetime (figure 18). The 4-biphenylthio

series have higher emission quantum yields and are redshifted compared to the phenylthio series, as summarized in Table 1.

Table 1 Photophysical properties of the asterisks (from figure 14).

	solid state			77K			sol DCM			sol DMF		
	Φ_{em}	λ_{em}/nm	τ (μs)	λ_{em}/nm	τ (ms)	λ_{em}/nm	Φ_{em}	λ_{em}/nm	Φ_{em}	τ_1 (ns)	τ_2 (ns)	
OCN	15.6%	564	12.2	534	7.3	652	0.41%	645	0.35%	0.7	23.8	
MCN	14.6%	587	5.34	518	24.7	629	0.98%	627	0.61%	0.8	4.7	
PCN	32.8%	562	2.38	548	3.08	615	0.60%	523	4.33%	6.9		
OCNB	28.6%	591	7.25	529	5.06	647	0.85%	644	0.38%	0.5	24.9	
MCNB	40.4%	590	5.28	523	4.06	624	1.61%	639	0.72%	0.31	6.7	
PCNB	41.0%	579	11.8	570	4.04	523		523	12.9%	7.0		

4.4 Conclusion

Seven novel asterisks were synthesized in excellent yield (>90%) and overall, ten asterisks, out of which four were with a π -extended system. All the asterisks were characterized by NMR (1H and ^{13}C) and HRMS. Photophysical studies were achieved with six asterisks. Absorption spectra was recorded in DMF and DCM, and emission spectra was recorded in DCM, DMF, DCM/MeOH 1:1 rigid matrix at 77K and in the solid state. The quantum yield of PCNB in the solid state is 41%, whereas, for others, the quantum yield was between 15-41%. We thus disclosed several new and highly phosphorescent emitters in the solid state, easily prepared, and from commercially available reagents. The benzene core of these asterisks is electron-poor because of two cyano groups. As a consequence, it is prone to sulfur and oxygen component exchanges in DCC, as similarly described for polymerization and depolymerization of polyarylene chalcogenides. [14] Thus, it may be possible that these series of phenylthio and 4-biphenylthio asterisks could be useful in dynamic nucleophilic aromatic substitutions toward some dynamic and self correcting materials having nice optical and emissive properties via rigidity-induced phosphorescence (RIP).

References of chapter 4

1. Y.-R. Wang, L. Feng, L. Xu, Y. Li, D.-D. Wang, J. Hou, K. Zhou, Q. Jin, G.-B. Ge, J.-N. Cui, L. Yang, *Chem. Commun.*, **2016**, 52, 6064-6067.

2. G. R. Kumar, S. K. Sarkar, P. Thilagar, *Chem. Eur. J.* **2016**, *22*, 17215-17225.
3. L. Wang, W. Wang, Z. Xie, *J. Mater. Chem. B*, **2016**, *4*, 4263-4266.
4. Y. Yuan, S. Xu, C.-J. Zhang, R. Zhang, B. Liu, *J. Mater. Chem. B* **2016**, *4*, 169-176.
5. O. Eiko, K. Sakamoto, T. Urano, *Color Material*, **2002**, *75*, 255-260
6. K. A. Volkov, G. V. Avramenko, V. M. Negrimovskii, E.A. Luk'yanets, *Russ. J. Gen. Chem.*, **2007**, *77*, 1108–1116.
7. S. Riebe, C. Vallet , F. V. Vight, D. G. Abradelo, C. Wölper, C. A. Strassert, G. Jansen, S. Knauer, J. Voskuhl, *Chem. Eur. J.* **2017**, *23*, 13660-13668.
8. P. Zeng, J. Wang, Y. Guo, R. Li, G. Mei, T. Peng, *Chem. Eng. J.*, **2019**, *373*, 651-659.
9. W. Ou, R. Zou, M. Han, L. Yu, C. Su, *Chin. Chem. Lett.*, **2020**, *31*, 1899-1902.
10. M. Villa, S. D'Agostino, P. Sabatino, R. Noel, J. Busto, M. Roy, M. Gingras, P. Ceroni, *New J. Chem.*, **2020**, 1-7.
11. H. Bhatia, I. Bhattacharjee, D. Ray, *J. Phys. Chem. Lett.* **2018**, *9*, 3808–3813.
12. Z. Nelson, N. A. Romero, J. Tiepelt, M. Baldo, T. M. Swager, *Macromolecules* **2021**, *54*, 6698-6704.

CHAPTER 5

PERSULFURATED BENZENE-CORED ASTERISKS WITH π -EXTENDED THIONAPHTHYL ARMS: SYNTHESIS, STRUCTURAL, PHOTOPHYSICAL AND COVALENT DYNAMIC PROPERTIES

5.0 Introduction

5.1 Objectives

5.2 Results and discussion

5.2.1 Synthesis

5.2.2 Mechanistic observation

5.3 Sulfur exchange components (the "sulfur dance")

5.4 Structural and supramolecular studies by sc-XRD

5.5 Conclusion

Note: This chapter is mostly taken from an article submitted for publication in a scientific journal. This work comprises some photophysical studies achieved by the group of Pr. Paola Ceroni, "G. Ciamician" department of chemistry at the University of Bologna. Sc-XRD studies were achieved by Dr. Michel Giorgi, from Aix-Marseille Université.

5.0 Introduction

Naphthalene is a special compound due to its structural (bicyclic polycyclic aromatic hydrocarbon) photophysical and physical properties. It is volatile because it sublimates readily at room temperature. Naphthalene is much more reactive than benzene toward electrophiles, notably for electrophilic aromatic substitutions. In spite of being toxic and an air pollutant, it is widely used as an intermediate to produce phthalic anhydride and pesticides. It can be found outdoor and indoor due to biomass burning, fuels, chemical industries, oil combustion, mothballs, pesticides, tobacco. Naphthalene derivatives have also found some uses in materials science and in photophysics. Naphthalene is an extension of the p -system of a benzene ring. It could thus be interesting to merge this unit with the known persulfurated benzene core asterisks, mentioned in the previous chapters.

The enhanced emission of light in rigid, constrained or crystalline state, is commonly called: "Aggregation-Induced Emission (AIE)". It has gained a wide attention in the last years^{[1],[2],[3],[4]} due to the development of light-emitting molecular systems

and devices, luminescent sensors and bioimaging. In most cases, the emission enhancement is triggered by crystallization or self-assemblies (aggregation), which causes restriction of intramolecular motions, thus favoring radiative deactivation of the excited state from the luminescent moiety.^[5] Some of the most emissive AIE systems are based on a family of persulfurated aromatic molecules,^[6] hereafter called molecular asterisks,^[7] where a central benzene ring is bound to six phenylthio groups. The parent compounds, hexakis(phenylthio) benzene (**3**)^[8] and hexakis (4-methylphenylthio)benzene (**4**)^[9], are known since 1957 and 1975, respectively. In spite of their early discovery, and being reported in patents since 1963,^[9] their exalted AIE properties were overlooked, and we disclosed them in 2013.^{[10],[11]} These compounds are not emissive in solution. However, when intramolecular motions are restricted in the solid state or in a rigid matrix, a bright green phosphorescence appears. A striking example of such phenomena is from (**4**), which is one of the most phosphorescent emitters known to date in the solid state, with an emission quantum yield reaching almost 100%.^[12] This phenomenon is called "Rigidification-Induced Phosphorescence" (RIP). Several structural and photophysical studies on this family of molecules have been carried out, but most of them focused on the functionalization of the outer phenyl rings at *para* or *ortho* positions (-H, -CH₃, -OCH₃).^{[12],[13],[14]} According to the Van Der Waals volume and the electronic contribution of these substituents, they could modulate the conformational dynamics, supramolecular interactions, and the opto-electronic properties of these asterisks. For instance, substituents like amide units^{[15],[16]} and chiral groups^{[17],[18]} were designed to generate Rigidification-Induced Phosphorescence (RIP) by some cohesive supramolecular interactions. Another example comes from the nano-organized formation of silica nanoparticles encapsulating covalently-bound phosphorescent asterisks in the search for new oxygen-sensing devices.^[16] The central persulfurated benzene core was also covalently-linked to some metal-chelating moieties like terpyridine^[19] or carboxylic acids^[20] to "turn on" phosphorescence by a selective complexation with some metal ions like Ag(I), Mg(II), Zn(II) or Pb(II). Structural rigidification occurs by ions complexation, thus generating a self-assembly of a supramolecular polymer (nanoparticles), with simultaneous enhanced phosphorescence by RIP in a dual mode detection of metal ions (simultaneous nanoparticles formation and light emission).

5.1 Objectives

Here, the purpose of this work is to report the consequences on the chemical, photophysical, and structural features of these molecular systems, after extending the peripheral π -system of a persulfurated benzene-cored asterisk (**3**). **Figure 1** lists a set of two regioisomeric asterisks (**5**) and (**6**) under study, with thionaphthyl substituents, along with a comparison (or guidance) with reference naphthalene derivatives (**1**) and (**2**). In short, most investigations on hexathio benzene-cored asterisks are relevant to the functionalization of the thiophenyl arms. However, an extension of the peripheral π -system with polycyclic aromatic hydrocarbons (PAH), such as naphthalene, has only been reported once in a structural study with (**6**),^[21] by overlooking at the chemical, photophysical and electronic properties. No comparison to other regioisomeric asterisks such as (**5**) was reported. Thus, an extension of the π -system surrounding a persulfurated benzene core could be important in search for new photophysical and electronic properties, due to electronic couplings with the central core. Additionally, a structural study is suited for evaluating the contribution of steric and electronic effects in search for new multi-responsive all-organic phosphorophores. To top it all off, we report new sulfur component exchange reactions in the frame of reversible S_NAr in Dynamic Covalent Chemistry (DCC) in a continuation of previous observations.²²

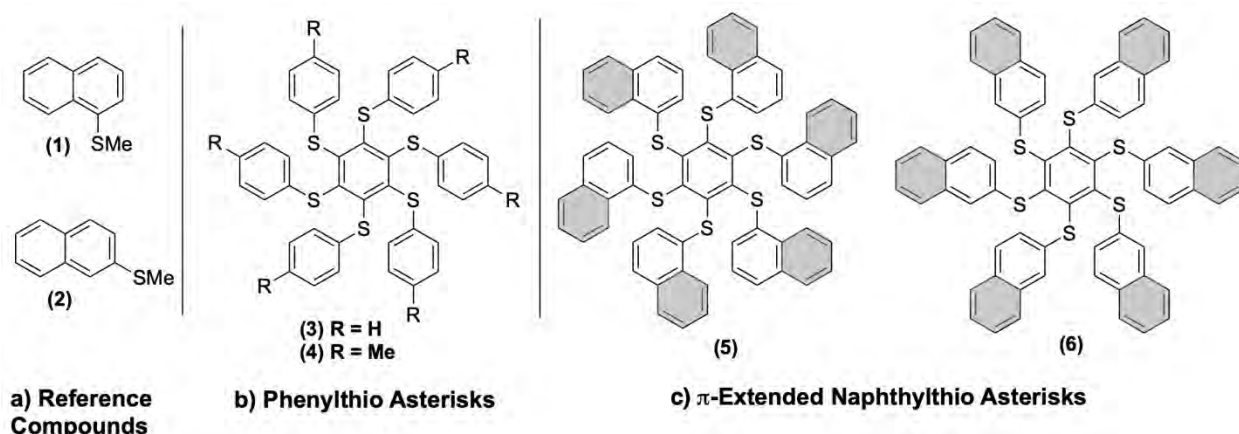


Figure 1. List of compounds under study: a) reference (methylthio)naphthalene regioisomers (**1**) and (**2**); b) reference hexakis(phenylthio) benzene (**3**) and hexakis(4-methylphenylthio)benzene (**4**); c) regioisomeric π -extended hexakis(naphthylthio) benzene asterisks (**5**) and (**6**) (gray rings indicate π -extension).

5.2 Results and discussion

5.2.1 Synthesis

Prior to some chemical, photophysical and structural studies on the π -extended thionaphthyl systems (**5**) and (**6**), the preparation of reference persulfurated benzene-cored asterisks (**3**)^[8] and (**4**)^[9] was achieved according to known literature methods. The reference thiomethylated naphthalene regioisomers (**1**)^[23] and (**2**)^[24] were also synthesized (see Supporting information), according to common procedures for methylating aromatic thiols. Thus, 1-naphthalenethiol reacted with an excess of iodomethane (potential carcinogen!) in the presence of dry potassium carbonate in DMF as a polar aprotic solvent. After sealing the mixture under argon in a pressure tube, it was stirred for four days at 50°C. However, the reaction was incomplete, and stirring was continued for seven days at 70°C, and then for four days at 80°C to ensure completion. These conditions were required because 1-naphthalenethiol is much less reactive at a peri position than for 2-naphthalenethiol. The latter reacted under milder conditions for two days and half at 40°C for providing 98% yield of the expected thioether (**2**).

The synthesis of the π -extended thionaphthyl systems (**5**) and (**6**) started from hexachlorobenzene (1.0 mol-eq) with a 1.5 fold excess of thiol (9.0 mol-eq) and potassium carbonate (9.0 mol-eq) in DMF. After bubbling argon for removing dioxygen and sealing the reaction tube, the mixture was vigorously stirred at 84°C for seven days in the case of asterisk (**5**). After purification by chromatography, it afforded (**5**) as a yellow solid in a 95% yield. A similar synthetic procedure was followed for (**6**), while heating at 80°C for four days. It afforded (**6**) as a yellow solid in a 73% yield.

5.2.2 Mechanistic observation

When synthesizing asterisk (**5**), we isolated the side-product (**7**) and its structure was determined by sc-XRD, as shown in **Figure 2**. An incomplete sulfuration of hexachlorobenzene led to a 1,2,3,4-tetrasulfurated benzene core, which underwent a double cyclization to produce dibenzothiophene units in a helical [5]dithiohelicene structure (**7**).

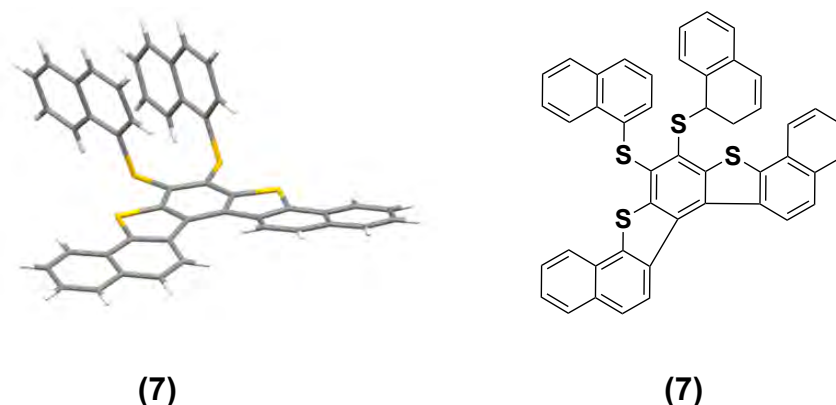
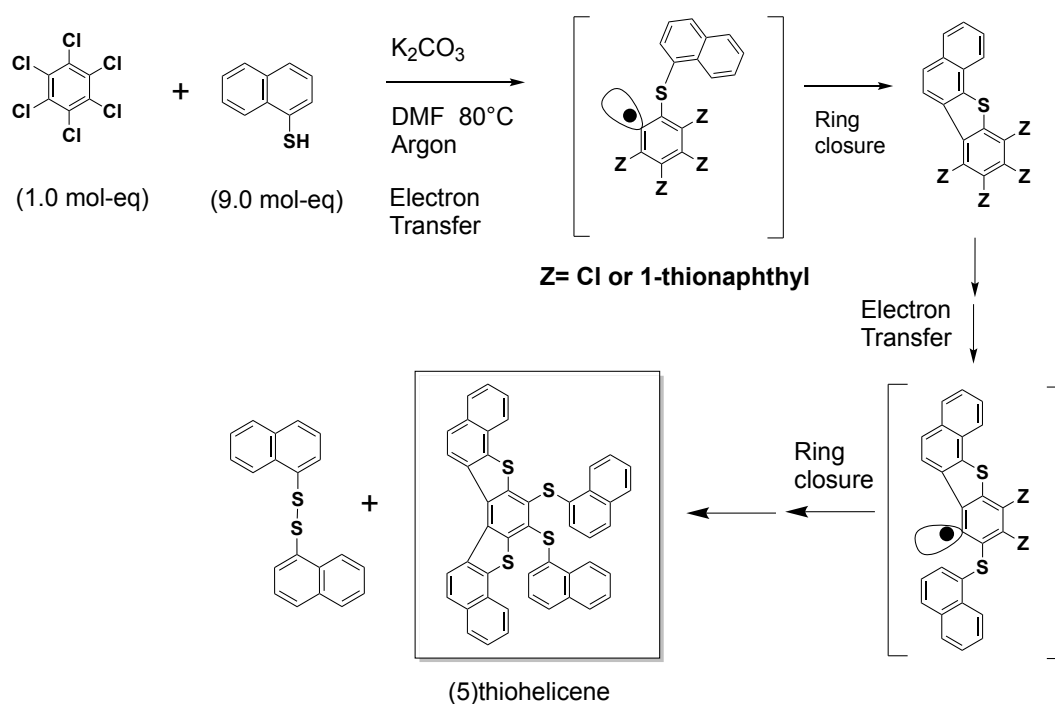


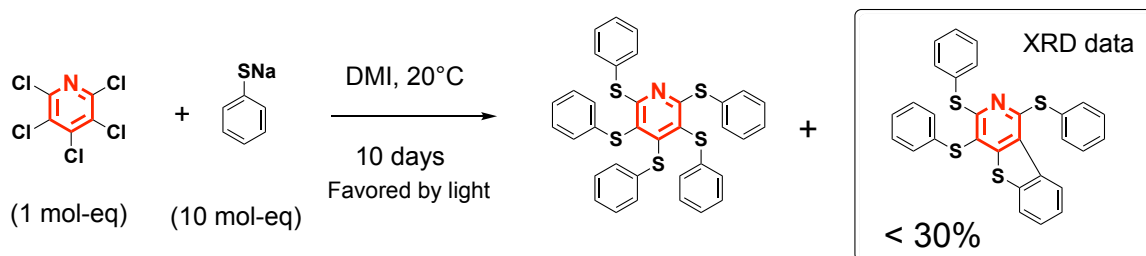
Figure 2. Structure determination by sc-XRD of by-product (7) isolated from the synthesis of (5). It incorporates two fused dibenzothiophene units in a [5]dithiohelicene structure.

A tentative mechanistic rationale for both cyclizations would involve two radical cyclizations (scheme 1). The latter could be initiated either from some radical nucleophilic substitutions ($S_{RN}1$), or from some electron-transfers coming from the thionaphthyl anions, as a reducing agent. It is not known at which stage of the sulfuration these radical processes could take place.



Scheme 1. A radical mechanism is tentatively proposed to explain the formation of (7) incorporating dibenzothiophene units, after the persulfuration of hexachlorobenzene.

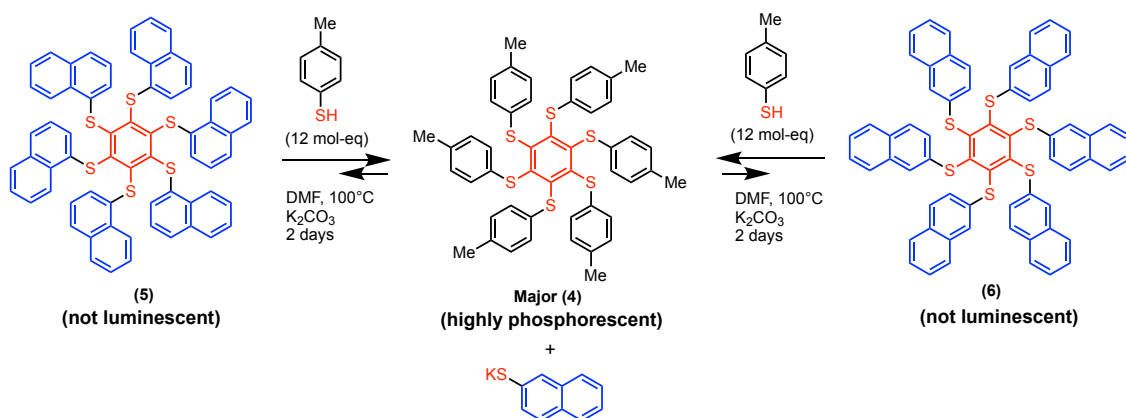
This mechanistic proposal is in agreement to a literature precedent for explaining the formation of a benzothienopyridine unit by a radical cyclization during the persulfuration of pentachloropyridine, as shown in **Scheme 2**.^[25]



Scheme 2. Proposed radical mechanism to explain the formation of a benzothienopyridine unit during the persulfuration of pentachloropyridine.

5.3 Sulfur exchange components (the "sulfur dance")

Continuing our studies on dynamic sulfur exchange reactions by S_NAr of potent uses in dynamic covalent chemistry (DCC), we investigated the exchanges of thionaphthyl units by thiophenyl ones (**scheme 3**). In light of leaving groups abilities, it is expected that a naphthylthio unit should be replaced with a preference to a 4-methylphenylthio one. Indeed, the naphthylthiolate anion is more stable than the 4-methylphenylthiolate anion. We thus ran experiments under conditions toward a full conversion of asterisk (**5**) or (**6**) into asterisk (**4**), by using a large excess of 4-methylbenzenethiol (12 mol-eq) in the presence of K_2CO_3 in DMF at 100°C. Analysis of both reaction mixtures indicated the presence of the corresponding naphthyl disulfides, as oxidized leaving groups, and the formation of asterisk (**4**) as a major component (>50% yield). It should be pointed out that poorly emissive asterisks (**5**) or (**6**) can be converted to (**4**) as one of the most phosphorescent solids known to date.^[12] These results convey new information on benzene-cored asterisks with π -extended systems, and broaden the scope of sulfur exchange reactions in the "sulfur dance" around a benzene core by dynamic S_NAr reactions.



Scheme 3. Sulfur component exchange reactions. Conversion of poorly emissive π -extended 1- or 2-naphthylthio benzene-cored asterisks (**5**) or (**6**) into highly phosphorescent asterisk (**4**) (solid state) in a > 50% yield.

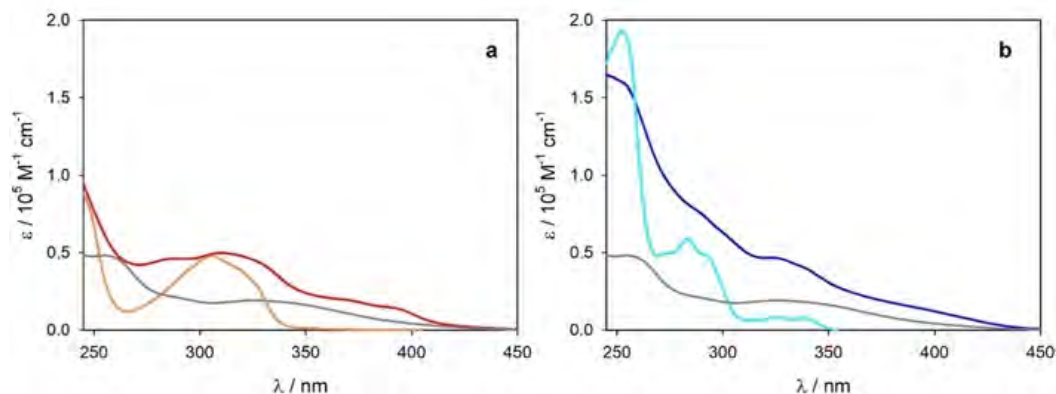


Figure 1. Absorption spectra in air-equilibrated CH_2Cl_2 solution : (a) Asterisk (**5**) (red line) and asterisks (**4**) (grey line) and model compound (**1**) (orange line), (b) Asterisk (**6**) (blue line) and asterisks (**4**) (grey line) and model compound (**2**) (cyan line). For the sake of comparison, the molar absorption coefficient of (**1**) and (**2**) has been multiplied by 6.

The absorption spectra of (**5**) and (**6**) are reminiscent of the numerical sum of the spectra of their model compounds, namely (**4**) and 6 times (**1**) or (**2**). The emission spectra of the asterisks and their model compounds in dichloromethane solution are reported in **Figure 4**, and compared to those recorded in $\text{CH}_2\text{Cl}_2/\text{MeOH}$ (1:1 V/V) in a rigid matrix at 77 K. Asterisk (**5**) shows two emission peaks at 350 and 430 nm (solid red line in **Figure 4a**). The high-energy band can be attributed to the naphthalene fluorescence by comparison with the model compound (**1**) (solid orange line in **Figure 4a**): the corresponding fluorescence quantum yield is strongly diminished (Table 1), demonstrating an efficient quenching mechanism. The same situation is observed in

the comparison between asterisk (**6**) and (**2**) emission spectra (**Figure 4b**). It is worth noting that the fluorescence bands of (**6**) are red-shifted compared to those of (**5**), in agreement with the red-shift observed for model compound (**2**) versus (**1**).

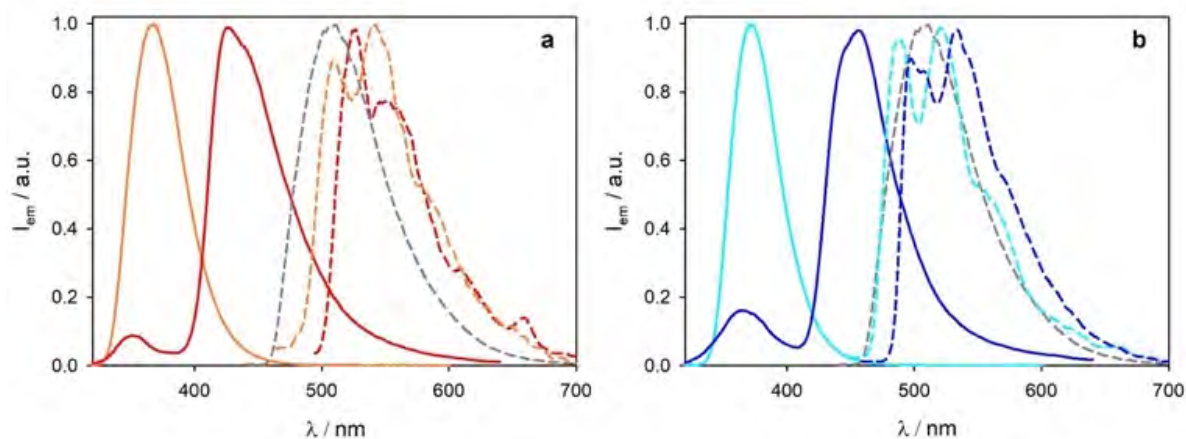


Figure 4. Normalized emission spectra in air-equilibrated CH_2Cl_2 solution at room temperature (solid lines) and in $\text{CH}_2\text{Cl}_2/\text{MeOH}$ 1:1 rigid matrix at 77 K (dashed lines) : (a) Asterisk (**5**) (red line) and asterisk (**6**) (grey line) and model compound (**1**) (orange line), (b) asterisk (**6**) (blue line) and asterisks (**4**) (grey line) and model compound (**2**) (cyan line). $\lambda_{\text{ex}} = 300$ nm.

The fluorescence band at 430-450 nm is somewhat reminiscent of the fluorescence of naphthalene excimers,^{[27],[28],[29]} but the very short lifetime (<0.2 ns, Table 1) rules out this assignment. It has never been observed for previously investigated hexakis(phenylthio) benzene-cored asterisks, and we tentatively attribute this emission to

the fluorescence decay of the per-(phenylthio)benzene core, suggesting a less efficient intersystem crossing to the lowest triplet state for asterisks (**5**) and (**6**) compared to (**4**). In solid state, asterisks (**5**) and (**6**) are not luminescent and the typical green phosphorescence of (**4**) (**Figure 4**) is not observed, confirming that the presence of the peripheral naphthalene units strongly affects the luminescence properties of the asterisks and the population of the triplet state of the persulfurated core.

Table 1. Most relevant photophysical data of the asterisks (**5**) and (**6**) in CH₂Cl₂ at 298 K and in CH₂Cl₂/MeOH (1:1 v/v) at 77 K.

Compound	298 K			77 K	
	λ_{em} (nm)	Φ_{em}	τ (ns)	λ_{em} (nm)	τ (s)
1-Thionaphthyl Asterisk (5)	350 430	<0.01% 0.17%	[a] <0.2	525	0.12
2-Thionaphthyl Asterisk (6)	365 455	0.2% 2.7%	[a] <0.2	535	0.30
1-MeS-Naphthalene(1)	370	1.9%	0.60	510	0.20
2-MeS-Naphthalene (2)	375	4.3%	1.56	490	0.31
4-Me-Thiophenyl Asterisk (4)	[b]	[b]	[b]	505	4.0x10 ⁻³

[a] The emission intensity is too weak to measure the corresponding lifetime.

[b] No emission is observed in DCM solution at 298 K and a strong phosphorescence in the solid state at 513 nm with Φ_{em} = 100% and τ = 3.0 μ s.^[12]

The emission spectra of (**5**) and (**6**) in a CH₂Cl₂/MeOH (1:1 v/v) rigid matrix at 77 K (dashed lines in **Figure 4**) show a vibrationally structured band with the highest energy peak at 550 nm. The model compounds (**1**) and (**2**) show a very similar emission spectra with a small blue shift. The corresponding lifetimes are in the second range, in agreement with the phosphorescence decay of (**1**) and (**2**) and 3 orders of magnitude higher than that observed for the phosphorescence of (**4**) (**Table 1**).

The absence of the typical emission of a per(phenylthio)benzene core in the solid state, and the phosphorescence with long lifetime in a rigid matrix at 77 K could be explained by an energy transfer from the triplet state of the persulfurated benzene-cored asterisks to the outer naphthalene moieties, as schematically depicted in **Figure 5**. This result is confirmed by the fact that excitation in the range 400-450 nm, where only the persulfurated core absorbs light, results in the typical naphthalene phosphorescence.

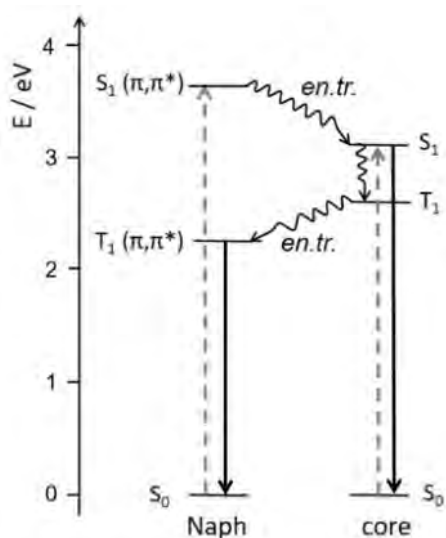


Figure 5. Schematic energy level diagram showing the absorption (dashed grey lines), emission (solid black lines), and non-radiative processes (wavy lines) occurring in asterisks (**5**) and (**6**) at 77 K.

5.4 Structural and supramolecular studies by sc-XRD

A structural study by sc-XRD (single-crystal X-ray diffraction) leading to the characteristics of both regioisomeric systems (**5**) and (**6**) is useful to better understand the systems, which itself, should be modulated by the conformational features, distortion of π -system and supramolecular interactions. **Figures 6** and **7** represents the two crystalline regioisomeric asterisks (**5**) and (**6**) after sc-XRD analysis.

In compound (**5**) the center of the central π cycle (centroid of Cg1) lies on the crystallographic center of symmetry and thus the asymmetric unit is only half of the asterisk. Two opposite S-naphthyl units are almost perpendicular to that ring (dihedral equal to $88.27(8)^\circ$) and they are engaged into symmetric intramolecular CH/ π interaction with it: the distance C5---Cg1 = $3.688(2)$ Å and the angle C5-H5---Cg1 is equal to 140° . The four remaining thionaphthyl units are parallel by adjacent pairs and have angles of $67.23(10)^\circ$ and $64.06(10)^\circ$ respectively with the central π cycle (**Figure 6**). They interact by pairs through intramolecular π - π stacking (dihedral equal to $6.32(7)^\circ$) but are also engaged into intermolecular CH/ π and π - π interactions with symmetry-related molecules within the lattice (**table S1**: see experimental part).

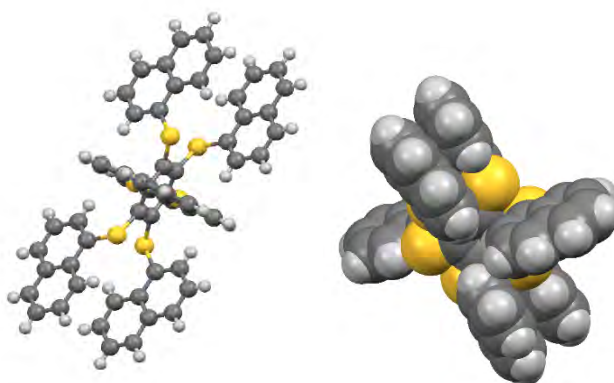


Figure 6: Structural and conformational analysis of **(5)** by sc-XRD.

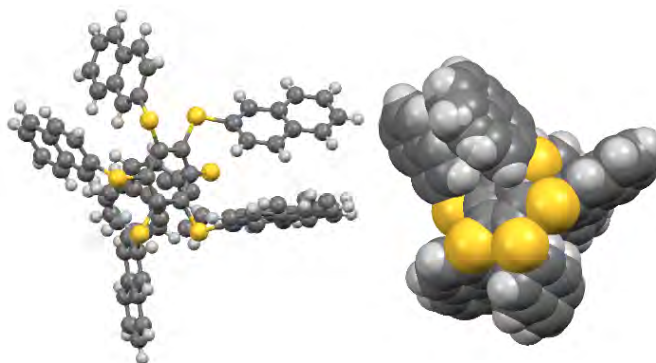


Figure 7: Structural and conformational analysis of **(6)** by sc-XRD

As shown in **Figure 7**, the behavior of **(6)** is different. The asymmetric unit is in general positioned within the unit cell, and the thionaphthyl substituents are not related by symmetry. They adopt an up-down-up-(down)₃ conformational sequence relative to the central π cycle. The dihedrals of the S-naphthyl group to the mean central ring have a large diversity and range from $63.0(5)^\circ$ to $117.5(5)^\circ$. Opposite to **(5)**, this arrangement only favors CH/ π interactions; no intra- or intermolecular π - π stacking is observed (**Table S2**, see experimental part).

These different organizations within both asterisks have a remarkable influence on the deformation of the central benzene ring. The central benzene core of **(5)** is not distorted (weighted average absolute torsion angle = 4.85°) while the puckering value Q for the ring in **(6)** is equal to $0.144(3)\text{\AA}$ with a weighted average absolute torsion angle equal to 8.01° (Figure 8).^{[30],[31]}



Figure 8: distorted central benzene core of (6)

In compound (5), the benzene core is protected from external influences by the symmetric arrangement of the substituents and the interactions they provide. On the contrary, the same ring in (6) is affected by the sum of the strains brought by all the asymmetric intra and intermolecular CH/ π interactions. The better accessibility of the benzene core in (6) is also reflected by the presence of several intermolecular S-H interactions (C(H)---S distances around 3.7 Å) while the C(H)---S distances in (5) are all longer than 3.8 Å. Interestingly, the distortion of the central benzene core in (6) is comparable to that observed in the previously published naphthalenethio benzene-cored asterisk, despite different arrangement of the naphthalene moieties.^[20] In that previous report, the puckering value Q is about 0.12 Å and the weighted average absolute torsion angle is equal to 8.45°, but the substituents are in a conformational sequence up-up-down-down-up-down. Unlike (6), this conformation allows the formation of some intermolecular π - π interactions.

5.5 Conclusion

We synthesized two regioisomeric persulfurated benzene-cored asterisks (5) and (6) for investigating the influence of peripheral π -extended systems on their photophysical, structural and dynamic chemical properties, compared to (3) and (4). The minor by-product (7) with a helical [5]dithiohelicene structure was isolated. It could result from radical cyclizations through S_{RN}1 or other electron-transfer mechanisms. This observation is important in the mechanism of persulfuration. We report different conformational behaviors, structural distortions of the core, and supramolecular interactions of regioisomers (5) and (6) in the crystalline state. The higher symmetry of compound (5) provides intramolecular π - π interactions with the naphthyl substituents, whereas a more disymmetrical order of (6) generates many C-H/ π interactions, and a strong distortion from planarity of the benzene core to accommodate these interactions. As for the photophysical features, the lifetimes of the two phosphorescent excited states of (5) and (6) are different from (4) at 77 K: a few ms for the persulfurated

asterisks (**4**)^{[11],[12]} and a few seconds for (**5**) and (**6**) or the thiomethylated naphthalenes (**1**) and (**2**).^[32] This difference is due to the nature of the electronic transitions of the two chromophores and the corresponding rate of spin-forbidden transitions: a charge-transfer electronic transition for the persulfurated asterisk and π , π^* electronic transition of a naphthalene unit. The lowest triplet excited state of a thionaphthalene unit and that of persulfurated benzene asterisks (**4-6**) are very close in energy. The absence of the typical emission of a per(phenylthio)benzene core in the solid state, and the phosphorescence with long lifetime in a rigid matrix at 77 K could be explained by an energy transfer from the triplet state of the persulfurated benzene core to the outer naphthalene moieties (**Figure 5**). In conclusion, a π -extension of the per(phenylthio) benzene unit inhibits phosphorescence. As for sulfur exchange reactions, both non emissive (**5**) and (**6**) are converted to highly emissive (**4**).^[11] All results convey new structural, photophysical, and predictive properties on π -extended per(phenylthio) benzene asterisks. The scope of dynamic S_NAr around a benzene core is broadened, in the frame of dynamic covalent chemistry, for making new optical and electronic materials.

References

- [1] J. Mei, Y. Hong, J. W. Y. Lam, A. Qin, Y. Tang, B. Z. Tang, *Adv. Mater.* **2014**, *26*, 5429-5479.
- [2] J. Mei, N. L. C. Leung, R. T. K. Kwok, J. W. Y. Lam, B. Z. Tang, *Chem. Rev.* **2015**, *115*, 11718-11940.
- [3] M. Baroncini, G. Bergamini, P. Ceroni, *Chem. Commun.* **2017**, *53*, 2081-2093.
- [4] M. Hayduk, S. Riebe, J. Voskuhl, *Chem. Eur. J.* **2018**, *24*, 12221-12230.
- [5] Y. Wang, G. Zhang, M. Gao, Y. Cai, C. Zhan, Z. Zhao, D. Zhang, B. Z. Tang, *Faraday Discuss.* **2017**, *196*, 9-30.
- [6] M. Gingras, J.-M. Raimundo, Y. M. Chabre, *Angew. Chem. Int. Ed.* **2006**, *45*, 1686-1712; *Angew. Chem.* **2006**, *118*, 1718.
- [7] M. Gingras, A. Pinchart, C. Dallaire *Angew. Chem. Int. Ed. Engl.* **1998**, *37*, 3149-315; *Angew. Chem.* **1998**, *110*, 3338.
- [8] R. Adams, Reifschneider, W.; Nair, M. D. *Croat. Chem. Acta* **1957**, *29*, 277-285; b) Adams, R.; Ferretti, A. *J. Am. Chem. Soc.* **1959**, *81*, 4927-4931.
- [9] a) B.F. Malichenko, L.P. Robota *Zh. Org. Khim.* **1975**, *11*, 778-78; b) A.D.U. Hardy, D.D. MacNicol, D.R. Wilson, *J. Chem. Soc. Perkin Trans II* **1979**, 1011-1019.
- [10] Some applicative areas of hexakis(arylthio)benzenes were disclosed in industry as early as in 1963. Patents on biocidal properties as herbicides, insecticides, anti-oxidant

- additives to lubricating oils, intermediates in dyestuffs and biologically active materials were reported: a) Reifschneider, W. Aralkyl Poly(thioethers), (Dow Chemicals Co.) US 3 100 802-A, **1963**. b) Reifschneider, W. Thioethers. (Dow Chemicals Co.), US 3 228 989, **1966**. c) Reifschneider, W. Hexakis thioethers (Dow Chemicals Co.), US 3 311 664, **1967** [Chem. Abstr. **1967**, 67, 402893]; d) Spivack, J. D. Compositions Stabilized with Poly(alkylthio)benzenes (Ciba-Geigy AG), DE 2 819 882, **1978** [Chem. Abstr. **1978**, 90,88309z].
- [11] G. Bergamini, A. Fermi, C. Botta, U. Giovanella, S. Di Motta, F. Negri, R. Peresutti, M. Gingras, P. Ceroni, *J. Mater. Chem. C* **2013**, 1, 2717-2724.
- [12] A. Fermi, G. Bergamini, R. Peresutti, E. Marchi, M. Roy, P. Ceroni, M. Gingras, *Dyes Pigm.* **2014**, 110, 113-122.
- [13] J.H.R. Tucker, M. Gingras, H. Brand, J.-M. Lehn, *J. Chem. Soc. Perkin Trans. II* **1997**, 1303-1307.
- [14] M. Villa, S. D'Agostino, P. Sabatino, R. Noel, J. Busto, M. Roy, M. Gingras, P. Ceroni, *New J. Chem.* **2020**, 44, 3249-3254.
- [15] H. Wu, C. Hang, X. Li, L. Yin, M. Zhu, J. Zhang, Y. Zhou, H. Ågren, Q. Zhang, L. Zhu, *Chem. Commun.* **2017**, 53, 2661-2664.
- [16] M. Villa, B. Del Secco, L. Ravotto, M. Roy, E. Rampazzo, N. Zaccheroni, L. Prodi, M. Gingras, S. A. Vinogradov, P. Ceroni, *J. Phys. Chem. C* **2019**, 123, 29884-29890.
- [17] M. Sleiman, A. Varrot, J.-M. Raimundo, M. Gingras, P. G. Goekjian *Chem. Commun.* **2008**, 6507-6509.
- [18] H. Wu, Y. Zhou, L. Yin, C. Hang, X. Li, H. Ågren, T. Yi, Q. Zhang, L. Zhu, *J. Am. Chem. Soc.* **2017**, 139, 785-791.
- [19] A. Fermi, G. Bergamini, M. Roy, M. Gingras, P. Ceroni, *J. Am. Chem. Soc.* **2014**, 136, 6395-6400.
- [20] M. Villa, M. Roy, G. Bergamini, M. Gingras, P. Ceroni, *Dalton Trans.* **2019**, 48, 3815-3818.
- [21] D. D. MacNicol, P. R. Mallinson, A. Murphy, G.J. Sym, *Tetrahedron Lett.* **1982**, 23, 4131-4134.
- [22] M. Villa, "Smart and Highly Phosphorescent Asterisks for (Bio)Sensors, Antennae, and Molecular Imaging", doctoral dissertation, Aix-Marseille Université, Marseille, France and University of Bologna, Bologna, Italy, Dec. 14 **2018**; <https://ecole-doctorale-250.univ-amu.fr/fr/soutenance/336>.
- [23] a) C. G. Overberger, S. P. Ligthelm, E. A. Swire, *J. Am. Chem. Soc.* **1950**, 72, 2856-2859; b) F. Taboury, *Ann. Chim. Phys.* **1908**, 15, 5-66.
- [24] a) A. Gasco, G. Di Modica, E. Barni, *Annali di Chimica* (Rome, Italy) **1968**, 58, 385-392; b) C. G. Overberger, S.P. Ligthelm, E.A. Swire *J. Am. Chem. Soc.* **1950**, 72, 2856-2859.

- [25] C.J. Gilmore, D.D. MacNicol *Tetrahedron Lett* **1984**, 38, 4303-4306.
- [26] B. Narayan, K. Nagura, T. Takaya, K. Iwata, A. Shinohara, H. Shinmori, H. Wang, Q. Li, X. Sun, H. Li, S. Ishihara, T. Nakanishi, *Phys. Chem. Phys. Chem.* **2018**, 20, 2970-2975.
- [27] D. Parker, J. A. G. Williams, *J. Chem. Soc., Perkin Trans. 2* **1995**, 1305-1314.
- [28] C. Saudan, V. Balzani, P. Ceroni, M. Gorka, M. Maestri, V. Vicinelli, F. Vögtle, *Tetrahedron* **2003**, 59, 3845-3852.
- [29] E. Marchi, M. Baroncini, G. Bergamini, J. Van Heyst, F. Vögtle, P. Ceroni, *J. Am. Chem. Soc.* **2012**, 134, 15277-15280.
- [30] A. Domenicano, A. Vaciago, C. A. Coulson, *Acta Cryst.* **1975**, B31, 221-234.
- [31] D. Cremer, J. A. Pople *J. Am. Chem. Soc.* **1975**, 97, 1354-1358.
- [32] A. C. M. Montalti, L. Prodi, M. Gandolfi, *Handbook of Photochemistry*, Boca Raton: CRC Press, **2006**.

CHAPTER 6

"THE SULFUR AND OXYGEN DANCE" AROUND ARENES AND HETEROARENES - DYNAMIC COVALENT NUCLEOPHILIC AROMATIC SUBSTITUTION

- 6.1 Introduction - Dynamic Covalent Chemistry (DCC)
- 6.2 Scope of reversible processes and reactions in DCC
- 6.3 Methods to verify the reversibility of a chemical process.
- 6.4 Summary of general applications relevant to DCC
- 6.5 Survey of reversible nucleophilic aromatic substitutions in the literature
- 6.6 Thesis work on DCC with polysulfurated benzene-cored asterisks

6.7 Manuscript submitted for publication entitled: "The Sulfur Dance" Around Arenes and Heteroarenes - Dynamic Covalent Nucleophilic Aromatic Substitution"

- 6.7.1 Introduction
- 6.7.2 Results and Discussion
- 6.7.3 Sulfur component exchanges
 - 6.7.3.1 Hexasulfurated asterisks
 - 6.7.3.2 Pentasulfurated asterisks.
 - 6.7.3.3 Tetrasulfurated asterisks.
 - 6.7.3.4 Pentasulfurated pyridine-cored asterisk.
- 6.7.4 Mechanistic considerations
- 6.7.5 Synthetic applications.
- 6.7.6 Demonstration of reversibility in S_NAr .
- 6.7.7 Conclusion

6.8 Additional data to the submitted manuscript:

Reversible nucleophilic reactions on tetra-, hexa-substituted and 1,2-dicyanotetra-substituted sulfurated /oxygenated aromatic systems with different aryl thiolates.

- 6.8.1 Reversible S_NAr on hexakis(phenylthio)benzene and hexakis(4-methyl phenylthio) benzene with phenyl thiolates
- 6.8.2 Reversible S_NAr on tetrasulfurated benzene and tetrasulfurated / tetraoxygenated 1,2-dicyano-benzene with different phenylthiolates.
- 6.8.3 Asterisk conversion to another one by sulfur exchange reactions

6.1 Dynamic Covalent Chemistry (DCC)

Dynamic combinational chemistry includes reversible covalent and non covalent bonds formation and bonds breaking simultaneously. [1] This is a new approach in supramolecular chemistry, which uses self-assembly processes to generate a library of chemical compounds. We are interested in DCC (Dynamic Covalent Chemistry), which allows a continuous interconversion between the constituents of a library. As a schematic representation, Emil Fischer's lock and key mechanism includes three processes (figure 1):

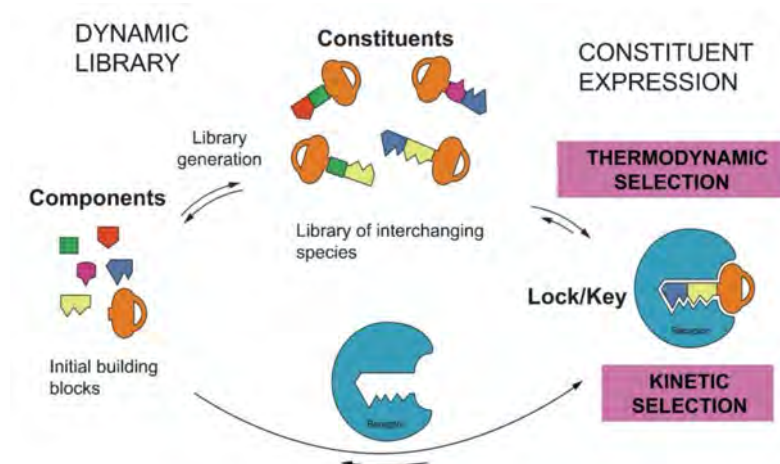


Figure 1: Emil Fischer's lock and key mechanism in Dynamic Covalent Chemistry (DCC). [2] Reprinted with permission from Nature Materials.

- 1) **Selection** of building blocks (for example-template(s) and ligand(s)) which are going to interact with each other reversibly.
- 2) **Conditions:** ligands such as aromatic thiolates/ ethers will interchange on the template.
- 3) **Subjection of a library:** results from binding strength and maybe other factors such as temperature, solvent, concentration, etc. All the building blocks must have functional groups which can help to undergo reversible exchanges on a template. [1]

As the name suggests, in dynamic covalent chemistry, the reaction is dynamic. Multiple reacting species have several competing reactions; hence, multiple products may exist in equilibrium. As shown in figure 2, the reaction can either be kinetically or thermodynamically controlled. The concentration of kinetic intermediates is more than the thermodynamic products ($[K.I.] > [T.P.]$) because of the low activation barrier. Moreover,

with time, intermediates equilibrate towards the global minimum, corresponding to the lowest overall Gibbs free energy (ΔG°) shown in green. The driving force for products to re-equilibrate towards the most stable products is referred to as thermodynamic control. [3] Kinetically controlled reactions are not common. Since 2010, Ognjen S. Milijanic's group have published some work on kinetically controlled reactions. Kinetic controlled processes can remove material from equilibrium and can give kinetically well defined and stable compounds that are no longer subject to equilibrium. [4a] For instance, kinetic self-sorting is guided by the Curtin-Hammett principle which states that for a reaction with a pair of reactive intermediates or reactants that operates under rapid/fast equilibrium conditions, the chemoselectivity will be guided by the relative differences in the rates of irreversible reactions that remove material from equilibrium. [4b]

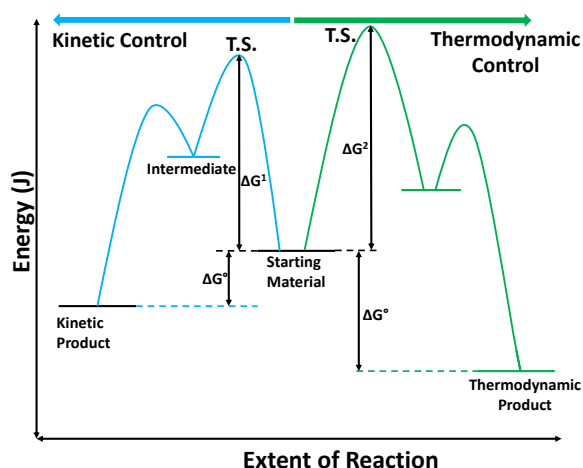


Figure 2: energy diagram for kinetically or thermodynamically controlled reactions. [3]

6.2 Scope of reversible processes and reactions in DCC

Reversible and exchange reactions can be divided into three main categories with some examples:

- 1) Bonding between C-C:** in aldol, two carbonyl groups generate a beta-hydroxy carbonyl unit. However, it needs a catalyst because the energy barrier between kinetic products and starting material makes reversible reactions too slow. [5] Diels-Alder reaction is often reversible at high temperatures, whereas retro-cycloaddition is

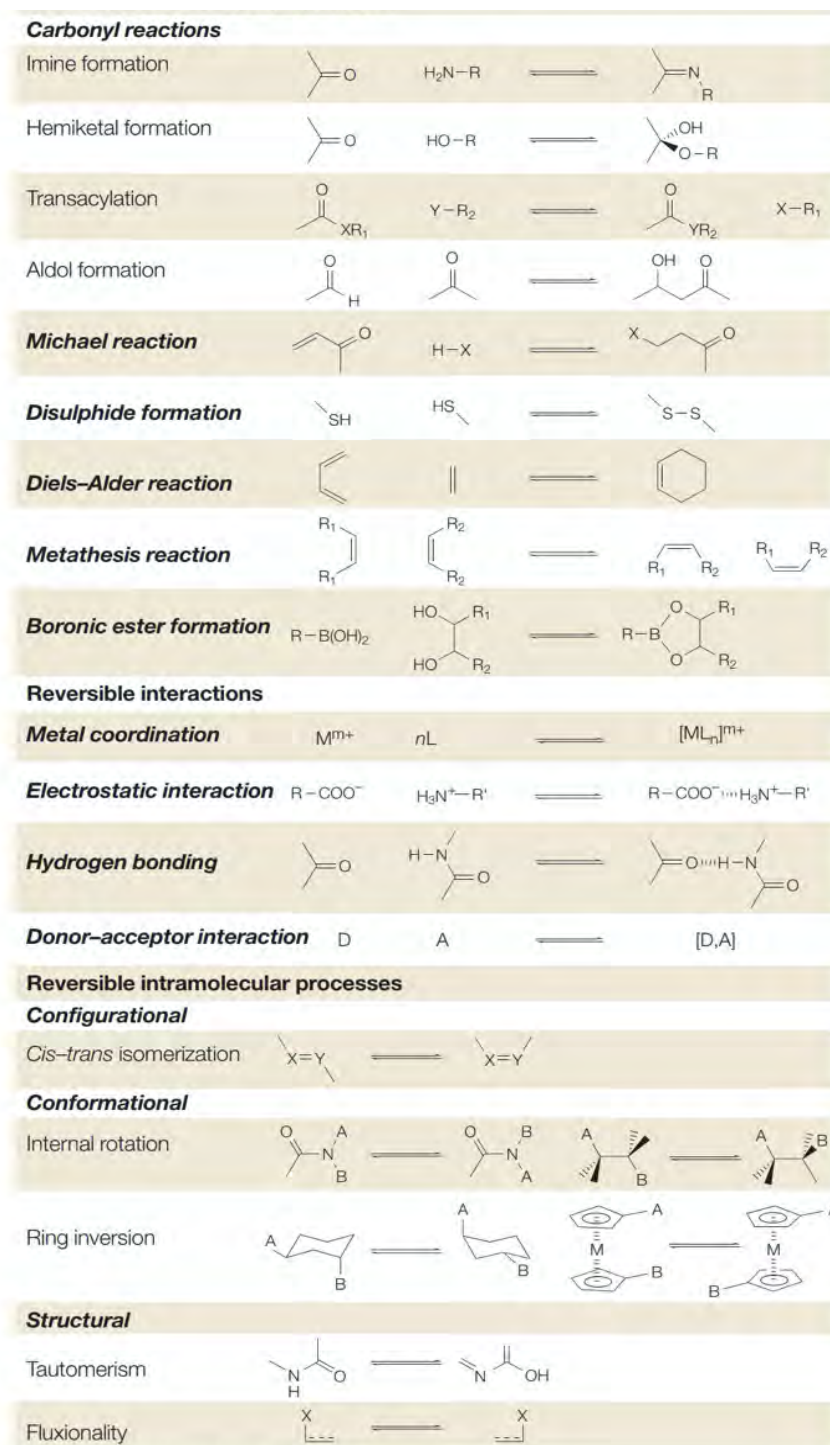
reversible at 40°C. [6] An olefin carbon and an alkyne carbon generate a C-C bond in olefin-alkyne metathesis. [7]

- 2) **Bonding between C-X (X=heteroatom):** here, a heteroatom can be N, O, S. This kind of carbon and heteroatom bond formation can be seen in esters. [7] Between carbonyl ester and an alcohol, and reverse esterification via hydrolysis. The second example is that imine-aminal formation is used in material chemistry for molecular switches, organic carbon framework, and self-sorting reactions. [8]
- 3) **Bonding between X-X (X=heteroatom):** between asymmetrical disulfides. [9] Disulfide exchange has been much exploited because it offers several attractions: the disulfide bond is relatively robust, but it exchanges under mild conditions. Disulfide dynamic covalent library (DCLs) can be simply generated by the dissolution of thiol building blocks in water at pH 8.0 under air, allowing for the screening of biologically relevant targets under near-physiological conditions. The exchange is generally accepted to proceed through the nucleophilic attack of a thiolate anion on the disulfide bond formed by the slow oxidation of the thiol building blocks. The process is reversible if thiolate anions are present in the solution. However, the oxidation process is irreversible. The exchange stops after the building blocks are fully oxidized, allowing for easy purification of the macrocycles formed and self-condensation of boronic acids or condensation with diols. [10]

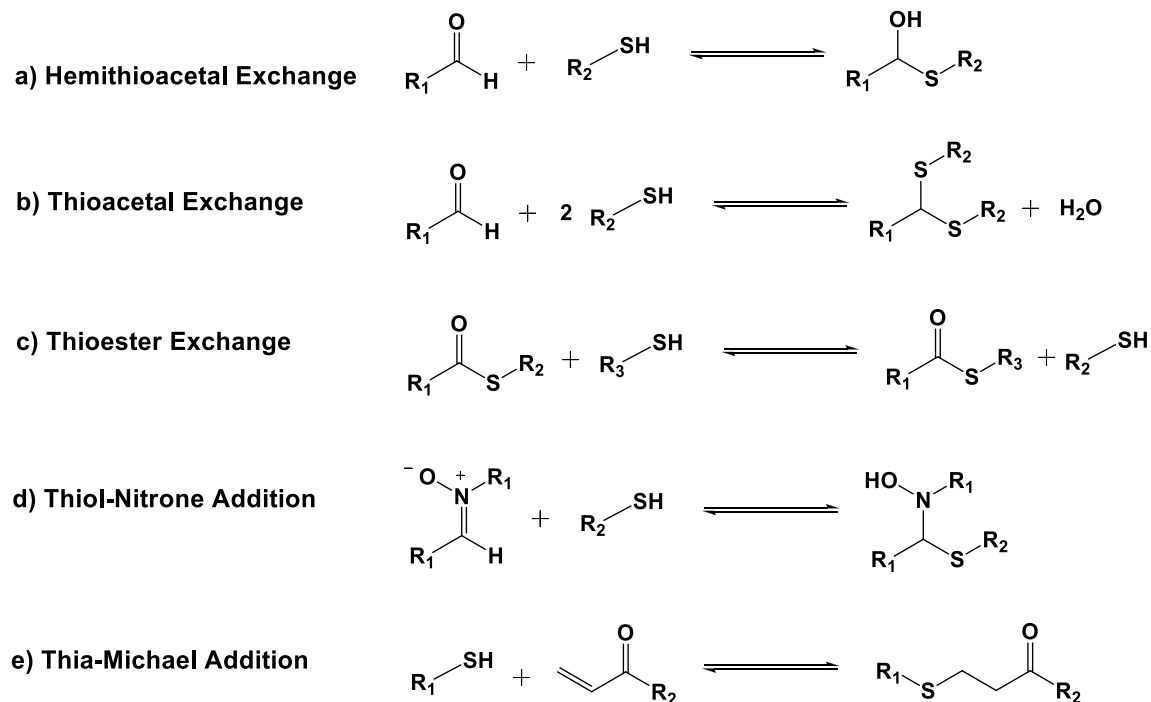
As discussed above, several types of reactions are reversible, and they often include sulfur in disulfide exchange. Additionally to the list of reversible processes in scheme 1, other types of reactions are presented in scheme 2 and they involve sulfur chemistry with their dynamic nature. Sulfur is often nucleophilic and also a leaving group. The C-S bonds follows similar reaction pathways like C-O bonds, but equilibration rates and catalysis are different. [11]

In all of the listed reversible reactions in schemes 1 and 2, scarce reversible nucleophilic aromatic substitution reactions have been reported so far. The group of professor Gingras published some pioneered results. Other work include specialized persulfurated benzenes or naphthalenes with 1,2-benzenedithiol or a polysulfurated 1,2-dicyanobenzene with thiols. [12-13] Due to the importance of nucleophilic aromatic

substitutions in chemistry, this is opening the way to a entire new domain in dynamic covalent chemistry.



Scheme 1 : summary of a few reversible processes of uses in DCC. [1] Reprinted with permission of Chemistry of Materials.



Scheme 2: summary of a few reversible processes with dynamic C-S bonds, by addition of sulfur nucleophiles to an electrophilic carbon atom. [13]

6.3 Methods to verify the reversibility of a chemical process

There are mainly two methods by which we can verify the reversibility of a dynamic covalent system:

1. Dual Entry-Point Analysis
2. Stationary State Perturbation

For the first method, two different systems (A-A and B-B) will generate a dynamic system reacting in the same compositions while maintaining the overall ratio of building blocks. Pathway independence is defining the characteristic of a system at equilibrium. A reverse reaction will be done with two different systems again (such as A-B and B-A). If the products distribution of the reaction above match with the products distribution of the reverse reaction, it provides evidence that the system is under thermodynamic control.

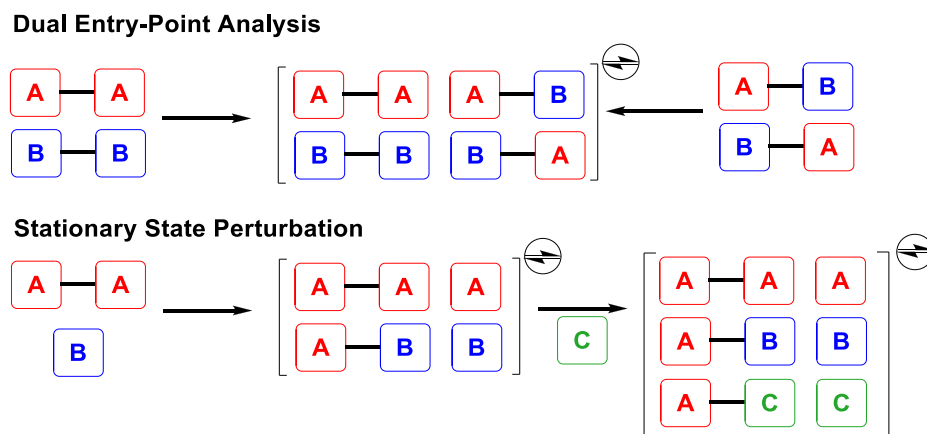


Figure 3: methods to test the reversibility of S_NAr in DCC. [13] Reprinted with permission from *Nat. Rev. Drug Discov.*

For the second method, starting from a system, let us say, A-A and B, reacting them under certain conditions and allowing them to attain a point where the system composition no longer changes. Then, adding a third component to the reaction mixture (component C) allowed it to evolve with time. Suppose the third component is incorporated into the reaction mixture, it indicates that the system was initially at equilibrium (after reacting A-A and B). A large excess of the third component can give precise results (5-10 eq.). [13]

6.4 Summary of general applications relevant to DCC

Dynamic covalent bonds are important, as they can provide a wide range of dynamic materials with many features relevant to the dynamics in DCC such as: adaptation, self-correction, self-healing, and self-replication. Figure 4 makes a summary of these functions. Dynamic covalent chemistry is thus involved in many applications related to organic synthesis, materials science, medicinal chemistry, nanoscience, biology, catalysis, and nanomedicine. [16-21].

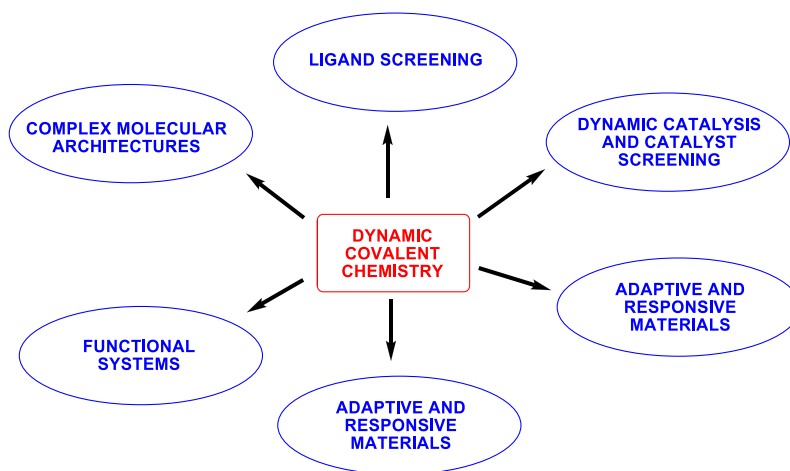


Figure 4: Applications of dynamic covalent chemistry

Large dynamic systems can be built by breaking and making new bonds via DCC with a sensitivity to their chemical environment, and can be controlled by an effector. To reach the thermodynamic equilibrium, the dynamic systems react to environmental changes, such as temperature, solvent, irradiation, electric field, complexing entities, etc. [14] As proposed, the lifetime of each bond is in the range $1 \text{ ms} < \tau < 1 \text{ min}$, which is stable enough to be detected by most analytical methods, yet dynamic enough to allow a swift adaption. [5]

Self-sorting: as the name indicates, when complex or unorganized systems start rearranging into more ordered or systematic forms under certain given conditions, it is known as self-sorting. As the covalent bonds are dynamic in DCC, they can self-sort or rearrange the bonds to get a stable thermodynamic product. [4]

Dynamic self-replication process: it is also a type of self-sorting process, components of dynamic mixture sort into several different systems, one of which is autocatalytic. For example, one component of an imine from the dynamic library catalyzed its formation from precursor aldehydes and amines. [4, 22]

Self-healing: dynamer is a type of polymer, which can be supramolecular or covalently, generated from monomers, and linked by reversible connections (covalent or non-covalent bonds formed via reversible reactions). From long and polydispersed polyethylene spacers, a flexible and elastic polymeric chains in solution can be cross-linked dynamically later with a suitable cross-linking agent. The darker rectangular region in the films in figure 5 is the area where self-healing takes place. [23]

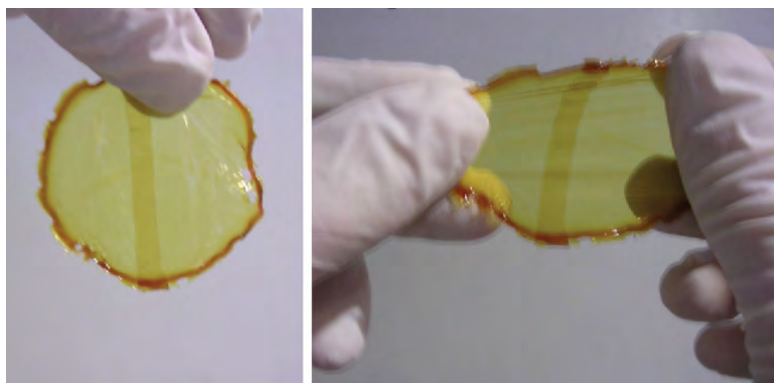


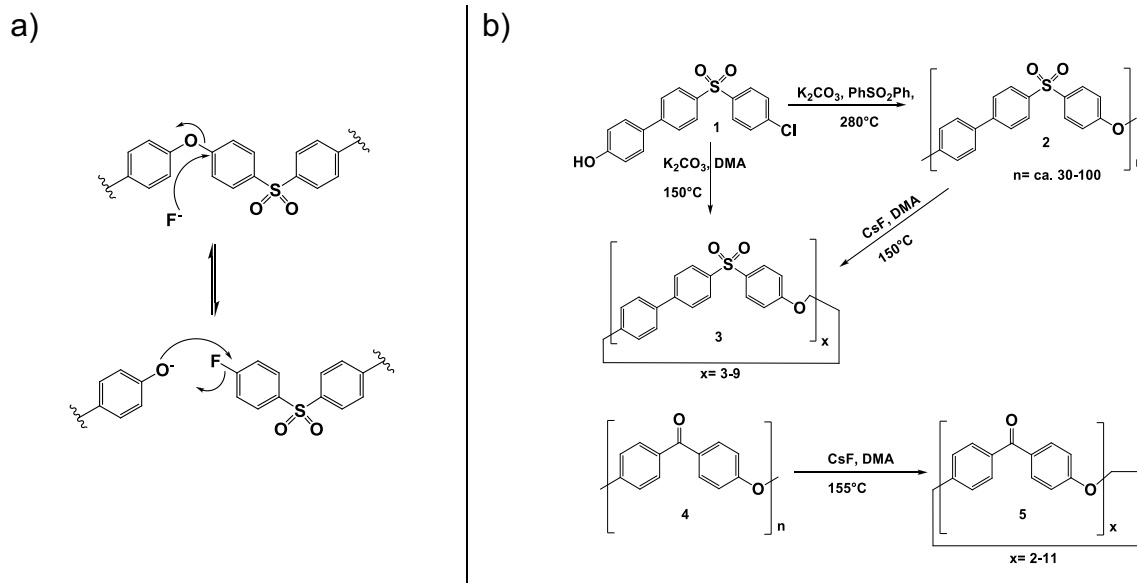
Figure 5 : self-healing thin films synthesized from Diels-Alder reactions. Reprinted with permission of Chemical Society Reviews. [23]

6.5 Survey of reversible nucleophilic aromatic substitutions in the literature

There are scarce reports of reversible nucleophilic aromatic substitutions in the literature. Many of them did not mention explicitly the reversibility and the chemical exchange of components in the frame of DCC. Sometimes, it could be deducted from some unwanted side-products observed in a chemical process. Recently, some attention has been paid to the reversibility of some nucleophilic aromatic substitution reactions (S_NAr). Our group has been pioneering this area in some doctoral thesis, some laboratory observations and in some publications. Here, we will make the first thorough survey on these reversible reactions of potential uses for DCC.

So far, only a few publications clearly mentioned nucleophilic aromatic substitution reactions in dynamic covalent chemistry. In 1997, some polymers were synthesized via ring-opening polymerization of a macrocyclic aromatic ether-ketones and ether sulfones. The catalytic transesterification of aromatic poly(ether sulfone)s and poly(ether ketone)s are possible at high temperatures with some nucleophiles (such as fluoride anions) and a strong base. The authors suggest a mechanism for polymer-macrocycle interconversion but without mentioning clearly DCC, which suggests a dynamic covalent nature in some aromatic nucleophilic substitution reactions (scheme 3a). Ring-opening polymerization is already known in this work, but they reported ring-closing depolymerization of aromatic poly(ether sulfone) (2) in a DMA (N,N-dimethylacetamide) solution at 150°C, by using cesium fluoride (CsF) as a catalyst. Polymer 2 equilibria is attained with CsF after 48

hours. No change in the molar mass distribution was observed, and some oligomers were recovered in a 95% yield by simply precipitating them in methanol. Fluorine elemental analysis reveals low levels of fluorine, and the formation of cyclic species. [24]

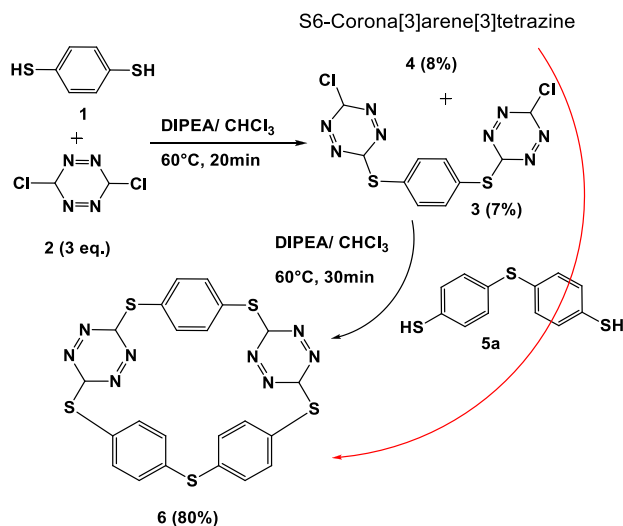


Scheme 3: a) mechanism of transesterification of aromatic poly(ether sulfone)s with fluoride; b) polycondensation of monomer (1) and (4) under high dilution conditions. [24]

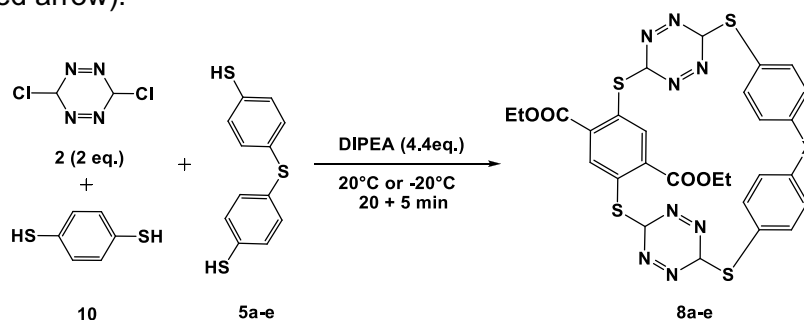
Novel type of persulfurated macrocycles, called corona[5]arenes, were synthesized by two methods. The first one is from macrocycle to macrocycle, and the second one is from a one-pot three-component method. A ring contraction of the persulfurated macrocycle from S6 to S5 was observed. From scheme 4, when compound 1 and 2 react, it generates S6-corona-[3]arene[2]tetrazine (4), the trimer (3) in 7% and 8% yield, and polar oligomers. A [3+2] macrocycle condensation of compound 3 with 5a in DIPEA (N,N-diisopropylethylamine) / CHCl₃ leads to S5-corona-[3]arene[2]tetrazine (6) in a 80% yield, and traces of compound 4. Accidentally, when S6-corona-[3]arene[2]tetrazine (6) reacts with dithiol (5a), it forms mainly S5-corona-[3]arene[2]tetrazine (6) (it is shown in scheme 4 with the red arrow). The reaction favored S5 rather than S6 due to more thermodynamically stability, and the S-C bonds strength of tetrazine in (4) is weaker than the S-C bond from S5-corona arene.

Several reactions were tried with different bases (DIPEA, DBU, NEt₃, and DABCO) and solvents (CHCl₃, DCM, ACN, and DCM) to find the best possible reaction conditions.

Among all solvents, DIPEA and CHCl_3 gave the best yields for S5-corona. Due to the dynamic nature of covalent S-C bond in tetrazine, they explored a one-pot three-component synthesis (scheme 5). By treating compound 2 (2 mol-eq.) and equimolar amount of both dithiols (10 and 5a-e).



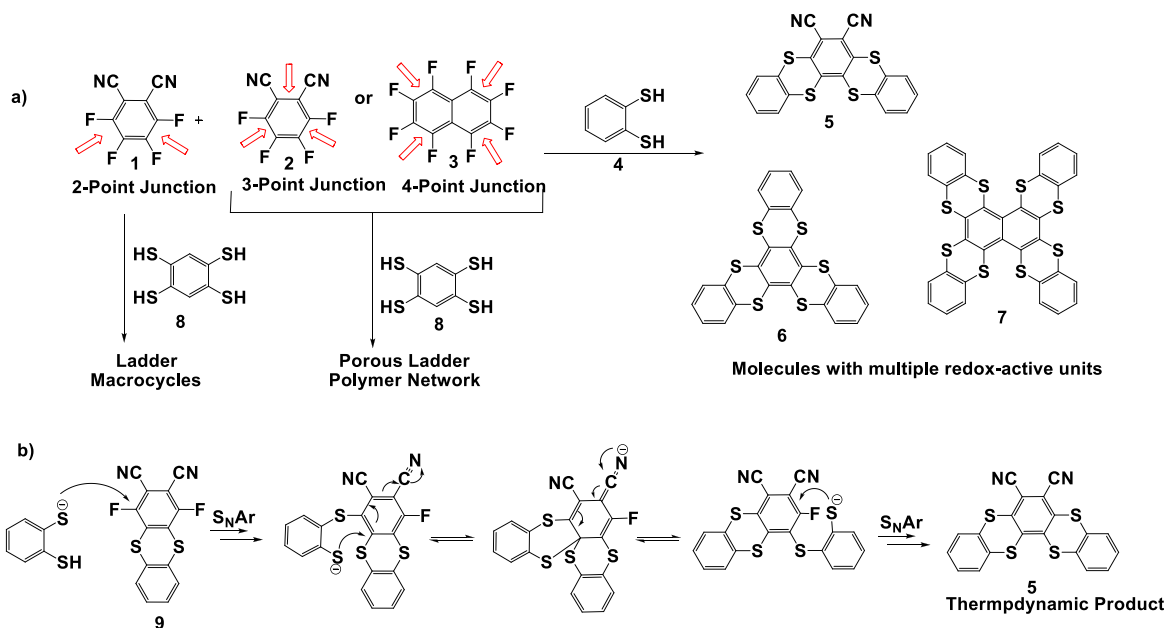
Scheme 4 : A [3+2] approach to synthesize S5-corona-[3]arene[2]tetrazine (6) from macrocycle to macrocycle (red arrow).



Scheme 5: a second method for making macrocycles (8a-e), in a one-pot three component reaction via an equilibrated process. [25]

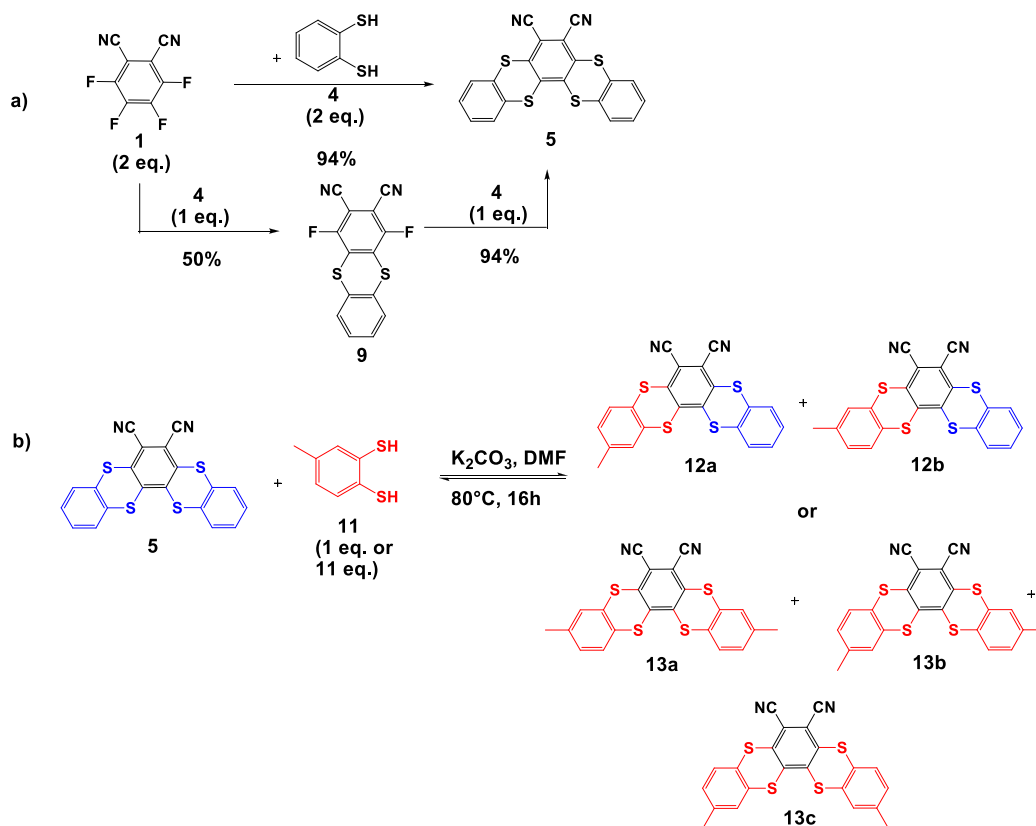
It was found that S5 was formed rapidly in good yield when the linker is S, CH_2 , CMe_2 , but the yield decreases to 11% when the linker is SO_2 . Some sc-XRD studies were achieved, and the macrocycles are useful hosts in supramolecular studies, with tunable cavities and electronic properties to study. [25]

In 2018, Swager and his group reported the dynamic and self-correcting nature of two, three, and four-point junctions to afford thianthrene-type molecules (scheme 6a) with two, three, and four thianthrene units.



Scheme 6: a) Formation of two, three and four point junctions by S_NAr ; b) Proposed mechanism for reaction of compound (9) with dithiol (4). [26]

Scheme 6a shows different substitutions with dithiol and tetrathiol to make ladder macrocycles, porous ladder polymer network, dianthrene, thianthrene, tetranthrene, etc. Thermodynamic and kinetic products were formed by treating compound (1) and (4) (dithiol, 1 mol-eq.) to produce the kinetic product (9), and the latter was treated with 1 mol-eq of dithiol to form compound (5), which is a thermodynamic product (scheme 6b). To check the reversibility in nucleophilic substitution reaction, (5) was treated with toluene-3,4-dithiol (11) and potassium carbonate as a base in DMF at 80°C for 16 hours and compared the spectra. When compound (11, 1 mol-eq) was added, two isomers with single substitution (12a and 12b) were observed by 1H NMR (figure 6b), whereas when 10 eq. of dithiol (11) was added three regioisomers with a double substitution were observed (13a to 13c). These results provide evidence for the reversibility of S_NAr under mild conditions in dynamic covalent chemistry. [26]



Scheme 7: a) Model reaction showing self-correcting and dynamic nature of S_NAr ; b) Exchange reaction of compound (5) and (11) with 1 eq. and 10 eq. of toluene-3,4-dithiol (11). [26]

In another macrocyclic system, dynamic nucleophilic aromatic substitutions were performed with disubstituted tetrazines to show the reversibility of S_NAr reactions. In 2021, phenols and arylthiols were used to synthesize disubstituted tetrazines at room temperature in good yields, instead of using amines and aliphatic alcohols, as they require harsh conditions and suffer from low yields (scheme 8). The reaction was achieved between p-cresol (1) and disubstituted tetrazine with 4-methoxyphenol (2-Tz-2) as the reference process. A reverse reaction was done to compare with the above forward reaction. The reverse reaction between 4-methoxyphenol (2) and cresol-substituted tetrazine (1-Tz-1), one mol-eq. of tetrazine, and 2 mol-eq. of the corresponding thiol/phenol led to the same distribution of products, including the neutral reaction, which started from Cl-Tz-Cl as shown in scheme 8.

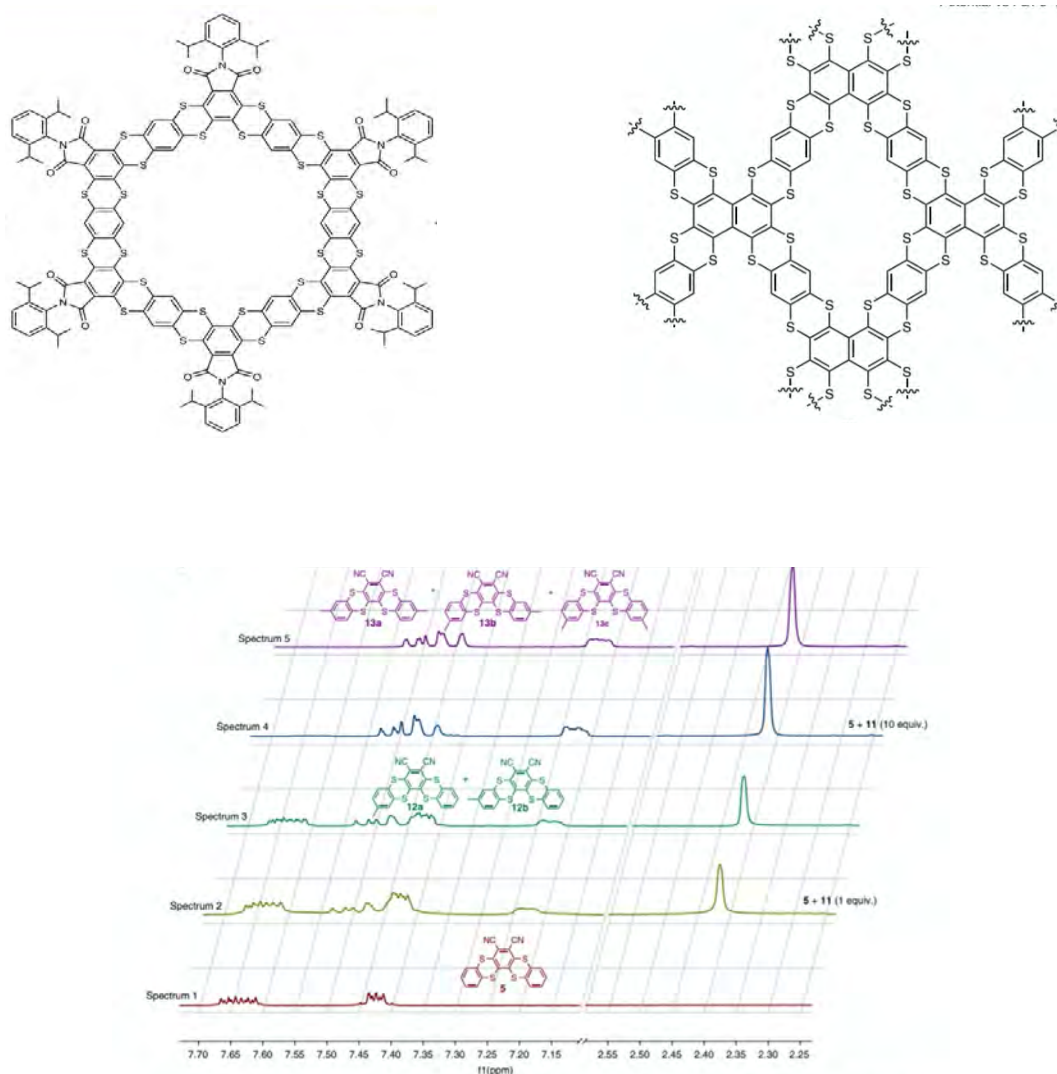
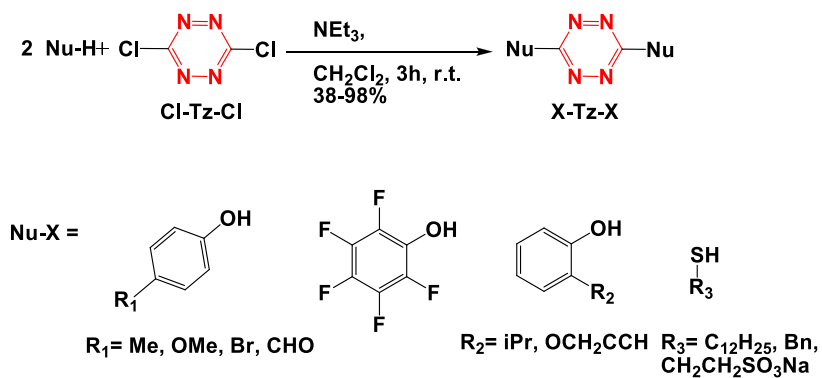
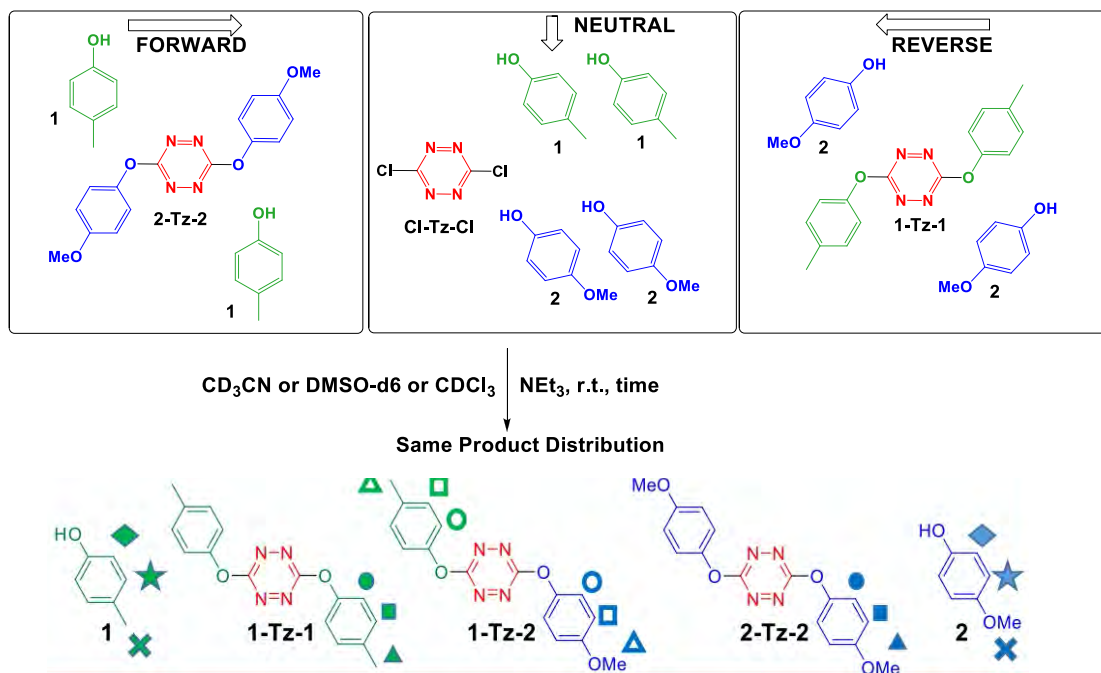


Figure 6: a) Examples of two and four point junction macrocycles synthesized via S_NAr ; b) Stacked 1H -NMR spectra's for reaction of compound (5) and (11) (scheme 4b). [26]

a)



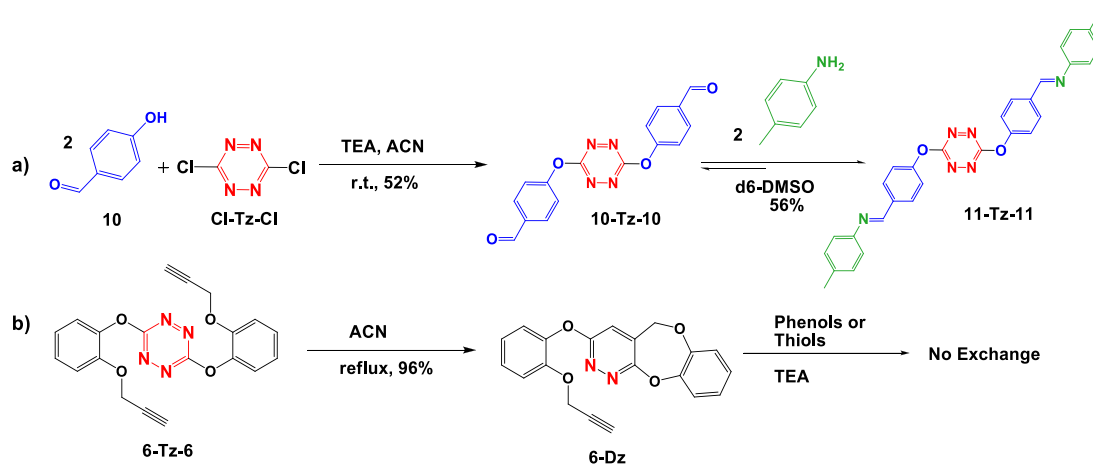
b)



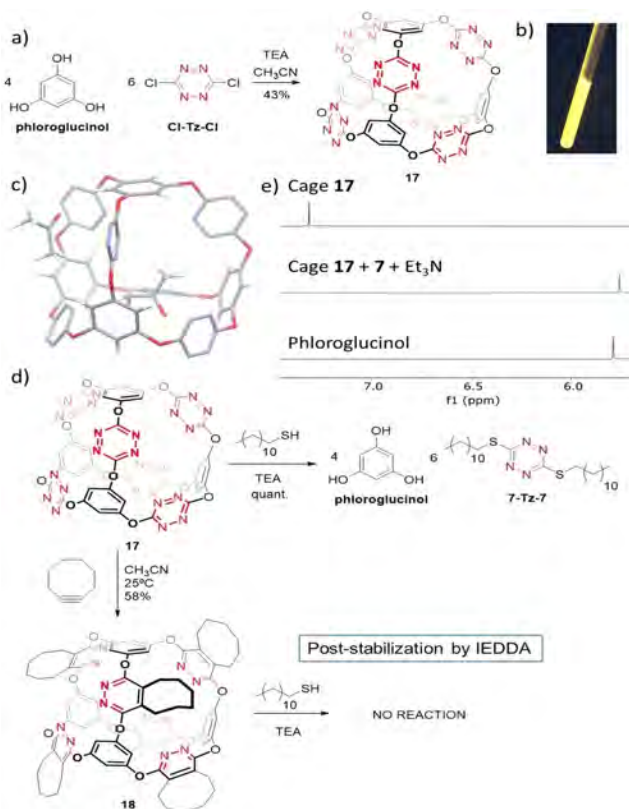
Scheme 8: a) synthesis of disubstituted tetrazines; b) reactions performed to test the reversibility of SNTZ reactions via forward, reverse and neutral reactions. [27]

Several reactions were tried in different solvents (D6-DMSO, CD_3CN , CDCl_3 , etc) and bases (TEA, DIPEA, NMM, pyridine, Cs_2CO_3). It was found that a less basic base takes a longer time to complete the reaction (such as NMM). The best one was DIPEA and TEA or Cs_2CO_3 in DMSO. A solvent like CD_3CN takes 2 hours at RT to reach equilibrium, whereas 0.5 h at 50°C . In CDCl_3 , the reaction is slow at RT, but it progresses at 50°C and attains an equilibrium after 15h. A base is required for the exchange reactions. Reversibility was further proven by increasing the concentration of one chemical species and shifting the equilibrium backward. It was also found that SnTz is compatible with imine chemistry. IEDDA (inverse electron demand Diels Alder) reaction was also achieved in DMSO to connect imine chemistry. Heating can convert exchangeable 6-Tz-6 into an unreactive 6-Dz by an intramolecular IEDDA reaction (scheme 9). Also, via SNTz clicking with phenols and de-clicked them with thiols was possible. This can be useful to synthesize responsive molecular architectures. A responsive tetrahedral and fluorescent cage was produced (cage 17) in a 43% yield, as shown in scheme 10, where each of four faces is an I- corona[6]arene. This chemistry has potential uses in the synthesis of porous

organic cages, interlocked structures, covalent adaptable networks, and COFs. Post-functionalization by IEDDA of the compounds obtained, allows the attachment of molecular fragments, and at the same time, it inhibits the exchange.



Scheme 9: a) combining SNTz with imine chemistry; b) heating converts exchangeable 6-Tz-6 into unreactive 6-Dz by an intramolecular IEDDA reaction [27]



Scheme 10: a), b) Synthesis of fluorescent cages; c) X-Ray structure of cage (17) (one molecule of acetone lies inside the cavity and the other outside); d) Cage 17 disabled by thiol (7) in presence of trimethylamine, post-stabilization by IEDDA; e) $^1\text{H-NMR}$ of pure (17), the crude disassembling reaction mixture after 30 min. in CD_3CN . [27]

REFERENCES FOR SECTIONS 6.1 TO 6.5:

1. O. Ramström, J.-M. Lehn, *Nat. Rev. Drug Discov.* **2002**, *1*, 26-36.
2. E. Fischer, *Chem. Ber.*, **1894**, *27*, 2985-2993.
3. https://commons.wikimedia.org/wiki/File:Thermodynamic_versus_kinetic_control.png#/media/File:Thermodynamic_versus_kinetic_control.png
4. a) C.-W. Hsu, O. Š. Miljanić, in *Dynamic Covalent Chemistry, Principles, Reactions and Applications*, (W. Zhang, Y. Jin, Eds), Chapter 6, Self-sorting through Dynamic Covalent Chemistry, Wiley, **2017**; b) J. I. Seeman. *Chem. Rev.* **1983**, *83*, 83-134.
5. Y. Zhang, P. Vongvilai, M. Sakulsombat, A. Fischer, O. Ramström, *Adv. Synth. & Cat.*, **2014**, *356*, 987-992.
6. R. C. Boutelle, B. H. Northrop, *J. Org. Chem.*, **2011**, *76*, 7994-8002.
7. G. C. Vougioukalakis, R. H. Grubbs, *Chem. Rev.* **2010**, *110*, 1746-1787.
8. Y. Jin, C. Yu, R. J. Denman, W. Zhang, *Chem. Soc. Rev.*, **2013**, *42*, 6634-6654.
9. K. Jeehong, B. Kangkyun, D. Shetty, N. Selvapalam, G. Yun, N. H. Kim, Y. H. Ko, K. M. Park, I. Hwang, *Angew. Chem. Int. Ed.*, **2015**, *54*, 2693-2697.
10. R. Nishiyabu, Y. Kubo, T. D. James, J. S. Fossey, *Chem. Commun.*, **2011**, *47*, 1124-1150.
11. a) Williamson and J. Scrugham, *Annalen*, **1854**, *7*, 237; b) Williamson and Scrugham, *Annalen* **1854**, *92*, 316.
12. Pisani, *Compt. Rend.*, **1854**, *39*, 852 ; (d) Pisani, *Annalen*, **1854**, *92*, 326.
13. F. Schaufelberger, B. J. J. Timmer, O. Ramström, in *Dynamic Covalent Chemistry, Principles, Reactions and Applications*, (W. Zhang, Y. Jin, Eds), Chapter 1, *Principles of Dynamic Covalent Chemistry*, Wiley, **2017**, pp 1-30.
14. F. Schaufelberger, B. J. J. Timmer, O. Ramström, in *Dynamic Covalent Chemistry, Principles, Reactions and Applications*, (W. Zhang, Y. Jin, Eds), Wiley, **2017**.
15. Y. Zhu, H. Yang, Y. Jin, W. Zhang, *Chem. Mater.*, **2013**, *25*, 3718-3723.
16. R. J. Wojtecki, M. A. Meador, S. J. Rowan, *Nat. Mater.*, **2011**, *10*, 14-27.
17. P. Nowak, V. Saggiomo, F. Salehian, M. Colomb-Delsuc, Y. Han, S. Otto, *Angew. Chem. Int. Ed.*, **2015**, *54*, 4192-4197.
18. P. Dydio, P.-A. R. Breuil, J. N. H. Reek, *Isr. J. Chem.*, **2013**, *53*, 61-74.
19. L. Tauk, A. P. Schröder, G. Decher, N. Giuseppone, *Nat. Chem.*, **2009**, *1*, 649-656.

20. I. M. Serafimova, M. A. Pufall, S. Krishnan, K. Duda, M. S. Cohen, R. L. Maglathlin, J. M. McFarland, R. M. Miller, M. Frödin, J. Taunton, *Nat. Chem. Biol.*, **2012**, *8*, 471-476.
21. K. Severin, Analytical Applications of Dynamic Combinatorial Chemistry, in *Dynamic Combinatorial Chemistry* (eds J. N. H. Reek, S. Otto), Wiley-VCH, Weinheim, **2010**.
22. M. L. Saha, M. Schmittel, *Org. Biomol. Chem.*, **2012**, *10*, 4651-4684.
23. N. Roy, B. Bruchmann, J.-M. Lehn, *Chem. Soc. Rev.*, **2015**, *44*, 3786-3807.
24. A. B. Haida, I. Baxter, H. M. Colquhoun, P. Hodge, F. H. Kohnke, D. J. Williams, *Chem. Commun.*, **1997**, 1533-1534.
25. Z. C. Wu, Q. H. Guo, M. X. Wang, *Angew. Chem. Int. Ed.*, **2017**, *56*, 7151-7155.
26. W. J. Ong, T. M. Swager, *Nat. Chem.*, **2018**, *10*, 1023-1030.
27. T. Santos, D. S. Rivero, Y. P. Pérez, E. M. Encinas, J. Pasán, A. H. Daranas, R. Carrillo, *Angew. Chem. Int. Ed.*, **2021**, *60*, 18783-18791.

6.6 Thesis work on reversible nucleophilic aromatic substitutions in DCC with polysulfurated benzene-cored asterisks

6.7 MANUSCRIPT SUBMITTED FOR PUBLICATION

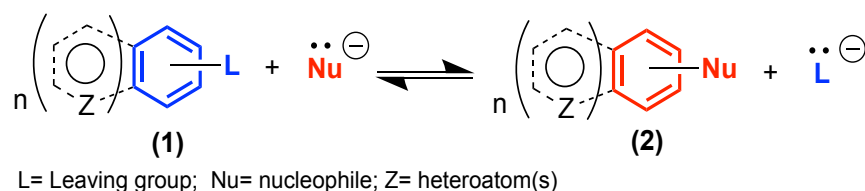
The following section refers to a manuscript submitted to a scientific journal on nucleophilic aromatic substitution reactions in the frame of DCC and organic chemistry, primarily based on this thesis work. The analytical separative methods and LC-HRMS analyses were performed at ISIS, Université de Strasbourg in the laboratory of professor Jean-Marie Lehn. Dr. Jean-Louis Schmitt contributed to these analyses.

"The Sulfur Dance" Around Arenes and Heteroarenes - Dynamic Covalent Nucleophilic Aromatic Substitutions"

6.7.1 Introduction

Nucleophilic aromatic substitutions are among the most frequently used reactions in organic chemistry.^[1] Such exchanges of chemical components may occur by different mechanisms (S_NAr ,^[2] $S_{RN}1$,^[3] cS_NAr ,^[4] S_NArH ^[5]). In the following, we will use the

denomination S_NAr for representing these different mechanistic possibilities of nucleophilic aromatic substitutions. Even if their reversibility was shown in rare cases,^[6] it was overlooked in spite of a great number of S_NAr reactions reported since 1854.^[7] It is conceptually of much interest in aromatic chemistry and in Dynamic Covalent Chemistry (DCC),^[8-13] beside a number of reversible reactions studied, with imines,^[14,15] esters,^[16] disulfides,^[17] dithioacetals,^[18] hemiacetals,^[19] metathesis,^[20] S_N2 ,^[21] and Diels-Alder reactions.^[22] Reversible S_NAr reactions could present a wide scope, involving several types of nucleophiles, leaving groups and aromatic or heteroaromatic substrates, without the need for metal catalysis, as schematically depicted in Scheme 1.



Scheme 1. Schematic representation of the reversibility of nucleophilic aromatic substitutions.

In order to explore these reversible reactions, we chose as model substrates, some thiaarenes and thiaheteroarenes^[23] (hereafter named "asterisks").^[24] A number of years ago, we investigated the REDOX properties of a range of persulfurated polyaromatic compounds,^[25] and we showed that per(thio)arenes are electron-acceptors in spite of a rich electronic density.^[26-28] Later on, some of us disclosed their potency as all-organic phosphorescent triplet emitters with quantum yields reaching near 100% in the crystalline state.^[29-31] Many are the most phosphorescent solids known to date. They also display "turn-on" phosphorescence upon supramolecular polymerization by metal-ion complexation, which makes them "smart" and sensitive to their environment by rigidification-induced phosphorescence (RIP).^[32, 33] In the course of these studies, we have observed sulfur exchange reactions by S_NAr .^[34] Due to the importance of reversibility in S_NAr reactions, we want to focus here on the general ability of thiaarenes and thiaheteroarenes to undergo facile component exchange. It could lead to a constitutional variation toward adaptative features, as is the case of processes occurring in the generation of macrocyclic compounds.^[35,36] Such features open new avenues in dynamic covalent chemistry (DCC). Among a plethora of nucleophiles and arenes, the exchange

of sulfurated groups around thiaarene or thiaheteroarene cores (often at room temperature) display a "sulfur dance" behavior, by analogy to the "halogen dance."^[37] Reversible nucleophilic aromatic substitutions (Scheme 1, Figure 1) on various aromatic or heteroaromatic core components as "DCC templates" present a manifold of synthetic, structural and physicochemical features. The latter combine luminescence, dyes and redox properties, as additional sensing, monitoring and imaging parameters during dynamic processes. The implementation of S_NAr in DCC opens the door to applications toward dynamic and adaptative assemblies^[38,39] and new materials with relatively non-toxic^[40] and easily available substrates.

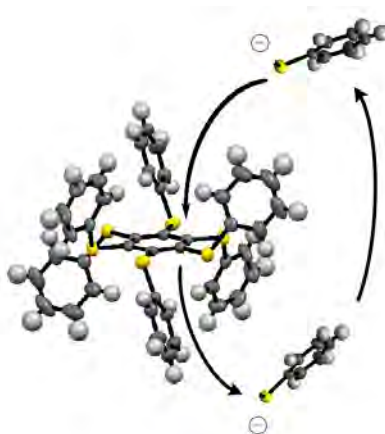
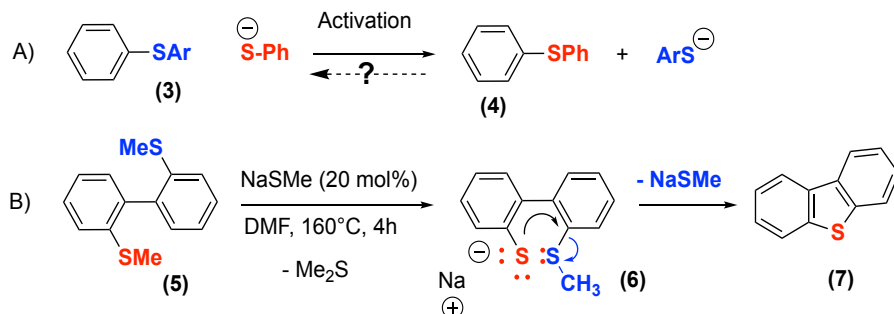


Figure 1. Representation of the "sulfur dance" DCC process. Reversible nucleophilic aromatic substitutions with continuous exchange of sulfur components (thiophenolate anion) around a per(thio)benzene core (DCC template).

6.7.2 Results and Discussion

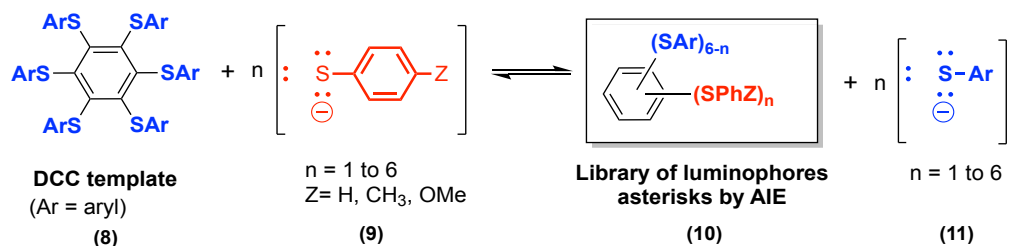
Reversible nucleophilic aromatic substitutions have rarely been reported in aromatic chemistry, and implemented in the context of DCC, in spite of their great importance.^[1,2] The classical S_NAr mechanism (i.e. addition-elimination) comprises two steps which were rarely shown to be reversible. It is rather surprising, as reversible exchanges leading to the formation of a *s*-complex in the first step have been occasionally reported in arene and heteroarene chemistry with activated electron-poor substrates in S_NAr .^[41] In general, they comprise NO_2 , F, Cl, Br, CN, RS, OR leaving groups, and carbon-, oxygen-, sulfur-, and nitrogen-centered nucleophiles. However, the elimination step was not shown to be reversible, and thiolate anions were considered as poor leaving groups in S_NAr . As for unactivated thiaarenes (e.g. aryl sulfides), intermolecular sulfur substitutions rarely occurs

without strong heating conditions (Scheme 2A). Intramolecular exchange of a sulfur group can proceed irreversibly at high temperatures (Scheme 2B).^[42] In short, exchange of sulfur components by nucleophilic aromatic substitution takes place, but with a proper activation.



Scheme 2. a) A general scheme of intermolecular, irreversible, sulfur component exchange by $\text{S}_{\text{N}}\text{Ar}$ with an unactivated aryl sulfide (3); b) Irreversible sulfur exchange by intramolecular $\text{S}_{\text{N}}\text{Ar}$ at 160°C .^[42]

We already observed many years ago that sulfur component exchange reactions of some per(thio)arenes and heteroarenes occur with arylthiolate anions (Scheme 3).^[34] Exchange reactions were also reported from 1,2-benzenedithiol derivatives with sulfurated arenes,^[35] and from thiophenols with 3,6-di(thio)tetrazines.^[36] Considering the intense activities in DCC, a general understanding of reversible nucleophilic aromatic substitutions is needed in view of the limited data available.^[34-36] They are promising reactions, distinct from functional groups and reversible reactions most extensively investigated in DCC. Exchanges of chemical components via $\text{S}_{\text{N}}\text{Ar}$,^[2] $\text{S}_{\text{RN}}1$,^[3] $\text{cS}_{\text{N}}\text{Ar}$,^[4] $\text{S}_{\text{N}}\text{ArH}$ ^[5] or by other substitution mechanisms are thus of broad significance in aromatic chemistry and for DCC. Furthermore, poly- or per(thio)arenes and thiaheteroarenes are particularly attractive because some possess remarkable exalted properties such as phosphorescence by RIP, with a sensitivity and responsiveness to their environment after a molecular rigidification (conformational restriction). Multiple reversible reactions surrounding an aromatic core (Scheme 3) amounts to performing DCC on a template ("the sulfur dance").



Scheme 3. A "DCC template" has been shown to provide a library of mixed substituted luminophores from reversible nucleophilic aromatic substitutions by the "sulfur dance."^[34]

6.7.3 Sulfur component exchanges.

We delineate the scope of these reversible S_NAr reactions with poly- and per(thio)arenes and a (thio)heteroarene. In Figure 2, we found that para-substituted asterisks with H, F, CN, Me, CO_2iPr or incorporating benzothiazolyl-2-thio, 1-naphthylthio, 2-naphthylthio and 1,2-dicyano groups are suitable systems for sulfur component exchanges, in the presence of thiophenolates between 25-90°C. Most importantly, there is no need for metal catalysis^[43,44] nor high temperatures (for instance S_NAr substitutions with thiolates can occur at 180°C).^[45]

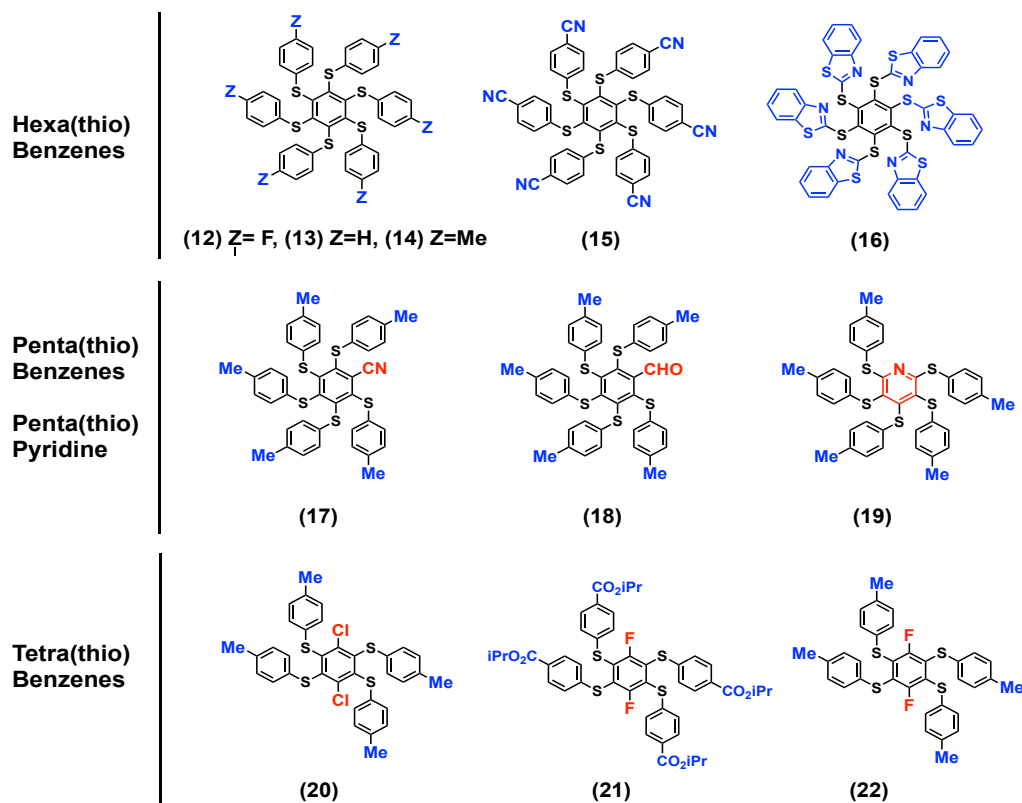


Figure 2. Asterisks undergoing S_NAr with *p*-substituted thiophenolate anions at 25°C (except for **13** and **14** at 70°C) for providing a library of asterisks.

The model substrates come from hexa- penta- or tetrasulfuration of the central aromatic core. The more electron-poor asterisks provide easier component exchanges at 25°C, as it is expected in a S_NAr mechanism with a σ -complex. Thus, para-substitution with electron-withdrawing groups on the arms and activating groups directly attached to

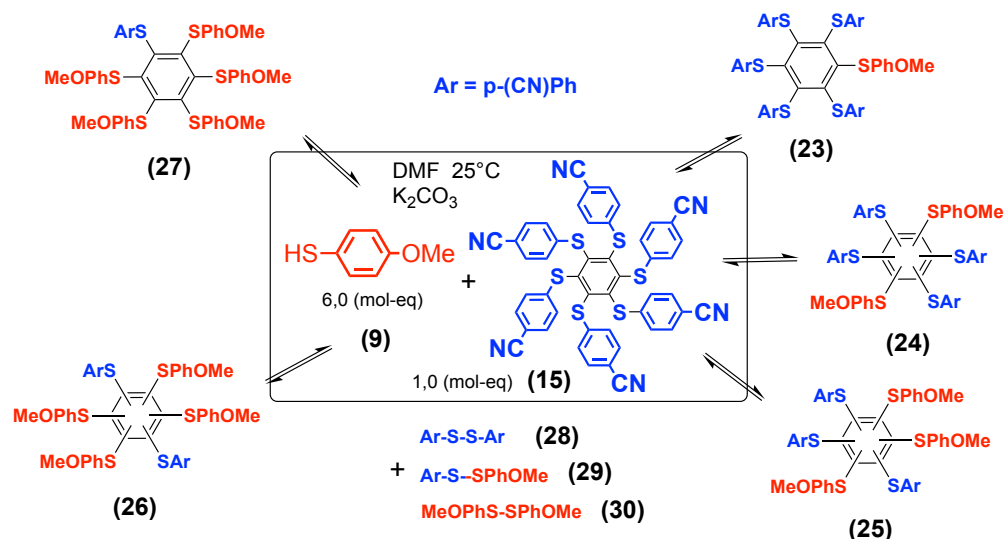
the aromatic core provide effective sulfur exchange dynamics at 25°C. A heteroaromatic core, such as pyridine, is also an effective substrate.^[46] This reactivity is in line with the reversibility observed for producing Meisenheimer complexes in S_NAr with activated substrates.^[41a-e]

Exchange of sulfur components was tested with the asterisks in Figure 2 at different temperatures and equivalents of thiols (*p*-methoxybenzenethiol or *p*-thiocresol). The reaction progress was monitored by ¹H NMR, and the crude mixture was further analyzed by ¹H, ¹³C NMR, HR LC-MS, after a comparison to authentic reference samples (when available). The release of thiolates and their subsequent oxidation to disulfides (mixed or symmetrical ones) further attests to these substitutions. In the next sections, we will detail these sulfur component exchanges, and indicate the generality of the "sulfur dance" process in reversible S_NAr reactions.

6.7.3.1 Hexasulfurated asterisks.

As a typical example, we reacted (15) (1.0 mol-eq.) with *p*-methoxybenzenethiol (6.2 mol-eq.) at 25°C for two days in the presence of K₂CO₃ in DMF (Figure 3a). The reaction mixture provided a library of at least five asterisks, and traces of unreacted (15). As observed by HR LC-MS, a product selectivity (~70%) was found for the asterisk with three *p*-methoxyphenylthio groups (unoptimized). The regioisomeric structures remain to be determined.

A)



B)

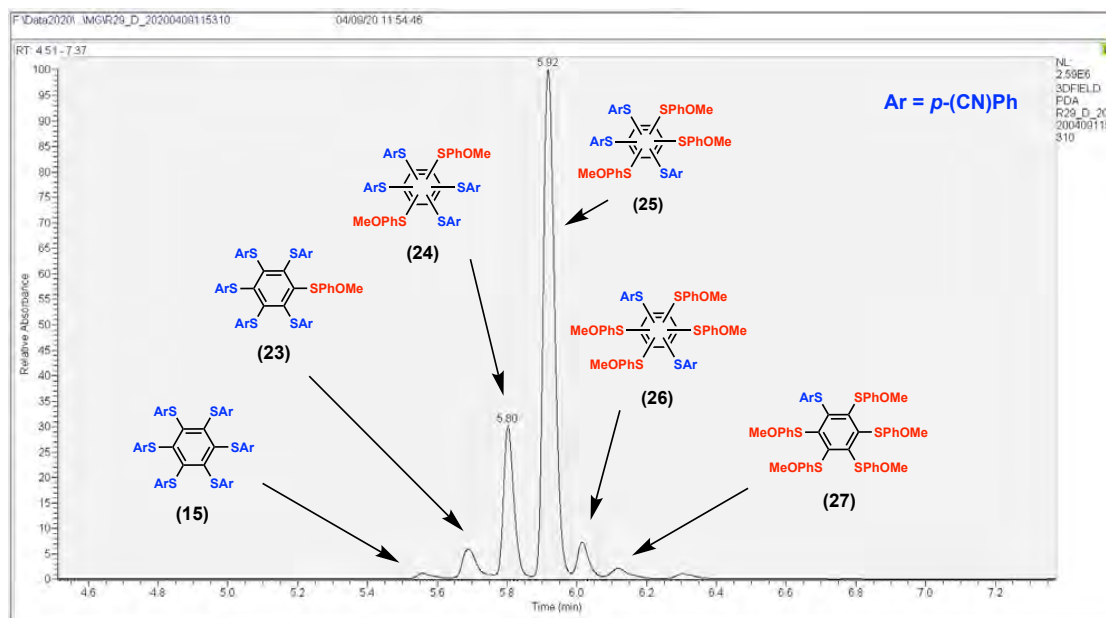


Figure 3. A) A sulfur component exchange system based on the reaction of **(15)** with *p*-methoxybenzenethiol and K_2CO_3 at $25^\circ C$ in DMF; B) A LC chromatogram shows selectivity in the products distribution, as determined by LC-HRMS. The regioisomeric structures remain to be determined.

Asterisks with electron-withdrawing fluoro substituents (**12**) or with benzothiazolyl-2-thio groups (**16**) provide easy exchange dynamics at $25^\circ C$, whereas para-substitution with H, Me or OMe or 1-naphthylthio- or 2-naphthylthio- groups requires higher temperature than $25^\circ C$.

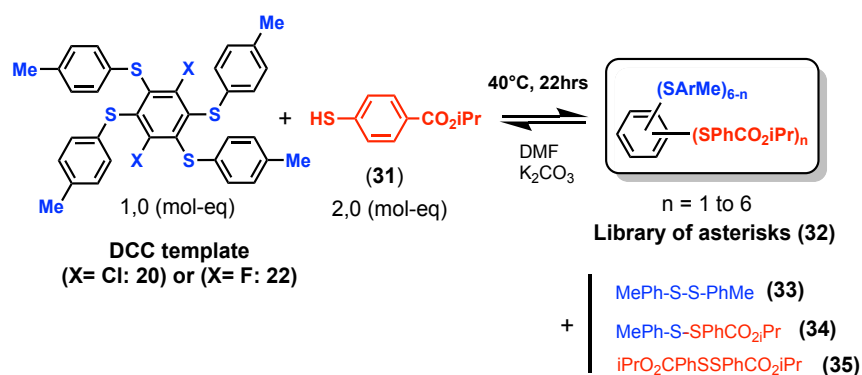
6.7.3.2 Pentasulfurated asterisks.

Asterisks (**17**) and (**18**) with CN and CHO activating groups directly attached to the benzene core were investigated. After reacting **(17)** (1.0 mol-eq.) with *p*-methoxybenzenethiol (6.2 mol-eq.) at $25^\circ C$ for 38 hours in the presence of K_2CO_3 in DMF, 1H NMR and LC-HRMS indicated a library of at least five asterisks incorporating one to five *p*-methoxyphenylthio groups and some unreacted (**17**). The exact regioisomeric structures are unknown at this stage. Under similar conditions, (**18**) afforded at least five asterisks incorporating one to five *p*-methoxyphenylthio groups after exchanges at $25^\circ C$. The selectivity in the products distribution was favorable to the incorporation of two and

three *p*-methoxyphenylthio groups (without optimization). In summary, both (17) and (18) are templates with effective dynamics to afford a non-statistical distribution of products with some selectivity.

6.7.3.3 Tetrasulfurated asterisks.

Asterisk (20) is activated by two Cl substituents toward S_NAr . It allows sulfur exchange components to make a library of asterisks in the presence of isopropyl-4-mercaptobenzoate (31) (2.1 mol-eq.) and K_2CO_3 in DMF at 40°C for 22 hrs (Scheme 4). The formation of three disulfides (33), (34) and (35) confirmed these exchanges. This sequence is representative of the last two sulfuration steps in scheme 5, starting from (40). Thus, sulfur component exchanges might occur before or after the last hexasulfuration step. Similar results were obtained with (22) (X=F) and with 1,2-dicyano-3,4,5,6-tetra(phenylthio) benzene.^[35]



Scheme 4. Exchanges of sulfur components of (20) and (22) with thiol (31) to make a library of asterisks.

A LC-MS analysis yields a non-statistical distribution of asterisks with mixed methyl and *p*-isopropoxyloxycarbonyl substituents. Scrambling reactions were observed after only 56% conversion of (20). Thus, isopropyl-4-mercaptobenzoate can displace a *p*-methylphenylthio group, and a library of asterisks decorated by several combinations of *p*-methyl and *p*-isopropoxyloxycarbonyl substituents is produced. Both asterisks containing six *p*-methyl or *p*-isopropoxyloxycarbonyl substituents are also detected. Regioisomeric structures have not been identified at this stage.

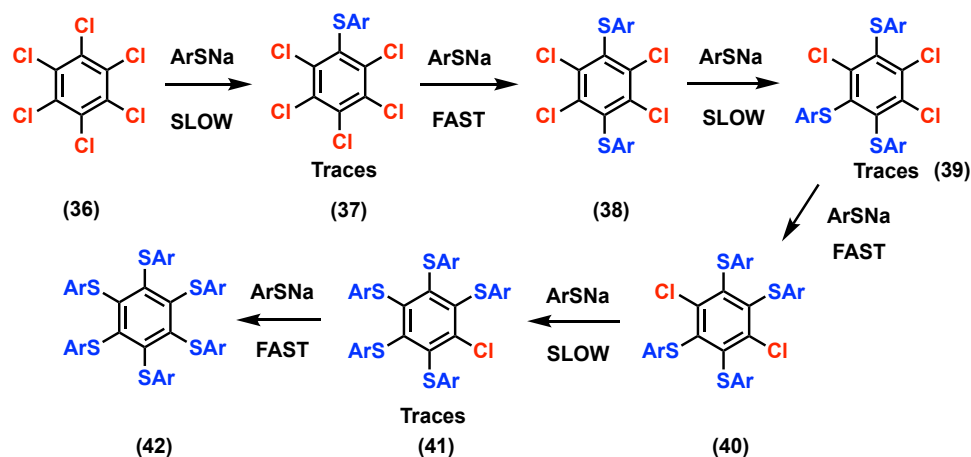
Reacting electron-poor (**21**) with *p*-thiocresol under similar conditions as in Scheme 4 led to the displacement of two F atoms for making about 40% of mixed hexa(thio)benzene asterisks decorated with *p*-methyl and *p*-isopropoxyloxycarbonyl substituents. Scrambling reactions are clearly evidenced by the hexasulfurated products distribution, where the incorporation of up to four isopropyl-4-mercapto-benzoate groups is observed. Additionally, some mixed disulfides are produced, indicating displacements of *p*-methylphenylthio groups. In summary, the tetrasulfurated asterisks (**20**), (**21**) and (**22**) also display exchange reactions, and are prone to the "sulfur dance" around the benzene core.

6.7.3.4 Pentasulfurated pyridine-cored asterisk.

In the thiaheteroaromatic series, we chose the pyridine-cored asterisk (**19**) (1.0 mol-eq.) to react with *p*-methoxybenzenethiol (5.8 mol-eq.) in the presence of K₂CO₃ in DMF at 25°C for 48 hours. Analysis of the mixture by LC-HRMS indicated the presence of at least five persulfurated asterisks incorporating one to five *p*-methoxyphenylthio groups, thus confirming the displacements of *p*-methylphenylthio groups around a pyridine core. The regioisomeric structures are not identified at this stage. Thus, exchanges of sulfur groups are also appropriate in this heteroaromatic system.

6.7.4 Mechanistic considerations.

Aromatic nucleophilic substitutions occurring with the "sulfur dance" raise questions about reaction mechanism, reversibility and reactivity. Thus, many parameters need to be circumscribed: a) the stepwise formation of the asterisks themselves (scope, kinetics and mechanisms), b) the thiolates exchange processes (scope and mechanism) on fully formed asterisks. As for the synthesis of persulfurated asterisks, literature precedents are indicative of a stepwise mechanism.^[23] It comprises six successive steps giving only traces of the odd mono-, tri-, and pentasubstituted products. A recent ¹⁹F NMR study with C₆F₆ confirmed this trend.^[47] Compounds (**39**) and (**41**) were never isolated. Pentakis(methylthio) chlorobenzene was detected in the methylthio series, but attempts to isolate it failed.^[48] Reversibility in each step of Scheme 5 has not been established, but it should not be excluded.



Scheme 5. Stepwise formation of a persulfurated benzene asterisk according to literature precedents and to the regioselectivity observed. In each step, reversible S_NAr reactions with thiolates cannot be excluded.^[22]

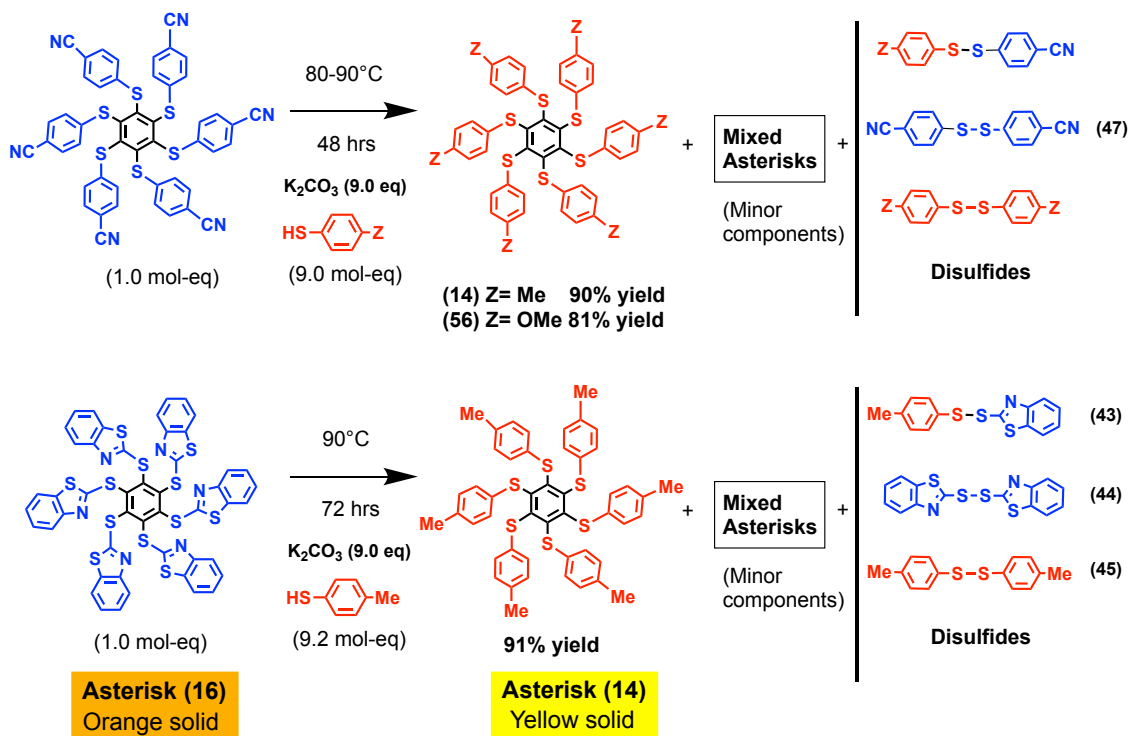
As for the degree of sulfuration, when reacting per-halogeno benzene with arenethiolates (4 to 5 mol-eq.), di-, tetra-, and hexasulfurated products (**38**), (**40**), and (**42**) are formed in polar aprotic solvents (Scheme 5).^[47] With an excess of thiolate (9 mol-eq.), the major product is hexasulfurated. In polar protic solvents (e.g. ethylene glycol/pyridine)^[49] and less polar aprotic ones (e.g. diglyme),^[45] sulfuration tends to stop after two or four substitutions under mild conditions.^[50] Polar aprotic solvents such as HMPA (hexamethylphosphoramide),^[51] DMI (1,3-dimethyl-2-imidazolidinone)^[52] and DMF^[53] favor hexasulfuration of a perhalobenzene at 25°C.^[54] In short, the solvent polarity and its aprotic nature have a strong influence towards rates and nucleophilicity of thiolates in these sulfurations. The fact that the amount of trisulfurated (**39**) and pentasulfurated products (**41**) is often negligible in most benzene persulfurations, indicates a fast conversion of these intermediates into tetra- and hexasulfurated products, (**40**) and (**42**) respectively.^{[23],[47],[50b]} This behavior is in agreement with fast scrambling hexasulfurations observed for (**20**), (**21**) and (**22**), even at 2 mol-eq.

Regioselectivity^[55] in each substitution step is summarized in Scheme 5. It follows that a divalent sulfur atom is ortho- and para-directing.^{[23],[47]} A nucleophilic aromatic sulfuration of a benzene ring may proceed by S_NAr , cS_NAr , $S_{RN}1$,^[56] S_NArH and *cine*-substitutions mechanisms according to the literature data. As for the role of sulfur, it stabilizes a negatively charged s- complex in S_NAr or presumably in a transition state (cS_NAr).

Stabilization of a carbanion by a divalent sulfur atom in s position is well known.^[57,58] One may see an analogy to the stabilization of a s-complex intermediate.

6.7.5 Synthetic applications.

Typical conversions between two asterisks are shown in Scheme 6. Instead of setting mild conditions at 25°C for producing a library of asterisks, we tried to overpass the activation energy required to most exchange reactions by heating at 90°C. As an example, we were successful in converting the hexa(thio)benzene asterisk (**16**) (reacting DCC template) into (**14**) in a 91% isolated yield. Thus, the asterisk (**16**) is transformed into (**14**), as the most phosphorescent solid known to date.^[29] Minor components are asterisks with mixed *p*-tolylthio- and benzothiazolyl-2-thio groups. Such nucleophilic aromatic substitutions are unprecedented in aromatic sulfur chemistry because six substitutions occur, even if thiophenolates are rarely used as leaving groups in S_NAr. Other examples of such conversions are presented in Scheme 6.



Scheme 6. Conversion of asterisks (**15**) and (**16**) (reacting templates) into asterisks (**14**) and (**56**) (product templates), with different photophysical properties, through dynamic sulfur exchanges at 80-90°C.

6.7.6 Demonstration of reversibility in S_NAr .

In addition to sulfur exchange components, a demonstration of covalent bonds dynamics is needed to implement S_NAr in DCC. Thus, we further explored the reversible nature of S_NAr in the "sulfur dance". We made use of two methods: 1) a convergence of the product distribution in reversible S_NAr systems starting from two different asterisks in the presence of thiols (Figure 4); 2) a thiol-promoted exchange of sulfur components between two asterisks (Figure 5).

As for the first method, it was tested between 70-100°C. Asterisk (**13**) reacted with *p*-thiocresol (9 mol-eq) to provide a library of mixed thiaarenes and (**14**) (Figure 4, reaction from left to right – **blue arrow**). When asterisk (**14**) reacted with thiophenol (9 mol-eq.), a similar library of mixed asterisks and (**13**) was produced (Figure 4 reaction from right to left – **red arrow**). The convergence of the product distribution in the two processes points to the reversible nature of the S_NAr process. As for the second method, we chose a thiolate anion to trigger exchanges of sulfur components between two asterisks. In short, we investigated the transformation of two different asterisks toward a library of mixed-substituted asterisks, with a small amount of thiolate anions as promoter, to initiate exchange reactions in DCC.

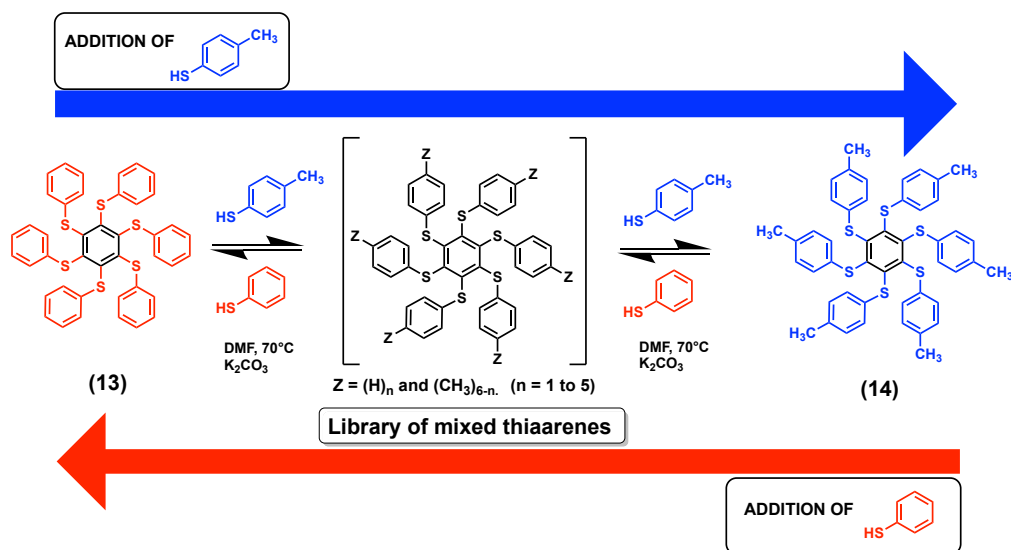
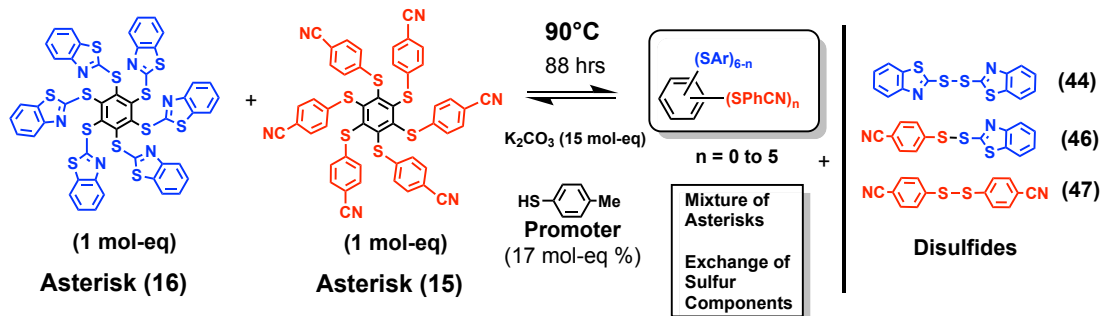


Figure 4: **blue arrow** (from left to right): reaction of asterisk (**13**) with *p*-thiocresol to provide a library of mixed thiaarenes and asterisk (**14**). **Red arrow** (from right to left) Reaction of asterisk (**14**) with thiophenol to provide a related library of mixed thiaarenes and (**13**). The library of asterisks was analyzed by ¹H NMR and HR LC-MS.

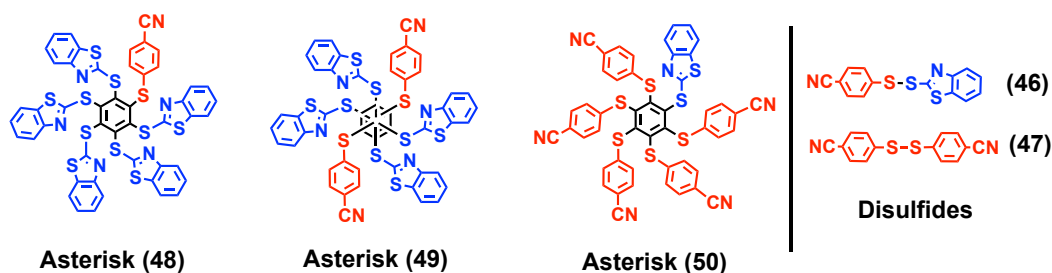
As shown in Figure 5a, an equimolar amount of asterisks (**15**) (1,0 mol-eq) and (**16**) (1,0 mol-eq) in DMF was treated with *p*-thiocresol as a promoter (17 mol-eq. % relative to each asterisk) in presence of K_2CO_3 (15 mol-eq.). The mixture was heated at 90°C for 88 hrs. LC-HRMS analysis clearly established a dynamic exchange of sulfur components between the two asterisks in the formation of a library of mixed asterisks incorporating benzothiazolyl-2-thio and *p*-cyanophenylthio arms in a non-statistical distribution (Figure 5b). Most importantly, the initiation of exchange reactions is confirmed by the detection of mixed minor asterisks structures (**51**), (**52**), (**53**) and (**54**) and disulfides (**43**) and (**55**) incorporating *p*-methylphenylthio moieties (Figure 5c). They originate from S_NAr reactions between *p*-thiocresol and the asterisks (**15**) and (**16**). This behavior is coherent with the S_NAr exchange reactions in Scheme 6. The release of *p*-cyanophenylthiolate and benzothiazolyl-2-thiolate anions promoted further scrambling reactions between the asterisks (**15**) and (**16**), as determined by the detection of a series of mixed asterisks (**48**), (**49**), (**50**) and disulfides (**46**) and (**47**) resulting from the exchanges of sulfur components (Figure 5b). Thus, this experiment unambiguously confirmed the dynamic and reversible nature of S_NAr in the "sulfur dance" surrounding an aromatic core.

A)



B)

Products from exchange of sulfur components



C)

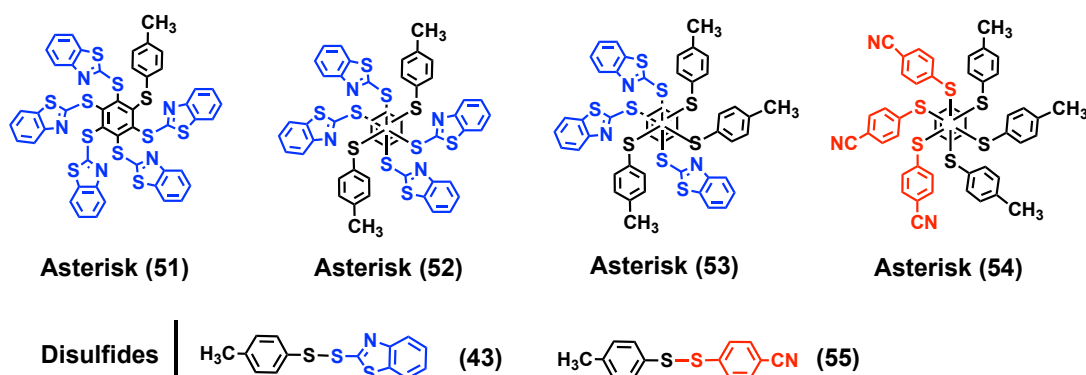
p-Thiocresol promoter incorporated into asterisks (15) and (16)

Figure 5: a) Exchange of sulfur components between asterisks (15) and (16) through reversible S_NAr in the "sulfur dance" promoted by *p*-thiocresol; b) Products resulting from reversible exchange of sulfur components from asterisks (15) and (16) as determined by LC-HRMS; c) Products resulting from the incorporation of *p*-thiocresol as a promoter into asterisks (15) and (16), as determined by LC-HRMS. Compounds (44) to (55) were identified after work.

6.7.7 Conclusion

Here, we indicate the generality of reversible nucleophilic aromatic substitutions (S_NAr) involving thiaarenes or thiaheteroarenes and thiols, which lead to sulfur exchange components, that one may consider as a sort of "sulfur dance". In this process, sulfur exchange reactions occur around an aromatic core, where thiolates behave both as nucleophiles and leaving groups in S_NAr , without the need for metal catalysis.^[43,44] The exchange of sulfur components between two asterisks, as well as the convergence of product distributions, starting from two different asterisks reacting with appropriate thiolates confirmed the reversible and dynamic nature of the sulfur dance process. The conversion of an asterisk (reacting template) into a library of asterisks at 25°C, may change to a selective formation of another asterisk (product template) at 90°C in high yield. These dynamic processes represent model studies on reversible nucleophilic aromatic substitutions of general significance in aromatic chemistry and in DCC. The "sulfur dance" around aromatic templates opens wider frontiers in view of the intrinsic adaptive and self-correcting features of DCC. It may also be implemented for the discovery of multifunctional, adaptive materials with tunable optical character such as

exalted and smart ("turn-on") luminescence of potential applications in the fields of imaging, nanoscience, and life sciences.^[59]

Experimental Section (see experimental part of the thesis, section for chapter 6)

Acknowledgements

We are extremely grateful to the Agence Nationale de la Recherche (ANR) in France (program PRC) for the grant ANR-20-CE07-0031 Acronym: "SulfurDance". We also acknowledge financial support from the Excellence Initiative of Aix-Marseille University – A*Midex, a French "Investissements d'Avenir" programme, and a doctoral contract to S.G.. M.V. acknowledges financial support from the French-Italian University for a doctoral contract (No C2-141 – Vinci program). A CNRS (No. PICS 07573) Program for International Scientific Collaborations with the Univ. of Bologna is thanked, as well as the University of Bologna, Aix-Marseille Université, CINaM and CNRS France. We thank Dr. Raymond Noël for providing us a few samples. This work was also supported by USIAS, the Institute for Advanced Study of the University of Strasbourg (JML) and the CNRS UMR 7006 ISIS (JLS).

Keywords: Sulfur • Dynamic Covalent Chemistry • S_NAr • ThiaArenes • Reversible reactions

References of the article (above) submitted for publication:

- [1] D. G. Brown, J. Boström, *J. Med. Chem.* **2016**, *59*, 4443.
- [2] F. Terrier, in *Modern Nucleophilic Aromatic Substitution*, Wiley-VCH, Weinheim, Germany **2013**.
- [3] (a) R. A. Rossi, A. B. Pierini, A. B. Penenory, *Chem Rev.* **2003**, *103*, 71; (b) J. F. Bunnett, *Acc. Chem. Res.* **1978**, *11*, 413.
- [4] (a) S. Rohrbach, A. J. Smith, J. H. Pang, D. L. Poole, T. Tuttle, S. Chiba, J. A. Murphy, *Angew. Chem. Int. Ed.* **2019**, *58*, 16368; *Angew. Chem.* **2019**, *131*, 16518; (b) E. E. Kwan, Y. Zeng, H. A. Besser, E. N. Jacobsen, *Nature Chem.* **2018**, *10*, 917; (c) C. N. Neumann, T. Ritter, *Acc. Chem. Res.* **2017**, *50*, 2822; (d) S. D. Schimler,

- M. A. Cismesia, P. S. Hanley, R. D. J. Froese, M. J. Jansma, D. C. Bland, M. S. Sanford, *J. Am. Chem. Soc.* **2017**, *139*, 1452; (e) D. J. Leonard, J. W. Ward, J. Clayden, *Nature* **2018**, *562*, 105.
- [5] (a) M. Makosza, *Chem. Soc. Rev.* **2010**, *39*, 2855; (b) M. Makosza, *Acc. Chem. Res.* **1987**, *20*, 282.
- [6] For an early discussion on reversible S_NAr: J. F. Bunnett, R. E. Zahler, *Chem. Rev.* **1951**, *49*, p. 301.
- [7] (a) Williamson and Scrugham, *J.* **1854**, *7*, 237; (b) Williamson and Scrugham, *Annalen* **1854**, *92*, 316; (c) Pisani, *Compt. Rend.*, **1854**, *39*, 852 ; (d) Pisani, *Annalen*, **1854**, *92*, 326.
- [8] J.-M. Lehn, *Chem. Eur. J.* **1999**, *5*, 2455.
- [9] J.-M. Lehn, *Chem. Soc. Rev.* **2007**, *36*, 151.
- [10] F. B. L. Cougnon, J. K. M. Sanders, *Acc. Chem. Res.* **2012**, *45*, 2211.
- [11] Y. Jin, C. Yu, R. J. Denman, W. Zhang, *Chem. Soc. Rev.* **2013**, *42*, 6634.
- [12] M.C.T. Fyfe, J. F. Stoddart, *Acc. Chem. Res.* **1997**, *30*, 393–401.
- [13] P. T. Corbett, J. L. Leclaire, L. Vial, K.R. West, J.-L. Wietor, J.K.M. Sanders, S.Otto, *Chem. Rev.* **2006**, *106*, 3652.
- [14] M. E. Belowich, J. F. Stoddart, *Chem. Soc. Rev.* **2012**, *41*, 2003.
- [15] A. Ciesielski, M. El Garah, S. Haar, P. Kovaricek, J.-M. Lehn, P. Samori, *Nature Chem.* **2014**, *6*, 1017.
- [16] R.-C. Brachvogel, M. von Delius, *Eur. J. Org. Chem.* **2016**, 3662.
- [17] S. P. Black, J. K. M. Sanders, A. R. Stefankiewicz, *Chem. Soc. Rev.* **2014**, *43*, 1861.
- [18] A. G. Orrillo, A. M. Escalante, R. L. E. Furlan, *Chem. Eur. J.* **2016**, *22*, 6746.
- [19] D. Drahonovsky, J.-M. Lehn, *J. Org. Chem.* **2009**, *74*, 8428.
- [20] R. Gu, K. Flidrova, J.-M. Lehn, *J. Am. Chem. Soc.* **2018**, *140*, 5560.
- [21] S. Kulchat, J.-M. Lehn, *Chem. Asian J.* **2015**, *10*, 2484.
- [22] P.J. Boul, P. Reutenauer, J.-M. Lehn, *Org. Lett.* **2005**, *7*, 15.
- [23] M. Gingras, J.-M. Raimundo, Y. M. Chabre, *Angew. Chem. Int. Ed.* **2006**, *45*, 1686; *Angew. Chem.* **2006**, *118*, 1718.
- [24] M. Gingras, A. Pinchart, C. Dallaire, *Angew. Chem. Int. Ed. Engl.* **1998**, *37*, 3149; *Angew. Chem.* **1998**, *110*, 3338.

- [25] J. H. R. Tucker, M. Gingras, H. Brand, J.-M. Lehn, *J. Chem. Soc. Perkin Trans. II* **1997**, 1303.
- [26] M. Mayor, J.-M. Lehn, *J. Am. Chem. Soc.* **1999**, *121*, 11231.
- [27] M. Mayor, J.-M. Lehn, K.M. Fromm, D. Fenske, *Angew. Chem. Int. Ed. Engl.* **1997**, *36*, 2370; *Angew. Chem.* **1997**, *109*, 2468.
- [28] M. Mayor, J.-M. Lehn, *Helv. Chim. Acta* **1997**, *80*, 2277.
- [29] G. Bergamini, A. Fermi, C. Botta, U. Giovanella, S. Di Motta, F. Negri, R. Peresutti, M. Gingras, P. Ceroni, *J. Mater. Chem. C* **2013**, *1*, 2717.
- [30] A. Fermi, G. Bergamini, R. Peresutti, E. Marchi, M. Roy, P. Ceroni, M. Gingras, *Dyes and Pigments* **2014**, *110*, 113.
- [31] M. Villa, S. D'Agostino, P. Sabatino, R. Noël, J. Busto, M. Roy, M. Gingras, P. Ceroni, *New J. Chem.* **2020**, *44*, 3249.
- [32] A. Fermi, G. Bergamini, M. Roy, M. Gingras, P. Ceroni, *J. Am. Chem. Soc.* **2014**, *136*, 6395.
- [33] M. Villa, M. Roy, G. Bergamini, M. Gingras, P. Ceroni, *Dalton Trans.* **2019**, *48*, 3815.
- [34] (a) Pinchart, A. *Synthèses d'architectures moléculaires de sulfure de phénylène et de noyaux aromatiques persulfurés* Ph.D. Thesis, Université Libre de Bruxelles, Belgium and Université de Paris XI Orsay, France, Sept. 26 **2000**, pp. 163-165; <http://www.theses.fr/2000PA112189>; (b) R. Noël, *Étude et développement de substrats microporeux pour l'adsorption du radon et son application en physique du neutrino*, doctoral dissertation, Aix-Marseille Université, Marseille, France, Dec. 13, **2015**; <https://tel.archives-ouvertes.fr/tel-01521979>; (c) M. Villa, *Smart and Highly Phosphorescent Asterisks for (Bio)Sensors, Antennae, and Molecular Imaging*, doctoral dissertation, Aix-Marseille Université, Marseille, France and University of Bologna, Bologna, Italy, Dec. 14 **2018**; <https://ecole-doctorale-250.univ-amu.fr/fr/soutenance/336>; (d) M. Villa, B. Del Secco, L. Ravotto, M. Roy, E. Rampazzo, N. Zaccheroni, L. Prodi, M. Gingras, S. Vinogradov, P. Ceroni, *J. Phys. Chem. C* **2019**, *123*, 29884.
- [35] W. J. Ong, T. M. Swager, *Nature Chem.* **2018**, *10*, 1023.
- [36] With 3,6-di(thio)tetrazines: (a) T. Santos, D. S. Rivero, Y. Pérez-Pérez, E. Martín-Encinas, J. Pasán, A. H. Daranas, R. Carillo, *Angew. Chem. Int. Ed.* **2021**, *60*,

- 18783; *Angew. Chem.* **2021**, 133, 18931; (b) Z-C. Wu, Q.-H. Guo, M.-X. Wang, *Angew. Chem. Int. Ed.* **2017**, 56, 7151; *Angew. Chem.* **2017**, 129, 7257.
- [37] M. Schnürch, M. Spina, A. F. Khan, M. Mihovilovic, P. Stanetty, *Chem. Soc. Rev.* **2007**, 36, 1046.
- [38] N. Roy, B. Bruchmann, J.-M. Lehn, *Chem. Soc. Rev.* **2015**, 44, 3786.
- [39] Y. Liu, J.-M. Lehn, A.K.H. Hirsch, *Acc. Chem Res.* **2017**, 50, 376.
- [40] Unpublished preliminary MTT tests.
- [41] (a) F. Terrier, *Chem. Rev.* **1982**, 82, 78; (b) S. Kurbatov, S. Lakhdar, R. Goumont, F. Terrier, *Org. Prep. Proc. Int.* **2012**, 44, 289; (c) R.O. Al-Kaysi, I. Gallardo, G. Guirado, *Molecules* **2008**, 13, 1282; (d) E. Buncel, F. Terrier, *Org. & Biomol. Chem.* **2010**, 8, 2285; (e) M. Makosza, *Chem. Eur. J.* **2014**, 20, 5536; (f) K. Calfuman, S. Gallardo-Fuentes, R. Contreras, R. A. Tapia, P. R. Campodonico, *New J. Chem.* **2017**, 41, 12671; (g) Y-F. Kang, L.-Y. Niu, Q.-Z. Chin. Yang, *Chem. Lett.* **2019**, 30, 1791.
- [42] Y. Masuya, Y. Kawashima, T. Kodama, N. Chatani, M. Tobisu, *Synlett* **2019**, 30, 1995.
- [43] M. A. Rivero-Crespo, G. Toupalas, B. Morandi, *J. Am. Chem. Soc.* **2021**, 143, Doi.org/10.1021/jacs.1c09884
- [44] Z. Lian, B. N. Bhawal, P. Yu, B. Morandi, *Science* **2017**, 356, 1059.
- [45] S. D. Pastor, E. T. Hessel, *J. Org. Chem.* **1985**, 50, 4812.
- [46] L. Testaferri, M. Tiecco, M. Tingoli, D. Bartoli, A. Massoli, *Tetrahedron* **1985**, 41, 1373.
- [47] P. Dognini, P.M. Killoran, G.S. Hanson, L. Lewis Halsall, T. Chaudhry, Z. Islam, F. Giuntini, C.R. Coxon, *Peptide Science*, e24182, **2020**. Doi/org/10.1002/pep2.24182.
- [48] M. E. Peach, E. S. Rayner, *J. Fluor. Chem.* **1979**, 13, 447.
- [49] J. J. Jesudason, M. E. Peach, *J. Fluor. Chem.* **1988**, 41, 357.
- [50] (a) M. E. Peach, A. M. Smith, *J. Fluor. Chem.* **1974**, 4, 399; (b) K. R. Langille, M. E. Peach, *J. Fluor. Chem.* **1971/72**, 1, 407; (c) M. Kulka, *J. Org. Chem.* **1959**, 24, 235.
- [51] P. Cogolli, F. Maiolo, L. Testaferri, M. Tingoli, M. Tiecco, *J. Org. Chem.* **1979**, 44, 2642.

- [52] D. D. Mac Nicol, P. R. Mallinson, A. Murphy, G. J. Sym., *Tetrahedron Lett.* **1982**, **23**, 4131-4134.
- [53] M. E. Peach, E. S. Rayner, *J. Fluor. Chem.* **1979**, **13**, 447.
- [54] T. R. Crowell, M. E. Peach, *J. Fluor. Chem.* **1982**, **21**, 469.
- [55] E. Buncl, J. M. Dust, F. Terrier, *Chem. Rev.* **1995**, **95**, 2261.
- [56] (a) L. Grossi, S. Strazzari, *J. Chem. Soc., Perkin Trans 2*, **1999**, 2141; (b) S. Montanari, C. Paradisi, G. Scorrano, *J. Org. Chem.* **1993**, **58**, 5628; (c) B. C. Musial, M. E. Peach, *J. Fluor. Chem.* **1976**, **7**, 459; (d) S. D. Pastor, *Helv. Chim. Acta* **1988**, **71**, 859.
- [57] D. Seebach, E. J. Corey, *J. Org. Chem.* **1975**, **40**, 231.
- [58] C. F. Bernasconi, K. W. Kittredge, *J. Org. Chem.* **1998**, **63**, 1944.
- [59] Some applicative areas of hexakis(arylthio)benzenes were disclosed in industry as early as in 1963. Patents on biocidal properties as herbicides, insecticides, anti-oxidant additives to lubricating oils, intermediates in dyestuffs and biologically active materials were reported: (a) W. Reifschneider, Aralkyl Poly(thioethers), (Dow Chemicals Co.) US 3 100 802-A, **1963**; (b) W. Reifschneider, Thioethers. (Dow Chemicals Co.), US 3 228 989, **1966**; (c) W. Reifschneider, Hexakis thioethers (Dow Chemicals Co.), US 3 311 664, **1967** [Chem. Abstr. **1967**, **67**, 402893]; (d) J. D. Spivack, Compositions Stabilized with Poly(alkylthio)benzenes (Ciba-Geigy AG), DE 2 819 882, **1978** [Chem. Abstr. **1978**, **90**,88309z].

ADDITIONAL DATA TO THE SUBMITTED ARTICLE

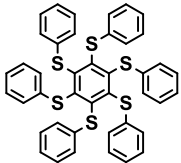
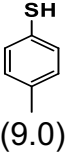
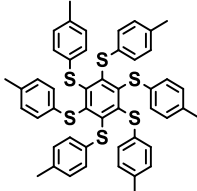
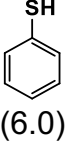
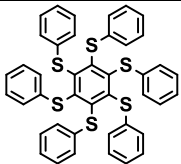
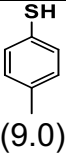
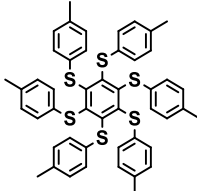
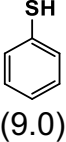
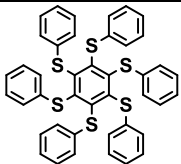
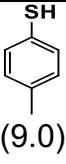
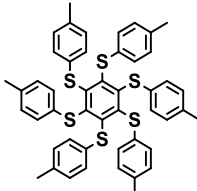
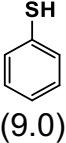
6.8 Reversible S_NAr on tetra-, hexasulfurated and 1,2-dicyano-tetrasulfurated / tetraoxygenated benzene with different phenyl thiolates

6.8.1 Reversible S_NAr on hexakis(phenylthio)benzene and hexakis(4-methylphenylthio) benzene with phenyl thiolates

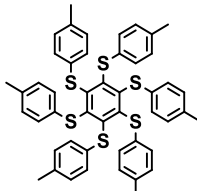
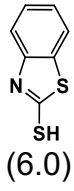
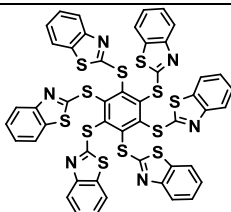
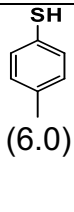
As shown in Table 1, fourteen reactions were run to investigate the sulfur-sulfur exchange between two persulfurated asterisks (hexakis(phenylthio) benzene and hexakis(4-methylphenylthio) benzene) and one heteroarasterisk. Different aryl thiolates such as 4-

methylbenzenethiol, thiophenol, and 4-benzothiazole were used. Three bases and two different solvents were tested to determine the S_NAr reversibility conditions. The bases are potassium carbonate (K_2CO_3), potassium tert-butoxide (t-BuOK) and cesium carbonate (Cs_2CO_3) whereas the polar aprotic solvents include DMF (N,N-dimethylformamide) and DMI (1,3-dimethyl-2-imidazolidinone).

Table 1: List of reactions tested for S_NAr reversibility on persulfurated benzenes toward DCC.

Assay no.	Starting Asterisk	Thiolate (mol-eq)	Temp (°C)	Time (Hrs)	Solvent	Base (mol-eq)	1H NMR Exchanges
R-124		 (9.0)	100	72	DMF	K_2CO_3	Yes
R-177		 (6.0)	100	72	DMF	K_2CO_3	Yes
R-181		 (9.0)	100	87	DMF	tBuOK	Yes
R-180		 (9.0)	100	87	DMF	tBuOK	Yes
R-183		 (9.0)	100	87	DMF	Cs_2CO_3	Yes
R-182		 (9.0)	100	87	DMF	Cs_2CO_3	Yes

R-179			100	41	DMI	K ₂ CO ₃	Yes
R-178			100	41	DMI	K ₂ CO ₃	Yes
R-174			90	40	DMI	Cs ₂ CO ₃	Yes
R-175			90	40	DMI	tBuOK	Yes
R-169			70	41	DMI	Cs ₂ CO ₃	Yes, but not much
R-168			70	41	DMI	Cs ₂ CO ₃	Yes, but not much
R-171			50	43	DMI	tBuOK	No
R-170			50	43	DMI	tBuOK	No
R-171			50	43	DMI	tBuOK	Yes

R-172		 (6.0)	60	40	DMI	tBuOK	Yes
R-173		 (6.0)	60	40	DMI	tBuOK	Yes

- All reactions were run under argon in a degassed solvent in a sealed pressure tube, as a closed reaction vessel.
- Solvents were kept under activated molecular sieves 3Å (activated at 250°C for 3 hours)
- t-BuOK was used as received.
- Cs₂CO₃ and K₂CO₃ salts were dried in an oven at 200°C.

Several reactions were tried from R-124 to R-173 by changing temperature, time, solvent, and bases. DMF is a common solvent used for most S_NAr reactions. Another solvent such as DMI (b.p. 225°C) was chosen because of its high polarity, thermal and chemical stability even at high temperatures. It can effectively promote nucleophilic substitution reactions. Cesium carbonate was selected because of its good solubility in polar solvents but also because of the "cesium effect", [2] making thiolate anions more nucleophilic from a loose ion pair with Cs⁺, compared to K⁺ from K₂CO₃. [1] Potassium tertiary butoxide was chosen as a strong base, being fully soluble in DMF or DMI.

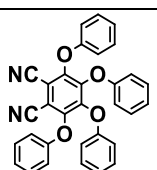
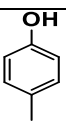
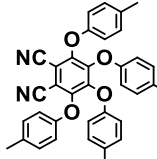
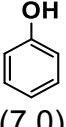
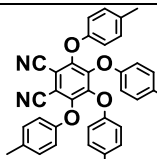
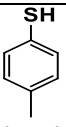
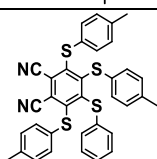
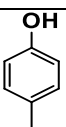
The most important parameter for dynamic covalent S_NAr reactions is the temperature effect on S_NAr for sulfur/sulfur exchange reactions. All reactions run at temperature higher than 70°C provides sufficient lability of the sulfur substituents on moderately or slightly deactivated starting asterisks. Reactions run at 50-60°C are favored if the base is strong and the arylthiol is fully deprotonated. Thus, the thiolate anions are produced at a higher concentration.

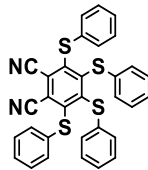
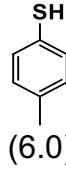
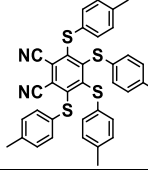
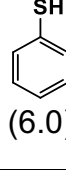
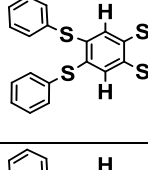
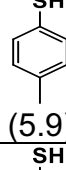
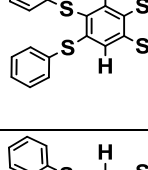
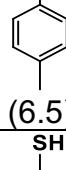
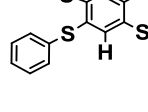
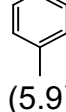
Although DMI gave satisfactory results, we prefer to use DMF for convenience for the purification, and removal of the solvent. Potassium carbonate seems to be convenient for these reactions at lower cost. t-BuOK is not stable at high temperatures. For further results, an experimental section is available for Chapter 6).

6.8.2 Reversible S_NAr on tetrasulfurated benzene and tetrasulfurated / tetraoxygenated 1,2-dicyano-benzene with different phenyl thiolates.

Ten more reactions were run to check S/S, S/O and O/O exchanges by S_NAr as shown in Table 2. All reactions were run in DMF using potassium carbonate as a base at temperatures higher or equal to 90°C. 1,2-Dicyanobenzene substituted with phenyloxy or phenylthio groups have shown some S/S, S/O, O/O exchanges. These reactions are usually considered easier, according to the results of Swager et al. The tetrasulfurated benzene substrates are expected to require higher temperature if the Meisenheimer complex is formed. The lower stability of this complex is due to a decrease in the number of sulfur substituents to stabilize it. Some data are being analyzed in Strasbourg by LC-HRMS.

Table 2: List of reactions tested for S_NAr on 1,2-dicyano-tetrasulfurated benzene and 1,2-dicyano-tetraoxygenated benzene and 1,2,4,5-tetrasulfurated benzene for S/S, S/O and O/O exchanges in DCC.

Assay no.	Starting Asterisk	Thiolate (mol-eq)	Temp (°C)	Time (Hrs)	Solvent	Base (mol-eq)	¹ H NMR Exchanges
R-224		 (6.0)	RT → 90 →	48 18	DMF	K ₂ CO ₃	RT- No 90°C- Yes
R-225		 (7.0)	RT → 90 →	48 18	DMF	K ₂ CO ₃	RT- No 90°C- Yes
R-227		 (6.0)	90	48	DMF	K ₂ CO ₃	Yes
R-228		 (6.0)	88	48	DMF	K ₂ CO ₃	Yes

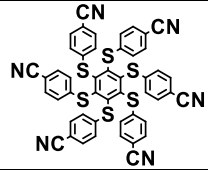
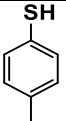
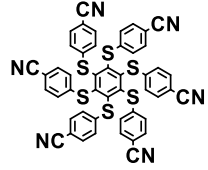
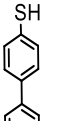
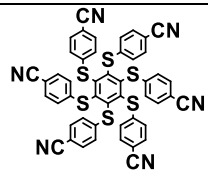
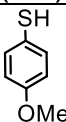
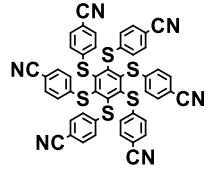
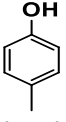
R-230		 (6.0)	90	72	DMF	K ₂ CO ₃	Yes
R-231		 (6.0)	90	72	DMF	K ₂ CO ₃	Yes
R-232		 (5.9)	90 → 116 →	48 18	DMF	K ₂ CO ₃	in progress
R-233		 (6.5)	118	48	DMF	K ₂ CO ₃	Yes
R-234		 (5.9)	150	111	DMF	K ₂ CO ₃	Yes

- All reactions were run under argon in a degassed solvent in a sealed pressure tube, as a closed reaction vessel.
- Solvents were kept under activated molecular sieves 3Å (activated at 250°C for 3 hours)
- K₂CO₃ salts were dried in an oven at 200°C.

6.8.3 Asterisk conversion to another one by sulfur exchange reactions

In Table 3, we were successful in converting an asterisk to another one by using an excess of thiol in the presence of K₂CO₃ at 90°C. Hexakis(4-cyanophenylthio)benzene asterisk is an electron-deficient asterisk to provide these conversions in isolated yields ranging from 79-90%. These reactions are additional to the ones presented in the submitted manuscript. These types of reactions are not found in the literature and further studies are required to extend the scope of them. It definitively shows that S_NAr are dynamic.

Table 3: asterisk conversion to another one by sulfur or oxygen component exchanges.

Assay no.	Starting Asterisk	Thiolate (mol-eq)	Temp (°C)	Time (Hrs)	Solvent	Base (mol-eq)	¹ H NMR Exchanges
R-109		 (9.0)	90	48	DMF	K ₂ CO ₃	Yes Yield= 90%
R-113		 (9.0)	90	40	DMF	K ₂ CO ₃	Yes Yield= 79%
R-115		 (9.0)	90	48	DMF	K ₂ CO ₃	(R-25) RT- Yes 90°C- Yes Yield= 81%
R-226		 (6.0)	RT → 90 →	48 18	DMF	K ₂ CO ₃	RT- mainly starting material 90°C- Yes

1. T. Flessner, S. Doye, *J. Prakt. Chem.* **1999**, 341, 436-444.
2. G. Dijkstra, W. H. Kruizinga, R. M. Kellogg, *J. Org. Chem.*, **1987**, 52, 4230-4234.

CHAPTER 7

EXPERIMENTAL PART OF THE THESIS

CHAPTER 7: GENERALITIES

Materials and general procedures: All reagents, solvents and chemicals were purchased from Sigma-Aldrich, Fisher, Alfa-Aesar or TCI Europe and used directly unless otherwise stated (purity: reagent or analytical grade). Solvents were stored for several days over freshly activated 3Å or 4Å molecular sieves (activated for 3 hours at 250°C). Reactions were monitored by TLC, ^1H , ^{19}F , ^{13}C NMR spectroscopy or LC-MS and LC-HRMS.

Thin-Layer chromatography (TLC): TLC analyses were performed on precoated silica gel (Alugram® SilG/UV254gel) aluminium plates from Macherey-Nagel. Compounds were visualized with UV-light (254 or 365 nm)

Flash chromatography was performed over silica gel 60, Merck type 230-400 mesh (40-63µm).

NMR spectroscopy

NMR (CINaM, Aix-Marseille Univ.): most spectra ^1H (399.78 MHz), ^{13}C (100.53 MHz) and ^{19}F (376.17 MHz) were recorded on **JEOL ECX-400** spectrometer with internal reference signals from residual protic solvent CHCl_3 at 7.26 ppm and $\text{DMSO-}d_6$ at 2.50 ppm, along with TMS. As for ^{13}C NMR spectra, the central resonance of the triplet for CDCl_3 at 77.16 ppm and the signal for $\text{DMSO-}d_6$ at 39.52 ppm were used as internal references.^[1] As for ^{19}F NMR spectra, the internal reference was C_6F_6 signal at -164.90 ppm relative to CFCl_3 (0 ppm). The resonance multiplicities in the ^1H NMR spectra are described as “s” (singlet), “d”(doublet), “t” (triplet), “q” (quarted), “sept” (septet) “m” (multiplet) or “b” (broad).

NMR (Univ. of Bologna): a **Varian ARX Inova 400** NMR spectrometer was used in a few cases for recording ^1H NMR (400.72 MHz) and ^{13}C NMR (100.76 MHz) spectra.

Mass spectroscopy

LC-MS (APCI and ESI+) (CINaM, Aix-Marseille Univ.): analyses were performed with a C18 Phenomenex Luna (3µm; 100 x 2 mm) column on a Shimadzu LCMS-2020 fitted with two LC-20AD prominence pumps equipped with a DGU-20AD prominence line degasser, a SIL-20AHT prominence auto-sampler, a CTO-20A prominence column oven, a SPD-20A prominence UV/Vis detector, a FCV-20AH valve unit, a Parker NitroFloLab nitrogen generator and either an APCI SET or an ESI SET detector. Positive or negative modes were used for both APCI and ESI mode.

GC-MS (CINaM, Aix-Marseille Univ.): Low resolution mass spectra (LRMS-EI) were recorded on a Shimadzu GC-MS QP2010SE instrument equipped with a DI2010 direct introduction unit with an electronic impact ionization source at 70eV. Direct introduction of the sample in the electronic impact (EI) detector.

LC-HRMS (ESI+) (ISIS, Univ. of Strasbourg): Analyses were performed using a Dionex RSLC U3000HPLC system (Thermo) with a chromatography column Acclaim Phenyl-1, (3 μ m; 150 x 2.1 mm). The mobile phase was water with 0.1% formic acid (method A) or acetonitrile with 0.1% formic acid (method B). Full MS spectra were acquired using Exactive series 2.9 sp4 software in a positive ion mode at a 3.5 kV spray voltage setting on a Thermo Scientific Exactive Plus EMR. Resolution of full MS and HCD scans were 140,000 and data were acquired in profile mode and processed using Xcalibur 4.3.

HRMS (ESI+) (Spectropôle of Marseille): High resolution mass spectra were recorded at the Spectropôle of Marseille (France) in triplicate with double internal standards. Oligomers of poly(propylene glycol) were used as internal standards. Ionization was facilitated by some adducts with Ag⁺, NH₄⁺ or Na⁺ ions. Two spectrometers were used: a) SYNAPT G2 HDMS (Waters) instrument equipped with an ESI source and a TOF analyzer in a positive mode. b) QStar Elite (Applied Biosystems SCIEX) instrument equipped with an atmospheric ionization source (API). The samples were ionized under ESI with an electrospray voltage of 5500 V; orifice voltage: 10V, and air pressure of the nebulizer at 20 psi. A TOF analyzer was used in a positive mode. Most high-resolution mass spectra (ESI+) were recorded in triplicate using double internal standards at the Spectropole (<https://fr-chimie.univ-amu.fr/spectropole/>).

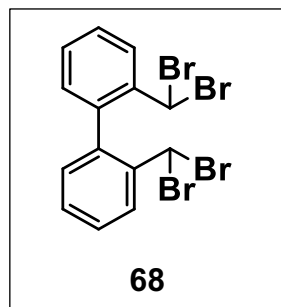
FT-IR: Infrared absorption spectra were directly recorded on solids or neat liquids on a Perkin-Elmer Spectrum 100 FT-IR Spectrometer equipped with a universal ATR accessory (contact crystal: diamond).

Melting points (uncorrected) were recorded with an Electrothermal 9200 digital melting point apparatus with a ramp rate temperature (rate increase of temperature) using samples in glass capillaries.

(1) Gottlieb, H.E., Kotlyar, V., Nudelman, A., "NMR Chemical shifts of common laboratory solvents as trace impurities", *J. Org. Chem.* **1997**, 62, 7512-7515.

EXPERIMENTAL SECTION FOR CHAPTER 2

Experimental Section for Scheme 1:



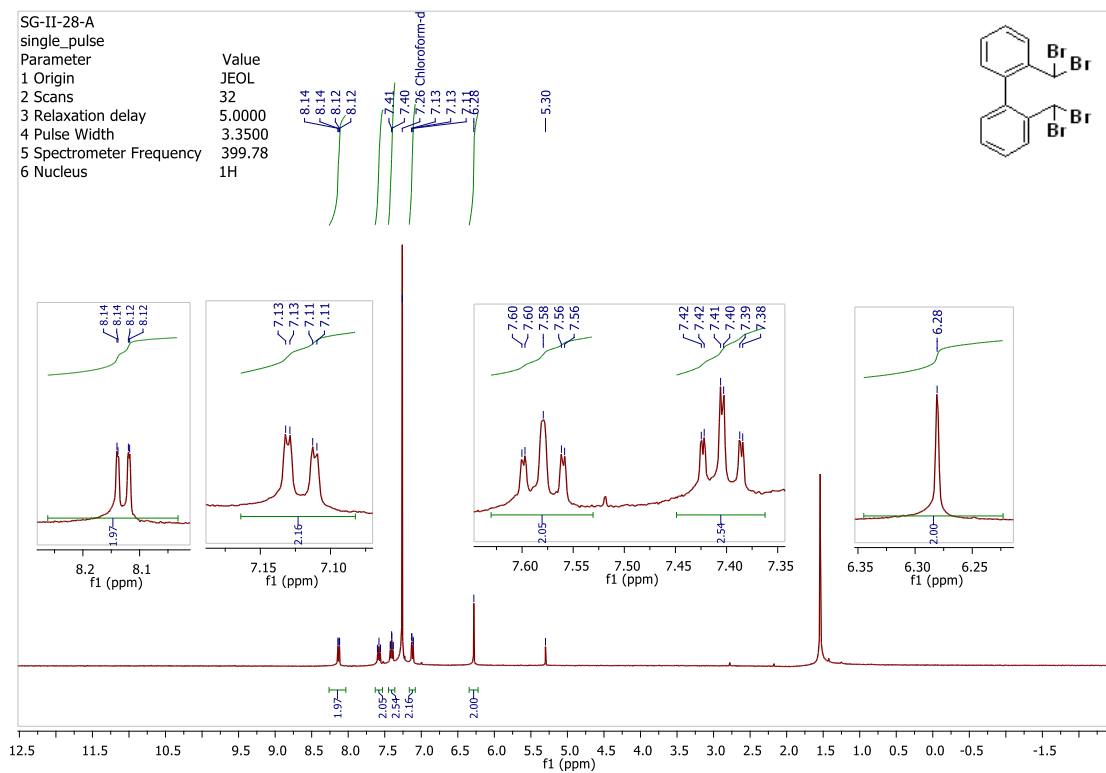
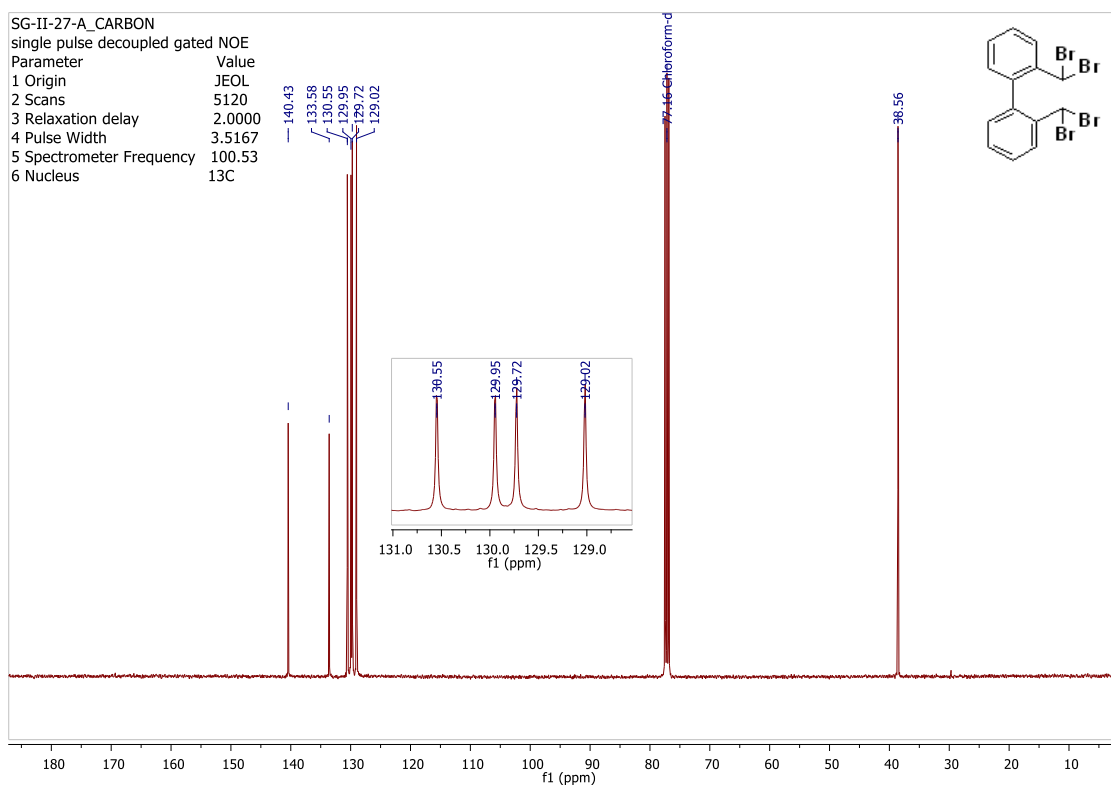
Procedure for compound-68 (R-33): In an oven-dried sealed tube, 2,2'-bis(bromomethyl)-1,1'-biphenyl (**50**) (100.8 mg, 0.296 mmol, 1.00 mol-eq.) was added and dissolved in CCl₄ (0.8 mL). The tube was purged with argon for 15 minutes. To this solution N-bromosuccinimide (575.9 mg, 3.235 mmol, 10.93 mol-eq.) and benzoyl peroxide (3.8 mg, 0.0157 mmol, 0.05 mol-eq.) were added. The reaction mixture was stirred for 50 hrs at 84°C. The consistency of the reaction mixture changed with time from thick to fluent. A NaOH solution (2 M) was poured into the mixture after cooling to 20°C, and it was extracted with toluene (4×10 mL). The organic phases were collected and dried over anhydrous MgSO₄, filtered and evaporated to dryness. **Mass: 136.7 mg, Yield: 93.4%.**

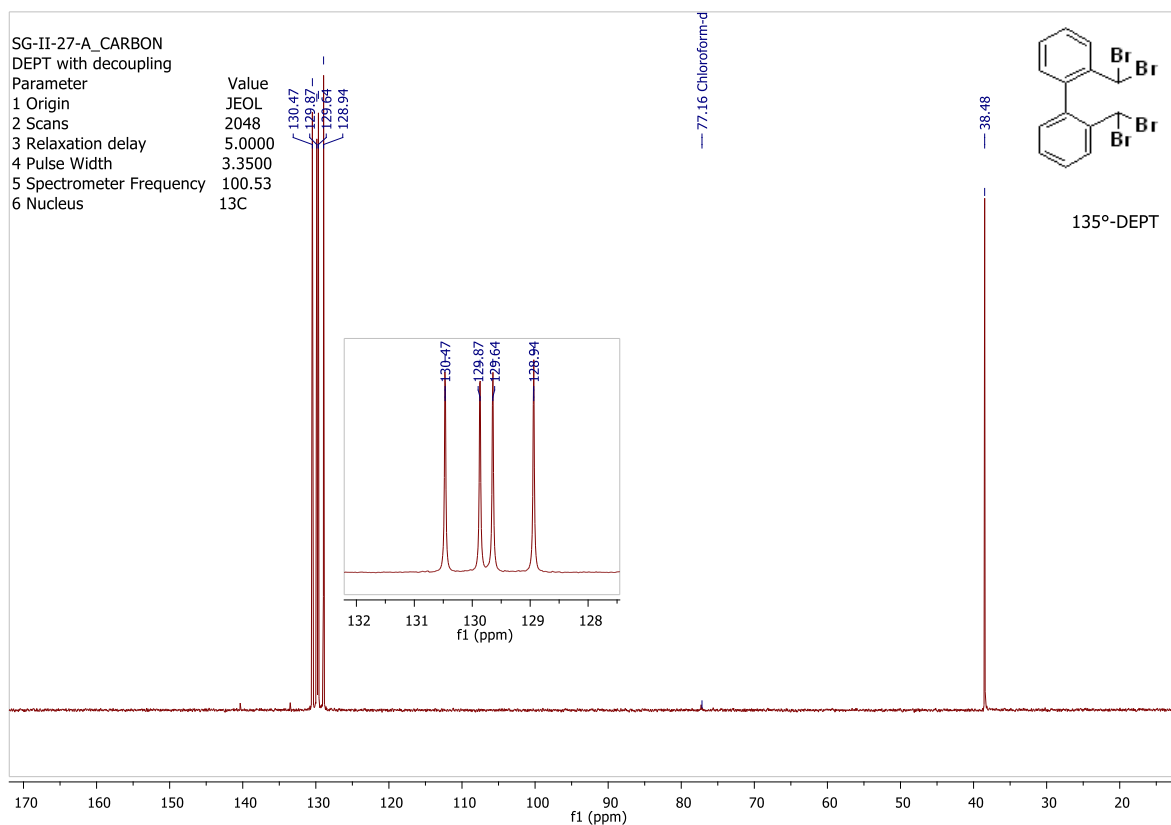
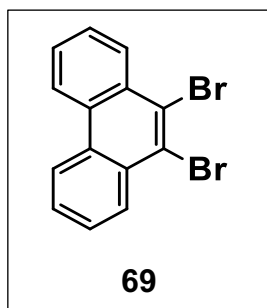
RESULTS: ¹H-NMR (**SG-II-28-A**) indicates the desired product 2,2'-bis(dibromomethyl)-1,1'-biphenyl (**2**).

SG-II-28-A: ¹H NMR (399.78 MHz, CDCl₃): δ = 8.13 (dd, J = 8.0, 0.8 Hz, 2H), 7.57 (td, J = 8.3, 1.2 Hz, 2H), 7.40 (td, J = 7.5, 1.2 Hz, 2H), 7.12 (dd, J = 7.7, 1.2 Hz, 2H), 6.29 (s, 2H) ppm. ¹³C-NMR (100.53 MHz, CDCl₃) (**SG-II-27-A**) δ = 140.43, 133.58, 130.55, 129.95, 129.72, 129.02, 38.56; **M.p.:** 127.6-130°C; **TLC** (tol:cyclohex: 10/90 v/v), R_f = 0.68

Reaction Number	Starting material (1) (g, mmol, eq.)	Reagent (g, mmol, eq.)	Solvent (CCl ₄) (mL)	Time	Temperature	%Yield
R-33	0.100, 0.294, 1	NBS (0.575, 3.234, 11); Benzoyl peroxide (0.004, 0.016, 0.05)	0.8	50hrs.	85°C	93.4
R-43	0.501, 1.473, 1	NBS (2.879, 16.178, 11); Benzoyl peroxide (0.018, 0.073, 0.05)	6.0	50hrs.	84°C	94.1

Table 1: reactions performed to synthesize 2,2'-bis(dibromomethyl)-1,1'-biphenyl (**68**)

 ^1H NMR (399.78 MHz, CDCl_3) ^{13}C NMR (100.53 MHz, CDCl_3)

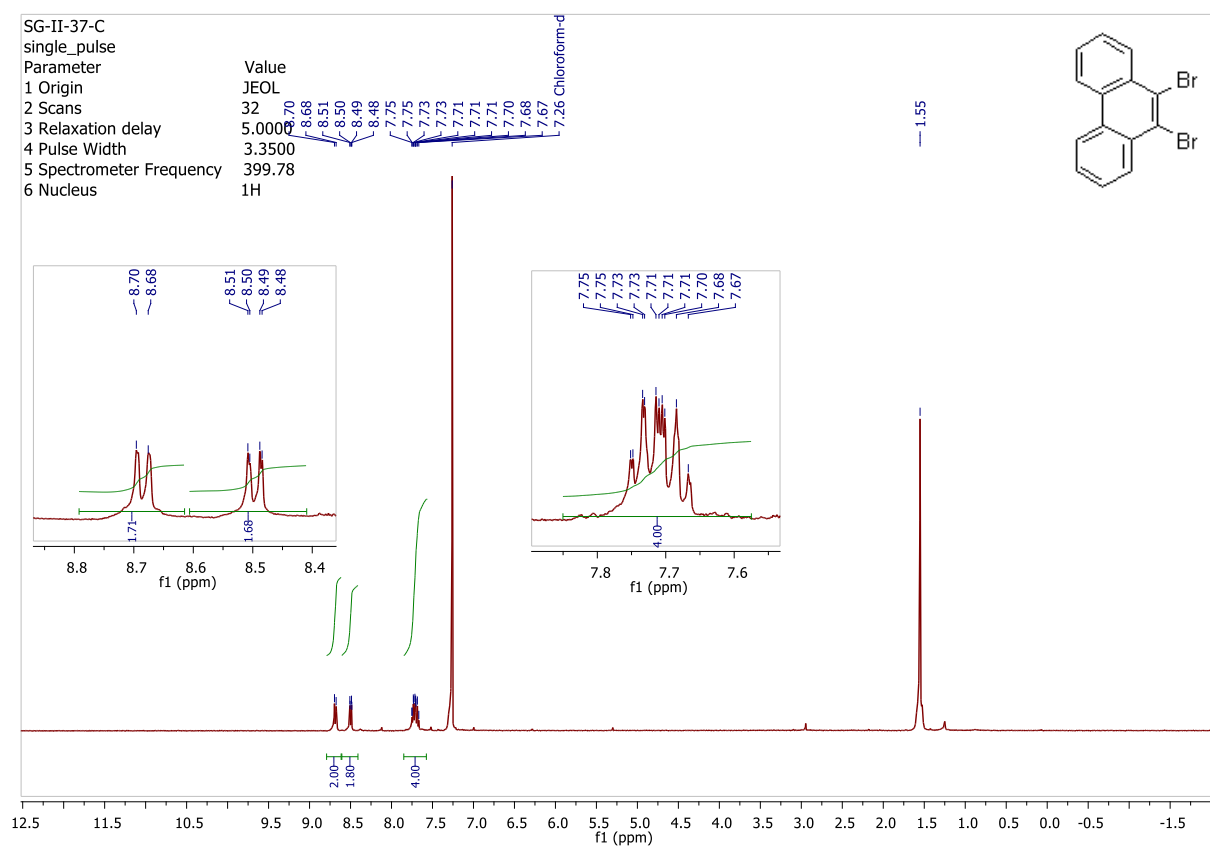
¹³C NMR (100.53 MHz, DEPT135, CDCl₃)

Procedure for compound-69 (R-46): In an oven-dried sealed tube, 2,2'-bis(dibromomethyl)-1,1'-biphenyl (**68**) (100.5mg, 0.202mmol, 1.00 mol-eq.), was added and dissolved in dry DMF (1.5 mL—dried with molecular sieves 3Å). The tube was purged with argon for 15 min.. The reaction mixture was stirred for 30 min. in an ice bath. To this solution, potassium tert-butoxide (455.4 mg, 4.058 mmol, 20 eq.) was added rapidly and stirring was continued for 24 hrs at 60°C and then for 24 hrs at 80°C. The reaction mixture was extracted with DCM (mL) and water (5×20mL). The combined organic layers were dried over MgSO₄, filtered, and evaporated to dryness. **Mass: 57.3 mg, Yield: 85%.**

RESULTS: $^1\text{H-NMR}$ (**SG-II-37-C**) indicates 9,10-dibromo-phenanthrene (**3**). **SG-II-37-C:** $^1\text{H NMR}$ (399.78 MHz, CDCl_3): $\delta = 8.69$ (dd, $J = 8.0, 1.1$ Hz, 2H), 8.48 (dd, $J = 7.9, 1.3$ Hz, 2H), m (7.75-7.67, 4H); M.p.: 178.6-180.0°C, **TLC** (tol:cyclohex: 10/90 v/v), $R_f = 0.5$.

Reaction Number	Starting material (2) (g, mmol, eq.)	Reagent (g, mmol, eq.)	Solvent (DMF) (mL)	Time	Temperature	%Yield
R-46	100.5, 0.202, 1	tBuOK (455.4, 4.058, 20)	1.5	48hrs.	60°C for 24hrs., 80°C for 24hrs.	85

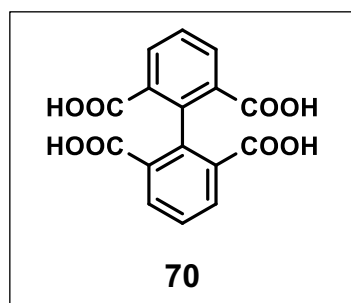
Table-2: reactions performed to synthesize 9,10-dibromo-phenanthrene (69).



$^1\text{H NMR}$ (399.78 MHz, CDCl_3)

1. M. Mansø, L. Fernandez, Z. Wang, K. Moth-Poulsen, M. Brøndsted Nielsen, *Molecules* **2020**, *25*, 322.
2. S. Goretta, C. Tasciotti, S. Mathieu, M. Smet, W. Maes, Y. M. Chabre, W. Dehaen, R. Giasson, J.-M. Raimundo, C. R. Henry, C. Barth, M. Gingras, *Org. Lett.*, **2009**, *11*, 3846-3849.

Experimental Section For Scheme-2:



Procedure for compound-70 (R-4): To pyrene (**1**) (5.00 g, 24.72 mmol, 23 mol-eq.) in CH₂Cl₂ (100 mL) was added MeCN (100 mL) and water (210 mL). To the resulting biphasic solution was added NaIO₄ (51.09 g., 238.90 mmol, 221 mol-eq.) followed by Ru(III)Cl₃ (0.225 g., 1.08 mmol, 1.0 mol-eq.). The solution warmed somewhat as the reaction

began but it was not vigorous. The reaction was run for 20 hrs (overnight) while stirring and it was filtered to afford a yellow solid. The mixed solid (tetraacid/tetraone) was extracted with acetone (320 mL), and the filtrate was concentrated under reduced pressure. The residue was identified as a mixture of the desired tetraacid and the corresponding tetraone. The crude product was grounded to a fine powder and it was triturated and refluxed twice for ~ 2 hrs. in DCM, and the solid was collected after a warm filtration. The tetraacid (biphenyl-2,2',6,6'-tetracarboxylic acid) was collected as a pale yellow powder: **Mass: 6.2247 g.; yield: 76.2%.**

RESULTS: ¹H-NMR (**SG-I-59-C**) mainly indicates the tetraacid (**5**, biphenyl-2,2',6,6'-tetracarboxylic acid) (Major) and (**SG-I-59-B**) tetraone (**11**, pyrene-4,5,9,10-tetraone) as side product.

SG-I-59-C: ¹H NMR (399.78 MHz, DMSO-d₆): δ = 12.46 (br, COOH), 7.96 (d, J=7.6Hz, 4H), 7.45 (t, J=7.7, 2H); ¹³C NMR (DMSO-d₆, d, ppm): 167.49, 142.08, 132.33, 131.82, and 126.48); **M.p.:** 393°C [16, 41-42]

Side Product: Compound-14 (Tetraone)

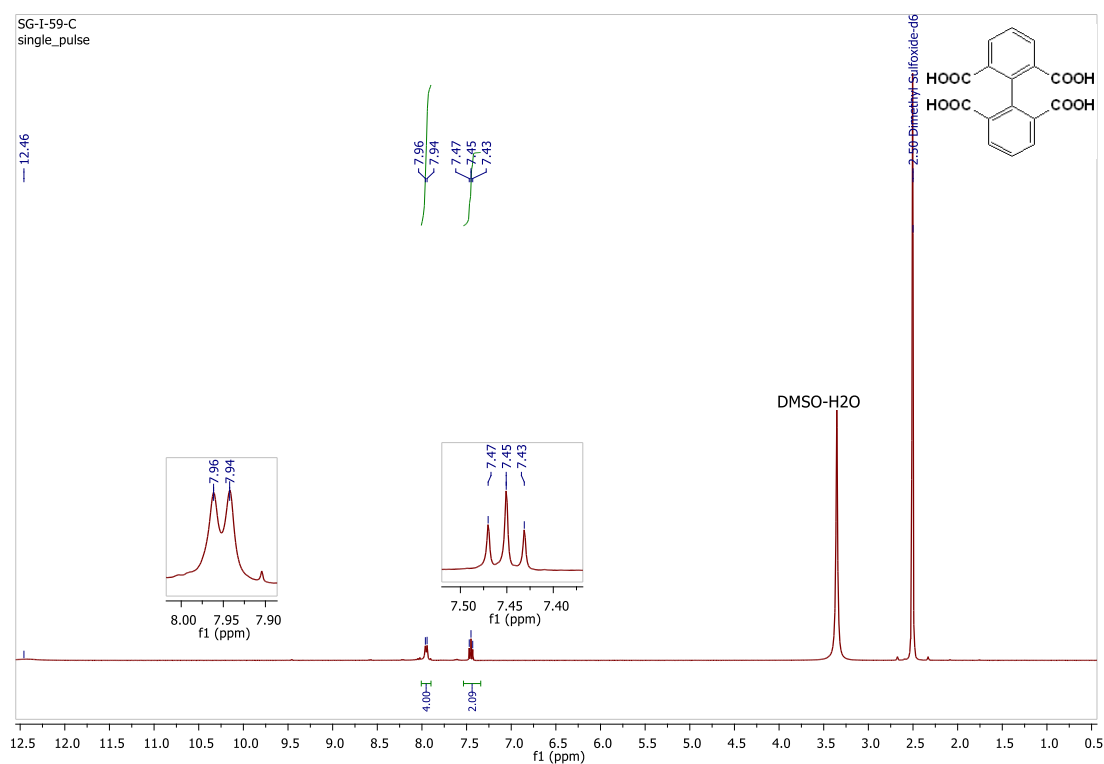
M.p >350 °C; **SG-I-59-B:** ¹H NMR (300 MHz, DMSO-d₆) δ 8.3 (d, 4H, J=7.7Hz), 7.71 (t, 2H, J=7.7Hz); ¹³C NMR (N/A, solubility too low) Ref.: [16, 41-42].

Reference:

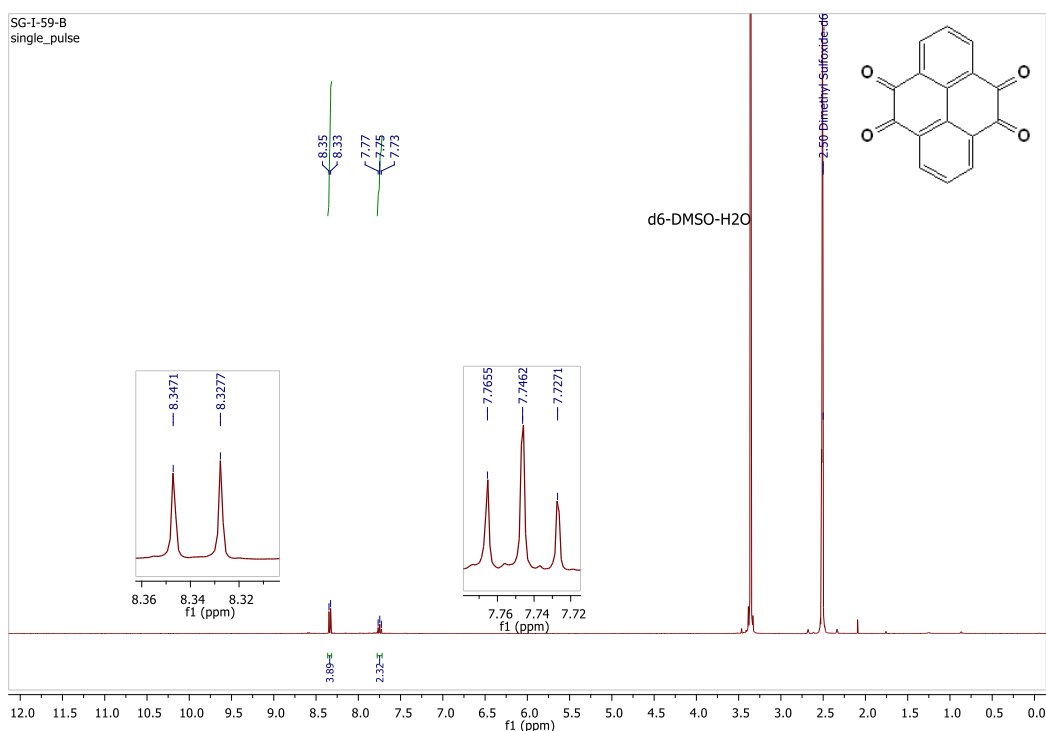
16. J. Hu, D. Zhang, F. W. Harris, *J. Org. Chem.* **2005**, *70*, 707-708.
41. K. E. Pryor, G.W. Shipps Jr, D.A. Skyler, J. Rebek Jr, *Tetrahedron*, **1998**, *54*, 4107-4124
42. K. Sakayori, Y. Shibasaki, M. Ueda, *J. Polym. Sci., Part A: Polym. Chem.*, **2006**, *44*, 6385-6393.

Reaction Number	Starting material (4, pyrene) (g, mmol, eq.)	Reagent (g, mmol, eq.)	Solvent (CH ₂ Cl ₂ /H ₂ O/ MeCN) (mL)	Time	Temp	%Yield
R-1	0.787, 0.389, 18.5	NaIO ₄ (0.806, 3.768, 179); RuCl ₃ (0.004, 0.021, 1)	1.6, 2.4, 1.6	16hrs	RT	50
R-2	0.788, 3.900, 24	NaIO ₄ (8.054, 37.654, 239); RuCl ₃ (0.033, 0.158, 1)	16, 24, 16	17hrs	RT	72.2
R-4	5.0, 24.721, 23	NaIO ₄ (51.098, 238.9, 221), RuCl ₃ (0.225, 1.08, 1)	100, 210, 100	20hrs.	RT	76.2
R-10	9.082, 44.498, 21	NaIO ₄ (91.835, 429.35, 206), RuCl ₃ (0.432, 2.082, 1)	160, 240, 160	31hrs.	RT	74.0

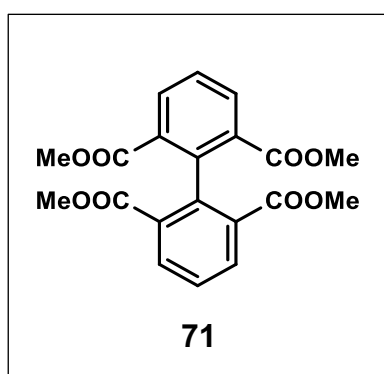
Table-3: Reactions performed to synthesize biphenyl-2,2',6,6'-tetracarboxylic acid (70)



¹H NMR (399.78 MHz, CDCl₃)



^{13}C NMR (100.53 MHz, CDCl_3)



Procedure for compound-71 (R-9): In an oven-dried round bottom flask, biphenyl-2,2',6,6'-tetracarboxylic acid) (**70**), (303.6 mg, 0.9193 mmol, 1.0 mol-eq.), potassium carbonate (377.4 mg, 2.731 mmol, 3.0 mol-eq.) iodomethane (0.6 mL, 1.368 g, 9.638 mmol, 10 mol-eq.) and DMF were added to the reaction mixture and stirred for 5 hrs. at room temperature. The solvent was evaporated under reduced pressure, and the reaction

mixture was extracted with toluene (5×20mL) and water (20 mL). In order to get pure tetraester (**6**), the resulting residue was purified by column chromatography on silica gel with a gradient of eluent of 30% acetone in hexane: **Mass: 299.5 mg, Yield: 85.3%.**

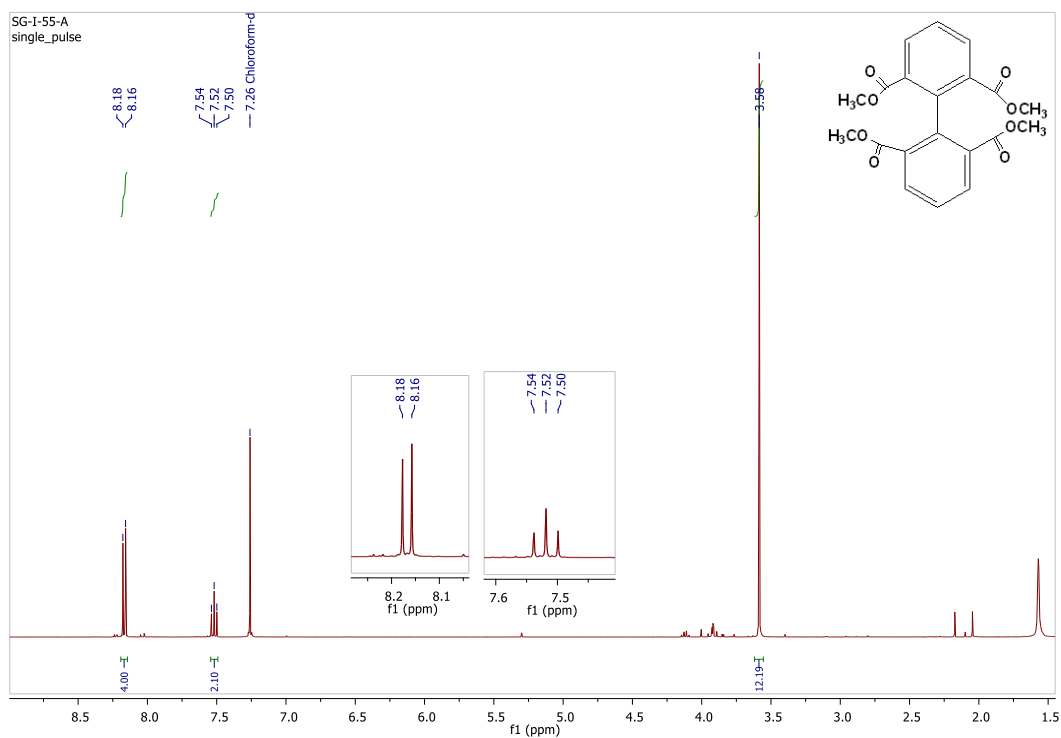
RESULTS: ^1H -NMR (**SG-I-55-A**) and ^{13}C -NMR (**SG-I-55-B**) mainly indicated [1,1'-biphenyl]-2,2',6,6'-tetramethyl ester (**71**). ^1H NMR **SG-I-55-A** (399.78 MHz, CDCl_3): δ = 8.17 (d, $J=7.8\text{Hz}$, 4H), 7.52 (t, $J=7.8\text{Hz}$, 2H), 3.58 (s, 12H); ^{13}C NMR **SG-I-55-B** (100.53 MHz, CDCl_3): δ = 166.68, 142.48, 133.34, 130.80, 127.27, 52.19; **M.p.:** 125-126°C [48-49], **TLC** (acet/cyclohex: 30/70 v/v), R_f = 0.5.

48. S. Dana, D. Chowdhury, A. Mandal, F. A. S. Chipem, M. Baidya, *ACS Catal.*, **2018**, *8*, 10173-10179.

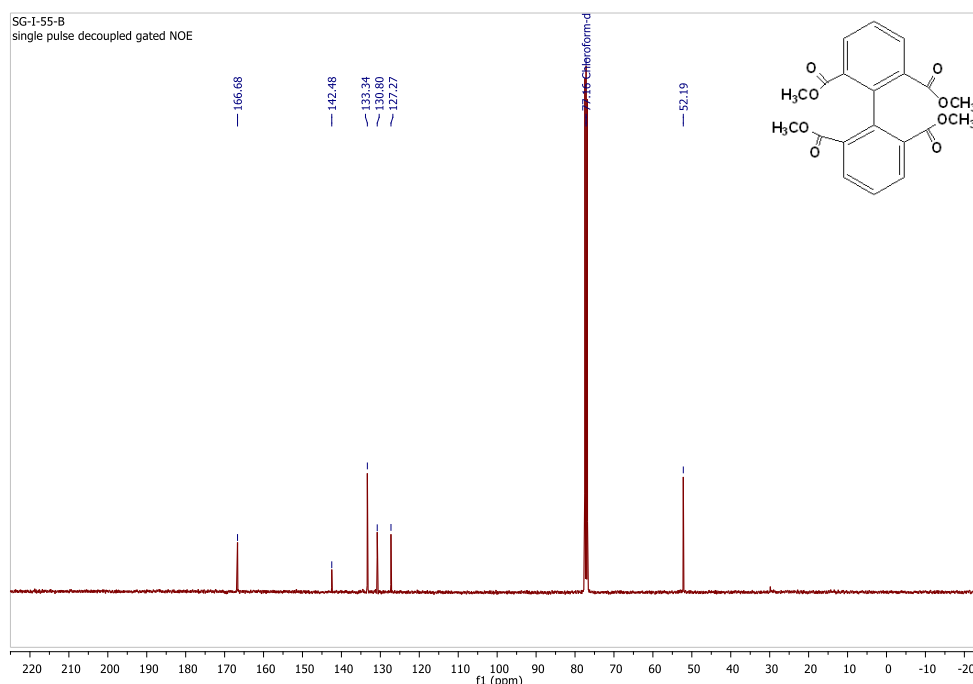
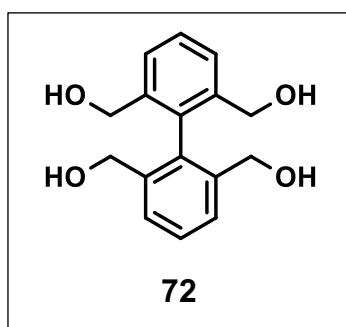
49. S. Gundala, C. L. Fagan, E. G. Delany, S. J. Connon, *Synlett* , **2013**, 24, 1225-1228.

Table-4: Reactions performed to synthesize [1,1'-Biphenyl]-2,2',6,6'-tetramethyl ester (71)

Reaction Number	Starting material (5)(g, mmol, eq.)	Reagent (g, mmol, eq.)	Solvent (DMF) (mL)	Time	Temperature	%Yield
R-7	0.026, 0.077, 1	K ₂ CO ₃ (0.033, 0.238, 3); MeI (0.114, 0.803, 10, 0.05mL)	3.6	5hrs.	80°C	42.7
R-9	0.303, 0.919, 1	K ₂ CO ₃ (0.377, 2.731, 3); MeI (1.368, 9.638, 10, 0.6mL)	0.3	5hrs.	80°C	85.3
R-17	4.041, 0.013, 1	K ₂ CO ₃ (5.031, 0.036, 2.7); MeI (22.8, 0.1606, 12, 10mL)	110	6hrs.	80°C	58.6



¹H NMR (399.78 MHz, CDCl₃)

¹³C NMR (100.53 MHz, CDCl₃)

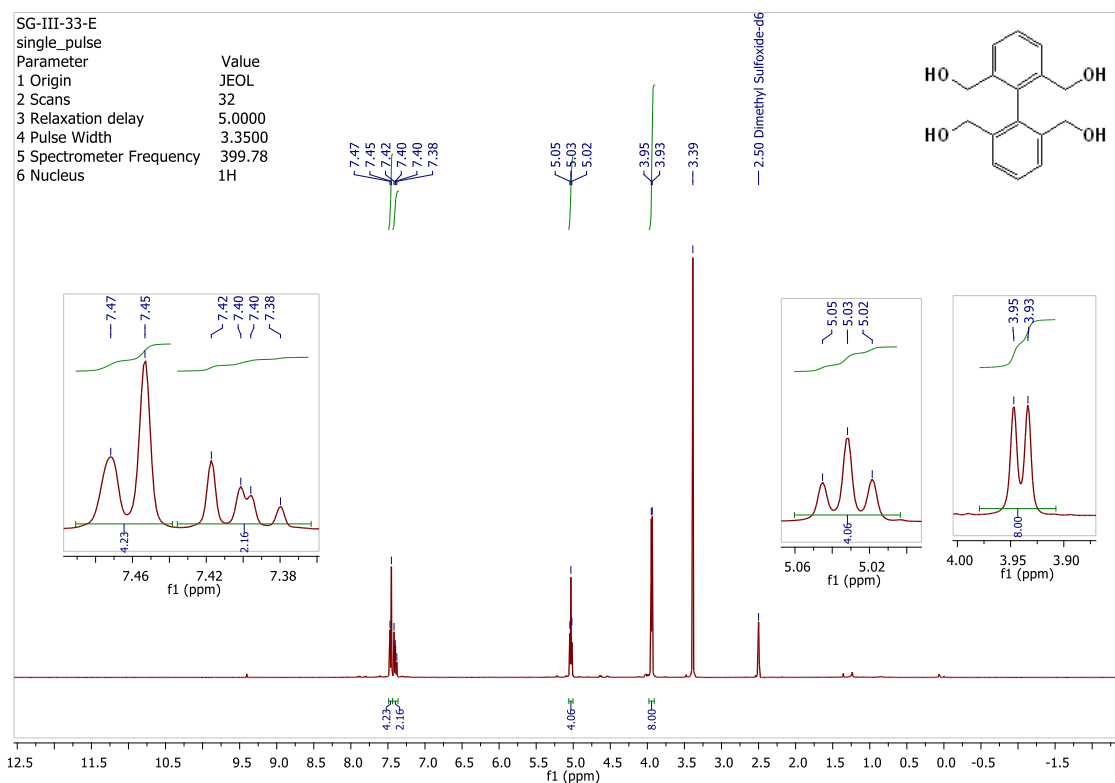
Procedure for compound-72 (R-13): In an oven-dried sealed tube, [1,1'-biphenyl]-2,2',6,6'-tetramethyl ester (71) (25.84 mg, 0.067 mmol, 1.00 mol-eq.) was added, and argon was purged for 15 min. in the tube. Diisobutylaluminium hydride in hexane (1.1 mL, 1M) was added under argon to a stirred mixture of tetraester. The reaction mixture was stirred

at room temperature for 17 hrs and was quenched with a saturated solution of sodium tartrate. The product was extracted with ether (3×5 mL) and water (5 mL). The combined organic layers were dried over MgSO₄, filtered. **(Mass: 10.1mg, Yield: 57.1%). RESULTS:** ¹H-NMR (**SG-III-33-E**) mainly indicating 2,2',6,6'-tetrakis(hydroxymethyl)biphenyl (tetra alcohol) (7).

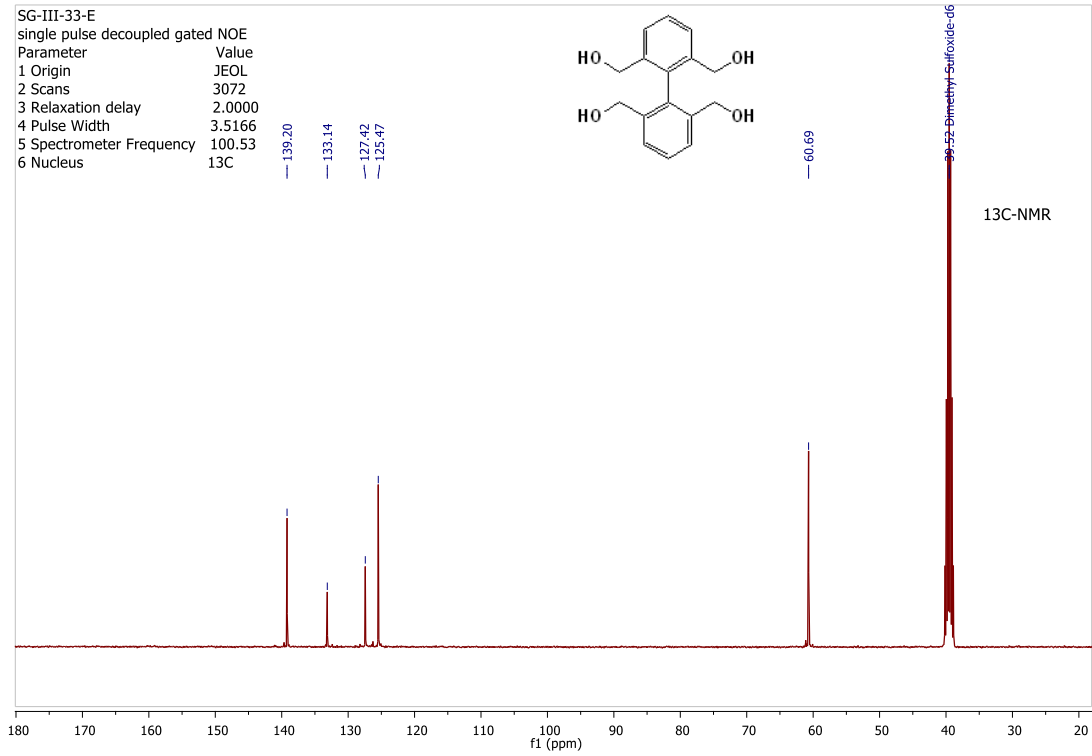
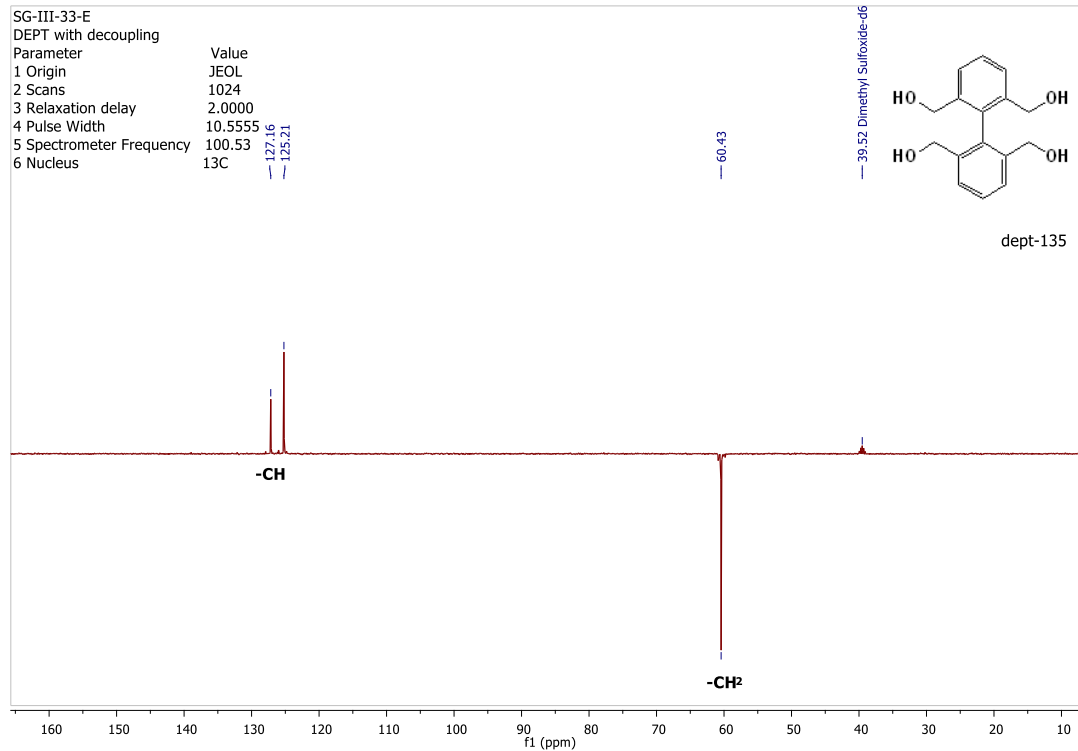
SG-III-33-E: ¹H NMR (399.78 MHz, DMSO-d₆): δ = 7.47 (m, 4H, J=7.4 Hz), 7.40 (td, 2H, J=8.5, 2.1 Hz), 5.03 (t, 4H, J=5.35 Hz, OH), 3.94 (d, 8H, J=5.32); **SG-III-33-E:** ¹³C-NMR (100.53 MHz, DMSO-d₆): δ = 139.20, 133.14, 127.42, 125.47, 60.69; **SG-III-33-E:** 135°-dept, NMR (100.53 MHz, DMSO-d₆): δ = 127.16, 125.21 (-CH, +ve peak), 60.43 (-CH₂, -ve peak); **M.p.:** 171.2-172°C, **TLC** (MeOH:DCM: 05/95 v/v), R_f = 0.4.

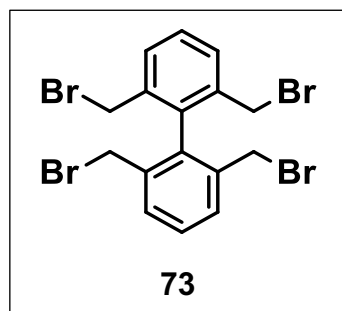
Reaction Number	Starting material (6) (g, mmol, eq.)	Reagent (mL, M)	Time	Temperature	%Yield
R-13	0.026, 0.067, 1	DiBAL-H in Hexane (1.1, 1M)	15hrs.	0°C	57.0
R-14	0.100, 0.259, 1	DiBAL-H in DCM (2.7, 1M)	48hrs.	0°C	43.0
R-18	1.301, 3.368, 1	DiBAL-H in DCM (40, 1M)	18hrs.	0°C	89.7
R-95	1.00, 2.588, 1	DiBAL-H in DCM (25, 1M)	24hrs.	0°C	40.0

Table-5: Reactions performed to synthesize 2,2',6,6'-tetrakis(hydroxymethyl)biphenyl (72)



¹H NMR (399.78 MHz, CDCl₃)

 ^{13}C NMR (100.53 MHz, CDCl_3) ^{13}C NMR DEPT 135 (100.53 MHz, CDCl_3)



Procedure for compound-73 (R-41): In an oven-dried sealed tube, 2,2',6,6'-tetrakis(hydroxymethyl)biphenyl (72) (330.6 mg, 1.205 mmol) was added, and argon was purged for 15 minutes in the tube. Phosphorus tribromide (2 mL, excess) was added under argon to a stirred mixture in an ice bath for 30minutes, and then the bath was removed, and

stirring was continued at room temperature for 24 hrs. The reaction mixture was quenched slowly with ice-cold water. A calcium oxide tube was used over the mouth of the flask for trapping HBr fumes. The reaction mixture was extracted with toluene (6×15 mL) and water (15 mL). The combined organic layers were dried over MgSO₄, filtered and evaporated. The crude product was purified by column chromatography over SiO₂ using 30% toluene/cyclohexane as an eluent. **(Mass: 32.24mg, Yield: 50.9%).**

RESULTS: ¹H-NMR (**SG-IV-62-C**) and ¹³C-NMR (**SG-IV-62-D**) indicates 2,2',6,6'-tetrakis(bromomethyl)biphenyl (**8**).

SG-IV-62-C: ¹H NMR (399.78 MHz, TMS): δ = 7.61 (d, 4H, J=7.67 Hz); 7.51 (td, 2H, J=6.9, 1.6 Hz); 4.23 (s, 8H); **SG-IV-62-D:** ¹³C NMR (100.53 MHz, TMS): δ = 136.66, 135.21, 131.62, 130.07, 32.24; **M.p.:** 167.5-168°C [51-52]; **TLC** (acet:cyclohex: 30/70 v/v), **R_f** = 0.51

51. M. Gingras, C. Collet, *Synlett*, **2005**, 2337-2341.

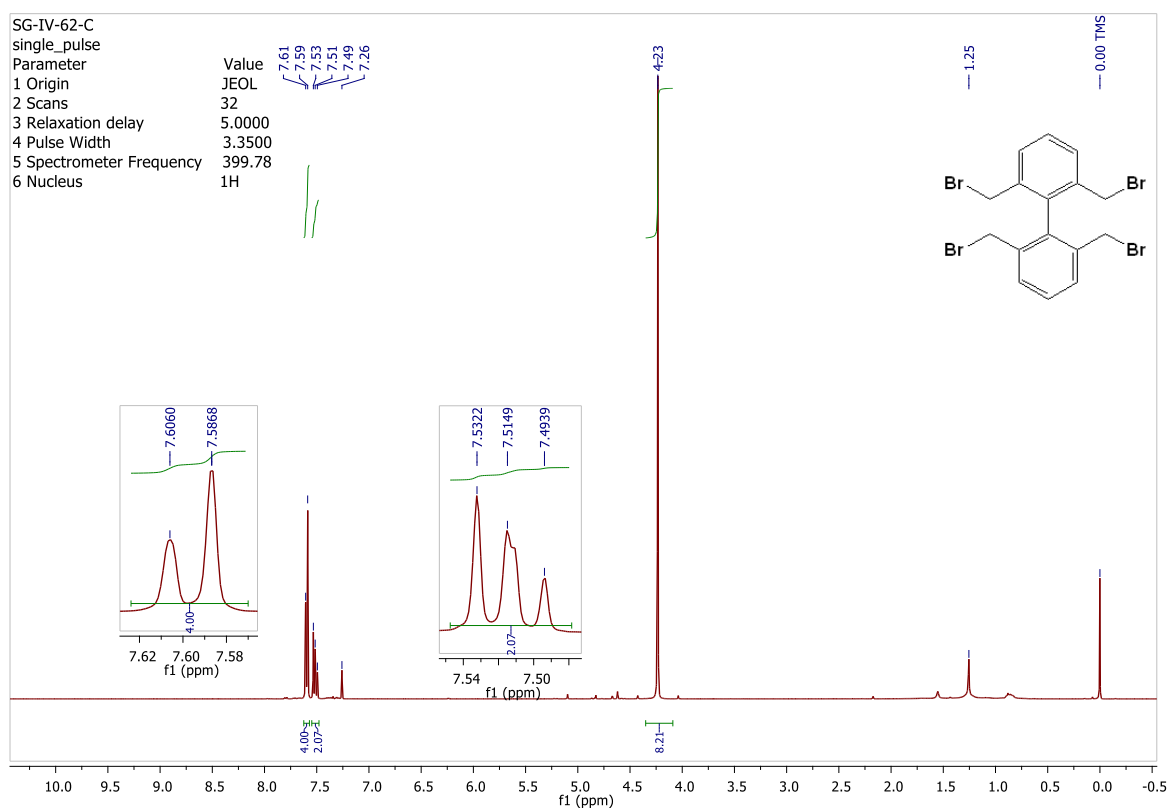
52. T. J. Seiders, E. L. Elliott, G. H. Grube, J. S. Siegel, *J. Am. Chem. Soc.*, **1999**, 121, 7804-7813.

Reaction Number	Starting material (7) (mg, mmol, eq.)	Reagent	Solvent (DCM) (mL)	Time	Temp.	%Yield
R-15	10.9, 0.039	PBr ₃ (0.08 mL)	0.3	3.5hrs.	50-55°C	30.7
R-19	100.5, 0.366	PBr ₃ (1.2 mL)	1.8	4hrs.	50-55°C	15.1
R-20	100.9, 0.367	PBr ₃ (0.15 mL)	1.8	4hrs.	50-55°C	15.1
R-32	15.4, 0.057, 1	Ph ₃ PBr ₂ (20.7mg, 0.491 mmol, 8.7eq.)	0.5	168hrs.	RT	11.8

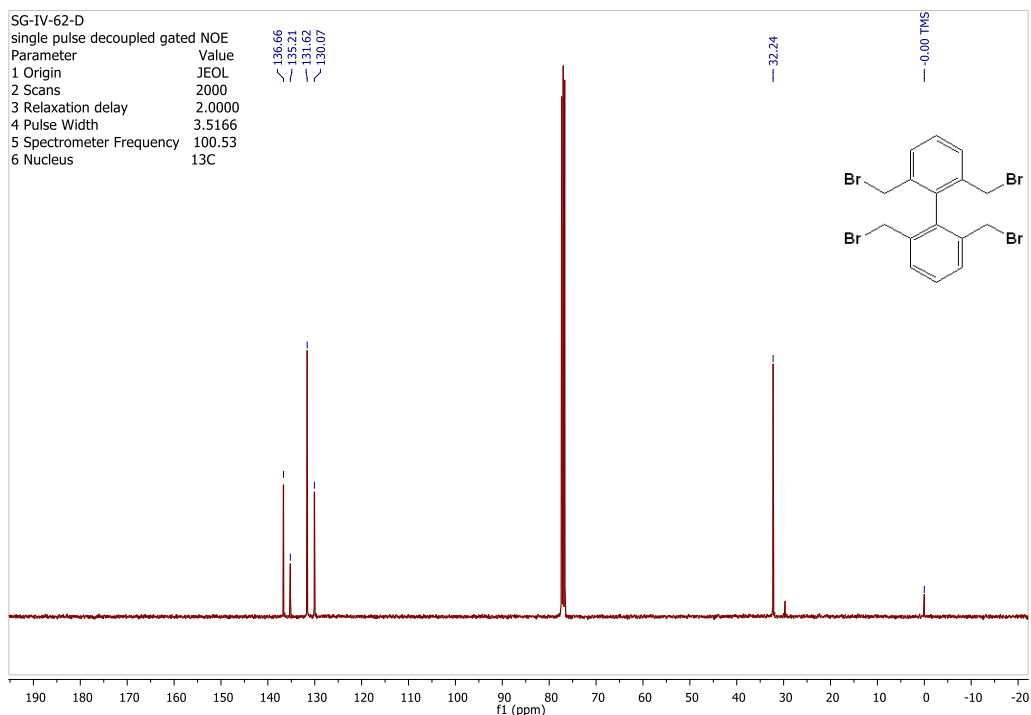
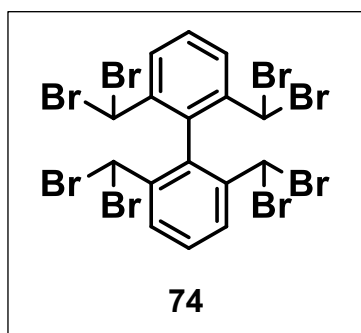
R-34	15.8, 0.057	PBr ₃ (0.09 mL)	1.0	21hrs.	RT	49.7
R-36	200.0, 0.729	PBr ₃ in DCM(1.16 mL)	--	24hrs.	RT	49.7

R-41	330.6, 1.205	PBr ₃ in DCM (2.0 mL)	--	24hrs.	RT	50.9
R-162	201.1, 0.733	PBr ₃ in DCM (1.2mL)	--	2days	RT	48

Table-6: Reactions performed to synthesize 2,2',6,6'-tetrakis(bromomethyl)biphenyl (73)



¹H NMR (399.78 MHz, CDCl₃)

 ^{13}C NMR (100.53 MHz, CDCl_3)

Procedure for compound-9 (R-74): In an oven-dried sealed tube, 2,2',6,6'-tetrakis(bromomethyl)biphenyl (73) (250.0 mg, 0.475 mmol, 1.00 mol-eq.) was added, The tetrabromo was dissolved in CCl_4 (6.0 mL) and argon was purged for 15 minutes in the tube. To this solution was added N-bromosuccinimide (2.966 mg, 16.665 mmol, 35 mol-eq.) and benzoyl peroxide (0.182 mg, 0.749 mmol, 0.6 mol-eq.). The reaction mixture was stirred for 13 days at 90-94°C. The peroxide was added from time to time, and the reaction was monitored by ^1H NMR, after collecting small aliquots and extraction with $\text{CDCl}_3/\text{NaOH}$ solution (2M). After completion, a NaOH solution was added to the reaction mixture after cooling to RT, and it was extracted with toluene (5×30mL) and water (30mL). The combined organic layers were dried over MgSO_4 , filtered and evaporated. (**Mass: 336.7mg, Yield: 84%**)

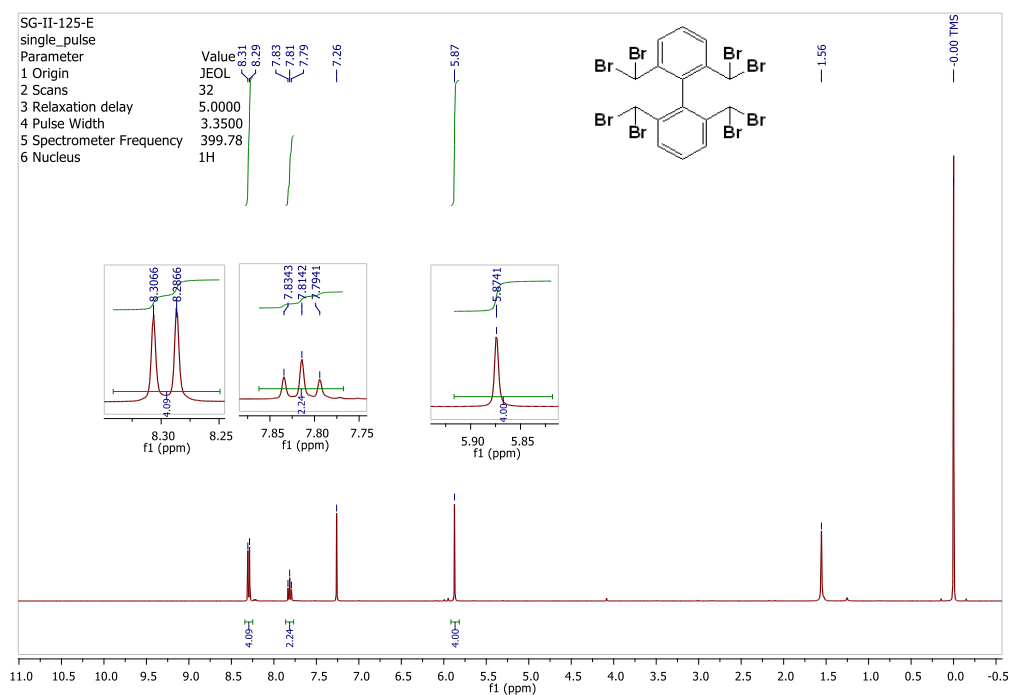
RESULTS: ^1H -NMR (SG-II-125-E) indicates the product 2,2',6,6'-tetrakis(dibromomethyl)biphenyl (74).

SG-II-125-E: ^1H NMR (399.78 MHz, TMS): δ = 8.30 (d, 4H, J = 7.9 Hz), 7.81 (t, 2H, J =8.0 Hz), 5.87 (s, 4H); ; **SG-IV-125-F:** ^{13}C NMR (100.53 MHz, TMS): δ = 140.75, 133.09, 132.01, 123.54, 77.33, 77.01, 76.69, 37.38; **SG-IV-125-F:** ^{13}C 135°-dept NMR

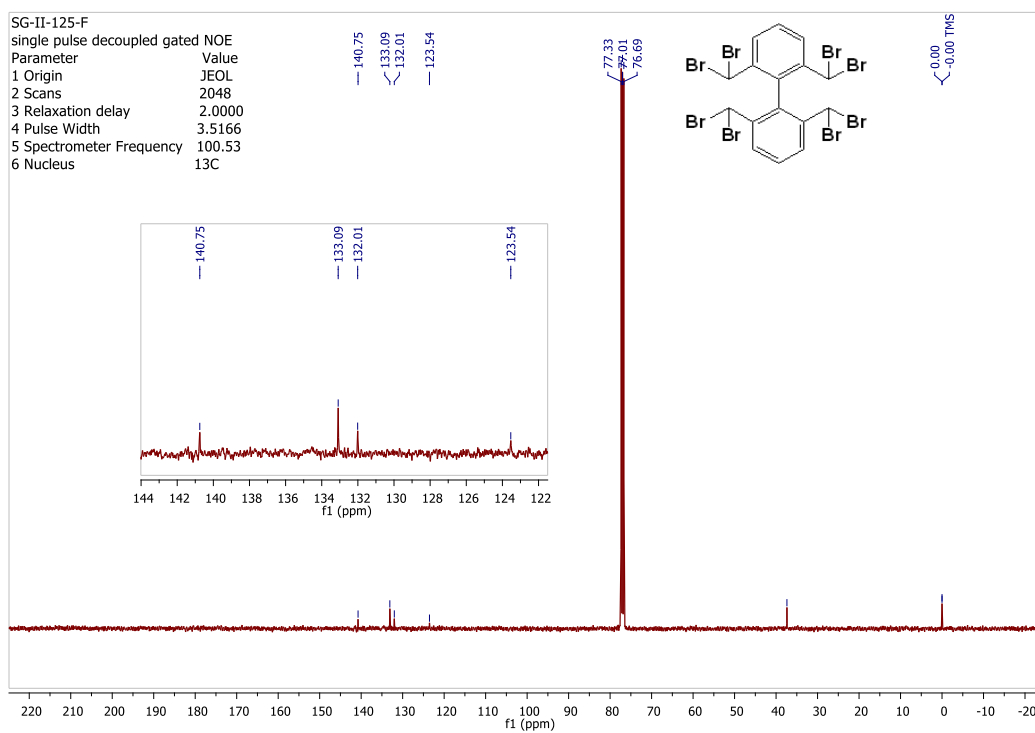
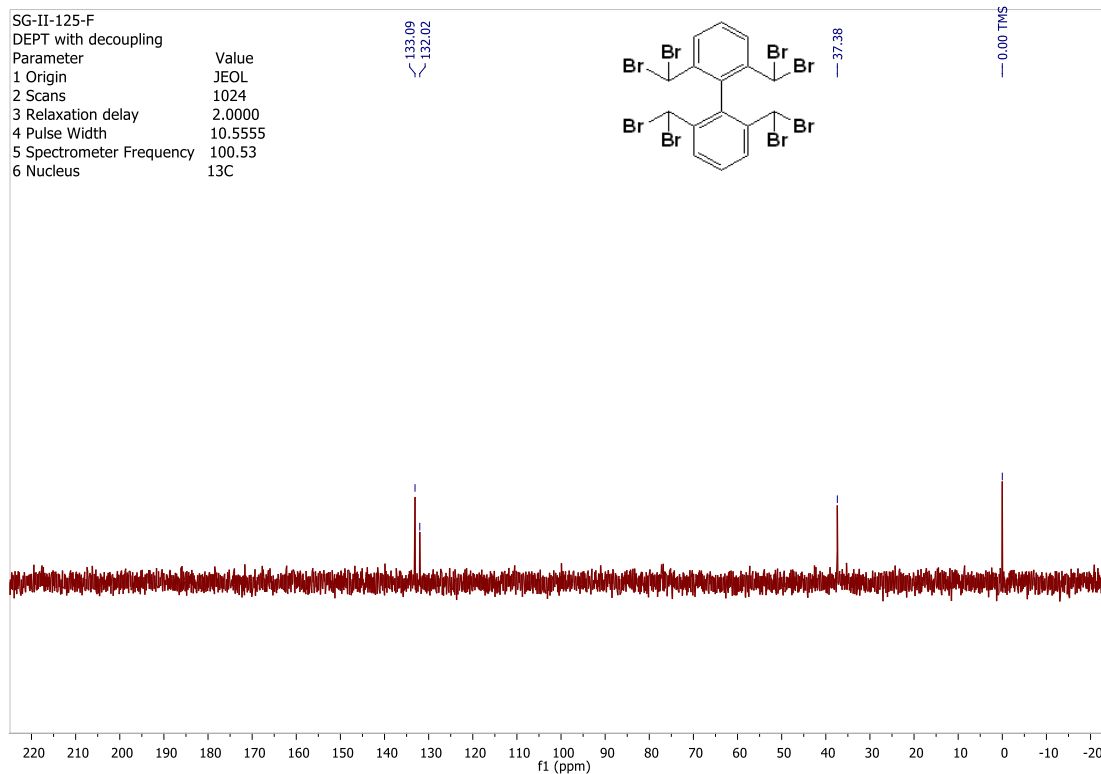
(100.53 MHz, TMS): δ = 133.09, 132.02, 37.38; TLC (tol:cyclohex: 10/90 v/v), R_f = 0.58.

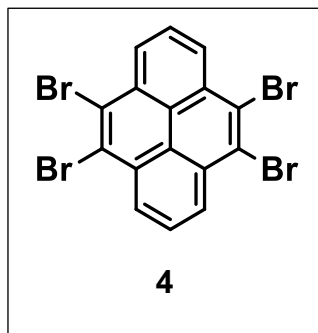
Reaction Number	Starting material (8) (mg, mmol, eq.)	Reagent (g, mmol, eq.)	Solvent (CCl ₄) (mL)	Time	Temperature	%Yield
R-23	25.4, 0.048, 1	NBS (187.3, 1.052, 22); Benzoyl peroxide (4.1, 0.017, 0.3)	0.4	24hrs.	67-70°C	75.7 (Failed)
R-39	25.2, 0.048, 1	NBS (254.2, 1.428, 30); Benzoyl peroxide (5.91, 0.024, 0.5)	0.25	187hrs.	84°C	17 (not exact should be more)
R-40	75.8, 0.144, 1	NBS (963.4, 5.428, 37); Benzoyl peroxide (15.3, 0.063, 0.4)	1.0	173hrs.	84°-94°C	48 (not exact should be more)
R-47	250.0, 0.475, 1	NBS (2.966, 16.665, 35); Benzoyl peroxide (0.182, 0.749, 0.6)	6.0	13days	90°-94°C	84 (not exact should be more)

Table-7: Reactions performed to synthesize 2,2',6,6'-etrakis(dibromomethyl)biphenyl (74)



¹H NMR (399.78 MHz, CDCl₃)

¹³C NMR (100.53 MHz, CDCl₃)¹³C NMR DEPT 135 (100.53 MHz, CDCl₃)



Procedure for compound-4 (R-44): In an oven-dried sealed tube, 2,2',6,6'-tetrakis(dibromomethyl)biphenyl (**74**) (15.5 mg, 0.018 mmol, 1.0 mol-eq.) was dissolved in dry DMF (0.3 mL—dried with molecular sieves 3Å) and argon was purged for 15 minutes in the tube. To this solution was added potassium tert-butoxide (60.2 mg, 0.536 mmol, 29 mol-eq.). The reaction

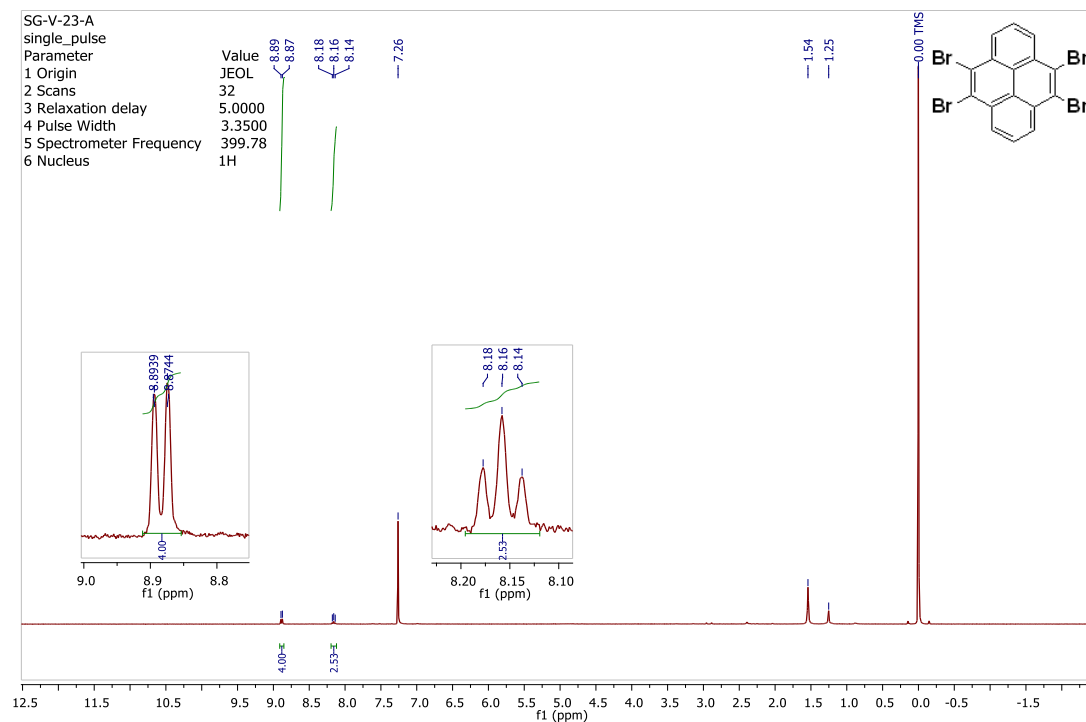
mixture was stirred for 30 minutes in an ice bath, the color changed from pale brown to dark brown after 20 minutes. Stirring was continued for 24 hrs. at 50°C, and it was extracted with DCM and water (5×5mL). The combined organic layers were dried over MgSO₄, filtered and evaporated. (**Mass: 7.8mg, Yield: 85%**)

RESULTS: ¹H-NMR (**SG-V-23-A**), indicates the product 4,5,9,10-tetrabromo pyrene (**10**)

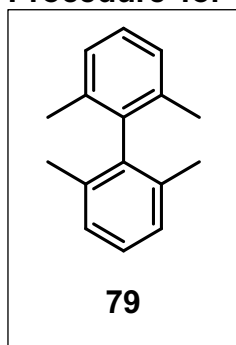
SG-V-23-A: ¹H NMR (399.78 MHz, TMS): δ = 8.89 (d, 4H, J=7.8 Hz), 8.15 (t, 2H, J=7.7 Hz); ¹³C NMR was not possible due to insolubility in most solvents. **M.p.:** 387°C (dec); **TLC** (tol:cyclohex: 90/10 v/v), **R_f** = 0.58

Reaction Number	Starting material (9) (mg, mmol, eq.)	Reagent (mg, mmol, eq.)	Solvent (DMF) (mL)	Time	Temperature	%Yield
R-42	6.9, 0.008, 1	tBuOK (39.7, 0.354, 43)	0.3	24hrs.	RT	56.6
R-44	15.5, 0.018, 1	tBuOK (60.2, 0.536, 29)	0.3	24hrs.	50°C	84.8
R-45a	15.0, 0.017, 1	tBuOK (79.8, 0.711, 40)	0.3	24hrs.	80°C	XXX
R-45b	11.0, 0.013, 1	tBuOK (40.8, 0.364, 28)	0.3	2hrs.	80°C	89

Table-8: reactions performed to synthesize 2,4,5,9,10-tetrabromo pyrene (**4**)

 ^1H NMR (399.78 MHz, CDCl_3)**Experimental Section For Scheme-6:**

Procedure for compound-79 (R-59): In an oven-dried sealed tube, FeCl_3 (10.0,

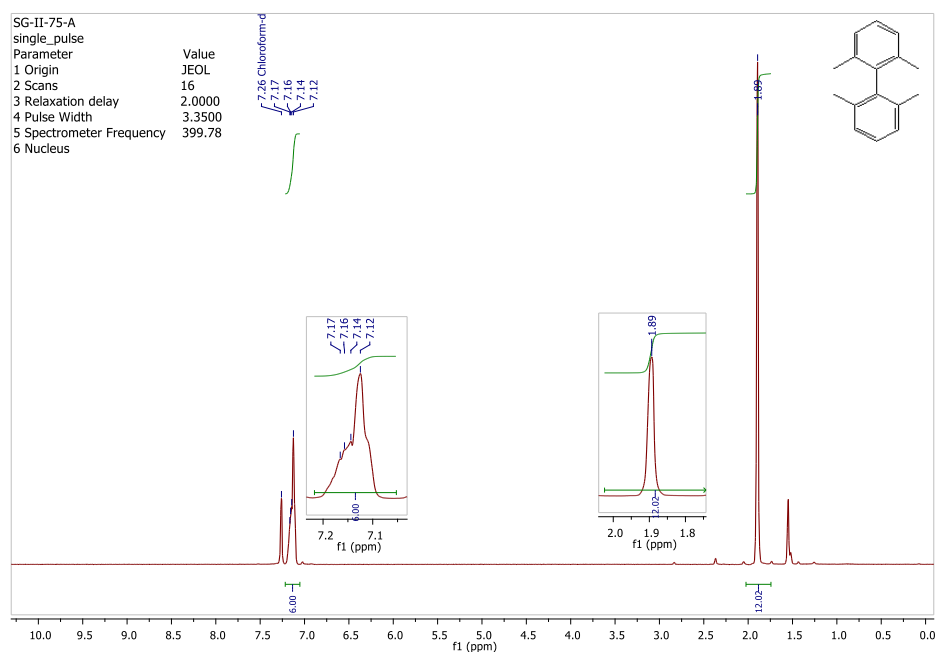


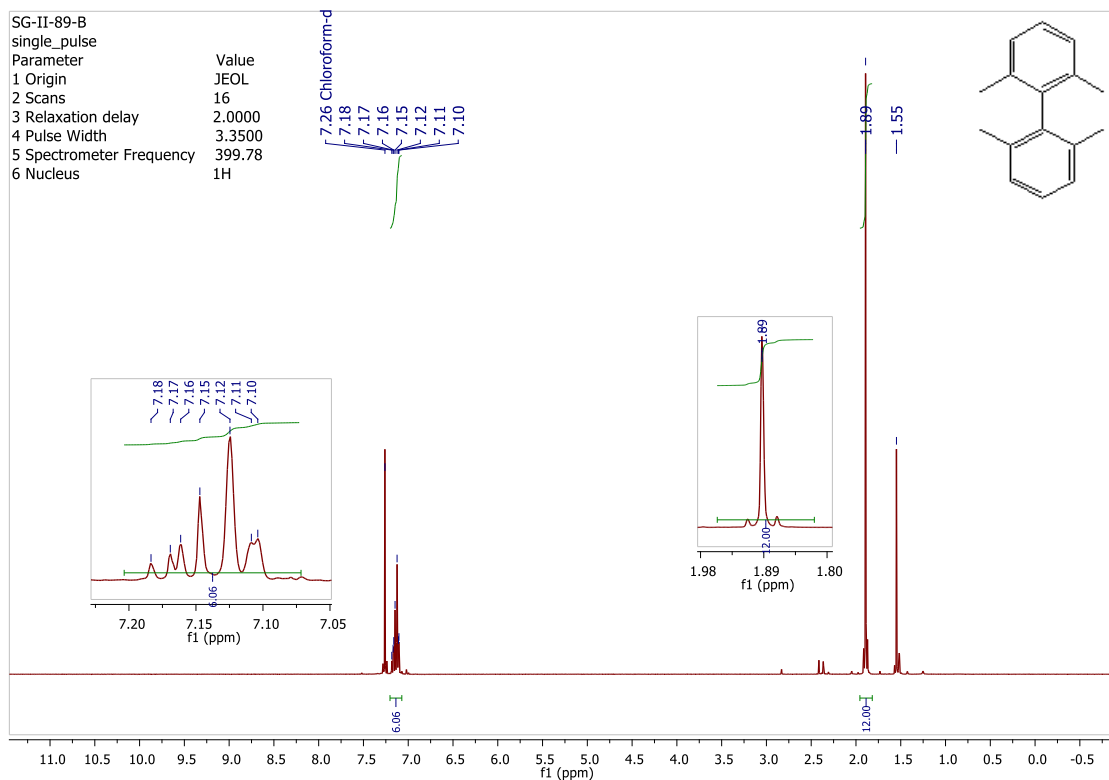
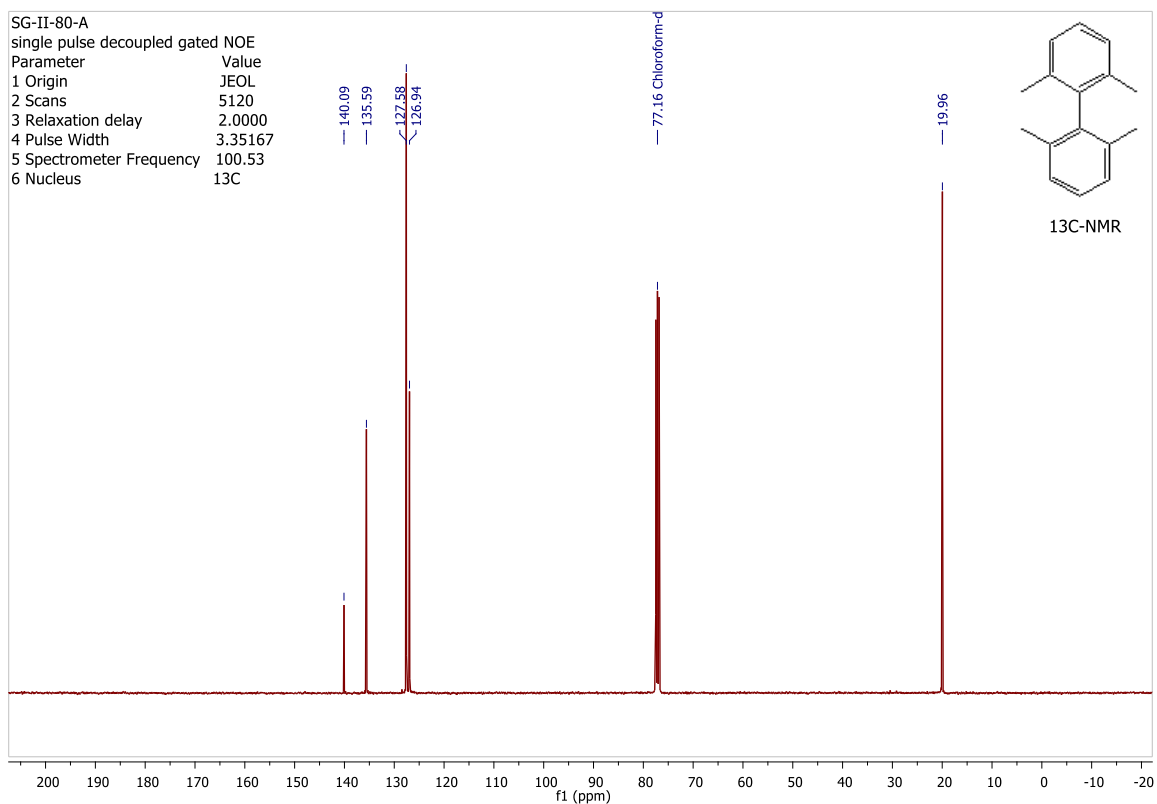
2.725, 16.803, 1.0 mol-eq.) was added followed by 1,2-dichloroethane (12.0 mL, 151.576 mmol, 9.0 mol-eq.). A solution of 2,6-dimethylphenylmagnesium bromide (13) was slowly added to the reaction tube via a syringe. The reaction mixture was stirred for 2 hours and 30 minutes in ice-cold water bath under argon conditions to attain room temperature slowly and it was refluxed at

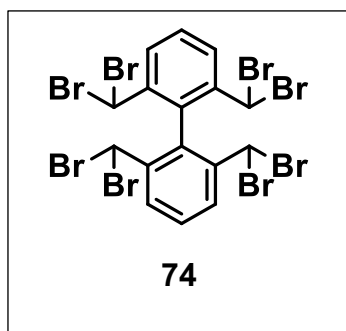
70°C for 3 hours and 30 minutes. Later, the reaction was quenched by adding HCl (1N). It was extracted with CHCl_3 (5 \times 30mL) and water (30mL). The combined organic layers were dried over MgSO_4 , filtered, and evaporated. It was purified by column chromatography over silica gel using 100% cyclohexane as an eluent. (**Mass: 2.546 g., Yield: 80.7%**).

RESULTS: ^1H -NMR **SG-II-75-A/ SG-II-89-A** and ^{13}C -NMR (**SG-II-80-A**): indicates 2,2',6,6'-tetrabromobiphenyl (**79**), **SG-II-75-A/ SG-II-89-A**: ^1H NMR (399.78 MHz, TMS): $\delta = 7.17$ - 7.12 (m, 6H), 1.89 (s, 12H); ^{13}C -NMR (**SG-II-80-A**): 140.09, 135.59, 127.58, 126.94, 19.96; **M.p.:** 66 - 67°C ; TLC (acetone: cyclohex: 30/70 v/v), $R_f = 0.5$.

Reaction Number	Starting material (13) (mL, gm, mmol, eq.)	Reagent (mol%, g, mmol, eq.)	Solvent (1,2-DCE) (mL, gm, mmol, eq.)	Time	Temperature	%Yield
R-49	5.0, 1.046, 5.00, 14	FeCl ₃ (3.9, 0.058, 0.357, 1.0)	0.7, 8.842, 24	3hrs	65°C	--
R-50	5.0, 1.046, 5.00, 5.0	FeCl ₃ (4.0, 0.165, 1.022, 1.0)	1.9, 23.999, 23	6hrs	75°C	16.9
R-52	5.0, 1.046, 5.00, 5.0	FeCl ₃ (4.0, 0.164, 1.013, 1.0)	1.9, 23.999, 23	1hr 45min.	65-70°C	33.2
R-54	5.0, 1.046, 5.00, 5.0	FeCl ₃ (4.0, 0.165, 1.016, 1.0)	1.9, 23.999, 23	5hrs	68-70°C	62
R-56	5.0, 1.046, 5.00, 1.8	FeCl ₃ (10.0, 0.459, 2.834, 1.0)	2.0, 25.263, 9.0	4:30-5.0hrs	70°C	77
R-57	40.0, 8.375, 40.0, 1.7	FeCl ₃ (10.3, 3.761, 23.189, 1.0)	16.0, 202.101, 8.7	20hrs 30min.	69°C (2hrs 30min.) and 80°C (1 hr.)	73.6
R-59	30.0, 6.281, 30.0, 1.8	FeCl ₃ (10.0, 2.725, 16.803, 1.0)	12.0, 151.576, 9.0	7hrs	70°C (4hrs 30min.)	80.7

Table-9: Reactions performed to synthesize 2,2',6,6'-tetramethylbiphenyl (79)¹H NMR (399.78 MHz, CDCl₃)

 ^1H NMR (399.78 MHz, CDCl_3) ^{13}C NMR (100.53 MHz, CDCl_3)

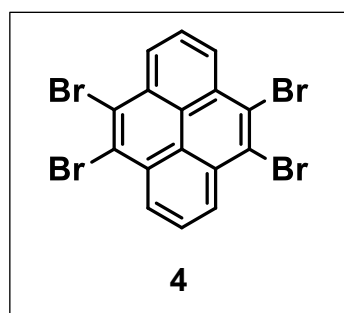


Procedure for compound-74 (R-58): In an oven-dried sealed tube, 2,2',6,6'-tetramethylbiphenyl (73) (250.0 mg, 0.475 mmol, 1.0 mol-eq.) was added, The tetrabromide was dissolved in CCl₄ (4.0 mL) and the tube was purged with argon for 15 minutes. To this solution was added N-bromosuccinimide (2.562 g., 14.395 mmol, 30 mol-eq.) and benzoyl peroxide (0.094g, 0.385mmol, 0.8eq.). The reaction mixture was stirred for 7 days at 94°C. Peroxide was added from time to time, and the reaction was monitored by ¹H NMR, after collecting small aliquots and extraction with CDCl₃/NaOH solution (2M). A NaOH solution was added to the reaction mixture after cooling to RT, and it was extracted with toluene (5×30mL). The combined organic layers were dried over MgSO₄, filtered and evaporated. (**Mass: 355.3 mg, Yield: 89%**). **RESULTS:** ¹H-NMR (**SG-II-85-B**) indicates the desired product 2,2',6,6'-tetrakis (dibromomethyl)biphenyl (**74**). **SG-II-125-E:** ¹H NMR (399.78 MHz, TMS): δ = 8.30 (d, 4H, J= 7.9 Hz), 7.81 (t, 2H, J=8.0 Hz), 5.87 (s, 4H);); **SG-IV-125-F:** ¹³C NMR (100.53 MHz, TMS): δ = 140.75, 133.09, 132.01, 123.54, 77.33, 77.01, 76.69, 37.38; **SG-IV-125-F:** 135°-dept NMR (100.53 MHz, TMS): δ = 133.09, 132.02, 37.38; **TLC** (tol:cyclohex: 10/90 v/v), **R_f** = 0.58

Reaction Number	Starting material (13) (gm, mmol, eq.)	Reagent (g, mmol, eq.)	Solvent (CCl ₄) (mL)	Time	Temp. °C	%Yield
R-53	0.016, 0.0763, 1	NBS (0.448, 2.515, 33); Benzoyl peroxide (0.0186, 0.0764, 1.0)	1.5	10days	25-50 (for 4 days) and 94 (for 6 days)	72.8
R-58	0.100, 0.476, 1	NBS (2.562, 14.395, 30); Benzoyl peroxide (0.094, 0.385, 0.8)	4.0	7days	94	88.7
R-67	1.0g, 4.774 mmol, eq.	NBS (25.436, 142.915, 30); Benzoyl peroxide	28	Stopped heating after 4days,	94	54

		(0.485, 1.993, 0.4)		Quenched after 11 days		
R-71	1.0g, 4.774 mmol, 1 eq.	NBS (25.484, 143.184, 30); Benzoyl peroxide (0.699, 2.875, 0.6)	30	3days	94	98 (very small trace of side product)
R-72	2.5g, 11.896 mmol, eq.	NBS (63.594, 357.309, 30); Benzoyl peroxide (1.299, 5.341, 0.4)	70	3days	94	71 (pure)

Table-10: reactions performed to synthesize 2,2',6,6' tetrakis(dibromomethyl)biphenyl) (**74**)



PROCEDURE: To oven-dried sealed tube, (2,2',6,6'-Tetrakis(dibromomethyl)biphenyl) (**74**) (15.2mg, 0.018mmol, 1eq.) was added and argon was purged for 15minutes in the tube. The octabromo (compound-9) was dissolved in dry DMF (0.5mL–dried with molecular sieves 3Å). To this solution was added Potassium tert-butoxide (67.4mg,

0.600mmol, 34eq.). The reaction mixture was stirred for 15minutes in an ice bath, and it was observed that the color changed from brown to dark brown after 15minutes. The stirring was continued for 48hrs. at 50°C) and it was extracted with DCM and water (4×5mL). The combined organic layers were dried over MgSO₄, filtered. (**Mass: 8.6mg, Yield: 92%**)

RESULTS: ¹H-NMR (**SG-II-55-A**), mainly indicating the desired product (**4**, 4,5,9,10-tetrabromopyrene) [12-13] and traces of starting material (**74**).

SG-V-23-A: ¹H NMR (399.78 MHz, TMS): δ = 8.89 (d, 4H, J=7.8 Hz), 8.15 (t, 2H, J=7.7 Hz); **M.p.:** 387°C (dec.); **TLC** (tol:cyclohex: 10/90 v/v), **R_f** = 0.58

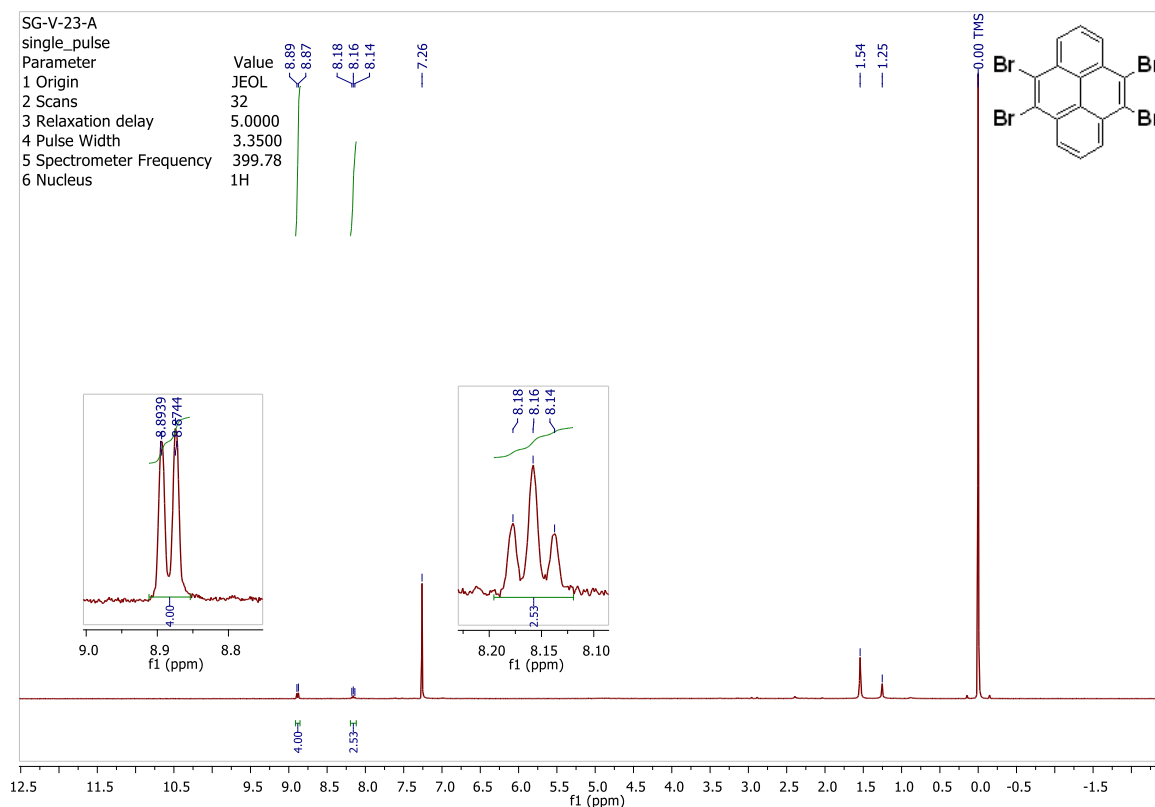
Table-11: Reactions performed to synthesize 24,5,9,10-tetrabromo pyrene (4)

Reaction Number	Starting material (9) (mg, mmol, eq.)	Reagent (mg, mmol, eq.)	Solvent (DMF) (mL)	Time	Temperature	%Yield
R-51	15.2, 0.018, 1	tBuOK (67.4, 0.600, 34)	0.5	48hrs.	50°C	92 Desired+ Trace of Starting material
R-69	100, 0.118, 1	tBuOK (401.3, 3.576, 30)	1.5	48hrs.	50°C	81.6
R-80	100, 0.118, 1	tBuOK (416.4, 3.710, 31)	1.5	48hrs.	50°C	55 Desired+ Trace of Starting material
R-86	30.4, 0.036, 1	tBuOK (191.,0, 1.702, 47)	0.6	5days	80°C & 50°C	Failed
R-87	30.1, 0.035, 1	tBuOK (0.182, 1.622, 46)	0.6	3days	60°C	Failed
R-88	30.5, 0.036, 1	tBuOK (0.160, 1.428, 39)	0.6	2days	50°C	Working, poor yield
R-89	250.0, 0.297, 1	tBuOK (1000.0, 10.821, 36)	4.0	2days	50°C	Failed, Not desired product
R-90	100.0, 0.118, 1	tBuOK (419.5, 3.738, 32)	1.5	2days	50°C	Failed, Not desired product
R-91	100.0, 0.118, 1	tBuOK (0.653, 5.825, 49)	1.5	2days	50°C	Failed, Not desired product

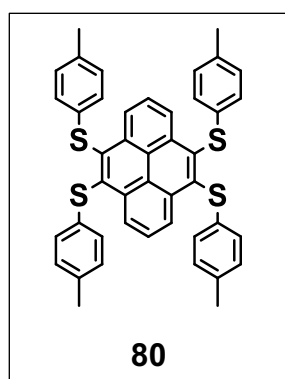
Reaction Number	Starting material (9) (mg, mmol, eq.)	Reagent (mg, mmol, eq.)	Solvent (DMF) (mL)	Time	Temperature	%Yield
R-92 In DMSO	15.1, 0.017, 1	tBuOK (161.6, 1.440, 80)	0.5	2days	50°C	Failed
R-93	30.1, 0.035, 1	tBuOK (114.6, 1.021, 29)	0.6	2days	50°C	Failed, Not desired product
R-94	50.3, 0.059, 1	tBuOK (20.6, 1.835, 31)	0.4	2days	30°C	Successful
R-101	250.0, 0.297, 1	tBuOK (1000.0, 8.91, 30)	1.5	2days	30°C	Failed, Not desired product
R-136	31.1, 0.037, 1	tBuOK (42.4, 0.378, 10)	0.6	24hours	Room temperature	Mixture of products
R-137	31.8, 0.037, 1	tBuOK (61.2, 0.545, 14)	0.6	24hours	Room temperature	Mixture of products
R-138	31.0, 0.0368, 1	tBuOK (40.4, 0.360, 9.8)	0.6	24hours	45-47° C	Mixture of products
R-140	31.9, 0.0379, 1	tBuOK (119.4, 1.064, 28)	0.45	18hrs.	50°C	Not completed, Mixture of products
R-141	32.4, 0.0385, 1	tBuOK (45.6, 0.406, 10.5)	0.6	3-4days	50°C	Not completed, Mixture of products

Reaction Number	Starting material (9) (mg, mmol, eq.)	Reagent (mg, mmol, eq.)	Solvent (DMF) (mL)	Time	Temperature	%Yield
R-144	30.1, 0.0357, 1	tBuOK (39.9, 0.355, 10)	0.6	2days	50°C	Not desired compound
R-150	30.4, 0.0361, 1	tBuOK (44.0, 0.392, 10.8)	0.6	2days	50°C	17.6%
R-151 (high dilution)	29.9, 0.0355, 1	tBuOK (122.9, 1.095, 31)	6.0	4days	50°C	Mixture of products
R-152	32.9, 0.0390, 1	tBuOK (134.4, 1.197, 30.6)	1.0	2days	50°C	Mixture of products
R-153	60.9, 0.0723, 1	tBuOK (103.2, 0.919, 12.7)	1.2	18hrs. and 30hrs.	40°C and 47°C	35%
R-155	60.7, 0.0721, 1	tBuOK (108.8, 0.969, 13)	1.2	2days	50°C	65%
R-156 (adding solution of t-BuOK)	60.9, 0.0723, 1	tBuOK in DMF (0.6M, 1.2mL)+ tBuOK (49.8, 0.443, 6)	-	4days	50°C	Mixture of products
R-157	90.1, 0.107, 1	tBuOK (129.3, 1.152, 10.7)	1.2	3days	47-50°C	74%
R-158	181.1, 0.215, 1	tBuOK (246.1, 2.193, 10)	1.6	2days	50°C	99%
R-159	812.6, 0.965, 1	tBuOK (1319.1, 11.755, 12)	2.5+ 3	18hrs.	Room temperature	Turned black, failed

Reaction Number	Starting material (9) (mg, mmol, eq.)	Reagent (mg, mmol, eq.)	Solvent (DMF) (mL)	Time	Temperature	%Yield
R-165	180.6, 0.215, 1	tBuOK (245.3, 2.186, 10)	1.5	4days	50°C	69%
R-167	250.3, 0.297, 1	tBuOK (336.3, 2.997, 10)	1.6	2days	47-50°C	--
R-188	50.4, 0.0598, 1	tBuOK (67.3, 0.599, 10)	1.2	4days	50°C	Starting material+ product
R-192	50.3, 0.0597, 1	tBuOK (135.0, 1.203, 20)	1.2	2days	50°C	Mixture of products
R-205	180.5, 0.214, 1	tBuOK (248.8, 2.217, 10)	1.6	24hrs. and 24hrs.	40°C and 47°C	90.6%
R-210	180.8, 0.215, 1	tBuOK (246.6, 2.197, 10)	1.6	3days	50°C	97.6%
R-213	250.8, 0.298, 1	tBuOK (333.3, 2.967, 10)	1.8	2days	50°C	>83%
R-248	250.2, 0.297, 1	tBuOK (365.8, 3.259, 11)	1.8	2days	50°C	92%
R-249	250.3, 0.297, 1	tBuOK (368.5, 3.284, 11)	1.8	2days	50°C	81%
R-257 (freeze thaw pump)	250.5, 0.297, 1	tBuOK (334.8, 2.984, 10)	1.8	2days	50°C	65%
R258 (freeze thaw pump)	821.7, 0.976, 1	tBuOK (1.776g, 15.826, 16)	5.0	30mins	50°C	71.5%



^1H NMR (399.78 MHz, CDCl_3)



Procedure for compound-80 (R-81): In an oven-dried sealed tube, (4,5,9,10-tetrabromopyrene) (**4**) (10.0mg, 0.019mmol, 1eq.), 4-methyl thiophenol (9.7mg, 0.078mmol, 4eq.) and Potassium carbonate (10.6mg, 0.077mmol, 4eq.) were added and argon was purged for 15minutes in the tube. To this dry DMF (0.5mL–dried with molecular sieves 3\AA) was added and the reaction mixture was stirred for 4days at 137°C and it was observed that the color was changed from white to yellow after 15minutes. Mainly 2 spots were observed by UV-vis in 5% Acetone/cyclohex). The reaction was extracted with toluene ($4\times 20\text{mL}$) and water (20mL). The combined organic layers were dried over MgSO_4 , filtered. The crude product was purified by chromatography over silica gel (eluent: cyclohexane /Acetone: 95/5) to yield a bright yellow solid.

RESULTS: ^1H NMR **SG-II-174-F** (CDCl_3 , 400MHz), ^{13}C -NMR **SG-II-174-G** (CDCl_3 , 400MHz) indicates desired asterisk at 137°C in DMF.

SG-II-174-F: ^1H NMR (399.78 MHz, TMS): δ =9.01 (d, 4H, J=8.0 Hz), 7.89 (t, 2H, J=7.9 Hz), 6.95 (d, 8H, J=8.2), 6.86 (d, 8H, J=8.0 Hz), 2.14 (s, 12H); **SG-II-174-G:** ^{13}C NMR (101 MHz,) δ 135.81, 134.83, 132.47, 132.38, 130.59, 130.24, 128.94, 127.88, 127.82, 21.38; **M.p.:** 287.3-290°C; **TLC** (acetone/Cyclohex: 30/70 v/v), **R_f** = 0.68

NMR study with time

^1H -NMR **SG-II-173-A:** Reaction mixture Stirred 24hrs at RT (137°C)

^1H -NMR **SG-II-173-B:** Reaction mixture Stirred 67hrs (~3days) at RT (137°C)

^1H -NMR **SG-II-173-C:** Reaction mixture Stirred 89hrs (~ 4days) at RT (137°C)

^1H -NMR **SG-II-173-D:** Reaction mixture after workup but not dried under vacuum, same as above

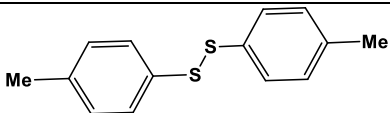
^1H -NMR **SG-II-173-E:** Reaction mixture dried under vacuum overnight

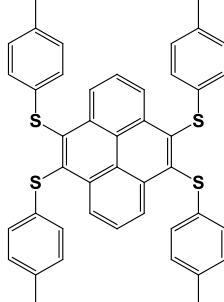
COLUMN

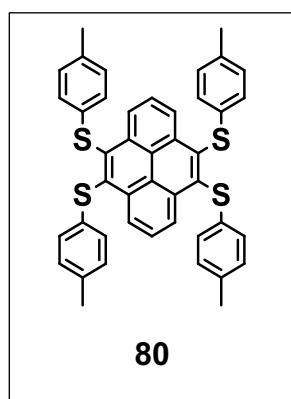
Fraction [8], (1st spot on TLC): ^1H -NMR **SG-II-174-B** colorless product indicates methyl disulfide containing **Me** group (**MePhSSPhMe**). **Mass: 0.4 mg**

Fraction [9-10], (mixture of 1st and 2nd spot on TLC): product indicates mixture of two spots, methyl disulfide containing **Me** group (**MePhSSPhMe**) and asterisk

Fraction [11-12], (2nd spot on TLC): ^1H -NMR **SG-II-174-C & SG-II-174-E** yellow product indicates asterisk. **Mass: 2.6 mg**

Fractions no ^1H -NMR	Mass (mg)	Mmol	Approx. relative ratio (mol %)	Tentative assignment of structure by ^1H NMR (isolated products)
Fraction [8] SG-II-174-B	0.4			
Fractions[9-10] SG-II-174-E	--			Mixture of two spots (Disulfide+ Asterisk)

Fractions[11-12] SG-II-174-F (1H-NMR) SG-II-174-G (13C-NMR)	2.6			
---------------------------------------------------------------------------------------	-----	--	--	-------------------------------------------------------------------------------------



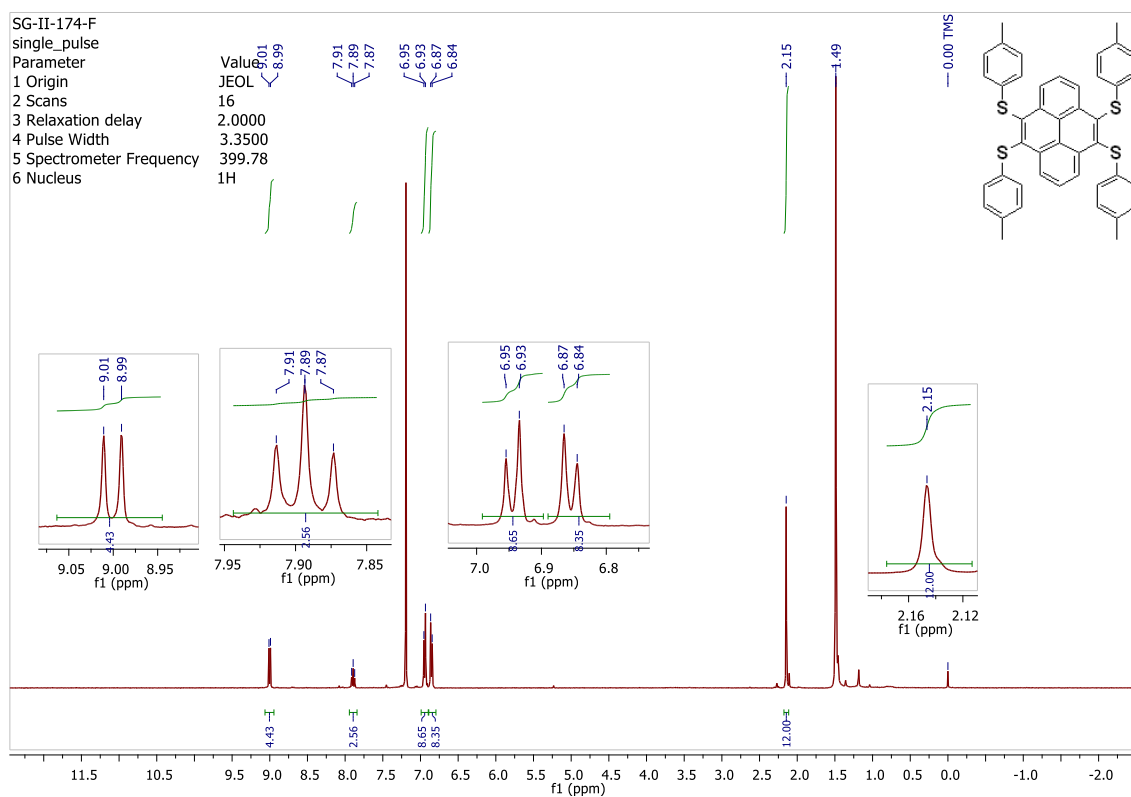
Procedure for compound-80 (R-161): In an oven-dried sealed tube, (4,5,9,10-tetrabromopyrene) (**4**) (90.5mg, 0.175mmol, 1eq.), 4-methyl thiophenol (86.9mg, 0.699mmol, 4eq.) and Potassium carbonate (97.3mg, 0.704mmol, 4eq.) were added and argon was purged for 15minutes in the tube. To this, dry DMF (0.5mL–dried with molecular sieves 3Å) was added and purged Ar for 5minutes. The reaction mixture was stirred for 5days at 133°C and it was observed the color changed

from white to yellow after 15minutes. The reaction mixture was monitored by thin layer chromatography (SiO₂, 5% Acetone/ cyclohex). Mainly 2 spots were observed by UV-vis in 5% Acetone/cyclohex). The the crude product was triturated with a solution of ethanol/H₂O (5mL each) and filtered. (**Mass: 119.0mg, %Yield: 98.6%**)

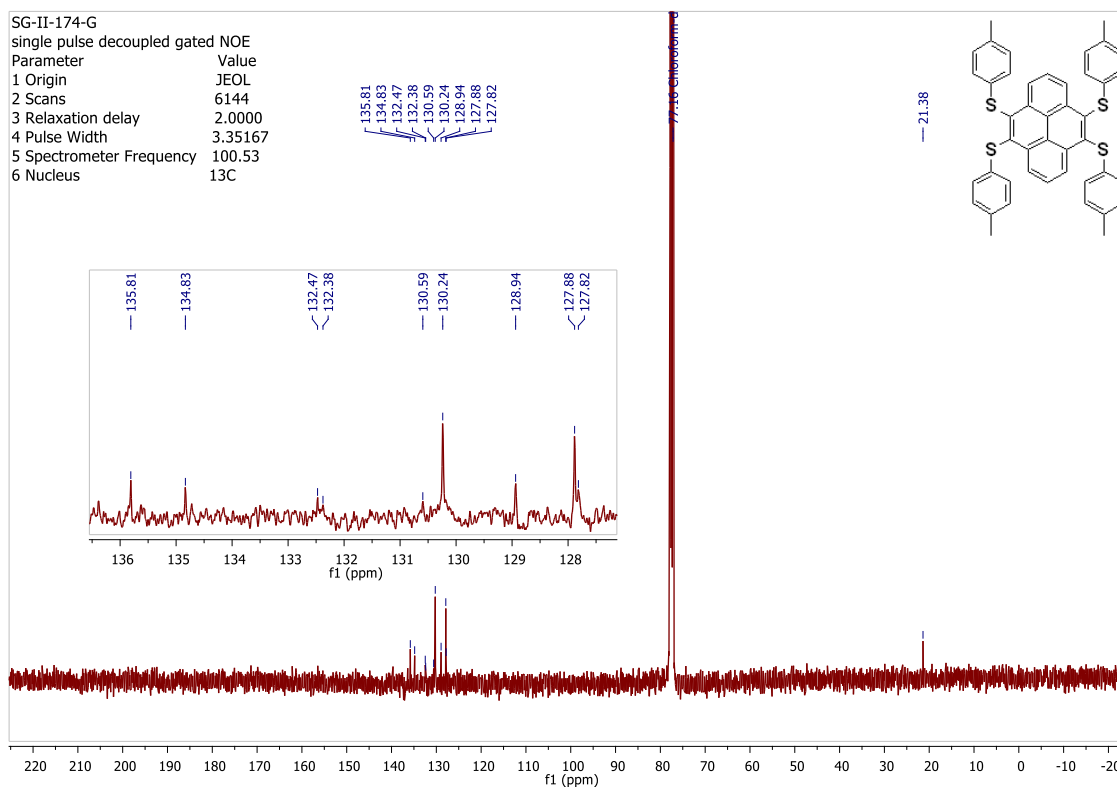
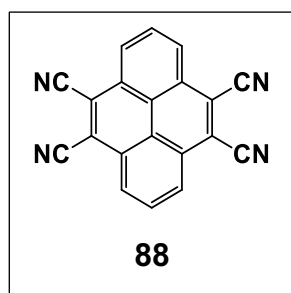
RESULTS: SG-II-174-F: 1H NMR (399.78 MHz, TMS): δ =9.01 (d, 4H, J=8.0 Hz), 7.89 (t, 2H, J=7.9 Hz), 6.95 (d, 8H, J=8.2), 6.86 (d, 8H, J=8.0 Hz), 2.14 (s, 12H); **SG-II-174-G:** 13C NMR (101 MHz,) δ 135.81, 134.83, 132.47, 132.38, 130.59, 130.24, 128.94, 127.88, 127.82, 21.38; **M.p.:** 287.3-290°C; **TLC** (acetone/ Cyclohex: 30/70 v/v), **Rf** = 0.68

Reaction Number	Starting material (mg, mmol, eq.)	Reagent (mg, mmol, eq.)	Solvent (DMF) (mL)	Time	Temperature	%Yield
R-81	Br-Py (10.0, 0.019, 1) Thiol (9.7, 0.078, 4)	K ₂ CO ₃ (10.6, 0.077, 4)	0.5	4days	137°C	--
R-161	Br-Py (90.5, 0.175, 1) Thiol (86.9, 0.699, 4)	K ₂ CO ₃ (10.6, 0.077, 4)	1.0	5days	133°C	98.6%

Table-12: Reactions performed to synthesize 4,5,9,10-tetrathiotolyl pyrene (**80**)



¹H NMR (399.78 MHz, CDCl₃)

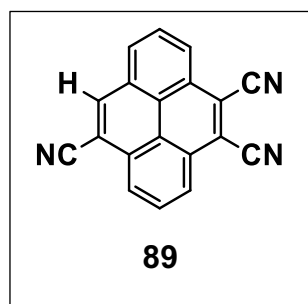
¹³C NMR (100.53 MHz, CDCl₃)

Procedure for compound-88 (R-250): In an oven-dried sealed tube, 4,5,9,10-tetrabromopyrene, **4** (25.1mg, 0.0485mmol, 1eq.) was added, copper (I) cyanide (35.0mg, 0.391mmol, 8eq.) was added and argon was purged for 15minutes in the tube. To this, dry NMP (0.5mL–dried with molecular sieves 3Å) was added and purged Ar for 5minutes. The reaction mixture was stirred for

2hours at 196°C and it was observed the color changed to dark brown after 2-3 minutes. Mainly 4 spots were observed by UV-vis in 80% DCM/cyclohex). The reaction mixture was purified by column chromatography (SiO₂, 80% DCM/ cyclohex). (**Mass: 2.1mg+ crystals**)

RESULTS: ¹H-NMR (**SG-V-145-C**) mainly indicating the desired product 4,5,9,10-tetracyanopyrene (**88**).

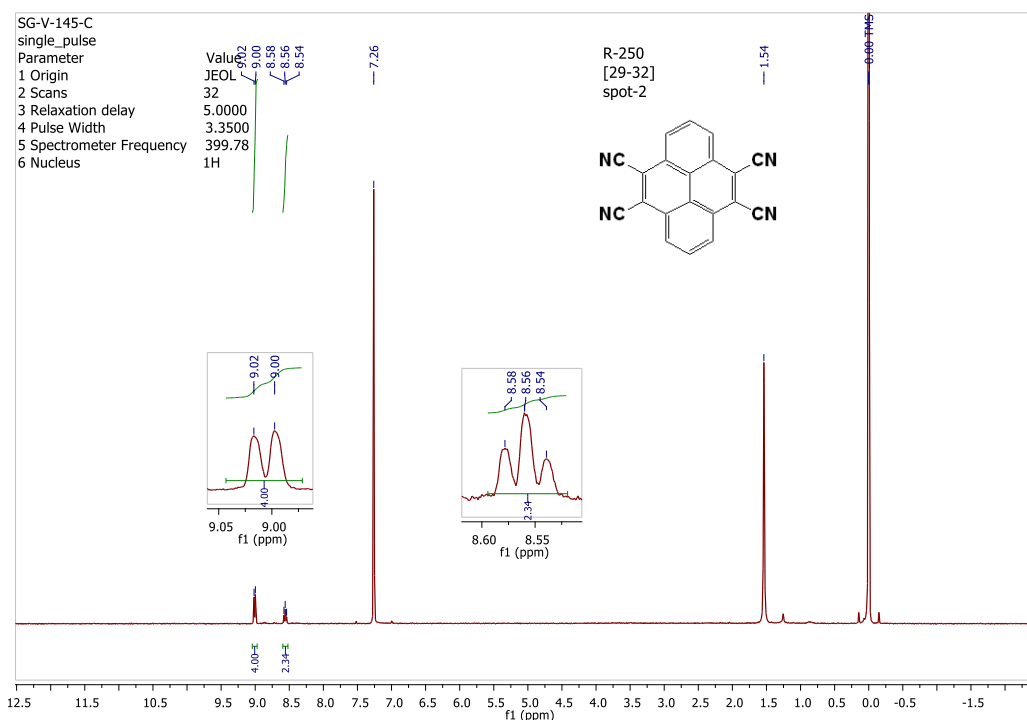
SG-V-145-C: ¹H NMR (399.78 MHz, CDCl₃): 9.02 (d, 4H, J=7.8Hz), 8.56 (t, 2H, J=7.36Hz); **SG-V-145-F:** Dept-135°-NMR (100.53 MHz, CDCl₃, Crystallized in tube) 130.25, 129.70, 127.65, 127.23; **M.p.:** 378-380°C; **TLC** (DCM:Cyclohex: 80/20 v/v), **R_f**= 0.62



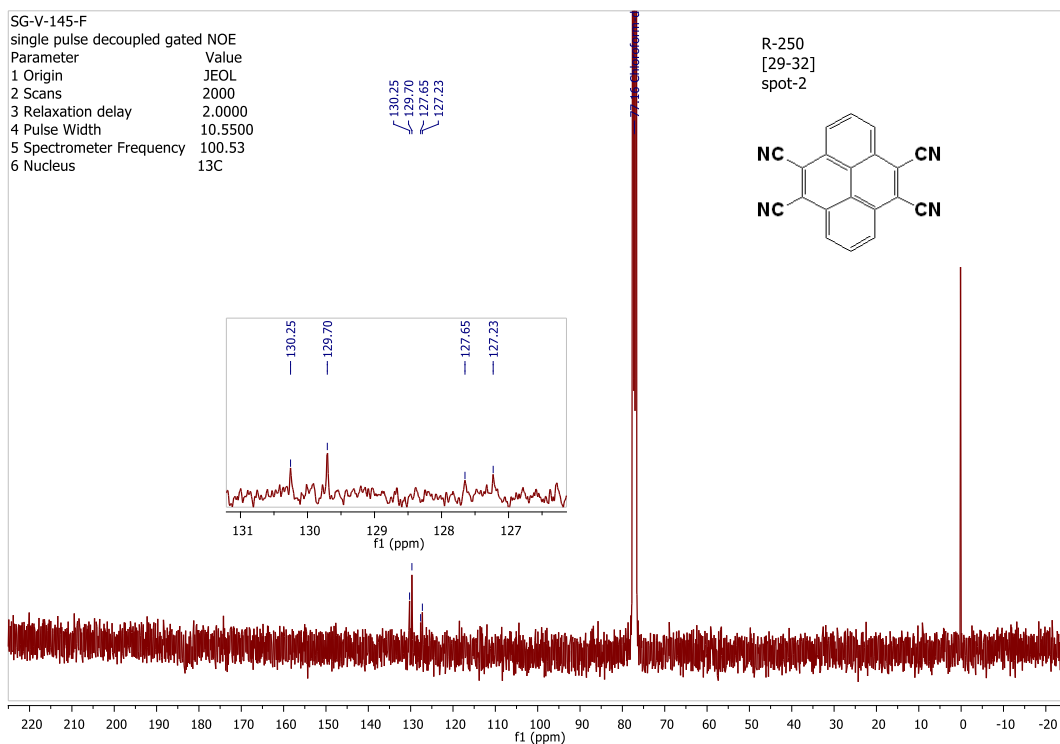
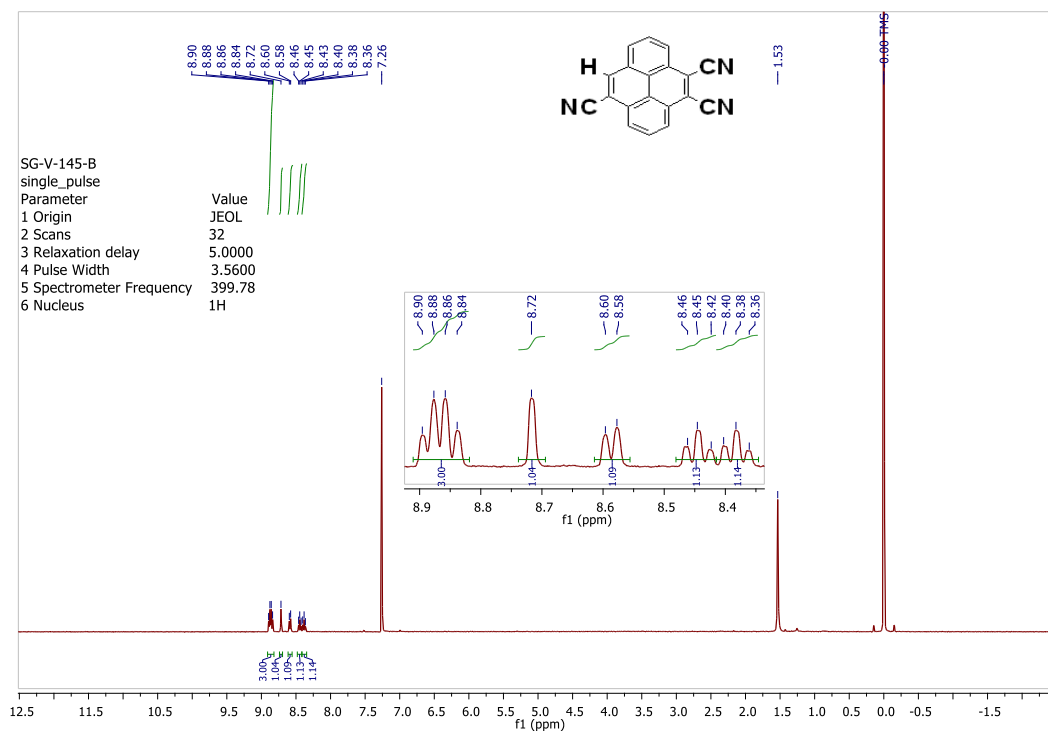
Byproduct: SG-V-145-B: ^1H NMR (399.78 MHz, CDCl_3): 8.90 (q, 3H, $J=7.55, 7.79\text{Hz}$), 8.72 (s, 1H), 8.60 (d, 1H, $J=7.54\text{ Hz}$), 8.46 (t, 1H, $J=6.41\text{ Hz}$), 8.40 (t, 1H, $J=8.05\text{ Hz}$); **SG-V-145-E:** ^{13}C -NMR (100.53 MHz, CDCl_3 , Crystallized in tube) 136.48, 131.33, 129.32, 129.22, 129.04, 128.47, 128.38, 128.20, 128.07, 126.88, 125.55, 116.36, 115.37, 114.68; **TLC** (DCM:Cyclohex: 80/20 v/v), $R_f= 0.68$; **Mass: 4.8 mg**

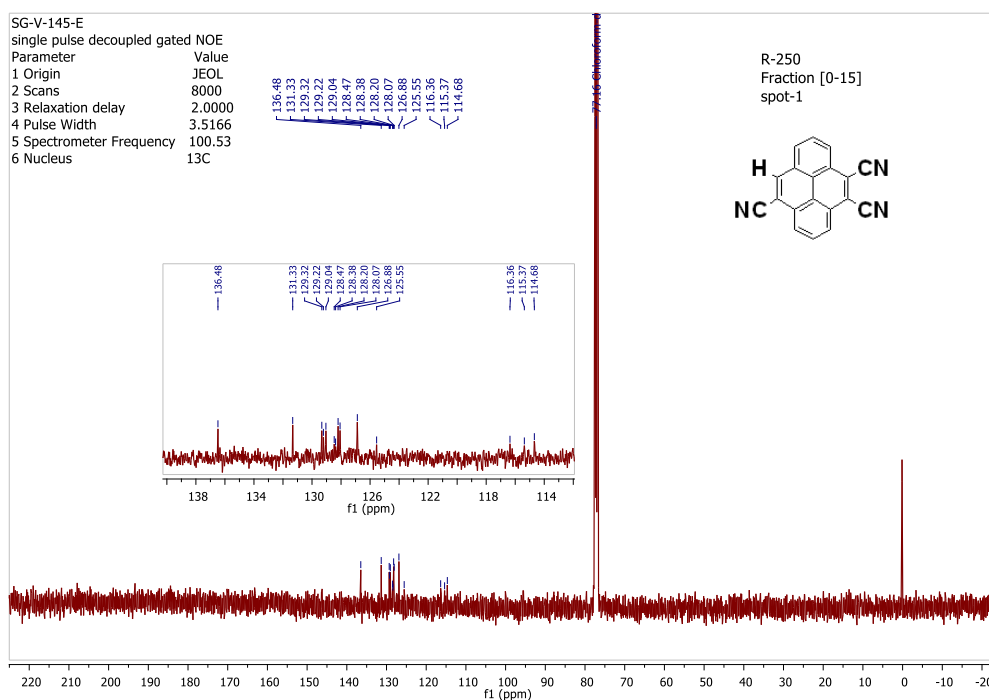
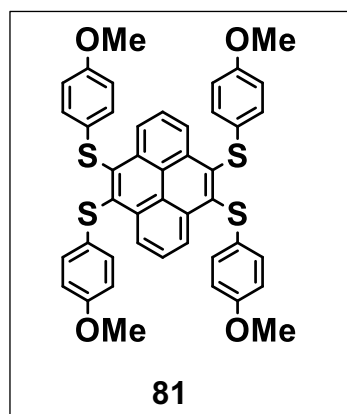
Reaction Number	Starting material (mg, mmol, eq.)	Reagent CuCN (mg, mmol, eq.)	Solvent (NMP) (mL)	Time	Temperature	%Yield
R-250	Br-Py (25.1, 0.0485, 1)	(35.0, 0.391, 8)	0.5	2hrs.	196°C	--

Table-13: Reactions performed to synthesize 4,5,9,10-tetracyanopyrene (**89**)



^1H NMR (399.78 MHz, CDCl_3)

 ^{13}C NMR (100.53 MHz, CDCl_3) ^1H NMR (399.78 MHz, CDCl_3)

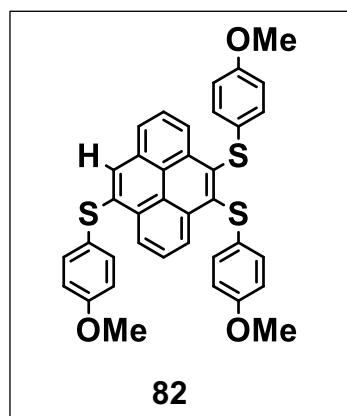
¹³C NMR (100.53 MHz, CDCl₃)

Procedure for compound-81 (R-263): In an oven-dried sealed tube, (4,5,9,10-tetrabromopyrene) (**4**) (171.8mg, 0.332mmol, 1eq.), 4-methoxybenzene thiol (239.4mg, 0.21mL, 1.707mmol, 5eq.) and Potassium carbonate (230.3mg, 1.666mmol, 5eq.) were added and argon was purged for 15minutes in the tube. To this, dry DMF (2.0mL—dried with molecular sieves 3Å) was added and purged argon for 5minutes. The reaction mixture was stirred for

3days at 67°C and it was observed the color changed to yellow after 2-3 minutes. The reaction mixture was monitored by thin layer chromatography (SiO₂, 80% Tol/ Cyclohex). This solid is extracted with toluene (3 x 30mL) and water (30mL). The organic phase was dried over anhydrous Na₂SO₄, filtered and the solvent was evaporated off. Mainly 5 spots were observed by UV-vis in 80% Tol/ Cyclohex). The reaction mixture was purified by column chromatography (SiO₂, 80% DCM/ cyclohex).
(Mass: 135.1mg+ crystals in two tubes, Yield: >60%)

RESULTS: SG-V-181-D1: ¹H NMR (399.78 MHz, TMS): δ =9.11 (d, 4H, J=8.04 Hz), 7.97 (t, 2H, J=8.03 Hz), 7.12 (d, 8H, J=8.82 Hz), 6.68 (d, 8H, J=8.8 Hz), 3.69 (s, 12H);

SG-V-181-D1: ¹³C NMR (101 MHz,) δ 158.05, 139.62, 131.99, 129.77, 128.53, 128.31, 127.22, 126.46, 114.67, 55.24; **SG-V-181-D1:** ¹³⁵-Dept NMR (101 MHz,) δ 129.79, 128.32, 127.22, 114.69, 55.24, **M.p.:** 206-211°C; **TLC** (DCM/ Cyclohex: 50/50 v/v), **R_f** = 0.4



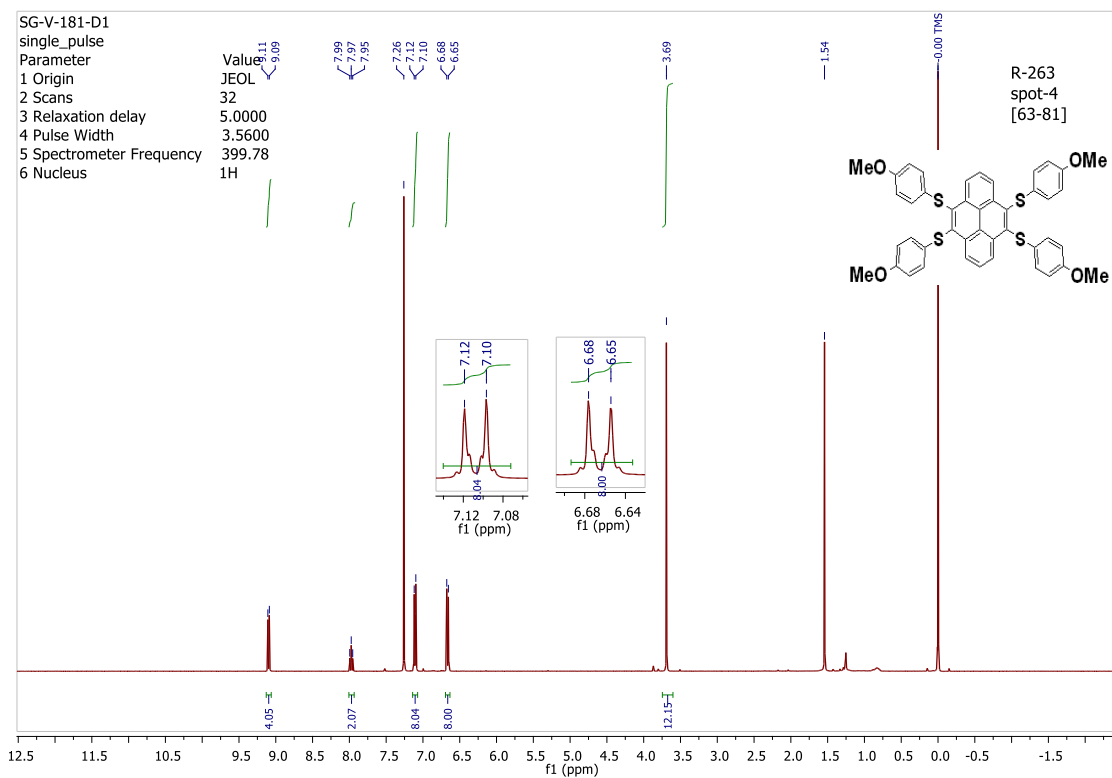
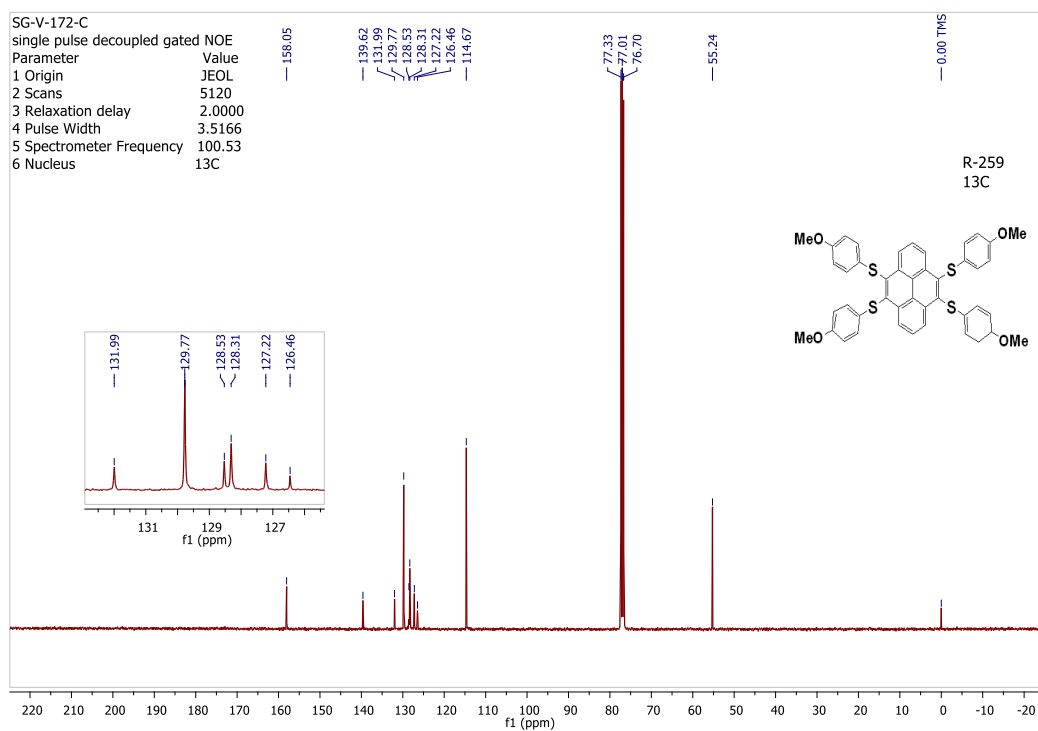
Byproduct: SG-V-181-C: ¹H NMR (399.78 MHz, TMS): δ = 9.08 (d, 1H, J=8.02 Hz), 8.96 (d, 1H, J=7.9 Hz), 8.73 (d, 1H, J=7.89 Hz), 8.02 (t, 2H, J=7.85 Hz), 7.93 (t, 1H, J=7.82 Hz), 7.88 (s, 1H), 7.49 (d, 2H, J=8.71 Hz), 7.09 (d, 4H, J=8.75 Hz), 6.93 (d, 2H, J=8.72 Hz), 6.66 (d, 4H, J=8.68 Hz), 3.83 (s, 3H),

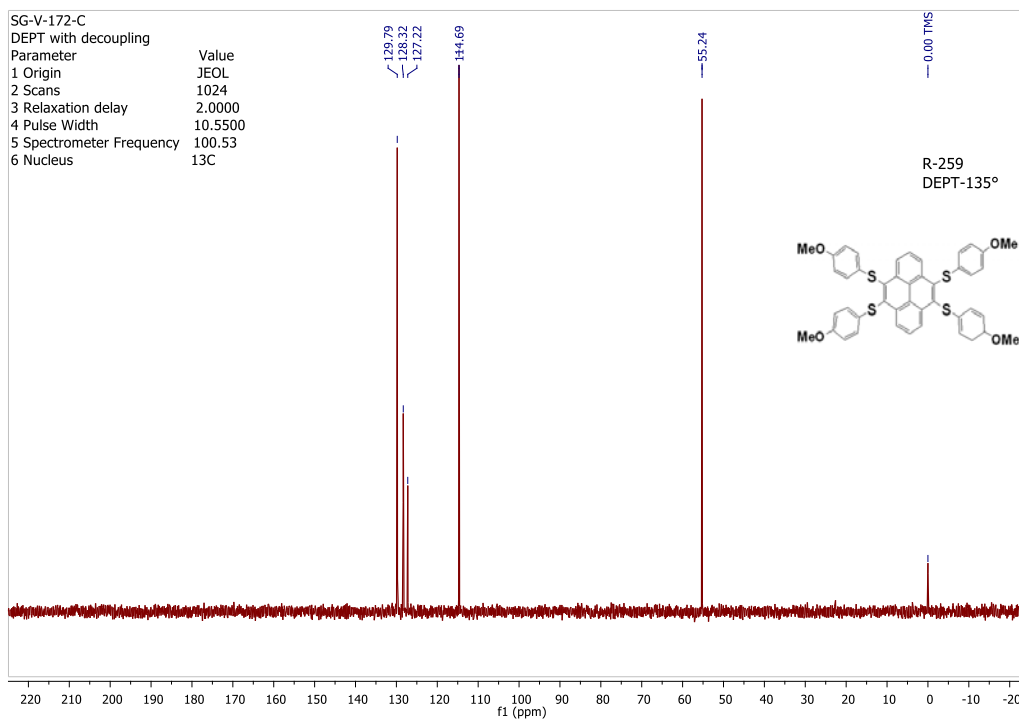
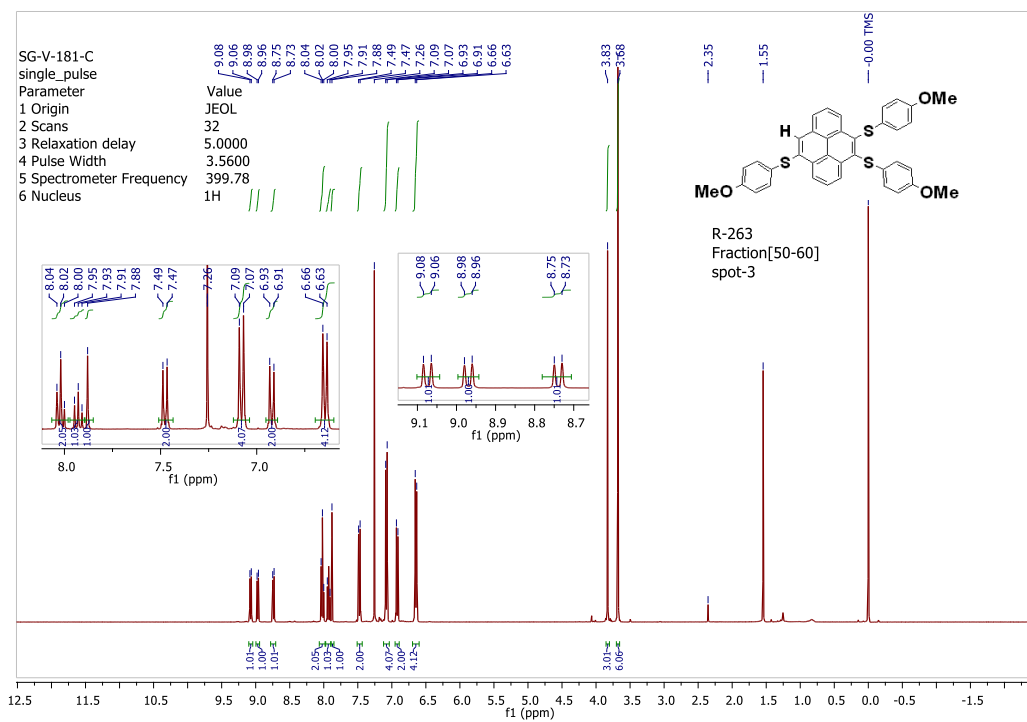
3.68 (s, 6H); **SG-V-172-C:** ¹³C NMR (101 MHz,) δ 159.72, 157.94, 139.62, 139.58, 134.50, 134.44, 132.17, 131.67,

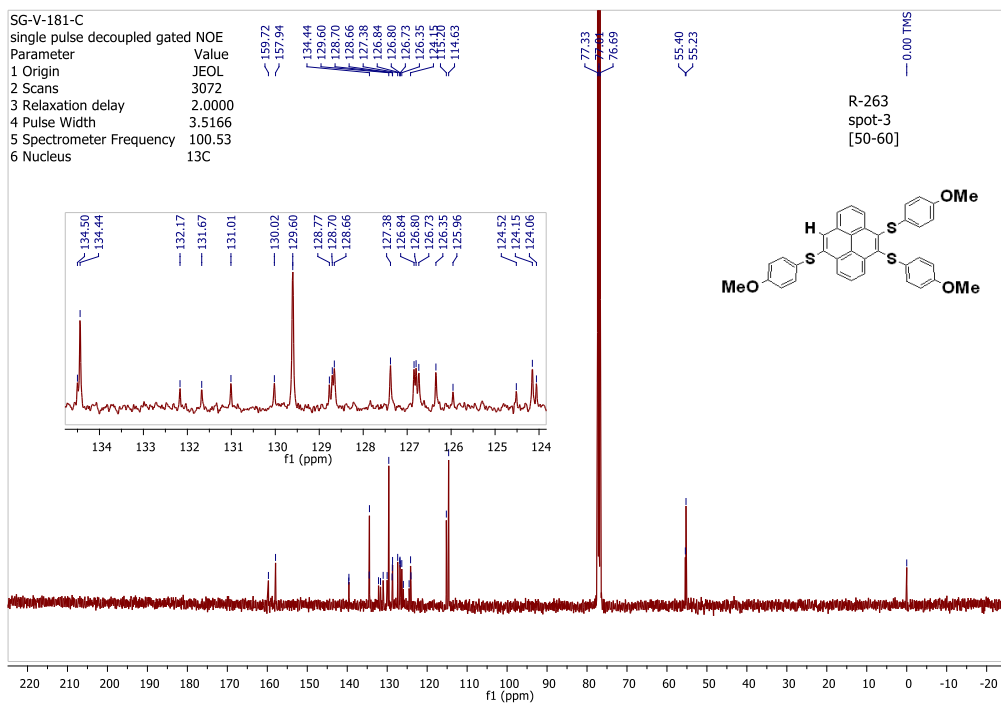
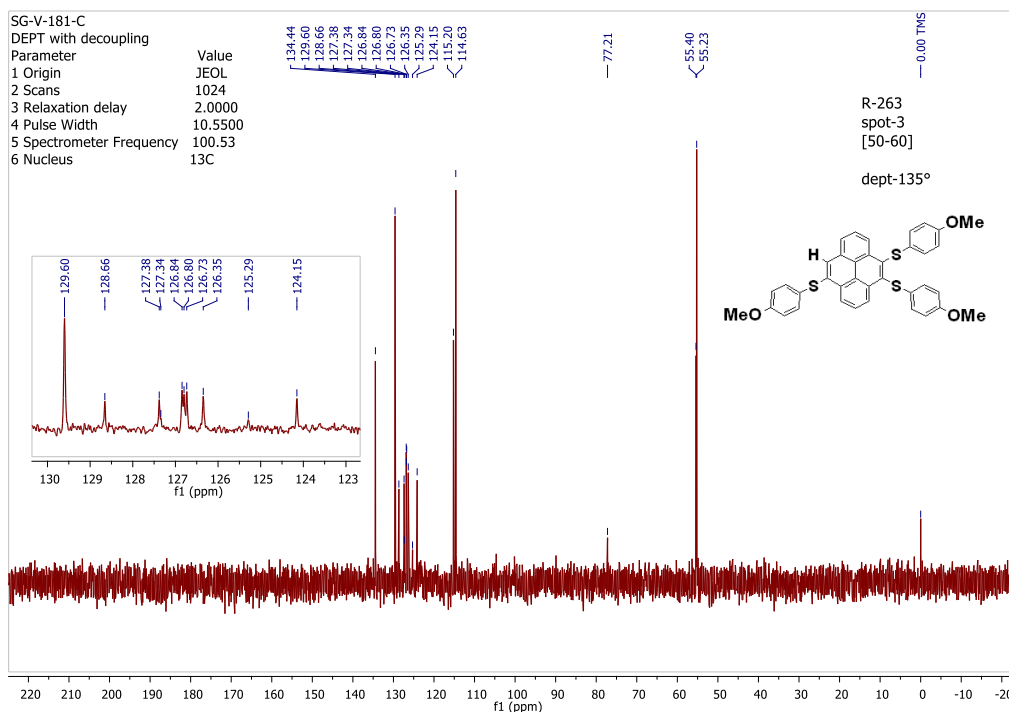
131.01, 130.02, 129.60, 128.77, 128.70, 128.66, 127.38, 126.84, 126.80, 126.73, 126.35, 125.96, 124.52, 124.15, 124.06, 115.20, 114.63, 55.40, 55.23; **SG-V-172-C:** ¹³⁵-Dept NMR (101 MHz,) δ 134.44, 129.60, 128.66, 127.38, 127.34, 126.84, 126.80, 126.73, 126.35, 125.29, 124.15, 115.20, 114.63, 55.40, 55.23, **M.p.:** 162-164.7°C; **TLC** (DCM/ Cyclohex: 30/70 v/v), **R_f** = 0.4

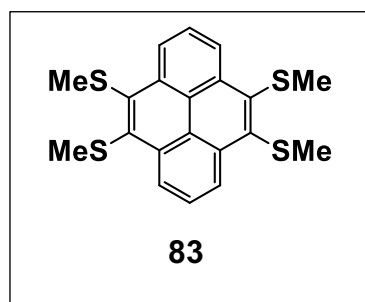
Reaction Number	Starting material (mg, mmol, eq.)	Reagent Methoxy_thiol (mg, mmol, eq.)	Solvent (DMF) (mL)	Time	Temp.	%Yield
R-256	Br-Py (50.1, 0.0967, 1)	(57.0, 0.05mL, 0.406, 4.2)	1.0	2days	100°C	--
R-263	Br-Py (171.8, 0.332, 1)	(239.4, 0.21mL, 1.707, 5)	2.0	3days	67°C	>60%

Table-14: Reactions performed to synthesize compound-81 and 82

 ^1H NMR (399.78 MHz, CDCl_3) ^{13}C NMR (100.53 MHz, CDCl_3)

 ^{13}C NMR (100.53 MHz, CDCl_3) ^1H NMR (399.78 MHz, CDCl_3)

 ^{13}C NMR (100.53 MHz, CDCl_3) ^{13}C NMR DEPT 135 (100.53 MHz, CDCl_3)



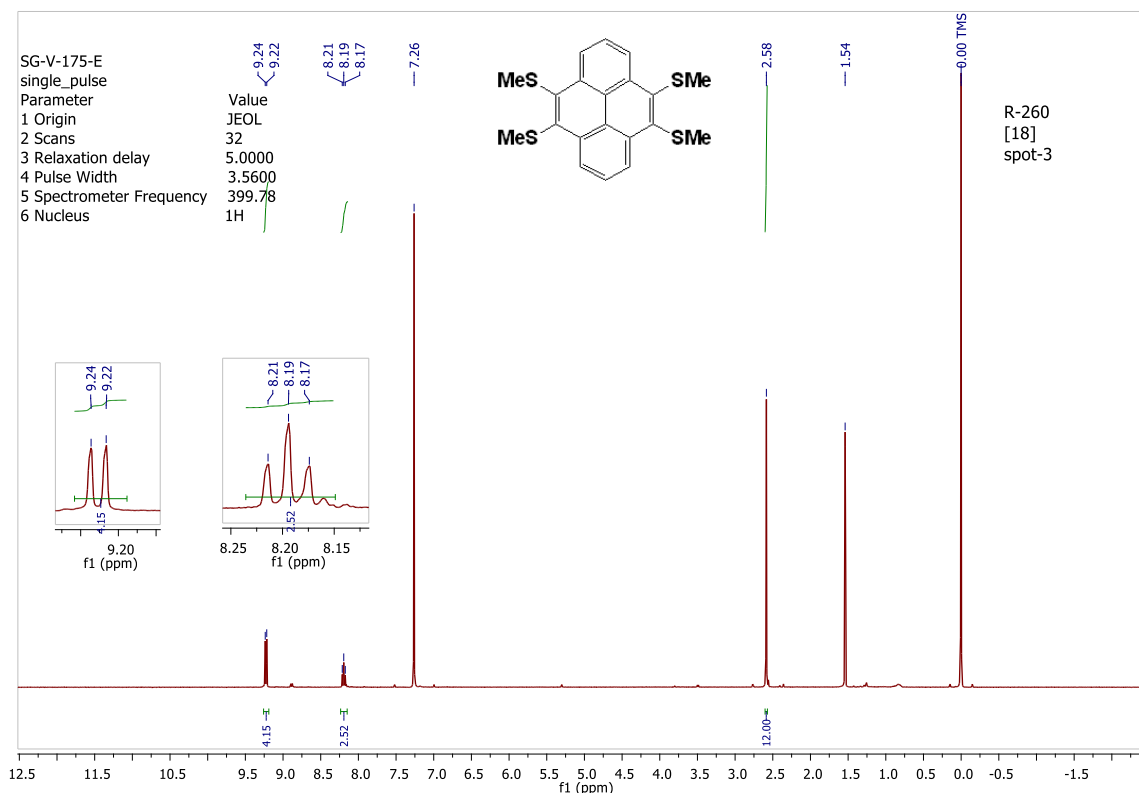
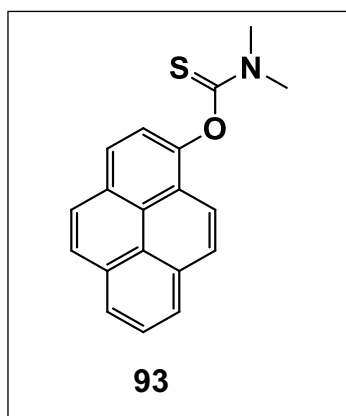
Procedure for compound-83 (R-260): In an oven-dried sealed tube, (4,5,9,10-tetrabromopyrene) (**4**) (30.2mg, 0.0583mmol, 1eq.), sodium methanethiolate (66.3mg, 0.946mmol, 16eq.) were added and argon was purged for 15minutes in the tube. To this, dry DMF (1.0mL–dried with molecular sieves 3Å) was added and purged argon for

5minutes. The reaction mixture was stirred for 5 days at 85°C. The reaction mixture was monitored by thin layer chromatography (SiO₂, 80% Tol/ Cyclohex). The reaction mixture was quenched with 0.1N HCl (5-10mL) and the reaction mixture was further extracted with toluene (3 x 20mL) and water (20mL). The organic phase was dried over anhydrous sodium sulfate, filtered and the solvent was evaporated off. Mainly 5 spots were observed by UV-vis in 50% Tol/ Cyclohex). The reaction mixture was purified by column chromatography (SiO₂, 50% DCM/ cyclohex). (**Mass: 0.2mg**)

SG-V-175-E: ¹H NMR (399.78 MHz, CDCl₃): 9.24 (d, 4H, J=8.01 Hz), 8.19 (t, 2H, J=7.92 Hz), 2.58 (s, 12H); **TLC** (Tol:Cyclohex: 50/50 v/v), R_f= 0.62

Reaction Number	Starting material (mg, mmol, eq.)	Reagent (NaSH(Me)) (mg, mmol, eq.)	Solvent (DMF) (mL)	Time	Temp.	%Yield
R-260	Br-Py (30.2, 0.058, 1)	(66.3, 0.946, 16)	1.0	5days	85°C	--
R-270	Br-Py (108.4, 0.209, 1)	(294.4, 4.200, 20)	2.0	4days	85°C	--

Table-15: Reactions performed to synthesize compound-83

 ^1H NMR (399.78 MHz, CDCl_3)

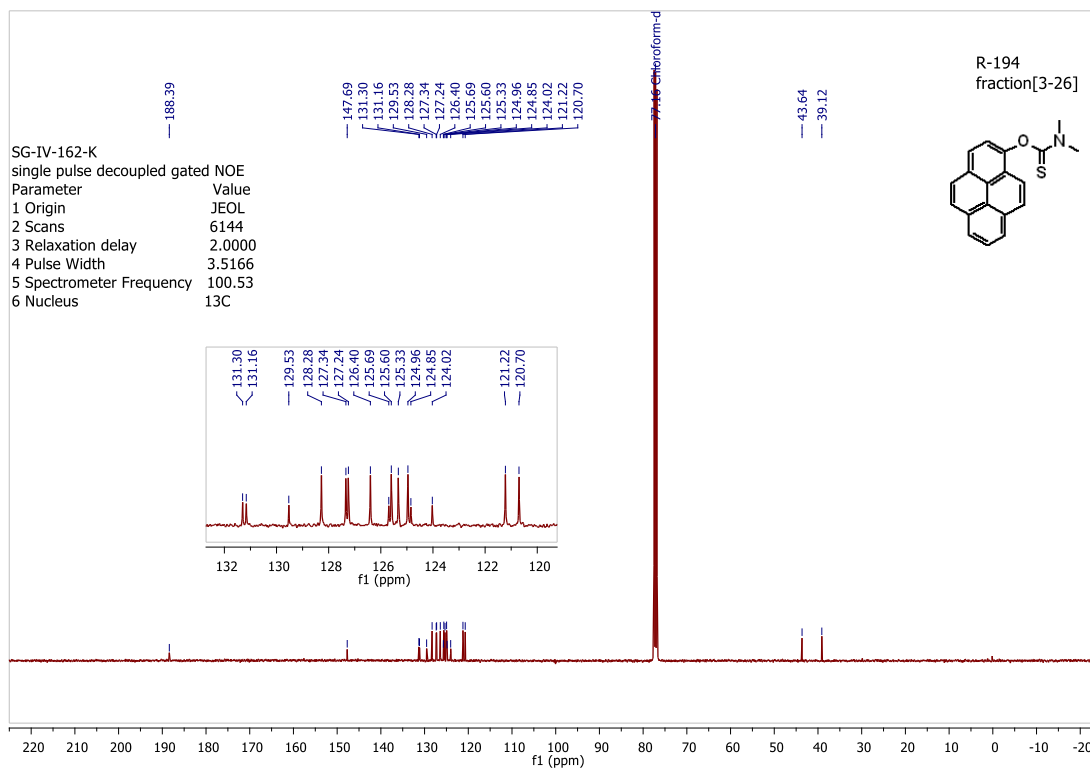
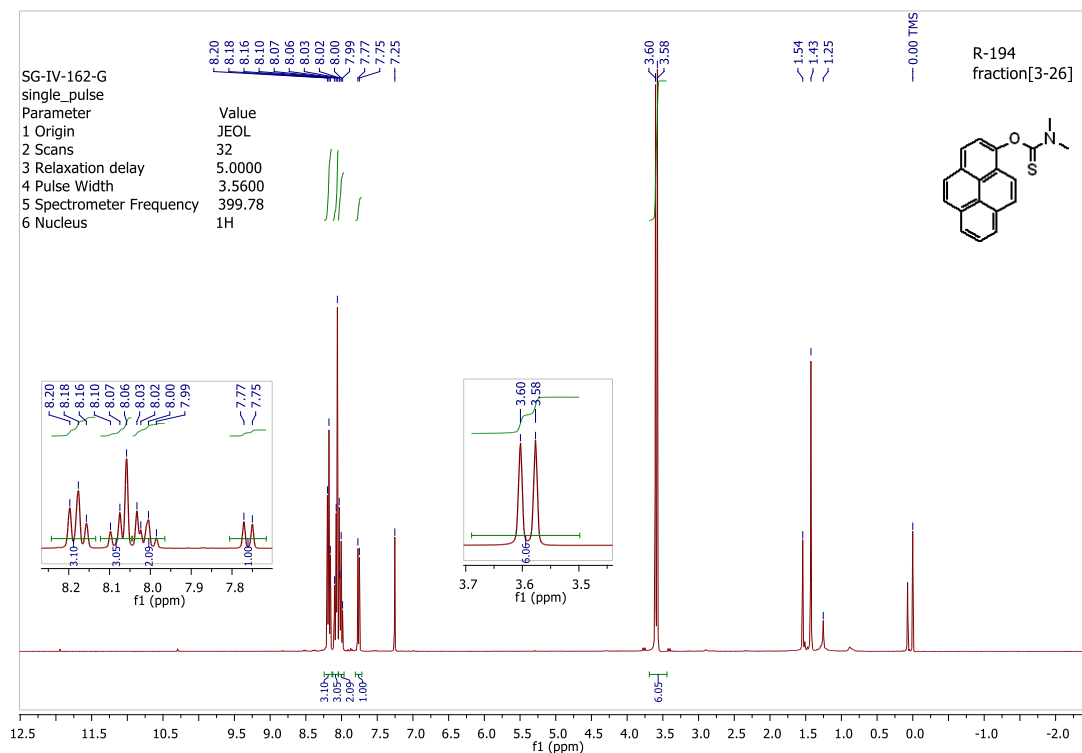
Procedure for compound-93 (1-Pyrenyl-O-thiocarbamate) (R-211): In an oven-dried sealed tube, 1-hydroxypyrene (2.500g, 11.351mmol, 1eq.), and (DABCO) 1,4-diazabicyclo[2.2.2]octane (3.817g, 34.029mmol, 3.0eq.) were added and argon was purged for 15minutes in the tube. To this, dry DMF (2.0mL–dried with molecular sieves 3Å) was added and purged argon for 5minutes. N,N-dimethylthiocarbamoyl chloride (1.968g, 15.922mmol, 1.4eq.) was added to the reaction mixture . The reaction mixture was stirred for 4days and 15hours at 112-115°C. The reaction mixture was quenched with 1M HCl (20mL) and the reaction mixture was further extracted with toluene (5 x 20mL) and water (30mL). The organic phase was dried over anhydrous sodium sulfate, filtered and the solvent was evaporated off. Mainly three spots were observed by UV-vis in 80% DCM/ Cyclohex). The reaction mixture was purified by column chromatography (SiO_2 , 80% DCM/ cyclohex). (**Mass: 2.414g , Yield: 99%**)

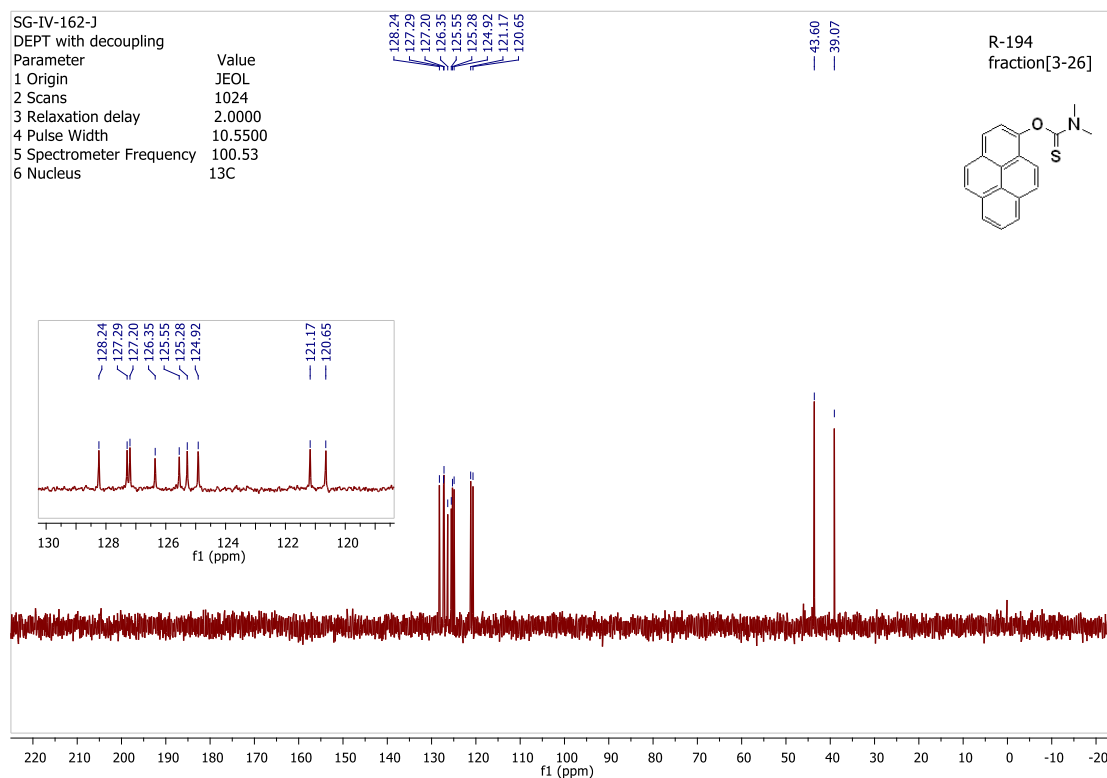
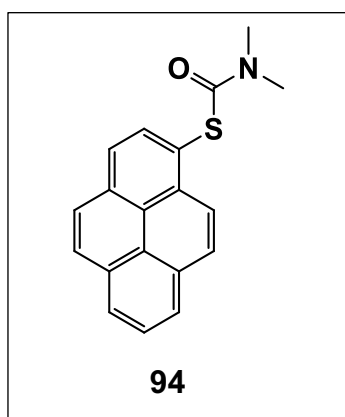
1.4eq.) was added to the reaction mixture . The reaction mixture was stirred for 4days and 15hours at 112-115°C. The reaction mixture was quenched with 1M HCl (20mL) and the reaction mixture was further extracted with toluene (5 x 20mL) and water (30mL). The organic phase was dried over anhydrous sodium sulfate, filtered and the solvent was evaporated off. Mainly three spots were observed by UV-vis in 80% DCM/ Cyclohex). The reaction mixture was purified by column chromatography (SiO_2 , 80% DCM/ cyclohex). (**Mass: 2.414g , Yield: 99%**)

RESULTS: SG-IV-162-G: ¹H NMR (399.78 MHz, TMS): δ =8.18 (t, 3H, J=7.88 Hz), 8.10-7.99 (m, 5H), 7.77 (d, 1H, J=8.3 Hz), 3.60 (d, 6H); **SG-IV-162-K:** ¹³C NMR (101 MHz,) δ 188.39, 147.69, 131.30, 131.16, 129.53, 128.28, 127.34, 127.24, 126.40, 125.69, 125.60, 125.33, 124.96, 124.85, 124.02, 121.22, 120.70, 43.64, 39.12; **SG-IV-162-J:** ¹³⁵-Dept NMR (101 MHz,) δ 128.24, 127.29, 127.20, 126.35, 125.55, 125.28, 124.92, 121.17, 120.65, 43.60, 39.07, **M.p.:** 137-139°C (from literature); **TLC** (DCM/ Cyclohex: 90/20 v/v), **R_f** = 0.6

Reaction Number	Starting material (mg, mmol, eq.)	Reagent (mg, mmol, eq.)	DABCO (mg, mmol, eq.)	Solvent (DMF) (mL)	Time	Temp °C	%Yield
R-194	OH-Py (30.7, 0.139, 1)	(27.34, 0.221, 1.6)	(49.02, 0.437, 3.1)	0.8	24hrs 21hrs	100 115°	39%
R-195	OH-Py (100.9, 0.458, 1)	(78.9, 0.638, 1.4)	(152.8, 1.362, 3)	1.5	48hrs .	115	58%
R-198	OH-Py (297.4, 1.350, 1)	(234.8, 1.899, 1.4)	(459.9, 4.100, 3)	3.0	93hrs .	115	99%
R-211	OH-Py (2.500g, 11.350mmol, 1)	(1.968g, 15.922mmol, 1.4)	(3.817g, 34.029mmol, 3)	25.0	4days & 15hrs .	112- 115	99%

Table-16: Reactions performed to synthesize compound-93



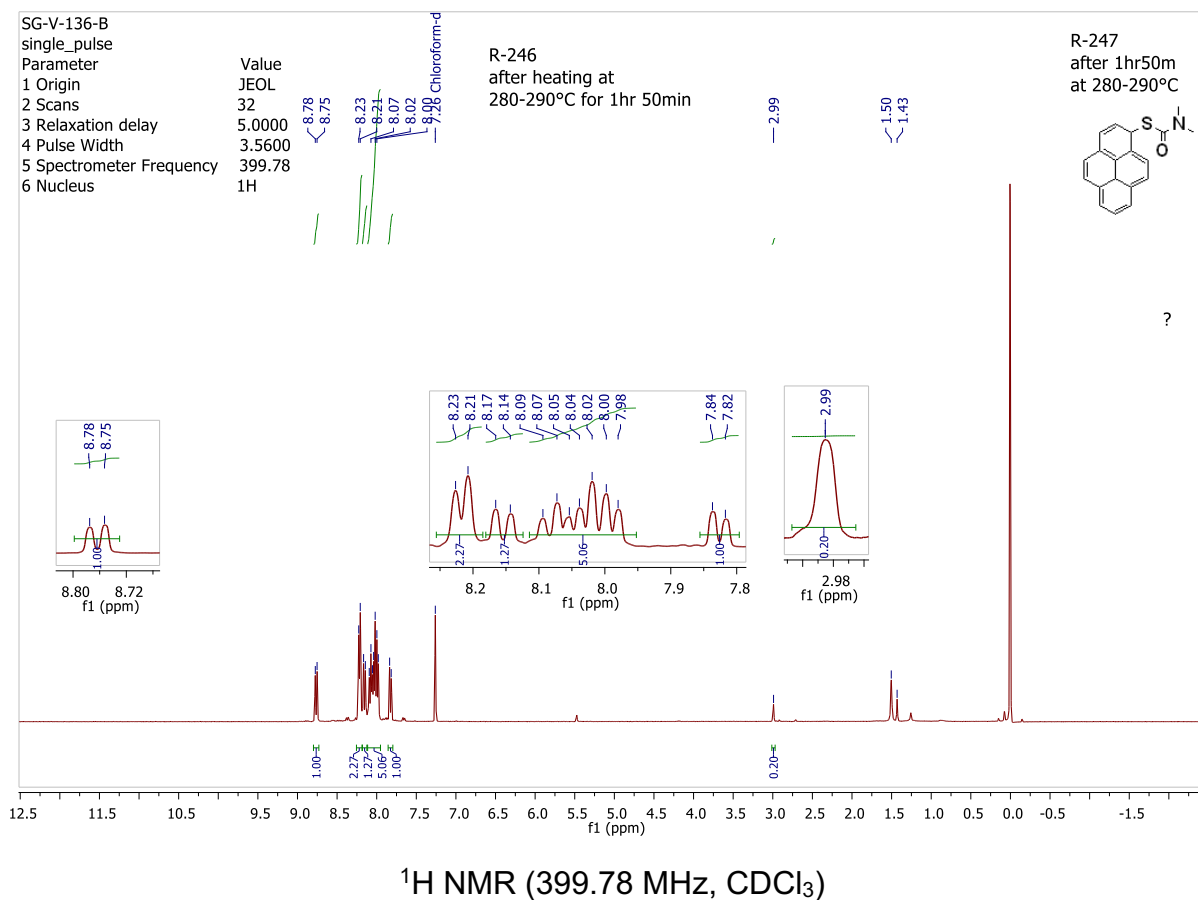
¹³C NMR DEPT 135 (100.53 MHz, CDCl₃)

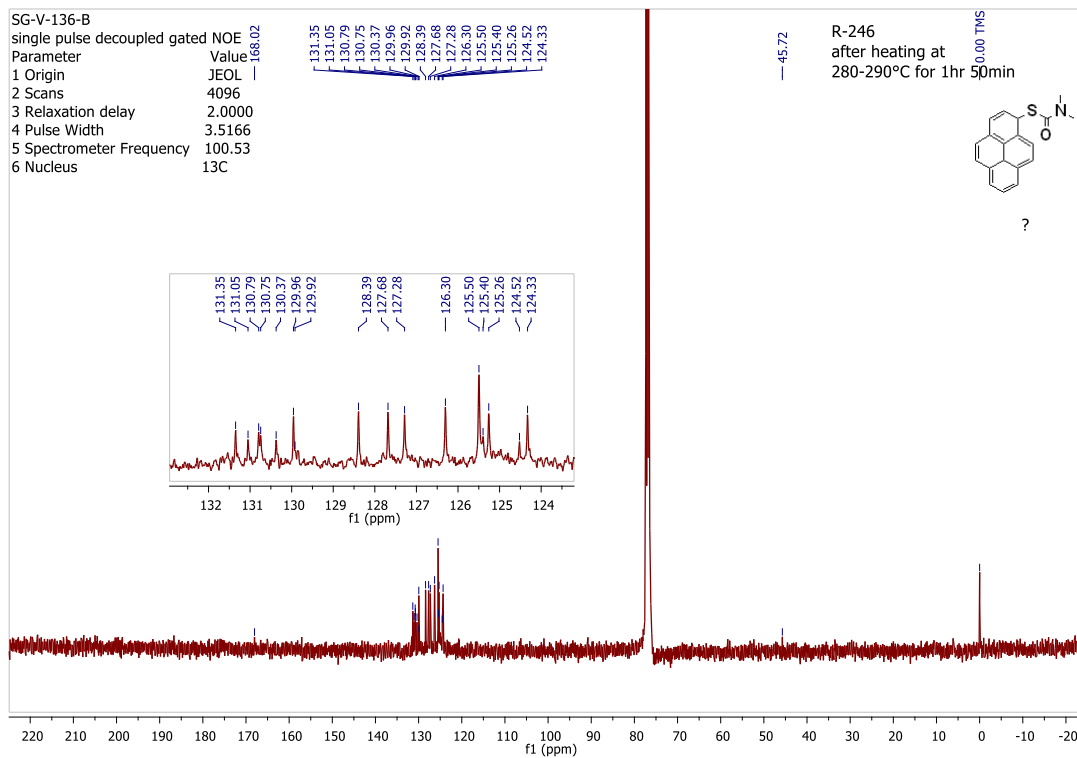
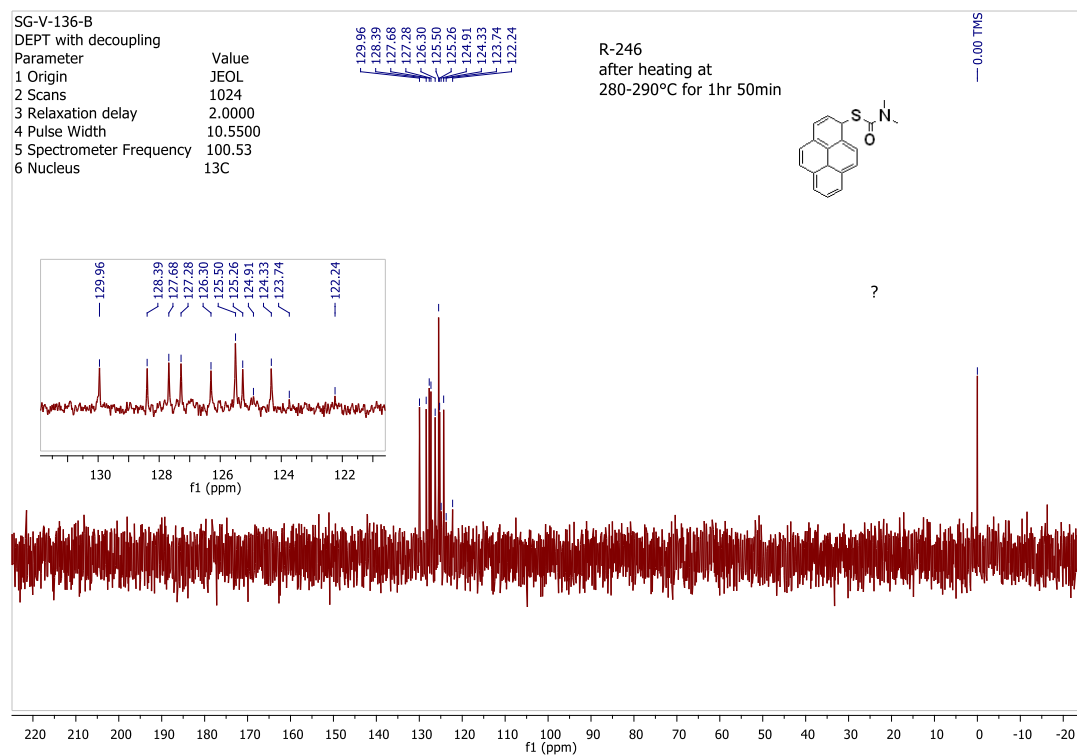
Procedure for compound-94 (1-Pyrenyl-S-thiocarbamate) (R-247): In an oven-dried sealed tube, 1-Pyrenyl-O-thiocarbamate (**93**) (32.79mg, 0.138mmol, 1eq.). The reaction mixture was heated for 1hour and 50mins. at 280-290°C. The reaction mixture was transferred to the round bottom flask with dichloromethane. The reaction mixture was purified by column chromatography (SiO₂, 50% DCM/ cyclohex). (**Mass: 26.8mg , Yield: 82%**)

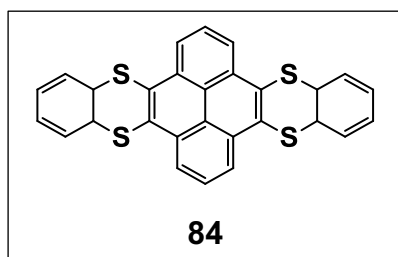
RESULTS: SG-V-136-B: ¹H NMR (399.78 MHz, TMS): δ = 8.78 (d, 1H, J=8.9 Hz), 8.23 (d, 2H, J= 7.5 Hz), 8.17 (d, 1H, J=8.8 Hz), 8.09- 7.98 (m, 5H), 7.84 (d, 1H, J= 7.8 Hz); **SG-V-136-B:** ¹³C NMR (101 MHz,) δ 168.02, 131.35, 131.05, 130.79, 130.75, 130.37, 129.96, 129.92, 128.39, 127.68, 127.28, 126.30, 125.50, 125.40, 125.26, 124.52, 124.33, 45.72; **SG-V-136-B:** ¹³⁵-Dept NMR (101 MHz,) δ 129.96, 128.39, 127.68, 127.28, 126.30, 125.50, 125.26, 124.91, 124.33, 123.74, 122.24, **M.p.:** 127-129°C (from literature); **TLC** (DCM/ Cyclohex: 50/50 v/v), **R_f** = 0.46

Reaction Number	Starting material (mg, mmol.)	Time	Temperature	%Yield
R-200	(11.12, 0.047)	1hr.50mins.	280-290°C	--
R-204	(14.4, 0.0609)	1hr.50mins.	280-290°C	--
R-247	(32.79, 0.138)	1hr.50mins.	280-290°C	82%
R-268	(500.9, 2.119)	1hr.55mins.	280-290°C	78%

Table-17: Reactions performed to synthesize compound-94



 ^{13}C NMR (100.53 MHz, CDCl_3) ^{13}C NMR DEPT 135 (100.53 MHz, CDCl_3)



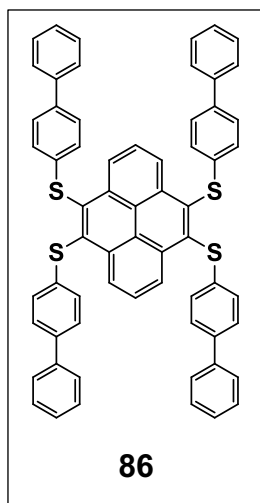
Procedure for compound-84 (R-253): In an oven-dried sealed tube, (4,5,9,10-tetrabromopyrene) (**4**) (30.7mg, 0.0592mmol, 1eq.), 1,2-benzenedithiol (18.4mg, 0.129mmol, 2.2eq.) and copper oxide (18.5mg, 0.129mmol, 2.2eq.) were added and argon was purged

for 15minutes in the tube. To this, distilled pyridine/ quinoline (1:4 ratio) (0.3:1.2 mL—dried with molecular sieves 3Å) was added and purged argon for 5minutes. The reaction mixture was stirred for 18 hours at 160°C. The reaction mixture was monitored by thin layer chromatography (SiO₂, 80% Tol/ Cyclohex). This solid is extracted with toluene (3 x 30mL) and water (30mL). The organic phase was dried over anhydrous Na₂SO₄, filtered and the solvent was evaporated off. Mainly 2 spots were observed by UV-vis in 80% DCM/ Cyclohex). The reaction mixture was purified by column chromatography (SiO₂, 80% DCM/ cyclohex). Further analyses are in progress.

Reaction Number	Starting material (mg, mmol, eq.)	Reagent (mg, mmol, eq.)	Solvent (pyridine/ quinoline) (mL)	Time	Temperature	%Yield
R-252	Br-Py (30.4, 0.058, 1)	Dithiol (18.6, 0.131, 2.2) Cu ₂ O (18.6, 0.129, 2.2)	1.2/0.3	16hrs.	160°C	mixture
R-253	Br-Py (30.7, 0.059, 1)	Dithiol (18.4, 0.129, 2.2) Cu ₂ O (18.5, 0.129, 2.2)	0.3/1.2	18hrs.	160°C	mixture

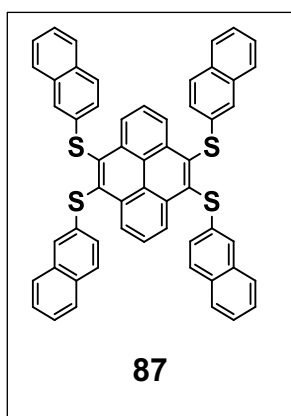
Table-18: Reactions performed to synthesize compound-84

Procedure for compound-86 (R-251): In an oven-dried sealed tube, 4,5,9,10-tetrabromopyrene (30.7mg, 0.0593mmol, 1.00 mol-eq.), 4-biphenyl thiol (47.7mg, 0.256mmol, 4.3eq.) and potassium carbonate (36.0mg, 0.260mmol, 4.4eq.) were added and the tube was purged with argon for 15 min.. Dry DMF (1.4mL—dried over molecular sieves 3Å) was injected and the tube was purged with Ar for 5 min.. The



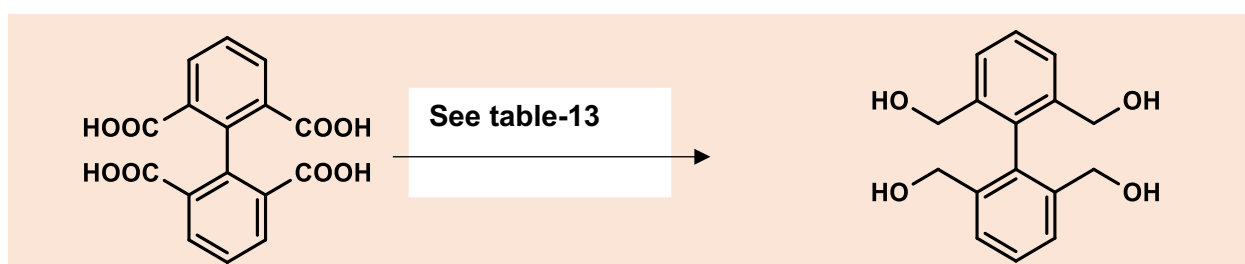
reaction mixture was sealed and stirred for 2 days at 140°C. The color changed to bright yellow after 2-3 minutes. After trituration with acetone (5-10 mL), a yellow product is obtained, insoluble in most solvents. (**Mass: 44.5 mg, Yield: 80%**), **M.p.:** 336-338°C. Further analyses are in progress.

Procedure for compound-87 (R-267): In an oven-dried sealed tube, 4,5,9,10-



tetrabromopyrene (59.0 mg, 0.114 mmol, 1 eq.), 2-naphthalene thiol (43.1 mg, 0.269 mmol, 2.4 eq.) and Potassium carbonate (38.1 mg, 0.276 mmol, 2.4 eq.) was added and argon was purged for 15 minutes in the tube. To this, dry DMF (1.0 mL—dried with molecular sieves 3 Å) was added and purged Ar for 5 minutes. The reaction mixture was stirred for 3 days at 65°C and it was observed the color changed to bright yellow after 2-3 minutes. Compound is insoluble in CDCl₃. Further analyses are in progress. **M.p.:** turned black at 327°C. Further analysis are in progress.

Attempts made but Failed



Reaction Number	Starting material (2, Tetraacid) (mg, mmol, eq.)	Reagent	Time	Temperature	%Yield
R-3	21.4, 0.065, 1	BF ₃ .OEt ₂ in THF ^[15] (111 μL); NaBH ₄ (62.8, 1.66, 25)	18 hrs.	56°C	18 hrs.

R-5	52.0, 0.157, 1	LiAlH ₄ in THF ^[16] (4.5mL, 1M)	18hrs.	0°C	18hrs.
R-6	25.5, 0.077, 1	BH ₃ -THF ^[17] (0.45mL, 1M)	18hrs.	RT	18hrs.
R-16	25.5, 0.077, 1	DiBAL-H in DCM ^[5] (1mL, 1M)	18hrs.	0°C	18hrs.

Table-19:

Reaction-8

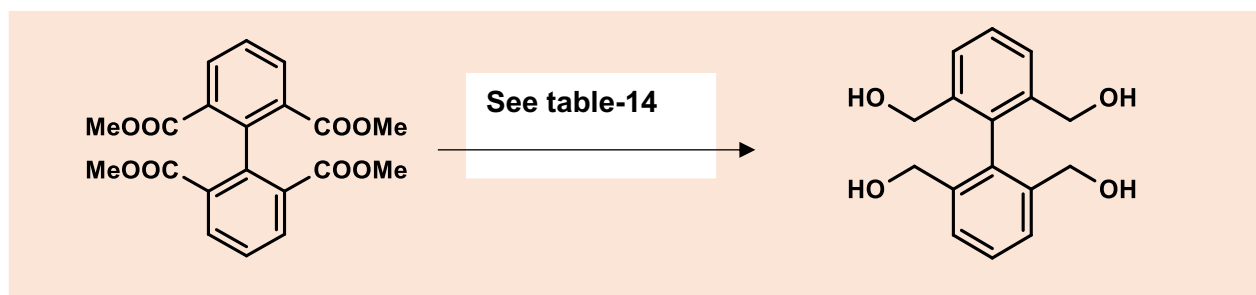


Table-20:

Reaction Number	Starting material 4, (Tetraester) (mg, mmol, eq.)	Reagent	Time	Temperature	%Yield
R-8	12.4, 0.032, 1	LiAlH ₄ in THF ^[15] (0.4mL, 1M)	18hrs.	0°C	--
R-12	30.6, 0.0792, 1	LiAlH ₄ in THF ^[15] (0.7mL, 1M)	18hrs.	0°C	--

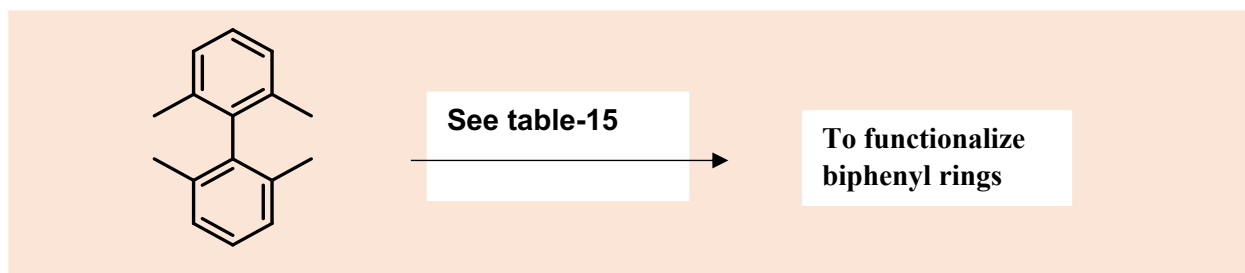
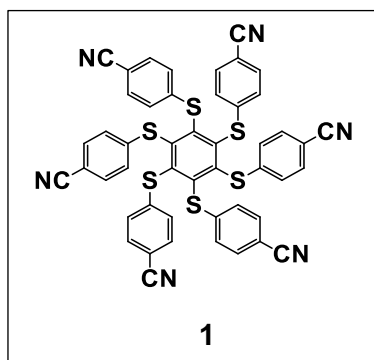


Table-21:

Reaction Number	Starting material (13)(mg, mmol, eq.)	Reagent	Solvent	Time	Temperature	%Yield
R-60	5.0, 0.024, 1	Br ₂ (5.43μL, 16.8, 0.105, 4.5)	CDCl ₃ (30μL)	16-18hrs.	25-28°C	--
R-61	4.0, 0.019, 1	Br ₂ (8.0μL, 24.9, 0.156, 8)	CDCl ₃ (30μL)	1hr.	25-28°C	--



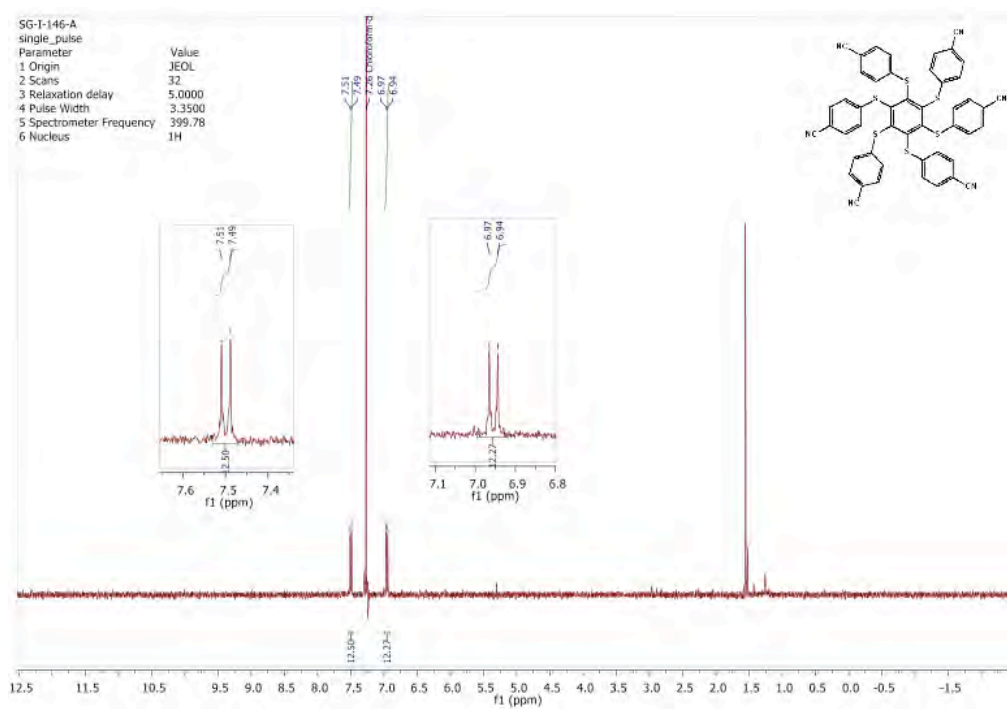
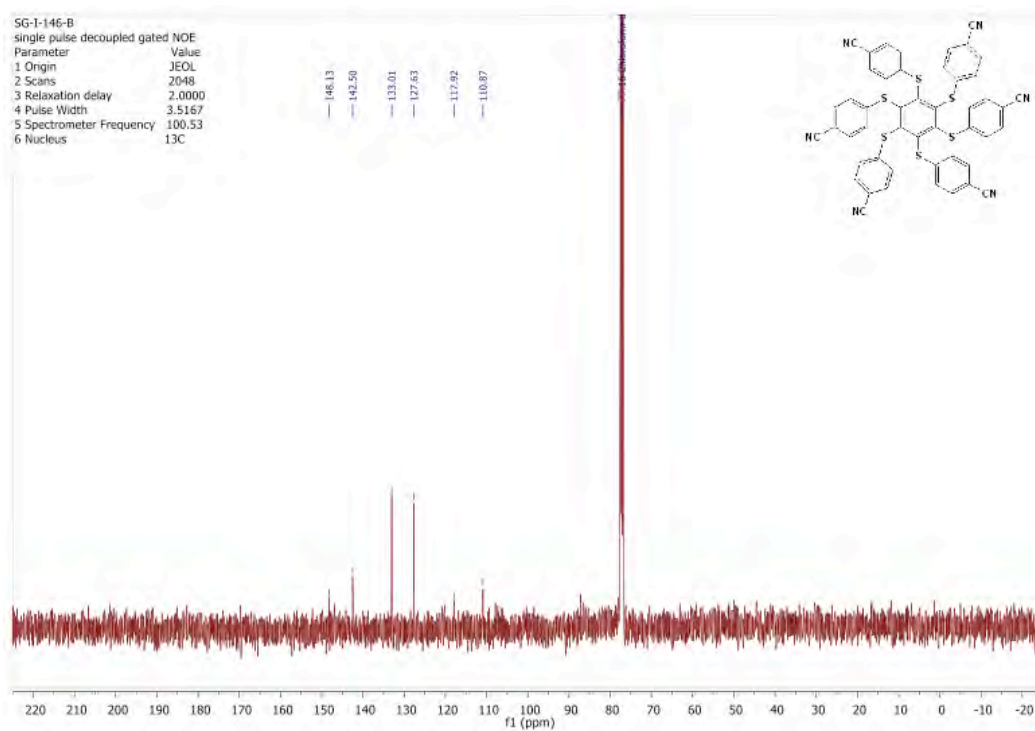
Procedure for asterisk-1 (R-27): Hexachlorobenzene (100.9 mg, 0.354 mmol, 1.00 eq.), 4-mercaptobenzonitrile (284.7 mg, 2.106 mmol, 6.00 eq.) and dry potassium carbonate (292.0 mg, 2.112 mmol, 6.02 eq.) were introduced into an oven-dried sealed tube. Under an argon atmosphere, dry DMF (0.5 mL, kept over 3Å molecular sieves) was injected via a syringe and the tube was purged

with argon for 15-20 minutes before being sealed. The heterogeneous mixture was stirred at 40°C in an oil bath for 16h. It turned from colorless to a bright yellow color in a few minutes. After cooling to 25°C and adding a solution of ethanol/water (50:50 v/v; 10 mL) a bright yellow solid precipitated. After filtration and drying under vacuum, the corresponding product (**1**) was obtained as a bright yellow solid (284 mg.; 0.324 mmol; 92% yield).

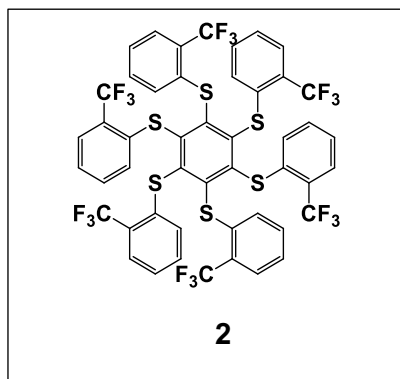
M.p.: 282-286°C; **TLC** (SiO₂, *n*-hex/EtOAc: 70/30 v/v) R_f = 0.29; **¹H NMR** (399.78 MHz, CDCl₃, ppm): δ = 7.50 (d_{app}, *J* = 8.4 Hz, 12H), 6.95 (d_{app}, *J* = 8.5 Hz, 12H); **¹³C NMR** (100.53 MHz, CDCl₃ ppm): δ = 148.1, 142.5, 133.0, 127.6, 117.9, 110.9; **¹H NMR** (200.13 MHz, DMSO-d₆, ppm): δ = 7.30 (d_{app}, ³*J* = 8.2 Hz, 12H), 7.76 (d_{app}, ³*J* = 8.2 Hz, 12H); **¹³C NMR** (50.32 MHz, DMSO-d₆ ppm): δ = 147.9, 144.3, 133.8, 128.1, 119.4, 109.4; **HRMS (ESI+)** calculated for [C₄₈H₂₄N₆S₆ +H⁺]: 877.0459 Da, found [M+H⁺] 877.0447 *m/z*; [C₄₈H₂₄N₆S₆ +Na⁺]: 899.0279 Da, found [M+Na⁺] 899.0272 *m/z*.

Table 25:

Reaction Number	Hexachloro benzene (mg, mmol, eq.)	Thiol (mg/ g, mmol, eq.)	K ₂ CO ₃ (mg/ g, mmol, eq.)	Solvent (dry DMF) (mL)	Time	Temperature (°C)	Yield
R-27	(100.9, 0.354, 1.0)	(284.7mg, 2.106, 6.00)	(292.0, 2.112, 6.02)	0.5	16hrs.	40°C	92%
R-201	(394.7, 1.386, 1.0)	(1.501g, 11.100, 8.0)	(1.535g, 11.111, 8.0)	10.0	48hrs.	40°C	98%

 ^1H NMR (399.78 MHz, CDCl_3) ^{13}C NMR (100.53 MHz, CDCl_3)

Procedure for asterisk-2 (R-122): In an oven-dried sealed tube, purged with argon, was added Hexachlorobenzene (0.355g, 1.247mmol, 1.00 eq.) , 2-(trifluoromethyl)benzene thiol (1.5mL, 2.025g, 11.365mmol, 9.0eq.), and dry potassium carbonate (1.557g, 11.268 mmol, 9.0 eq.) were introduced into an oven-dried sealed tube. Under an argon atmosphere, dry DMF (16.0 mL, kept over 3Å molecular sieves) was injected via a syringe and the tube

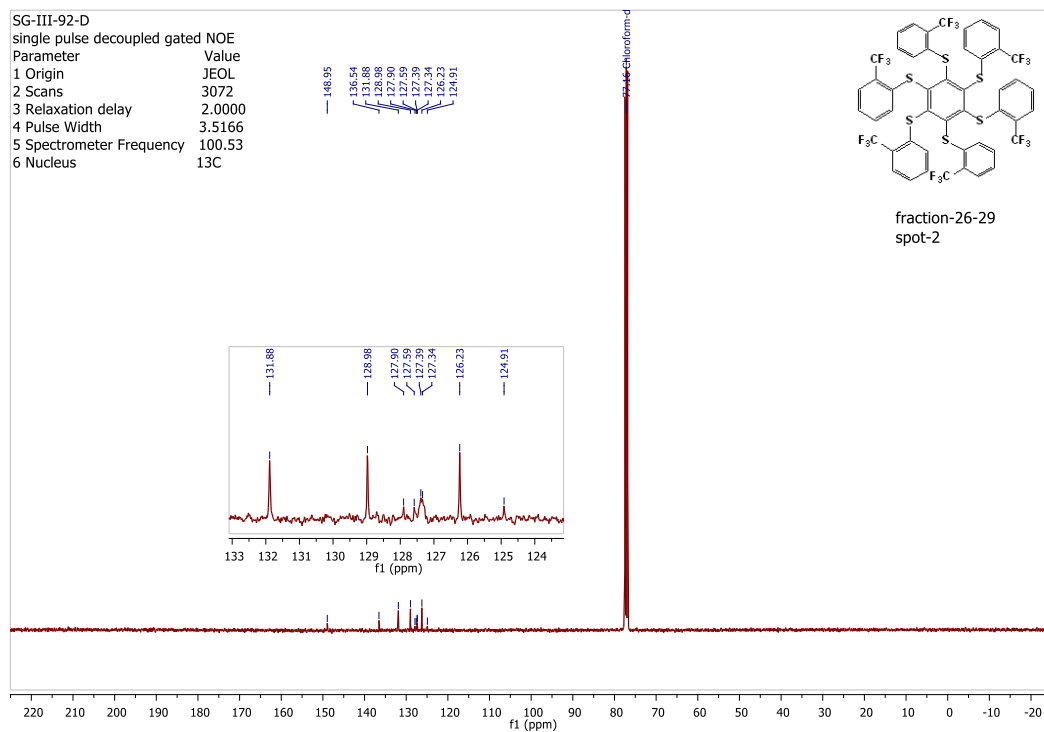
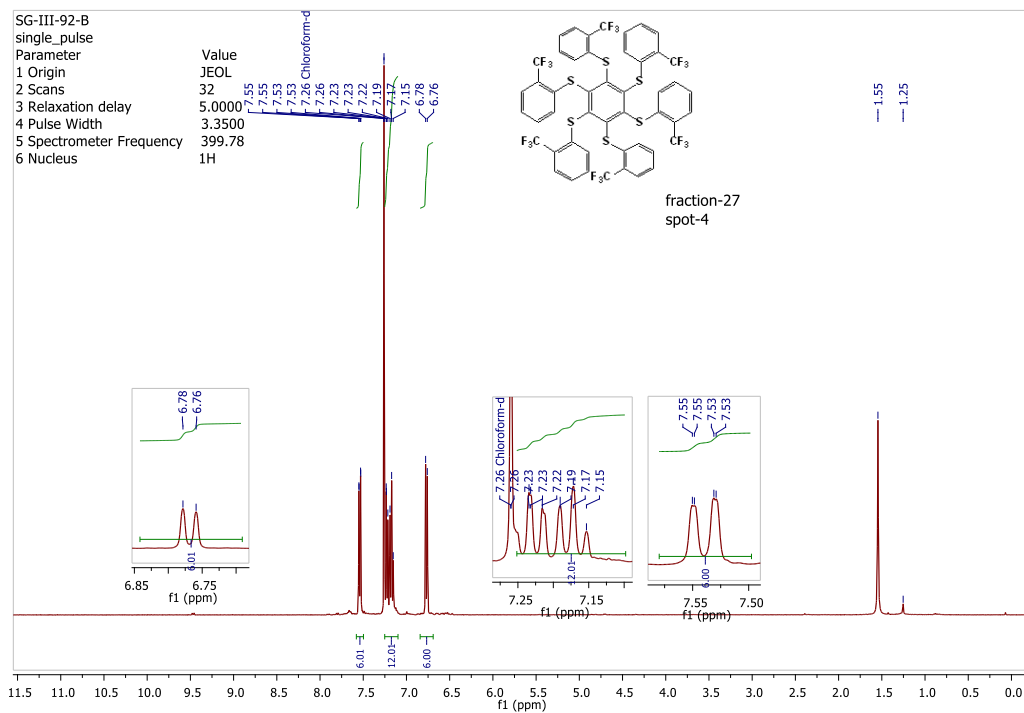


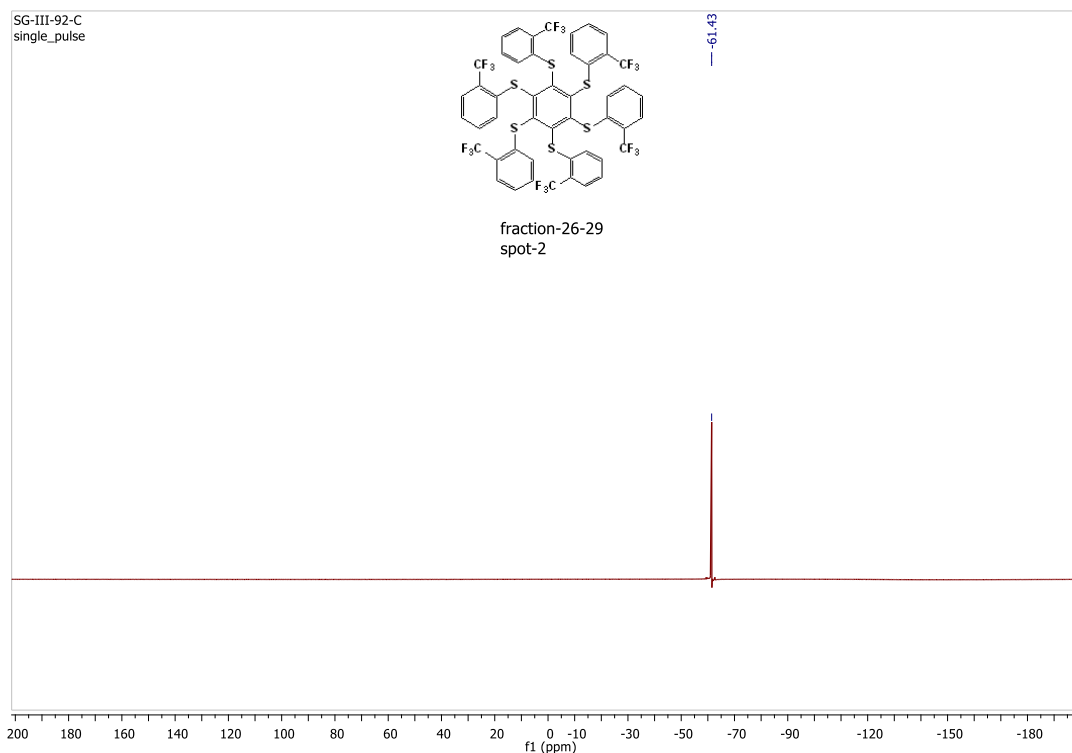
was purged with argon for 15-20 minutes before being sealed. The heterogeneous mixture was stirred at 60°C in an oil bath for 5days. It turned from colorless to a bright yellow color in a few minutes. Column chromatography (acetone/cyclohex, 30/70, v/v) was done to separated the ast-2 and was dried under vacuum, the corresponding product (**2**) was obtained as a bright yellow solid (97% yield).

M.p.: 207.2-210.2°C; **TLC** (SiO₂, acetone/cyclohex 30:70 v/v) R_f = 0.61; **¹H NMR** (399.78 MHz, CDCl₃, ppm), **SG-III-92-B:** δ = 7.55 (dddd, 6H, J= 7.66 Hz), 7.17 (t, 6H, J= 10.1 Hz), 7.23 (t, 6H, J= 10.1 Hz), 6.78 (d, 6H, J= 7.75 Hz); **¹³C NMR** (100.53 MHz, CDCl₃ ppm), **SG-III-92-D:** δ = 158.5, 147.8, 131.0, 128.7, 114.5, 55.4; **¹⁹F NMR** (CDCl₃ ppm), **SG-III-92-C:** -61.43.

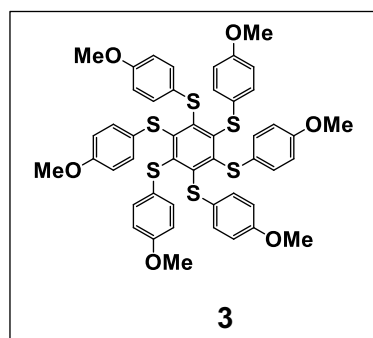
Table 26:

Reaction Number	Hexachloro benzene (mg, mmol, eq.)	Thiol (mL, mg/g, mmol, eq.)	K ₂ CO ₃ (mg/ g, mmol, eq.)	Solvent (dry DMF) (mL)	Time	Temperature (°C)	Yield
R-111	(17.8, 0.0625, 1.00)	(0.75mL, 100.0mg, 5.879, 90)	(78.3, 0.566, 9.0)	1.0	68hrs.	60°C	>80%
R-122	(355.3, 1.247, 1.0)	(1.5mL, 2.025g, 11.365, 9.0)	(1.557g, 11.268, 9.0)	16.0	5days	60°C	97%



 ^{19}F NMR (376,17 MHz, CDCl_3)

Procedure for asterisk-3 (R-28): In an oven-dried sealed tube, purged with argon, was

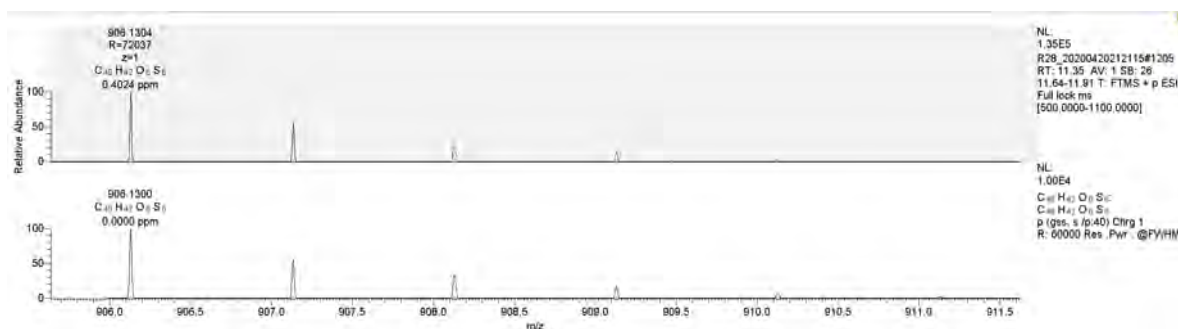


added hexachlorobenzene (600.1 mg, 2.107mmol, 1eq.), dried potassium t-butoxide (2.127mg, 18.954mmol, 9eq.), 4-cyanobenzenebenzene thiol (1.282mg, 9.481mmol, 9.5eq.), 4-methoxybenzenebenzene thiol (1.16mL, 9.477mmol, 9.5eq.) and dry DMF (4.0 mL, dried and kept over activated molecular sieves 3\AA). Argon was bubbled through the mixture for 5-10 minutes. The color changed

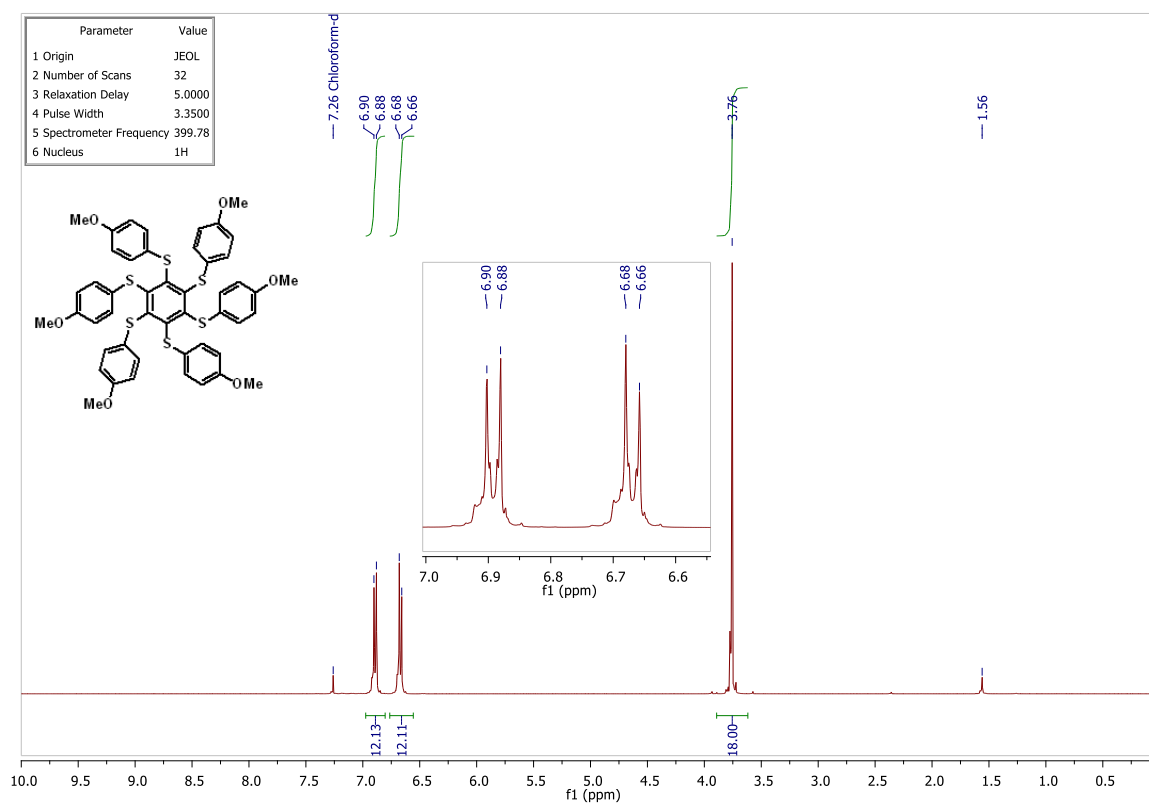
from off white to yellow. The tube was sealed and the reaction was stirred at room temperature (25°C) for 18 hours in an oil bath. Most DMF was removed on a rotary evaporator under reduced pressure. The crude was triturated in ethanol and water (1:1, v/v) while stirring for two hours, filtration, and drying afforded a yellow solid. **Yield= >90%**

M.p.: $161\text{-}162^\circ\text{C}$ (lit. $161\text{-}163^\circ\text{C}^5$; $158\text{-}159^\circ\text{C}^4$); **TLC** (SiO_2 , DCM/acetone 95:5 v/v) R_f = 0.84; **^1H NMR** (399.78 MHz, CDCl_3 , ppm): δ = 6.89 (d_{app} , J = 8.7 Hz, 12H), 6.67 (d_{app} ,

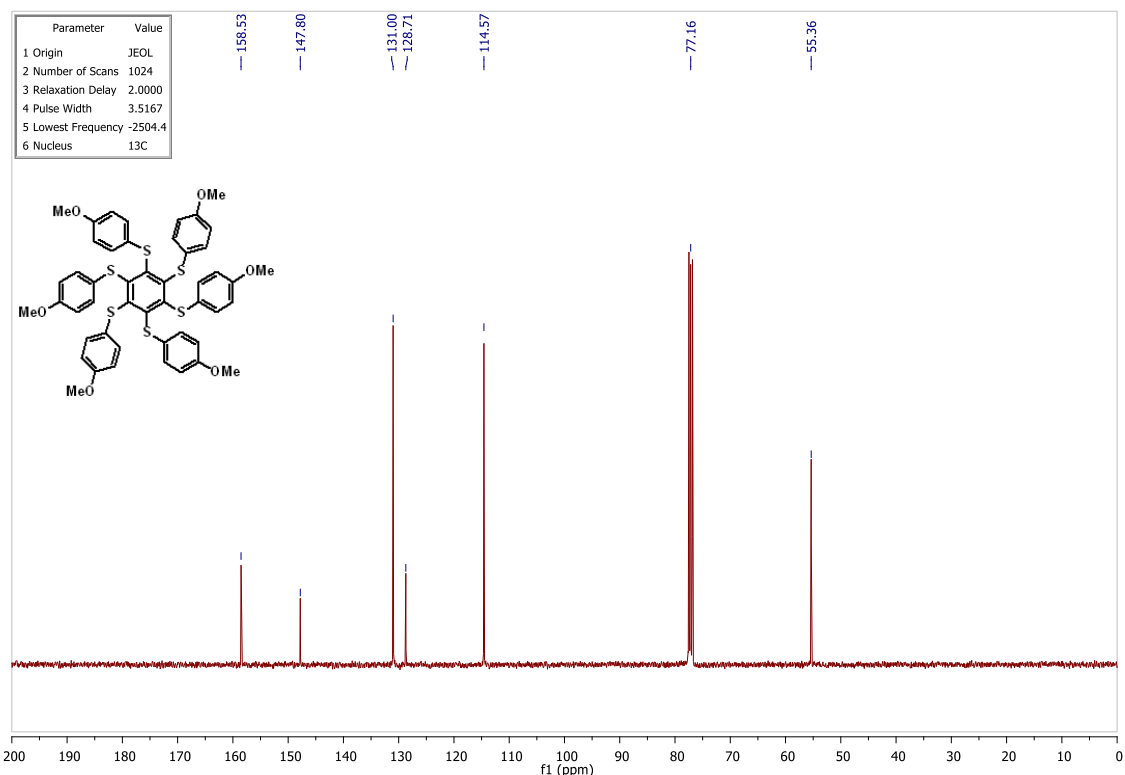
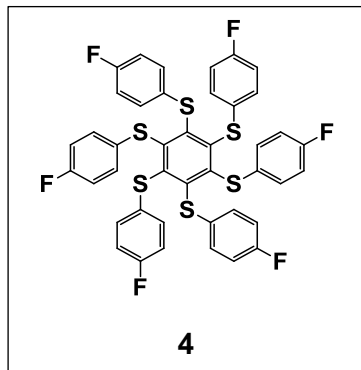
$J = 8.7$ Hz, 12H), 3.76 (s, 18H); ^{13}C NMR (100.53 MHz, CDCl_3 ppm): $\delta = 158.5, 147.8, 131.0, 128.7, 114.5, 55.4$; HRMS (ESI+) calculated for $[\text{C}_{48}\text{H}_{42}\text{O}_6\text{S}_6 + \text{H}^+]$: 907.1378 Da, found $[\text{M}+\text{H}^+]$ 907.1376 m/z .



HRMS (ESI, positive mode) for (3)



^1H -NMR spectrum of (3) (CDCl_3 , 399.78 MHz)

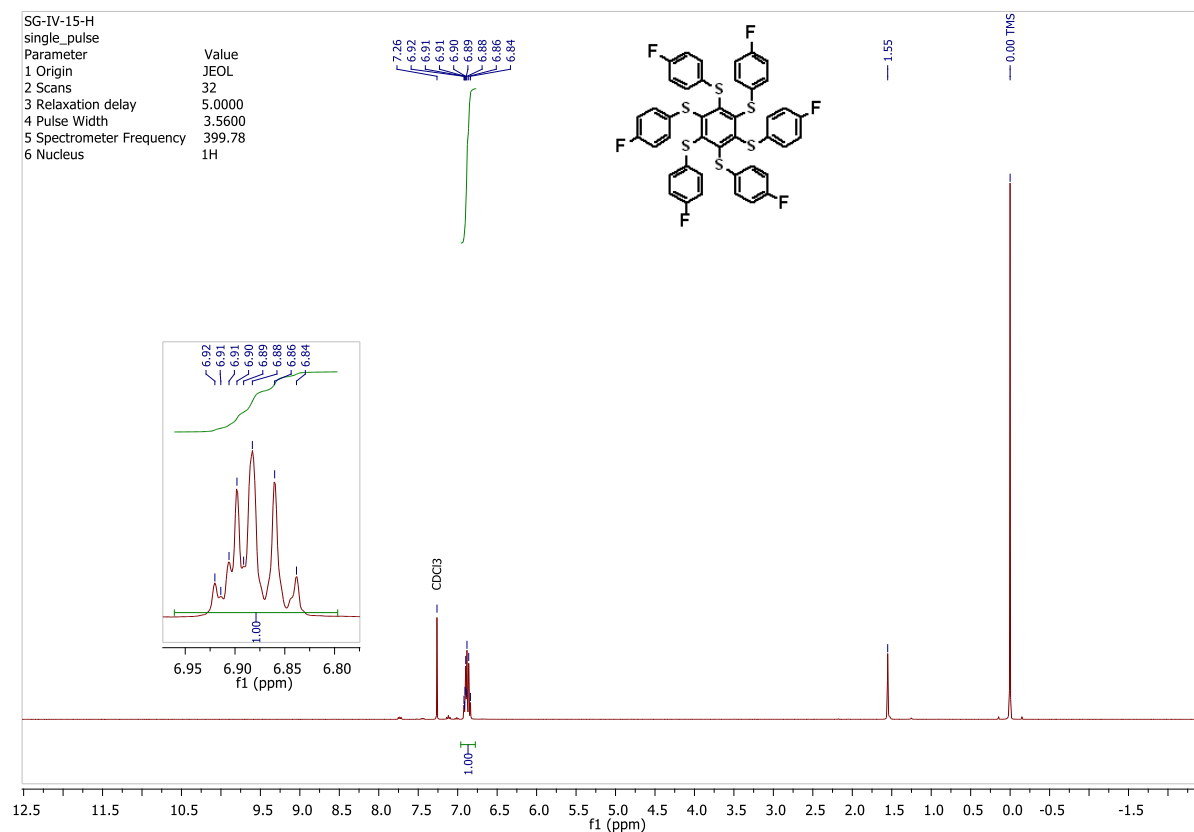
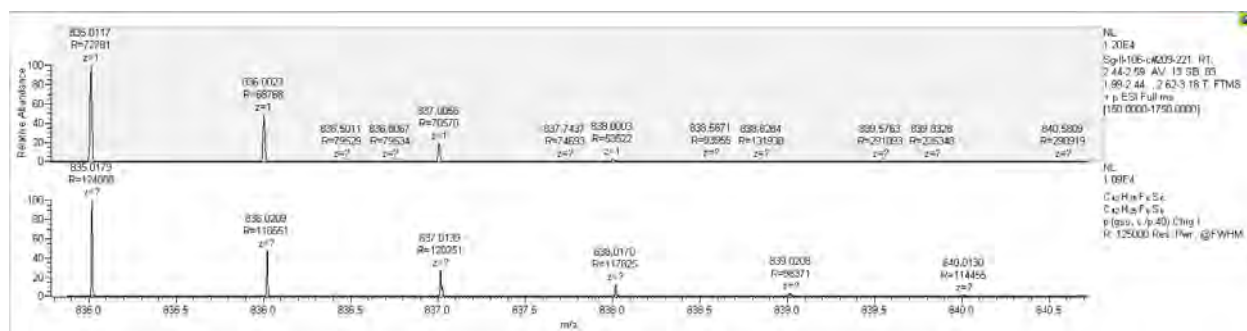
¹³C-NMR spectrum of (3) (CDCl₃, 399.78 MHz)

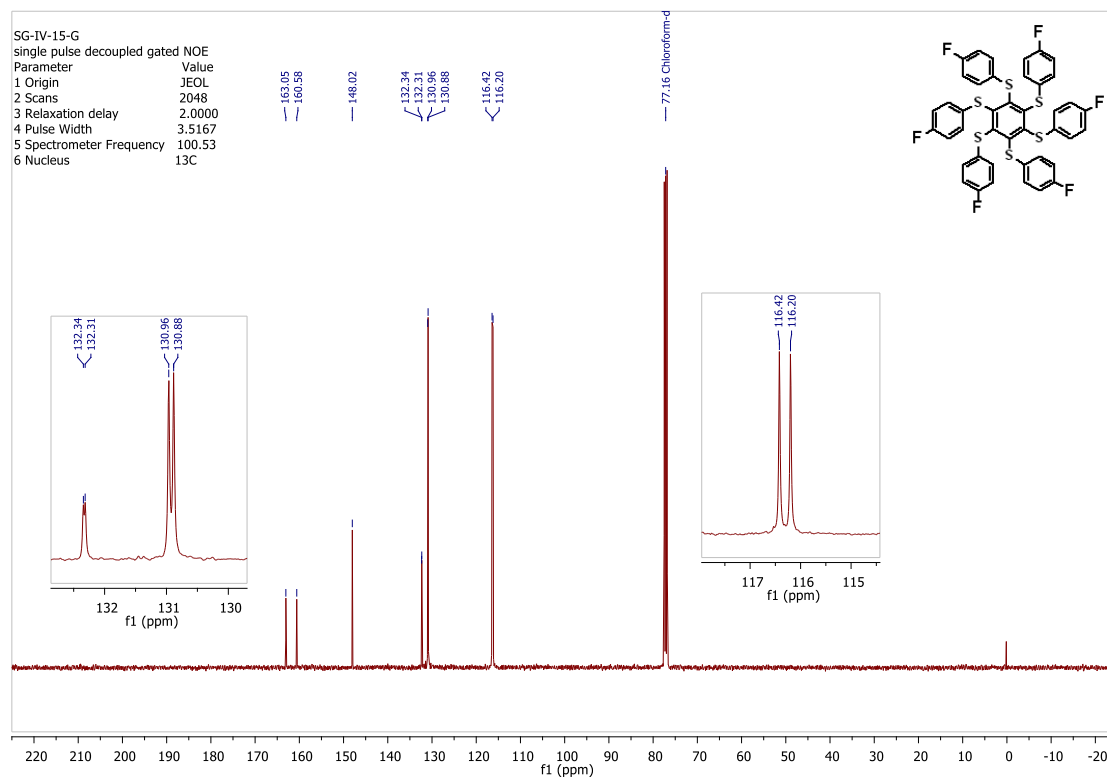
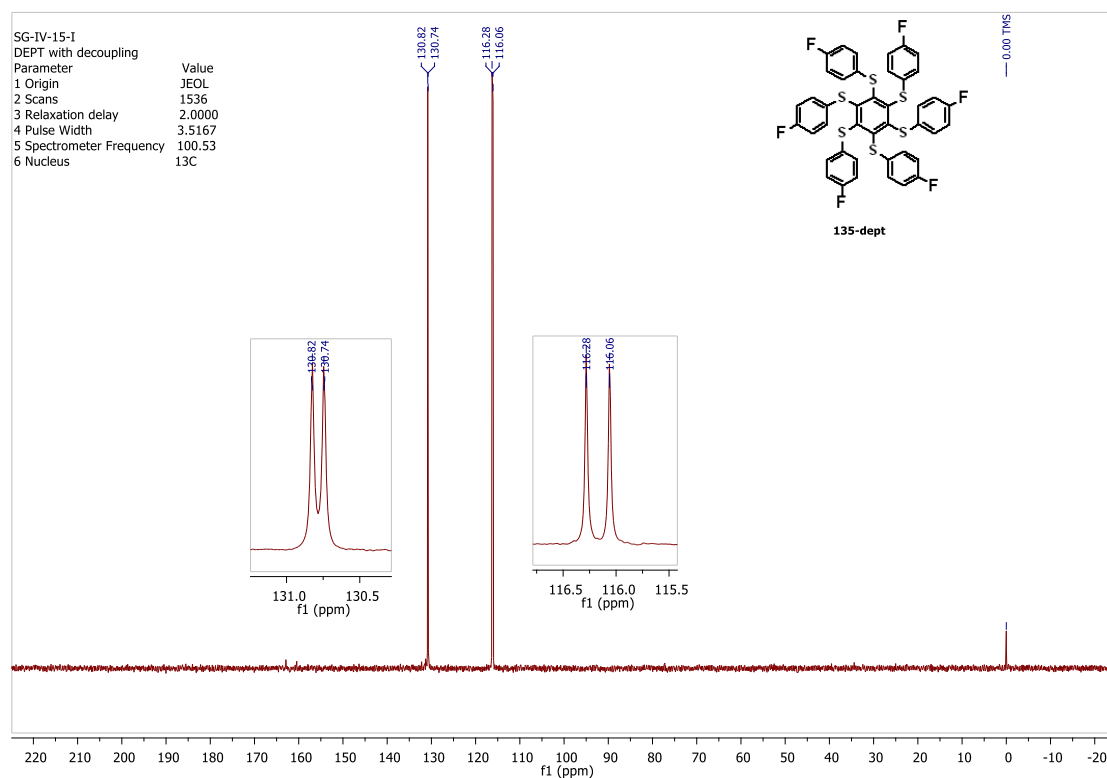
Procedure for asterisk-4 (R-146): In an oven-dried sealed tube, purged with argon, was added hexachlorobenzene (0.447 g, 1.57 mmol, 1.00 mol-eq.), dried potassium carbonate (1.945 g, 14.07 mmol, 8.96 mol-eq.), *p*-fluorothiophenol (1.804 g, 14.08 mmol, 1.50 mL, 8.97 mol-eq.) and dry DMF (6.0 mL, dried and kept over activated molecular sieves 3Å). Argon was bubbled

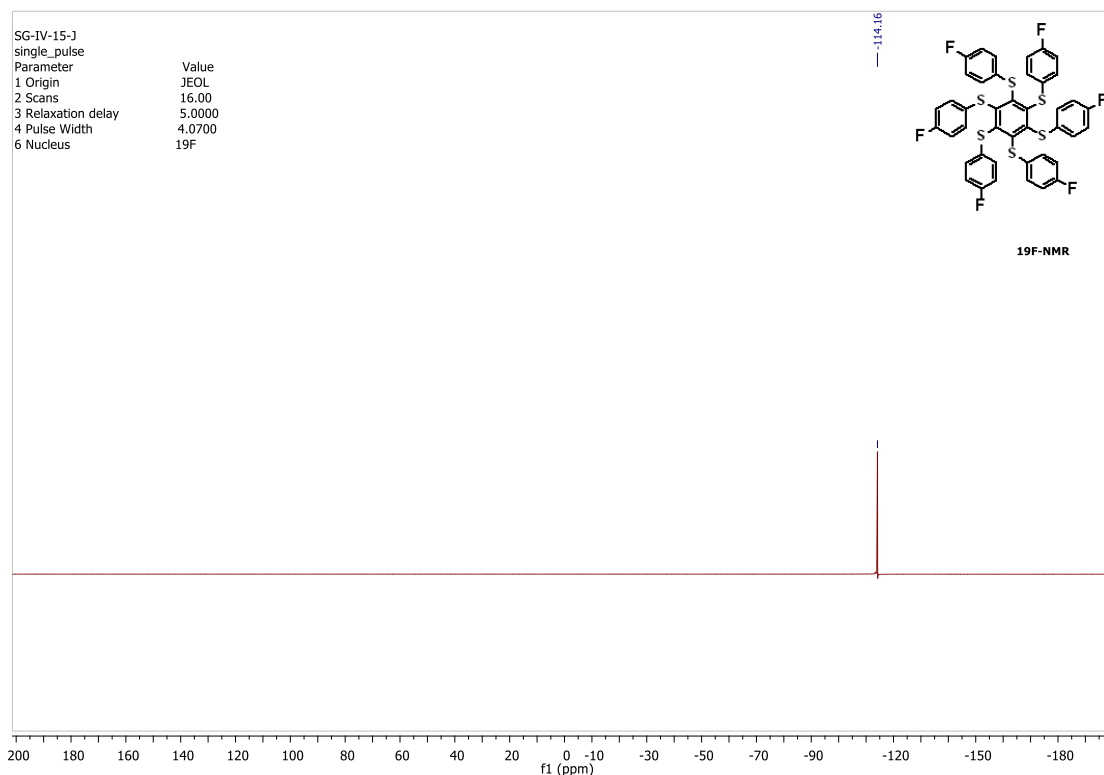
through the mixture for 5-10 minutes. The tube was sealed and the reaction was stirred at 27°C for 3 days. Most DMF was removed on a rotary evaporator under reduced pressure. To the reaction mixture was added EtOH (30 mL) and H₂O (30 mL) at 25°C while stirring vigorously. A solid was formed and stirring was continued for 3 hrs. After filtration, the solid was dried *in vacuo* to afford a pure yellow solid (1.230 g, 1.473 mmol, 94% yield).

M.p. 117-118°C; **TLC** (SiO₂, tol./*n*-hex. 50:50 v/v) R_f = 0.33; **¹H NMR** (399.78 MHz, CDCl₃, ppm): δ = 6.82-6.94 (m, 24H); **¹³C NMR** (100.53 MHz, CDCl₃, ppm): δ = 161.8

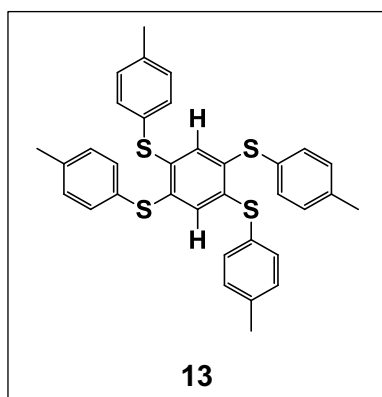
(d, $^1J_{C-F} = 248,0$ Hz), 148.0, 132.3, $^4J_{C-F}=3.3$ Hz), 130.9 (d, $^3J_{C-F}= 7.9$ Hz), 116.2 (d, $^2J_{C-F}= 22.2$ Hz); ^{19}F NMR (376.17 MHz, $CDCl_3$) : -114.16 (s); **MS** (EI, 70 eV) calculated for $[C_{42}H_{24}F_6S_6]$: 834 Da, found $[M^+]$ 834 m/z , $[M - (F-Ph-SH)]$ 707 m/z ; **HRMS (ESI+)** calculated for $[C_{42}H_{25}F_6 S_6 + H^+]$: 835.0179 Da, found $[M^+]$ 835.0117 m/z .



 ^{13}C -NMR $\{^1\text{H}\}$ spectrum of (4) (CDCl_3 , 100.53 MHz) ^{13}C -NMR DEPT 135 spectrum of (4) (CDCl_3 , 100.53 MHz)



¹⁹F-NMR spectrum of (4) (CDCl₃, 376,17 MHz)



Procedure for asterisk-13 (R-215): In an oven-dried sealed tube, purged with argon, was added 1,2,4,5-tetrabromobenzene (2.509 g, 6.374 mmol, 1.00 mol-eq.), dried potassium carbonate (4.389 g, 31.758 mmol, 5.0 mol-eq.), 4-methylbenzene thiol (3.944 g, 31.759 mmol, 5.0 mol-eq.) and dry DMF (20.0 mL, dried and kept over activated molecular sieves 3Å). Argon was bubbled through the mixture for 5-10 minutes. The tube was

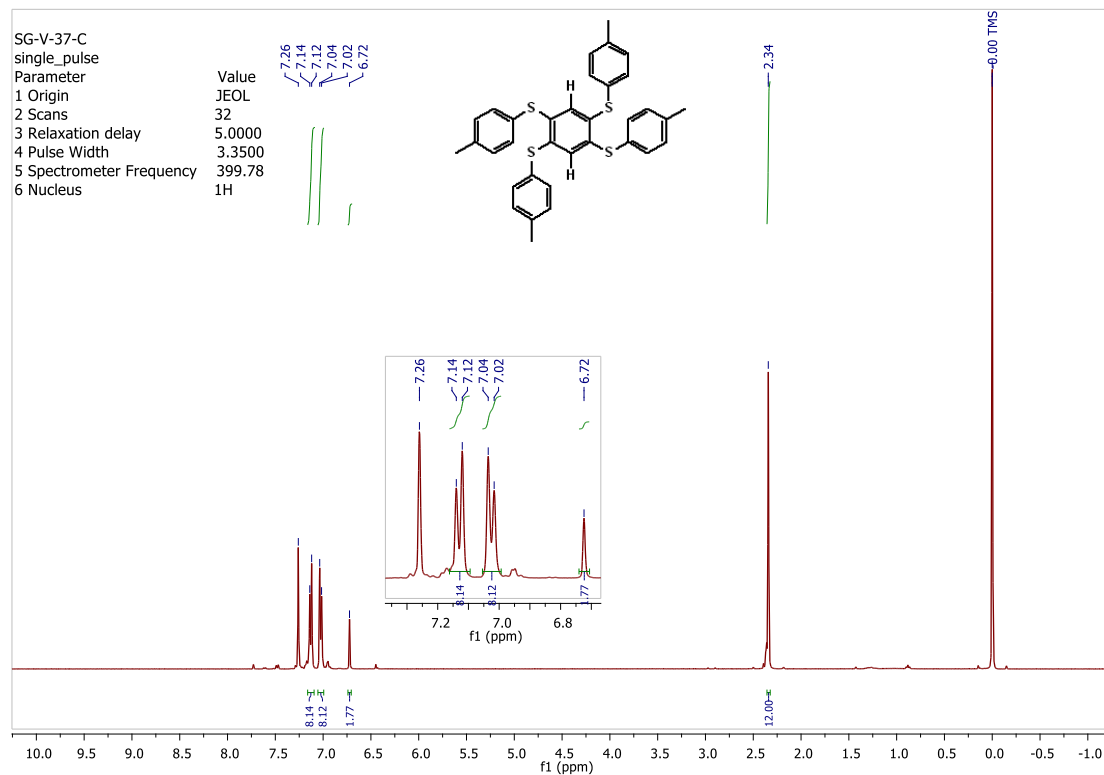
sealed and the reaction was stirred at 80°C for 3 days and 70°C for 18 hours. Most DMF was removed on a rotary evaporator under reduced pressure. To the reaction mixture was added EtOH (10 mL) and H₂O (15 mL) at 25°C while stirring vigorously. A solid was formed and stirring was continued for 3 hrs. After filtration, the solid was dried *in vacuo* to afford a white solid and was recrystallized from toluene. (3.83 g, 91.3% yield).

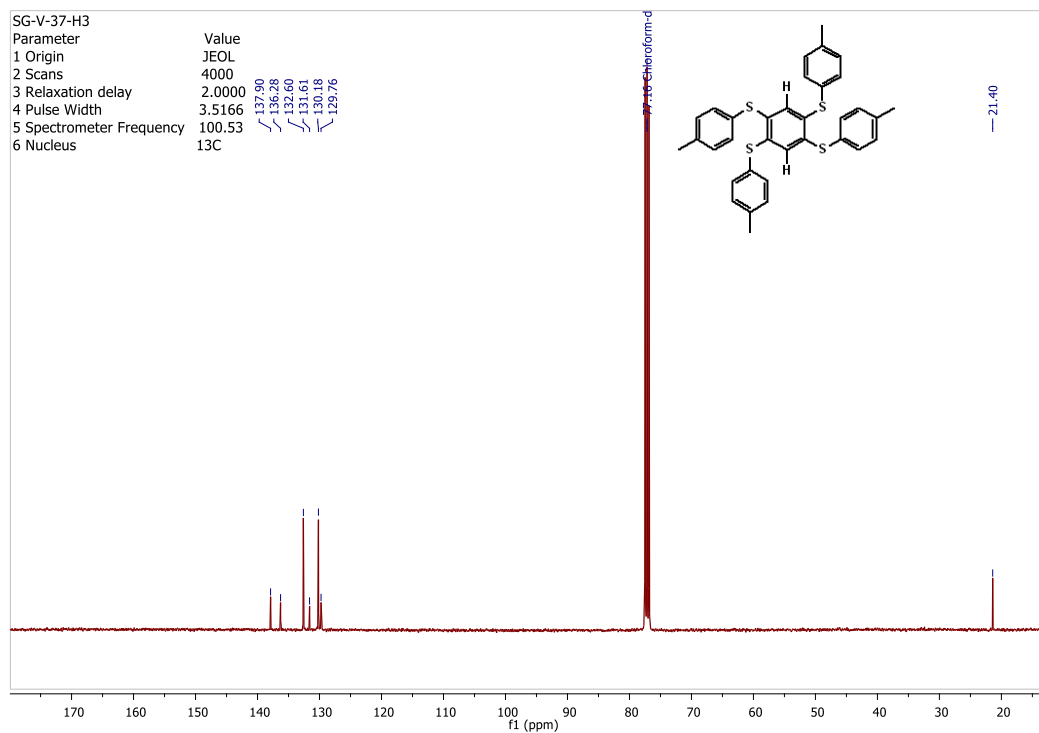
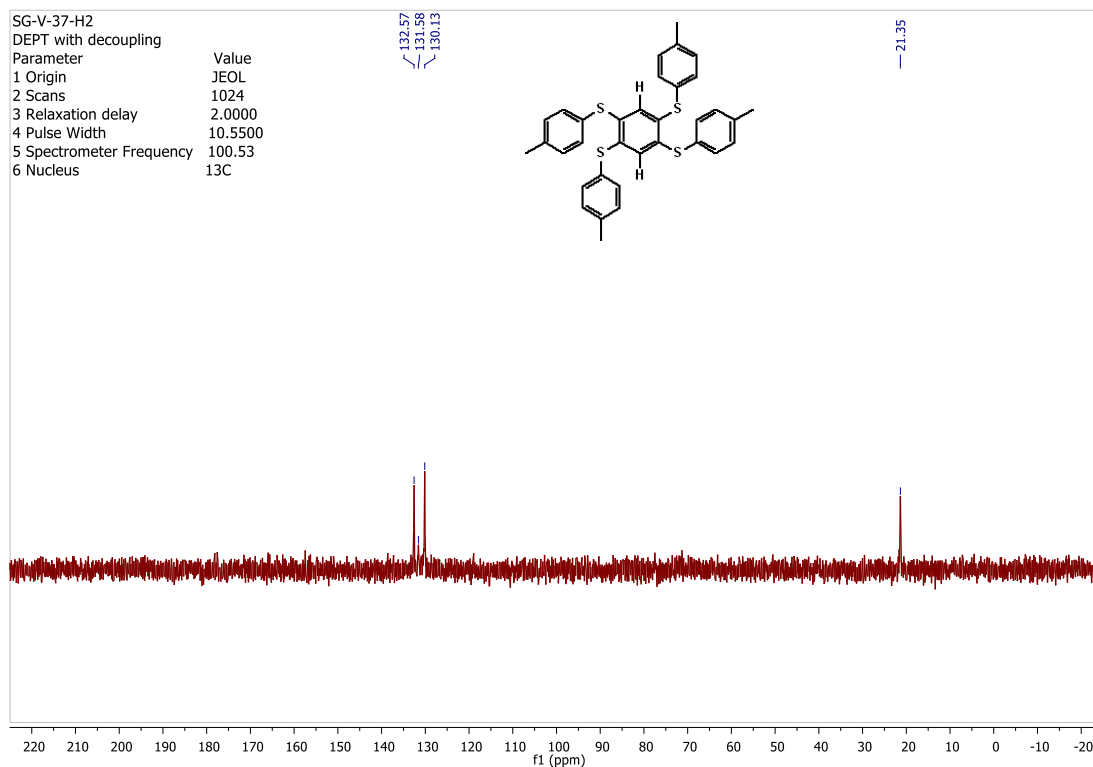
M.p. 232-236°C; **TLC** (SiO₂, acetone/cyclohex. 30:70 v/v) R_f = 0.62; **¹H NMR** (399.78 MHz, CDCl₃, ppm), **SG-V-37-C:** δ = 7.14 (d, 8H, J= 7.75 Hz), 7.04 (d, 8H, J=7.72 Hz),

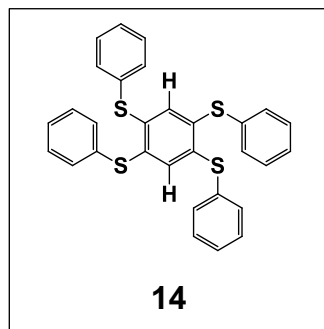
7.02 (s, 2H), 2.34 (s, 12H); **13C NMR** (100.53 MHz, CDCl₃ ppm), **SG-V-37-H3**: δ = 137.90, 136.28, 132.60, 131.61, 130.18, 129.76, 21.40; **135°-Dept NMR** (100.53 MHz, CDCl₃), **SG-V-37-H2**: 132.57, 131.58, 130.13, 21.35

Table 27:

Reaction Number	Hexachloro benzene (g, mmol, eq.)	Thiol (g, mmol, eq.)	K ₂ CO ₃ (mg/ g, mmol, eq.)	Solvent (dry DMF) (mL)	Time	Temperature (°C)	Yield
R-147	(0.500, 1.271, 1.00)	(0.788, 6.348, 5.0)	(0.876, 6.341, 5.0)	9.0	4days	80°C	15%
R-215	(2.509, 6.374, 1.00)	(3.944, 31.759, 5.0)	(4.389, 31.758, 5.0)	20.0	3days 18hrs.	80°C 70°C	91%

¹H NMR (399.78 MHz, CDCl₃)

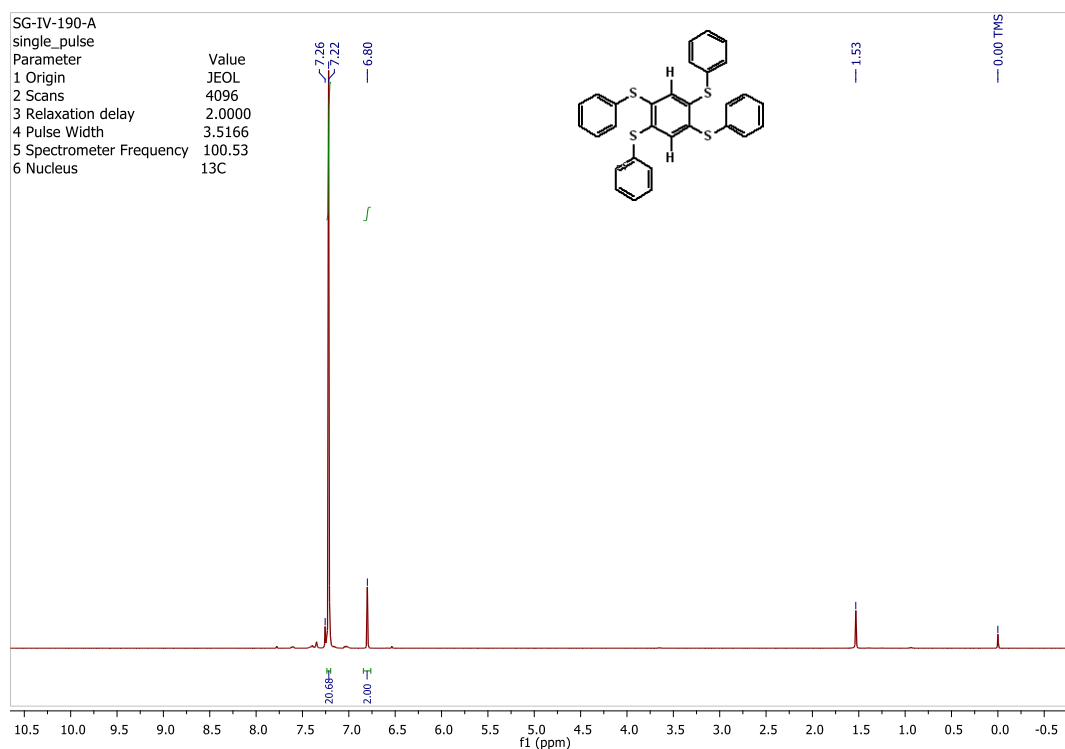
¹³C NMR (100.53 MHz, CDCl₃)¹³C-NMR DEPT 135 (CDCl₃, 100.53 MHz)



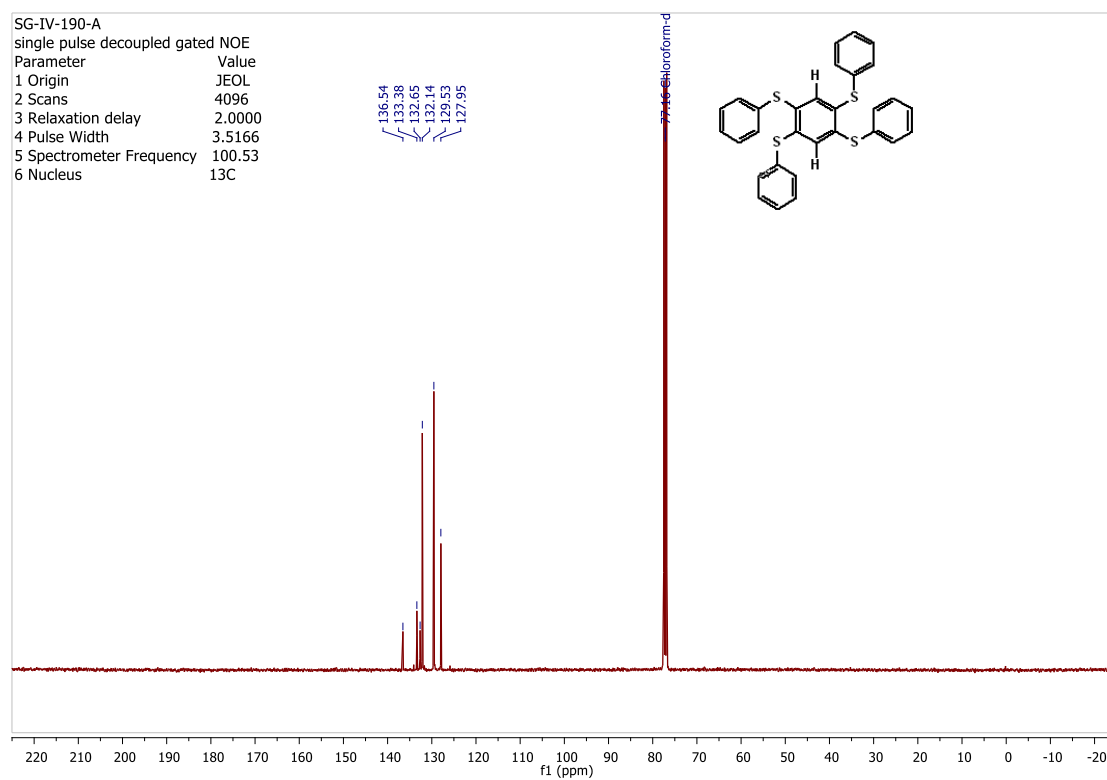
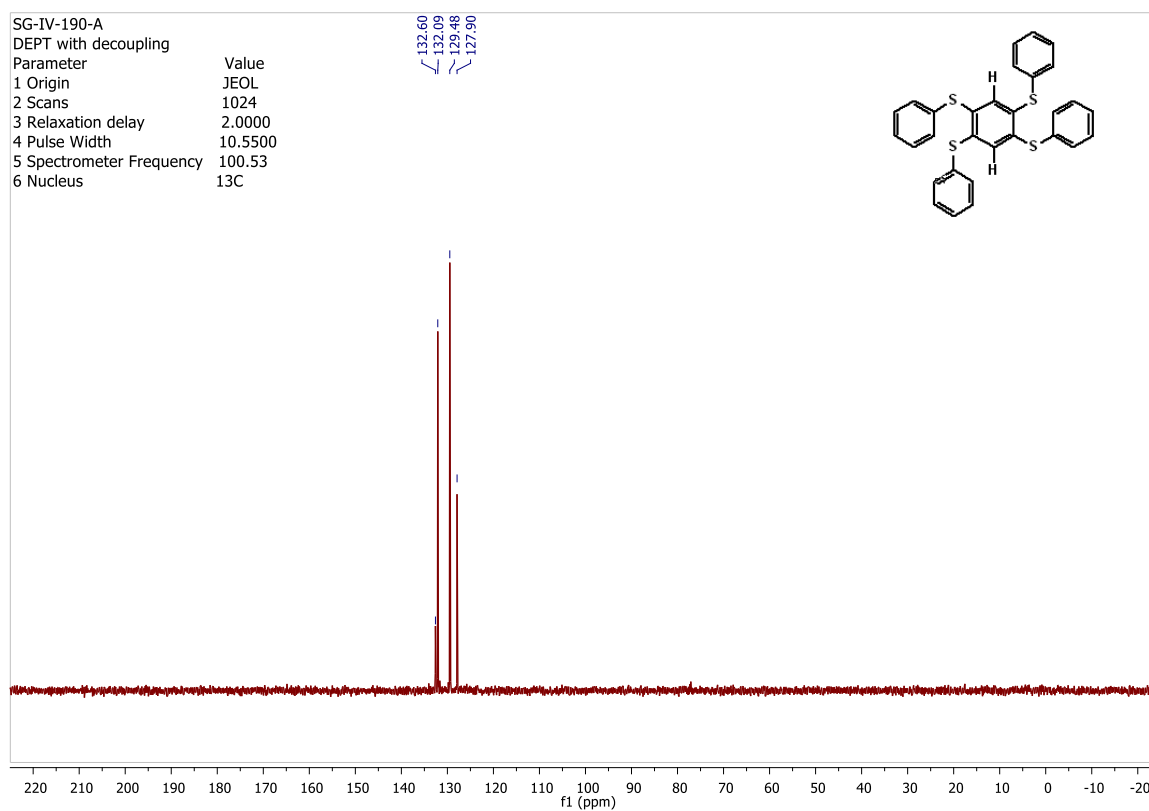
Procedure for asterisk-14 (R-203): In an oven-dried sealed tube, purged with argon, was added 1,2,4,5-tetrafluorobenzene (2.5mL, 3.36 g, 0.022 mol, 1.00 mol-eq.), dried potassium carbonate (15.467 g, 0.111 mol, 5.0 mol-eq.), thiophenol (11.5 mL, 12.42 g, 0.111 mol, 5.0 mol-eq.) and dry DMF (20.0 mL, dried and kept over activated molecular sieves 3Å). Argon was bubbled through the mixture for 5-10 minutes.

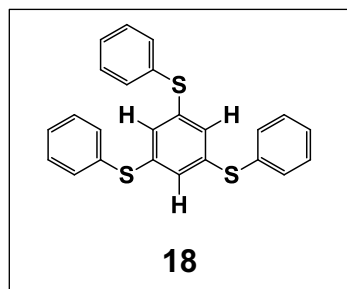
The tube was sealed and the reaction was stirred at 80°C for 3 days and 70°C for 18 hours. Most DMF was removed on a rotary evaporator under reduced pressure. To the reaction mixture was added EtOH (10 mL) and H₂O (15 mL) at 25°C while stirring vigorously. A solid was formed and stirring was continued for 3 hrs. After filtration, the solid was dried *in vacuo* to afford a white solid and was recrystallized from n-butanol. (10.00 g, 98% yield).

M.p. 147.6-149.6°C; **TLC** (SiO₂, acetone/cyclohex. 30:70 v/v) R_f = 0.46; **¹H NMR** (399.78 MHz, CDCl₃, ppm), **SG-IV-190-A**: δ = 7.22 (s, 20H), 6.80 (s, 2H); **¹³C NMR** (100.53 MHz, CDCl₃ ppm), **SG-IV-190-A**: δ =136.54, 133.38, 132.65, 132.14, 129.53, 127.95; **¹³⁵-DeptNMR** (100.53 MHz, CDCl₃), **SG-IV-190-A** : 132.60, 132.09, 129.48, 127.90



¹H NMR (399.78 MHz, CDCl₃)

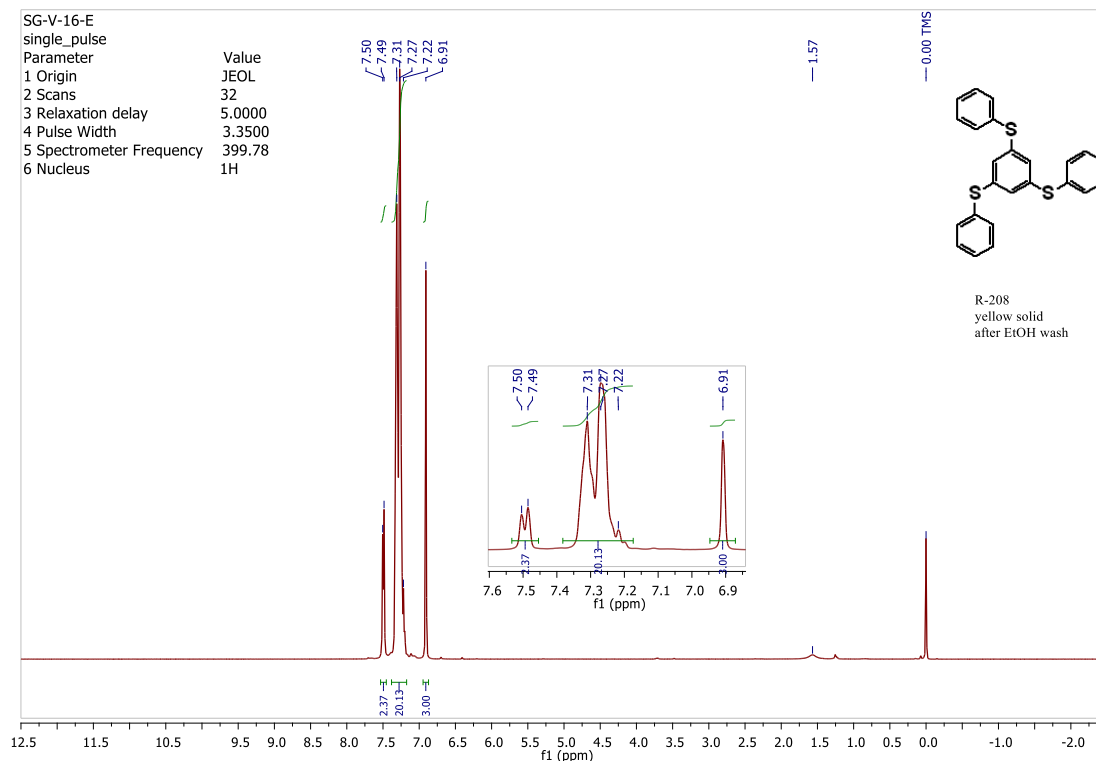
 ^{13}C -NMR (CDCl_3 , 100.53 MHz) ^{13}C -NMR DEPT 135 (CDCl_3 , 100.53 MHz)



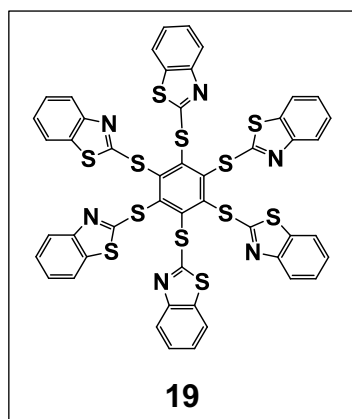
Procedure for asterisk-18 (R-208): In an oven-dried sealed tube, purged with argon, was added 1,3,5-tribromobenzene (7.810 g, 24.814 mmol, 1.00 mol-eq.), dried potassium carbonate (13.726 g, 99.322 mmol, 4.0 mol-eq.), thiophenol (10.0 mL, 10.943 g, 99.32 mmol, 4.0 mol-eq.) and dry DMF (30.0 mL, dried and kept over

activated molecular sieves 3Å). Argon was bubbled through the mixture for 5-10 minutes. The tube was sealed and the reaction was stirred at 80°C for 18 hours and 150°C for 48 hours. Most DMF was removed on a rotary evaporator under reduced pressure. To the reaction mixture was added EtOH (20 mL) and H₂O (20 mL) at 25°C while stirring vigorously. A solid was formed and stirring was continued for 3 hrs. After filtration, the solid was dried *in vacuo* to afford a white solid and was recrystallized from toluene. (**Yield= >90%**)

M.p. 38.5-41°C; **TLC** (SiO₂, tol/cyclohex. 10:90 v/v) R_f = 0.43; **¹H NMR** (399.78 MHz, CDCl₃, ppm), **SG-V-16-E**: δ = 7.50 (d, 2H, J= 7.55 Hz), 7.31 (d, 20H, J= 15.9 Hz), 6.91 (s, 3H).



¹H NMR (399.78 MHz, CDCl₃)



Procedure for asterisk-19 (R-96): In an oven-dried sealed tube, purged with argon, was added hexachlorobenzene (0.200 g, 0.702 mmol, 1.00 mol-eq.), dried potassium carbonate (1.163 g, 8.415 mmol, 11.99 mol-eq.), 2-mercaptobenzothiazole (1.000 g, 5.979 mmol, 8.517 mol-eq.) and dry DMF (3.5 mL, dried and kept over activated molecular sieves 3Å). Argon was bubbled through the mixture for 5-10 minutes. The color changed from yellow

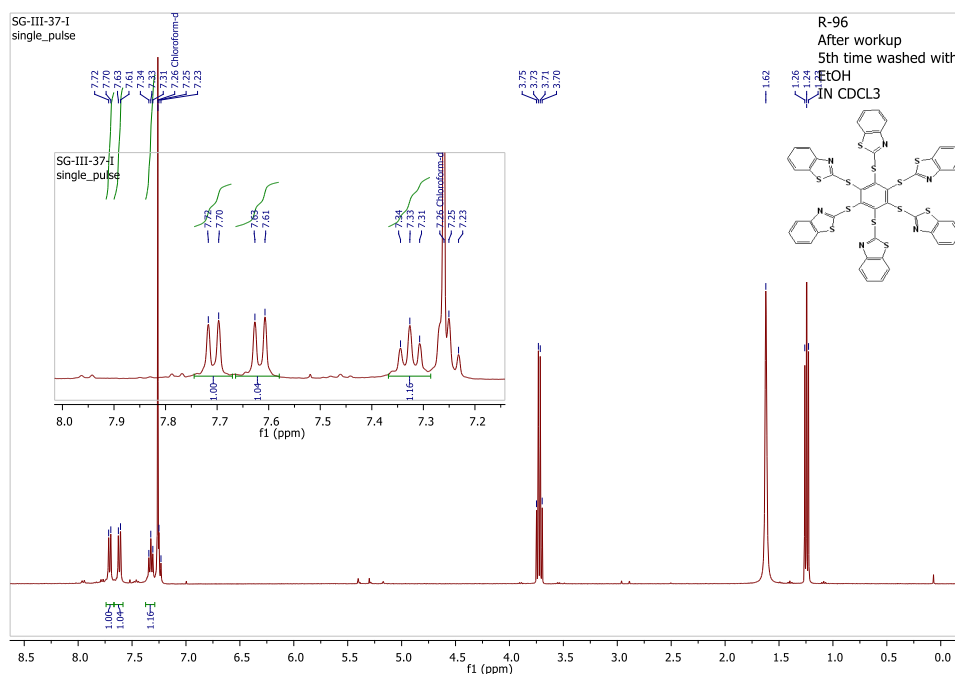
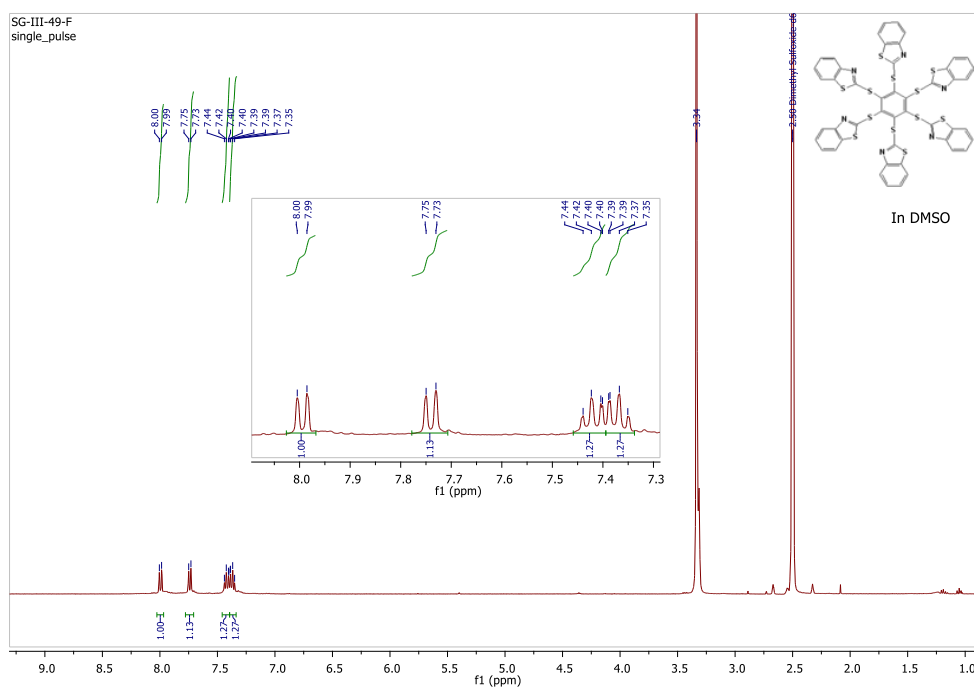
to orange. The tube was sealed and the reaction was stirred at 60°C for 5 days in an oil bath. Most DMF was removed on a rotary evaporator under reduced pressure. To the reaction mixture was added DCM (15 mL) and the organic layer was washed with H₂O (2×15mL) to remove remaining DMF. The organic phase was dried over anhydrous MgSO₄, filtered and DCM evaporated to afford a yellow-orange solid. It was triturated with EtOH (5×10 mL) at 25°C with a strong stirring for several minutes, and the supernatant was removed. It was repeated four times. The solid was then dried *in vacuo* to afford a pure yellow solid (0.634 g, 5.93 mmol, 84% yield).

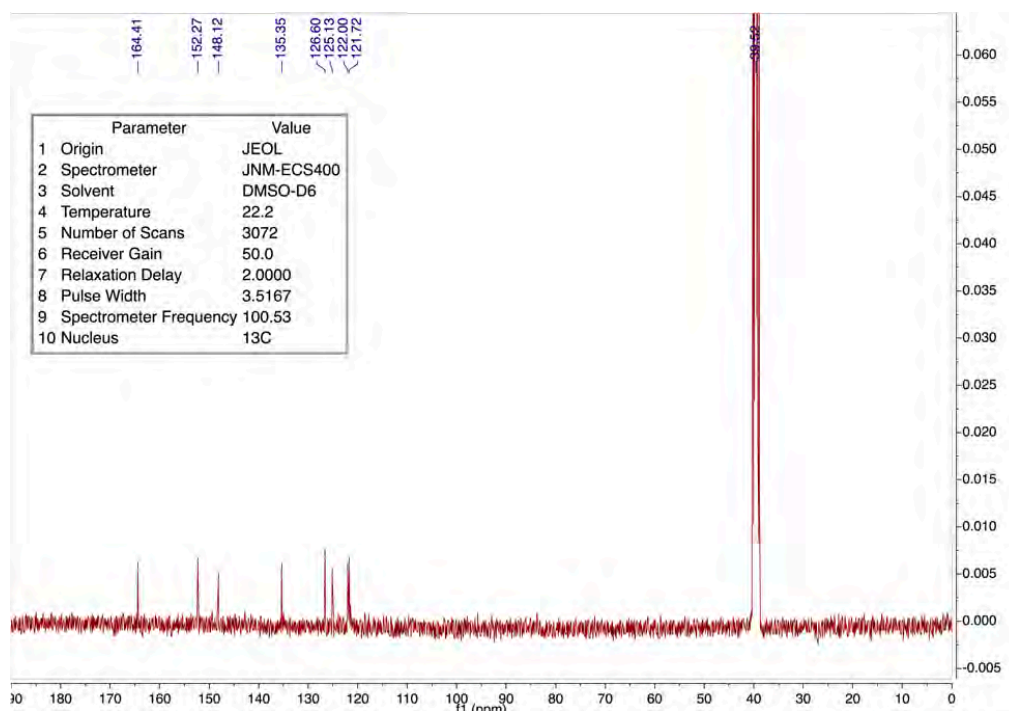
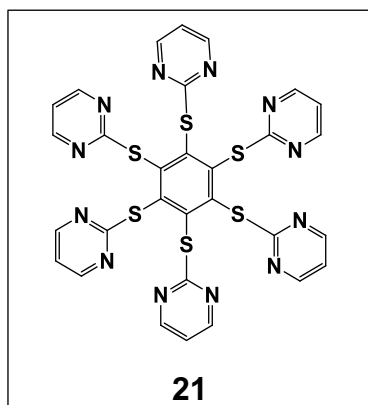
M.p.: 218-234°C (dec.); **TLC** (SiO₂, EtOAc/cyclohex. 10:90 v/v) R_f = 0.43; (SiO₂, DCM 100%) R_f = 0.23; **¹H NMR** (SG-III-49G, 399.78 MHz, DMSO-d₆, ppm): δ = 7.99 (d, J = 8.0 Hz, 1H), 7.74 (d, J = 7.8 Hz, 1H), 7.42 (ddd, J= 7.9, 7.3, 1.3 Hz, 1H), 7.36 (dd, J= 7.6, 7.5, 1.2 Hz, 1H); **¹H NMR** (SG-III-49-E, 399.78 MHz, CDCl₃, ppm): δ = 7.71 (d, J = 8.0 Hz, 1H); 7.62 (d, J= 7.8 Hz, 1H), 7.32 (dd, J = 7.8, 7.5 Hz, 1H), 7.24 (dd, J= 7.8, 7.5 Hz, 1H); **¹³C NMR** (SG-III-37-K, 100.53 MHz, DMSO-d₆, ppm): δ = 164.4, 152.3, 148.1, 135.3, 126.6, 125.1, 122.0, 121.7; **¹³C NMR** (SG-III-49-E, 100.53 MHz, CDCl₃, ppm): δ = 164.8, 153.0, 148.8, 135.9, 126.3, 124.9, 122.3, 121.1.

Table 28:

Reaction Number	Hexachloro benzene (mg, mmol, eq.)	Thiol (g, mmol, eq.)	K ₂ CO ₃ (g, mmol, eq.)	Solvent (dry DMF) (mL)	Time	Temperature (°C)	Yield
R-96	(0.200, 0.702, 1.00)	(1.000, 5.979, 8.5)	(1.163, 8.415, 12.0)	15.0	5days	60°C	84%

R-99	(2.0, 7.022, 1.0)	(10.643, 63.635, 9.0)	(11.436, 82.745, 12.0)	17.0	5days	60°C	37.2%
------	-------------------	------------------------	------------------------	------	-------	------	-------

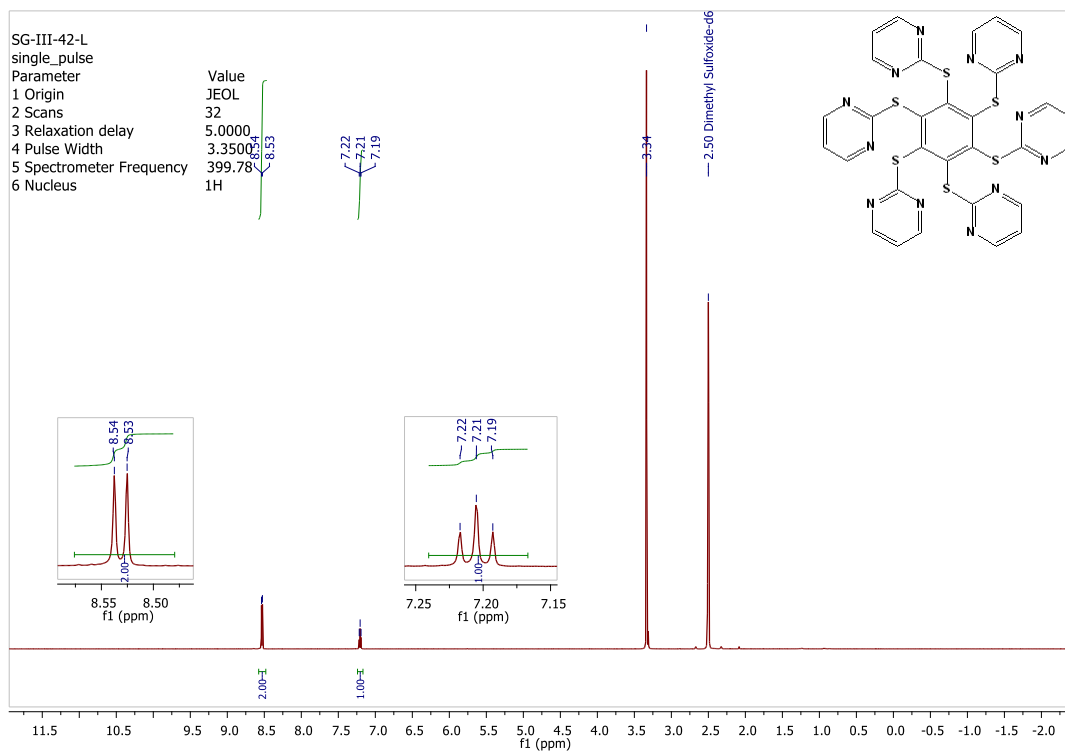
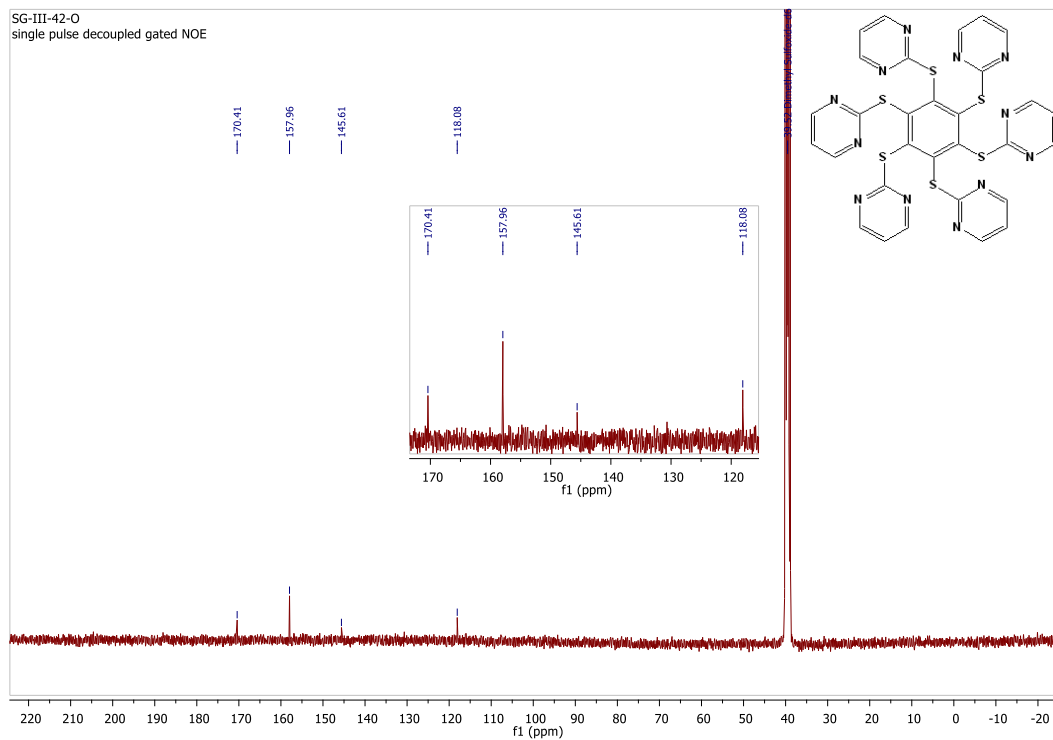
¹H NMR (399.78 MHz, CDCl₃)¹H NMR (399.78 MHz, DMSO-D₆)

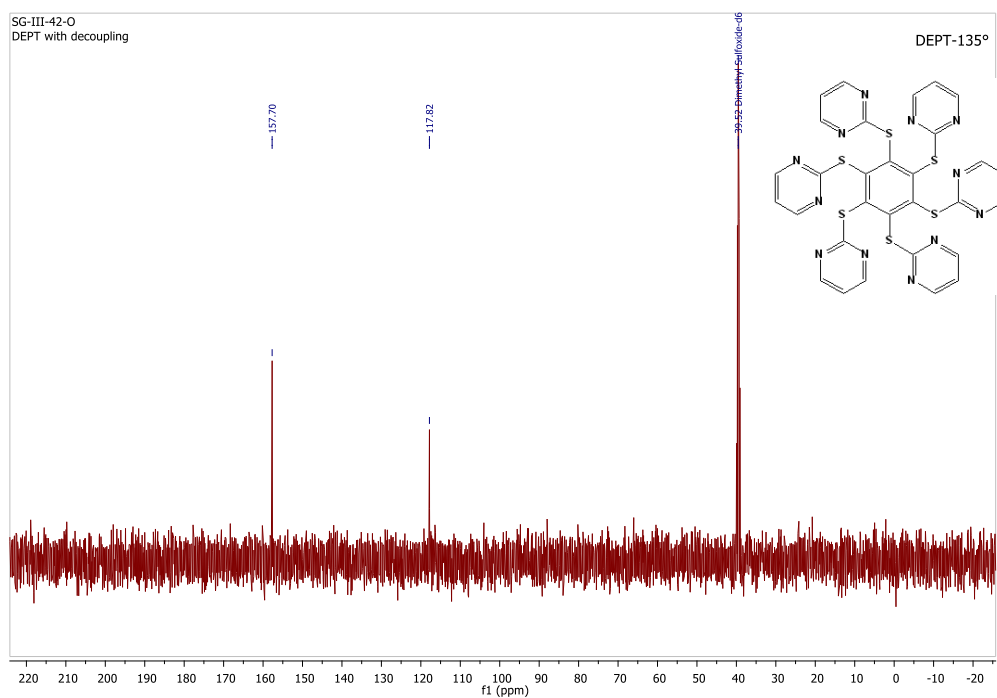
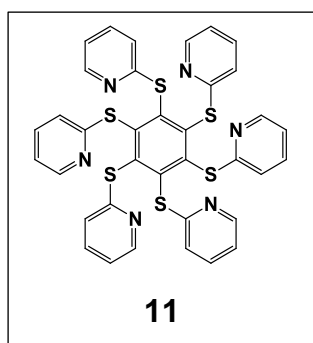
¹³C-NMR (CDCl₃, 100.53 MHz)

Procedure for asterisk-20 (R-97): In an oven-dried sealed tube, purged with argon, was added hexachlorobenzene (2.00g, 7.023mmol, 1.0eq.), dried Potassium carbonate (11.629g, 84.143mmol, 12eq.), 2-Mercaptopyrimidine (7.015g, 62.547mmol, 9eq.) and dry DMF (44.0 mL, dried and kept over activated molecular sieves 3Å). Argon was bubbled through the mixture for 5-10 minutes. The tube was sealed and the reaction was

stirred at 60°C for 12 days in an oil bath. Most DMF was removed on a rotary evaporator under reduced pressure. To the reaction mixture was added DCM (3 ×20mL) and H₂O, the organic layers were collected. The organic phase was dried over anhydrous MgSO₄, filtered and DCM evaporated to afford a pale-orange solid. Mass : 4.85g, Yield = 94%

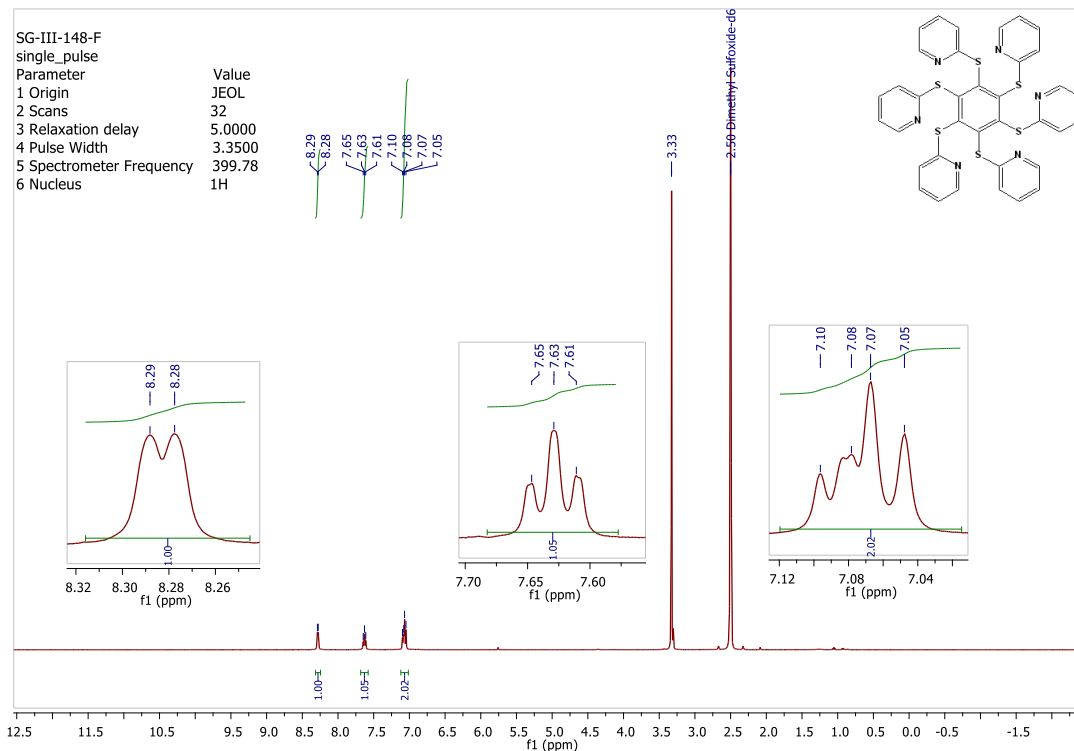
SG-III-42-L: ¹H NMR (399.78 MHz, DMSO-d₆): δ = 8.54 (d, 2H, J= 4.9 Hz), 7.21 (t, 1H, J= 4.8 Hz); ¹³C NMR (100.53 MHz, DMSO-d₆), **SG-III-42-O:** 170.41, 157.96, 145.61, 118.08; (¹³⁵-DEPT) NMR (DMSO-d₆), **SG-III-42-O:** 157.70, 117.82; **M.p:** 321-327°C

 ^1H NMR (399.78 MHz, CDCl_3) ^{13}C -NMR (CDCl_3 , 100.53 MHz)

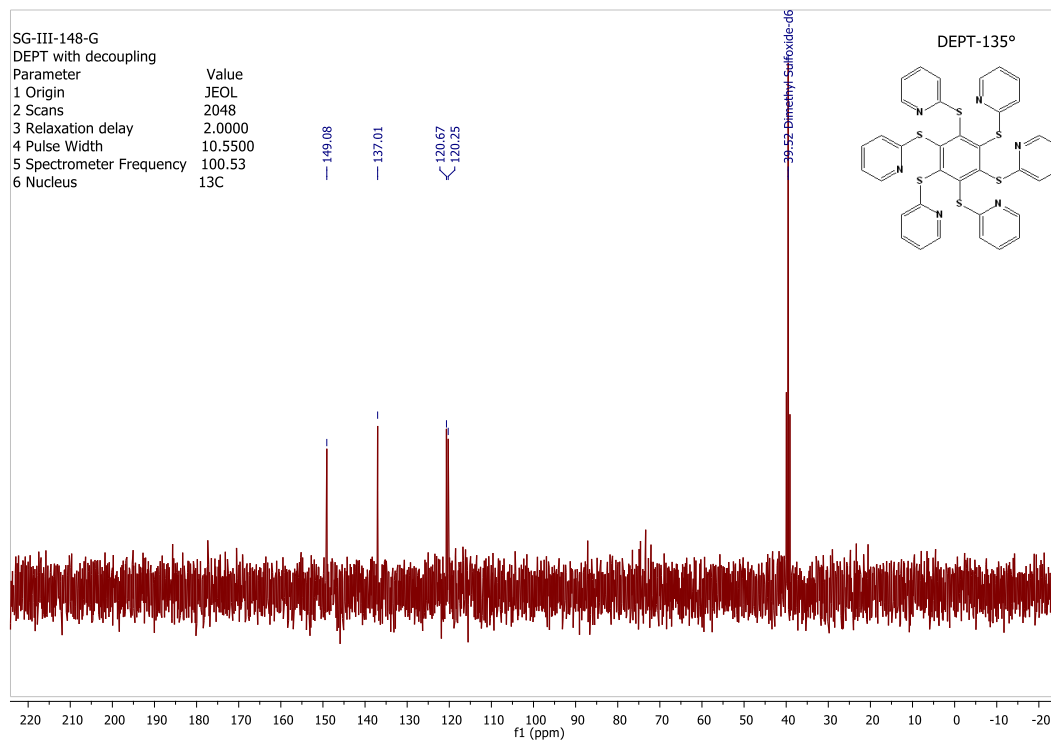
 ^{13}C -NMR DEPT 135 (CDCl_3 , 100.53 MHz)

Procedure for asterisk-11 (R-125): In an oven-dried sealed tube, purged with argon, was added hexachlorobenzene (C_6Cl_6) (213.4mg, 0.749mmol, 1.0eq.), dried Potassium carbonate (621.8mg, 4.499mmol, 6eq.), 2-mercaptopyridine (500.3mg, 4.500mmol, 6eq.) in dry DMF (3 mL, dried and kept over activated molecular sieves 3\AA). Argon was bubbled through the mixture for 5-10 minutes. The tube was sealed and the reaction was stirred at 60°C for 6 days in an oil bath. Most DMF was removed on a rotary evaporator under reduced pressure. The color was changed from yellow to canary (bright) yellow. The reaction mixture was triturated with EtOH (20 mL) and H_2O (20mL) at 25°C with a strong stirring for several minutes, and the supernatant was removed. The solid was then dried *in vacuo* to afford a pale orange solid. Mass: 473.7mg, Yield= 86%

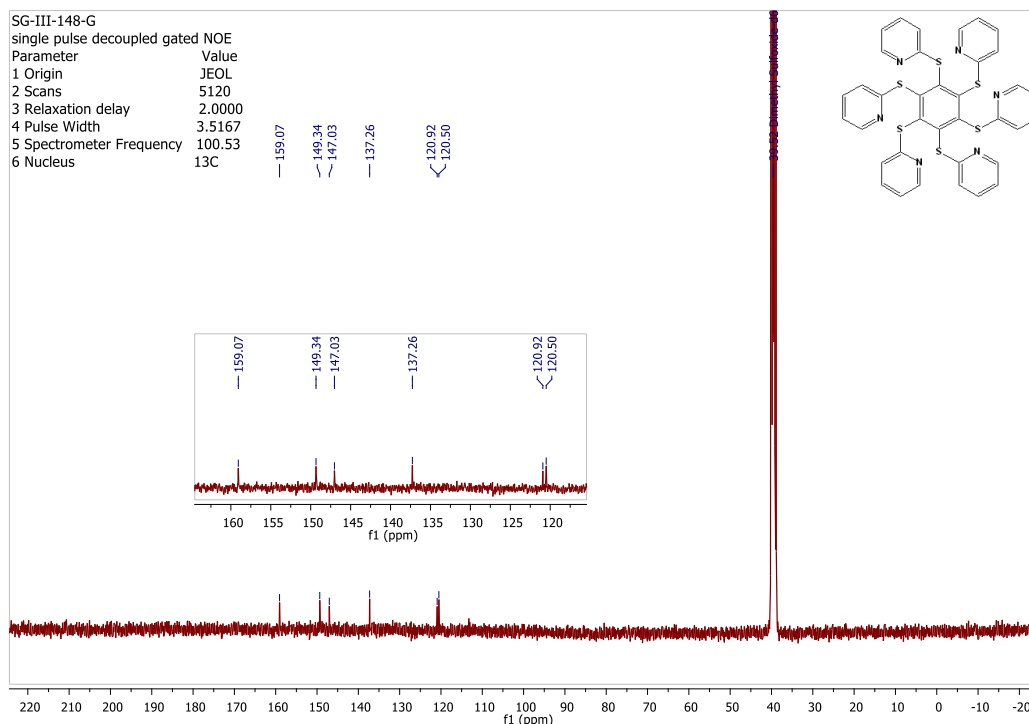
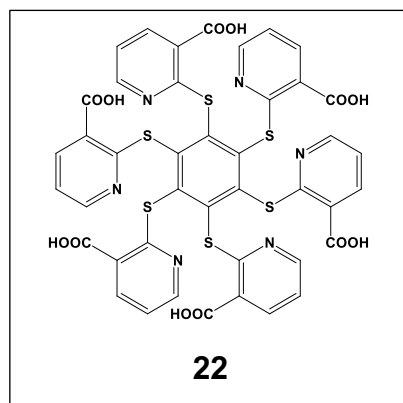
SG-III-148-F: ^1H NMR (399.78 MHz, DMSO-d_6): δ = 8.29 (d, 1H, J = 4.2 Hz), 7.63 (t, 1H, J = 7.1 Hz), 7.10-7.05 (m, 2H); ^{13}C NMR (100.53 MHz, DMSO-d_6), **SG-III-148-G:** 159.07, 149.34, 147.03, 137.26, 120.92, 120.50; Dept-135° NMR (100.53 MHz, DMSO-d_6) **SG-III-148-G:** 149.08, 137.01, 120.67, 120.25; **M.p:** $204.9\text{-}237^\circ\text{C}$



¹H NMR (399.78 MHz, CDCl₃)



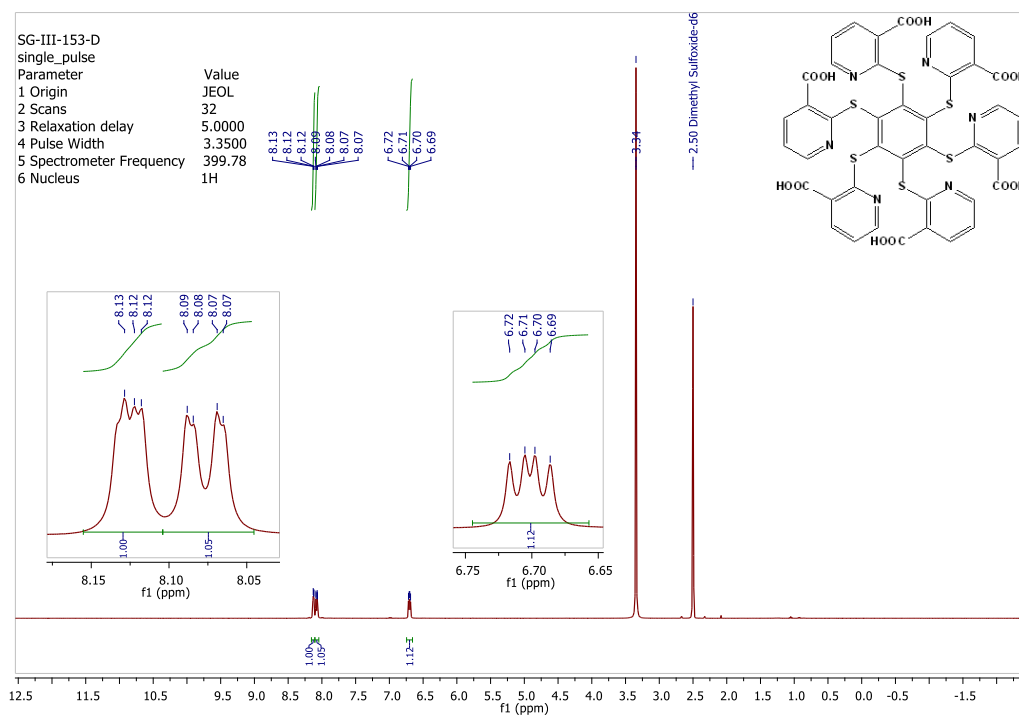
¹³C-NMR DEPT 135 (CDCl₃, 100.53 MHz)

 ^{13}C -NMR (CDCl_3 , 100.53 MHz)

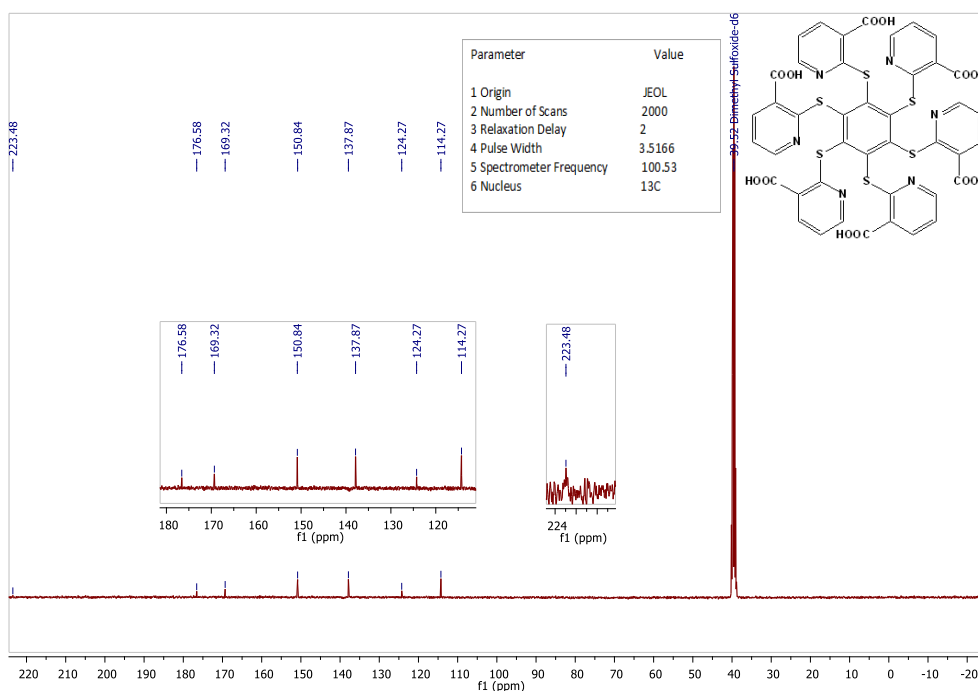
Procedure for asterisk-22 (R-126): In an oven-dried sealed tube, purged with argon, was added hexachlorobenzene (C_6Cl_6) (305.9mg, 1.074mmol, 1.0eq.), dried Potassium carbonate (890.9mg, 6.446mmol, 6eq.), 2-mercaptonicotinic acid (1000.3mg, 6.463mmol, 6eq.) in dry DMF (10mL, dried and kept over activated molecular sieves 3\AA). Argon was bubbled through the mixture for 5-10 minutes. The tube was sealed and the reaction was stirred at 60°C for 8 days in an oil bath. Most DMF was removed on a rotary evaporator under reduced pressure. The color was changed from yellow to canary (bright) yellow. The reaction mixture was triturated with EtOH (5mL) and H_2O (5mL) and filtered to get the light green solid. Again, the reaction mixture was triturated with EtOH (5mL), H_2O (5mL) and added DCM (10mL) & acetone (5mL) yellow solid precipitated out and filtered to get pale yellow solid, and the supernatant was removed. The solid was then dried *in vacuo* to afford a pale-yellow solid. **Mass:**

919.6mg, Yield= 86%

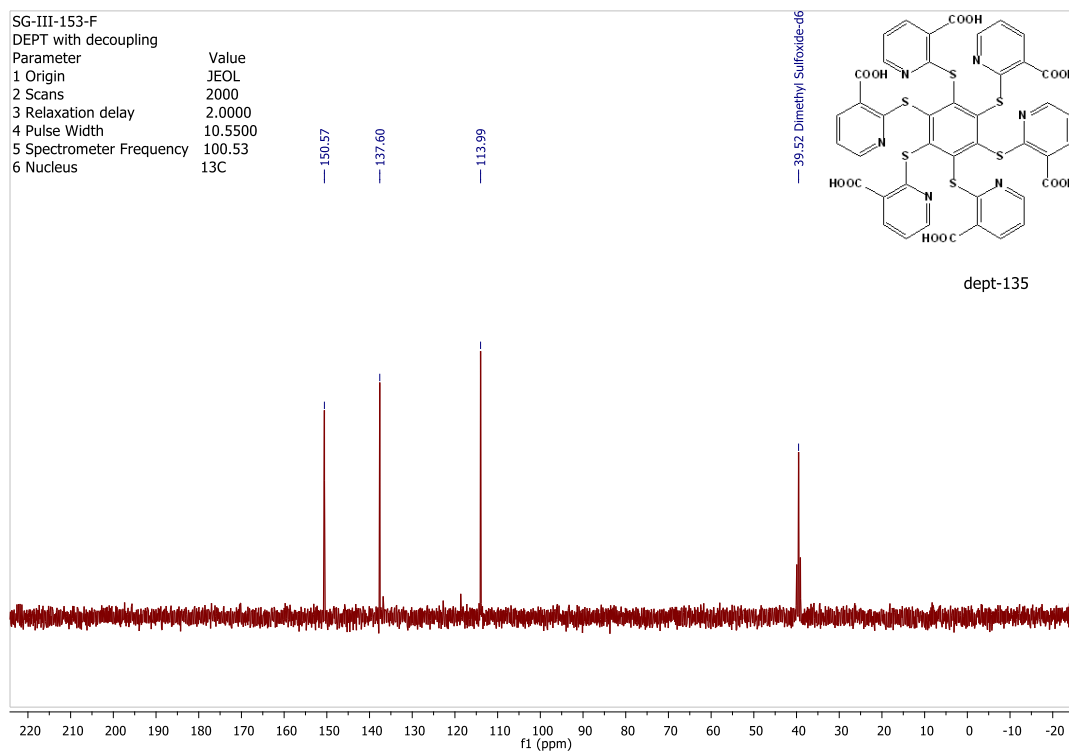
SG-III-153-D: ^1H NMR (399.78 MHz, DMSO- d_6): δ = 8.13-8.07 (m, 2H), 6.71 (dd, 1H);
 ^{13}C NMR (100.53 MHz, DMSO- d_6), **SG-III-153-E:** 223.48, 176.58, 169.32, 150.84,
 137.87, 124.27, 114.27 ; Dept-135° NMR (100.53 MHz, DMSO- d_6), **SG-III-153-F:**
 150.57, 137.60, 113.99; **M.p.** : 101-105.9°C



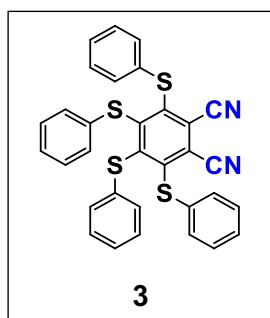
^1H NMR (399.78 MHz, CDCl_3)



^{13}C -NMR (CDCl_3 , 100.53 MHz)

 ^{13}C -NMR DEPT 135 (CDCl_3 , 100.53 MHz)

EXPERIMENTAL SECTION FOR CHAPTER 4



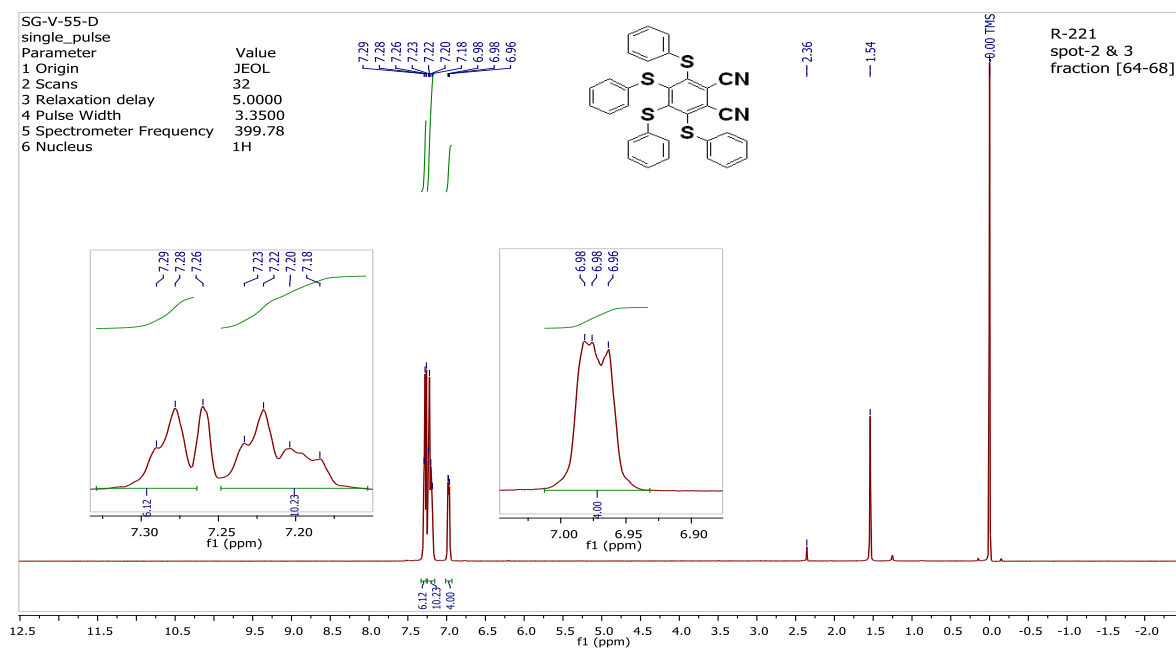
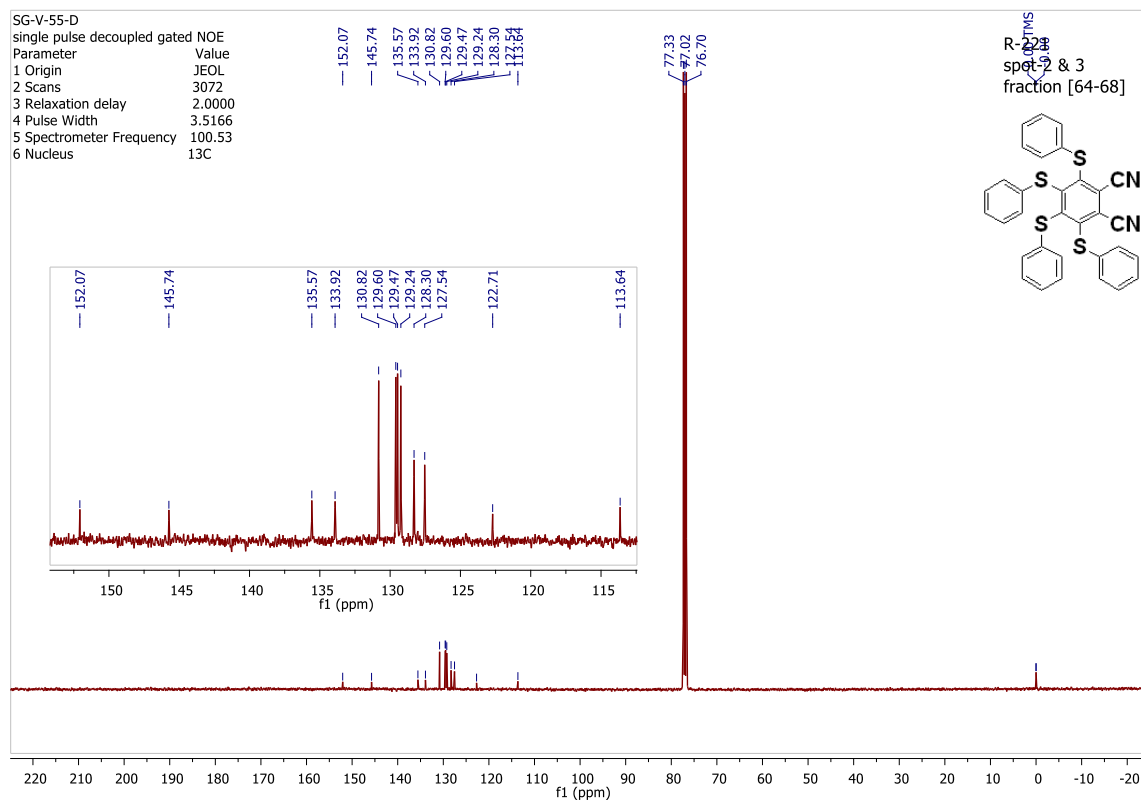
Procedure for asterisk-3 (R-221): In an oven-dried sealed tube, purged with argon, was added (1) tetrafluorophthalonitrile (1.0g, 4.997mmol, 1eq.), dried potassium carbonate (3.468 g, 25.098 mmol, 5.0 mol-eq.), thiophenol (2.5 mL, 2.753 g, 24.988 mmol, 5.0 mol-eq.) and dry DMF (8.0 mL, dried and kept over activated molecular sieves 3Å). Argon was bubbled through the mixture for 5-10 minutes. The color changed from off white to yellow. The

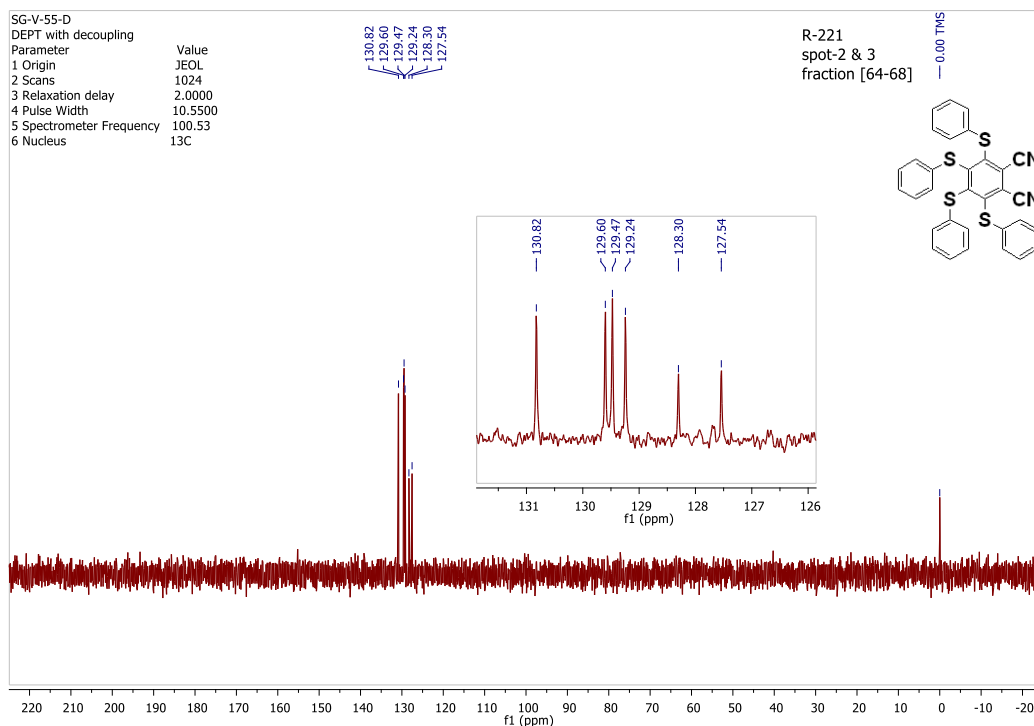
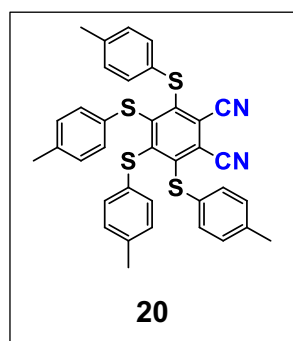
tube was sealed and the reaction was stirred at 50°C for 18 hours in an oil bath. Most DMF was removed on a rotary evaporator under reduced pressure. To the crude mixture was added H₂O (15 mL), and the solid was filtered and the residue was purified using column chromatography (eluent: toluene/ cyclohexane). **Mass: 1.677g. Yield= >60%**

SG-V-55-D: ¹H NMR (399.78 MHz, CDCl₃): δ = 7.29-7.26 (m, 6H), 7.23-7.18 (m, 10H), 6.98-6.96 (m, 4H); ¹³C NMR (100.53 MHz, TMS), **SG-V-55-D:** 152.07, 145.74, 135.57, 133.92, 130.82, 129.60, 129.47, 129.24, 128.30, 127.54, 122.71, 113.64; (135°-DEPT) NMR (CDCl₃), **SG-V-55-D:** 130.82, 129.60, 129.47, 129.24, 128.30, 127.54; **M.p.:** 150-153°C; **TLC** (acetone:Cyclohex: 30/70 v/v), **R_f**= 0.5

Table 29:

Reaction Number	Hexachloro benzene (g, mmol, eq.)	Thiol (mL, g, mmol, eq.)	K ₂ CO ₃ (g, mmol, eq.)	Solvent (dry DMF) (mL)	Time	Temperature (°C)	Yield
R-209	(1.008g, 5.037, 1.00)	(3mL, 3.304g, 29.986, 6.0)	(4.147, 30.006, 6.0)	14.5	5days 18hrs.	60°C 80°C	--
R-221	(1.0g, 4.997, 1.0)	(2.5 mL, 2.753 g, 24.988, 5.0)	3.468g, 25.098, 5.0	8.0	18hrs.	50°C	>60%

 ^1H NMR (399.78 MHz, CDCl_3) ^{13}C -NMR (CDCl_3 , 100.53 MHz)

 ^{13}C -NMR DEPT 135 (CDCl_3 , 100.53 MHz)

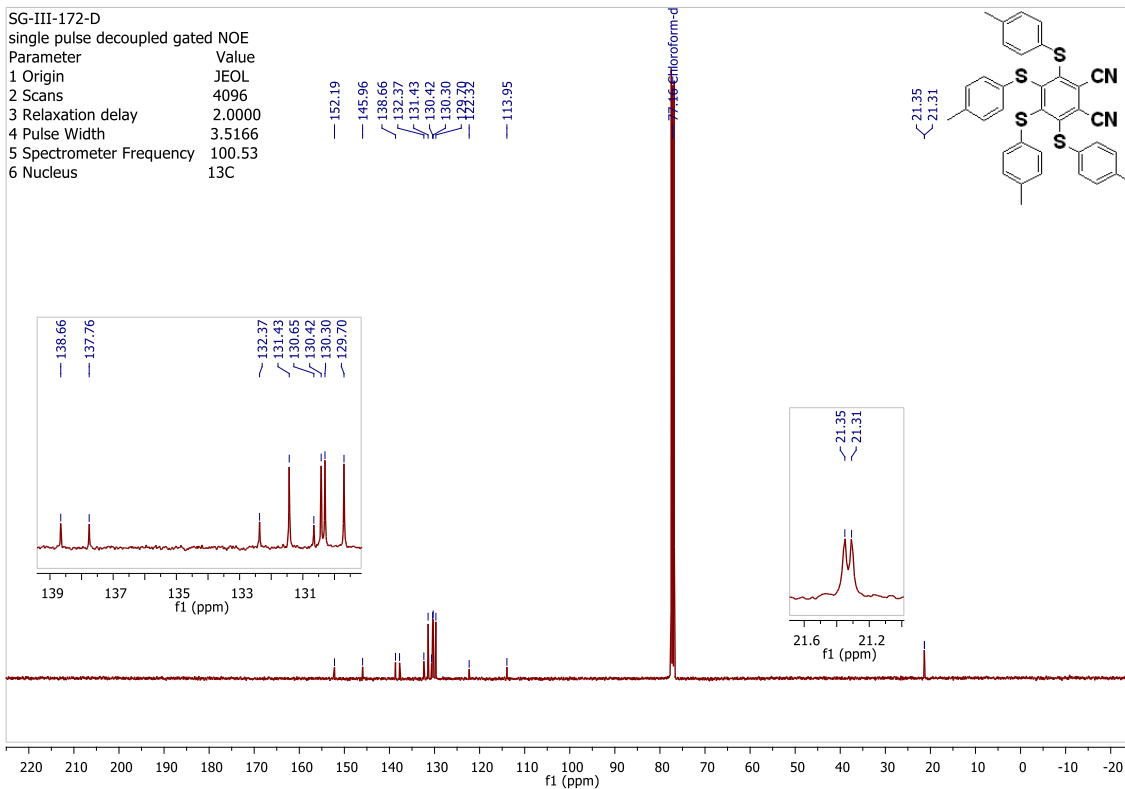
Procedure for asterisk-20 (R-131): In an oven-dried sealed tube, purged with argon, was added (1) tetrafluorophthalonitrile (200.0 mg, 0.999mmol, 1eq.), dried potassium carbonate (829.0mg, 5.998mmol, 6eq.), 4-methylthiophenol (74.3mg, 5.985mmol, 6eq.) and dry DMF (2.0 mL, dried and kept over activated molecular sieves 3\AA). Argon was bubbled through the mixture for 5-10 minutes. The color changed from off white to

yellow. The tube was sealed and the reaction was stirred at 60°C for 42 hours in an oil bath. Most DMF was removed on a rotary evaporator under reduced pressure. It was triturated with EtOH (10 mL) and H₂O (10 mL) at 25°C overnight and filtered to get yellow solid. **Mass: 588.0 mg, Yield= 95%**

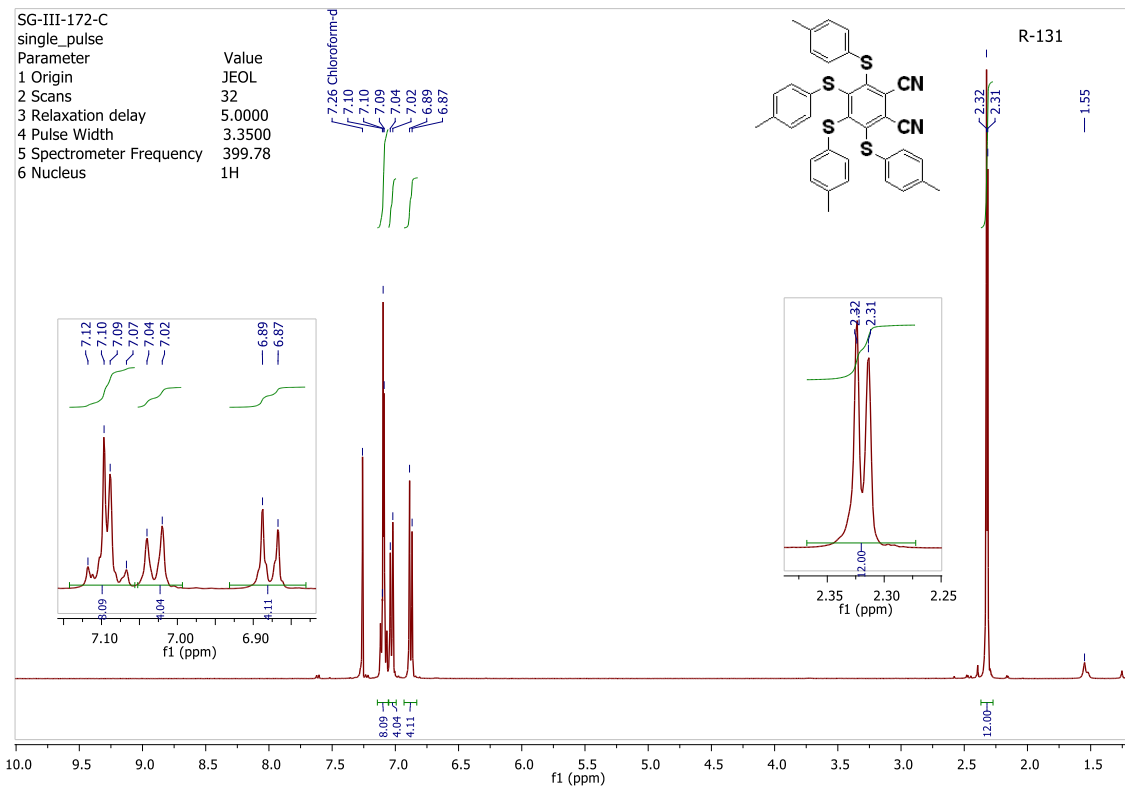
SG-III-172-C: ^1H NMR (399.78 MHz, CDCl_3): δ = 7.12 (d, 8H, J = 8.5 Hz), 7.04 (d, 4H, J = 8.0 Hz), 6.89 (d, 4H, J = 4H), 2.32 (d, 12H, J = 4.0 Hz); ^{13}C NMR (100.53 MHz, CDCl_3), **SG-III-172-D:** 152.19, 145.96, 138.66, 137.76, 132.37, 131.43, 130.65, 130.42, 130.30, 129.70, 122.32, 113.95, 21.35, 21.31; ($^{135^\circ}$ -DEPT) NMR (CDCl_3), **SG-III-172-D:** 131.23, 130.22, 130.10, 129.50, 21.15, 21.11; **M.p.:** $113\text{--}117^\circ\text{C}$; **TLC** (acetone:Cyclohex: 30/70 v/v), **R_f** = 0.58

Table 30:

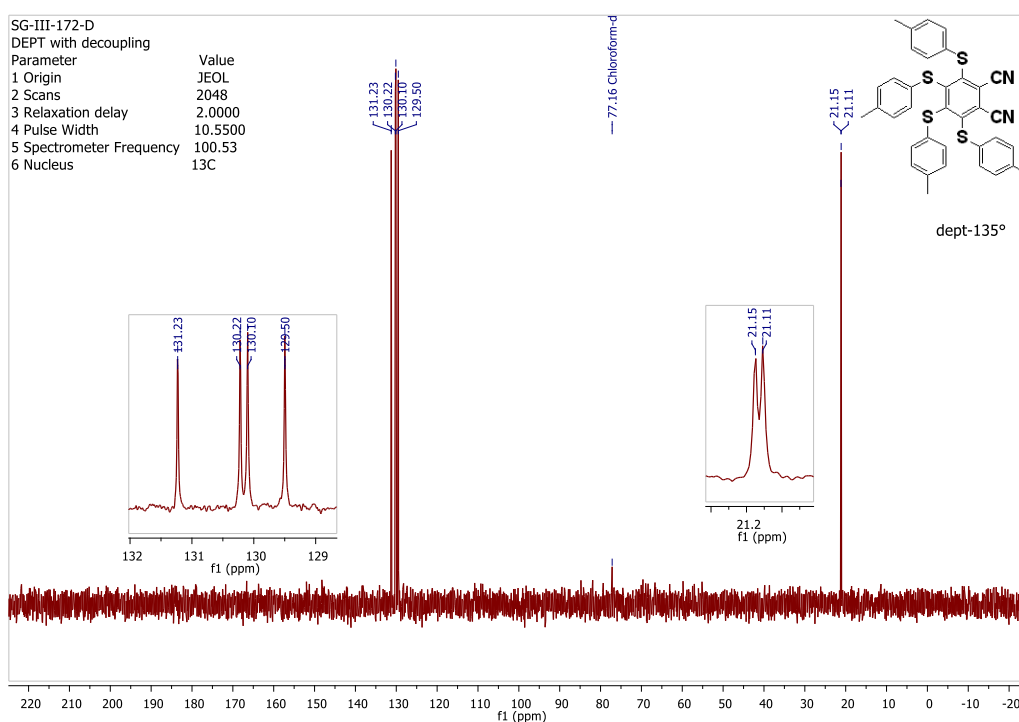
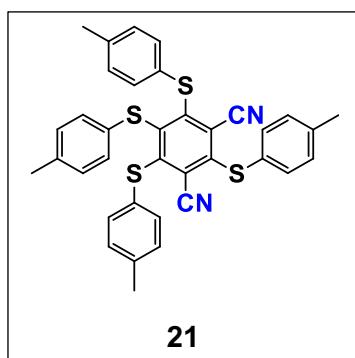
Reaction Number	Hexachloro benzene (mg, mmol, eq.)	Thiol (mg, mmol, eq.)	K ₂ CO ₃ (g, mmol, eq.)	Solvent (dry DMF) (mL)	Time	Temperature (°C)	Yield
R-116	100.5, 0.502, 1.00	95.80mg, 0.771, 1.5	(103.9, 0.752, 1.5)	1.0	48hrs.	28°C	24%
R-123	100.3, 0.501, 1.0	95.23, 0.766, 1.5	104.20, 0.754, 1.5	0.5	5days	30°C	--
R-127	100.2, 0.501, 1.0	93.80, 0.755, 1.5	104.1, 0.753, 1.5	2.0	6days	60°C	--
R-131	200.0, 0.999, 1.0	743.4, 5.986, 6.0	829.0, 5.998, 6.0	2.0	42hrs.	60°C	95%
R-133	100.9, 0.504, 1.0	374.9, 3.018, 6.0	416.3, 3.012, 6.0	1.0	7days	73-75°C	>90%
R-246	400.5, 2.001, 1.0	1.485g, 11.959, 6.0	1.656g, 11.981, 6.0	6.0	24hrs. 2days	60°C 30°C	90%



¹H NMR (399.78 MHz, CDCl₃)



¹³C-NMR (CDCl₃, 100.53 MHz)

 ^{13}C -NMR DEPT 135 (CDCl_3 , 100.53 MHz)

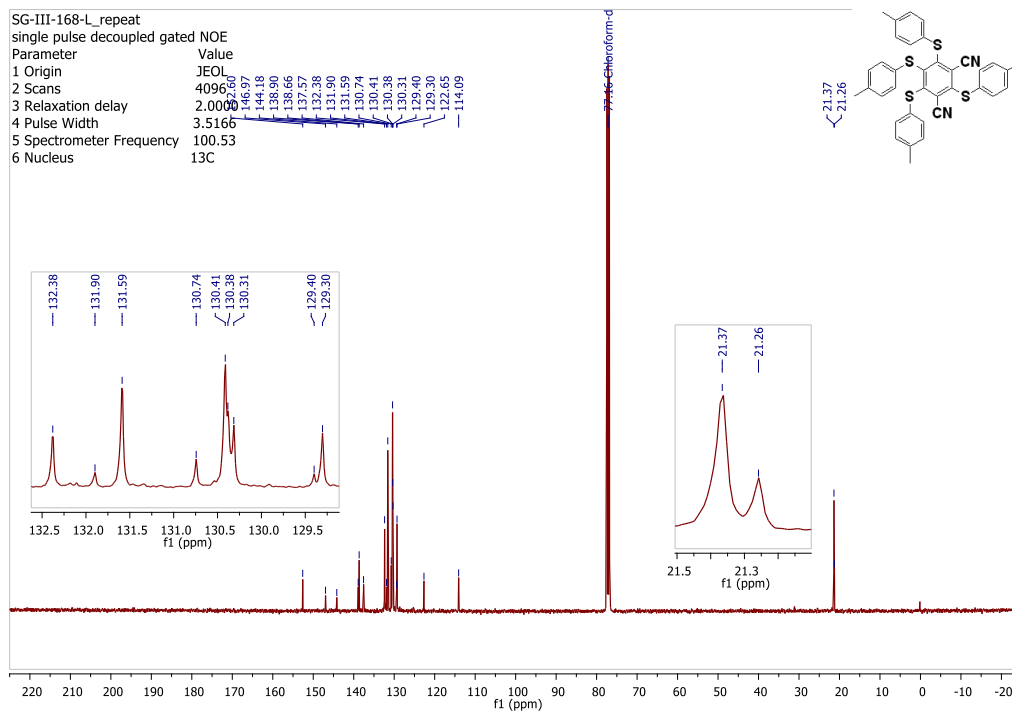
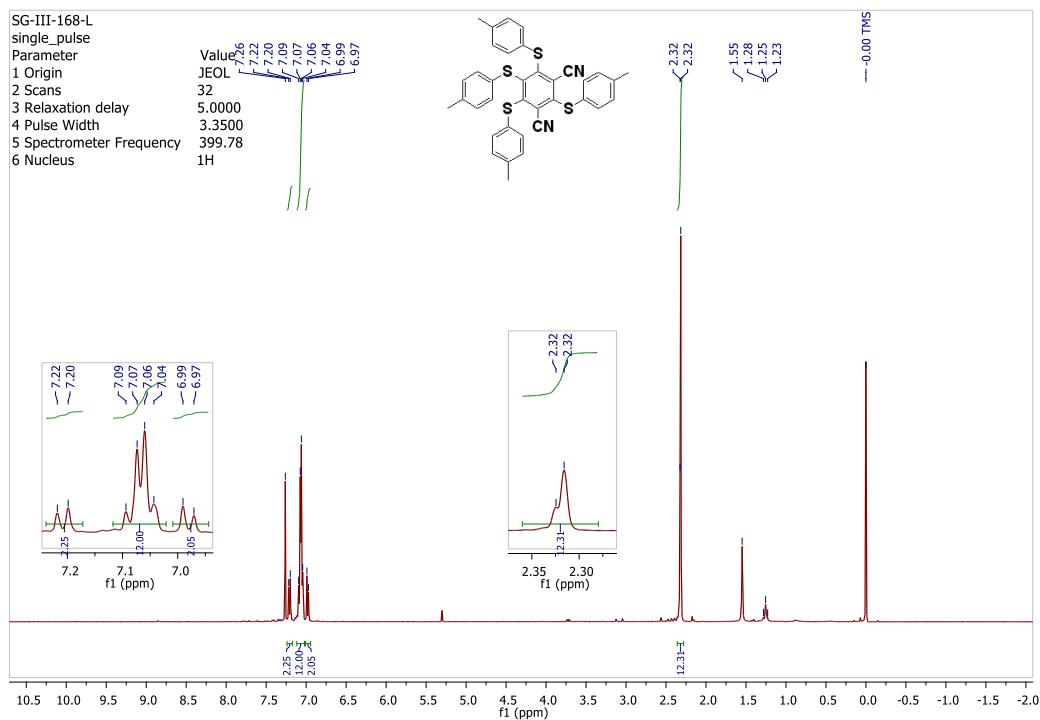
Procedure for asterisk-21 (R-130): In an oven-dried sealed tube, purged with argon, was added (**10**) tetrafluoroisophthalonitrile (200.4 mg, 1.001mmol, 1eq.), dried potassium carbonate (828.5mg, 5.995 mmol, 6eq.) and 4-methylthiophenol (74.3mg, 5.985mmol, 6eq.) and dry DMF (4.5 mL, dried and kept over activated molecular sieves 3Å). Argon was bubbled through the mixture for 5-10

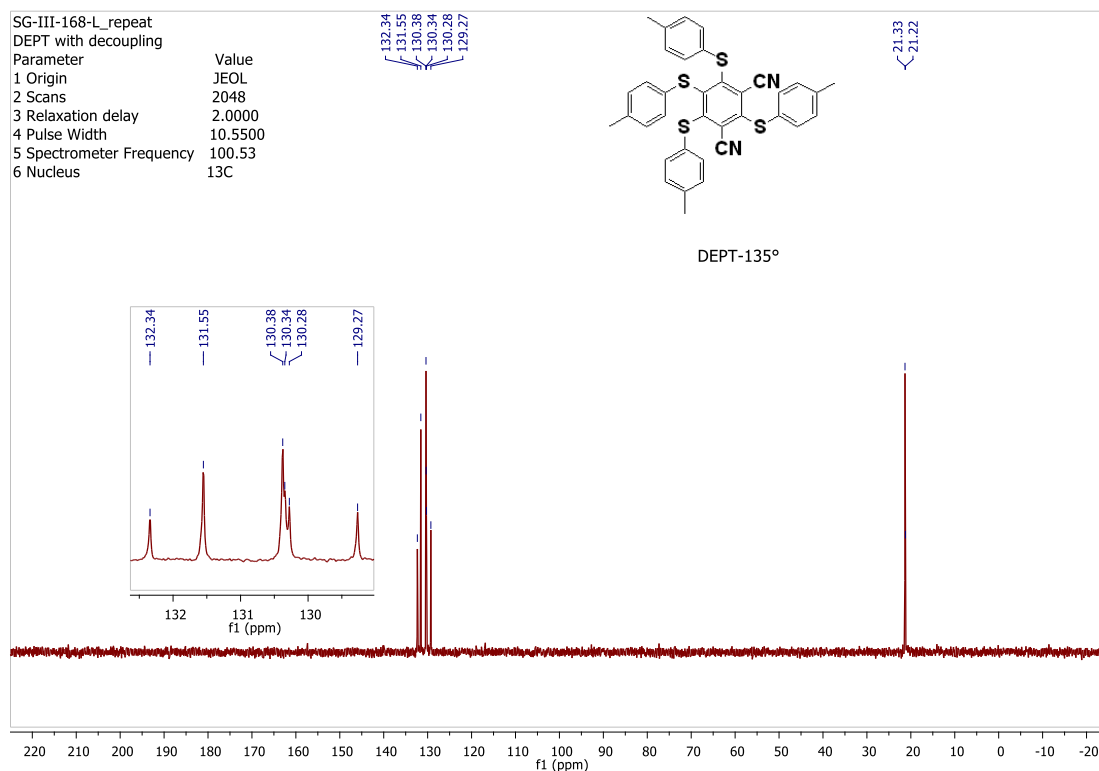
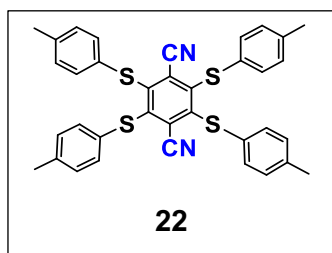
minutes. The color changed from off white to yellow. The tube was sealed and the reaction was stirred at 60°C in an oil bath for 8days and for 24hrs. at 75°C. Most DMF was removed on a rotary evaporator under reduced pressure. It was triturated with EtOH (10 mL) and H₂O (10 mL) at 25°C overnight and filtered to get yellow solid.

Mass: 292.0 mg, Yield= 47%

SG-III-168-L: ^1H NMR (399.78 MHz, TMS): δ = 7.22 (d, 2H, J=7.8 Hz), 7.09 (d, 12H, J= 8.1 Hz), 6.99 (d, 2H, J= 7.9 Hz), 2.32 (singlet with one shoulder, 12H); ^{13}C NMR (100.53 MHz, CDCl_3) **SG-III-168-L_repeat:** 152.60, 146.97, 144.18, 138.90, 138.66, 137.57, 132.38, 131.90, 131.59, 130.74, 130.41, 130.38, 130.31, 129.40, 129.30, 122.65, 114.09, 21.37, 21.26; ($^{135^\circ}$ -DEPT) NMR (CDCl_3), **SG-III-168-L_repeat:**

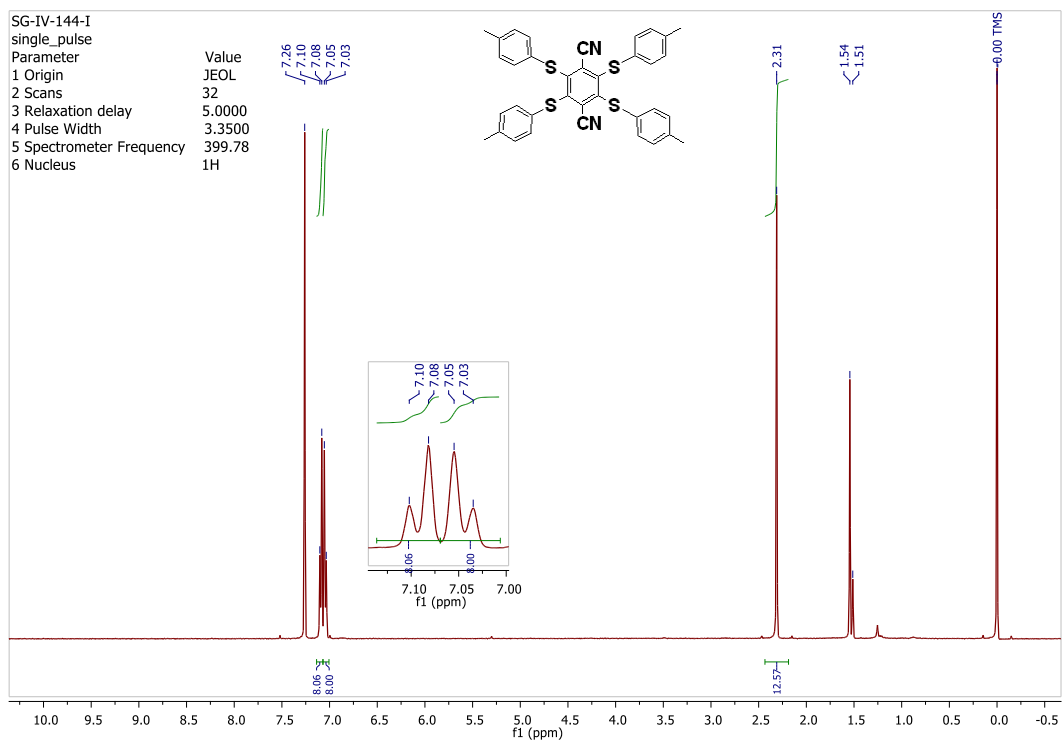
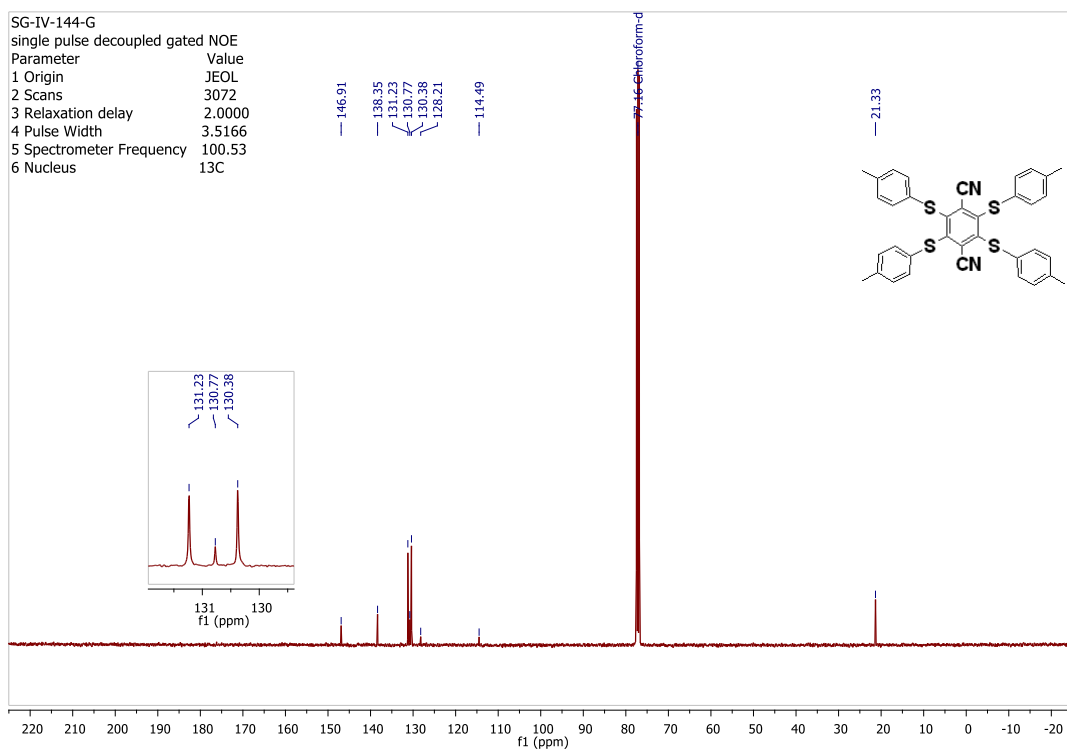
132.34, 131.55, 130.38, 130.34, 130.28, 129.27, 21.33, 21.22; **M.p.:** 165-168°C; **TLC**
(acetone:Cyclohex: 30/70 v/v), **R_f**= 0.58

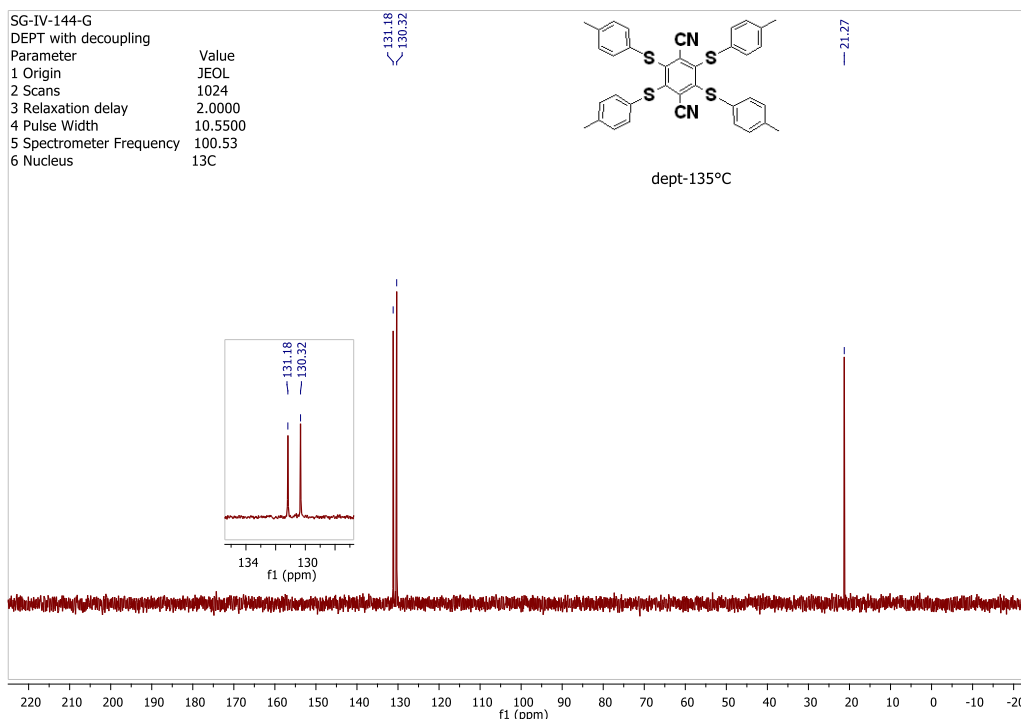
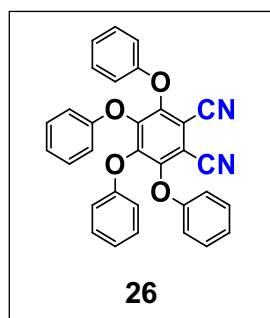


¹³C-NMR DEPT 135 (CDCl₃, 100.53 MHz)

Procedure for asterisk-22 (R-189): In an oven-dried sealed tube, purged with argon, was added (14) tetrafluoroterephthalonitrile (201.0mg, 1.004mmol, 1eq.), dried potassium carbonate (829.6mg, 6.003mmol, 6eq.) and 4-methylthiophenol (74.4mg, 5.993mmol, 6eq.) and dry DMF (6.5 mL, dried and kept over activated molecular sieves 3Å). Argon was bubbled through the mixture for 5-10 minutes. The color changed from off white to yellow. The tube was sealed and the reaction was stirred at 60°C in an oil bath for 4 days. Most DMF was removed on a rotary evaporator under reduced pressure. It was triturated with EtOH (10 mL) and H₂O (10 mL) at 25°C for 40 minutes and filtered to get yellow solid. **Mass: 560.6 mg, Yield= 90%**

SG-IV-144-I: ¹H NMR (399.78 MHz, TMS): δ = 7.10 (d, 8H, J= 8.1 Hz), 7.05 (d, 8H, J= 8.0 Hz), 2.31 (s, 12H); ¹³C NMR (100.53 MHz, CDCl₃) **SG-IV-144-G:** 146.91, 138.35, 131.23, 130.77, 130.38, 128.21, 114.49, 21.33; (135°-DEPT) NMR (CDCl₃), **SG-IV-144-G:** 131.18, 130.32, 21.27; **M.p.:** 266-268°C; **TLC** (tol:Cyclohex: 80/20 v/v), **R_f**= 0.58

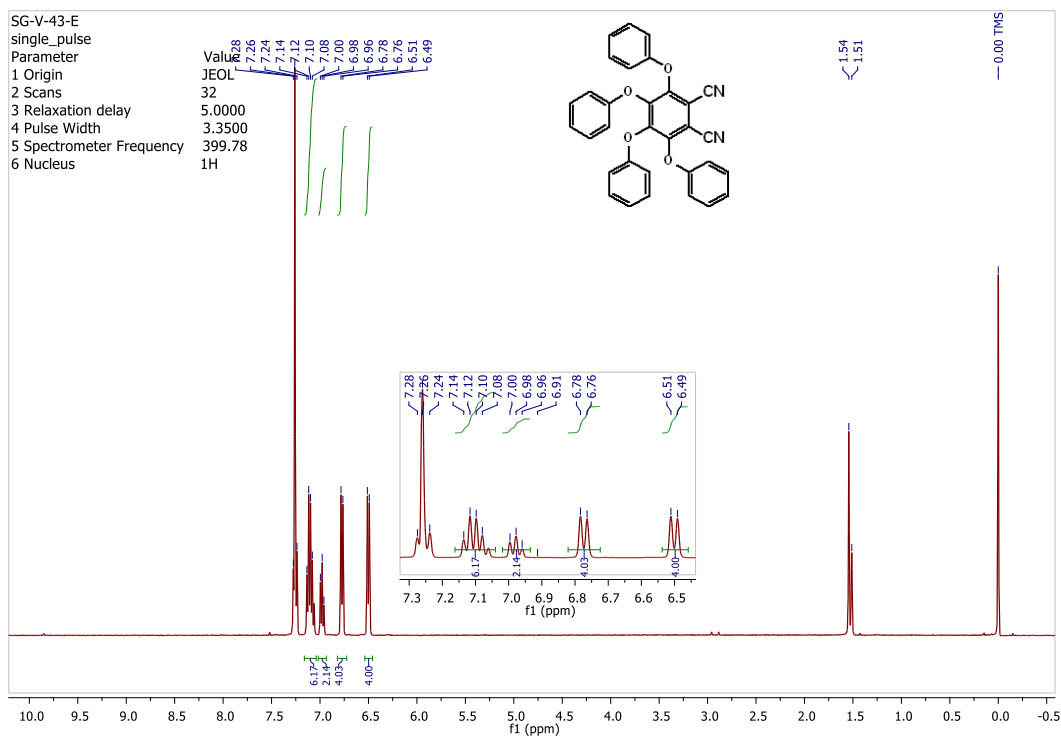
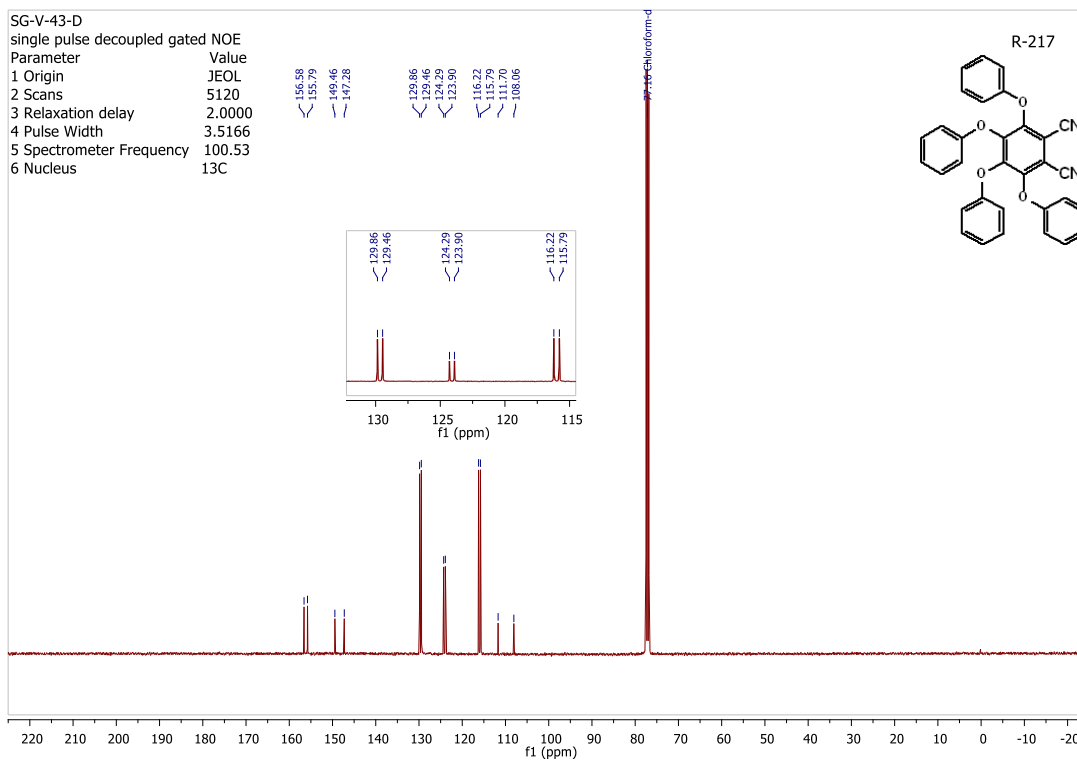
 ^1H NMR (399.78 MHz, CDCl_3) ^{13}C -NMR (CDCl_3 , 100.53 MHz)

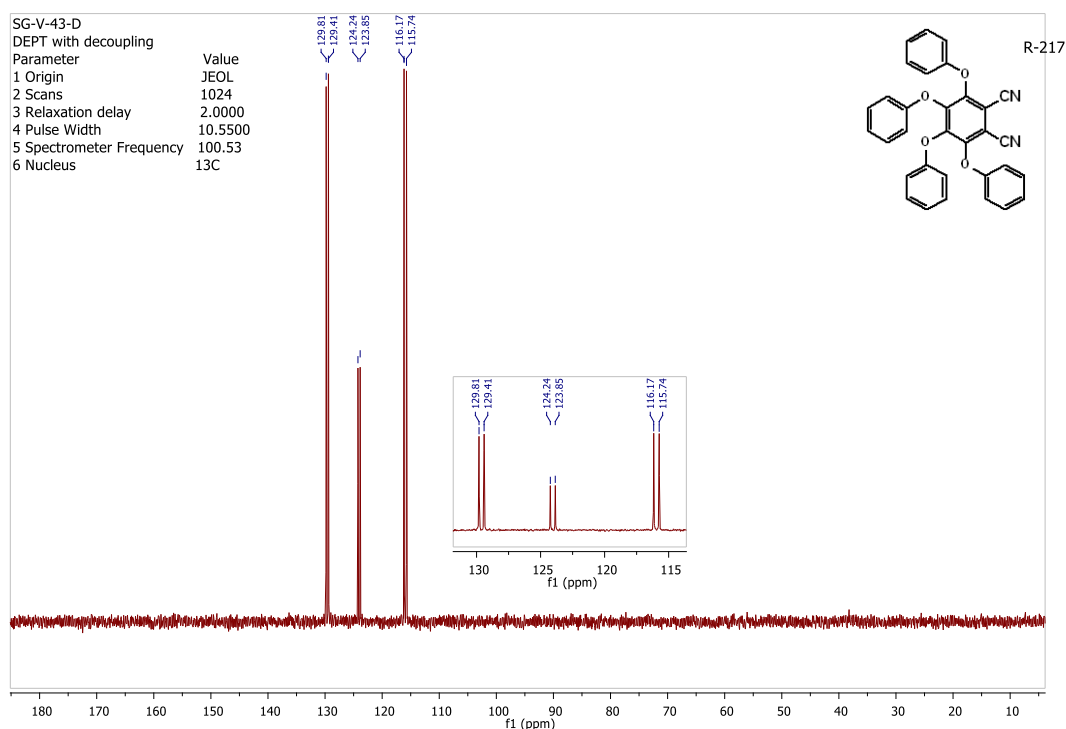
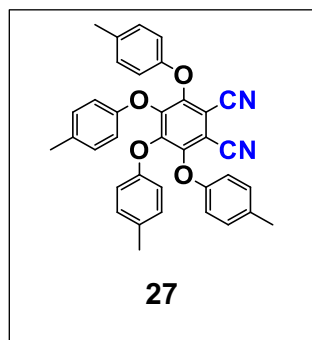
¹³C-NMR DEPT 135 (CDCl₃, 100.53 MHz)

Procedure for asterisk-26 (R-217): In an oven-dried sealed tube, purged with argon, was added (1) tetrafluorophthalonitrile (1.507gm, 7.536mmol, 1eq.), dried potassium carbonate (4.587gm, 33.191mmol, 4.4eq.) and phenol (3.108gm, 33.031mmol, 4.4eq.) and dry DMF (20 mL, dried and kept over activated molecular sieves 3Å). Argon was bubbled through the

mixture for 5-10 minutes. The color changed from off white to yellow. The tube was sealed and the reaction was stirred at 60°C in an oil bath for 18 hours. The reaction mixture was quenched with NaOH (1M, 15mL). It was triturated with EtOH (10 mL) and H₂O (10 mL) at 25°C for 2 hours and filtered to get white solid. **Mass: 3.716 gm, Yield= 99.8%**

SG-V-43-E: ¹H NMR (399.78 MHz, TMS): δ = 7.28 (t, 4H, J= 7.9 Hz), 7.14-7.08 (m, 6H), 6.98 (t, 2H, J=7.4 Hz), 6.78 (d, 4H, J= 7.8 Hz), 6.51 (d, 4H, J= 7.8 Hz); ¹³C NMR (100.53 MHz, CDCl₃) **SG-V-43-D:**156.58, 155.79, 149.46, 147.28, 129.86, 129.46, 124.29, 123.90, 116.22, 115.79, 111.70, 108.06; (135°-DEPT) NMR (CDCl₃), **SG-V-43-D:**129.81, 129.41, 124.24, 123.85, 116.17, 115.74; **M.p.:** 158.2-160°C; **TLC** (acetone:Cyclohex: 30/70 v/v), **R_f**= 0.50

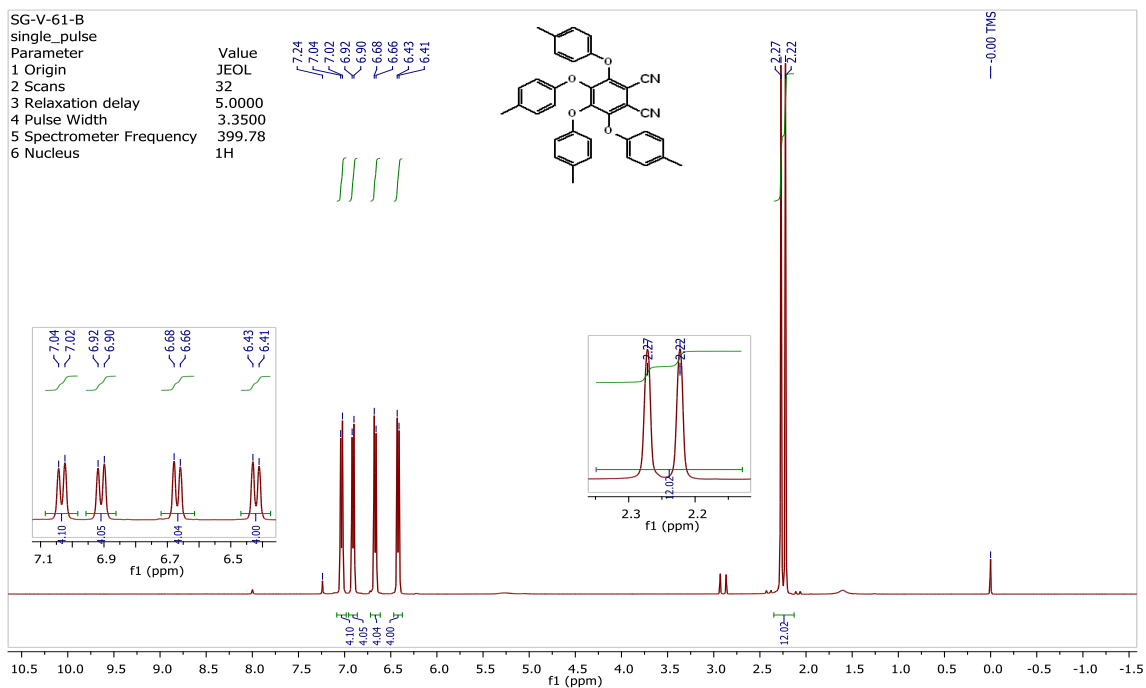
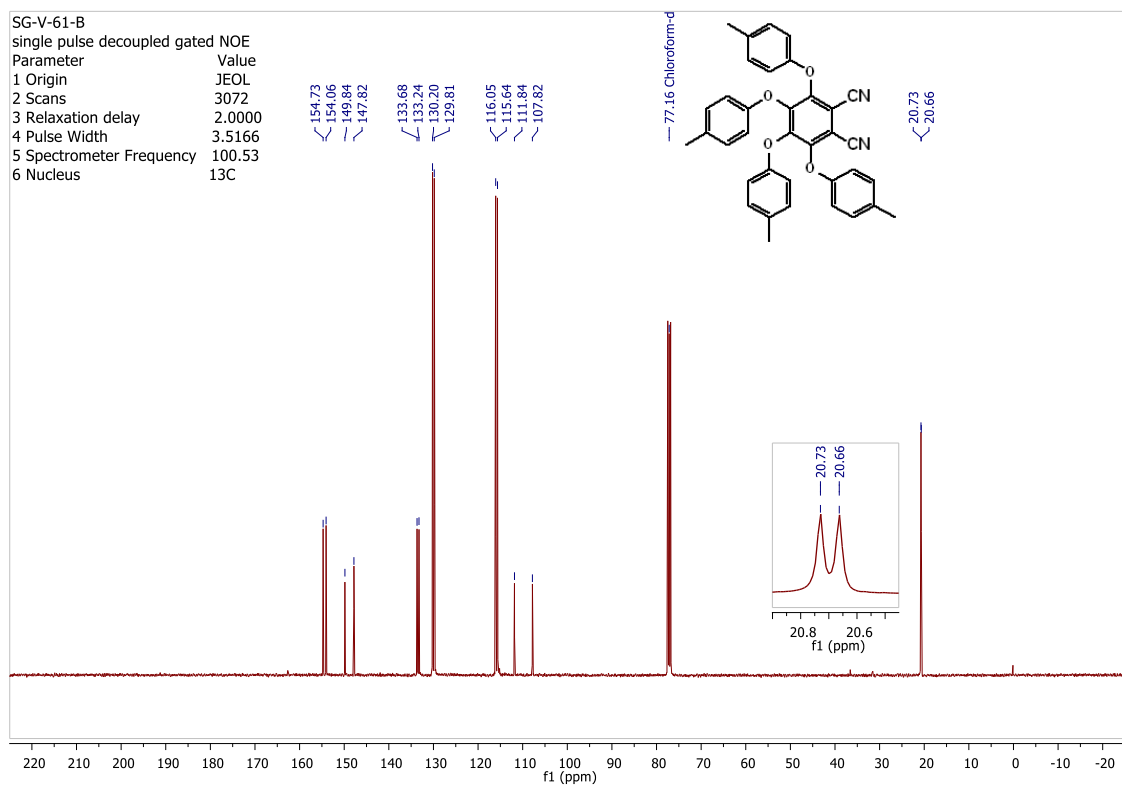
¹H NMR (399.78 MHz, CDCl₃)¹³C-NMR (CDCl₃, 100.53 MHz)

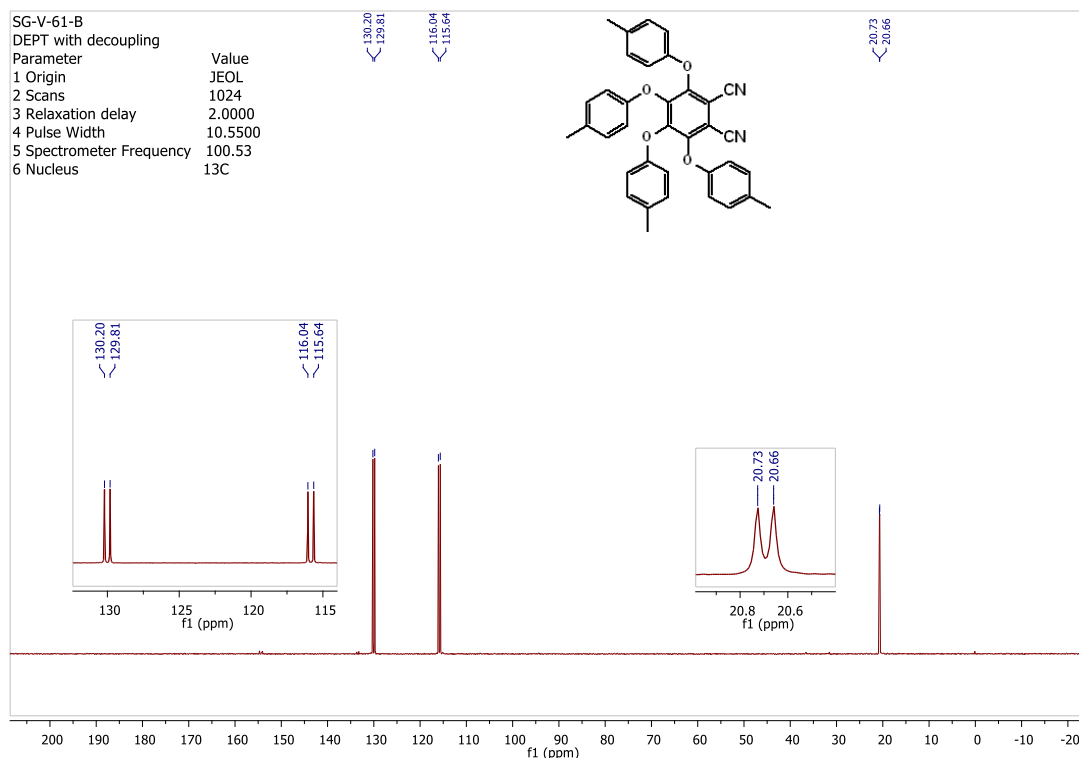
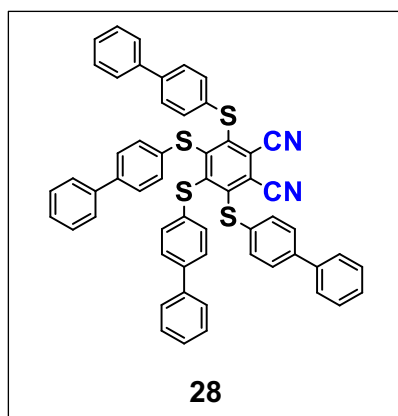
¹³C-NMR DEPT 135 (CDCl₃, 100.53 MHz)

Procedure for asterisk-27 (R-223): In an oven-dried sealed tube, purged with argon, was added (1) tetrafluorophthalonitrile (1.010gm, 5.048mmol, 1eq.), dried potassium carbonate (3.009gm, 21.773mmol, 4.3eq.) and p-cresol (2.30mL, 2.377gm, 21.989mmol, 4.4eq.) and dry DMF (8.0 mL, dried and kept over activated molecular sieves 3Å). Argon was bubbled through the mixture for 5-10 minutes. The color

changed from off white to yellow. The tube was sealed and the reaction was stirred at RT (25-28°C) in an oil bath for 2 days. The reaction mixture was quenched with NaOH (1M, 15mL). It was triturated with EtOH (10 mL) and H₂O (10 mL) at 25°C overnight and filtered to get white solid. **Mass: 2.64 gm, Yield= 94.6%**

SG-V-61-B: ¹H NMR (399.78 MHz, TMS): δ = 7.04 (d, 4H, J=7.9 Hz), 6.92 (d, 4H, J=7.9 Hz), 6.68 (d, 4H, J=7.8 Hz), 6.43 (d, 4H, J=7.8 Hz); ¹³C NMR (100.53 MHz, CDCl₃) **SG-V-61-B:** 154.73, 154.06, 149.84, 147.82, 133.68, 133.24, 130.20, 129.81, 116.05, 115.64, 111.84, 107.82, 20.73, 20.66; (¹³⁵-DEPT) NMR (CDCl₃), **SG-V-61-B:** 130.20, 129.81, 116.04, 115.64, 20.73, 20.66; **M.p.:** 184.9-186°C; **TLC** (acetone:Cyclohex: 30/70 v/v), **Rf= 0.51**

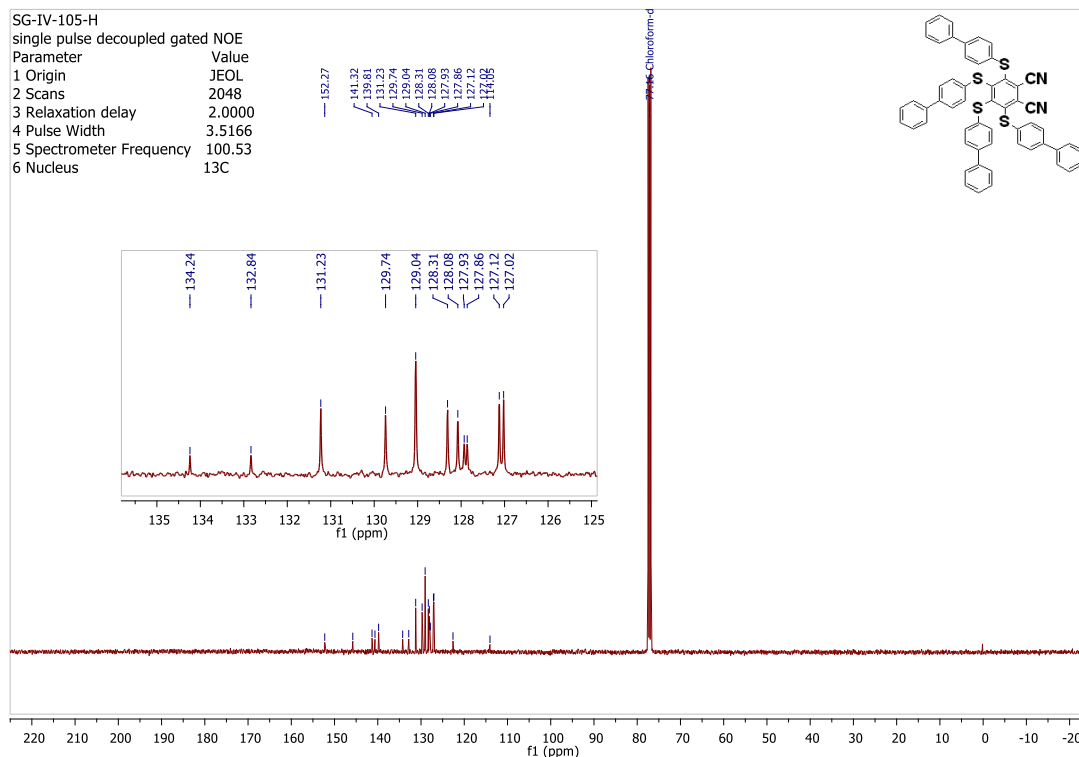
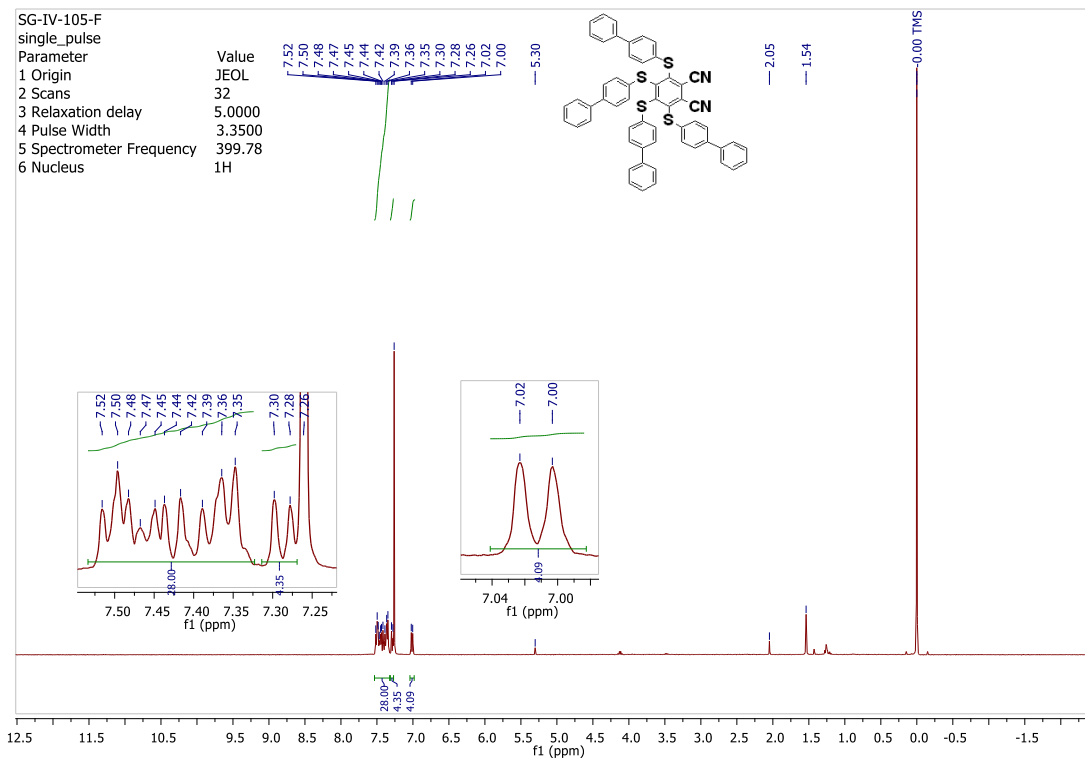
 ^1H NMR (399.78 MHz, CDCl_3) ^{13}C -NMR (CDCl_3 , 100.53 MHz)

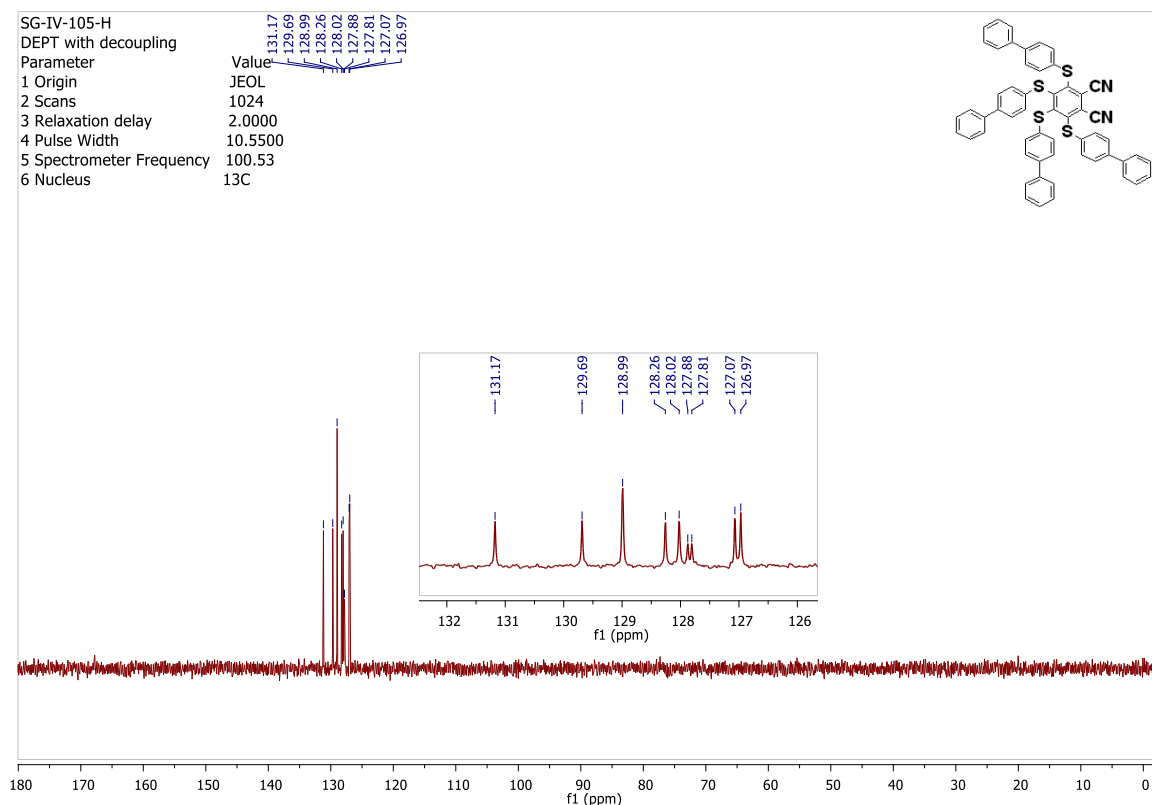
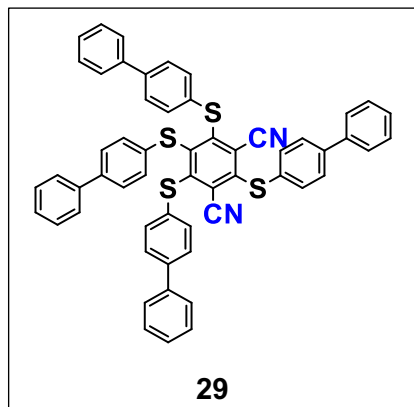
¹³C-NMR DEPT 135 (CDCl₃, 100.53 MHz)

Procedure for asterisk-28 (R-176): In an oven-dried sealed tube, purged with argon, was added (1) tetrafluorophthalonitrile (61.3mg, 0.306mmol, 1eq.), dried potassium carbonate (185.5mg, 1.342mmol, 4.4eq.) and 4-biphenyl thiol (250.8mg, 1.346mmol, 4.4eq.) and dry DMF (2.0 mL, dried and kept over activated molecular sieves 3Å). Argon was bubbled through the mixture for 5-10 minutes. The color changed

from off white to yellow. The tube was sealed and the reaction was stirred at 60°C in an oil bath for 7 days. To the crude mixture was added H₂O (15 mL), and the solid was filtered and the residue was purified using column chromatography (eluent: DCM/ cyclohexane). **Mass: 189.9 mg, Yield= 72%**

SG-IV-105-F: ¹H NMR (399.78 MHz, TMS): δ = 7.52-7.35 (m, 28H), 7.30 (d, 4H, J= 8.0 Hz), 7.02 (d, 4H, J= 7.9 Hz); ¹³C NMR (100.53 MHz, CDCl₃) **SG-IV-105-H:** 152.27, 145.78, 141.32, 140.65, 139.81, 134.24, 132.84, 131.23, 129.74, 129.04, 128.31, 128.08, 127.93, 127.86, 127.12, 127.02, 122.61, 114.05; (¹³⁵-DEPT) NMR (CDCl₃), **SG-IV-105-H:** 131.17, 129.69, 128.99, 128.26, 128.02, 127.88, 127.81, 127.07, 126.97; **M.p.:** 263-265°C; **TLC** (Tol:Cyclohex: 80/20 v/v), **R_f**= 0.43



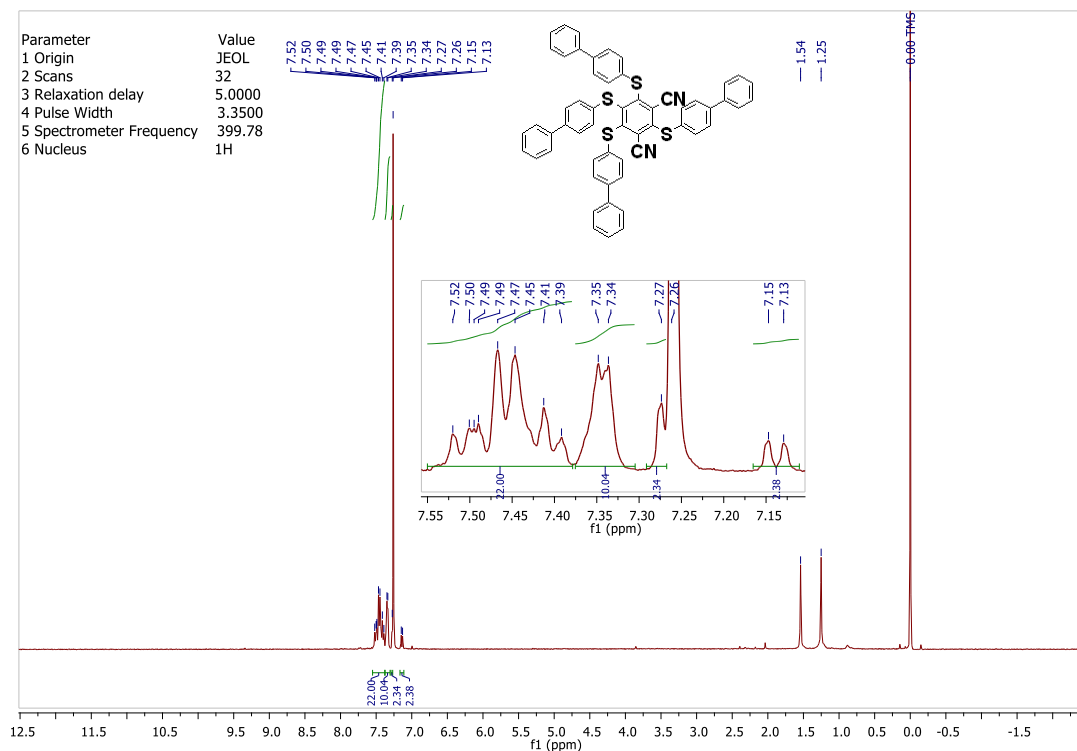
 ^{13}C -NMR DEPT 135 (CDCl_3 , 100.53 MHz)

Procedure for asterisk-29 (R-197): In an oven-dried sealed tube, purged with argon, was added (**10**) tetrafluoroisophthalonitrile (60.5mg, 0.302mmol, 1eq.), dried potassium carbonate (174.2mg, 1.260mmol, 4.2eq.) and 4-biphenyl thiol (234.7mg, 1.259mmol, 4.2eq.) and dry DMF (3.0 mL, dried and kept over activated molecular sieves 3\AA). Argon was bubbled through the mixture for 5-10 minutes. The color

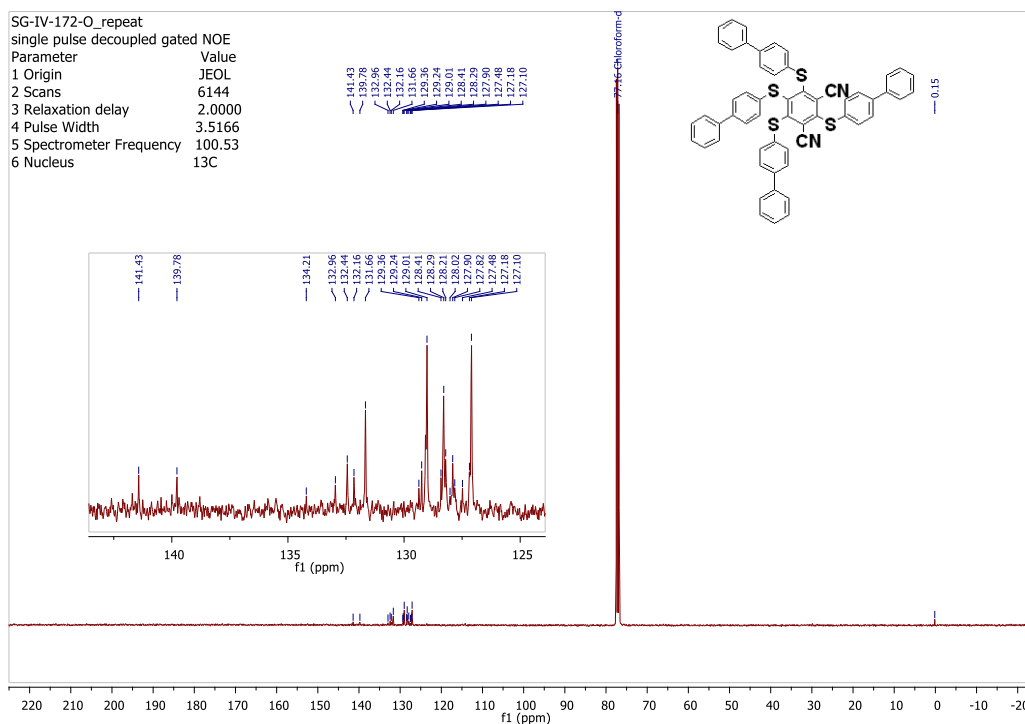
changed from off white to bright-yellow. The tube was sealed and the reaction was stirred at 60°C in an oil bath for 94 hours. The crude mixture was triturated with EtOH (10 mL) and H_2O (10 mL) at 50°C for 3hours and filtered to get yellow solid. **Mass: 184.0 mg, Yield= 70%.**

SG-IV-172-N: ^1H NMR (399.78 MHz, TMS): δ = 7.52-7.39 (m, 22H), 7.35-7.34 (m, 10H), 7.27 (d, 2H), 7.15 (d, 2H, J = 7.1 Hz); ^{13}C NMR (100.53 MHz, CDCl_3) **SG-IV-172-O_repeat:** 141.43, 139.78, 134.21, 132.96, 132.44, 132.16, 131.66, 129.36, 129.24, 129.01, 128.41, 128.29, 128.21, 128.02, 127.90, 127.82, 127.48, 127.18,

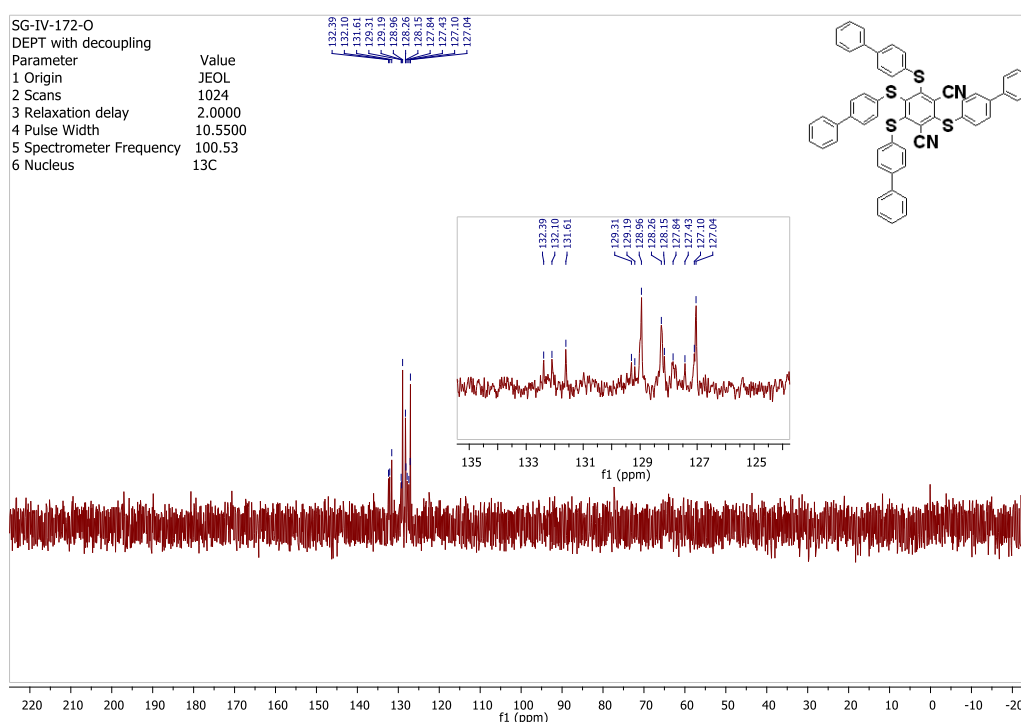
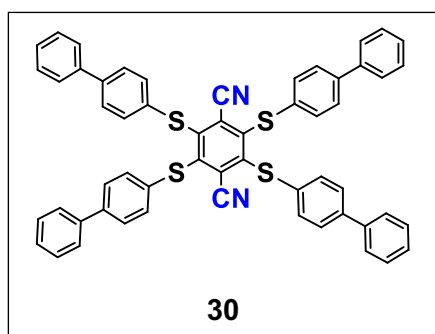
127.10; (135°-DEPT) NMR (CDCl₃), **SG-IV-172-O**: 132.39, 132.10, 131.61, 129.31, 129.19, 128.96, 128.26, 128.15, 127.84, 127.43, 127.10, 127.04; **M.p.**: 269.8-271°C; **TLC** (Tol:Cyclohex: 80/20 v/v), **R_f**= 0.57



¹H NMR (399.78 MHz, CDCl₃)

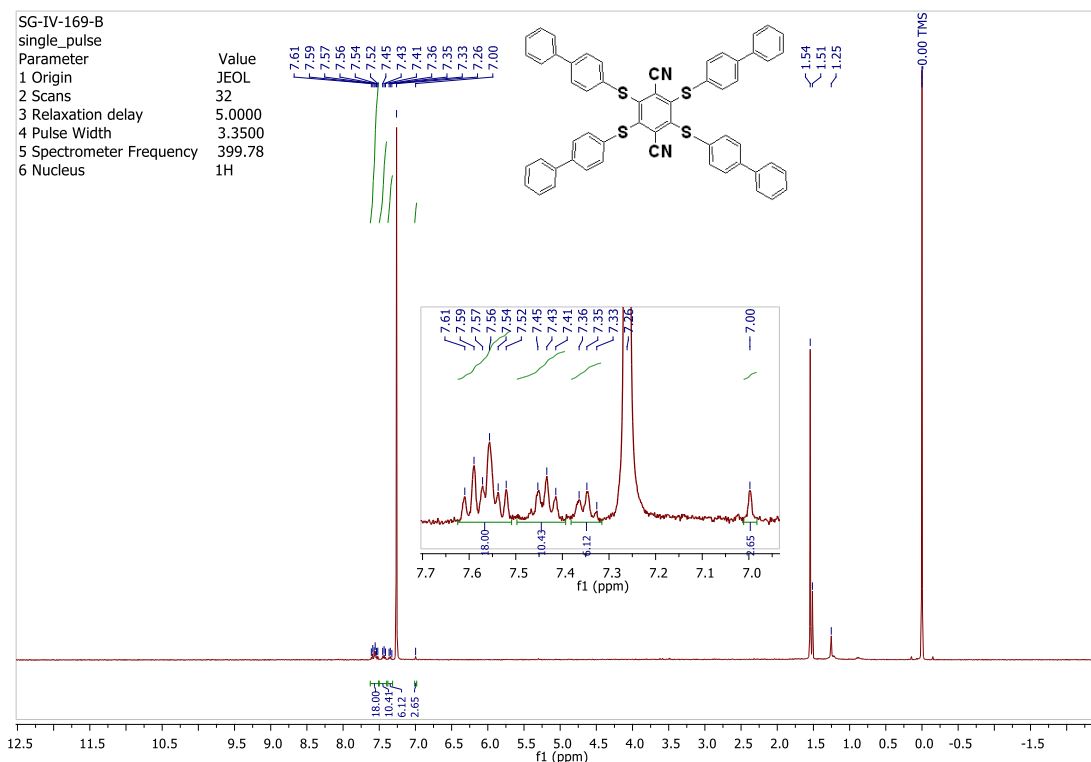


¹³C-NMR (CDCl₃, 100.53 MHz)

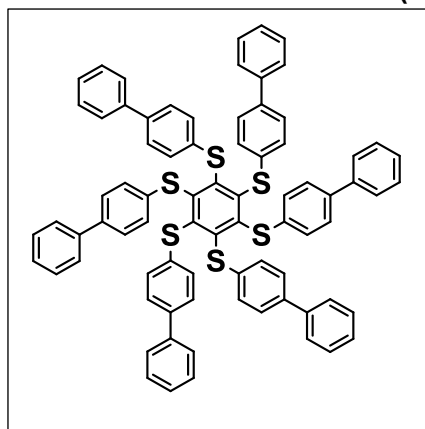
 ^{13}C -NMR DEPT 135 (CDCl_3 , 100.53 MHz)

Procedure for asterisk-30 (R-196): In an oven-dried sealed tube, purged with argon, was added (**14**) tetrafluoroterephthalonitrile (60.7mg, 0.303mmol, 1eq.), dried potassium carbonate (174.9mg, 1.265mmol, 4.2eq.) and 4-biphenyl thiol (234.9mg, 1.261mmol, 4.1eq.) and dry DMF (3.5 mL, dried and kept over activated molecular sieves 3\AA). Argon was bubbled through the mixture for 5-10 minutes. The color changed from off white to bright-yellow. The tube was sealed and the reaction was stirred at 64°C in an oil bath for 70 hours. The crude mixture was triturated with EtOH (5 mL) and H_2O (10 mL) at RT ($25\text{-}28^\circ\text{C}$) for 20 minutes and filtered to get red-orange solid. **Mass: 246.3 mg, Yield= 94%**

SG-IV-172-N: ^1H NMR (399.78 MHz, TMS): $\delta = 7.61\text{-}7.52$ (m, 18H), 7.43 (t, 10H, $J = 7.7$ Hz), 7.35 (t, 6H, $J = 6.6$ Hz), 7.00 (s, 2H); ^{13}C NMR (100.53 MHz, CDCl_3); Not soluble to do ^{13}C -NMR; **M.p.:** $374.2\text{-}375.2^\circ\text{C}$; **TLC:** Not Soluble

 ^1H NMR (399.78 MHz, CDCl_3)

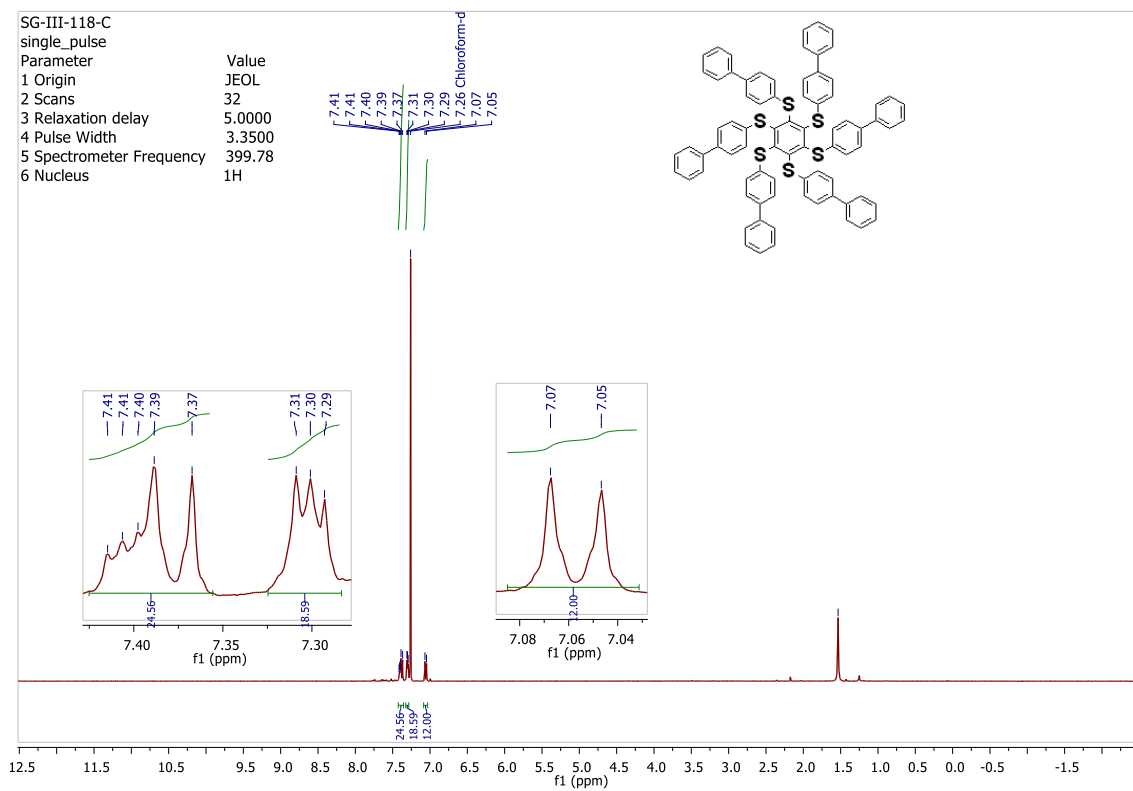
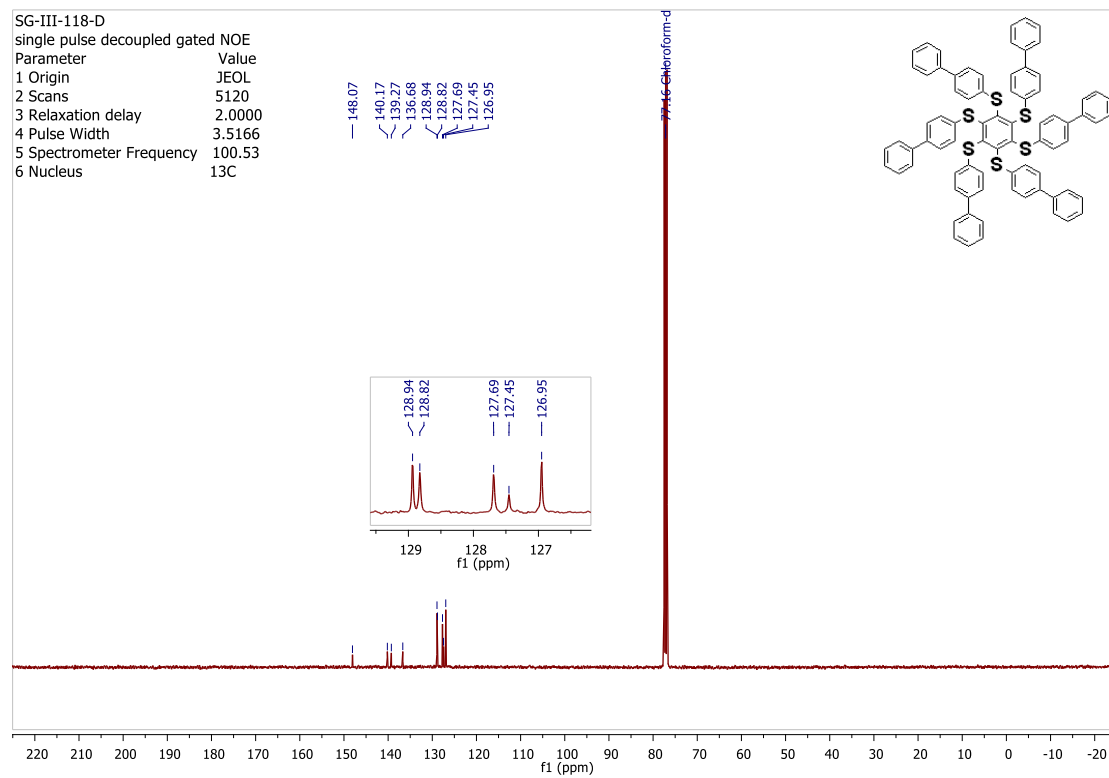
Procedure for asterisk-31 (R-117): In an oven dried sealed tube, purged with argon,

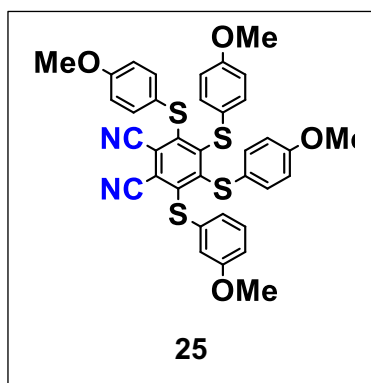


was added hexachlorobenzene (C_6Cl_6) (20.6mg, 0.072mmol, 1.0eq.), dried Potassium carbonate (87.4mg, 0.632mmol, 9eq.), biphenyl-4-thiol (118.7mg, 0.637mmol, 9eq.) in dry DMF (1mL -dried with molecular sieves 3\AA). Argon was bubbled through the mixture for 5-10minutes in the tube. The tube was sealed and the reaction was stirred at 90°C for 40hours. Most DMF was removed on a rotary

evaporator under reduced pressure. The reaction mixture was extracted with H_2O (35mL) and toluene ($4 \times 35\text{mL}$). The collected organic phase was dried over anhydrous MgSO_4 , filtered. The crude mixture was triturated with EtOH (30 mL) at RT ($25\text{-}28^\circ\text{C}$) and was filtered to get yellow-orange solid. **Mass: 68.8mg, Yield= 82%**

SG-III-118-C: ^1H NMR (399.78 MHz, TMS): $\delta = 7.41\text{-}7.37$ (m, 24H), $7.31\text{-}7.29$ (m, 18H), 7.07 (d, 12H, $J = 6.3$ Hz); ^{13}C NMR (100.53 MHz, CDCl_3) **SG-III-118-D:** 148.07, 140.17, 139.27, 136.68, 128.94, 128.82, 127.69, 127.45, 126.95; **M.p.:** $250\text{-}252.8^\circ\text{C}$; **TLC** (Tol:Cyclohex: 30/70 v/v), **Rf**= 0.40

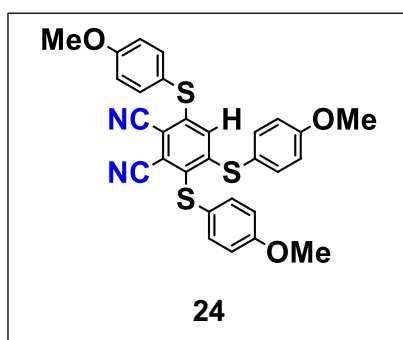
 ^1H NMR (399.78 MHz, CDCl_3) ^{13}C -NMR (CDCl_3 , 100.53 MHz)

**Procedure for asterisk-24 and asterisk-25 (byproduct)**

(R-241): In an oven-dried sealed tube, purged with argon, was added (1) tetrafluorophthalonitrile (201.1 mg, 1.005mmol, 1eq.), dried potassium carbonate (830.8mg, 6.011mmol, 6eq.), 4-methoxythiophenol (843.6mg, 0.74mL, 6.017mmol, 6eq.) and dry DMF (2.0 mL, dried and kept over activated molecular sieves 3Å). Argon was

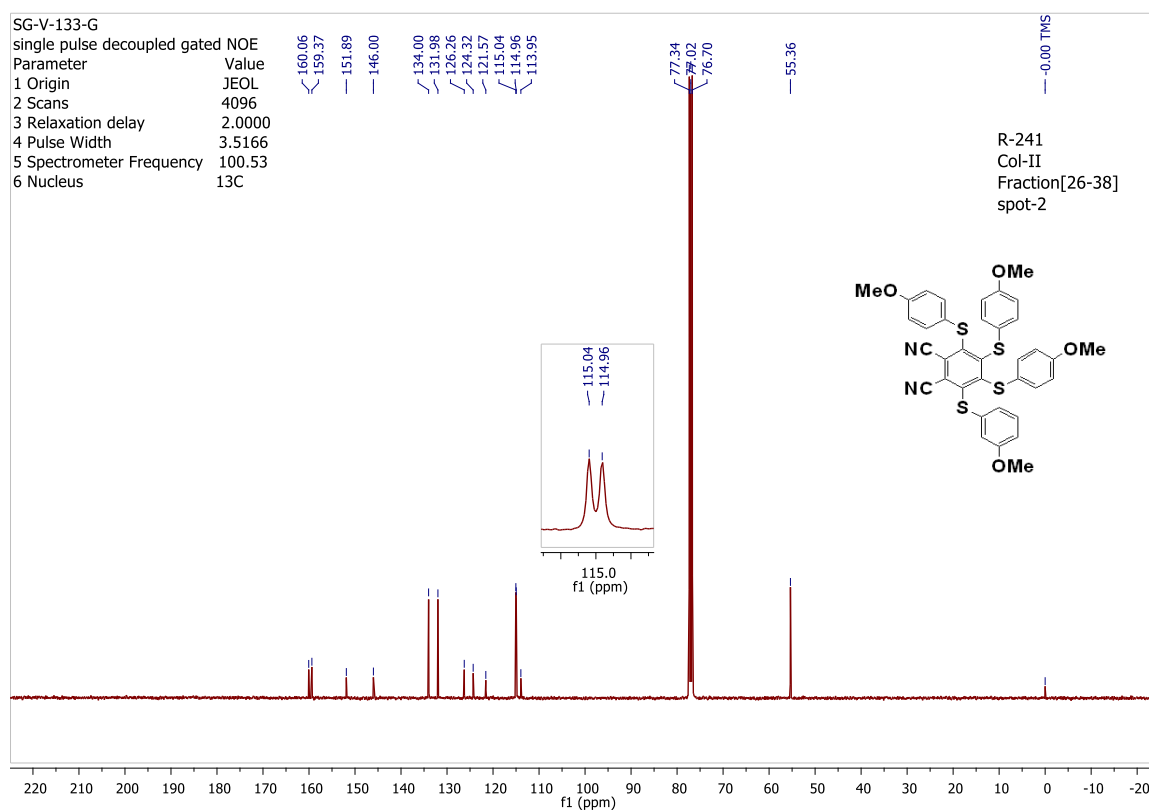
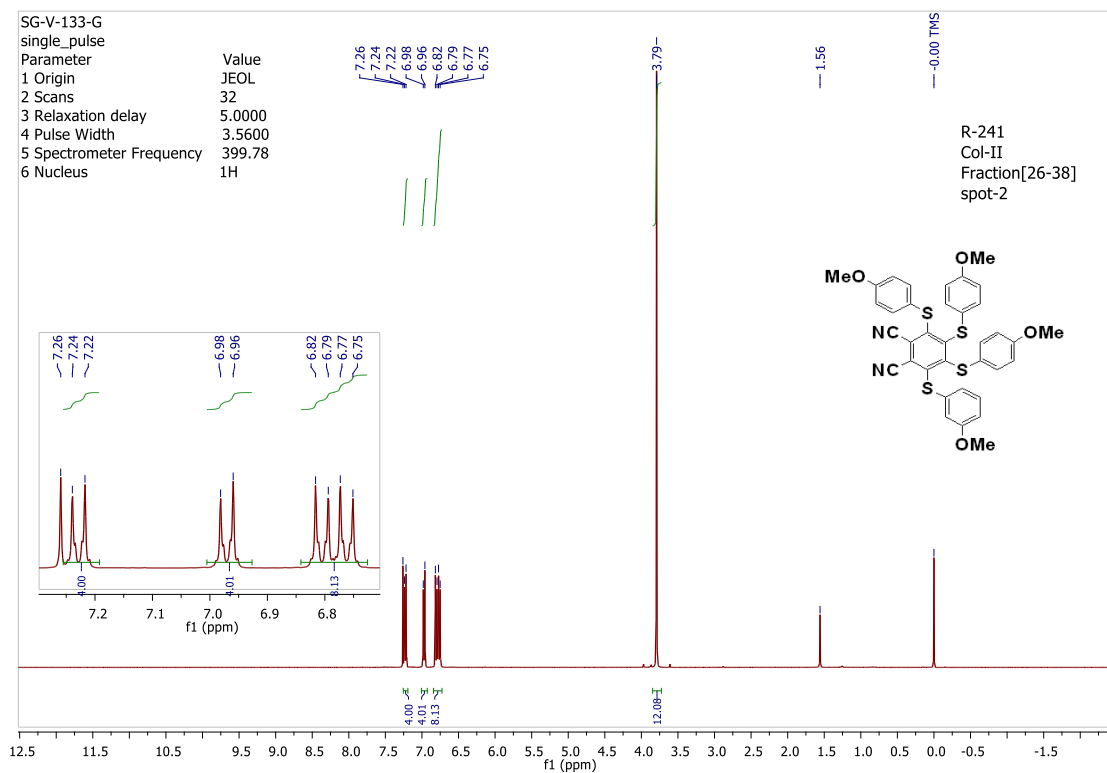
bubbled through the mixture for 5-10 minutes. The color changed from off white to yellow. The tube was sealed and the reaction was stirred at 60°C for 3 days in an oil bath. Most DMF was removed on a rotary evaporator under reduced pressure. It was triturated with EtOH (10 mL) and H₂O (20 mL) at 25°C overnight and filtered to get yellow solid. The solid was purified by doing two columns. First using column chromatography (eluent: Acetone/ cyclohexane, 30/70 v/v) and column chromatography (eluent: DCM/ cyclohexane, 80/20 v/v). **Mass: 243.3 mg, Yield= 39%**

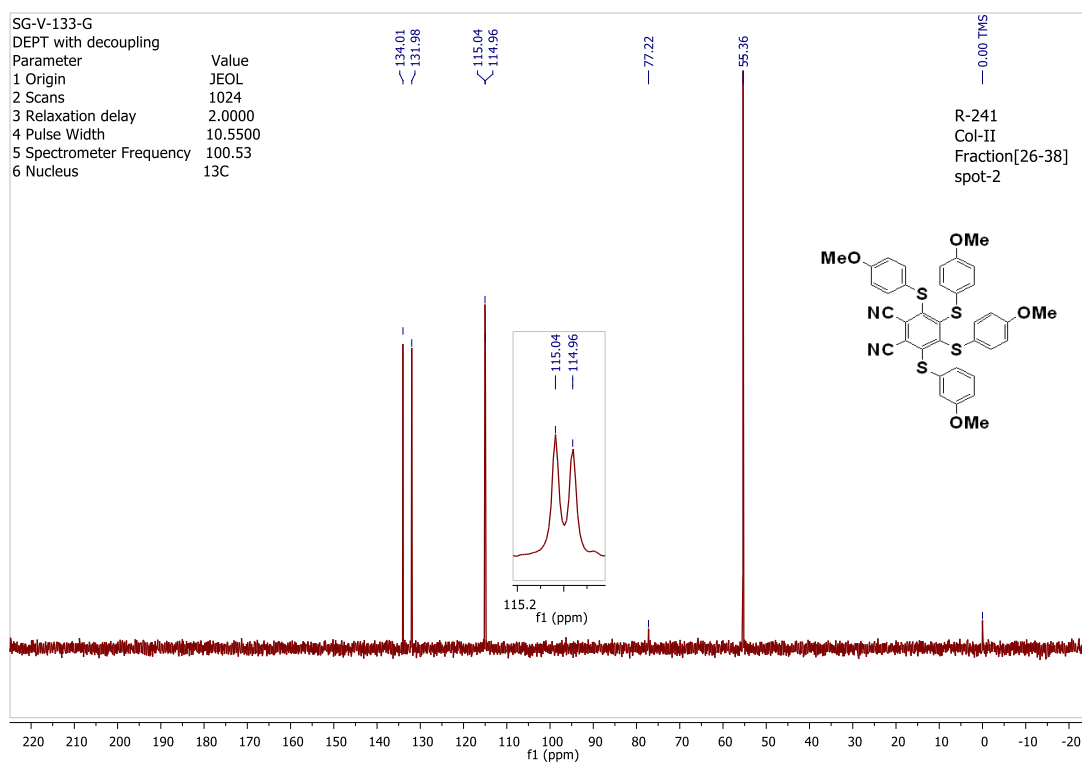
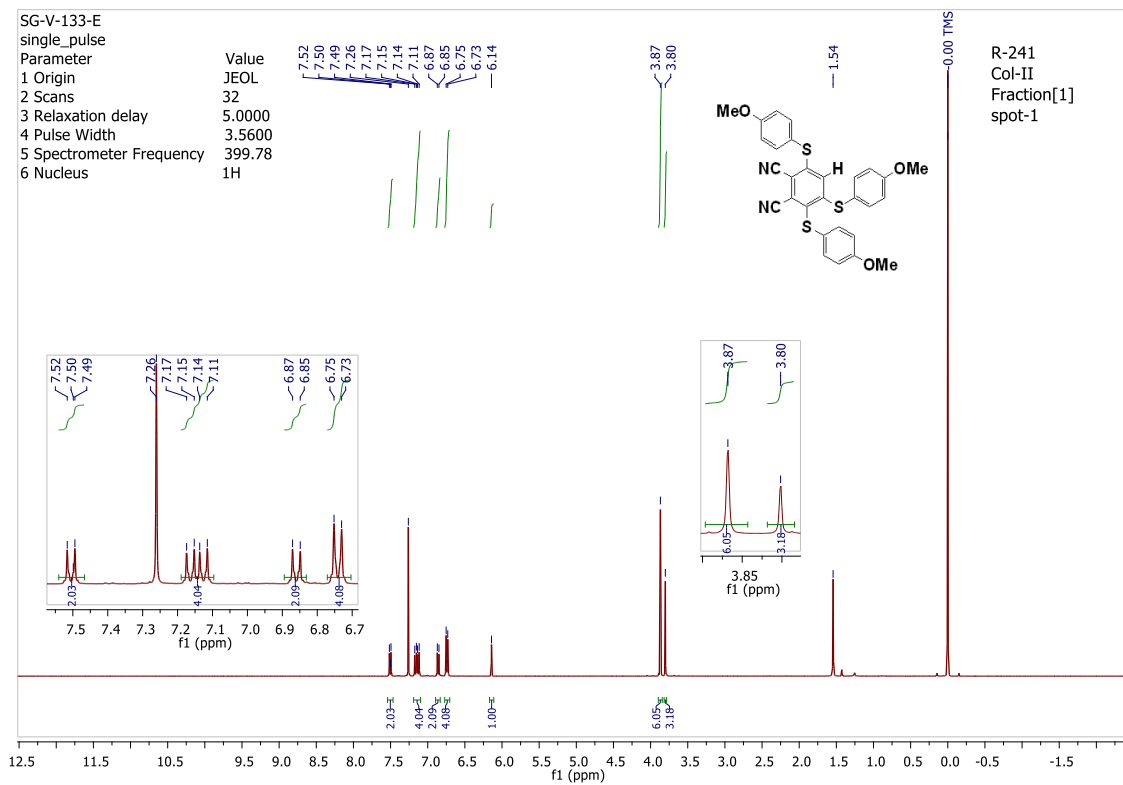
SG-V-133-G: ¹H NMR (399.78 MHz, CDCl₃): δ =7.24 (d, 4H, J= 8.75 Hz), 6.98 (d, 4H, J= 8.71 Hz), 6.82 (d, 4H, J= 8.76 Hz), 6.77 (d, 12H, J= 8.96 Hz), 3.79 (s, 12H); ¹³C NMR (100.53 MHz, CDCl₃), **SG-V-133-G:** 160.06, 159.37, 151.89, 146.00, 134.00, 131.98, 126.26, 124.32, 121.57, 115.04, 114.96, 113.95, 55.36; (135°-DEPT) NMR (CDCl₃), **SG-V-133-G:** 134.01, 131.98, 115.04, 114.96, 55.36; **M.p.:** 129-133°C; **TLC** (DCM:Cyclohex: 50/50 v/v), **R_f**= 0.4

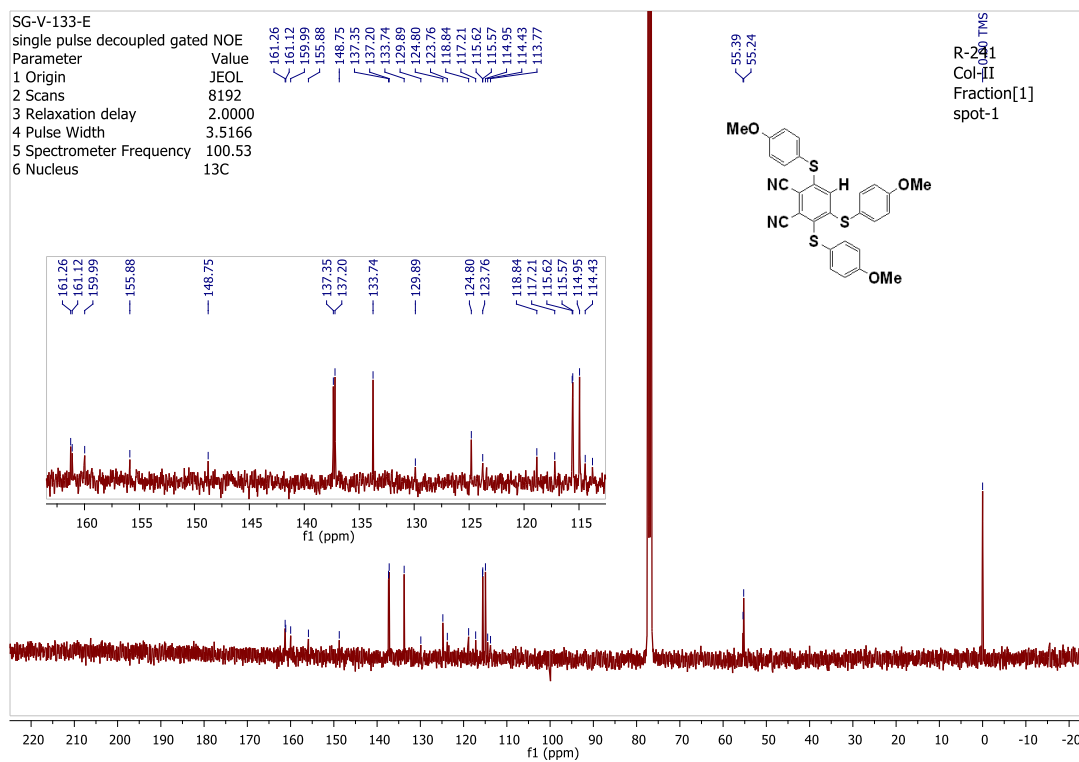
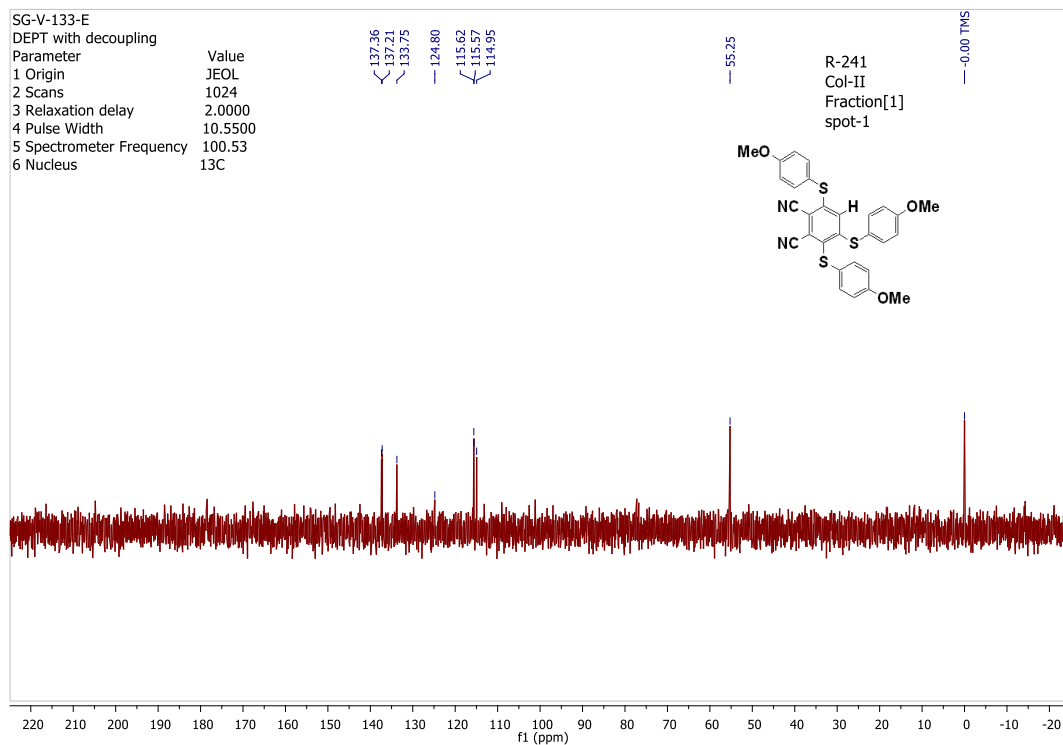


SG-V-133-E: ¹H NMR (399.78 MHz, CDCl₃): δ =7.50 (d, 2H, J= 8.77 Hz), 7.17 (d, 2H, J= 8.74 Hz), 7.14 (d, 2H, J= 8.71 Hz), 6.87 (d, 2H, J= 8.81 Hz), 6.75 (d, 4H, J= 8.66 Hz), 3.87 (s, 6H), 3.80 (s, 3H); ¹³C NMR (100.53 MHz, CDCl₃), **SG-V-133-E:** 161.26, 161.12, 159.99, 155.88, 148.75, 137.35, 137.20, 133.74, 129.89, 124.80, 123.76, 118.84, 117.21, 115.62,

115.57, 114.95, 114.43, 113.77, 55.39, 55.24; (135°-DEPT) NMR (CDCl₃), **SG-V-133-E:** 137.36, 137.21, 133.75, 124.80, 115.62, 115.57, 114.95, 55.25; **M.p.:** 190-193°C; **TLC** (DCM:Cyclohex: 80/20 v/v), **R_f**= 0.4, Mass: 44.3mg



 ^{13}C -NMR DEPT 135 (CDCl_3 , 100.53 MHz) ^1H NMR (399.78 MHz, CDCl_3)

 ^{13}C -NMR (CDCl_3 , 100.53 MHz) ^{13}C -NMR DEPT 135 (CDCl_3 , 100.53 MHz)

PERSULFURATED BENZENE-CORED ASTERISKS WITH Π -EXTENDED THIO-NAPHTHYL ARMS: SYNTHESIS, STRUCTURAL, PHOTOPHYSICAL AND COVALENT DYNAMIC PROPERTIES

Note:

This section is mostly taken from an article submitted for publication in a scientific journal with a supporting information.

This work comprises some photophysical studies achieved by the group of Pr. Paola Ceroni, "G. Ciamician" department of chemistry at the University of Bologna, Italy.

Sc-XRD studies were achieved by Dr. Michel Giorgi, from Aix-Marseille Université, France.

Some LC-HRMS experiments were performed by Dr. Jean-Louis Schmitt in the group of Pr. Jean-Marie Lehn at ISIS, University of Strasbourg, France

Supporting information

Persulfurated Benzene-Cored Asterisks with π -Extended ThioNaphthyl Arms: Synthesis, Structural, Photophysical and Covalent Dynamic Properties

Sapna Gahlot,^[a] Alessandro Gradone^{[b],[e]} Myriam Roy,^{[a],[c]} Michel Giorgi,^[c] Simone Conti,^[b] Paola Ceroni,^{[a],[b]} Marco Villa,^{*[a],[b]} and Marc Gingras^{*[a]}

Generalities

Materials and General Procedures. All reagents, solvents and chemicals were purchased from Sigma-Aldrich, Fisher, or Alfa-Aesar and used directly unless otherwise stated (purity: reagent or analytical grade). Solvents were stored for several days over freshly activated 3 Å molecular sieves (activated for 3 h at 250 °C). All the reactions were monitored by TLC.

Thin-Layer chromatography (TLC): TLC analyses were performed on precoated silica gel (Alugram® SilG/UV254gel) aluminium plates from Macherey-Nagel. Compounds were visualized with UV-light (254 or 365 nm)

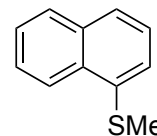
Flash chromatography was performed over silica gel 60, Merck type 230-400 mesh (40-63µm).

Melting points (uncorrected) were recorded with an Electrothermal 9200 digital melting point apparatus with a ramp rate temperature (rate increase of temperature) using samples in glass capillaries.

NMR spectra ¹H (399.78 MHz) and ¹³C (100.53 MHz) were recorded on JEOL ECX-400 spectrometer signals of the residual protic solvent CHCl₃ at 7.26 ppm was used as internal references, along with TMS when needed. As for ¹³C NMR spectra, the central resonance of the triplet for CDCl₃ at 77.16 ppm was used as internal references.^[1] The resonance multiplicities in the ¹H NMR spectra are described as “s” (singlet), “d”(doublet), “m” (multiplet) or “b” (broad).

Photophysical measurements: Photophysical measurements were carried out in dichloromethane at 298 K. Luminescence measurements at 77 K were performed in dichloromethane/methanol (1:1 v/v). UV–vis absorption spectra were recorded with a PerkinElmer I40 spectrophotometer using quartz cells with path length of 1.0 cm. Emission spectra were obtained with either a Perkin Elmer LS55 spectrofluorometer, equipped with a Hamamatsu R928 phototube, or an Edinburgh FLS920 spectrofluorometer. Excitation spectra in the visible range were acquired with the fluorimeter Perkin-Elmer LS55. Emission quantum yields were measured following the method of Demas and Crosby [G. A. Crosby, J. N. Demas, *J. Phys. Chem.* **1971**, 75, 991-1024.]. Standards used: [Ru(bpy)₃]²⁺ in air-equilibrated aqueous solution $\Phi = 0.0405$. [K. Suzuki, A. Kobayashi, S. Kaneko, K. Takehira, T. Yoshihara, H. Ishida, Y. Shiina, S. Oishi and S. Tobita, *Phys. Chem. Chem. Phys.* **2009**, 11, 9850–9860]. Lifetimes shorter than 10 µs were measured by the above-mentioned Edinburgh FLS920 spectrofluorimeter equipped with a TCC900 card for data acquisition in time-correlated single-photon counting experiments (0.5 ns time resolution) with 405 nm laser. Longer lifetimes (ms to s range) were measured by the PerkinElmer LS-55. The estimated experimental errors are: 2 nm on the absorption and emission band maximum, 5% on the molar absorption coefficient and luminescence lifetime, and 10% on the luminescence and photoisomerization quantum yields.

1-(Methylthio)naphthalene (1): 1-naphthalenethiol (80 μ L, 0.50 mmol, 1.0 mol-eq.) and dry potassium carbonate (516.0 mg, 3.73 mmol, 7.46 mol-eq.) were added to an oven-dried pressure tube under argon. Dry DMF (1.0 mL, dried over activated 3 \AA molecular sieves) was injected via a syringe, and argon was bubbled in the mixture for 15 min., and then iodomethane (0.10 mL, 228.0 mg, 1.6 mmol, 3.2 mol-eq.) was added via a syringe. The flask was sealed under argon and the reaction mixture was stirred for 4 days at 50 $^{\circ}$ C. Stirring continued for 7 days at 70 $^{\circ}$ C and then 4 days at 80 $^{\circ}$ C. After cooling to RT, the flask was opened and water was added (20 mL) while stirring. The aqueous phase was extracted with toluene (5 \times 15 mL). The combined organic layers were dried over anhydrous MgSO₄, filtered and concentrated *in vacuo*. Purification by column chromatography over silica gel using 100% cyclohexane as eluent provided the desired product as a colorless oil (11.6 mg, 0.067 mmol, 13% yield). **TLC** (SiO₂, acetone/cyclohex. 5:95 v/v) R_f = 0.6; **¹H NMR (399.78 MHz, CDCl₃, ppm)**: δ = 8.28 (br d, *J* = 7.9 Hz, 1H), 7.84 (br d, *J* = 8.2 Hz, 1H), 7.67 (br d, *J* = 7.6 Hz, 1H), 7.48-7.57 (m, 2H), 7.43 (dd, *J* = 7.5, 7.5 Hz, 1H), 7.39 (dd, *J* = 7.2, 1.3 Hz, 1H), 2.58 (s, 3H); **¹³C NMR (100.53 MHz, CDCl₃, ppm)**: δ = 135.94, 133.75, 131.77, 128.66, 126.37, 126.27, 125.96, 125.82, 124.41, 123.74, 16.35.



References: a) Gasco, A.; Di Modica, G.; Barni, E. *Annali di Chimica* (Rome, Italy) **1968**, *58*, 385-392; b) Overberger, C. G.; Lighthelm, Salomon P.; Swire, Edwin A. *J. Am. Chem. Soc.* **1950**, *72*, 2856-2859; c) Taboury, F. *Annales de Chimie et de Physique* **1908**, *15*, 5-66.

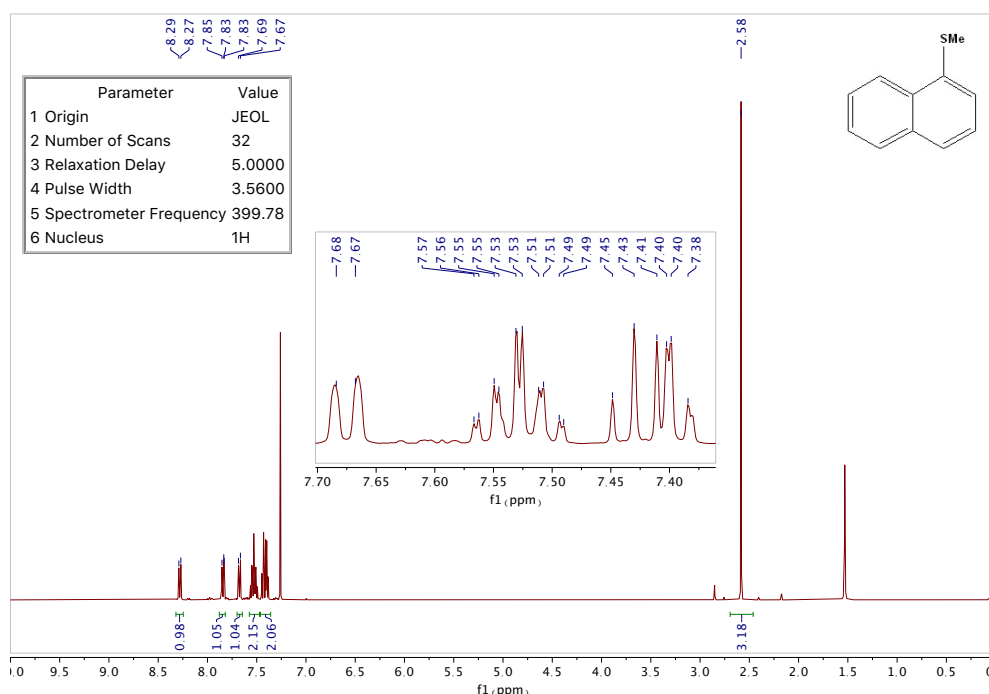


Figure S1 ¹H-NMR spectrum of (1) (CDCl₃, 399.78 MHz)

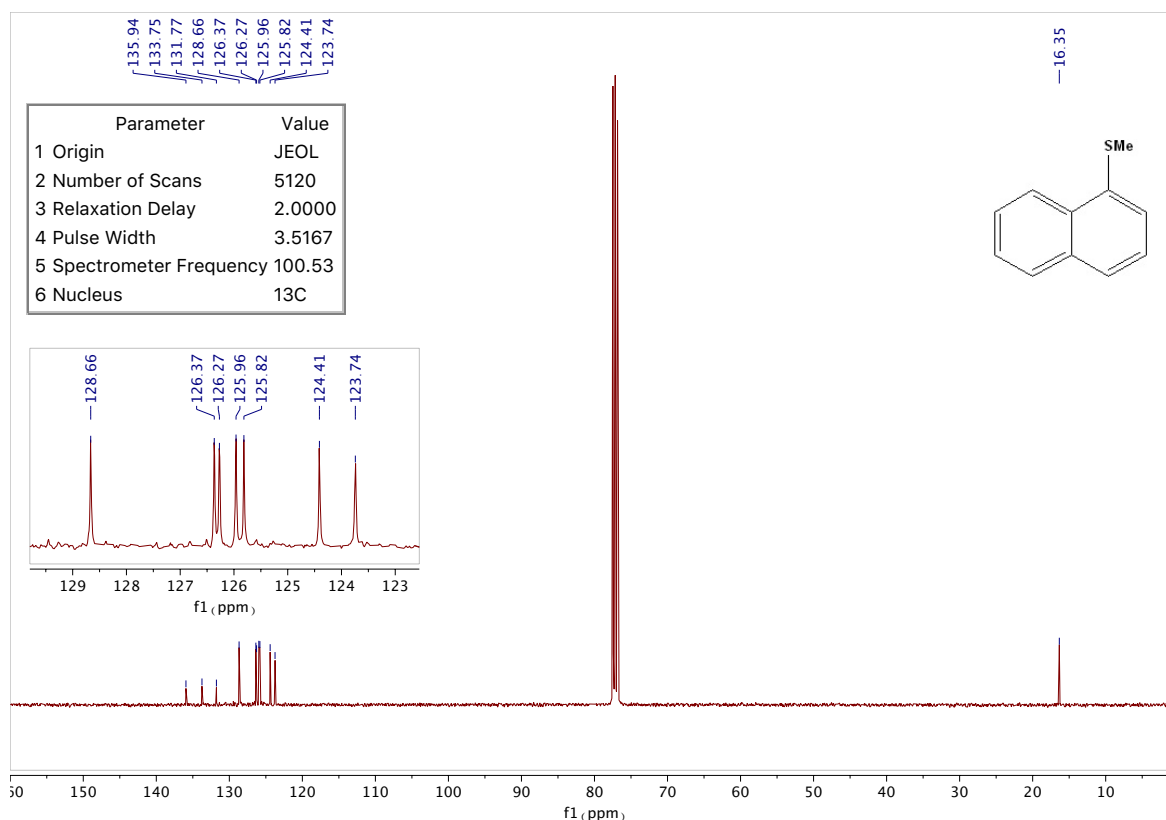
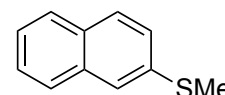


Figure S2 ^{13}C -NMR spectrum of **(1)** (CDCl_3 , 100.53 MHz)

2-(Methylthio)naphthalene (2): Into an oven-dried pressure tube was added 2-naphthalenethiol (301.0 mg, 1.87 mmol, 1.00 mol-eq.) and potassium carbonate (776.2 mg, 5.62 mmol, 3.01 mol-eq.) under argon. Dry DMF (1.0 mL, dried over activated 3\AA molecular sieves) was injected via a syringe and argon was bubbled through the mixture for about 15 min., and then iodomethane (350 μL , 5.62 mmol, 3.00 mol-eq.) was added via a syringe. The flask was sealed under argon and the reaction mixture was stirred for 2.5 days at 40°C . It was diluted with water (20 mL) and extracted with toluene (4×20 mL). The combined organic layers were dried over anhydrous MgSO_4 , filtered and concentrated *in vacuo*. The desired product was obtained as a colorless solid (322.0 mg, 1.85 mmol, 98%).



M.p.: $57\text{--}59^\circ\text{C}$; **TLC** (SiO_2 , acetone/cyclohex. 5:95 v/v) $R_f = 0.6$; **^1H NMR (399.78 MHz, CDCl_3 , ppm):** $\delta = 7.77$ (d, $J = 7.6$ Hz, 1H), 7.73 (d, $J = 8.0$ Hz, 2H), 7.60 (br s, 1H), 7.35–7.50 (m, 3H), 2.59 (s, 3H); **^{13}C NMR (100.53 MHz, CDCl_3 , ppm):** $\delta = 136.21, 134.01, 131.39, 128.32, 127.85, 126.93, 126.67, 125.78, 125.35, 123.43, 15.91$.

References: a) Gasco, A.; Di Modica, G.; Barni, E. *Annali di Chimica* (Rome, Italy) **1968**, *58*, 385–392; b) Overberger, C. G.; Ligthelm, Salomon P.; Swire, Edwin A. *J. Am. Chem. Soc.* **1950**, *72*, 2856–2859.

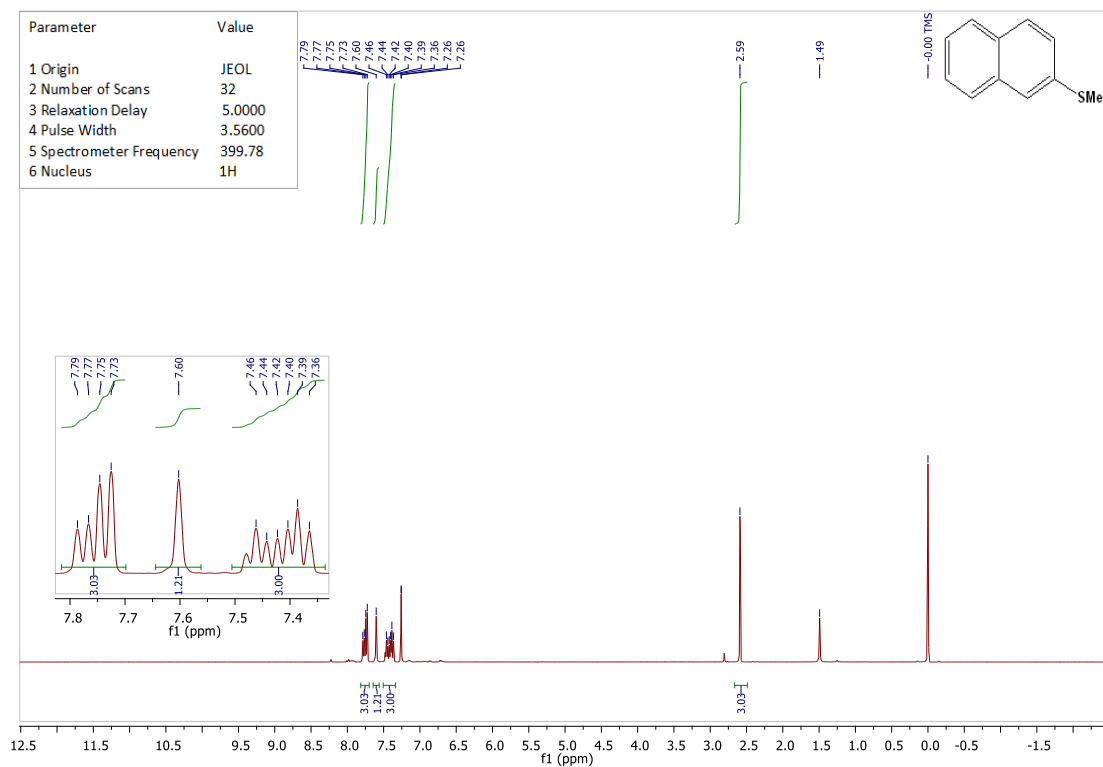


Figure S3 ¹H-NMR spectrum of **(2)** (CDCl₃, 399.78 MHz)

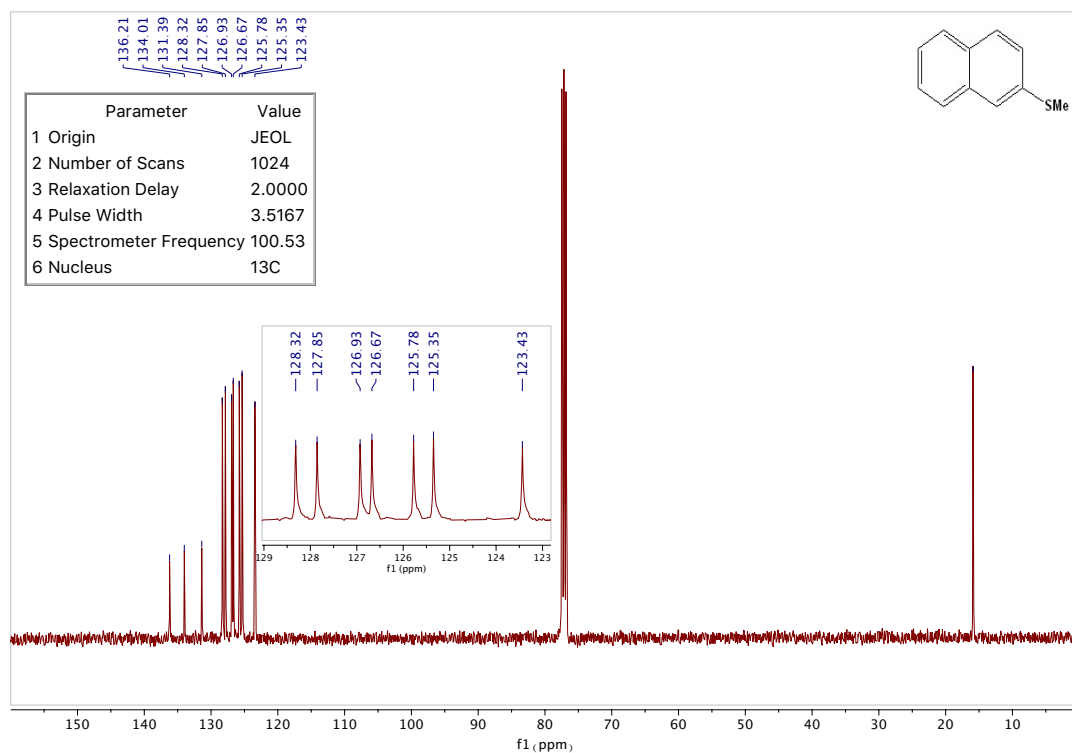
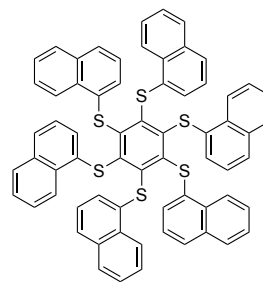


Figure S4 ¹³C-NMR spectrum of **(2)** (CDCl₃, 100.53 MHz)

Hexakis(1-naphthylthio)benzene (5). To an oven-dried pressure tube was added hexachlorobenzene (59.4 mg, 0.21 mmol, 1.00 mol-eq.) and potassium carbonate (259.7 mg, 1.88 mmol, 8.95 mol-eq.) under argon. Dry DMF (1.0 mL, dried over activated 3Å molecular sieves) was injected, and argon was bubbled for 15 min. through the mixture while stirring. 1-Naphthalenethiol was added via a syringe (0.26 mL, 300.0 mg, 1.87 mmol, 8.90 mol-eq.). The reaction mixture was stirred for 7 days at 84°C. After cooling down to 20°C and adding water (30 mL), it was extracted with chloroform (5×30 mL). The combined organic layers were dried over anhydrous MgSO₄, filtered and concentrated *in vacuo*. Purification by column chromatography over silica gel using 30% toluene/70% heptane as eluent provided the desired product (**5**) as a yellow solid (202.5 mg, 0.20 mmol, 95% yield).



M.p.: 210-213°C (*n*-hept/toluene 1:1 v/v); **TLC** (SiO₂, tol./cyclohex. 50:50 v/v) R_f = 0.56; **¹H NMR (399.78 MHz, CDCl₃, ppm):** δ = 7.89 (d, *J* = 8.2 Hz, 1H), 7.72 (d, *J* = 7.7 Hz, 1H), 7.54 (d, *J* = 8.0 Hz, 1H), 7.39 (dd, *J* = 7.4, 7.1 Hz, 1H), 7.25 (dd, *J* = 7.6, 6.5 Hz, 1H), 7.03 (dd, *J* = 7.6, 7.4 Hz, 1H), 6.83 (d, *J* = 6.8 Hz, 1H); **¹³C NMR (100.53 MHz, CDCl₃ ppm):** δ = 148.51, 134.97, 133.99, 131.46, 128.49, 127.06, 126.95, 126.21, 126.16, 125.47, 124.79; **¹³C NMR (DEPT135; 100.53 MHz, CDCl₃ ppm):** δ = 128.45, 127.02, 126.92, 126.17, 126.12, 125.44, 124.75; **HRMS (ESI+)** calculated for [C₆₆H₄₂S₆]: 1026.1605 Da; found [M⁺] 1026.1576 *m/z*.

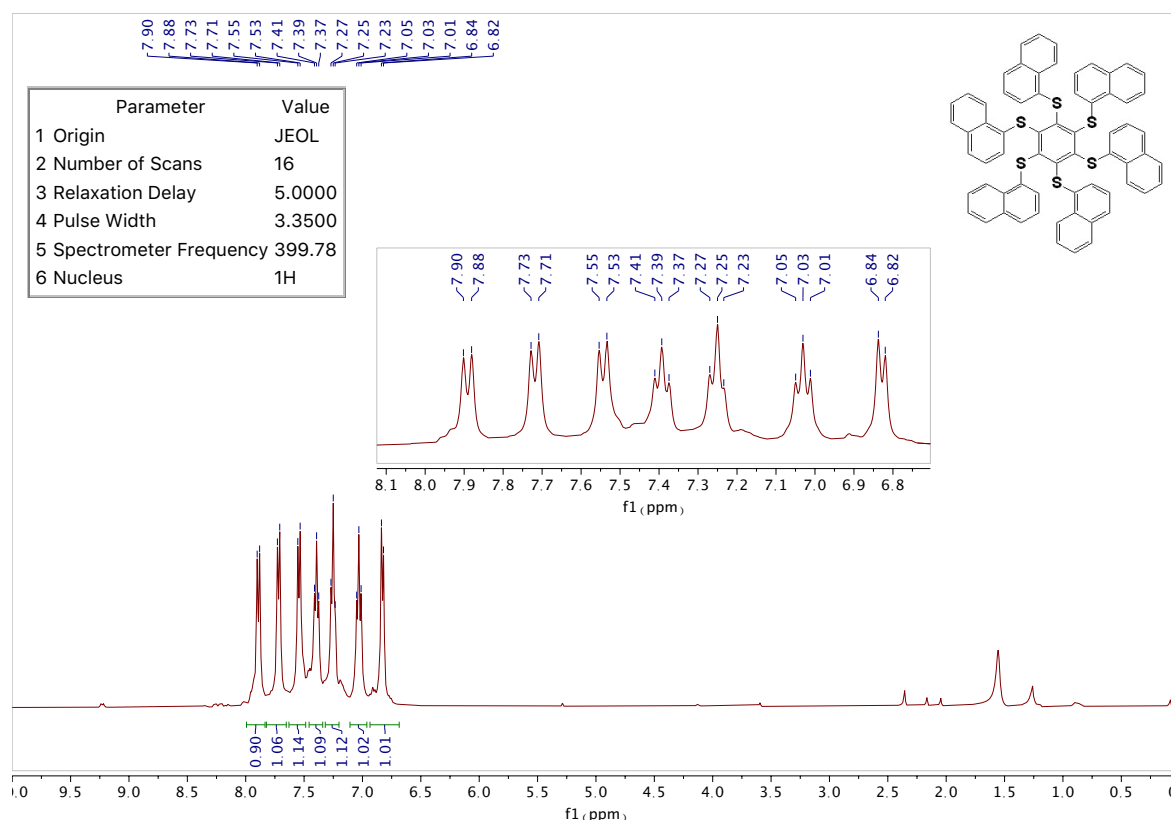


Figure S5 ¹H-NMR spectrum of (**5**) (CDCl₃, 399.78 MHz)

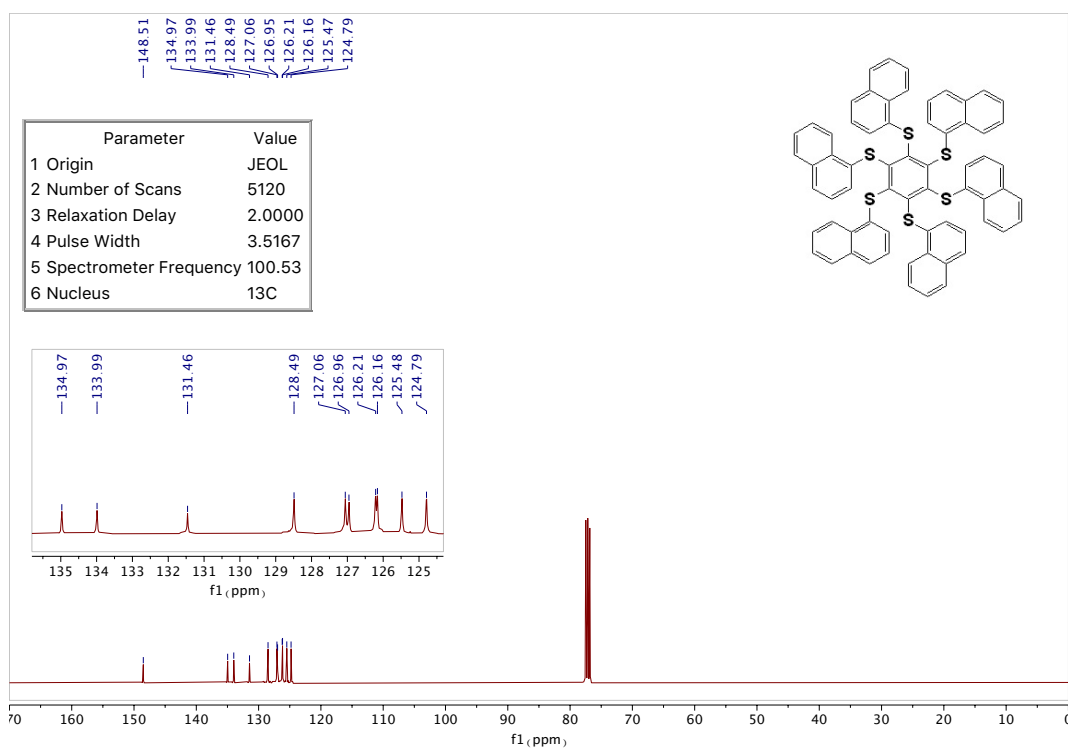


Figure S6 ^{13}C -NMR spectrum of (5) (CDCl_3 , 100.53 MHz)

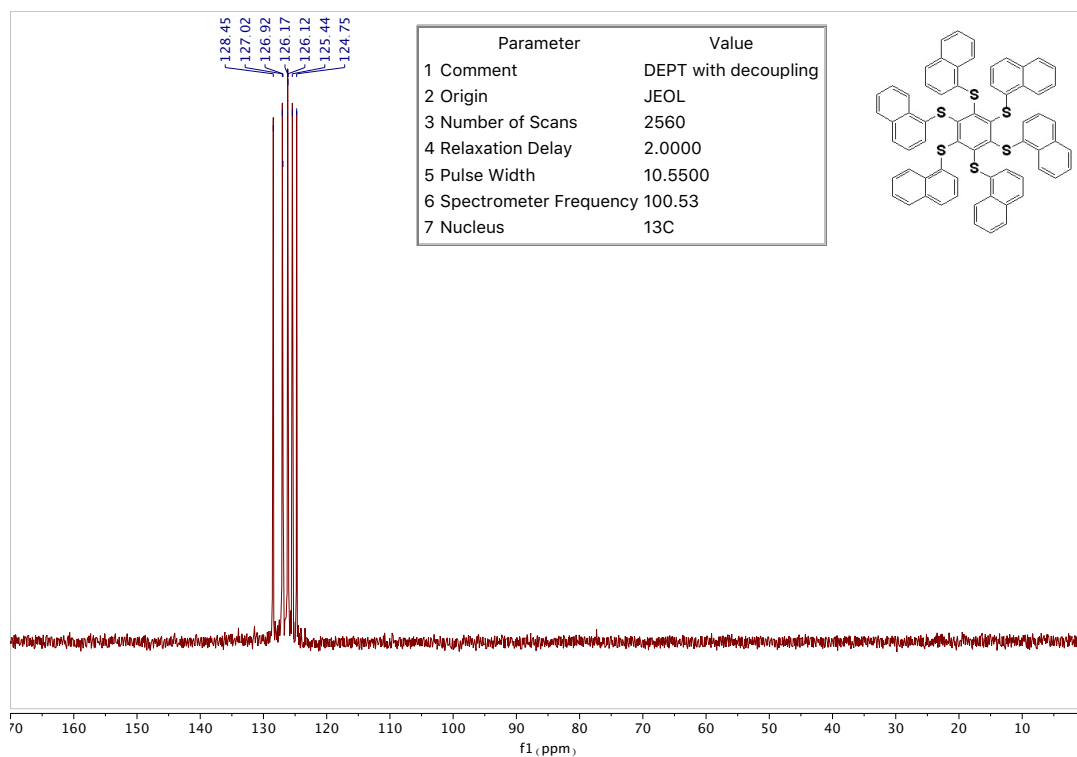


Figure S7 ^{13}C DEPT 135 NMR spectrum of (5) (CDCl_3 , 100.53 MHz)

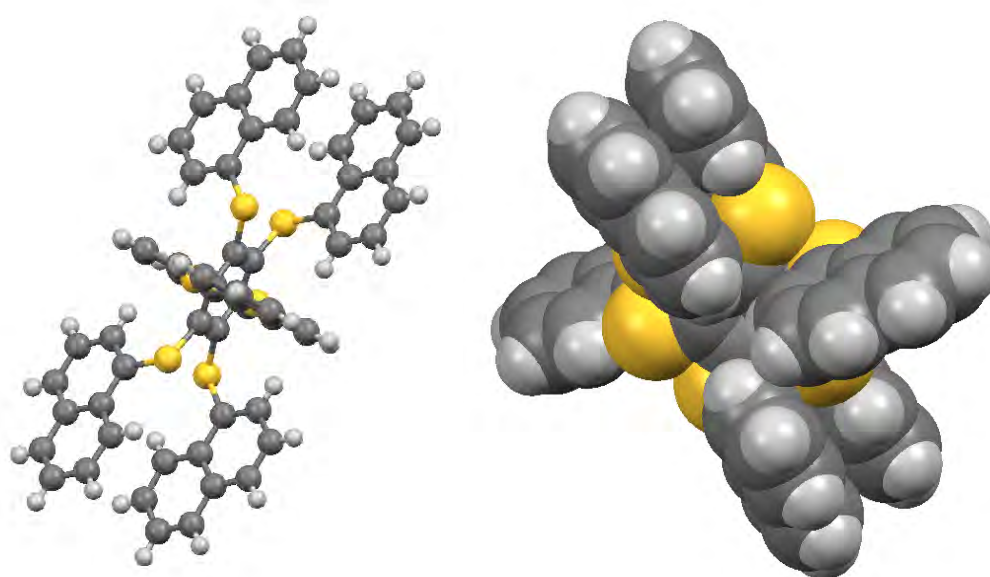
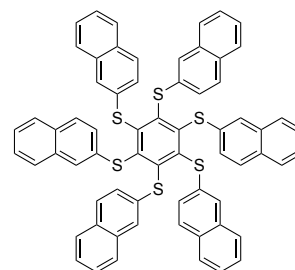


Figure S8 Structure determination of (5) by sc-XRD

Hexakis(2-naphthylthio)benzene (6). To an oven-dried sealed tube was added hexachlorobenzene (59.8 mg, 0.21 mmol, 1.00 mol-eq.) and dry potassium carbonate (259.2 mg, 1.87 mmol, 8.90 mol-eq.). Dry DMF (5.0 mL, dried over activated 3Å molecular sieves) was injected via a syringe and argon was bubbled for 15 minutes through the mixture. 2-Naphthalenethiol was added via a syringe (300.2 mg, 1.87 mmol, 8.90 mol-eq.). The reaction mixture turned from colorless to bright yellow and it was stirred for 4 days at 80°C (oil bath temperature). Most of DMF was removed *in vacuo* and the remaining crude solid was triturated with a solution of EtOH (20 mL) and H₂O (20 mL). Purification by column chromatography was achieved over silica gel using toluene/cyclohexane (5:95 v/v) as eluent. The eluent polarity was gradually increase to pure toluene to provide the desired product as a bright yellow solid (183.8 mg, 0.18 mmol, 73%).



M.p.: 193-195°C (*n*-hept/toluene 1:1 v/v); **TLC** (SiO₂, tol./cyclohex. 50:50 v/v) R_f = 0.53; **¹H NMR (399.78 MHz, CDCl₃, ppm):** δ = 7.58-7.63 (m, 1H), 7.44-7.49 (m, 1H), 7.39 (s, 1H), 7.34-7.40 (m, 3H), 7.05 (dd, *J* = 8.7, 1.8 Hz, 1H); **¹³C NMR (100.53 MHz, CDCl₃, ppm):** δ = 148.19, 134.94, 133.71, 131.95, 128.65, 127.83, 127.26, 127.23, 126.61, 126.43, 125.89; **¹³C NMR (DEPT135; 100.53 MHz, CDCl₃, ppm):** δ = 128.65, 127.83, 127.26, 127.23, 126.61, 126.43, 125.89; **HRMS (ESI+)** calculated for [C₆₆H₄₂S₆ + H⁺]: 1027.1684 Da; found [M + H⁺] 1027.1683 *m/z*.

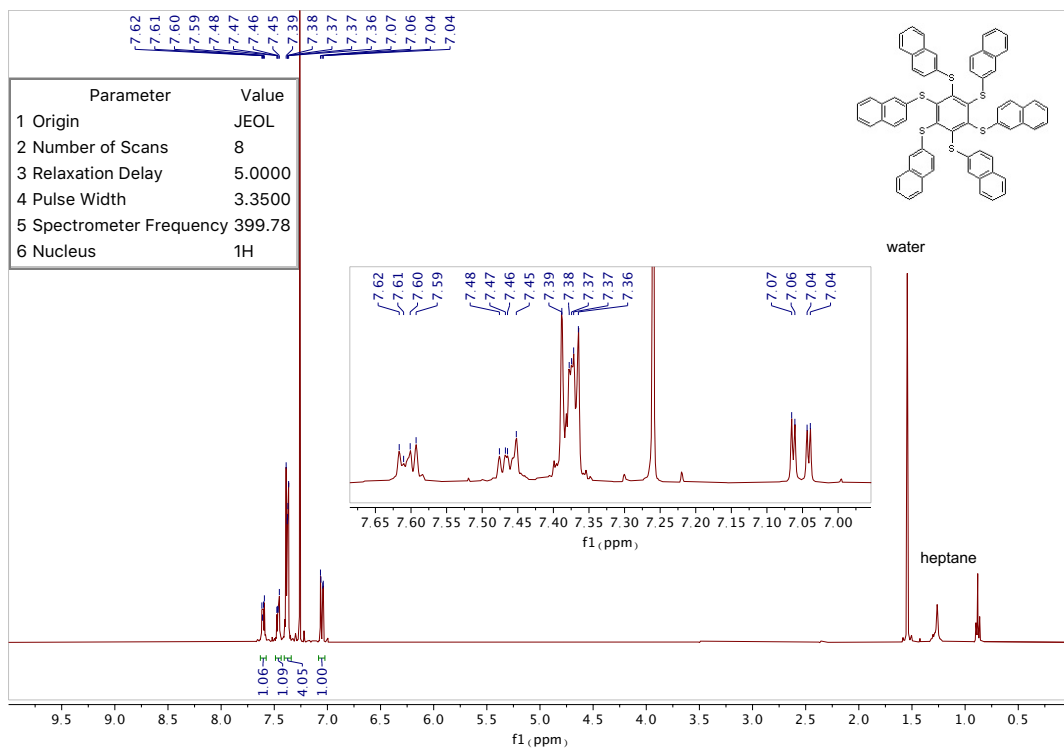


Figure S9 ^1H -NMR spectrum of (6) (CDCl_3 , 399.78 MHz)

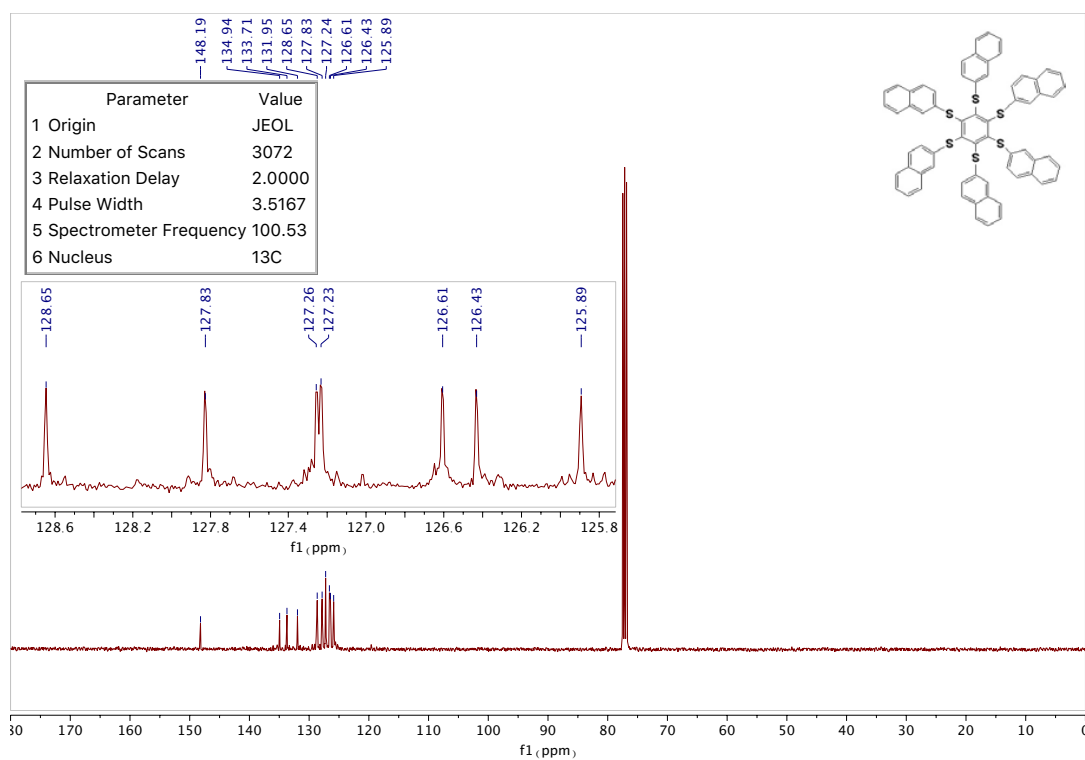


Figure S10 ^{13}C -NMR spectrum of (6) (CDCl_3 , 100.53 MHz)

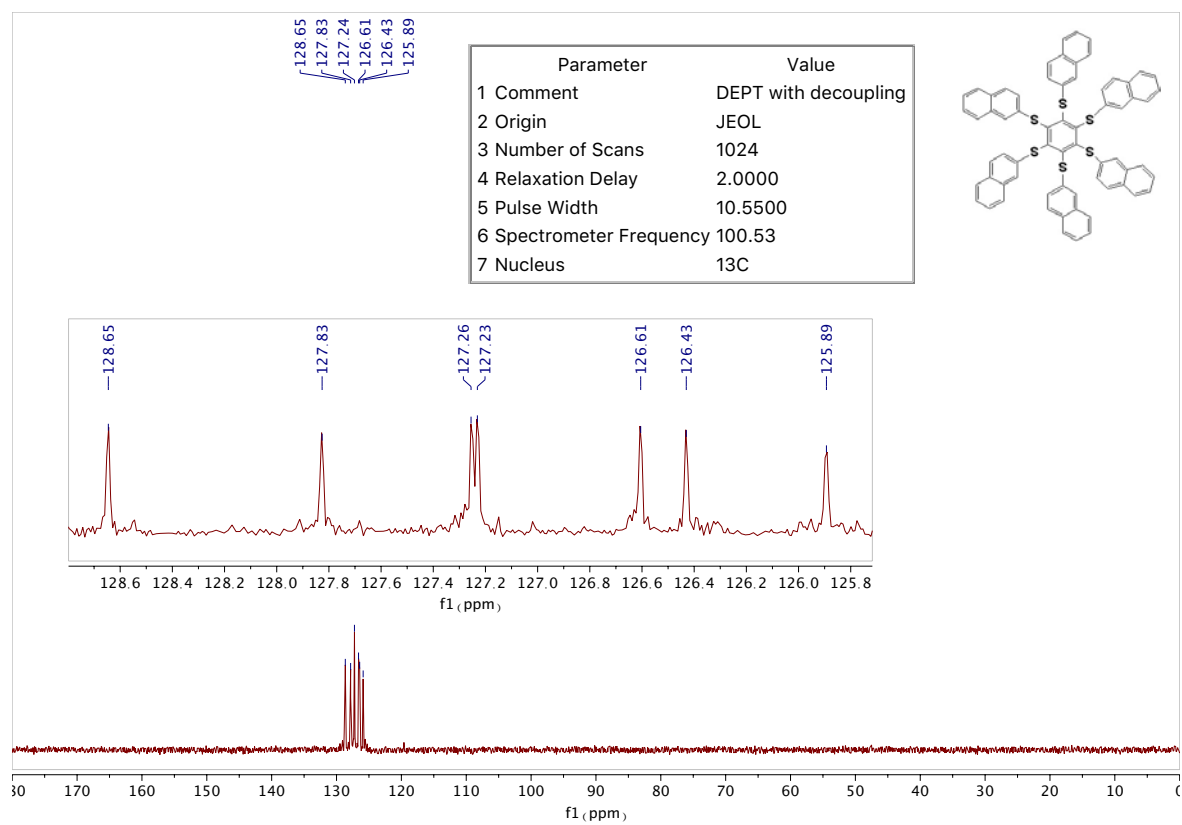


Figure S11 ^{13}C DEPT 135 NMR spectrum of **(6)** (CDCl_3 , 100.53 MHz)

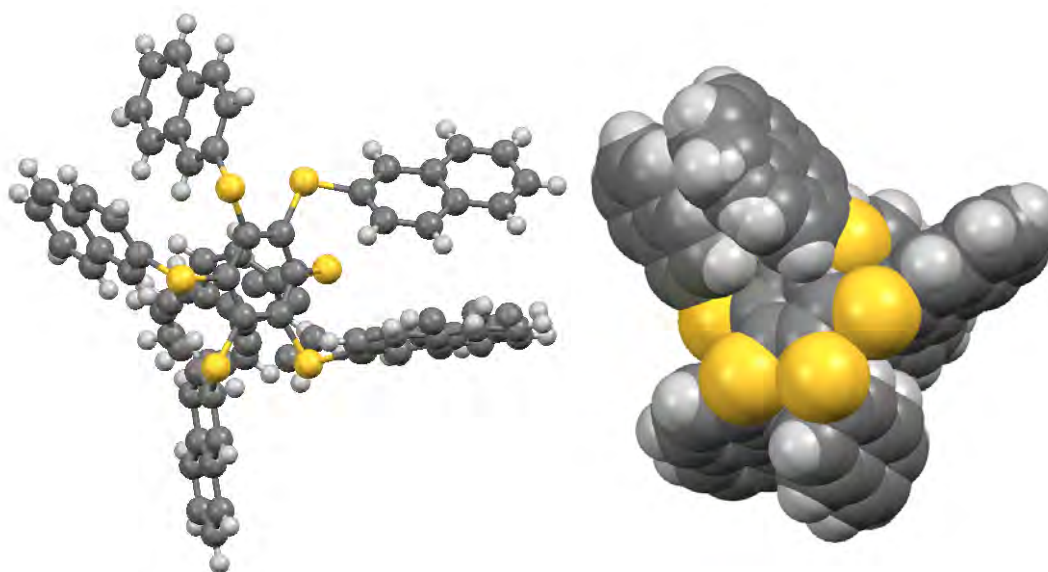


Figure S12 Structure determination of **(6)** by sc-XRD

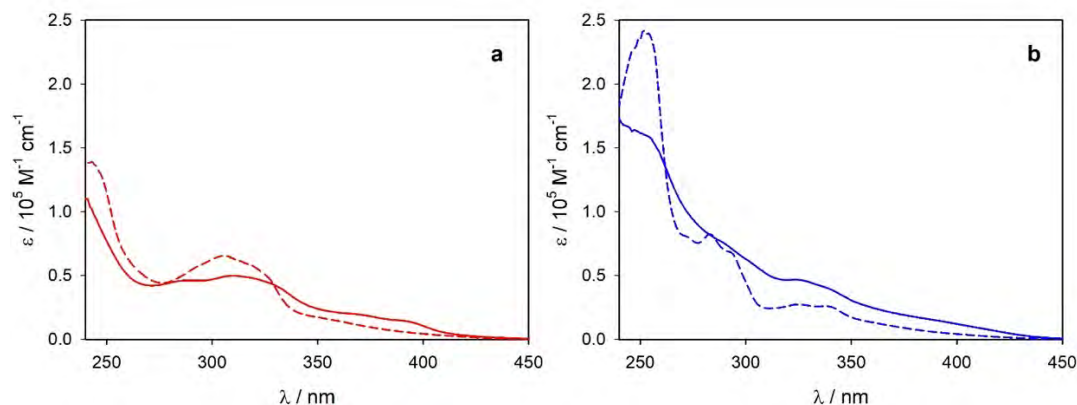


Figure S13: Absorption spectra in air-equilibrated CH_2Cl_2 solution of the compounds (5) and (6) (solid lines) and the corresponding spectra obtained by the mathematical addition of the respective model compounds (multiplied by 6 for the sake of comparison) with (4) profile (dash line): (a) Asterisk (5) (red solid line) and model compound (1) (red dashed line); (b) Asterisk (6) (blue solid line) and model compound (2) (blue dashed line).

Structural Studies on Compounds (5), (6) and (7)

For compound (5) the center of the central π cycle (centroid of Cg1) lies on the crystallographic center of symmetry and thus the asymmetric unit is only half of the asterisk. Two opposite S-Naphthyl are almost perpendicular to that ring (dihedral equal to $88.27(8)^\circ$) and they are engaged into symmetric intramolecular CH/ π interaction with it: the distance C5---Cg1 = $3.688(2) \text{ \AA}$ and the angle C5-H5---Cg1 is equal to 140° . The four remaining thionaphtyls are parallel by adjacent pairs and have angles of $67.23(10)^\circ$ and $64.06(10)^\circ$ respectively with the central π cycle (**Fig. S14**). They interact by pairs through intramolecular π - π stacking (dihedral equal to $6.32(7)^\circ$) but are also engaged into intermolecular CH/ π and π - π interactions with symmetry-related molecules within the lattice (**table S2**).

The behavior of (6) is somewhat different. The asymmetric unit is in general position within the unit cell, the thionaphtyls moieties are not related by symmetry and are positioned respectively in an up-down-up-(down)₃ sequence relatively to the central π cycle (**Fig. S15**). The dihedrals of the S-Naphthyl to the mean central ring have a large diversity and range from $63.0(5)^\circ$ to $117.5(5)^\circ$. Opposite to (5), this arrangement favors only CH/ π interactions, no π - π stacking being observed neither intramolecular nor intermolecular (**table S3**).

These different organizations within both asterisks have a remarkable influence on the deformation of the central benzene ring. For (5) the central benzene is not distorted (weighted average absolute torsion angle = 4.85°) while the puckering value Q for the ring in (6) is equal to $0.144(3) \text{ \AA}$ with a weighted average absolute torsion angle equal to 8.01° .^{5,6} Indeed in compound (5) the core benzene is protected from external influences by the symmetric arrangement of the substituents and the interaction they provide. On the contrary the same ring in (6) is affected by the sum of the strains brought by all the asymmetric intra and intermolecular CH/ π interactions. The better accessibility of the core benzene in (6) is also reflected by the presence of several intermolecular S-H interactions (C(H)---S distances around 3.7 \AA) while the C(H)---S distances in (5) are all longer than 3.8 \AA .

Interestingly the distortion of the central benzene in (6) is comparable to that observed in the previously published naphthalenethio benzene-cored asterisks, despite different arrangement of the naphthalene moieties.⁷ In this latter the puckering value Q is about 0.12 \AA and the weighted average absolute torsion angle is equal to 8.45° but the substituents are

in a sequence up-up-down-down-up-down. And unlike (6), this stereochemistry thus allows the formation of some intermolecular π - π interactions.

No distortion of the central benzene core is observed for compound (7): the weighted average absolute torsion angle is equal to 3.61°. The two thionaphtyls are perpendicular to the central ring (dihedrals equal to 77.11(16)° and 86.70(14)°) and are almost parallel together (dihedral equal to 12.12(15)°) and thus engaged into CH/ π interactions, with a perpendicular distance between their centroid equal to 3.7726(18) Å (Fig. S16). The central ring and the two dibenzothiophene are more or less on the same plane with dihedrals equal to 5.57(12)° and 9.16(12)° between the benzene core and its two substituents respectively.

X-Ray Crystallographic Studies on compounds (5), (6) and (7)

Crystals suitable for single crystal X-ray diffraction analysis were obtained by slow evaporation from a 50:50 heptane/toluene solution. They were measured on a Rigaku Oxford Diffraction SuperNova diffractometer at room temperature for (5) and (7) and at 180K for (6), at the CuK α radiation ($\lambda=1.54184$ Å). Data collection reduction and multiscan ABSPACK correction were performed with CrysAlisPro (Rigaku Oxford Diffraction). Using Olex2¹ the structures were solved by intrinsic phasing methods with SHELXT² and SHELXL³ was used for full matrix least squares refinement. H-atoms were introduced at geometrical positions and refined as riding atoms with their Uiso parameters constrained to 1.2Ueq(parent atom). Compound (6) co-crystallized with some highly disordered and unidentified molecules (with a content of 52 electrons for a volume of 256 Å³ in the asymmetric unit), most probably heptane, and a mask of solvent was applied during refinement⁴. Two naphthyl moieties were found to be disordered and were refined over two sites with occupation factors equal to 0.5.

Table S1. Crystal data and structure refinement for (5), (6) and (7)

Compound	(5)	(6)	(7)
Formula	C ₆₆ H ₄₂ S ₆	C ₆₆ H ₄₂ S ₆	C ₄₆ H ₂₆ S ₄
M _w	1027.35	1027.35	706.91
Crystal system	monoclinic	monoclinic	monoclinic
Measurement temperature/ K	295	295	295
Space group	P 2 ₁ /n	I 2/a	P 2 ₁ /c
a/ Å	14.4167(2)	29.3284(5)	16.5619(3)
b/ Å	13.19630(10)	10.2291(2)	7.6982(2)
c/ Å	14.8413(3)	40.0674(8)	25.9513(5)
β / °	117.301(2)	106.812(2)	90.936(2)
V/ Å ³	2509.00(8)	11506.6(4)	3308.27(12)
Z	2	8	4
Dc/g.cm ⁻³	1.36	1.186	1.419
Crystal colour	yellow	yellow	yellow
Crystal size/mm ³	0.04*0.24*0.3	0.02*0.06*0.08	0.03x0.03x0.24
μ (Mo-K α)/mm ⁻¹	2.852	2.488	2.906
N° of refl. measured	22059	40407	22573
N° of unique refl.	4809	11000	6311

N° of observed refl. [$F^2 > 4\sigma F^2$]	4320	8758	5475
N° parameters refined	325	781	451
R_1 [$F^2 > 4\sigma F^2$]	0.0411	0.0552	0.0627
wR_1 [$F^2 > 4\sigma F^2$]	0.1112 ^a	0.1475 ^b	0.1862
R_2 [all refl.]	0.0449	0.0683	0.701
wR_2 [all refl.]	0.1162 ^a	0.1571 ^b	0.1928 ^c
Goodness of fit [all refl.]	1.031	1.048	1.13
Residual Fourier/e. \AA^{-3}	-0.246; 0.645	-0.36; 0.392	-0.325; 0.42

^a $w=1/[(\sigma^2(F_o^2)+0.069P)^2+0.7174P]$ where $P=(F_o^2+2F_c^2)/3$

^b $w=1/[(\sigma^2(F_o^2)+0.0839P)^2+8.7684P]$ where $P=(F_o^2+2F_c^2)/3$

^c $w=1/[(\sigma^2(F_o^2)+0.087P)^2+3.8296P]$ where $P=(F_o^2+2F_c^2)/3$

Single-crystal X-ray diffraction analysis of compound (5)

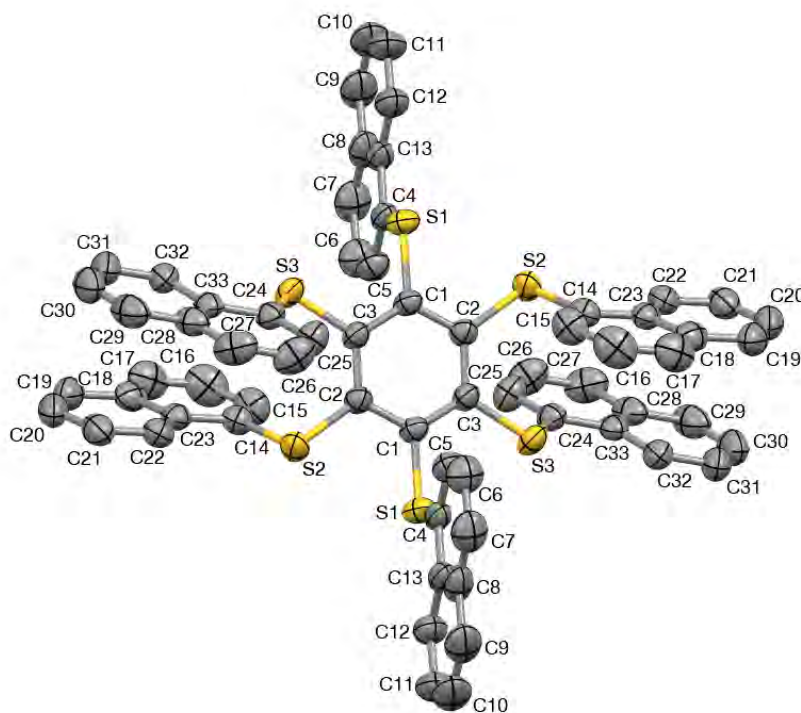


Figure S14. Ortep view (50% probability plot) of (5) showing the atom labelling. The H-atoms are omitted for clarity.

Table S2: Intra and intermolecular interactions for (5)

π - π interactions CgI/CgJ	Dihedral ($^\circ$)	Perpendicular distance (\AA)
Cg2/Cg3 ⁱ	0.73(14)	3.5772(11)
Cg3/Cg3 ⁱ	0.03(15)	3.5734(13)
Cg3/Cg8 ⁱ	0.37(12)	3.5787(13)
Cg5/Cg5 ⁱⁱ	0.00(11)	3.3819(9)
Cg8/Cg3 ⁱ	0.37(12)	3.5756(9)

Cg8/Cg8 ⁱ	0.00(9)	3.5789(9)
CH/ π interactions Cl/CgJ	Cl-CgJ (Å)	Cl-HI---CgJ (°)
C5/Cg1	3.688(2)	140
C17/Cg10 ⁱⁱⁱ	3.831(3)	155
C19/Cg7 ⁱⁱⁱ	3.691(3)	145
C29/Cg3 ^{iv}	3.614(3)	137
Cg1: C1/C2/C3/C1/C2/C3; Cg2: C4/C5/C6/C7/C8/C13; Cg3: C8/C9/C10/C11/C12/C13; Cg5: C18/C19/C20/C21/C22/C23; Cg7: C28/C29/C30/C31/C32/C33; Cg8: C4/C5/C6/C7/C8/C9/C10/C11/C12/C13; Cg10: C24/C25/C26/C27/C28/C29/C30/C31/C32/C33 Symmetry operations: <i>i</i> =1-x,2-y,1-z; <i>ii</i> =-x,1-y,1-z; <i>iii</i> =-0.5+x,0.5-y,-0.5+z; <i>iv</i> =0.5-x,-0.5+y,0.75-z		

Single-crystal X-ray diffraction analysis of compound (6)

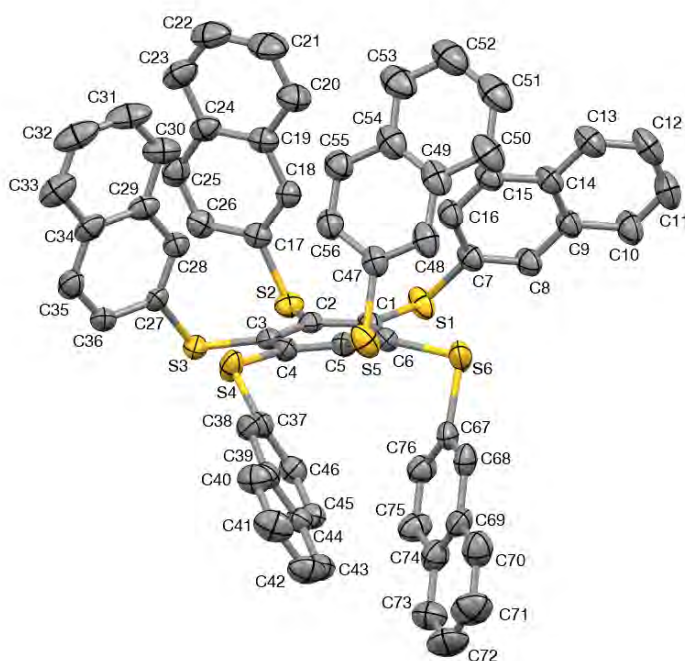


Figure S15. Ortep view (50% probability plot) of (6) showing the atom labelling. Only one of each disordered S-Naphthyl is shown and the H-atoms are omitted for clarity.

Table S3: Intra and intermolecular interactions for (6)

CH/ π interactions Cl/CgJ	Cl-CgJ (Å)	Cl-HI---CgJ (°)
C15/Cg11	3.599(4)	148
C15/Cg13	3.520(5)	149
C23/Cg6 ⁱ	3.607(4)	138
C25/Cg7 ⁱ	3.443(3)	131
C28/Cg4	3.446(3)	129
C30/Cg5	3.720(4)	138
C31/Cg1 ⁱⁱ	3.843(4)	154
C45/Cg15	3.688(4)	141

C45/Cg17	3.406(4)	150
C51/Cg9 ⁱⁱⁱ	3.568(5)	161
C71/Cg3 ^{iv}	3.483(6)	151
Cg1: C1/C2/C3/C4/C5/C6; Cg3: C9/C10/C11/C12/C13/C14; Cg4: C17/C18/C19/C24/C25/C26; Cg5: C19/C20/C21/C22/C23/C24; Cg6: C27/C28/C29/C34/C35/C36; Cg7: C29/C30/C31/C32/C33/C34; Cg9: C39/C40/C41/C42/C43/C44; Cg11: C49/C50/C51/C52/C53/C54; Cg13: C59/C60/C61/C62/C63/C64; Cg15: C69/C70/C71/C72/C73/C74; Cg17: C79/C80/C81/C82/C83/C84		
Symmetry operations: $i=1-x, 2-y, 1-z$; $ii=x, 1+y, z$; $iii=0.75-x, 0.75-y, 0.75-z$; $iv=0.75-x, 0.5-y, 0.75-z$		

Single-crystal X-ray diffraction analysis of compound (7)

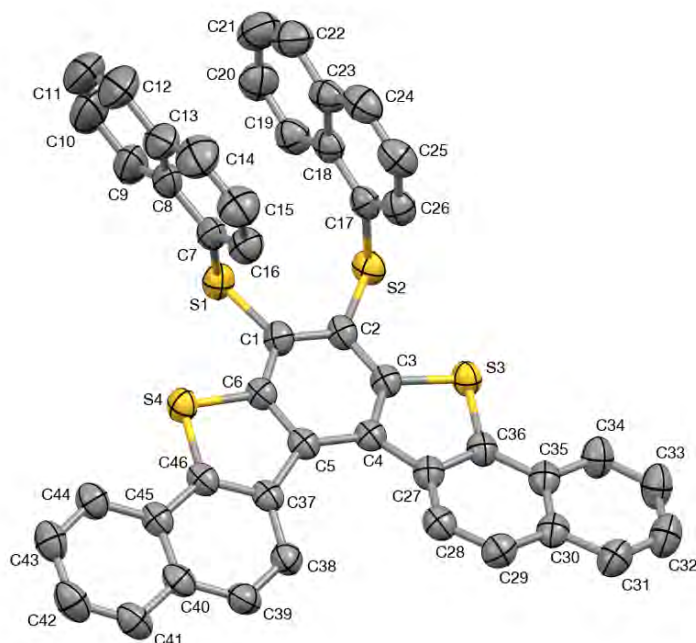
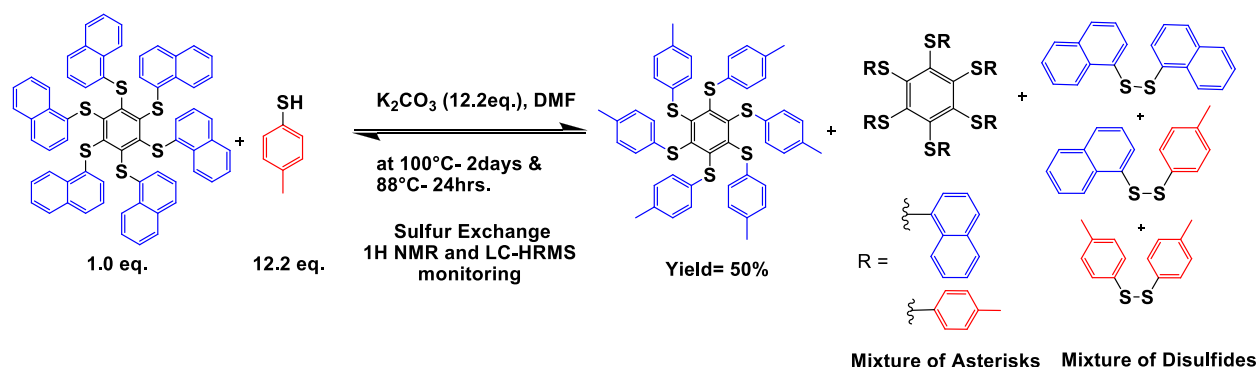


Figure S16. Ortep view (50% probability plot) of (7) showing the atom labelling. The H-atoms are omitted for clarity.

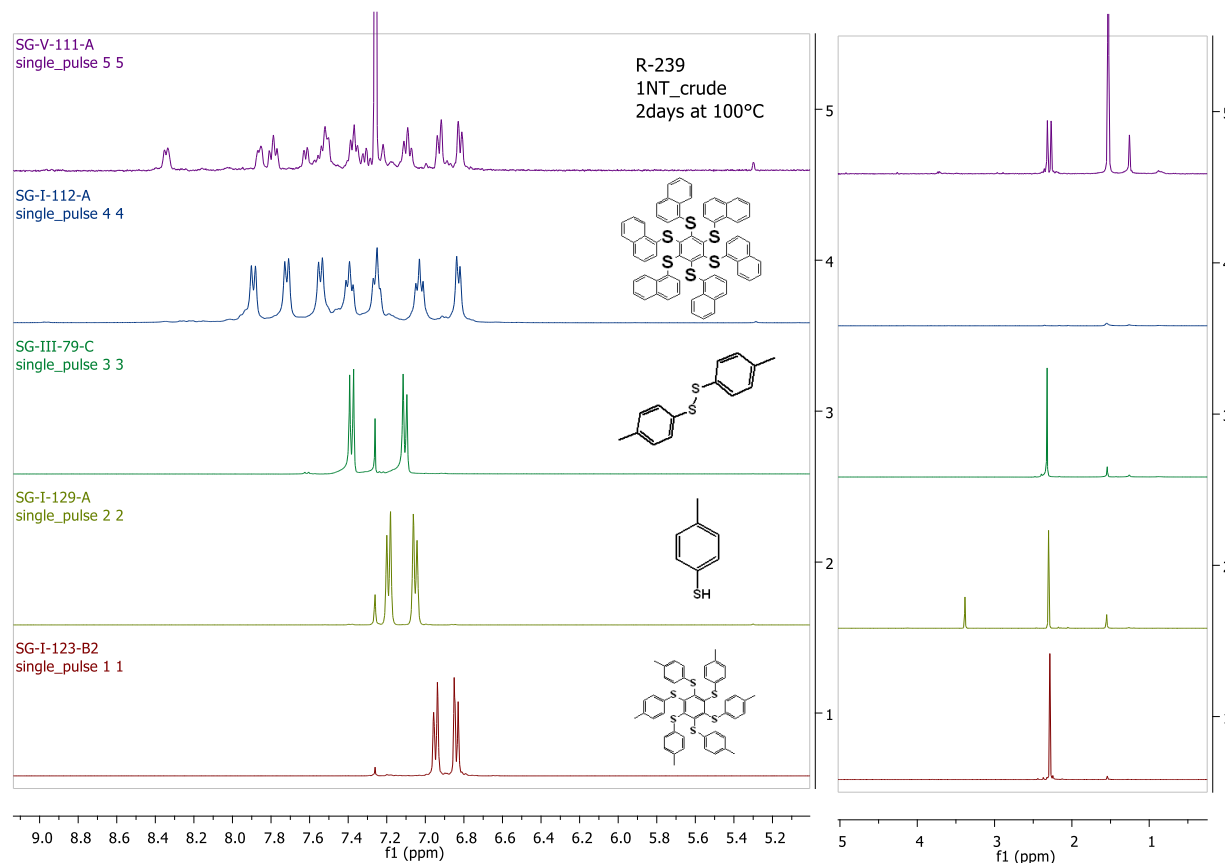
References

1. Dolomanov, O. V.; Bourhis, L. J.; Gildea, R. J.; Howard, J. A. K.; Puschmann, H. *J. Appl. Cryst.* **2009**, *42*, 339-341.
2. Sheldrick, G. M. *Acta Cryst.* **2015**, *A71*, 3-8.
3. Sheldrick, G. M. *Acta Cryst.* **2015**, *C71*, 3-8.
4. Rees, B.; Jenner, L.; Yusupov, M. *Acta Cryst.* **2005**, *D61*, 1299-1301.
5. Domenicano, A.; Vaciago, A.; Coulson, C.A. *Acta Cryst.* **1975**, *B31*, 221-234.
6. Cremer, D.; Pople, J.A. *J. Am. Chem. Soc.* **1975**, *97*, 1354-1358.
7. MacNicol, D.D.; Mallinson, P.R.; Murphy, A.; Sym, G.J. *Tetrahedron Lett.* **1982**, *23*, 4131-4134.

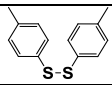
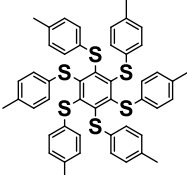
Sulfur Exchange Components in Dynamic Covalent Chemistry (DCC)

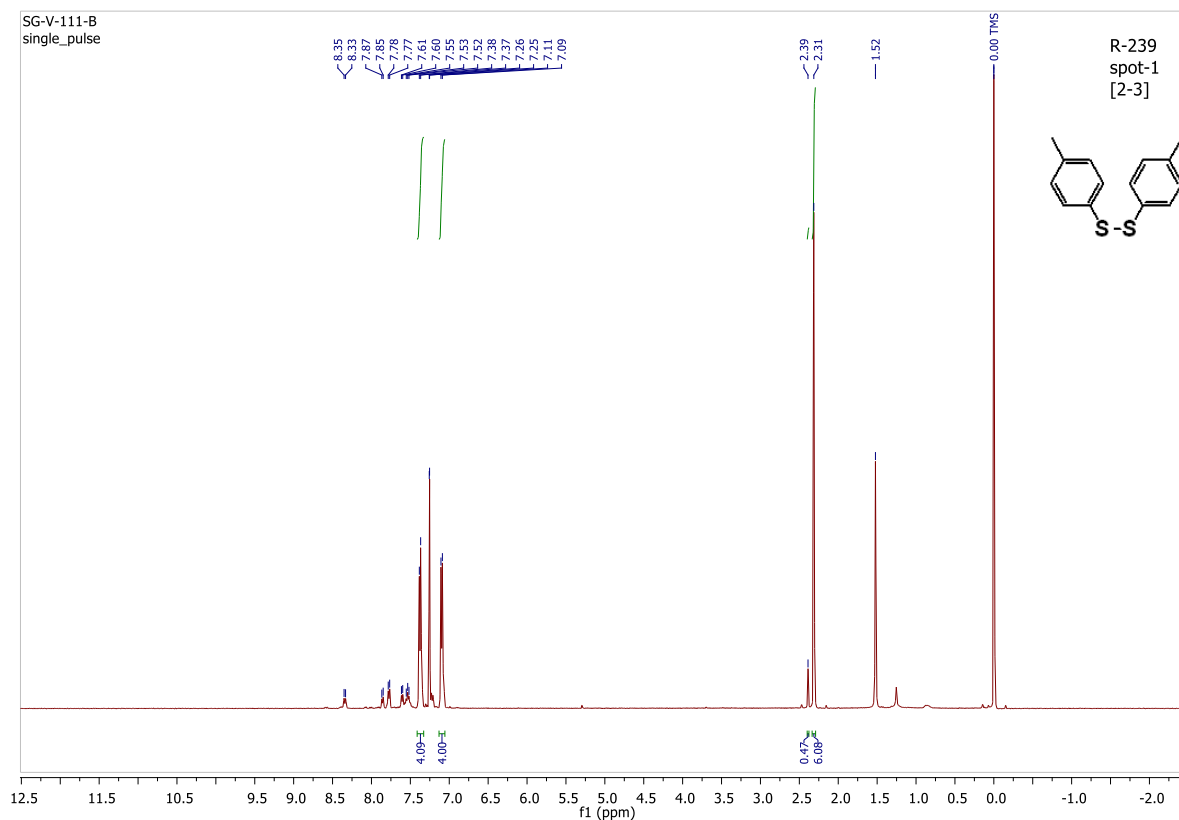


Procedure (R-239): In an oven-dried sealed tube, purged with argon, was added hexakis (1-naphthylthio) benzene (25.09 mg, 0.0244 mmol, 1,00 mol-eq), dried potassium carbonate (41.19 mg, 0.298 mmol, 12.2 mol-eq.), 4-methylbenzenethiol (37.10 mg, 0.298 mmol, 12.2 mol-eq.) and dry DMF (1.0 mL, dried with 3Å molecular sieves). Argon was bubbled through the mixture for 5-10 minutes. The tube was sealed under argon, and the reaction was stirred at 100°C in an oil bath for 2 days and at 88°C for 24 hours. Most DMF was removed by evaporation under vacuum. The crude was collected and a chromatography column on SiO₂ was achieved (eluent: toluene/cyclohexane : 30:70 v/v). Three spots were observed by TLC (toluene/cyclohexane : 50:50 v/v). Hexakis(4-methylphenylthio)benzene was collected (9.7 mg, 50% yield). ^1H and ^{13}C NMR spectra were identical to those from an authentic sample.

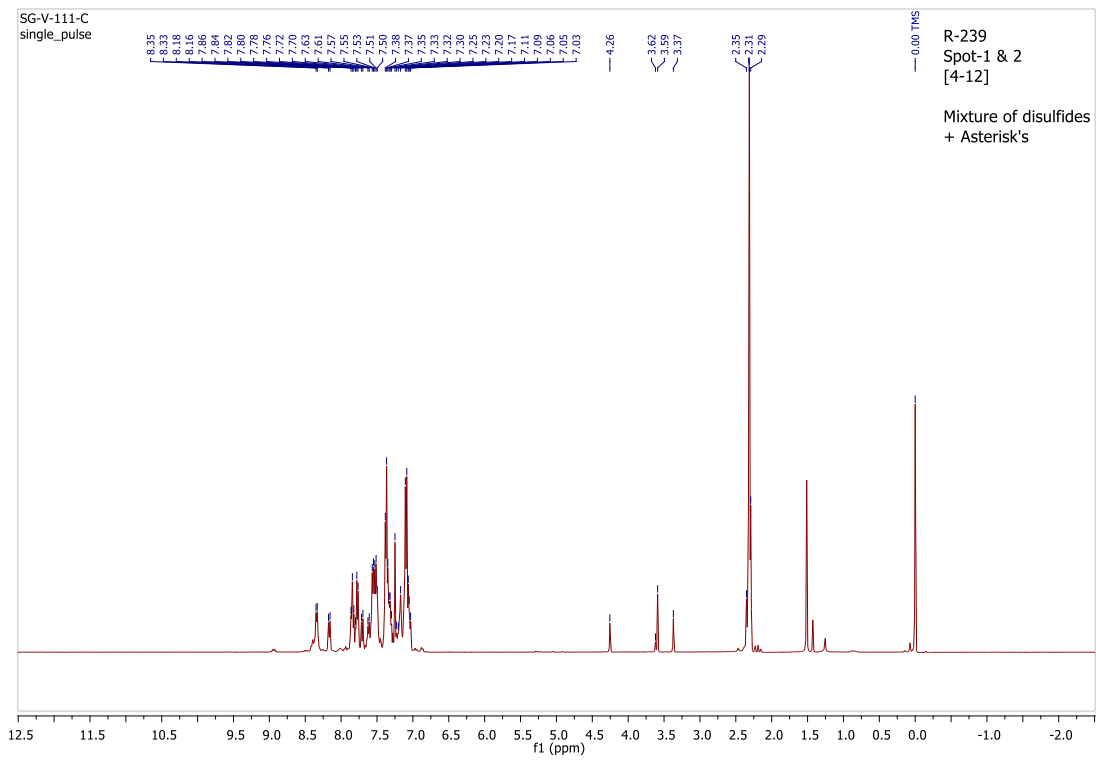


^1H NMR analysis of the crude mixture (CDCl_3 , 399.78 MHz)

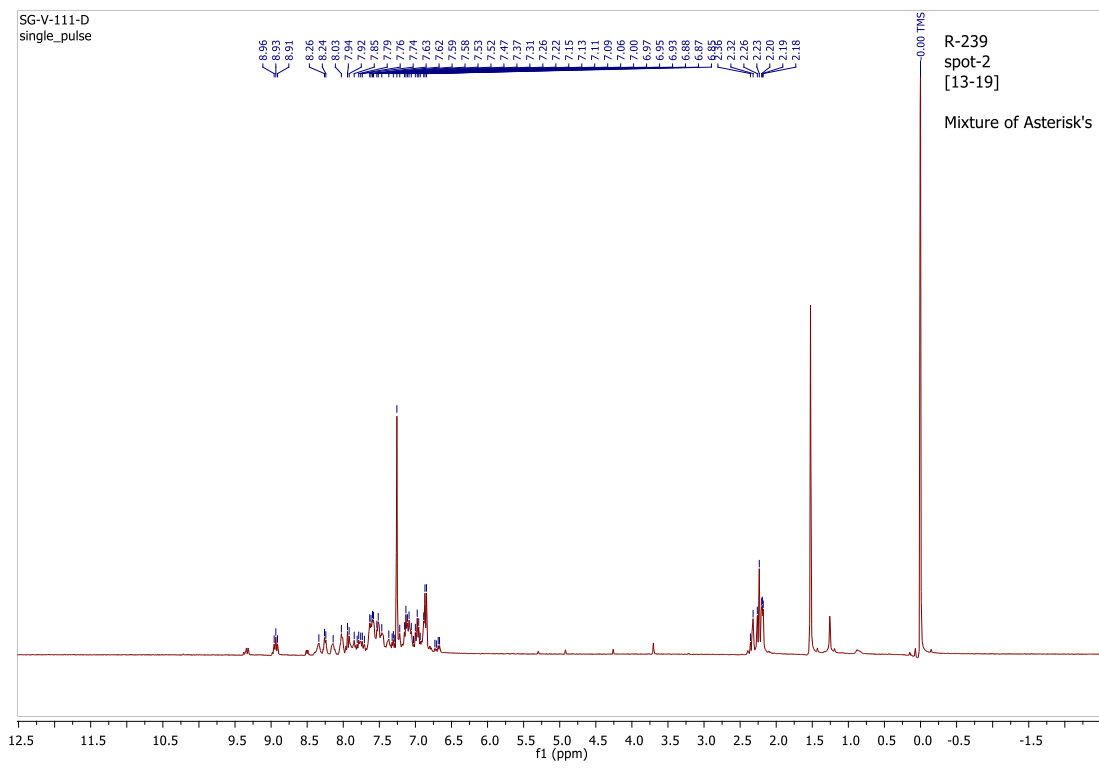
Spot [Fraction]	NMR	Mass (mg)	Compound
Spot-1 Fractions [2-3]	SG-V-111-B	--	
Spot-1 and 2 Fractions [4-12]	SG-V-111-C	29.2	Mixture of disulfides and compounds
Spot-2 Fractions [13-19]	SG-V-111-D	7.4	Mixture of compounds
Spot-3 Fractions [26-34]	SG-V-111-E	9.7	



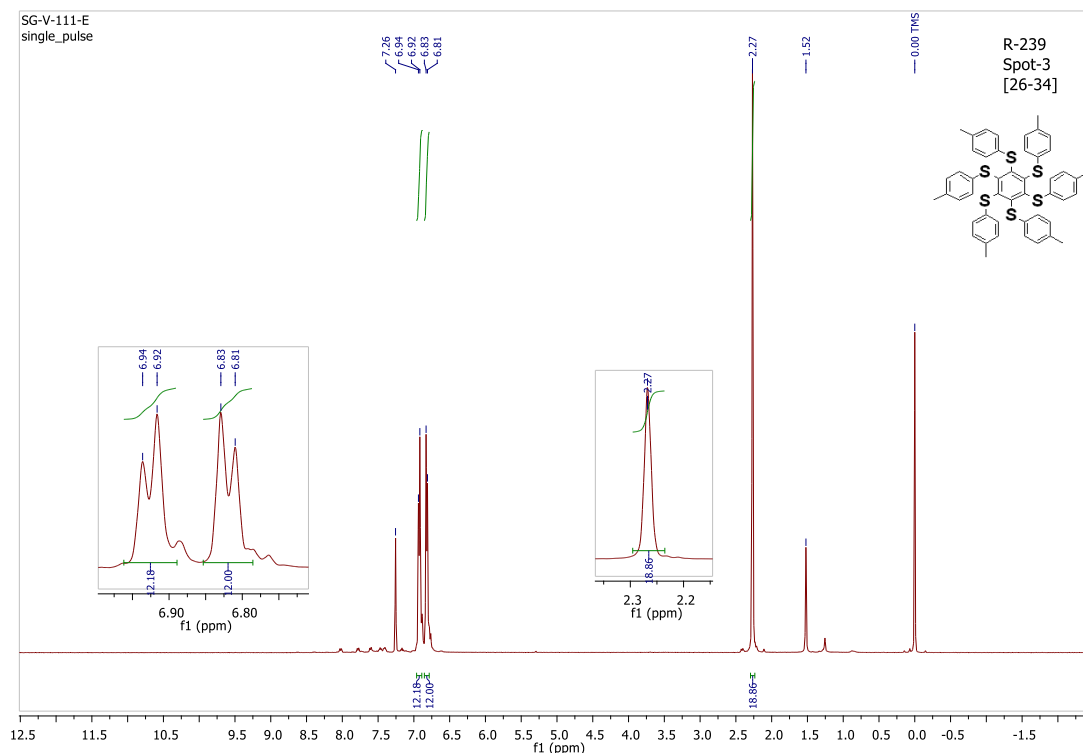
¹H-NMR SG-V-111-B (CDCl₃, 399.78 MHz)



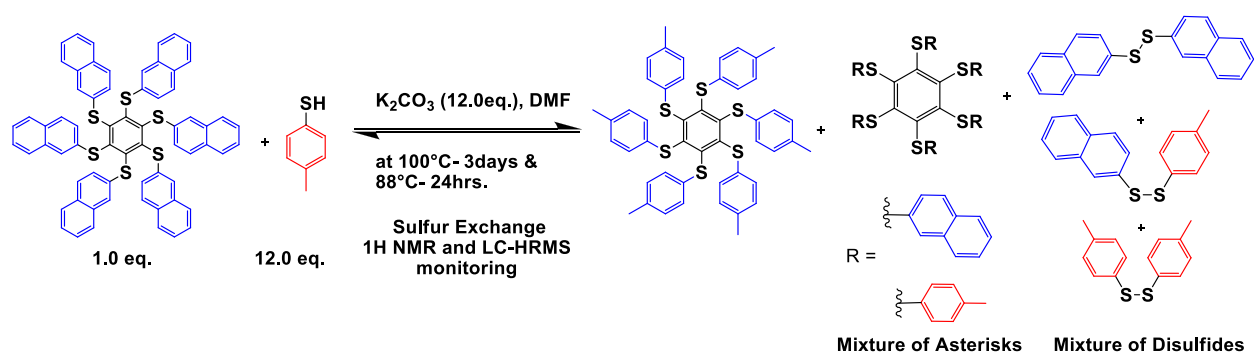
¹H-NMR SG-V-111-C (CDCl₃, 399.78 MHz)



¹H-NMR SG-V-111-D (CDCl₃, 399.78 MHz)

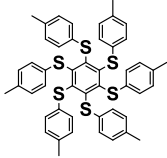


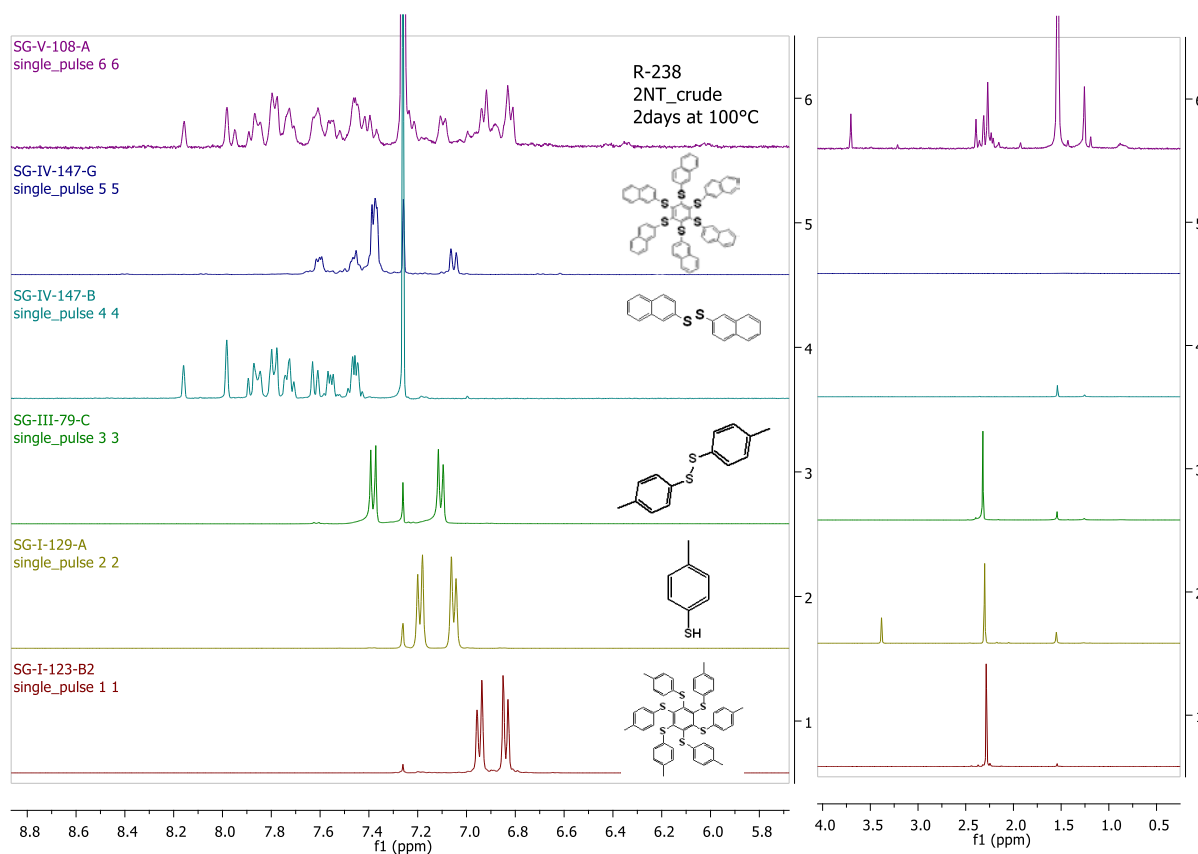
$^1\text{H-NMR}$ SG-V-111-E (CDCl_3 , 399.78 MHz)



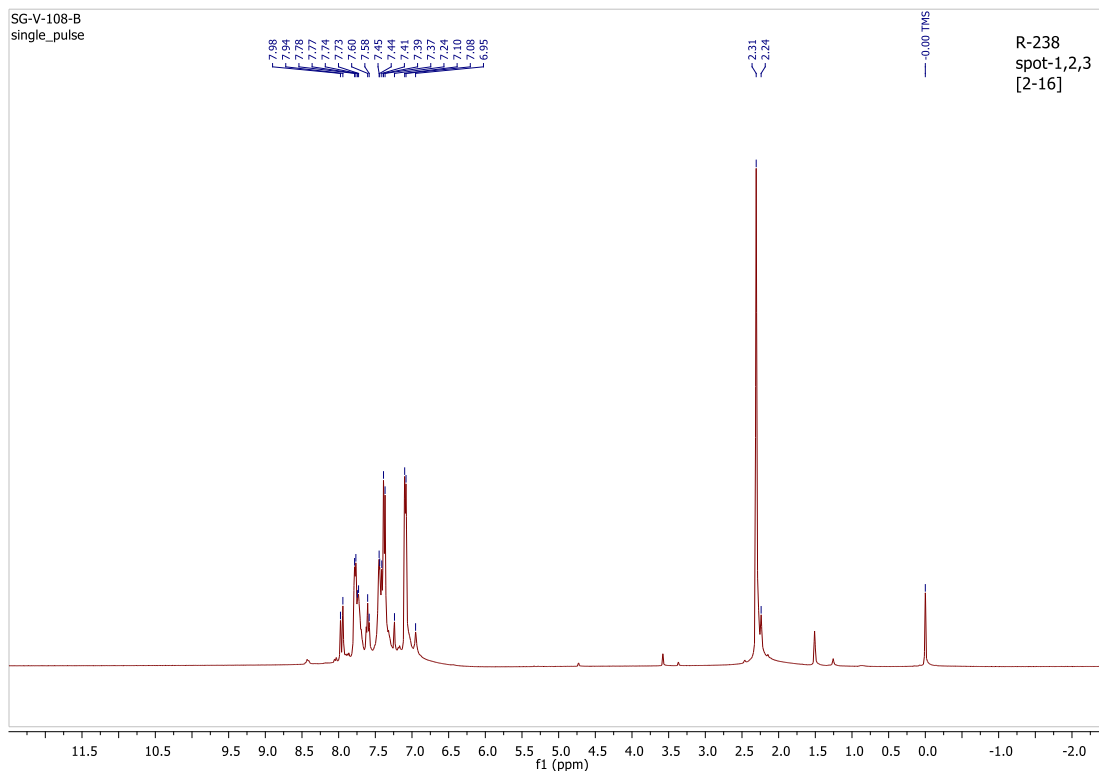
Procedure (R-238): In an oven-dried sealed tube, purged with argon, was added hexakis(2-naphthylthio)benzene (40.43 mg, 0.0393 mmol, 1,00 mol-eq), dried potassium carbonate (65.0 mg, 0.470 mmol, 12.0 mol-eq.), 4-methylbenzenethiol (57.70 mg, 0.465 mmol, 12.0 mol-eq.) and dry DMF (1.0 mL, dried with 3\AA molecular sieves). Argon was bubbled through the mixture for 5-10 minutes. The tube was sealed under argon, and the reaction was stirred at 100°C in an oil bath for 3 days and at 88°C for 24 hours. Most DMF was removed by evaporation under vacuum. The crude was collected and a chromatography column was achieved (eluent: 30% toluene/cyclohexane : 30:70 v/v). Five spots were observed by TLC (toluene/cyclohexane : 50:50 v/v).

$^1\text{H NMR}$ spectra SG-V-108-A: small workup with toluene (3 5 mL) and H_2O (5 mL), stirred for 2 days at 100°C

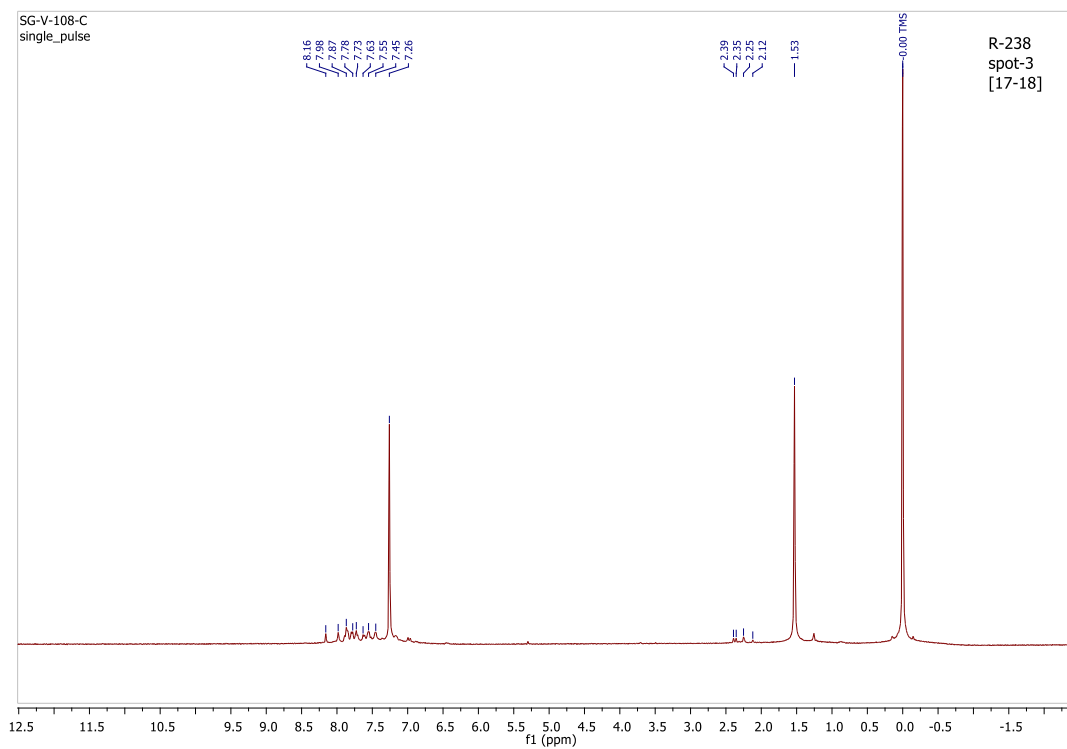
Spot [Fraction]	NMR	Mass (mg)	Compound
Spot-1,2 & 3 Fractions [2-16]	SG-V-108-B	--	Mixture of disulfides
Spot-3 Fractions [17-18]	SG-V-108-C	--	Mixture of disulfides and compounds
Mixture Fractions [19-22]	--	--	Mixture of compounds
Spot-4 Fractions [27-42]	SG-V-108-D	18.8	Mixture of asterisks
Spot-5 Fractions [49-60]	SG-V-108-E	25.8	 + other asterisks



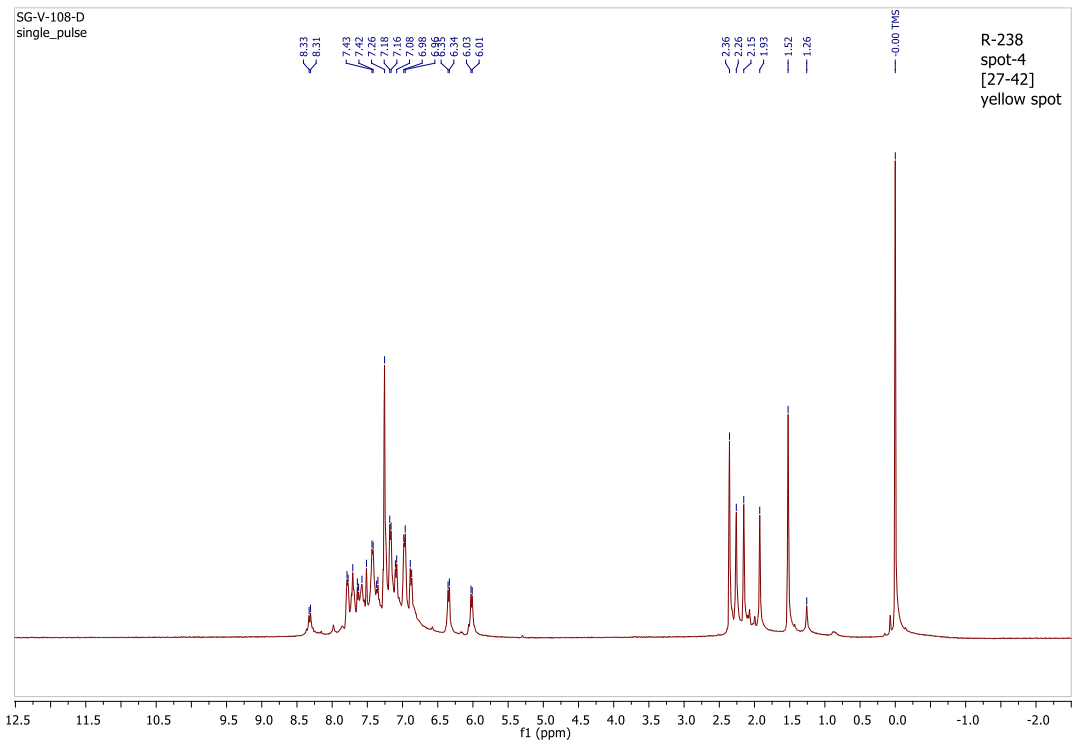
¹H NMR analysis of the crude mixture (CDCl₃, 399.78 MHz)



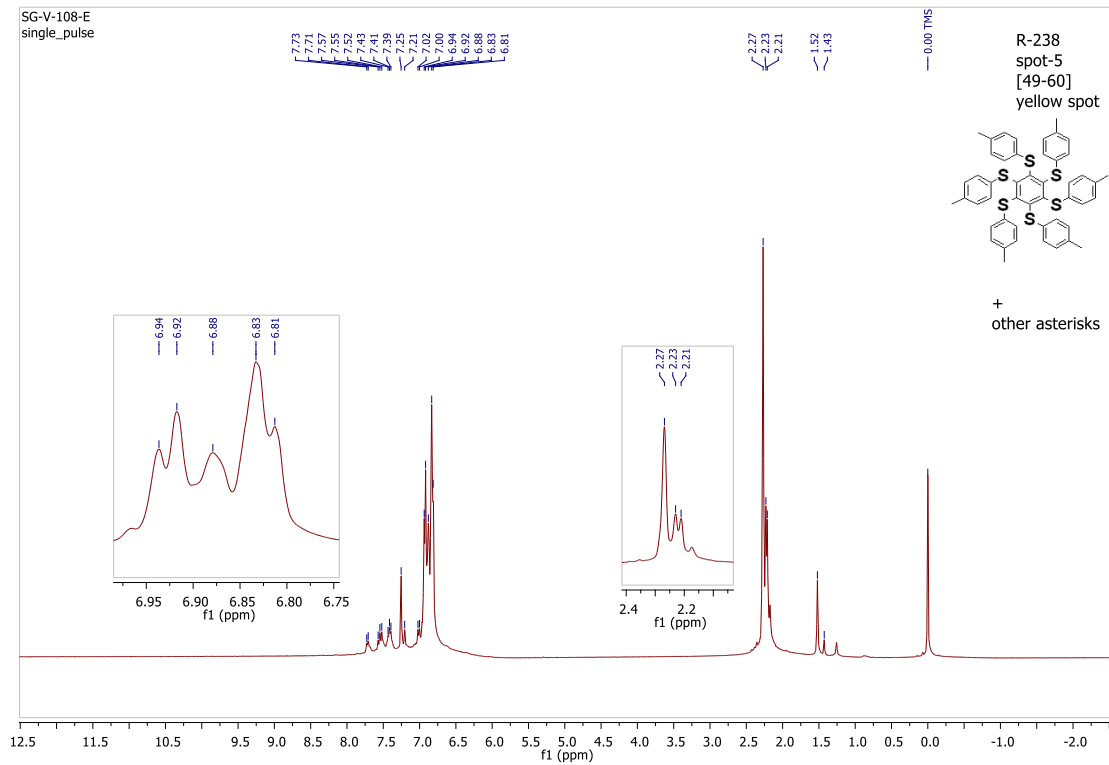
¹H-NMR SG-V-108-B (CDCl₃, 399.78 MHz)



¹H-NMR SG-V-108-C (CDCl₃, 399.78 MHz)



$^1\text{H-NMR}$ SG-V-108-D (CDCl_3 , 399.78 MHz)



$^1\text{H-NMR}$ SG-V-108-E (CDCl_3 , 399.78 MHz)

EXPERIMENTAL PART : CHAPTER 6

"THE SULFUR AND OXYGEN DANCE" AROUND ARENES AND HETEROARENES - DYNAMIC COVALENT NUCLEOPHILIC AROMATIC SUBSTITUTION

Note:

This section is mostly taken from an article submitted for publication in a scientific journal with a supporting information.

This work comprises some photophysical studies achieved by the group of Pr. Paola Ceroni, "G. Ciamician" department of chemistry at the University of Bologna, Italy.

Sc-XRD studies were achieved by Dr. Michel Giorgi, from Aix-Marseille Université, France.

LC-HRMS experiments were performed by Dr. Jean-Louis Schmitt in the group of Pr. Jean-Marie Lehn at ISIS, University of Strasbourg, France

Supporting Information

"The Sulfur Dance" Around Arenes and Heteroarenes – Dynamic Covalent Nucleophilic Aromatic Substitutions

Sapna Gahlot, Jean-Louis Schmitt,* Marco Villa, Myriam Roy, Paola Ceroni, Jean-Marie Lehn,* Marc Gingras*

Table of Contents

1.0	General information	SI-01
2.0	Synthesis and characterization of reference asterisks, thiols and disulfides:	SI-03
2.1	Hexa(thio) benzene asterisks	SI-03
2.2	Penta(thio) benzene asterisks	SI-17
2.3	Tetra(thio) benzene and pyridine asterisks	SI-23
2.4	Reference thiols, symmetrical and mixed disulfides	SI-31
2.5	Mixed hexa(thio) benzene asterisks	SI-51
3.0	Sulfur exchange reactions on hexa(thio) benzene asterisks page	SI-57
4.0	Sulfur exchange reactions on penta(thio) benzene asterisks	SI-65
5.0	Sulfur exchange reactions on tetra(thio) benzene asterisks	SI-75
6.0	Sulfur exchange reactions on tetra(thio) pyridine asterisks	SI-81
7.0	Conversion between two hexa(thio) benzene asterisks	SI-88
8.0	Demonstration of reversibility in S_NAr	SI-103
9.0	Exchange of sulfur components between two asterisks with a thiol as a promoter - demonstration of reversibility	SI-112

1.0 General Information

Materials and General Procedures: All reagents, solvents and chemicals were purchased from Sigma-Aldrich, Fisher, Alfa-Aesar or TCI Europe and used directly unless otherwise stated (purity: reagent or analytical grade). Solvents were stored for several days over freshly activated 3Å or 4Å molecular sieves (activated for 3 hours at 250°C). Reactions were monitored by TLC, 1H , ^{19}F , ^{13}C NMR spectroscopy or LC-MS and LC-HRMS.

Thin-Layer chromatography (TLC): TLC analyses were performed on precoated silica gel (Alugram® SiLG/UV254gel) aluminium plates from Macherey-Nagel. Compounds were visualized with UV-light (254 or 365 nm)

Flash chromatography was performed over silica gel 60, Merck type 230-400 mesh (40-63µm).

NMR spectroscopy

NMR (CINaM, Aix-Marseille Univ.): most spectra 1H (399.78 MHz), ^{13}C (100.53 MHz) and ^{19}F (376.17 MHz) were recorded on JEOL ECX-400 spectrometer with internal reference signals from residual protic solvent $CHCl_3$ at 7.26 ppm and $DMSO-d_6$ at 2.50 ppm, along with TMS. As for ^{13}C NMR spectra, the central resonance of the triplet for $CDCl_3$ at 77.16 ppm and the signal for $DMSO-d_6$ at 39.52 ppm were used as internal references.^[1] As for ^{19}F NMR spectra, the internal reference was C_6F_6 signal at -164.90 ppm relative to $CFCl_3$ (0 ppm). The resonance multiplicities

in the ^1H NMR spectra are described as “s” (singlet), “d”(doublet), “t” (triplet), “q” (quarted), “sept” (septet) “m” (multiplet) or “b” (broad).

NMR (Univ. of Bologna): a Varian ARX Inova 400 NMR spectrometer was used in a few cases for recording ^1H NMR (400.72 MHz) and ^{13}C NMR (100.76 MHz) spectra.

(1) Gottlieb, H.E., Kotlyar, V., Nudelman, A., "NMR Chemical shifts of common laboratory solvents as trace impurities", *J. Org. Chem.* **1997**, 62, 7512-7515.

Mass spectroscopy

LC-MS (APCI and ESI+) (CINaM, Aix-Marseille Univ.): Analyses were performed with a C18 Phenomenex Luna ($3\mu\text{m}$; 100 x 2 mm) column on a Shimadzu LCMS-2020 fitted with two LC-20AD prominence pumps equipped with a DGU-20AD prominence line degasser, a SIL-20AHT prominence auto-sampler, a CTO-20A prominence column oven, a SPD-20A prominence UV/Vis detector, a FCV-20AH valve unit, a Parker NitroFloLab nitrogen generator and either an APCI SET or an ESI SET detector. Positive or negative modes were used for both APCI and ESI mode.

GC-MS (CINaM, Aix-Marseille Univ.): Low resolution mass spectra (LRMS-EI) were recorded on a Shimadzu GC-MS QP2010SE instrument equipped with a DI2010 direct introduction unit with an electronic impact ionization source at 70eV. Direct introduction of the sample in the electronic impact (EI) detector.

LC-HRMS (ESI+) (ISIS, Univ. of Strasbourg): Analyses were performed using a Dionex RSLC U3000HPLC system (Thermo) with a chromatography column Acclaim Phenyl-1, ($3\mu\text{m}$; 150 x 2.1 mm). The mobile phase was water with 0.1% formic acid (method A) or acetonitrile with 0.1% formic acid (method B). Full MS spectra were acquired using Exactive series 2.9 sp4 software in a positive ion mode at a 3.5 kV spray voltage setting on a Thermo Scientific Exactive Plus EMR. Resolution of full MS and HCD scans were 140,000 and data were acquired in profile mode and processed using Xcalibur 4.3.

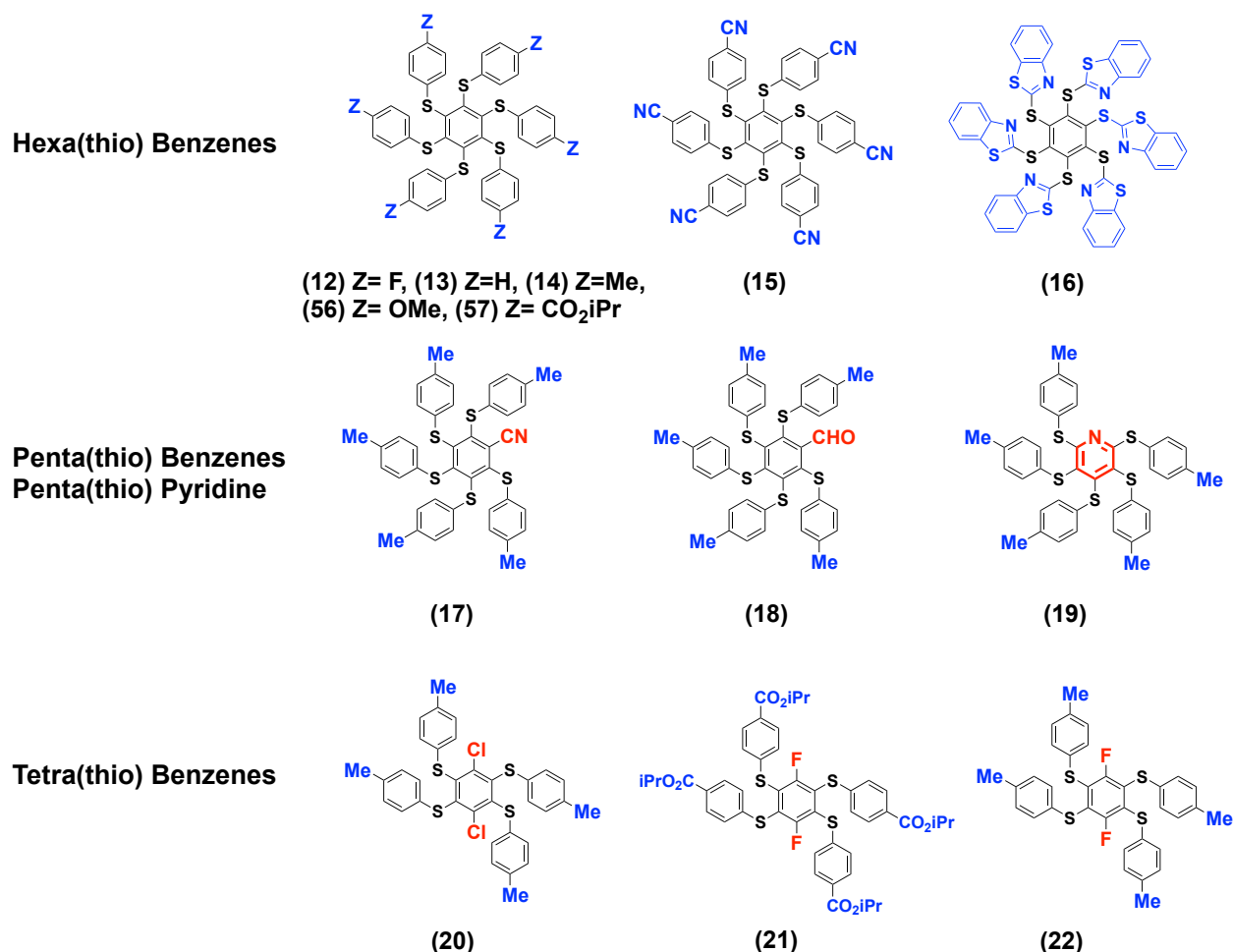
HRMS (ESI+) (Spectropôle of Marseille): High resolution mass spectra were recorded at the Spectropôle of Marseille (France) in triplicate with double internal standards. Oligomers of poly(propylene glycol) were used as internal standards. Ionization was facilitated by some adducts with Ag^+ , NH_4^+ or Na^+ ions. Two spectrometers were used: a) SYNAPT G2 HDMS (Waters) instrument equipped with an ESI source and a TOF analyzer in a positive mode. b) QStar Elite (Applied Biosystems SCIEX) instrument equipped with an atmospheric ionization source (API). The samples were ionized under ESI with an electrospray voltage of 5500 V; orifice voltage: 10V, and air pressure of the nebulizer at 20 psi. A TOF analyzer was used in a positive mode. Most high-resolution mass spectra (ESI+) were recorded in triplicate using double internal standards at the Spectropole (<https://fr-chimie.univ-amu.fr/spectropole/>).

FT-IR: Infrared absorption spectra were directly recorded on solids or neat liquids on a Perkin-Elmer Spectrum 100 FT-IR Spectrometer equipped with a universal ATR accessory (contact crystal: diamond).

Melting points (uncorrected) were recorded with an Electrothermal 9200 digital melting point apparatus with a ramp rate temperature (rate increase of temperature) using samples in glass capillaries.

2.0 Synthesis and characterization of reference asterisks, thiols and disulfides

List of reference asterisks for LC-MS and NMR analyses:

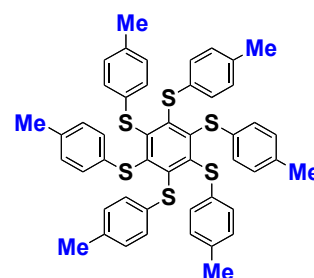


2.1 Hexa(thio) benzene asterisks

Hexakis(4-methylphenylthio)benzene (14)¹⁻⁸

Hexachlorobenzene (4.506 g, 15.82 mmol, 1.00 mol-eq.), dry potassium carbonate (19.66 g, 142.2 mmol; 8.99 mol-eq.) and *p*-thiocresol (18.06 g, 145.4 mmol; 9.19 mol-eq.) were added into a round bottom flask capped with a septum under an argon atmosphere. Dry DMF (100 mL) was injected via a syringe and the mixture was stirred at 60°C for 40 h. It turned yellow and the completion of the reaction was monitored by TLC (SiO₂, *n*-hex./EtOAc 85:15 v/v; R_f = 0.74). An aqueous

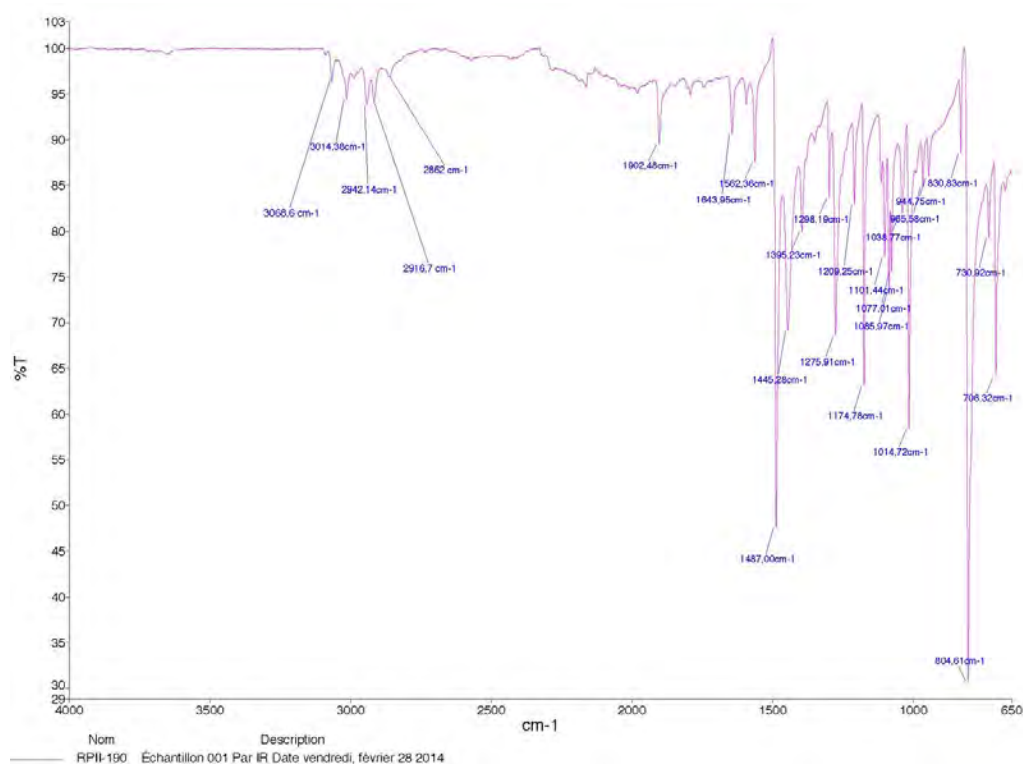
solution of NaOH (2 M, 100 mL) was poured into the flask while stirring, and a yellow precipitate appeared. After collecting the solid by filtration, the crude product was triturated with a solution of ethanol/H₂O (85:15 v/v; 50 mL) while stirring at reflux for 3 h. After cooling at RT, a filtration left a yellow solid, which was rinsed with ethanol (10 mL), with diethyl ether (20 mL), and then dried under high vacuum (11.55 g, 14.24 mmol, 90%). For analytical purity, it was recrystallized from warm toluene to afford bright yellow crystals.



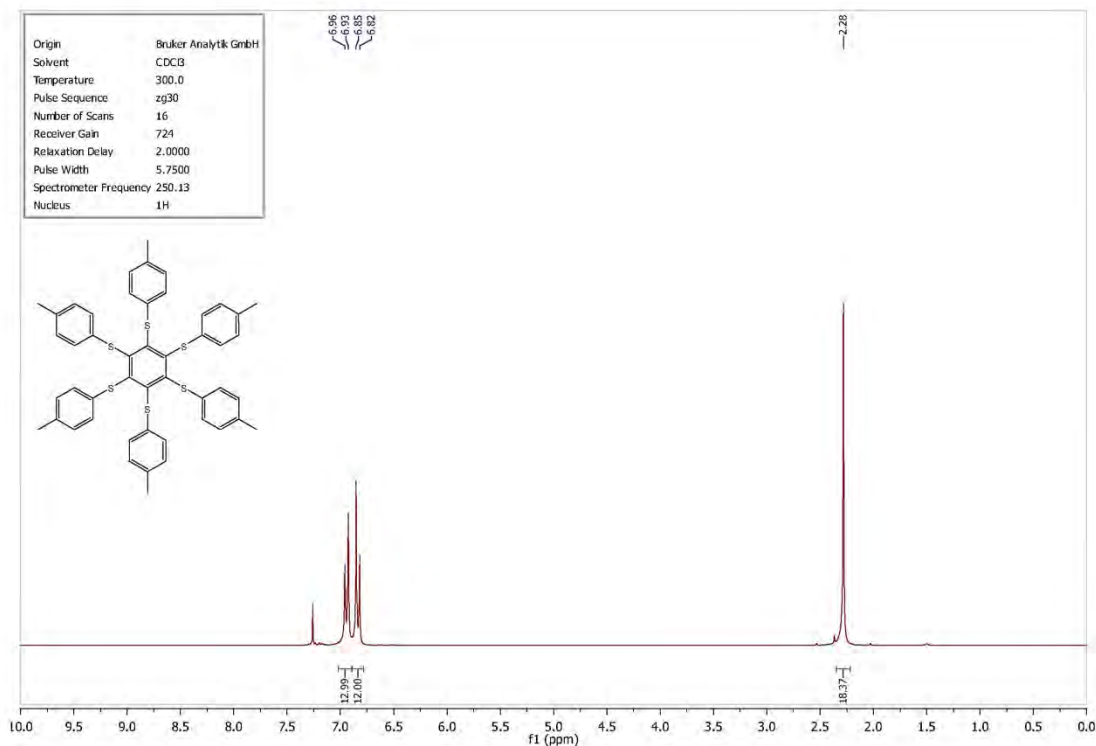
M.p.: 201.9-202.3°C (lit. 197-8°C⁶; 197-200°C⁷); **TLC** (SiO₂, *n*-hex/EtOAc 85:15 v/v) R_f = 0.74; **FT-IR** (ATR, diamond contact, neat, cm⁻¹) ν = 3069 (CH arom), 3014 (CH arom), 2942 (CH₃), 2862 (CH₃), 1487, 1445, 1276, 1174, 1015 (CH arom), 805 (strong, CH arom); **¹H NMR (250.13 MHz, CDCl₃, ppm):** δ = 6.94 (d_{app}, *J* = 8.1 Hz, 12H), 6.83 (d_{app}, *J* = 8.2 Hz, 12H); 2.28 (s, 18H); **¹³C NMR (62.90 MHz, CDCl₃, ppm):** δ = 147.9; 135.80, 134.42, 129.56, 128.52, 21.03; **LC-MS** (acetonitrile/water/0.1% formic acid; ESI+): 811 *m/z* [M+H]⁺, 833 *m/z* [M+Na]⁺; **Elemental analysis:** calculated %C 71.07 %H 5.22 %S 23.72, found %C 71.48 %H 5.39 %S 23.10.

References:

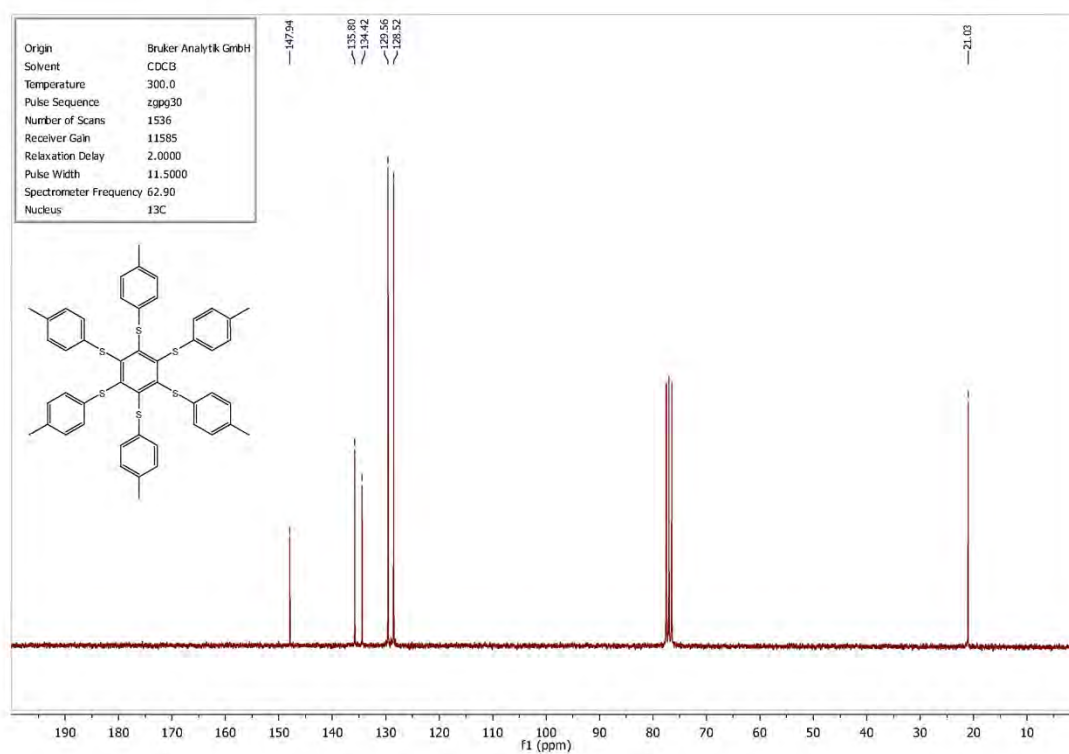
1. A. Fermi, G. Bergamini, R. Peresutti, E. Marchi, Roy, Myriam; P. Ceroni, M. Gingras, *Dyes and Pigments* (2014), 110, 113-122.
2. A. Fermi, G. Bergamini, M. Roy; M. Gingras, P. Ceroni, *J. Am. Chem. Soc.* (2014), 136, 6395-6400.
3. G. Bergamini, A. Fermi, C. Botta, U. Giovanella, S. Di Motta, F. Negri, R. Peresutti, M. Gingras, P. Ceroni, *J. Mater. Chem. C* (2013), 1(15), 2717-2724.
4. M. Arisawa, T. Suzuki, T. Ishikawa, M. Yamaguchi, *J. Am. Chem. Soc.* (2008), 130, 12214-12215
5. Y. Suenaga, K. Kitamura, T. Kuroda-Sowa, M. Maekawa, M. Munakata, *Inorg. Chim. Acta* (2002), 328, 105-110.
6. J.H.R. Tucker, M. Gingras, H. Brand, J.-M. Lehn, *J. Chem. Soc., Perkin Trans. 2: Physical Organic Chemistry* (1997), 7, 1303-1307.
7. A. D.U. Hardy, D.D. MacNicol, D.R. Wilson, *J. Chem. Soc., Perkin Trans. 2: Physical Organic Chemistry* (1979), 7, 1011-19.
8. B.F. Malichenko, L.P. Robota, *Zhurnal Organicheskoi Khimii* (1975), 11, 778-82.



FT-IR-ATR spectrum of (14)



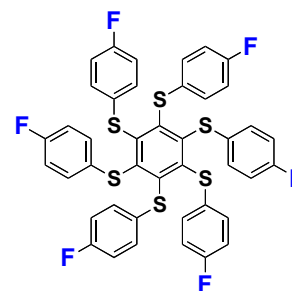
¹H-NMR spectrum of **14** (CDCl₃, 250.13 MHz)



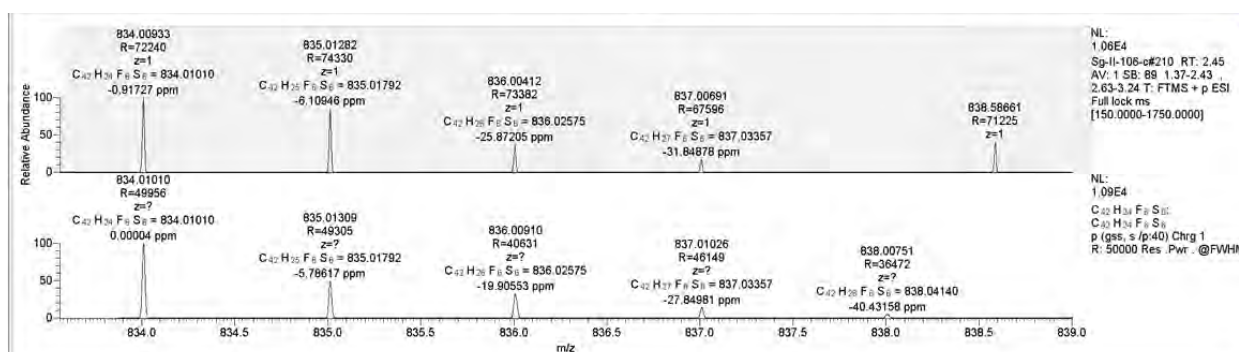
¹³C-NMR spectrum of **14** (CDCl₃, 62.90 MHz)

Hexakis(4-fluorophenylthio)benzene (**12**)

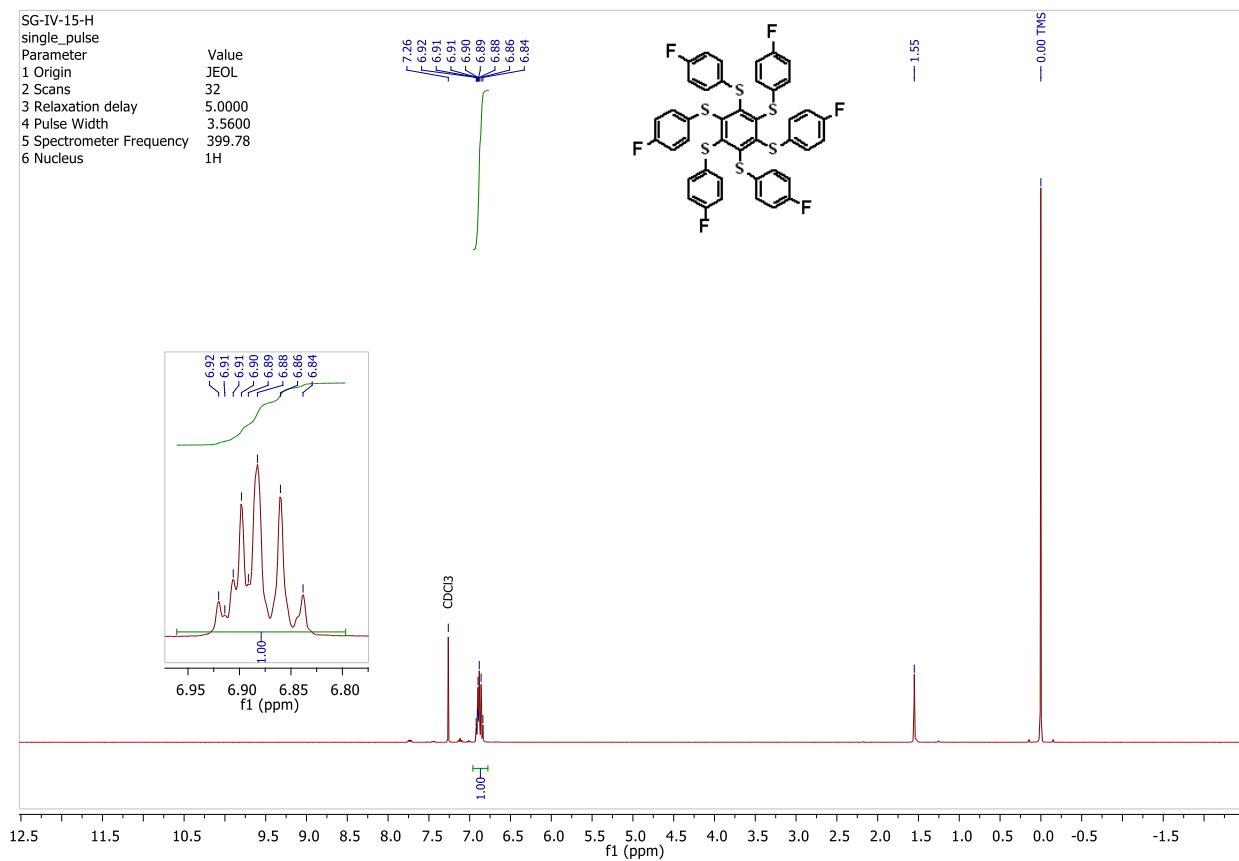
In an oven-dried sealed tube, purged with argon, was added hexachlorobenzene (0.447 g, 1.57 mmol, 1.00 mol-eq.), dried potassium carbonate (1.945 g, 14.07 mmol, 8.96 mol-eq.), *p*-fluorothiophenol (1.804 g, 14.08 mmol, 1.50 mL, 8.97 mol-eq.) and dry DMF (6.0 mL, dried and kept over activated molecular sieves 3Å). Argon was bubbled through the mixture for 5-10 minutes. The tube was sealed and the reaction was stirred at 27°C for 3 days. Most DMF was removed on a rotary evaporator under reduced pressure. To the reaction mixture was added EtOH (30 mL) and H₂O (30 mL) at 25°C while stirring vigorously. A solid was formed and stirring was continued for 3 hrs. After filtration, the solid was dried *in vacuo* to afford a pure yellow solid (1.230 g, 1.473 mmol, 94% yield).



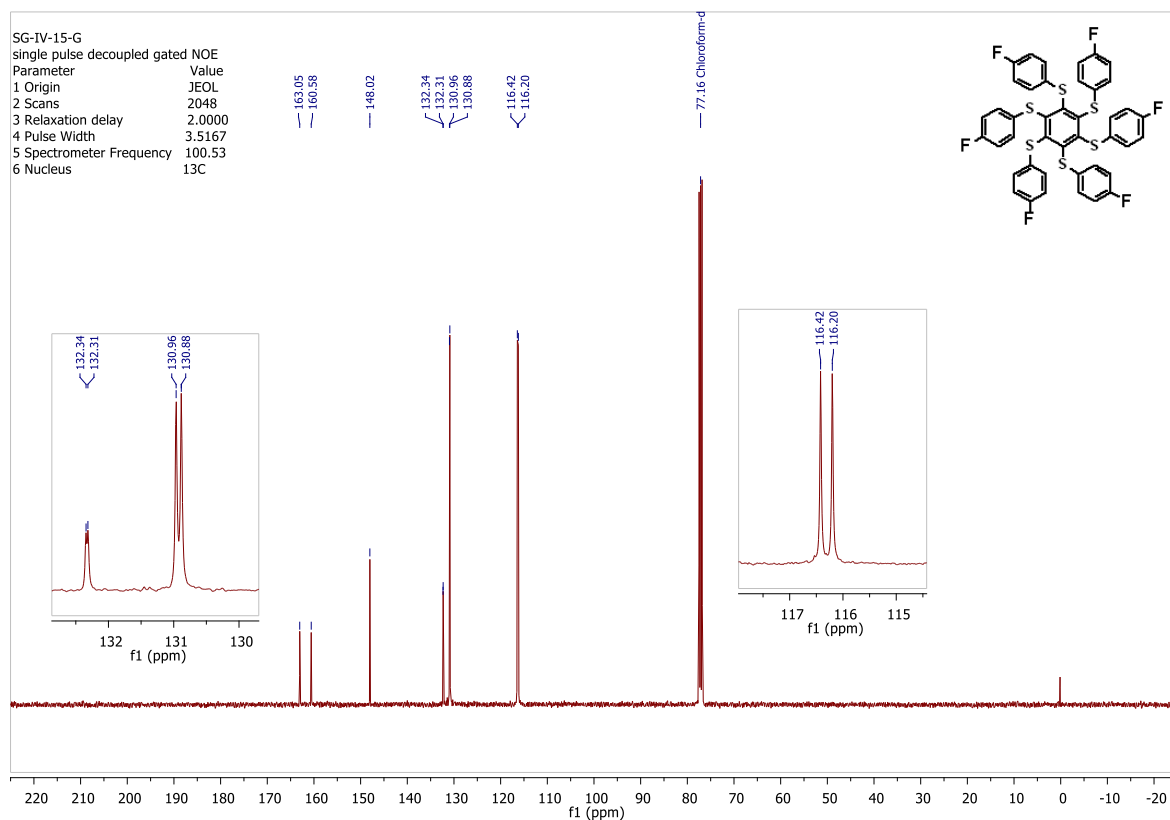
M.p. 117-118°C; **TLC** (SiO₂, tol./*n*-hex. 50:50 v/v) R_f = 0.33; **¹H NMR** (399.78 MHz, CDCl₃, ppm): δ = 6.82-6.94 (m, 24H); **¹³C NMR** (100.53 MHz, CDCl₃ ppm): δ = 161.8 (d, ¹J_{C-F} = 248,0 Hz), 148.0, 132.3, ⁴J_{C-F}=3.3 Hz), 130.9 (d, ³J_{C-F}= 7.9 Hz), 116.2 (d, ²J_{C-F}= 22.2 Hz); **¹⁹F NMR** (376.17 MHz, CDCl₃) : -114.16 (s); **MS** (EI, 70 eV) calculated for [C₄₂H₂₄F₆S₆]: 834 Da, found [M⁺] 834 *m/z*, [M – (F-Ph-SH)] 707 *m/z*; **HRMS (ESI+)** calculated for [C₄₂H₂₄F₆S₆]: 834.010 Da, found [M⁺] 834.009 *m/z*.



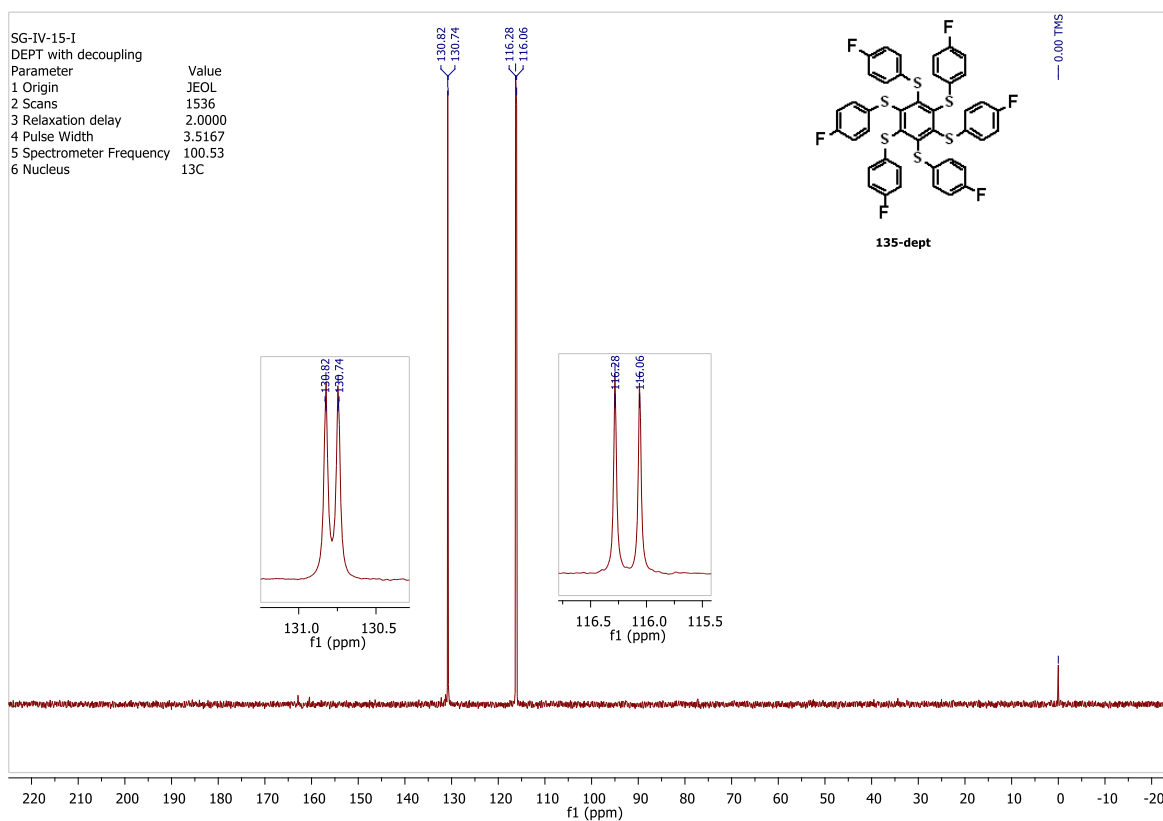
HRMS (ESI positive mode) of (**12**)



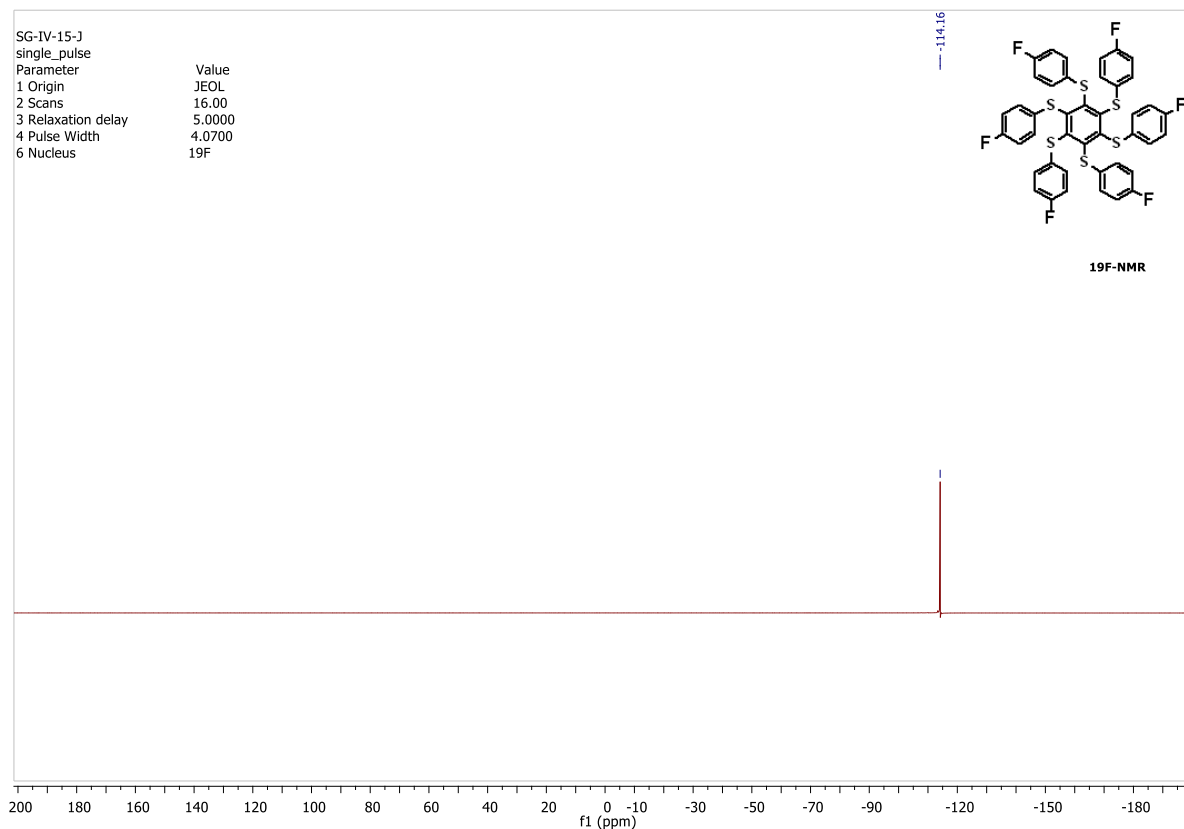
¹H-NMR spectrum of (**12**) (CDCl₃, 399.78 MHz)



¹³C-NMR {H} spectrum of (**12**) (CDCl₃, 100.53 MHz)



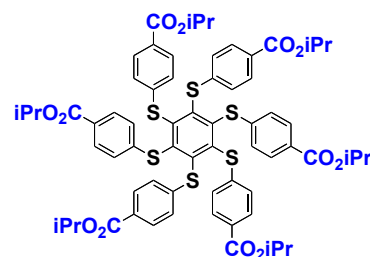
^{13}C -NMR DEPT 135 spectrum of (**12**) (CDCl_3 , 100.53 MHz)



^{19}F -NMR spectrum of (**12**) (CDCl_3 , 376,17 MHz)

Hexakis (4-isopropoxy carbonylphenylthio)benzene (57) ¹

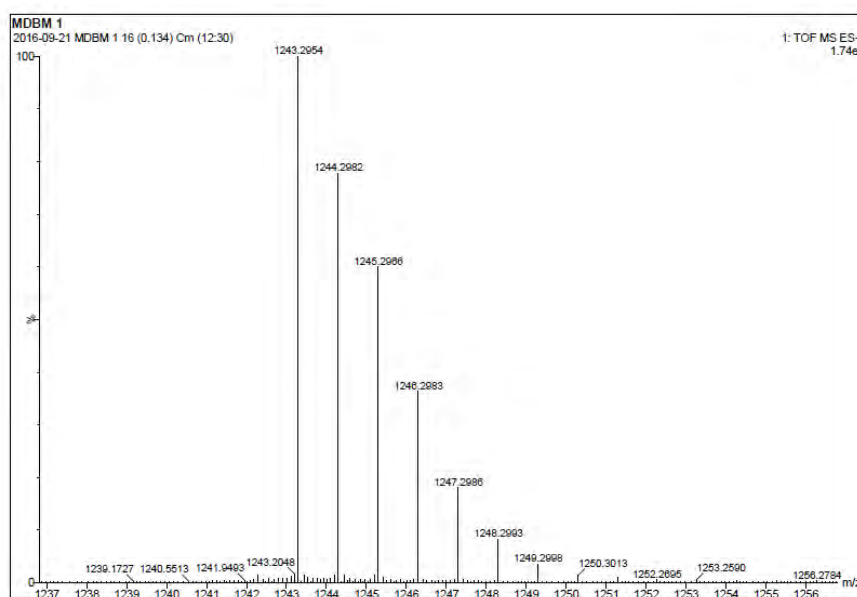
Hexachlorobenzene (676 mg, 2.37 mmol, 1.00 mol-eq), isopropyl-4-mercaptobenzoate (4.082 g, 20.83 mmol, 8.79 mol-eq) and dry potassium carbonate (3.809 g, 27.6 mmol, 11.7 mol-eq) were dried under high vacuum for 30 min. before being introduced into an oven-dried sealed tube. Under an argon atmosphere, dry DMF (10 mL, kept over activated 3Å molecular sieves) was added and the mixture was vigorously stirred at 60°C (oil bath temperature) for 4 days. Upon completion of the reaction, the reaction mixture was cooled down to room temperature and diluted with 150 mL of 1N HCl (aq.). A yellow-brown solid precipitated and the reaction mixture was extracted four times with toluene (4x50 mL). The combined organic phases were washed thrice with water (3x100 mL), dried over anhydrous MgSO₄, filtered and concentrated *in vacuo*. The crude yellow-orange solid was purified by trituration in ethanol (70 mL) under vigorous stirring and filtration. The collected solid was then recrystallized in warm isopropanol to give the desired compound as a yellow solid (2.830 g, 2.27 mmol, 96% yield).



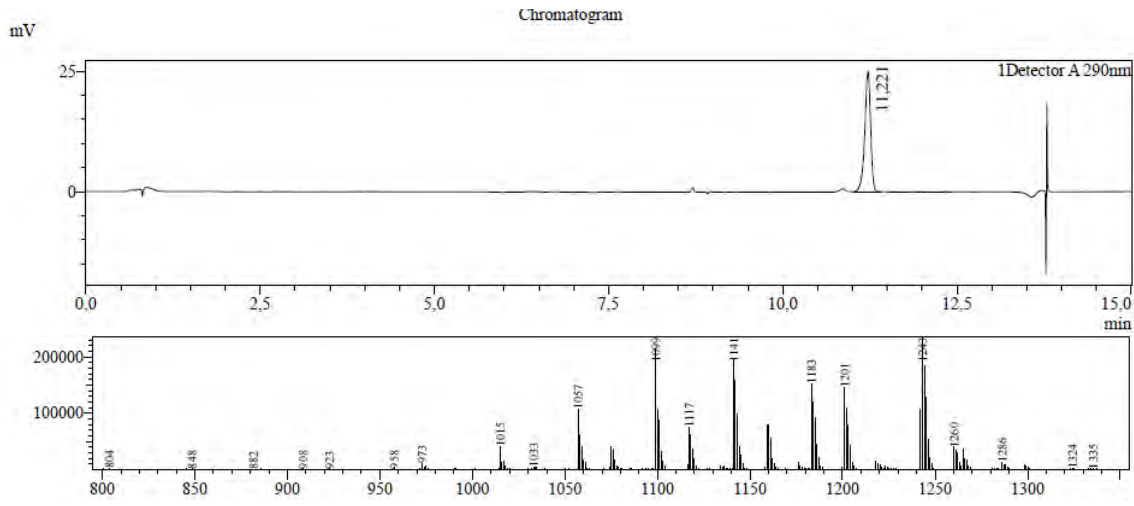
TLC (*n*-hept./EtOAc; 80:20 v/v) $R_f = 0.2$; **FT-IR** (ATR, diamond contact, neat, cm⁻¹) $\nu = 2977, 2940, 1708, 1592, 1270, 1179, 1091, 1012, 917, 852, 755, 687$; **¹H NMR** (399.78 MHz, CDCl₃, ppm): $\delta = 7.85$ (d_{app}, $J = 8.5$ Hz, 12H), 6.93 (d_{app}, $J = 8.4$ Hz, 12H), 5.22 (sept, $J = 6.3$ Hz, 6H), 1.36 (d, $J = 6.3$ Hz, 36H); **¹³C NMR** (100.53 MHz, CDCl₃ ppm): $\delta = 165.33, 148.11, 142.64, 130.42, 129.12, 126.97, 68.70, 22.06$; **LC-MS** (acetonitrile/water/ 0.1% formic acid; APCI: 1243 m/z [M+H]⁺); **HRMS (ESI+)** calculated for [C₆₆H₆₆O₁₂S₆ + H⁺]: 1243.2954 Da, found [M+H]⁺ 1243.2954 m/z ; **Elemental analysis**: calculated: %C 63.74 %H 5.35 %S 15.47, found: %C 63.31 %H 5.19 %S 15.45.

Reference:

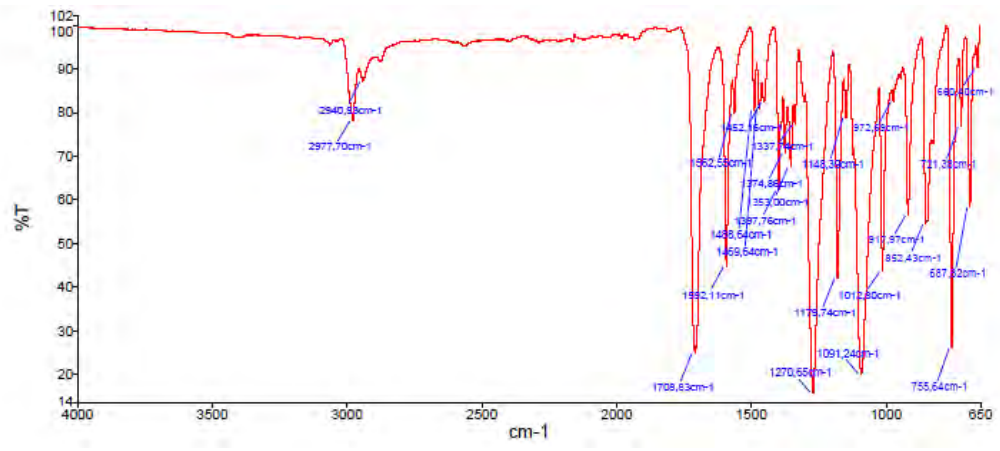
1. M. Villa, M. Roy, G. Bergamini, M. Gingras, P. Ceroni *Dalton Trans.* (2019), 48, 3815-3818.



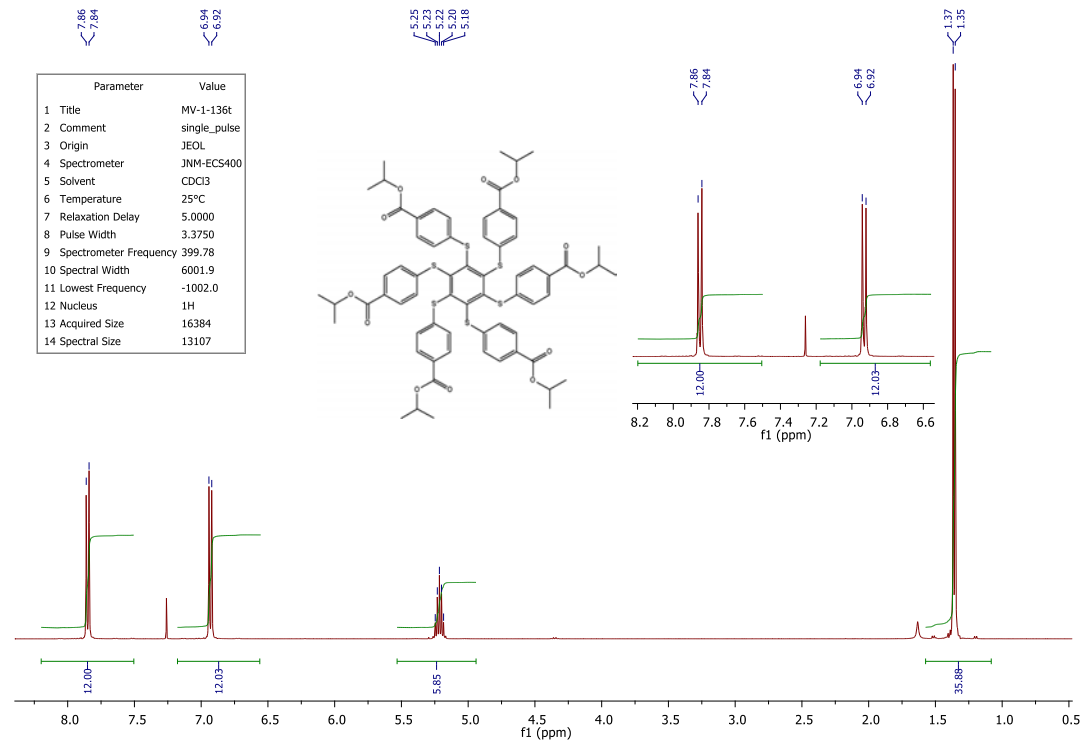
HRMS (ESI, positive mode) of (57)



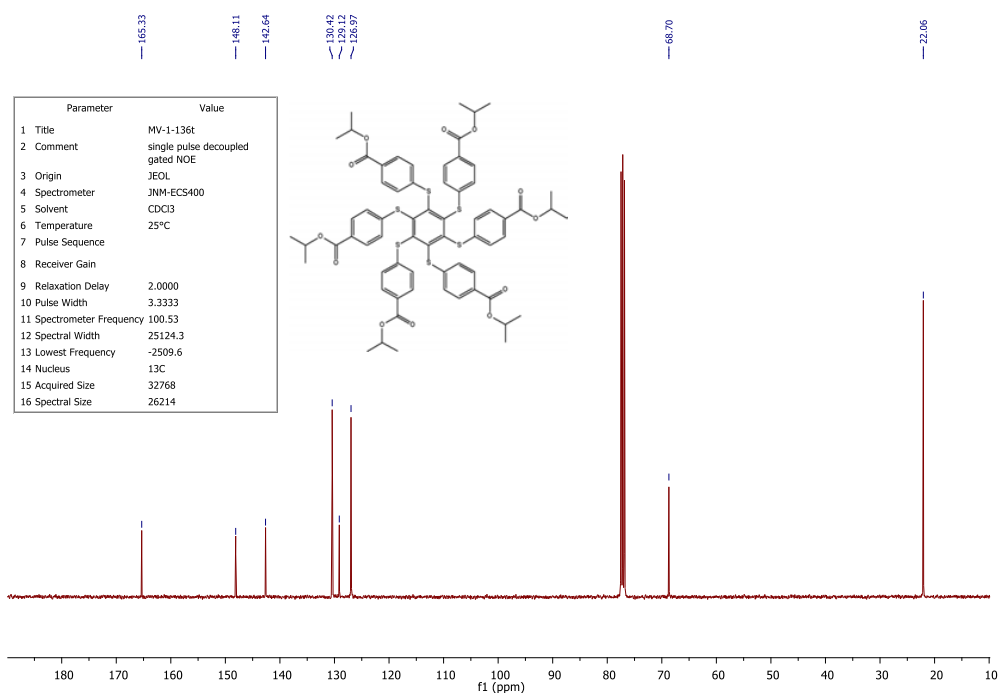
LC-MS: Reverse phase HPLC chromatogram of (57) and MS-APCI



FT-IR (ATR diamond contact) spectrum of (57)



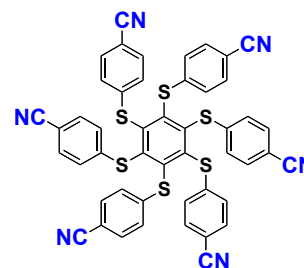
¹H-NMR spectrum of (57) (CDCl₃, 399.78 MHz)



^{13}C -NMR spectrum of (**57**) (CDCl_3 , 100.53 MHz)

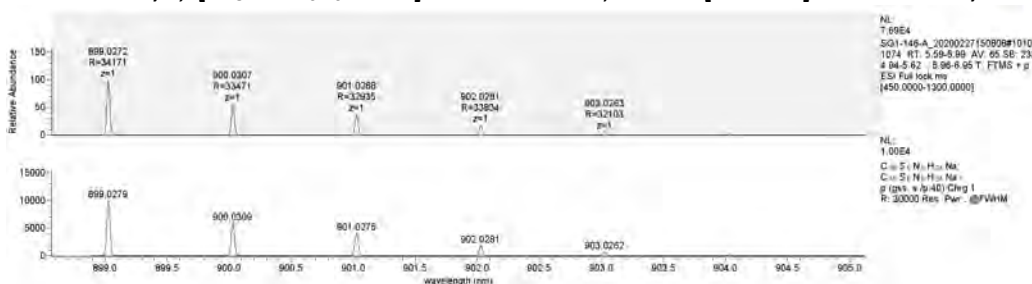
Hexakis(4-cyanophenylthio)benzene (**15**).

Hexachlorobenzene (100 mg, 0.351 mmol, 1.00 eq.), 4-mercaptobenzonitrile (285 mg, 2.106 mmol, 6.00 eq.) and dry potassium carbonate (292 mg, 2.112 mmol, 6.02 eq.) were introduced into an oven-dried sealed tube. Under an argon atmosphere, dry DMF (0.5 mL, kept over 3\AA molecular sieves) was injected via a syringe and the tube was purged with argon for 15-20 minutes before being sealed. The heterogeneous mixture was stirred at 40°C in an oil bath for 16h.

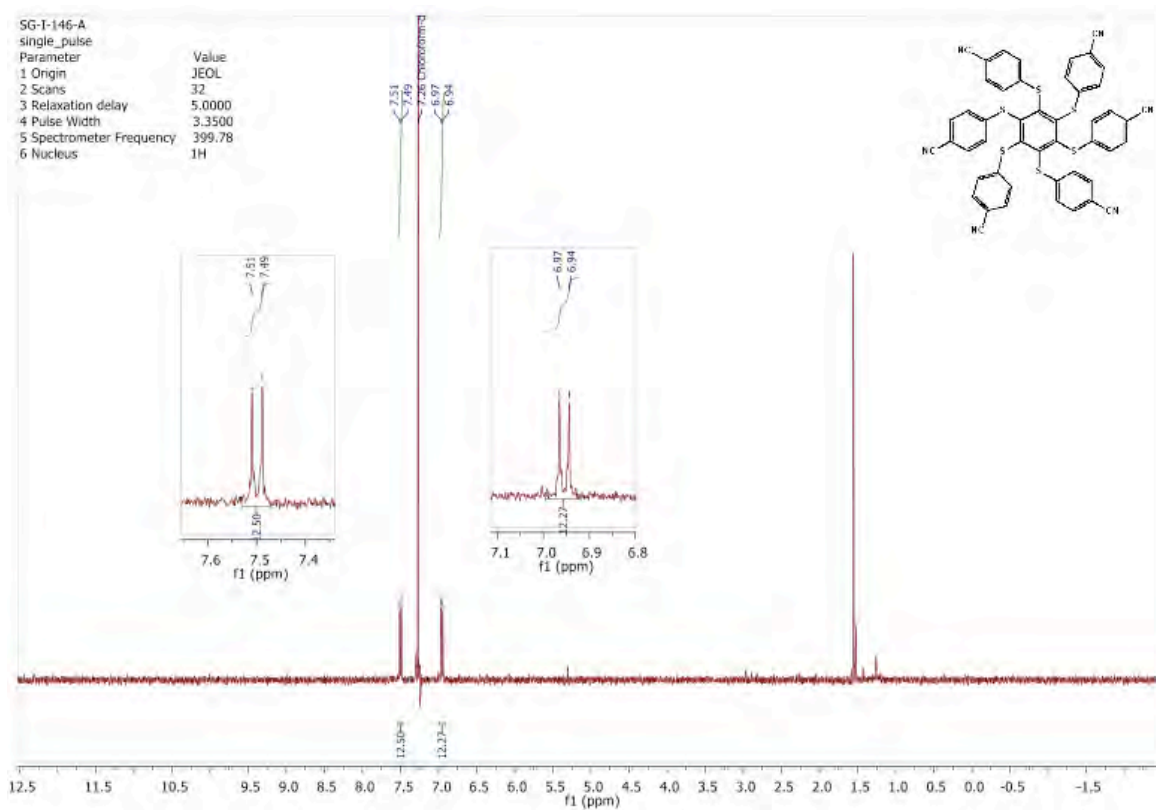


It turned from colorless to a bright yellow color in a few minutes. After cooling to 25°C and adding a solution of ethanol/water (50:50 v/v; 10 mL) a bright yellow solid precipitated. After filtration and drying under vacuum, the corresponding product (**15**) was obtained as a bright yellow solid (284 mg.; 0.324 mmol; 92% yield).

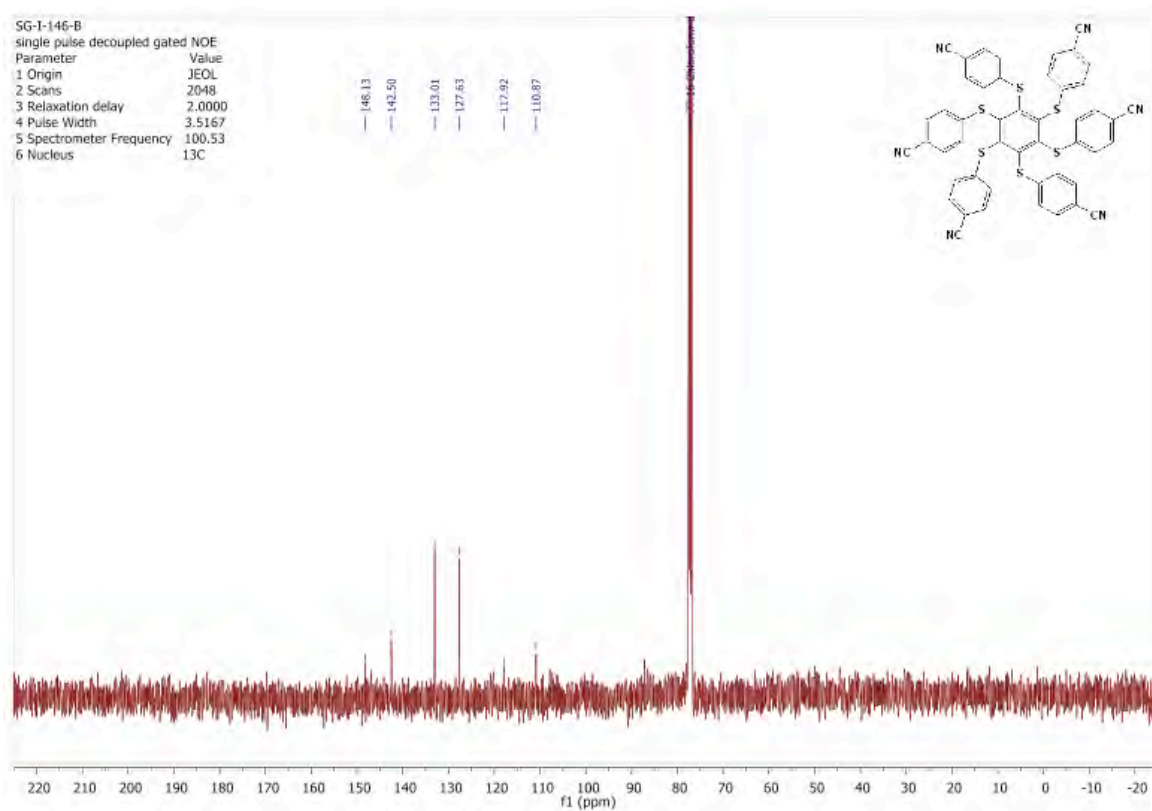
M.p.: $282\text{--}286^\circ\text{C}$; **TLC** (SiO_2 , *n*-hex/EtOAc: 70/30 v/v) $R_f = 0.29$; **^1H NMR** (399.78 MHz, CDCl_3 , ppm): $\delta = 7.50$ (d_{app} , $J = 8.4$ Hz, 12H), 6.95 (d_{app} , $J = 8.5$ Hz, 12H); **^{13}C NMR** (100.53 MHz, CDCl_3 ppm): $\delta = 148.1$, 142.5 , 133.0 , 127.6 , 117.9 , 110.9 ; **^1H NMR** (200.13 MHz, DMSO-d_6 , ppm): $\delta = 7.30$ (d_{app} , $^3J = 8.2$ Hz, 12H), 7.76 (d_{app} , $^3J = 8.2$ Hz, 12H); **^{13}C NMR** (50.32 MHz, DMSO-d_6 ppm): $\delta = 147.9$, 144.3 , 133.8 , 128.1 , 119.4 , 109.4 ; **HRMS (ESI+)** calculated for $[\text{C}_{48}\text{H}_{24}\text{N}_6\text{S}_6 + \text{H}^+]$: 877.0459 Da, found $[\text{M} + \text{H}^+]$ 877.0447 m/z ; $[\text{C}_{48}\text{H}_{24}\text{N}_6\text{S}_6 + \text{Na}^+]$: 899.0279 Da, found $[\text{M} + \text{Na}^+]$ 899.0272 m/z .



HRMS (ESI positive mode) of (**15**)



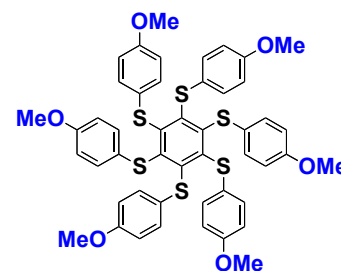
¹H-NMR spectrum of (**15**) (CDCl₃, 399.78 MHz)



¹³C-NMR spectrum of (**15**) (CDCl₃, 100.53 MHz)

Hexakis(4-methoxyphenylthio)benzene (56) ¹⁻⁶ (procedure taken from the PhD thesis of A. Pinchart)⁶

Into a two-necked 100 mL flask, fitted with a condenser, taken out of the oven and cooled under nitrogen, hexachlorobenzene (3.00 g.; 10.5 mmol) was added. 4-Methoxythiophenol (11.66 mL; 13.29 g.; 94.81 mmol) and dry 1,3-dimethyl-2-imidazolidinone (DMI, 30.0 mL) were injected via a syringe. Powdered NaH 95% (2.74 g., 114 mmol) was weighed in a dry flask taken out of the oven, which is then fixed with an elbow on the second neck of the flask containing the solution. The reaction medium is cooled by an ice bath. Oxygen

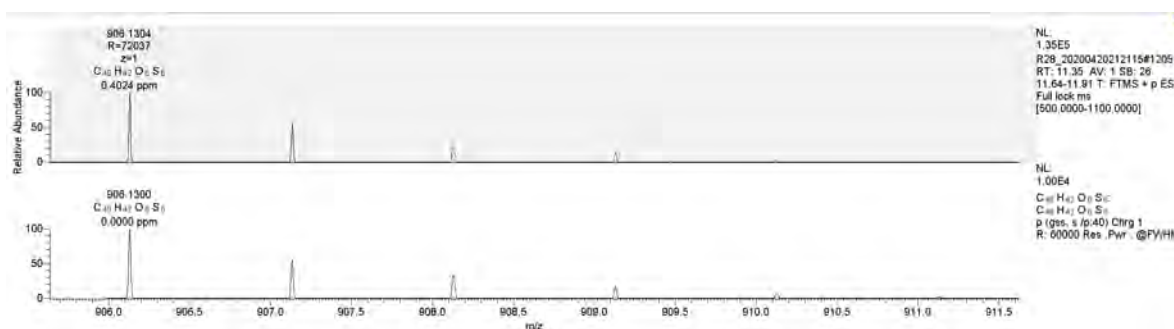


was removed by the use of vacuum and successive purges of nitrogen – freeze-thaw cycles (3 x 10 min). Sodium hydride was added carefully in small portions over 60 minutes. During the addition, a foam forms and the color of the solution became successively yellow, orange and red. At the end of the addition, the reaction medium was left for one hour at room temperature, with magnetic stirring. The flask was immersed in an oil bath at 80 ° C. After one hour, heating was stopped and the reaction was left at room temperature for two hours. A yellow precipitate formed on addition of 1M NaOH aqueous solution (1.25L). This solid is extracted with DCM (3 x 200 mL). The organic phase was dried over anhydrous Na₂SO₄, filtered and the solvent was evaporated off. A yellow oil was collected. After one night on the vacuum pump, the product solidified. Trituration in ethanol (150 mL) while stirring for two hours, filtration, and drying afforded a yellow solid (8.40 g.; 9.26 mmol; 88%).

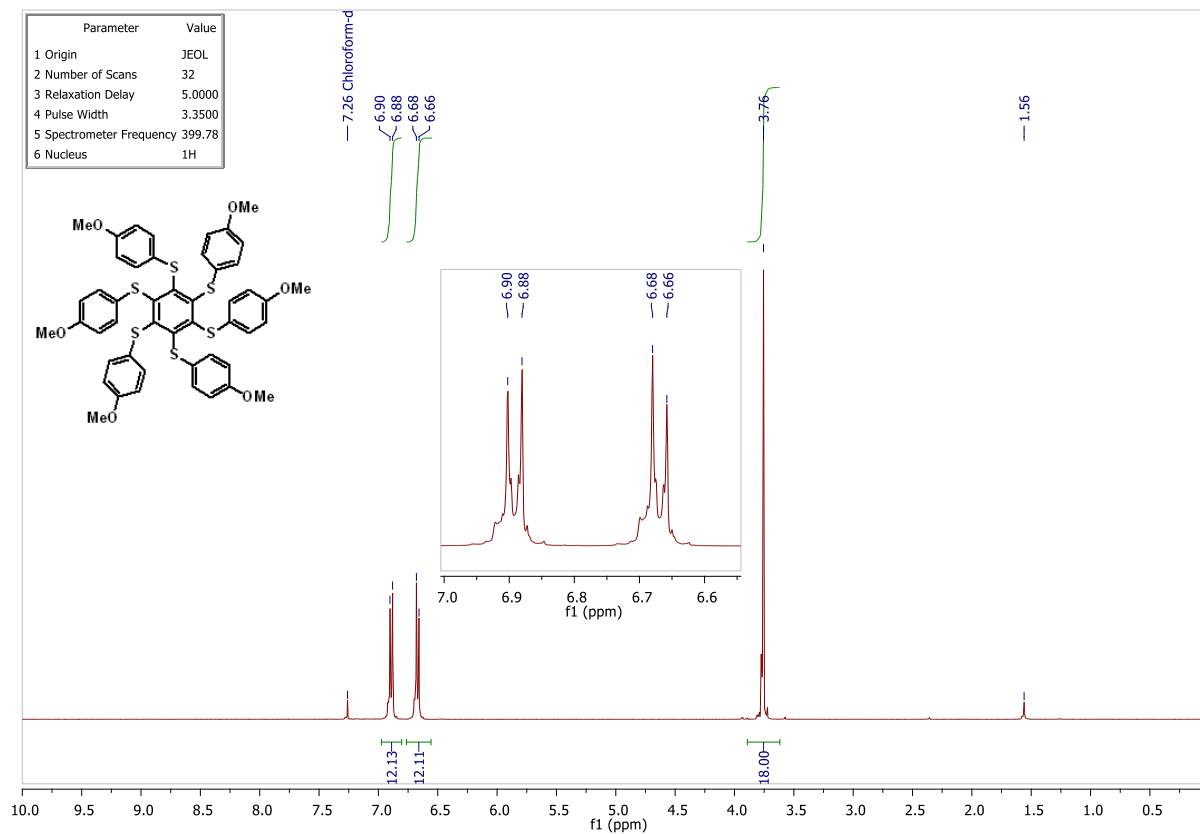
M.p.: 161-162°C (lit. 161-163°C⁵; 158-159°C⁴); **TLC** (SiO₂, DCM/acetone 95:5 v/v) R_f = 0.84; **¹H NMR** (399.78 MHz, CDCl₃, ppm): δ = 6.89 (d_{app}, J = 8.7 Hz, 12H), 6.67 (d_{app}, J = 8.7 Hz, 12H), 3.76 (s, 18H); **¹³C NMR** (100.53 MHz, CDCl₃, ppm): δ = 158.5, 147.8, 131.0, 128.7, 114.5, 55.4; **HRMS (ESI+)** calculated for [C₄₈H₄₂O₆S₆ + H⁺]: 907.1378 Da, found [M+H⁺] 907.1376 m/z.

References:

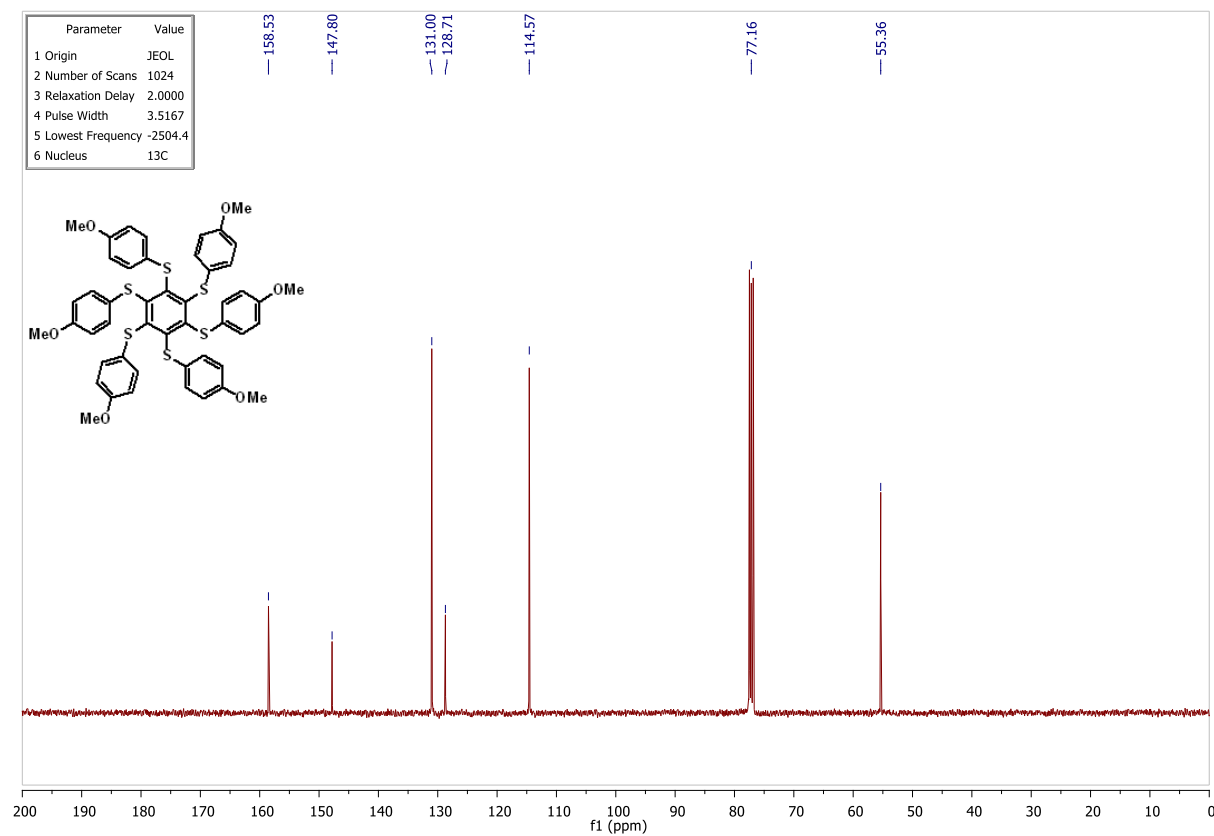
1. C. Aubert, C. Dallaire, G. Pepe, E. Levillain, G. Felix, M. Gingras, *Eur.J.Org.Chem.* (2012), 6145-6154.
2. C. Aubert, C. Dallaire, M. Gingras, *Tetrahedron Lett.* (2008), 49, 5355-5358.
3. J. N. Lowe, D.A. Fulton, S.-H. Chiu, A.M. Elizarov, S.J. Cantrill, S.J. Rowan, J.F. Stoddart, *J.Org. Chem.* (2004), 69, 4390-4402.
4. J.H.R. Tucker, M. Gingras, H. Brand, J.-M. Lehn, *J.Chem.Soc., Perkin Trans. 2: Physical Organic Chemistry* (1997), 7, 1303-1307.
5. T.D.P. Stack, R.H. Holm, *J.Am.Chem.Soc.* (1988), 110, 2484-94.
6. A. Pinchart, PhD dissertation, Université Libre de Bruxelles and Université de Paris-Sud Orsay, "Synthèse d'architectures moléculaires de sulfures de phénylène et de noyaux aromatiques persulfurés", sept. 26, 2000.



HRMS (ESI, positive mode) for (56)



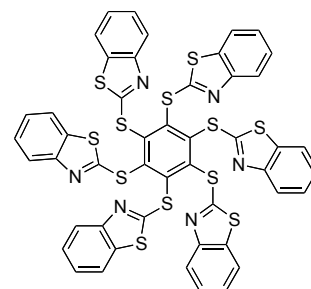
¹H-NMR spectrum of (**56**) (CDCl₃, 399.78 MHz)



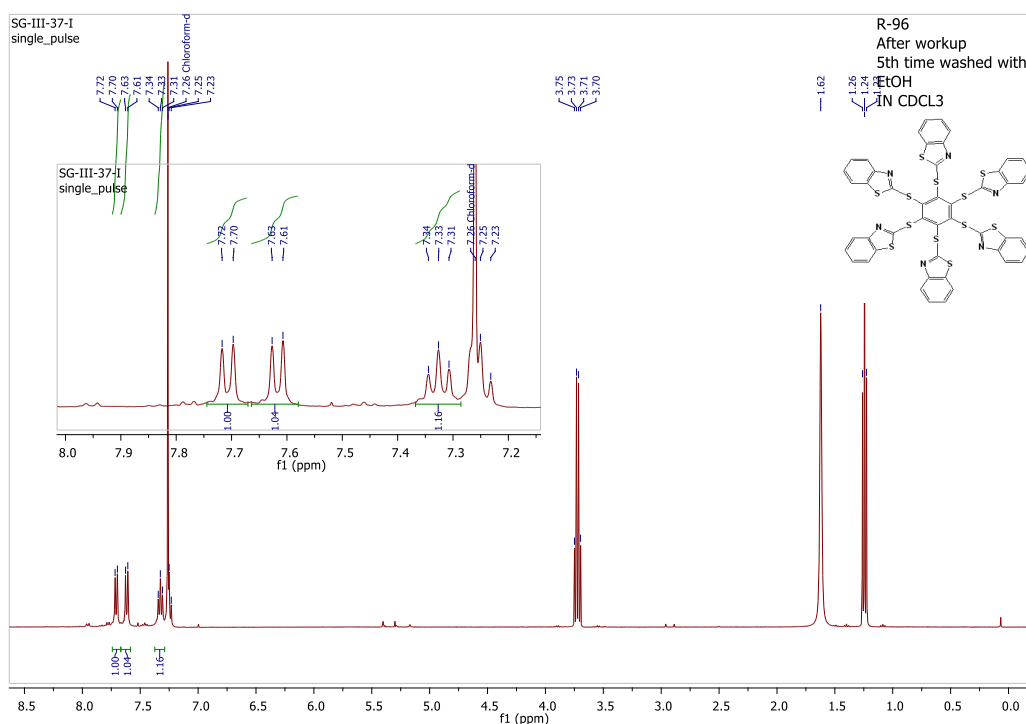
¹³C-NMR spectrum of (**56**) (CDCl₃, 100.53 MHz)

Hexakis(2-benzothiazolythio)benzene (16)

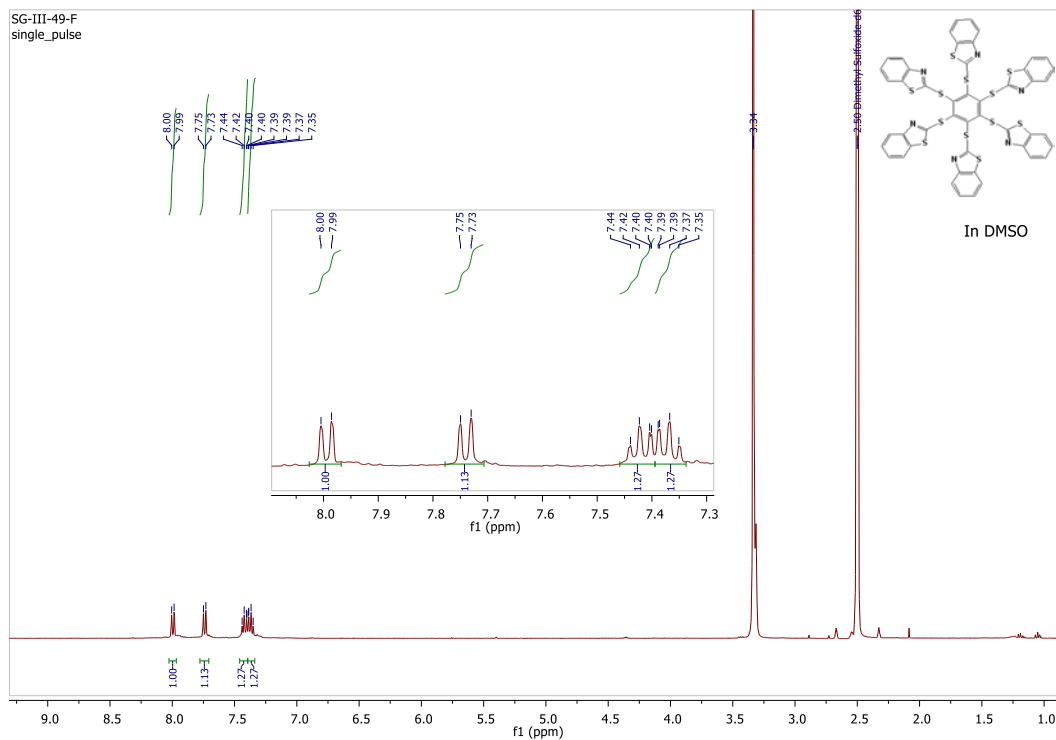
In an oven-dried sealed tube, purged with argon, was added hexachlorobenzene (0.200 g, 0.702 mmol, 1.00 mol-eq.), dried potassium carbonate (1.163 g, 8.415 mmol, 11.99 mol-eq.), 2-mercaptobenzothiazole (1.000 g, 5.979 mmol, 8.517 mol-eq.) and dry DMF (3.5 mL, dried and kept over activated molecular sieves 3Å). Argon was bubbled through the mixture for 5-10 min.. The color changed from yellow to orange. The tube was sealed and the reaction was stirred at 60°C for 5 days in an oil bath. Most DMF was removed on a rotary evaporator under reduced pressure. To the reaction mixture was added DCM (15 mL) and the organic layer was washed with H₂O (2×15mL) to remove remaining DMF. The organic phase was dried over anhydrous MgSO₄, filtered and DCM evaporated to afford a yellow-orange solid. It was triturated with EtOH (5×10 mL) at 25°C with a strong stirring for several minutes, and the supernatant was removed. It was repeated four times. The solid was then dried *in vacuo* to afford a pure yellow solid (0.634 g, 5.93 mmol, 84% yield).



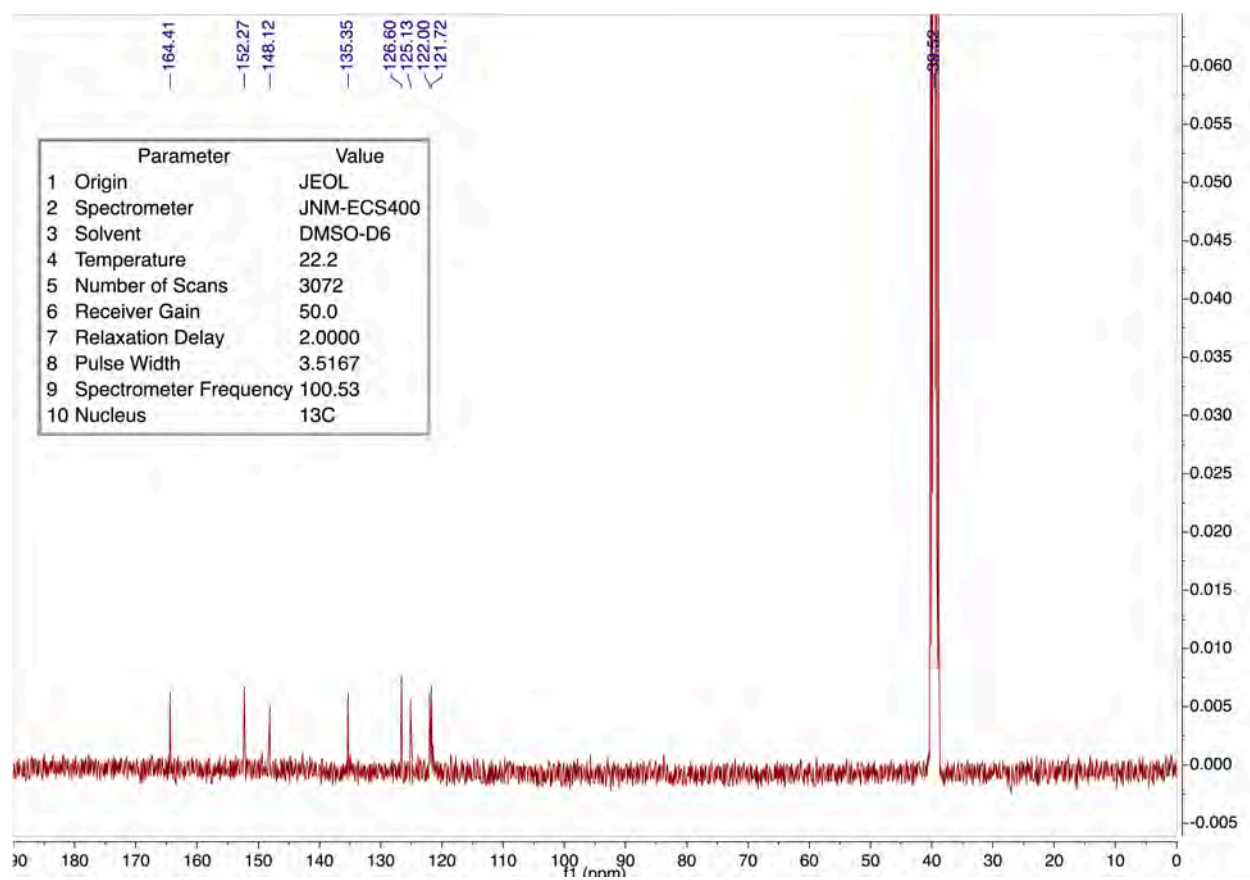
M.p.: 218-234°C (dec.); **TLC** (SiO₂, EtOAc/cyclohex. 10:90 v/v) R_f = 0.43; (SiO₂, DCM 100%) R_f = 0.23; **¹H NMR** (SGIII49G, 399.78 MHz, DMSO-d₆, ppm): δ = 7.99 (d, J = 8.0 Hz, 1H), 7.74 (d, J = 7.8 Hz, 1H), 7.42 (ddd, J = 7.9, 7.3, 1.3 Hz, 1H), 7.36 (dd, J = 7.6, 7.5, 1.2 Hz, 1H); **¹H NMR** (SGIII49E, 399.78 MHz, CDCl₃, ppm): δ = 7.71 (d, J = 8.0 Hz, 1H); 7.62 (d, J = 7.8 Hz, 1H), 7.32 (dd, J = 7.8, 7.5 Hz, 1H), 7.24 (dd, J = 7.8, 7.5 Hz, 1H); **¹³C NMR** (SGIII37K, 100.53 MHz, DMSO-d₆, ppm): δ = 164.4, 152.3, 148.1, 135.3, 126.6, 125.1, 122.0, 121.7; **¹³C NMR** (SGIII49E, 100.53 MHz, CDCl₃, ppm): δ = 164.8, 153.0, 148.8, 135.9, 126.3, 124.9, 122.3, 121.1. **MS (MALDI-TOF)** calculated for [C₄₈H₂₄N₆S₁₂ + H⁺]: 1068.87 Da, found 1068.70; **HRMS (ESI+)** calculated for [C₄₈H₂₄N₆S₁₂ + H⁺]: 1068.8789 Da; for [C₄₈H₂₄N₆S₁₂ + Na⁺]: 1090.8609 Da; for [C₄₈H₂₄N₆S₁₂ + K⁺]: 1106.8348 Da, found [M + H⁺] 1068.8791; [M + Na⁺] 1090.8610; [M + K⁺] 1106.8349.



¹H-NMR spectrum of (16) (CDCl₃, 399.78 MHz)



$^1\text{H-NMR}$ spectrum of **(16)** (DMSO- d_6 , 399.78 MHz)



$^{13}\text{C-NMR}$ spectrum of **(16)** (DMSO- d_6 , 100.53 MHz)

2.2 Penta(thio) benzene asterisks

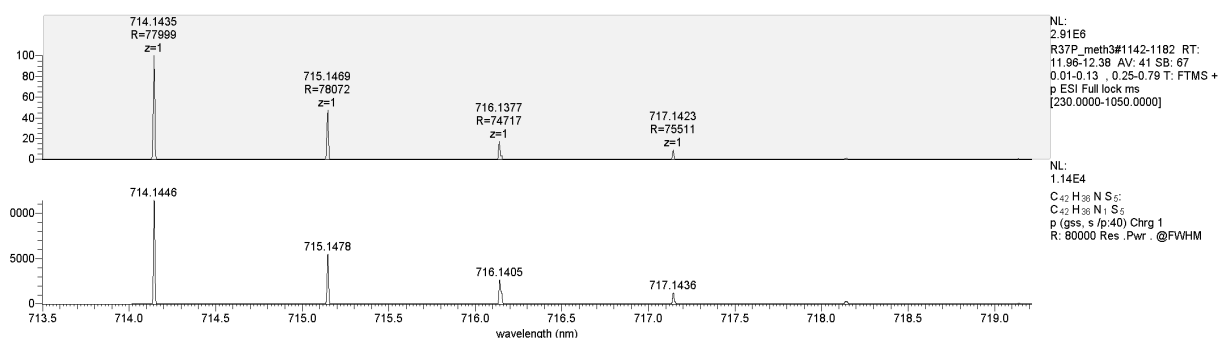
2,3,4,5,6-pentakis(4-methylphenylthio)benzotrile (17) ^{1,2}

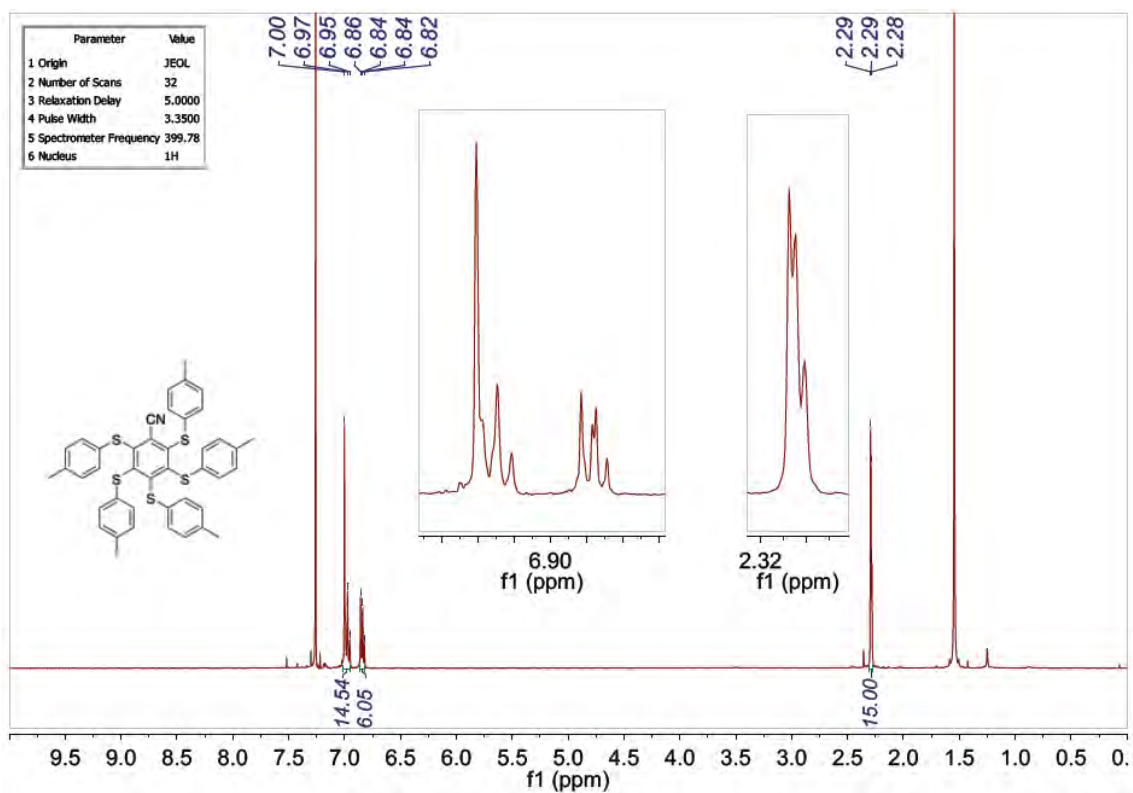
To a solution of 2,3,4,5,6-pentafluorobenzotrile (106 mg, 0.549 mmol, 1.00 eq.) in dry DMF (4.0 mL, kept over activated 3Å molecular sieves) was added dry potassium carbonate (572 mg, 4.14 mmol, 7.54 mol-eq.). The mixture was purged with argon for several minutes. 4-Methylbenzenethiol (482 mg, 3.88 mmol, 7.07 mol-eq.) was added and the reaction mixture was stirred at 20°C for 12 hours while changing color to bright yellow. Upon completion of the reaction (absence of ¹⁹F NMR signal), an aqueous solution of NaOH (2M, 50 mL) was added, and the mixture was extracted with DCM (3x30 mL). The organic layers were combined, dried over anhydrous MgSO₄, filtered and concentrated *in vacuo*. The crude product was then purified by column chromatography over silica gel using petroleum ether/DCM (80:20 v/v) as eluent. A bright yellow solid (17) was obtained (370 mg, 0.518 mmol, 94 % yield).

M.p.: 170.6-173.3°C; **TLC** (SiO₂, petroleum ether/DCM; 80:20 v/v) R_f = 0.16; **¹H NMR** (399.78 MHz, CDCl₃, ppm) δ = 7.01-6.94 (m, 14H), 6.84 (d, J = 8.2 Hz, 4H), 6.82 (d, J = 8.0 Hz, 2H), 2.295 (s, 6H), 2.290 (s, 6H), 2.28 (s, 3H); **¹³C NMR** (100.53 MHz, CDCl₃, ppm) δ = 153.24, 146.83, 146.76, 137.45, 136.94, 136.71, 133.61, 133.31, 131.98, 130.53, 130.07, 130.00, 129.97, 129.39, 128.96, 124.76, 115.39, 21.28, 21.27, 21.23; **HRMS (API+)** calculated for [C₄₂H₃₅NS₅ + NH₄]⁺: 731.1717 Da, found [M+NH₄]⁺ 731.1712 m/z. **HRMS (ESI+)** calculated for [C₄₂H₃₅N₁S₅ + H]⁺: 714.1446 Da, found [M+H]⁺ 714.1435 m/z.

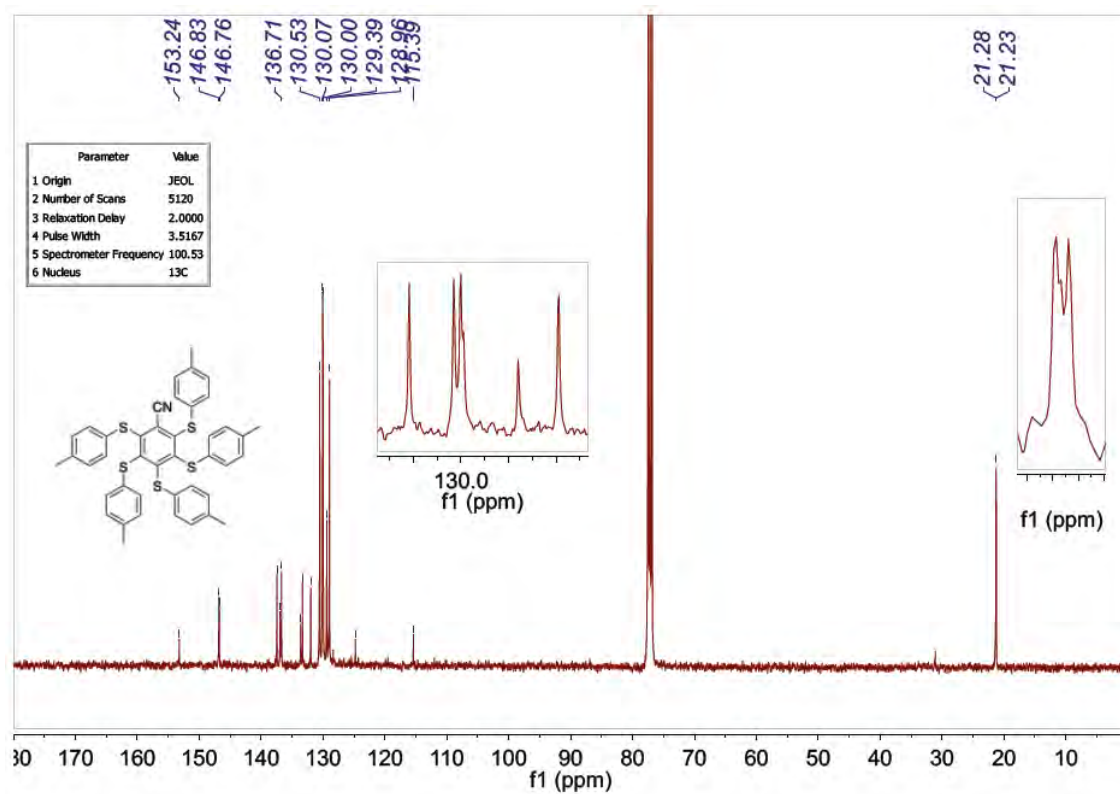
Reference:

1. M. Villa; S. D'Agostino; P. Sabatino; R. Noel; J. Busto; M. Roy; M. Gingras; P. Ceroni; *New J. Chem.* (2020), 44, 3249-3254.
2. R. Noel, *Étude et développement de substrats microporeux pour l'adsorption du radon et son application en physique du neutrino*, doctoral dissertation, Aix-Marseille Université, Déc. 13, 2015; <https://tel.archives-ouvertes.fr/tel-01521979>.





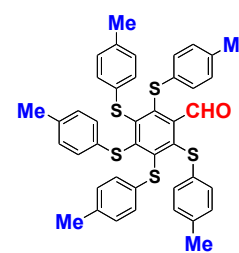
¹H-NMR spectrum of **(17)** (CDCl₃, 399.78 MHz)



¹³C-NMR spectrum of **(17)** (CDCl₃, 100.53 MHz)

2,3,4,5,6-pentakis(4-methylphenylthio)benzaldehyde (**18**)¹

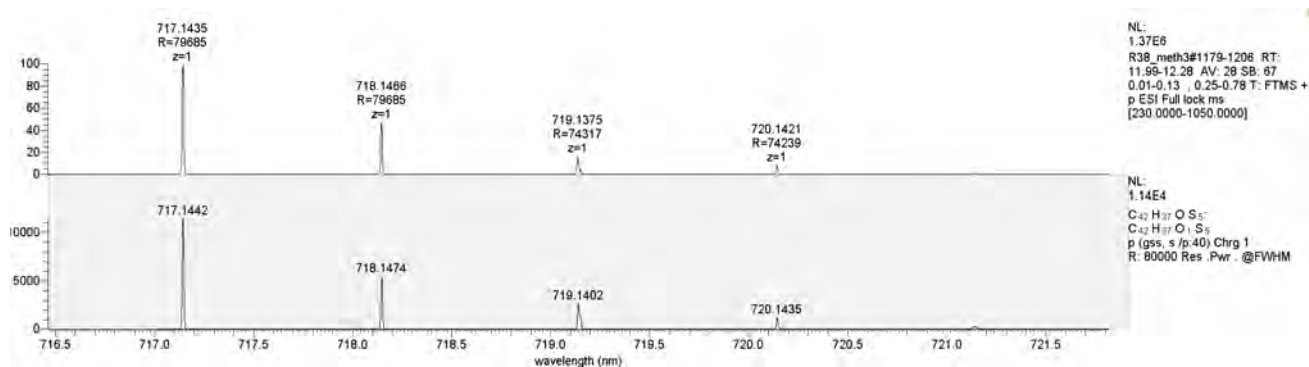
Pentafluorobenzaldehyde (500 mg, 2.55 mmol, 1.00 mol-eq.), was dissolved in dry DMI (6.0 mL), and potassium carbonate (2.82 g, 20.4 mmol, 8.00 mol-eq.) was added. The mixture was purged with argon for several minutes. The color of the mixture turned yellow. 4-Methyl-benzenethiol (2.37 g, 19.1 mmol, 7.49 mol-eq.) was added and the color changed to orange at 20°C. It was then heated to 40 °C (oil bath) and stirred overnight (12 hrs). Upon completion of the reaction (absence of ¹⁹F NMR signal), the mixture was treated with a saturated NaCl aqueous brine solution (100 mL) and extracted with Et₂O (4 x 30 mL). The organic layers were combined, dried over anhydrous MgSO₄ and filtered. After evaporating the solvent, a dark yellow oil was purified by column chromatography over silica gel using cyclohexane/DCM (90:10 v/v) as eluent. A yellow solid (**18**) was obtained (1.655 g, 2.32 mmol, 91% yield).



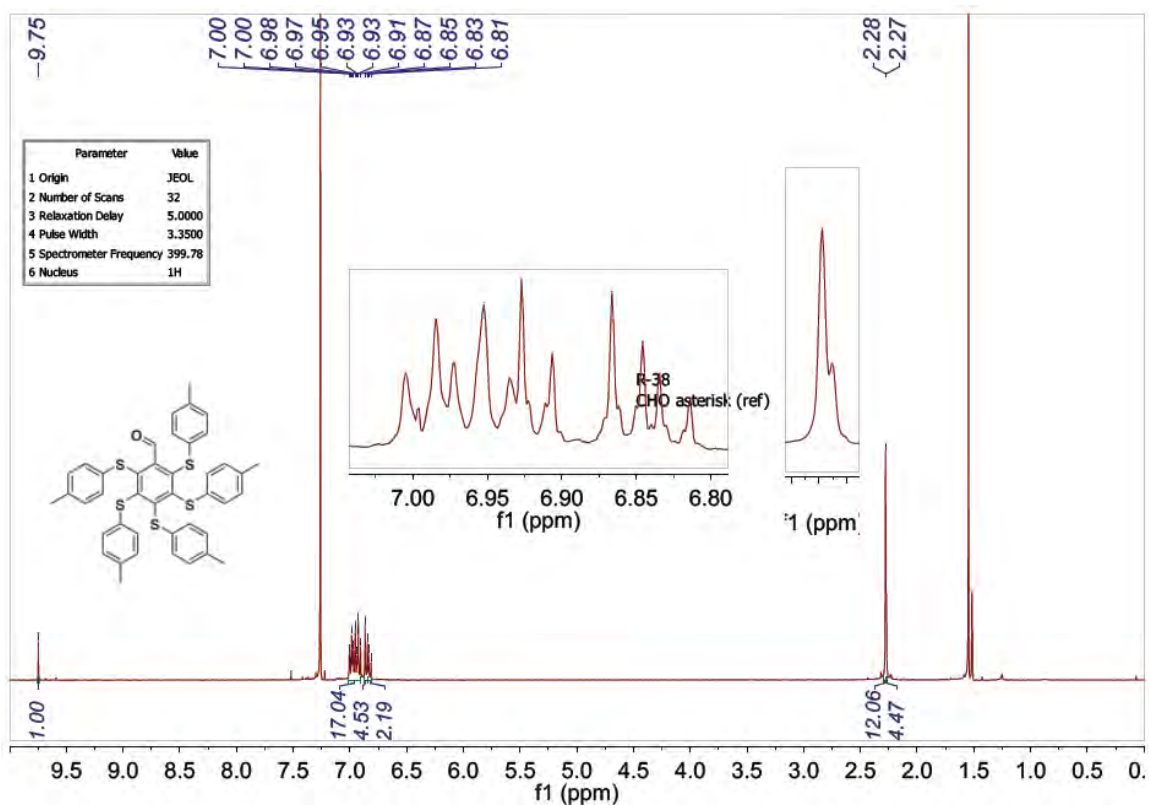
M.p.: 133.6-141.0°C; **TLC** (SiO₂, tol/cyclohex. 50:50 v/v) R_f = 0.47; **FT-IR** (ATR, diamond contact, neat, cm⁻¹) ν = 3018 (w), 2917 (w), 2862 (w), 1889 (w) 1698 (m), 1566 (w), 1489 (s), 1447(m), 1286 (m), 1162 (m), 1083 (m), 1015 (m), 926 (m), 796 (s), 734(m), 700 (m); **¹H NMR** (399.78 MHz, CDCl₃, ppm) δ = 9.75 (s, 1H), 6.99 (d, J = 8.3 Hz, 4H), 6.96 (d, J = 8.2 Hz, 4H), 6.94 (d, J = 8.3 Hz, 2H), 6.92 (d, J = 8.3 Hz, 4H), 6.86 (d, J = 8.3 Hz, 4H), 6.82 (d, J = 8.3 Hz, 2H), 2.28 (s, 12H), 2.27 (s, 3H); **¹³C NMR** (100.53 MHz, CDCl₃, ppm) δ = 190.69, 150.97, 147.28, 145.94, 141.46, 137.00, 136.39, 136.31, 134.12, 133.78, 133.15, 130.16, 129.87, 129.81, 129.49, 129.04, 128.72, 21.22 (3C); **HRMS (ESI+)** calculated for [C₄₂H₃₆O₁S₅+H⁺]: 717.1442 Da, found [M+H⁺] 717.1435 m/z.

Reference:

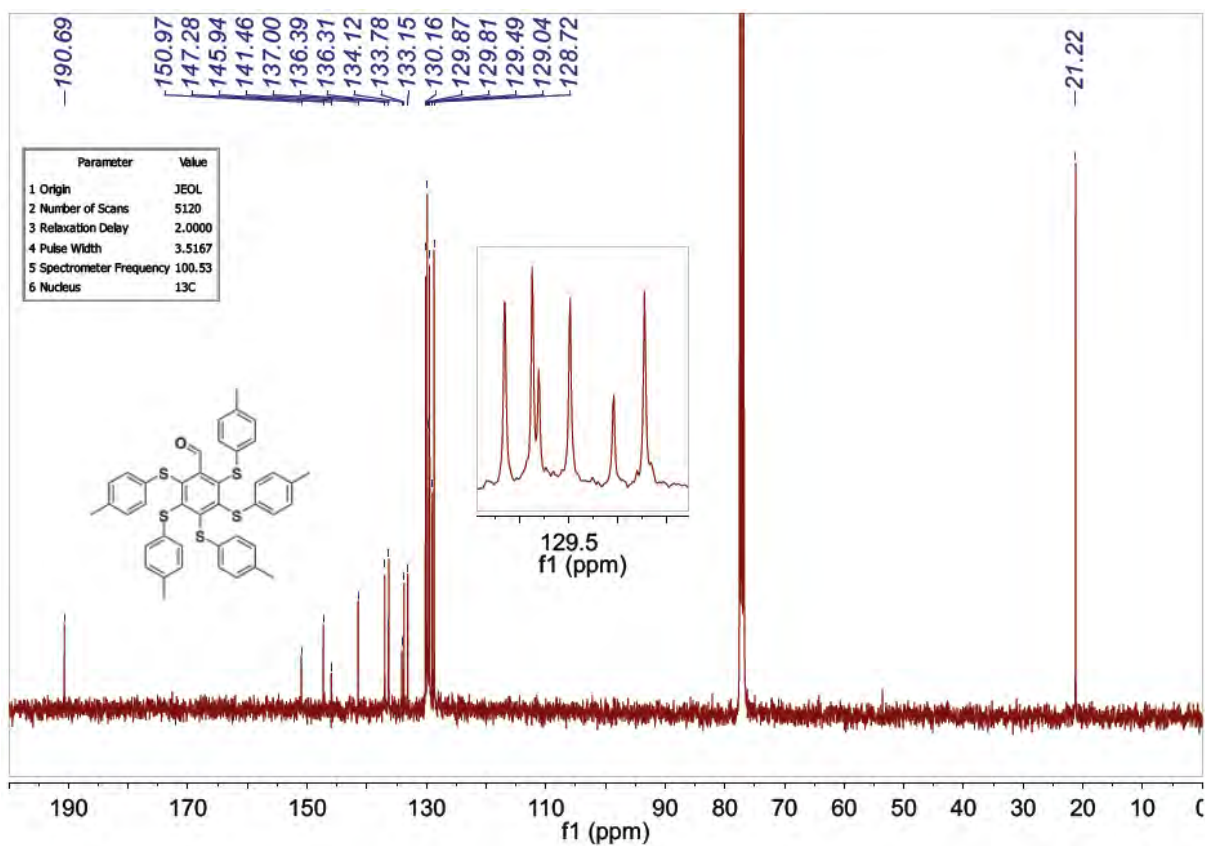
1. M. Villa; S. D'Agostino; P. Sabatino; R. Noel; J. Busto; M. Roy; M. Gingras; P. Ceroni, *New J. Chem.* (2020), 44, 3249-3254.



HRMS (ESI, positive mode) of (**18**)



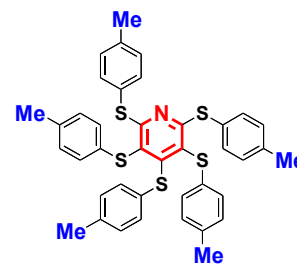
¹H-NMR spectrum of **(18)** (CDCl₃, 399.78 MHz)



¹³C-NMR spectrum of **(18)** (CDCl₃, 100.53 MHz)

2,3,4,5,6-pentakis(4-methylphenylthio)pyridine (**19**)¹

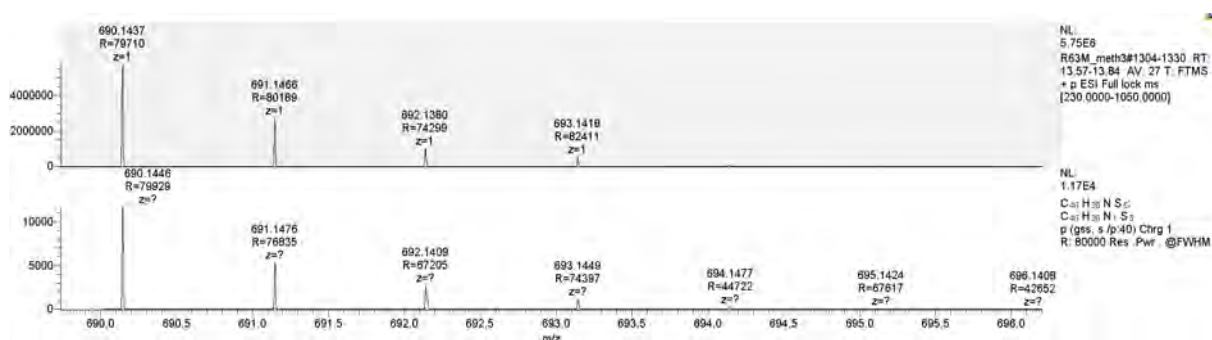
Under an argon atmosphere, pentafluoropyridine (128 mg, 0.757 mmol, 1.00 mol-eq.) and 4-methylbenzenethiol (930 mg, 7.49 mmol, 9.89 mol-eq.) were added in a 50 ml two-necked flask, followed by injection of DMI (5.0 ml, dried over activated 4Å molecular sieves) via a syringe. The mixture was cooled in an ice-bath (3°C) and powdered NaH (183 mg, 7.63 mmol, 10.0 mol-eq.) was slowly added. Upon addition of NaH, the mixture became light yellow and hydrogen was evolved. The reaction mixture was allowed to reach room temperature and it was stirred for six days. Ethanol (20 mL) was slowly added to the flask while stirring, and the resulting precipitate was collected by filtration under vacuum. TLC indicated that the crude product contained a slight impurity. A trituration in EtOH while stirring vigorously for 30 min. was carried out, and the solid was again collected by vacuum filtration. The pale-yellow powder (**19**) was then dried under high vacuum to afford a pure solid (510 mg; 0.739 mmol, 98% yield).



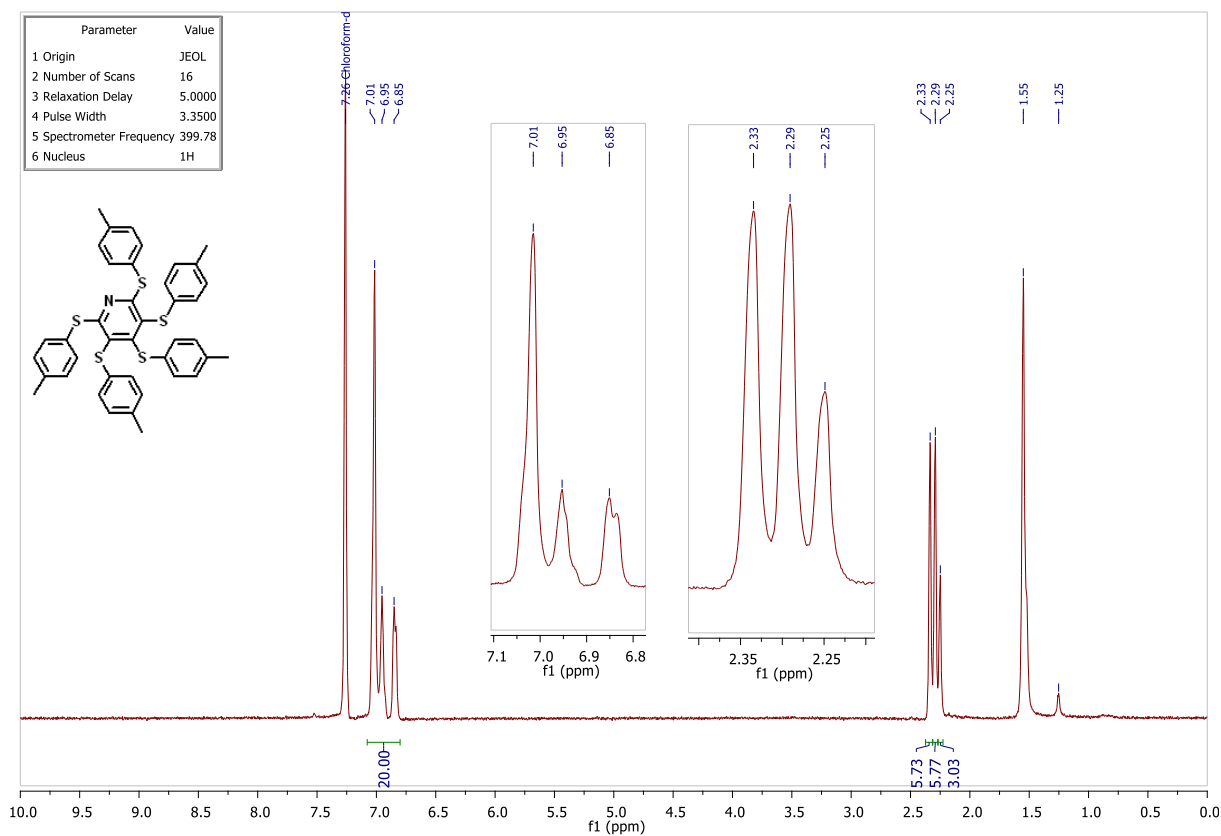
M.p.: 147-149°C (lit. 147-149°C)¹; **TLC** (SiO₂, acetone/cyclohex. 30:70 v/v) R_f = 0.70; (SiO₂, petroleum ether/DCM 50:50 v/v) R_f = 0.80; **¹H NMR** (399.78 MHz, CDCl₃, ppm) δ = 6.80-7.10 (m, 20H), 2.33 (s, 6H), 2.29 (s, 6H), 2.25 (s, 3H); **¹³C NMR** (100.53 MHz, CDCl₃, ppm) δ = 168.18, 158.66, 138.41, 137.17, 136.36, 135.22, 132.94, 132.64, 130.48, 130.15 (2C), 129.77, 128.11, 127.20, 126.05, 21.94, 21.50 (2C); **¹³C NMR** (125.77 MHz, CDCl₃, ppm) δ = 21.38, 21.41, 21.81, 125.98, 127.14, 128.03, 130.07, 130.25, 130.39, 132.55, 132.85, 135.04, 135.11, 136.26, 137.07, 138.30, 158.55, 168.07; **MS (MALDI-TOF)** calculated for [C₄₀H₃₅N₁S₅+H⁺]: 690.14 Da, found 690.10 m/z; **HRMS (ESI+)** calculated for [C₄₀H₃₅N₁S₅+H⁺]: 690.1446 Da, found [M+H⁺] 690.1437 m/z.

Reference:

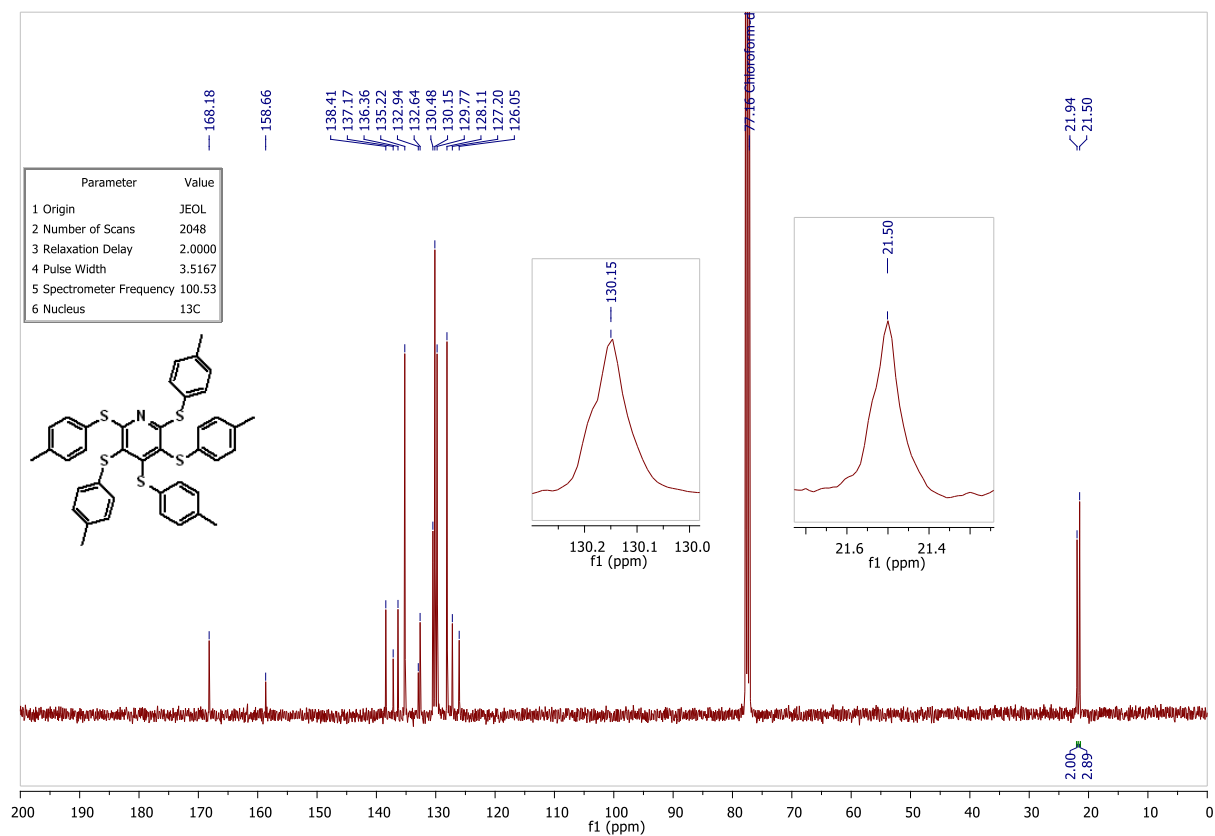
1. J.H.R. Tucker; M. Gingras; H. Brand; J.-M. Lehn, *J. Chem. Soc. Perkin Trans. 2: Physical Organic Chemistry* (1997), 7, 1303-1307.



HRMS (ESI, positive mode) of (**19**)



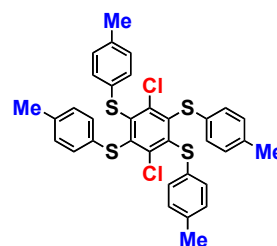
¹H-NMR spectrum of **(19)** (CDCl₃, 399.78 MHz)



¹³C-NMR spectrum of **(19)** (CDCl₃, 100.53 MHz)

2.3 Tetrathio benzene and pyridine asterisks

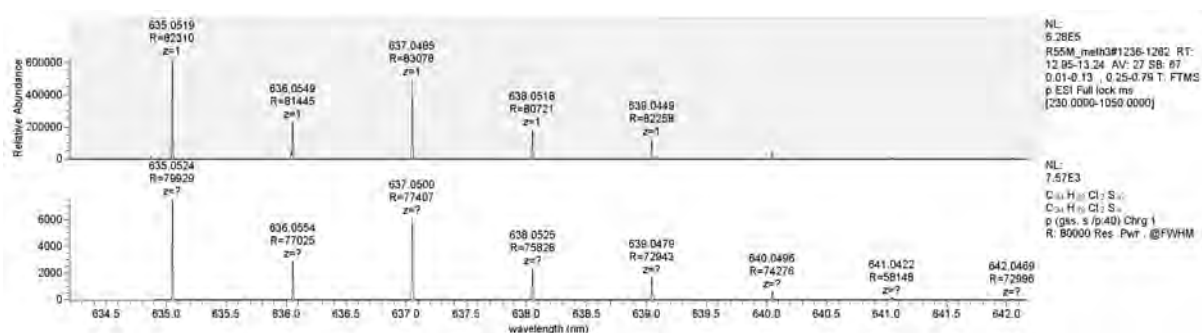
1,4-dichloro-2,3,5,6-tetrakis(4-methylphenylthio)benzene (20).¹ In a 50 mL two-necked flask, taken out of the oven and cooled under argon, hexachlorobenzene (100 mg, 0.351 mmol) and *p*-methylbenzenethiol (4.22 eq., 179 mg, 1.48 mmol) were added. DMI (5.0 mL) was injected. Powdered sodium hydride 95% (41 mg, 1.7 mmol) was weighed in a Gooch tube installed at a neck. Oxygen was removed by the use of high vacuum and successive purges of nitrogen – freeze-thaw cycles. The hydride was slowly added at 3°C (ice-bath temperature). The reaction mixture was stirred at room temperature for 3 hours. After cooling, EtOAc (20 ml) was added and a pale yellow solid precipitated. It was filtered, recovered and dried. After two triturations in ethanol while stirring vigorously and filtration, a pale yellow solid (**20**) was obtained (147 mg, 0.231 mmol, 66% yield).



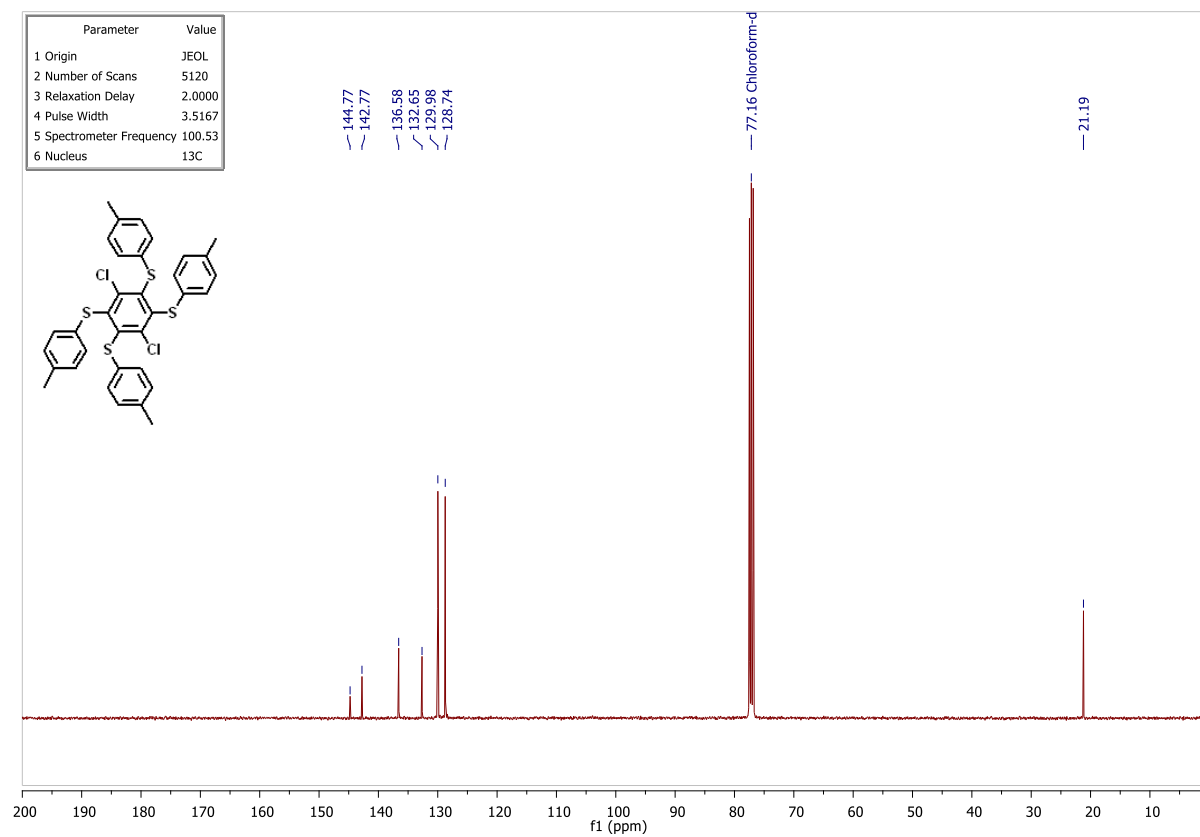
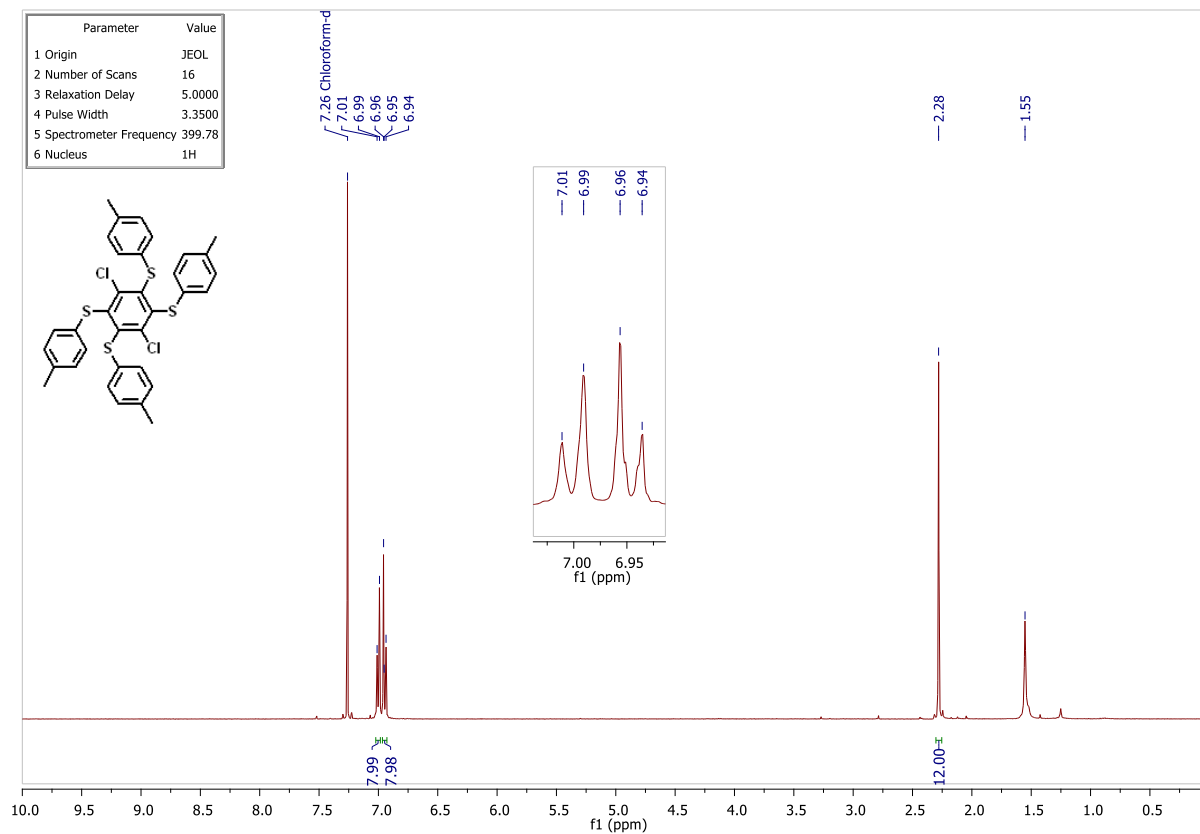
M.p.: 235-239°C (pale yellow solid); **TLC** (SiO₂, EtOAc/*n*-hex 10:90 v/v) : R_f = 0.50; **¹H NMR** (399.78 MHz, CDCl₃, ppm): δ = 7.00 (d_{app}, J = 8.2 Hz, 8H), 6.95 (d_{app}, J = 8.3 Hz, 8H), 2.28 (s, 12H); **¹³C NMR** (100.53 MHz, CDCl₃, ppm): δ = 144.8, 142.8, 136.6, 132.7, 130.0, 128.7, 21.19; **MS (EI)** m/e 635 (M⁺, 52%); **HRMS (ESI+)** calculated for [C₃₄H₂₈Cl₂S₄ +H⁺]: 635.0524 Da, found [M+H⁺] 635.0519 m/z.

Reference:

1. Pinchart, A. *Synthèses d'architectures moléculaires de sulfure de phénylène et de noyaux aromatiques persulfurés* PhD dissertation, Université Libre de Bruxelles et Université de Paris XI Orsay, Sept. 26 **2000**.

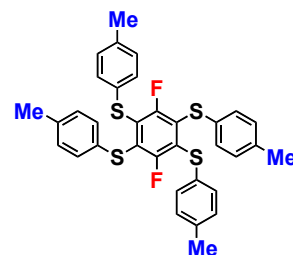


HRMS (ESI, positive mode) of (**20**)



1,4-difluoro-2,3,5,6-tetrakis(4-methylphenylthio)benzene (**22**)^{1,2,3}

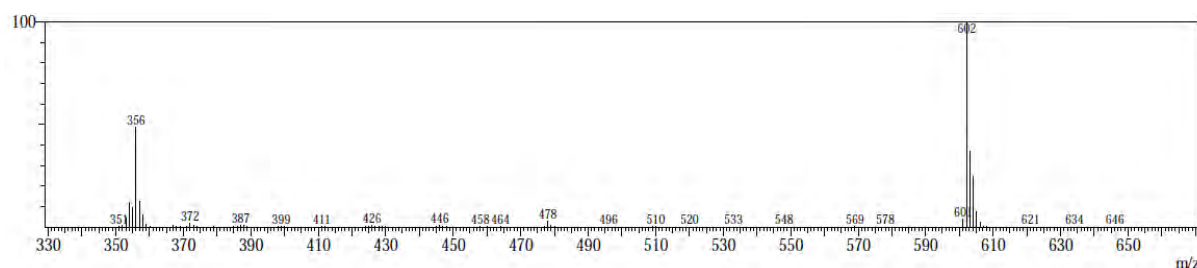
In a reaction tube, hexafluorobenzene (220 mg, 1.18 mmol, 1.00 mol-eq.) was dissolved in a solution of dry DMF and absolute EtOH (DMF/EtOH: 50:50 v/v, 2.0 mL). Dry potassium carbonate (817 mg, 5.91 mmol, 5.00 mol-eq.) was added. The mixture was purged with argon for several minutes. 4-Methyl-1-benzenethiol (587 mg, 4.73 mmol, 4.00 mol-eq.) was added. The tube was sealed and the reaction mixture was heated to 40°C and stirred 2 days. After completion of the reaction, the mixture was treated with an aqueous solution of NaOH (2M, 50 mL) and extracted with DCM (5x10 mL). The organic layers were combined, dried over anhydrous MgSO₄ and filtered. After removal the solvent *in vacuo*, the crude was purified by column chromatography over silica gel using cyclohexane/DCM as eluent to separate the disulfurated benzene molecule from the tetrasulfurated one. Crystallization by a slow evaporation of DCM provided transparent colorless needles of (**21**) (299 mg, 0.496 mmol, 42% yield).



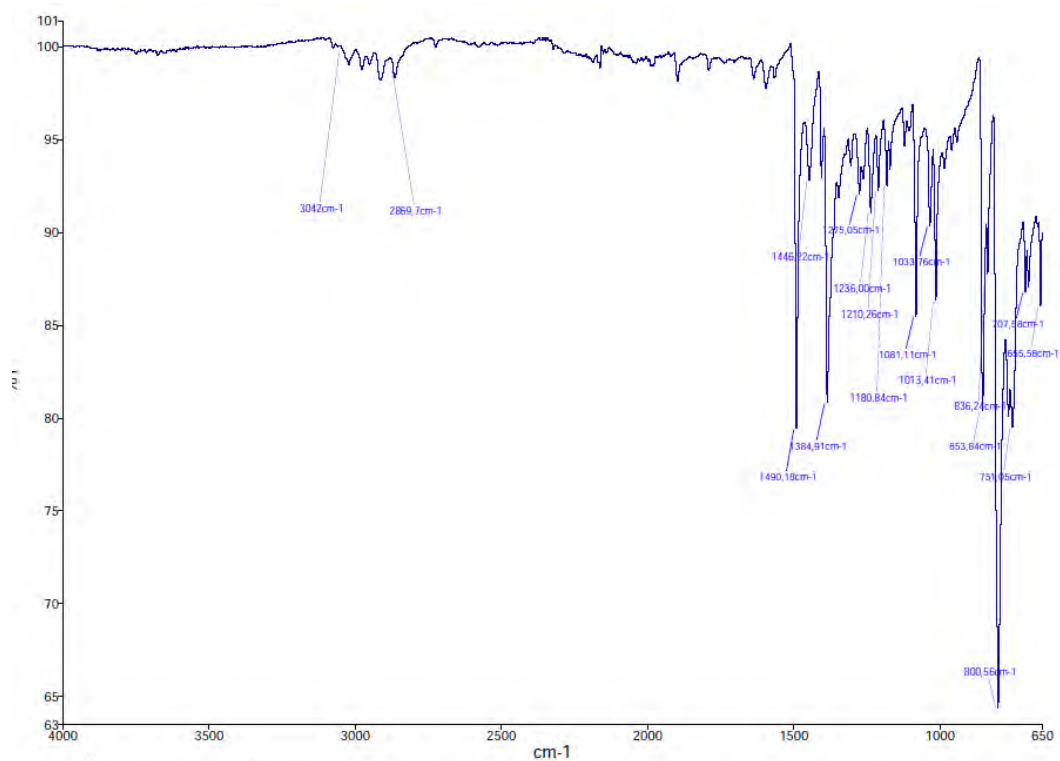
M.p.: 189.2-191.0°C (CH₂Cl₂); **FT-IR** (ATR, diamond contact, neat, cm⁻¹) ν = 3059 (w), 1579 (s), 1475 (s), 1440 (s), 1391 (s), 1378 (s), 1174 (m), 1081 (m), 1022 (m), 965 (m), 850 (s), 736 (s), 686 (s); **¹H NMR** (399.78 MHz, CDCl₃, ppm) δ = 7.08 (d_{app}, *J* = 8.2, 8H), 7.01 (d_{app}, *J* = 8.4, 8H), 2.30 (s, 12H); **¹³C NMR** (100.53 MHz, CDCl₃, ppm) δ = 159, 18 (dd, *J* = 251, 4 Hz), 137.15, 131.31, 130.06, 129.89, 129.23-129.01 (m, AA'XX' second order system), 21.17; **¹⁹F NMR** (376.17 MHz, CDCl₃, ppm) δ = -94.81; **MS** (EI, direct introduction GC-MS): 602 m/z [M]⁺.

Reference:

1. M. Arisawa; T. Suzuki; T. Ishikawa; M. Yamaguchi, *J. Am. Chem. Soc.* (2008), 130, 12214-12215.
2. B. F. Malichenko; L. P. Robota, *Zhurnal Organicheskoi Khimii* (1975), 11, 778-82.
3. Marco Villa, PhD thesis, University of Bologna and Aix-Marseille Université, december 14 (2018).

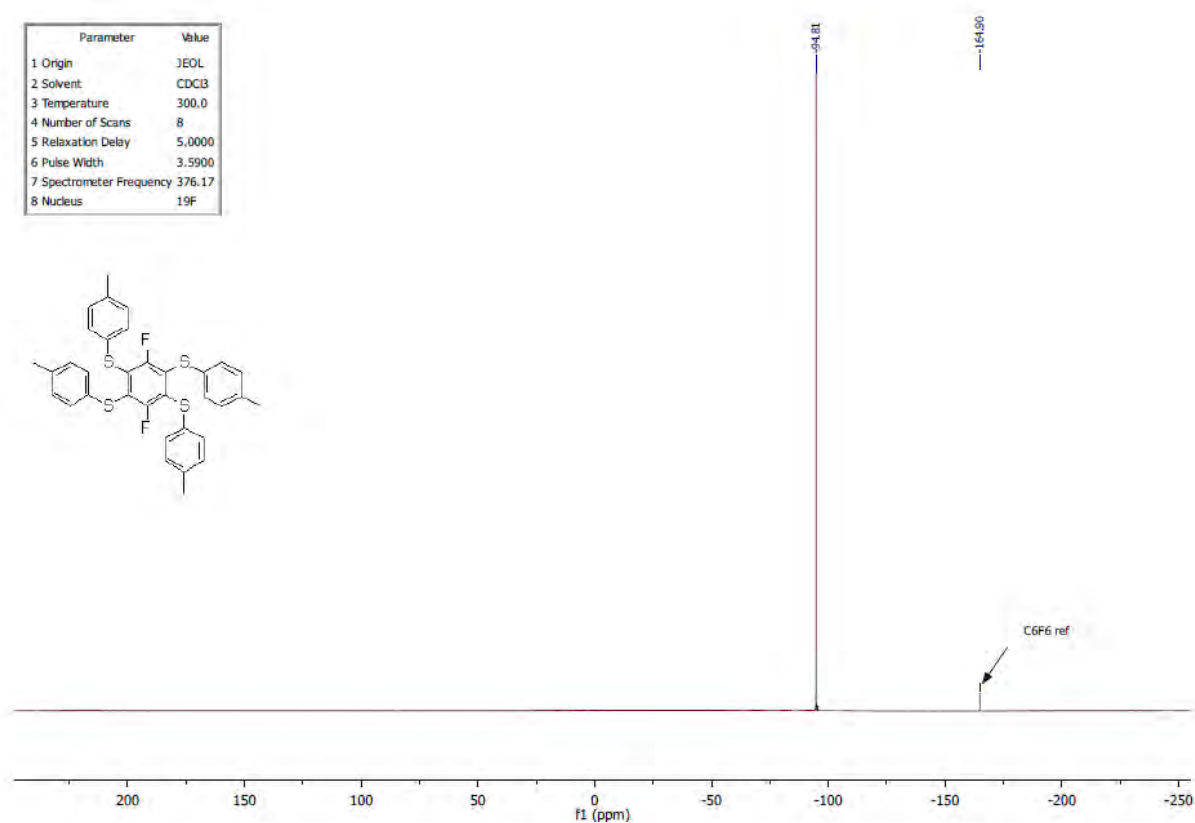


Reverse phase HPLC chromatogram of (**22**) and MS-APCI

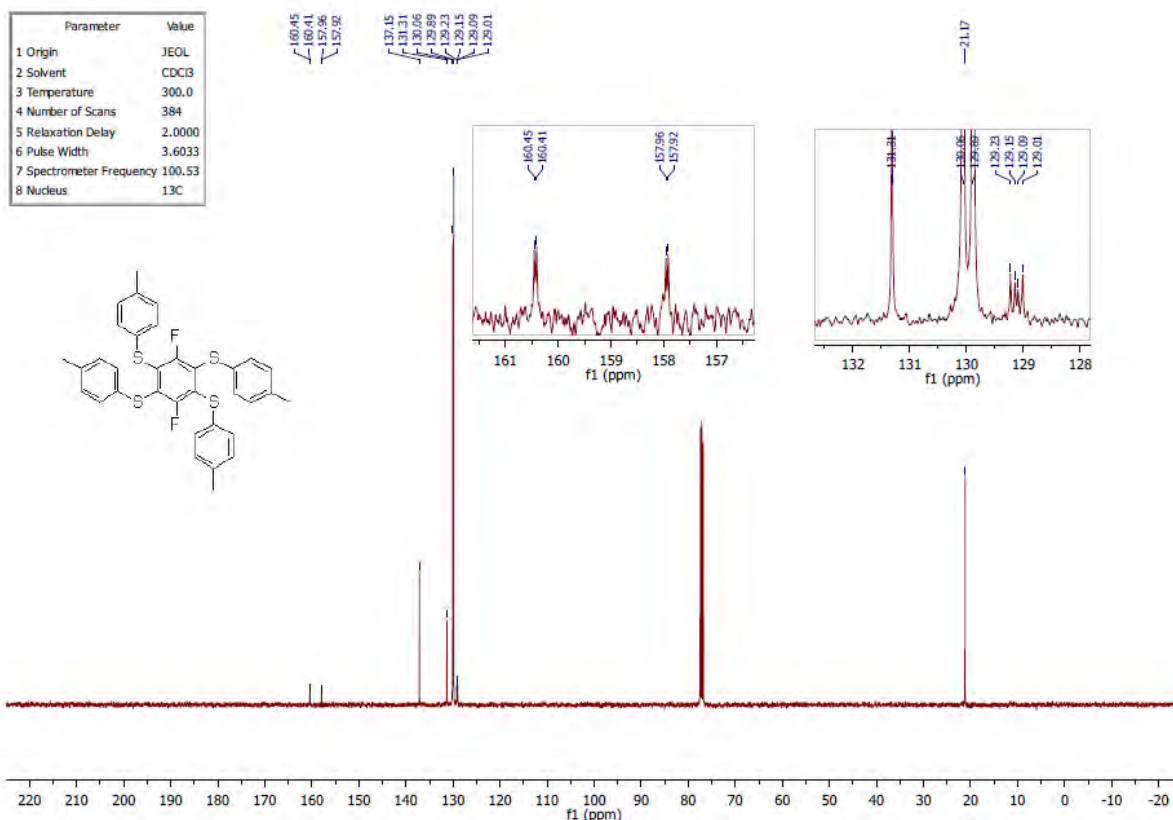


FT-IR spectrum of (22)

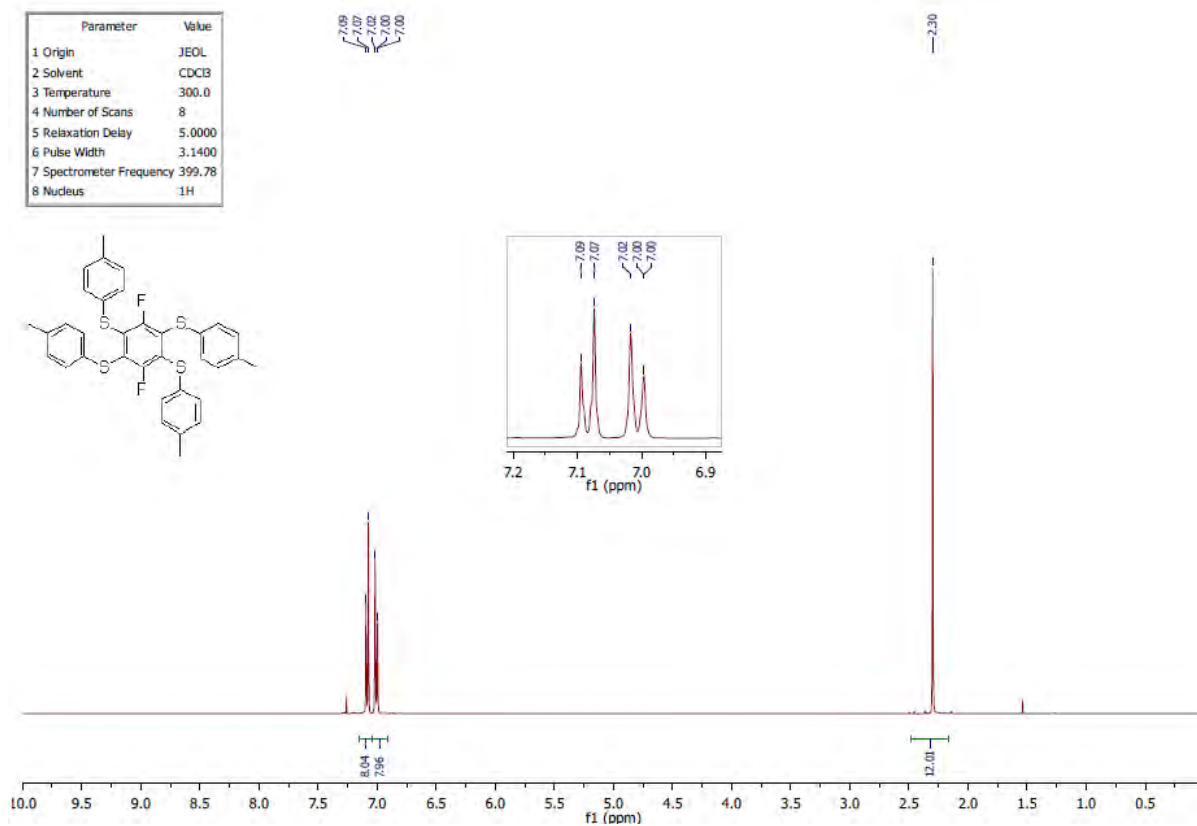
Parameter	Value
1 Origin	JEOL
2 Solvent	CDCl ₃
3 Temperature	300.0
4 Number of Scans	8
5 Relaxation Delay	5.0000
6 Pulse Width	3.5900
7 Spectrometer Frequency	376.17
8 Nucleus	¹⁹ F



¹⁹F-NMR spectrum of (22) (CDCl₃, 376.17 MHz)



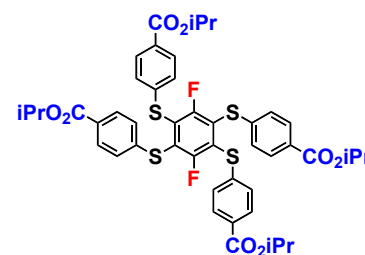
¹³C-NMR spectrum of **(22)** (CDCl₃, 100.53 MHz)



¹H-NMR spectrum of **(22)** (CDCl₃, 399.78 MHz)

1,4-difluoro-2,3,5,6-tetrakis(4-isopropylcarbonyloxy-phenylthio)benzene (**21**).

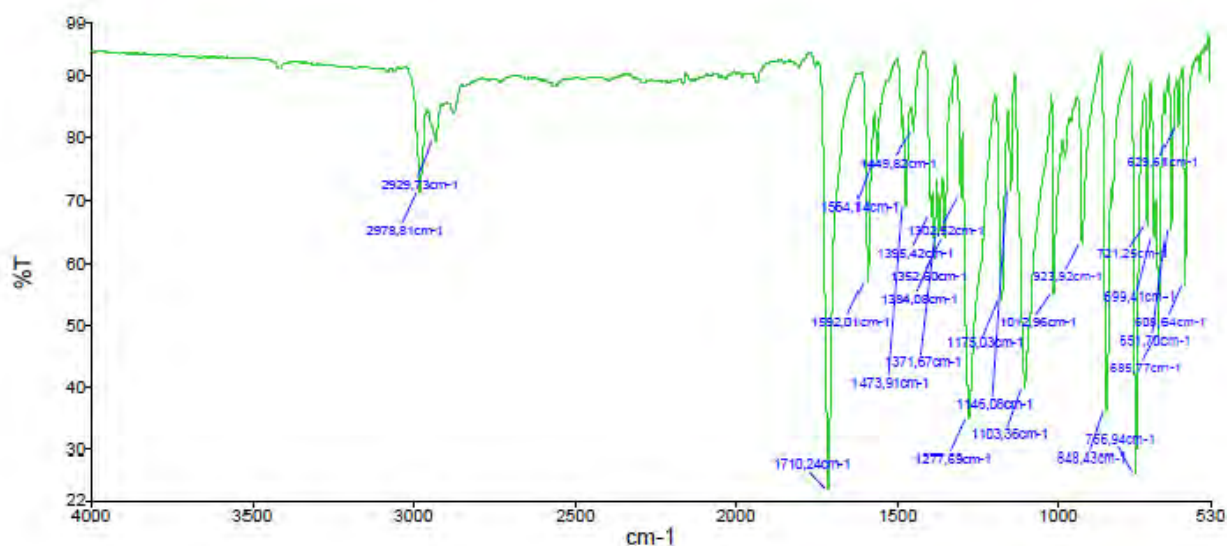
In an oven-dried glass tube were placed hexafluorobenzene (200 mg, 1.07 mmol, 1.00 mol-eq.), isopropyl-4-mercaptobenzoate (880 mg, 4.48 mmol, 4.19 mol-eq.) and dry potassium carbonate (623 mg, 4.51 mmol, 4.21 mol-eq.). All reagents were freshly dried under vacuum for about 30 min prior to use them. Under an argon atmosphere, dry DMF (5.5 mL) was injected via a syringe at 20°C and the mixture was vigorously stirred at 60°C (oil bath temperature) for 1 day. After cooling down to room temperature, an aqueous solution of HCl (1M, 100mL) was added, and the reaction mixture was extracted with toluene (3x25 mL). The combined organic phases were washed with water (5x25 mL), dried over anhydrous MgSO₄. After filtration and removal of solvents in vacuo, a brown-yellow crude product (**21**) was purified by chromatography over silica gel (eluent: *n*-hept./EtOAc: 90:10 v/v) to yield a pale yellow solid (855 mg, 0.96 mmol, 89% yield).



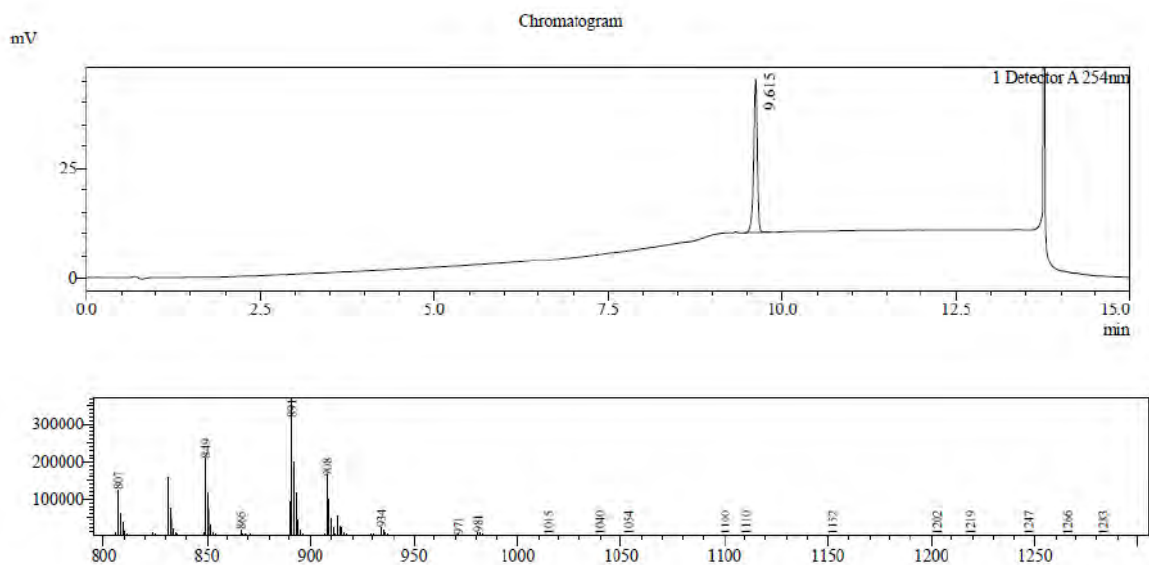
FT-IR (ATR, diamond contact, neat, cm⁻¹) ν = 2978, 2929, 1710, 1592, 1277, 1175, 1103, 848, 756, 685. **¹H NMR** (399.78 MHz, CDCl₃, ppm): δ = 7.88 (d_{app}, *J* = 8.5 Hz, 8H), 7.14 (d_{app}, *J* = 8.5 Hz, 8H), 5.22 (hept, *J* = 6.3 Hz, 4H), 1.35 (d, *J* = 6.2 Hz, 24H); **¹³C NMR** (100.53 MHz, CDCl₃, ppm): δ = 165.37, 159.65 (dd, *J*_{C-F} = 253, 4 Hz), 140.20, 130.43, 129.62, 128.62-128.64 (m, AA'XX' second order system), 128.03, 68.75, 22.05; **¹⁹F NMR** (376.17 MHz, CDCl₃, ppm): δ = - 89.31; **MS** (LC-MS acetonitrile/water/0.1% formic acid; APCI) 891 m/z [M+H]⁺.

Reference:

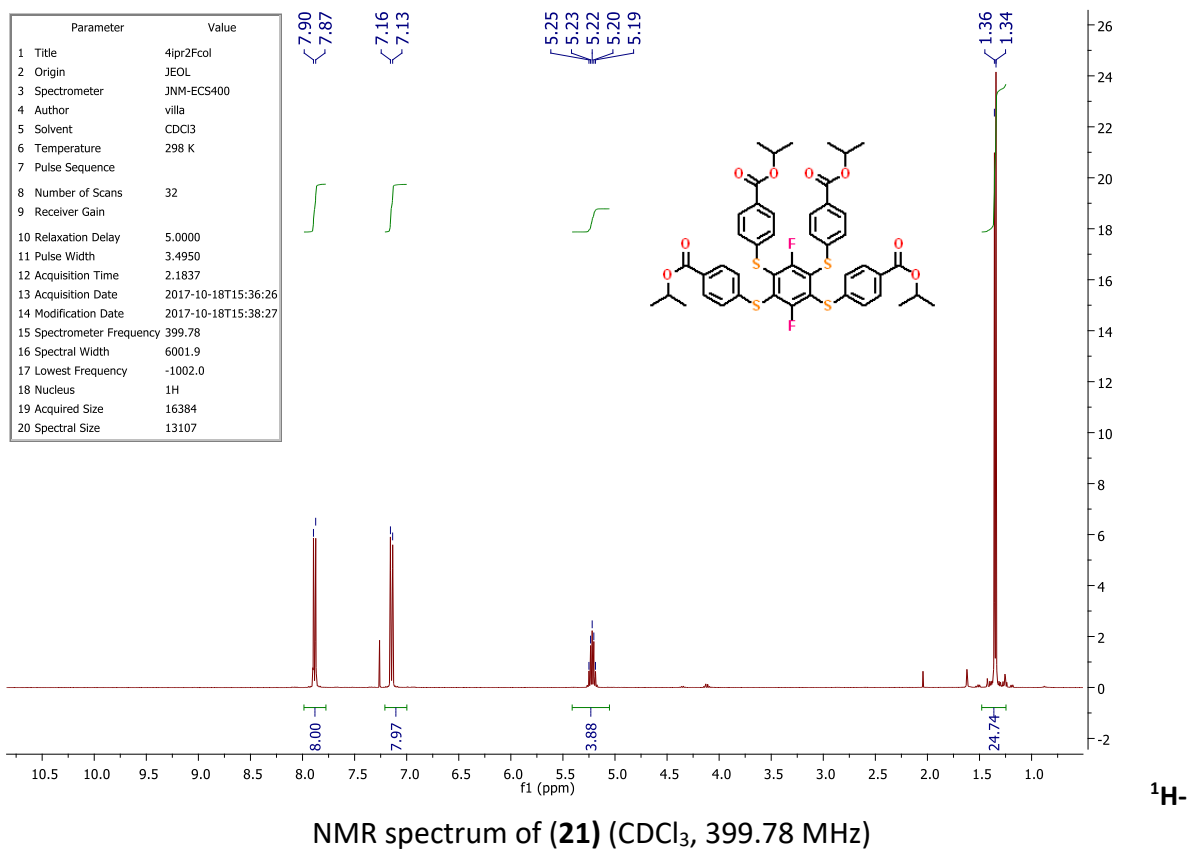
1. M. Villa; B. Del Secco; L. Ravotto; M. Roy; E. Rampazzo; N. Zaccheroni; L. Prodi; M. Gingras; S. Vinogradov; P. Ceroni, *J. Phys. Chem. C* 2019, 123, 29884-29890



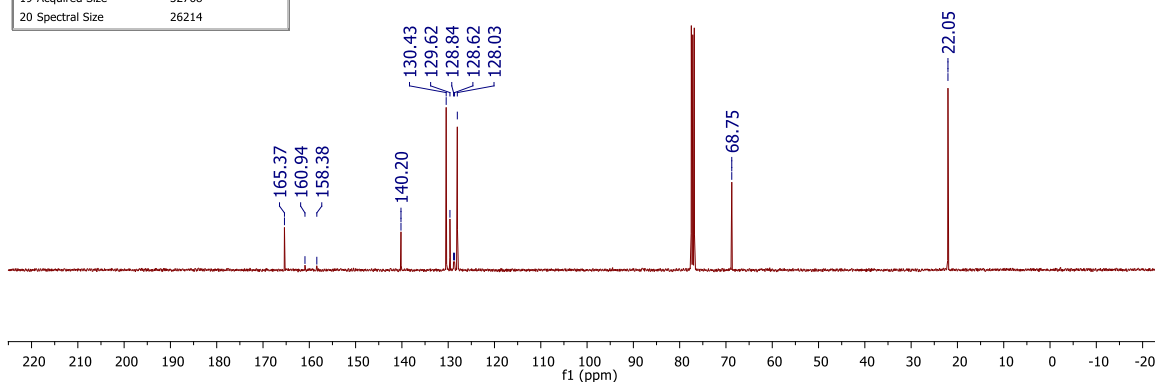
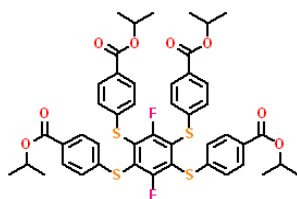
FT-IR spectrum of (**21**)



Reversed-phase HPLC chromatogram of **(21)** and MS-APCI

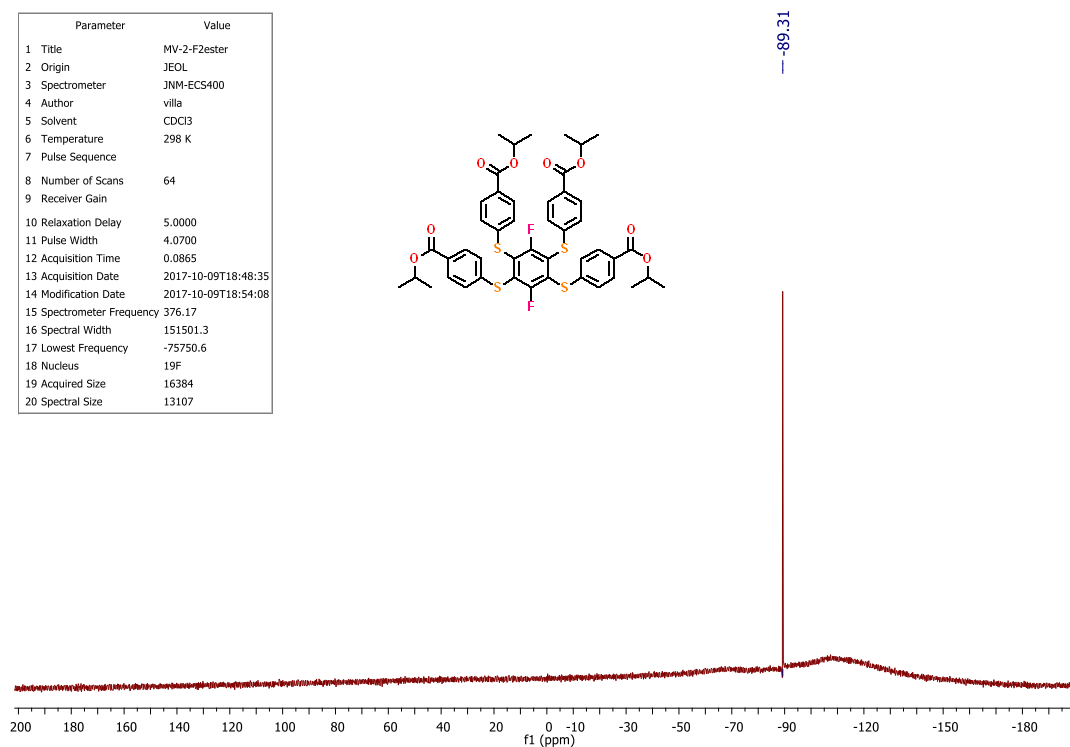
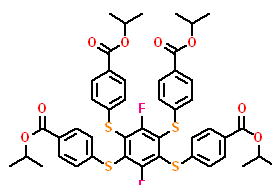


Parameter	Value
1 Title	4ipr2Fcol
2 Origin	JEOL
3 Spectrometer	JNM-ECS400
4 Author	villa
5 Solvent	CDCl3
6 Temperature	298 K
7 Pulse Sequence	
8 Number of Scans	1024
9 Receiver Gain	
10 Relaxation Delay	2.0000
11 Pulse Width	3.5333
12 Acquisition Time	1.0433
13 Acquisition Date	2017-10-19T03:24:23
14 Modification Date	2017-10-19T04:16:36
15 Spectrometer Frequency	100.53
16 Spectral Width	25124.3
17 Lowest Frequency	-2509.6
18 Nucleus	13C
19 Acquired Size	32768
20 Spectral Size	26214



¹³C-NMR spectrum of **(21)** (CDCl₃, 100.53 MHz)

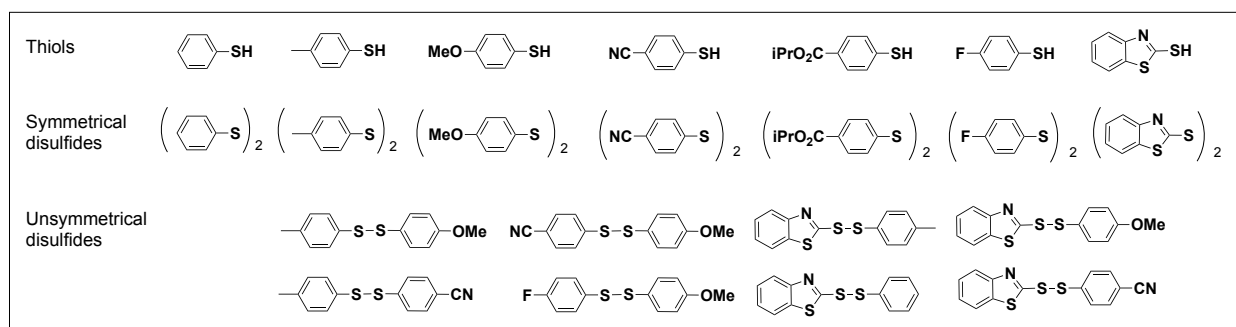
Parameter	Value
1 Title	MV-2-F2ester
2 Origin	JEOL
3 Spectrometer	JNM-ECS400
4 Author	villa
5 Solvent	CDCl3
6 Temperature	298 K
7 Pulse Sequence	
8 Number of Scans	64
9 Receiver Gain	
10 Relaxation Delay	5.0000
11 Pulse Width	4.0700
12 Acquisition Time	0.0865
13 Acquisition Date	2017-10-09T18:48:35
14 Modification Date	2017-10-09T18:54:08
15 Spectrometer Frequency	376.17
16 Spectral Width	151501.3
17 Lowest Frequency	-75750.6
18 Nucleus	19F
19 Acquired Size	16384
20 Spectral Size	13107



¹⁹F-NMR spectrum of **(21)** (CDCl₃, 376.17 MHz)

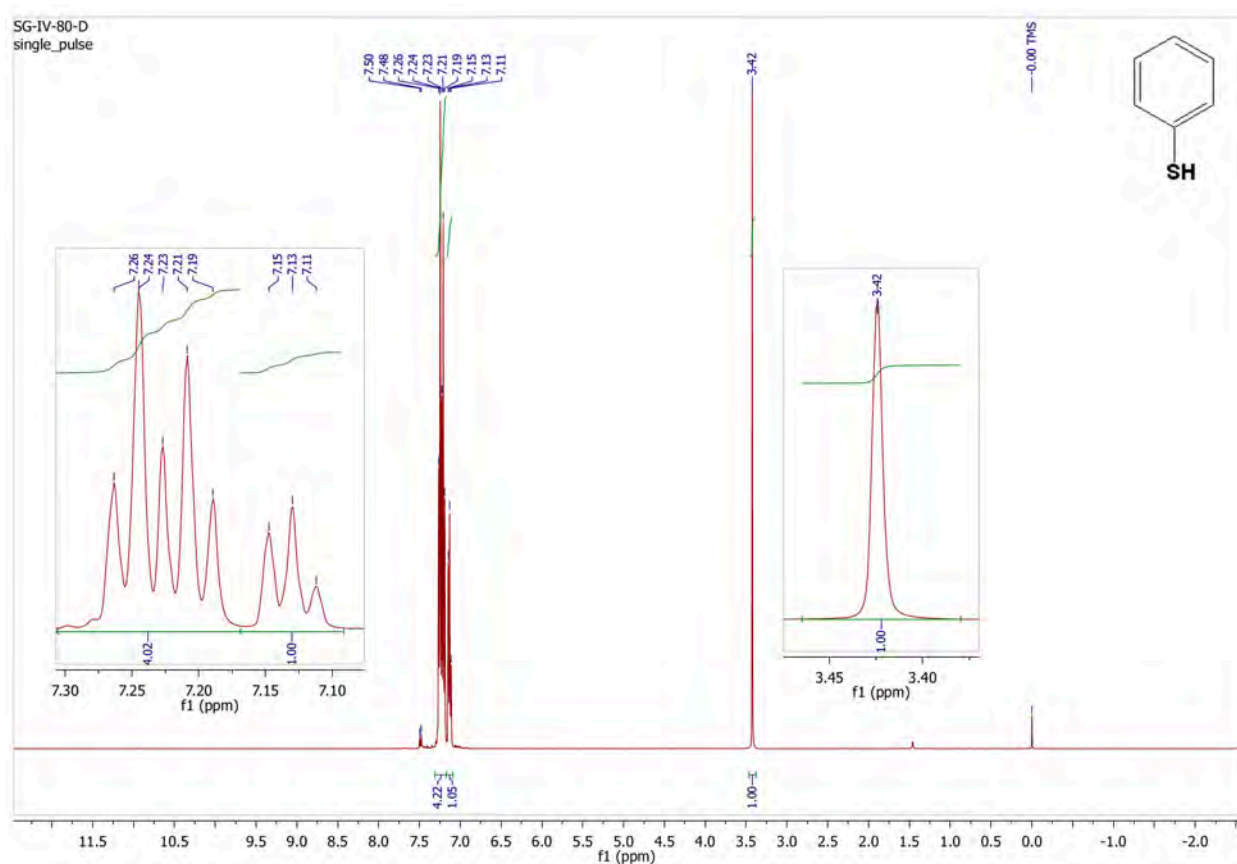
2.4 Reference thiols, symmetrical and mixed disulfides

List of thiols and disulfides as reference compounds in this work

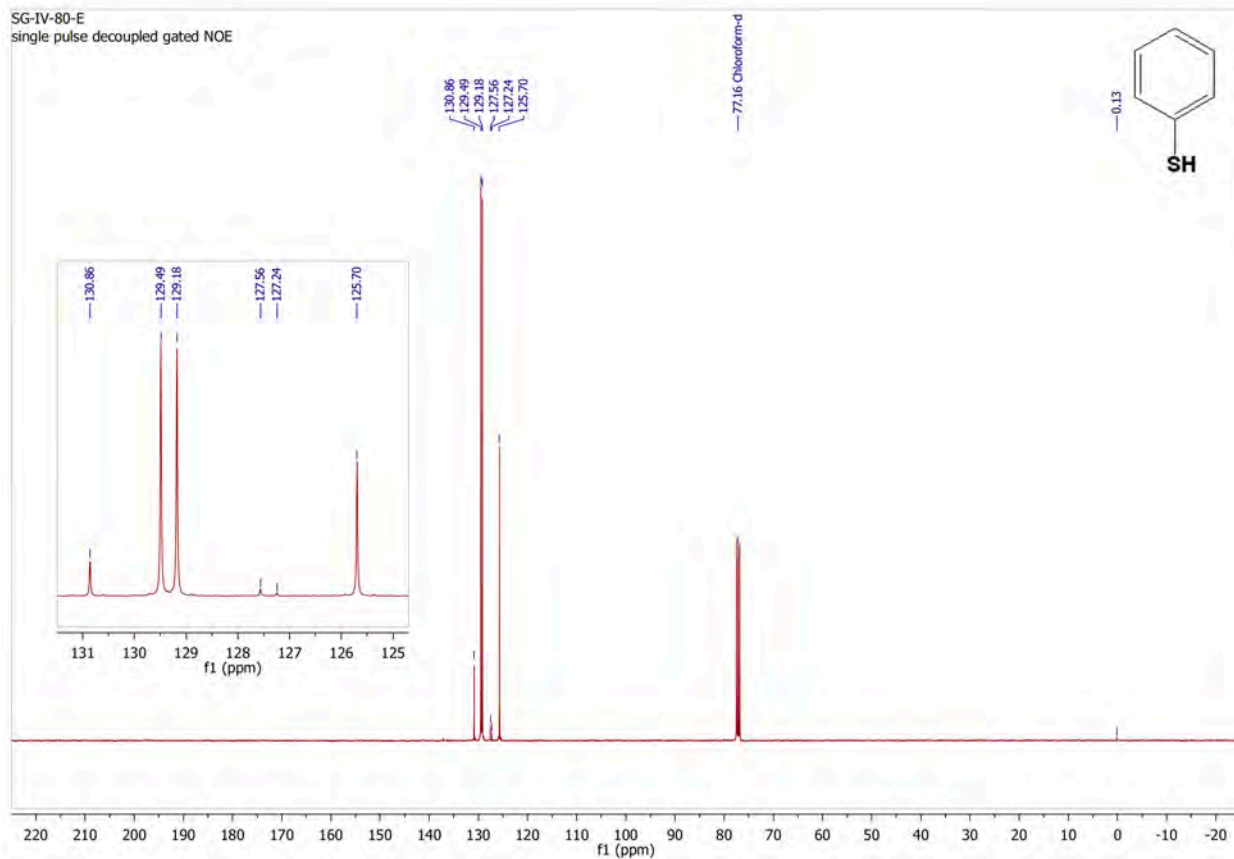


List of references thiols

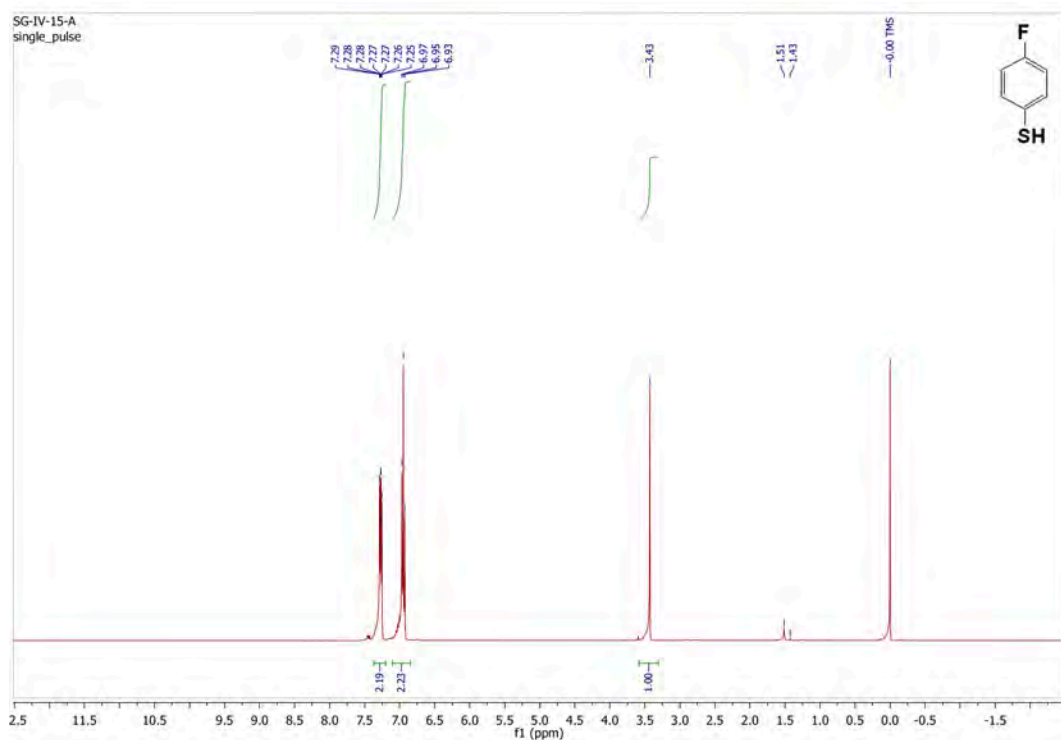
Thiophenol (commercial)

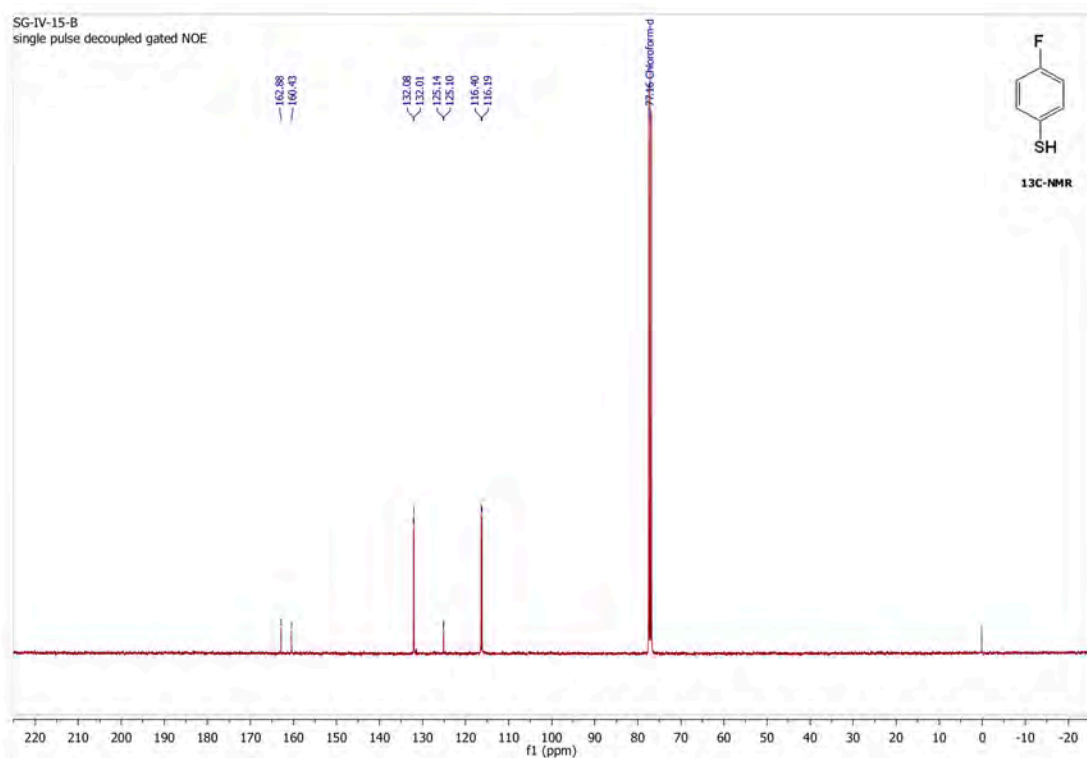


$^1\text{H-NMR}$ of thiophenol (CDCl_3 , 399.78 MHz)

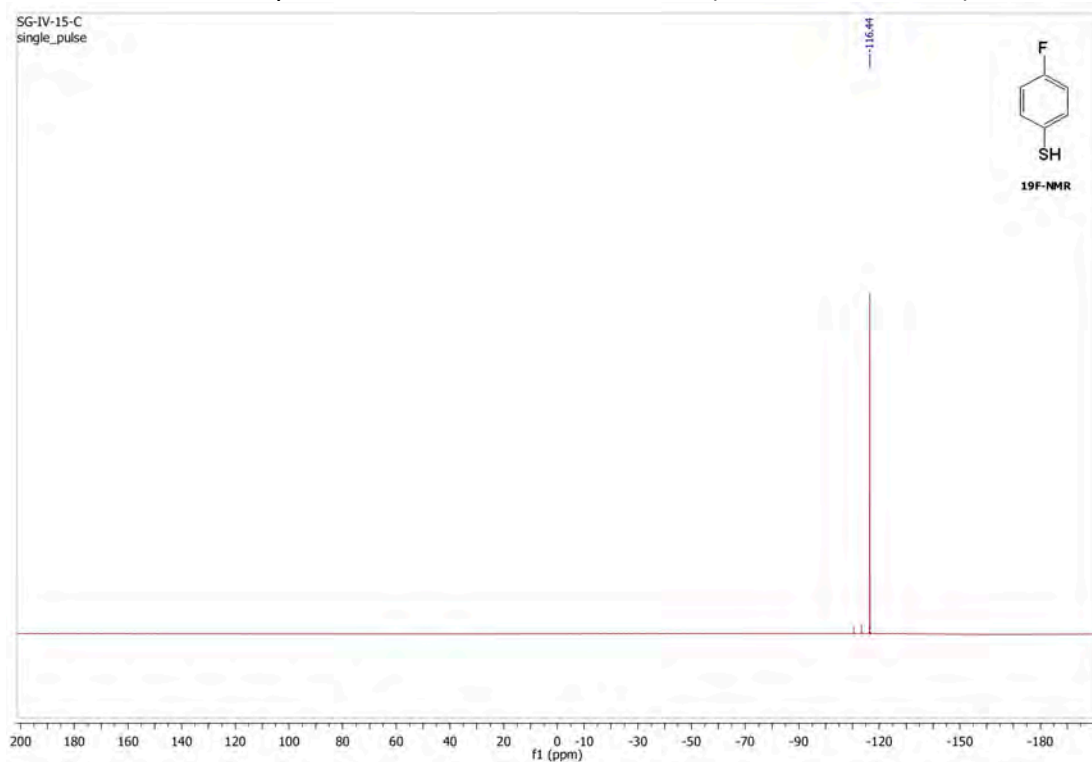


4-Fluorobenzenethiol (commercial)





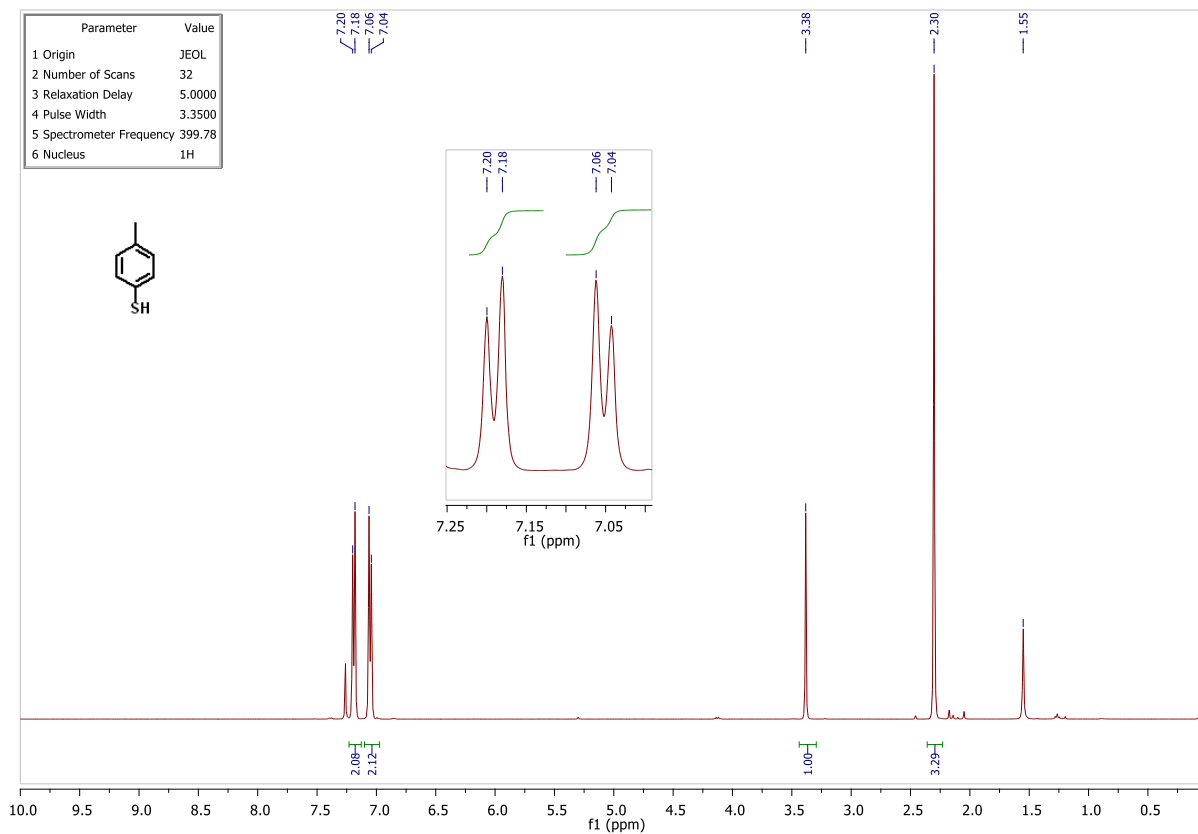
^{13}C -NMR spectrum of 4-fluorobenzenethiol (CDCl_3 , 100.53 MHz)



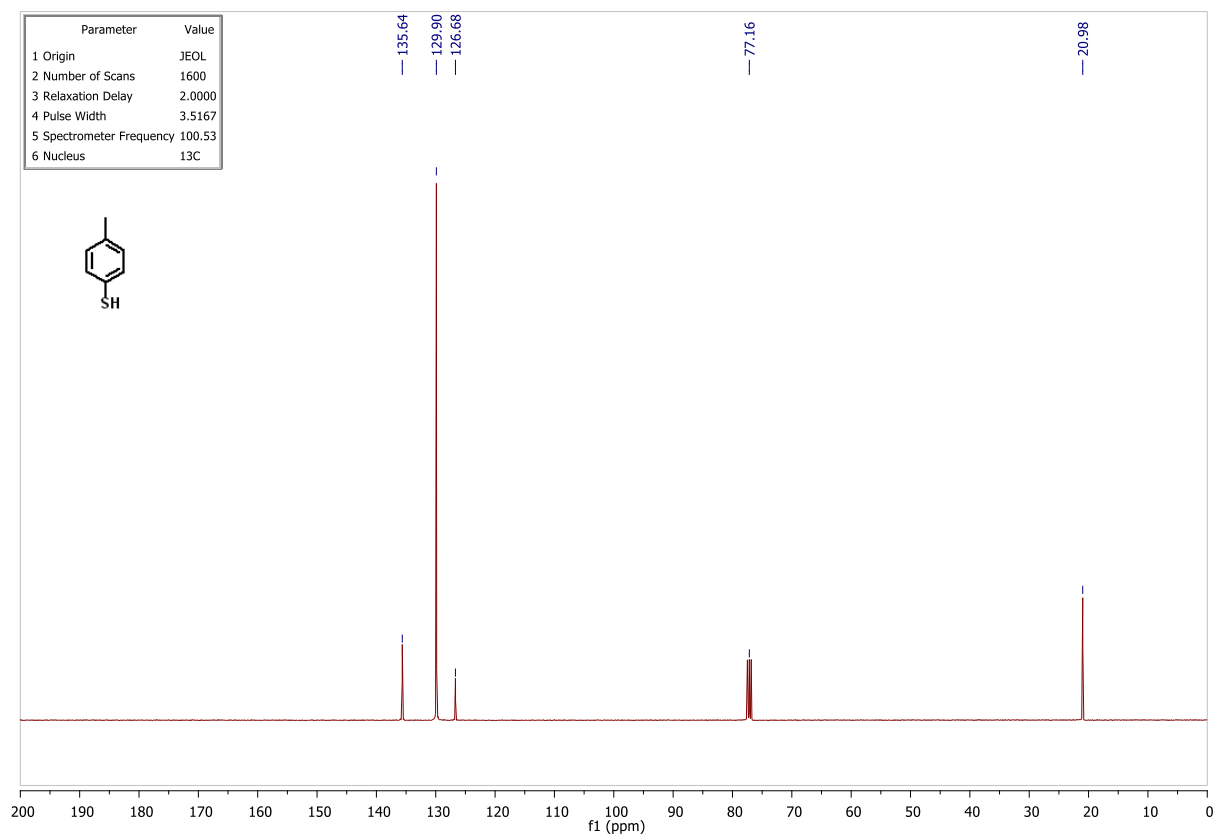
^{19}F -NMR of 4-fluorobenzenethiol (CDCl_3 , 376.17 MHz)

4-Methylbenzenethiol (commercial)

^1H NMR (399.78 MHz, CDCl_3 , ppm) δ = 7.19 (d, J = 7.8 Hz, 2H), 7.05 (d, J = 7.7 Hz, 2H), 2.38 (s, 3H); ^{13}C NMR (100.53 MHz, CDCl_3 , ppm) δ = 135.64, 129.90 (2C), 126.68, 20.98.



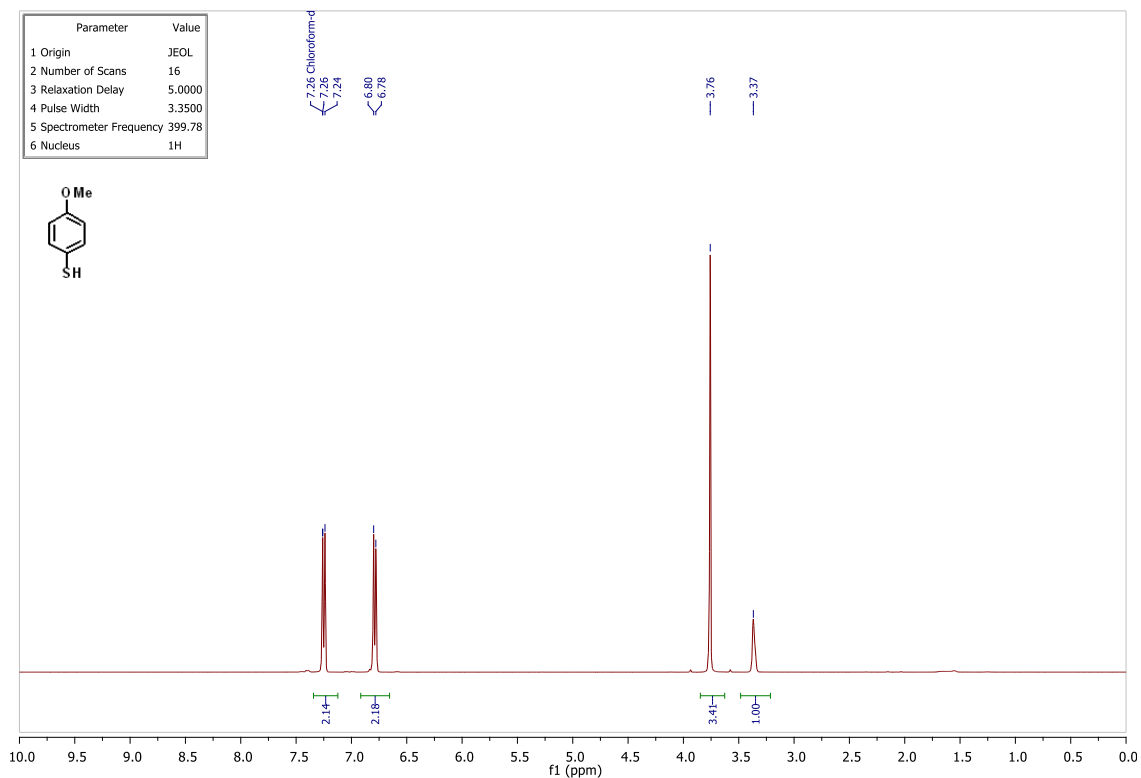
¹H-NMR of 4-methylbenzenethiol (CDCl₃, 399.78 MHz)



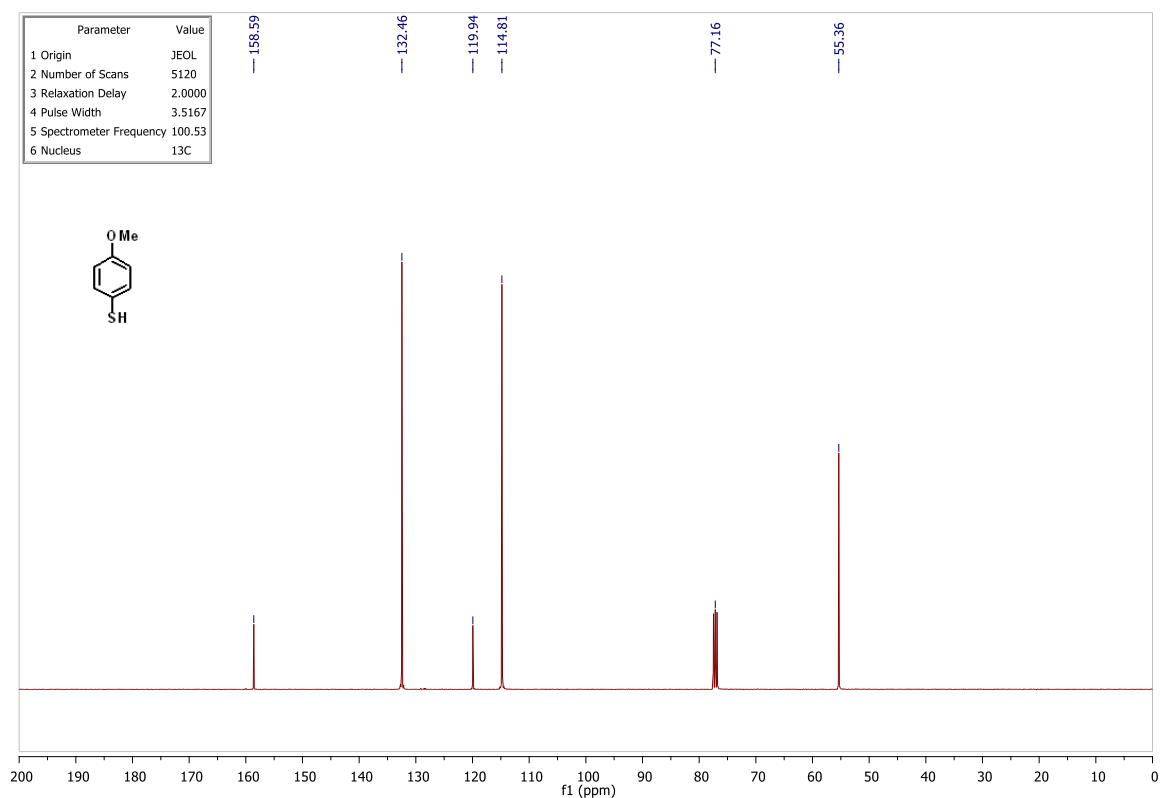
¹³C-NMR spectrum of 4-methylbenzenethiol (CDCl₃, 100.53 MHz)

4-Methoxybenzenethiol (commercial)

^1H NMR (399.78 MHz, CDCl_3 , ppm) $\delta = 7.25$ (d, $J = 8.2$ Hz, 2H), 6.79 (d, $J = 8.0$ Hz, 2H), 3.76 (s, 3H); ^{13}C NMR (100.53 MHz, CDCl_3 , ppm) $\delta = 158.59$, 132.46 , 119.94 , 114.81 , 55.36 .



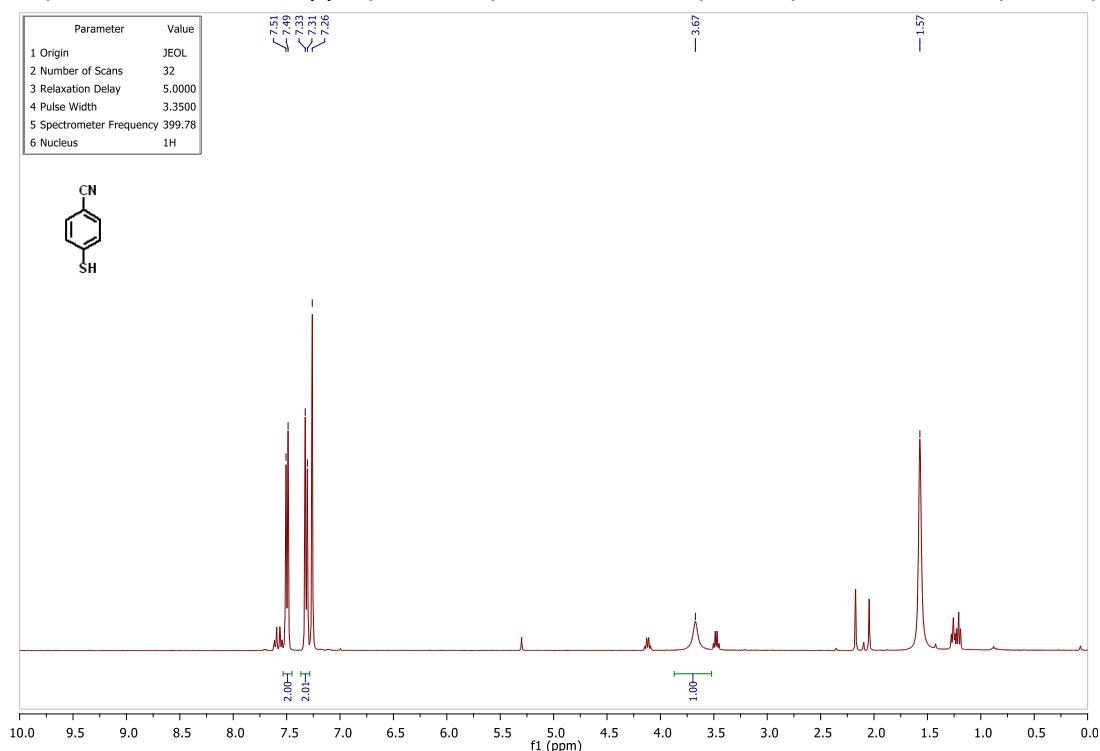
^1H -NMR of 4-methoxybenzenethiol (CDCl_3 , 399.78 MHz)



^{13}C -NMR spectrum of 4-methoxybenzenethiol (CDCl_3 , 100.53 MHz)

4-Cyanobenzenethiol (commercial)

$^1\text{H NMR}$ (399.78 MHz, CDCl_3 , ppm) δ = 7.50 (d, J = 8.0 Hz, 2H), 7.32 (d, J = 7.9 Hz, 2H), 3.67 (s, 1H).



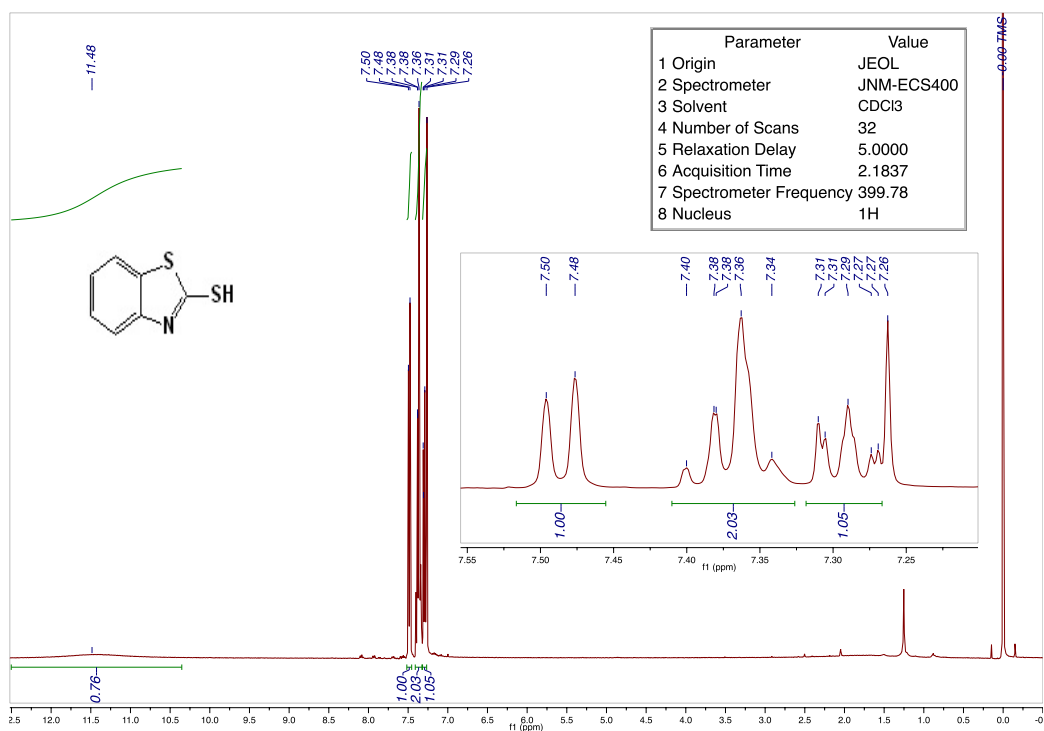
$^1\text{H-NMR}$ of 4-cyanobenzenethiol (CDCl_3 , 399.78 MHz)

Among some references:

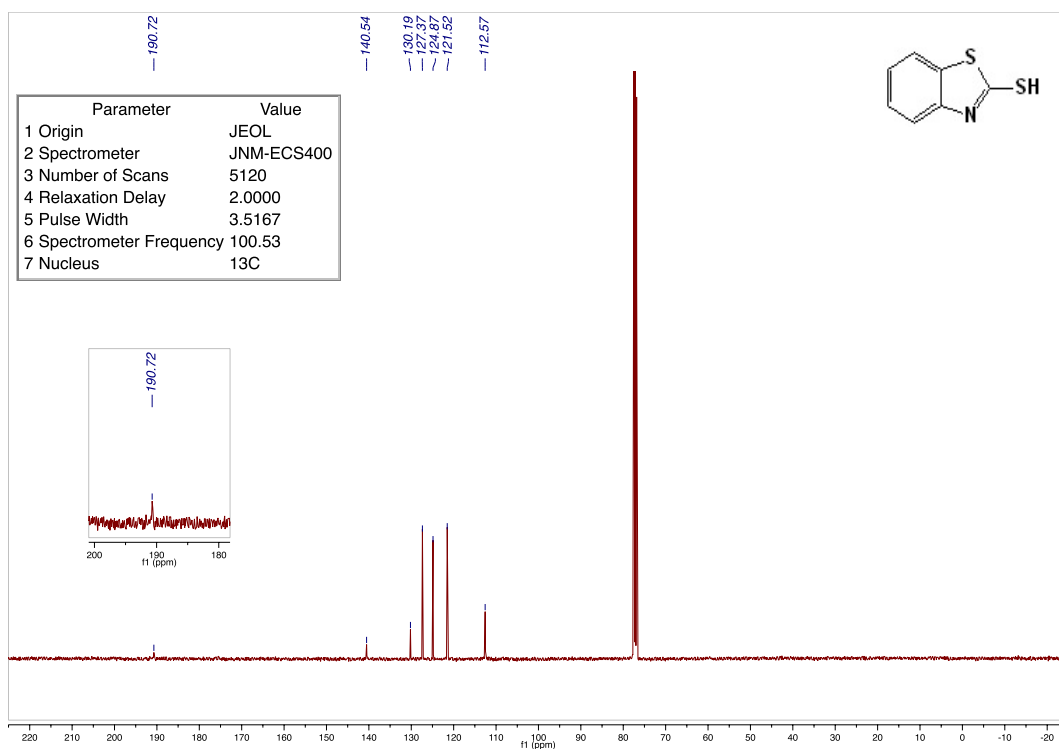
- 1) Z.-B. Dong; M. Balkenhohl; E. Tan; P. Knochel *Org. Lett.* (2018), 20, 7581-7584.
- 2) E. W. McClelland; L.A. Warren *J. Chem. Soc.* (1930), 1095-1102.
- 3) S. Krishnamurthy; D. Aimino *J. Org. Chem.* (1989), 54, 4458-62.
- 4) C. Combellas; S. Dellerue; G. Mathey; A. Thiebault *Tetrahedron Lett.* (1997), 38, 539-542.
- 5) S. Antonello; K. Daasbjerg; H. Jensen; F. Taddei; F. Maran *J. Am. Chem. Soc.* (2003), 125, 14.
- 6) J. Tobias; P. Knochel *Synlett* (2005), 1185-1187.

2-Mercaptobenzothiazole (commercial)

$^1\text{H NMR}$ (399.78 MHz, CDCl_3 , ppm): δ = 7.49 (d, J = 8.0 Hz, 1H), 7.33-7.41 (m, 2H), 7.29 (ddd, J = 8.1, 6.3, 1.9 Hz, 1H), 11.43 (br s, 1H, NH); $^{13}\text{C NMR}$ (100.53 MHz, CDCl_3 , ppm): δ = 190.7, 140.5, 130.2, 127.4, 124.9, 121.5, 112.6.



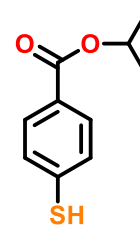
¹H-NMR of 2-mercaptobenzothiazole (CDCl₃, 399.78 MHz)



¹³C-NMR spectrum of 2-mercaptobenzothiazole (CDCl₃, 100.53 MHz)

Isopropyl 4-mercaptobenzoate: (31)

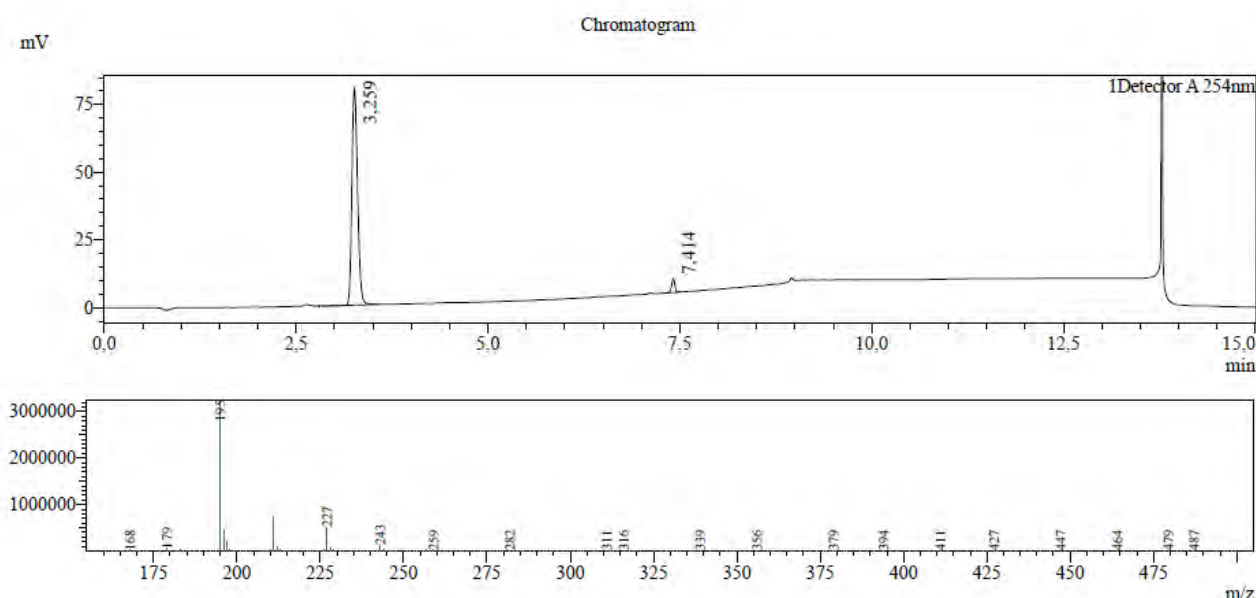
A solution of diisopropyl 4,4'-dithiobisbenzoate (**35**) (610 mg, 1.56 mmol, 1.00 mol-*eq*) and ground zinc powder (1.85 g, 28.29 mmol, 18.1 mol-*eq*) in acetic acid (10 mL) was heated to 90°C under an argon atmosphere. Upon completion of the reaction (about 12 hrs), the mixture was cooled to 20°C while stirring. To the mixture was added a 1 M HCl aqueous solution (50 mL), and the thiol was extracted with dichloromethane (3x20 mL). The combined organic phases were dried over anhydrous MgSO₄, filtered and concentrated under reduced pressure. After drying under high vacuum, an oil was recovered as the desired thiol (596 mg, 3.04 mmol, yield 97%).



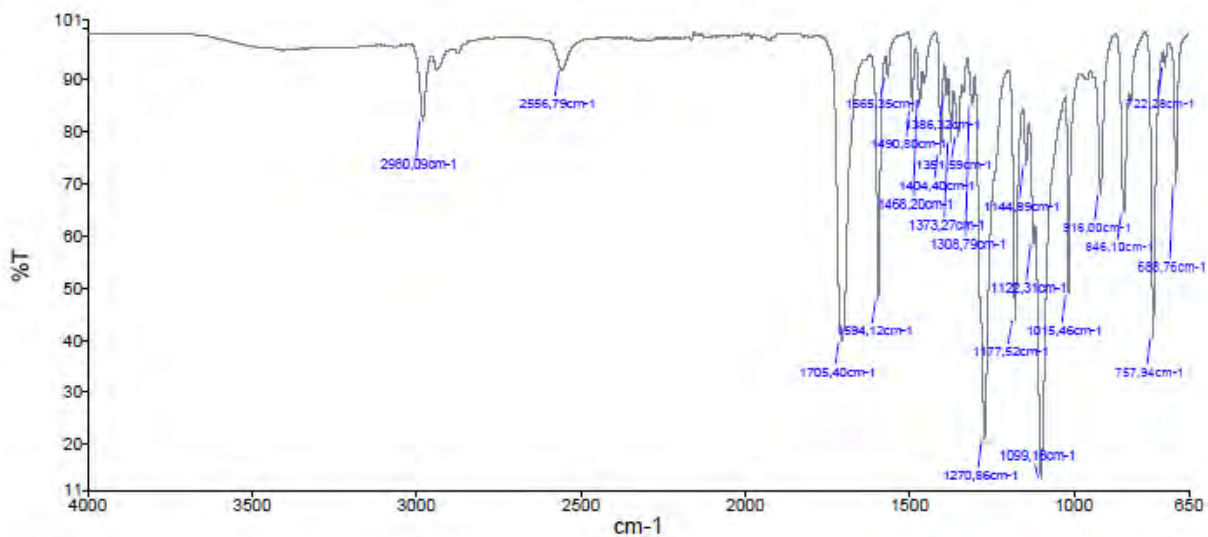
IR (ν , cm⁻¹): 2980, 2556, 1705, 1594, 1404, 1270, 1177, 1099, 1015, 918, 846, 757, 688; **¹H NMR** (δ , 400 MHz, CDCl₃): 7.87 (d, 2H, J=8.5), 7.26 (d, 2H, J=8.6), 5.25-5.18 (sept, 1H, J=6.2), 3.58 (s, 1H), 1.35 (d, 6H, J=6.3). **¹³C NMR** (δ , 100 MHz, CDCl₃): 165.73, 138.02, 130.26, 128.13, 127.98, 68.47, 22.03. **MS** (LC-MS, acetonitrile/water APCI): 195 m/z [M-H]⁻.

References:

- 1) M. Villa, M. Roy, G. Bergamini, P. Ceroni, M. Gingras *Chem Plus Chem* (2020), **85**, 1481-1486.
- 2) M. Villa; B. Del Secco; L. Ravotto; M. Roy; E. Rampazzo; N. Zaccheroni; L. Prodi; M. Gingras; S.A. Vinogradov; P. Ceroni *J. Phys. Chem. C* (2019), **123**, 29884-29890.
- 3) X. Yan; C. Li; X. Xu; Q. He; X. Zhao; Y. Pan, *Tetrahedron* (2019), **75**, 3081-3087.
- 4) M. Villa; M. Roy; G. Bergamini; M. Gingras; P. Ceroni *Dalton Trans.* (2019), **48**, 3815-3818.

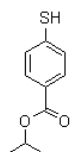
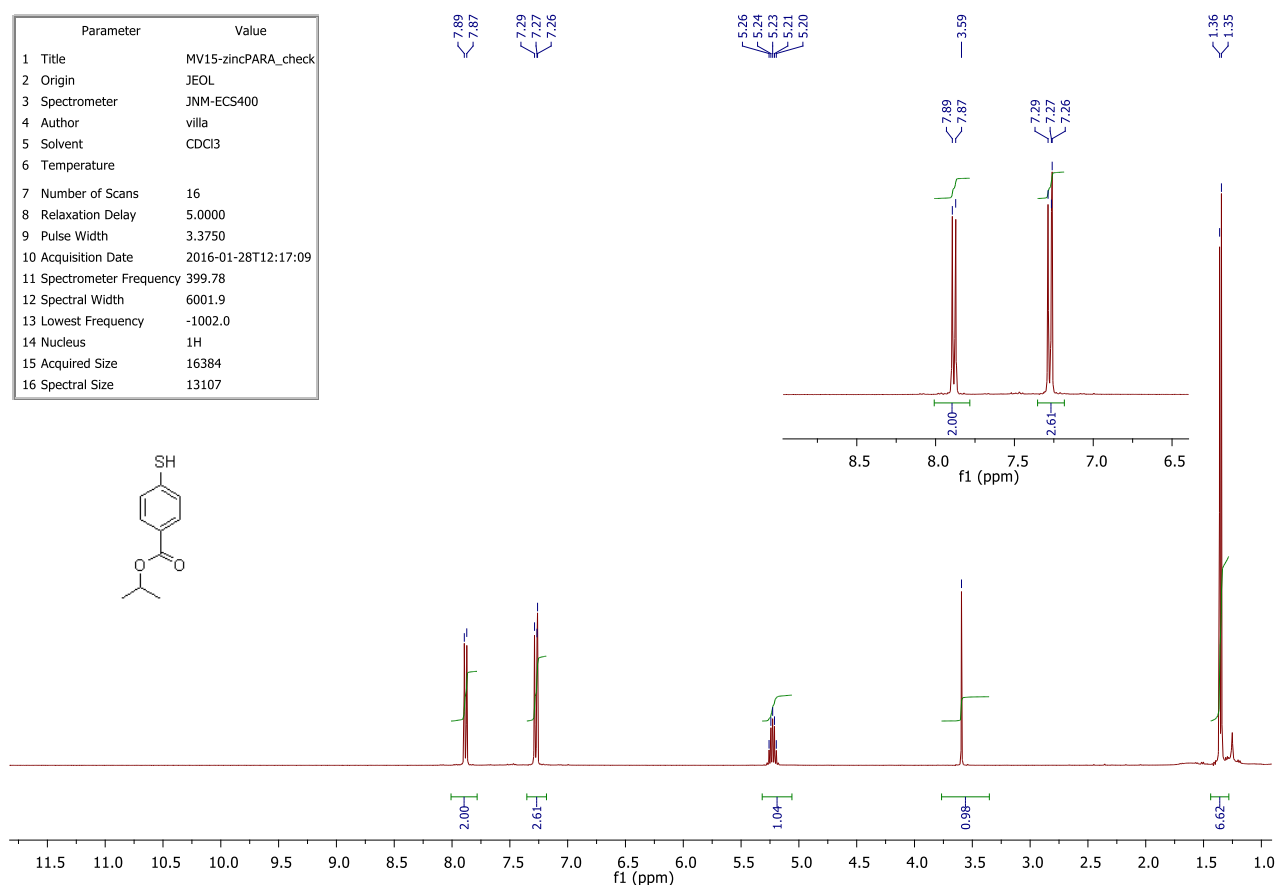


Reversed-phase HPLC chromatogram of Isopropyl 4-mercaptobenzoate and MS-APCI of different peaks (negative ionization).

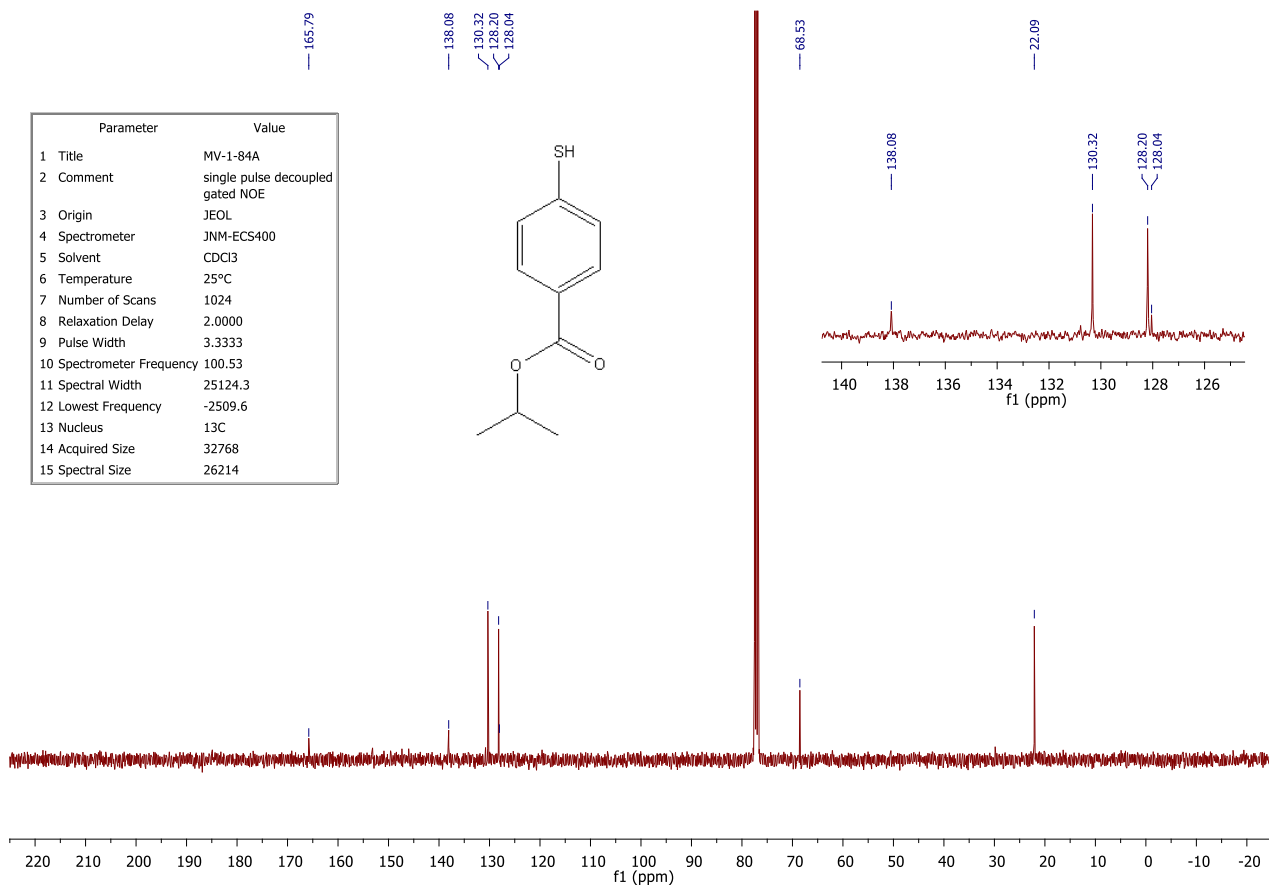


FT-IR spectrum of Isopropyl 4-mercaptobenzoate

Parameter	Value
1 Title	MV15-zincPARA_check
2 Origin	JEOL
3 Spectrometer	JNM-ECS400
4 Author	villa
5 Solvent	CDCl3
6 Temperature	
7 Number of Scans	16
8 Relaxation Delay	5.0000
9 Pulse Width	3.3750
10 Acquisition Date	2016-01-28T12:17:09
11 Spectrometer Frequency	399.78
12 Spectral Width	6001.9
13 Lowest Frequency	-1002.0
14 Nucleus	1H
15 Acquired Size	16384
16 Spectral Size	13107

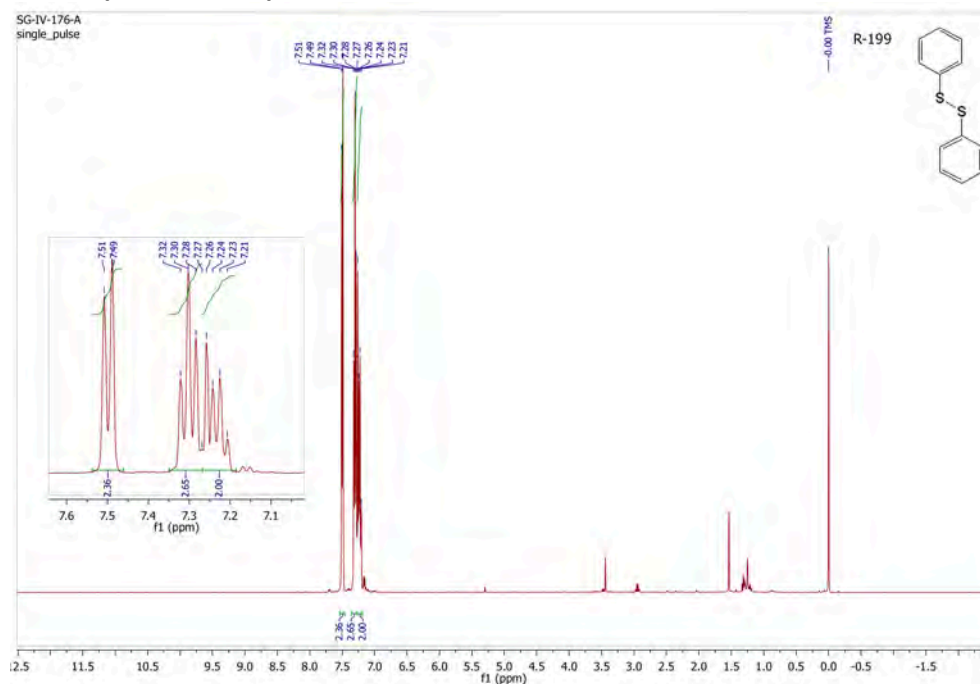


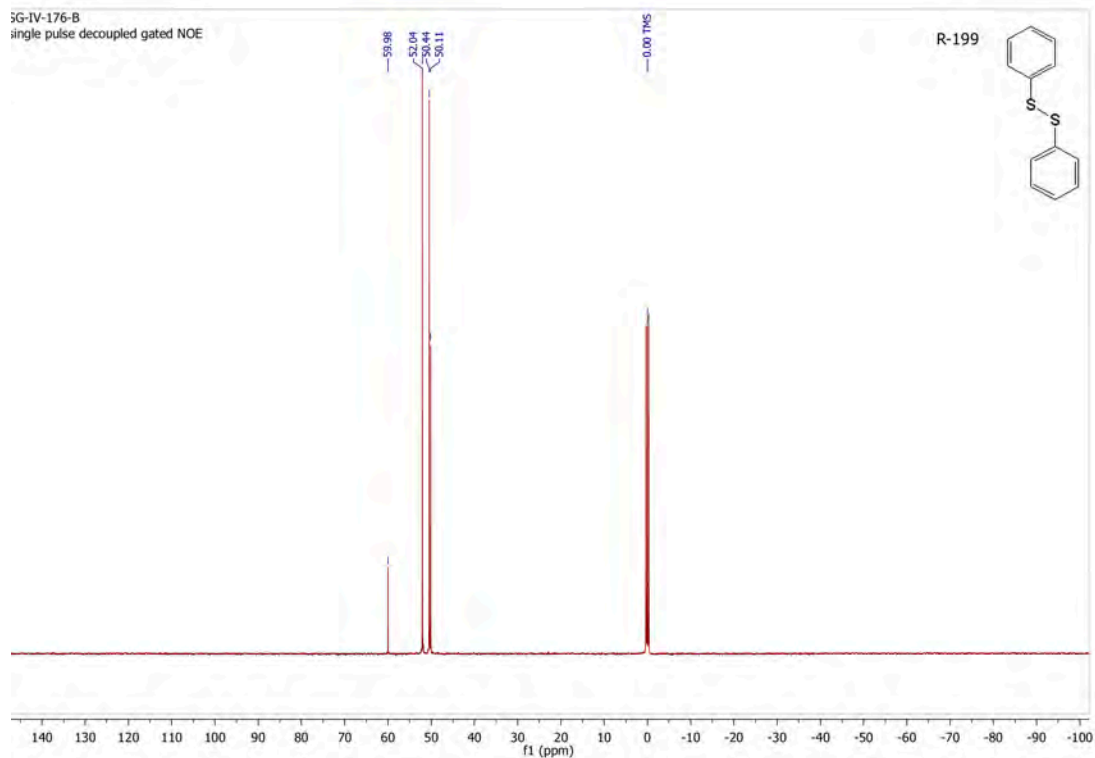
¹H-NMR spectrum of Isopropyl 4-mercaptobenzoate (CDCl₃, 399.78 MHz)



List of reference disulfides

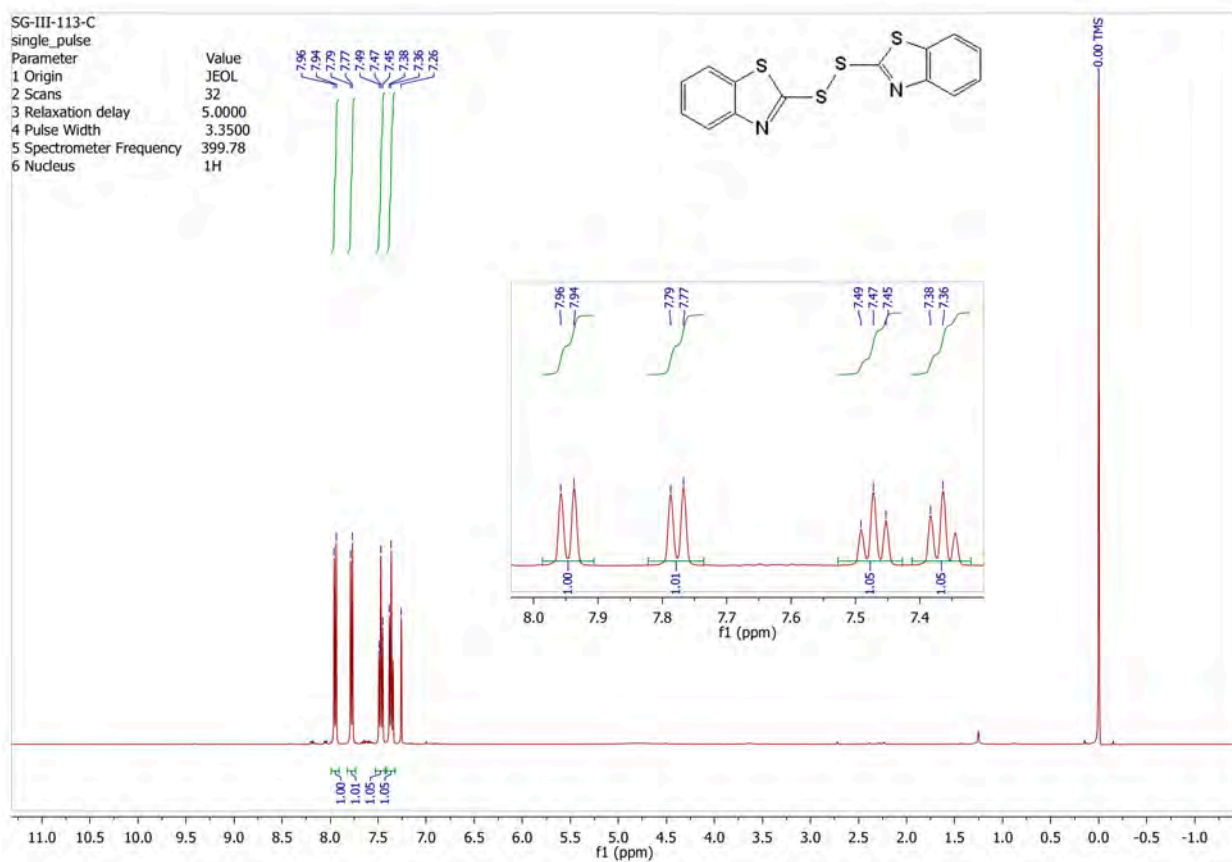
Phenyl disulfide (commercial)



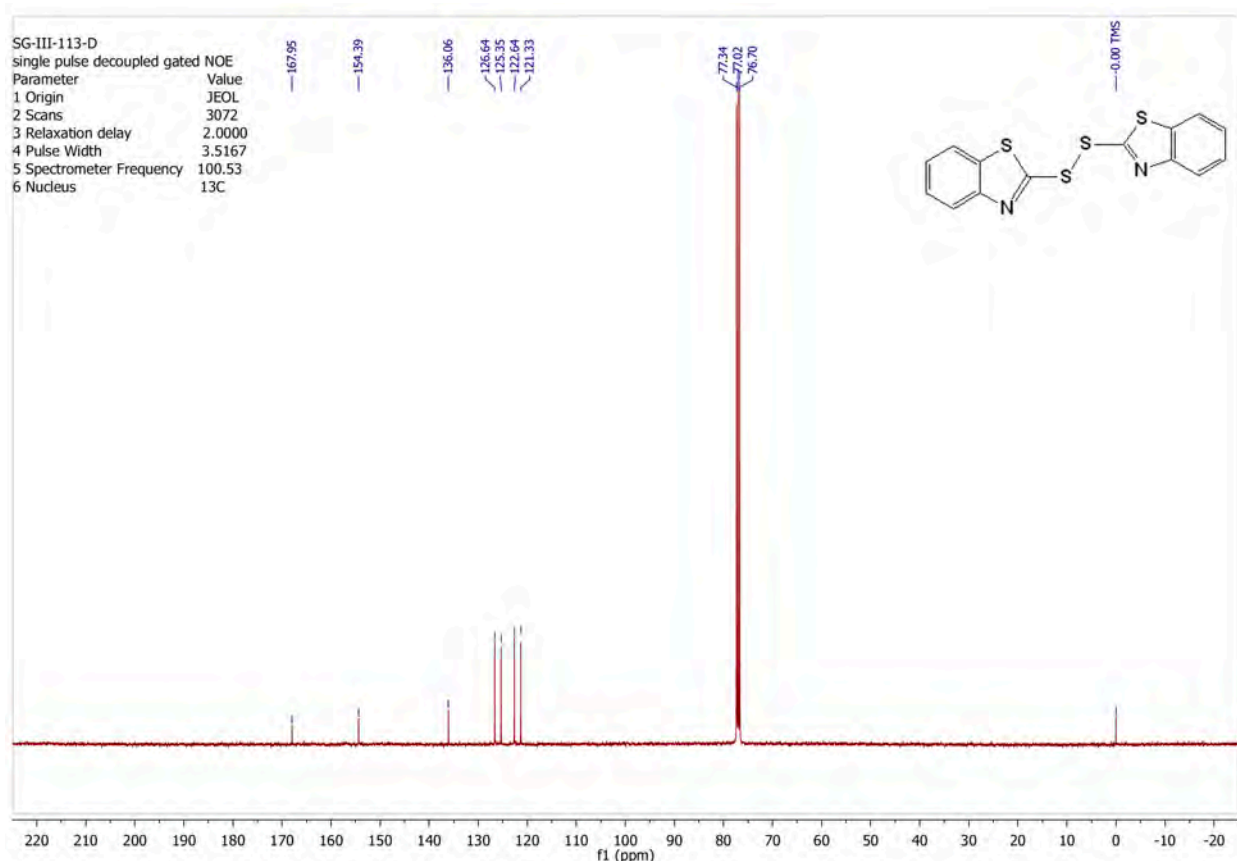


^{13}C -NMR spectrum of phenyl disulfide (CDCl_3 , 100.53 MHz)

2,2'-Dibenzothiazolyl disulfide (**44**) (commercial)



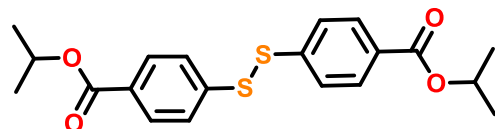
^1H -NMR spectrum of (**44**) (CDCl_3 , 399.78 MHz)



¹³C-NMR spectrum of **(44)** (CDCl₃, 100.53 MHz)

Diisopropyl 4,4'-dithiobisbenzoate (**35**)

To a solution of 4-mercaptobenzoic acid (1.980 g, 33.08 mmol, 1.00 mol-eq) in isopropanol (120 ml, 1.57 mol, 47.5 mol-eq) was added in a dropwise manner SOCl₂ (13.0 mL, 178 mmol, 5.38 mol-eq) at 0°C (ice-bath)



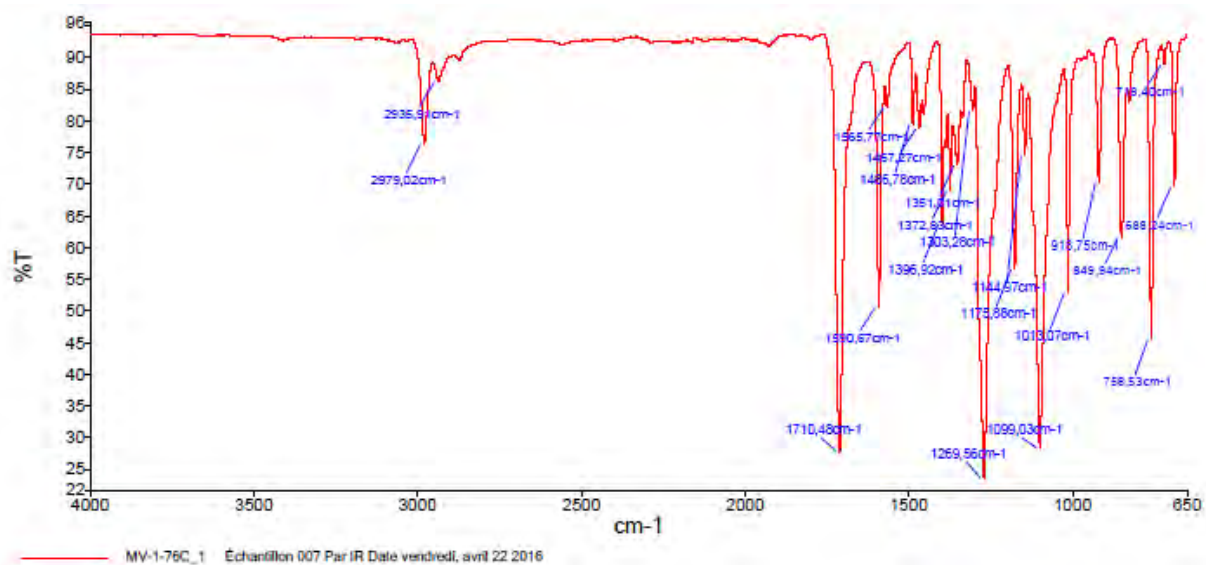
under an argon atmosphere. After removal of the bath, the mixture reached 20°C and then it was heated at 80°C for 7 days. Residual isopropanol was removed from the reaction mixture under reduced pressure, and the crude solid was dissolved in ethyl acetate and washed with an aqueous solution of Na₂CO₃. The aqueous phase was extracted further with ethyl acetate (3x100 mL). The combined organic phases were dried over anhydrous MgSO₄, filtered and evaporated under reduced pressure. The brown oil obtained was a mixture of disulfide and trisulfide (4:1 molar ratio) (2.501 g., 10.16 mmol, approximate yield of 97%).

TLC (SiO₂, cyclohex/dichloromethane 80:20 v/v) R_f = 0.4; **FT-IR** (ATR, diamond contact, neat, cm⁻¹) ν = 2979, 2935, 1714, 1571, 1373, 1352, 1280, 1105, 1072, 923, 748, 679; **¹H NMR** (399.78 MHz, CDCl₃, ppm) δ = 7.96 (d, J = 8.6 Hz, 4H), 7.51 (d, J = 8.5 Hz, 4H), 5.22 (sept, J = 6.2 Hz, 2H), 1.34 (d, J = 6.3 Hz, 12H); **¹³C NMR** (100.53 MHz, CDCl₃, ppm) δ = 165.55, 141.95, 130.37, 130.29, 129.74, 129.02, 126.13, 68.70, 22.07; **LC-MS** (acetonitrile/water, 0.1% formic acid), APCI: 391 m/z [M+H]⁺.

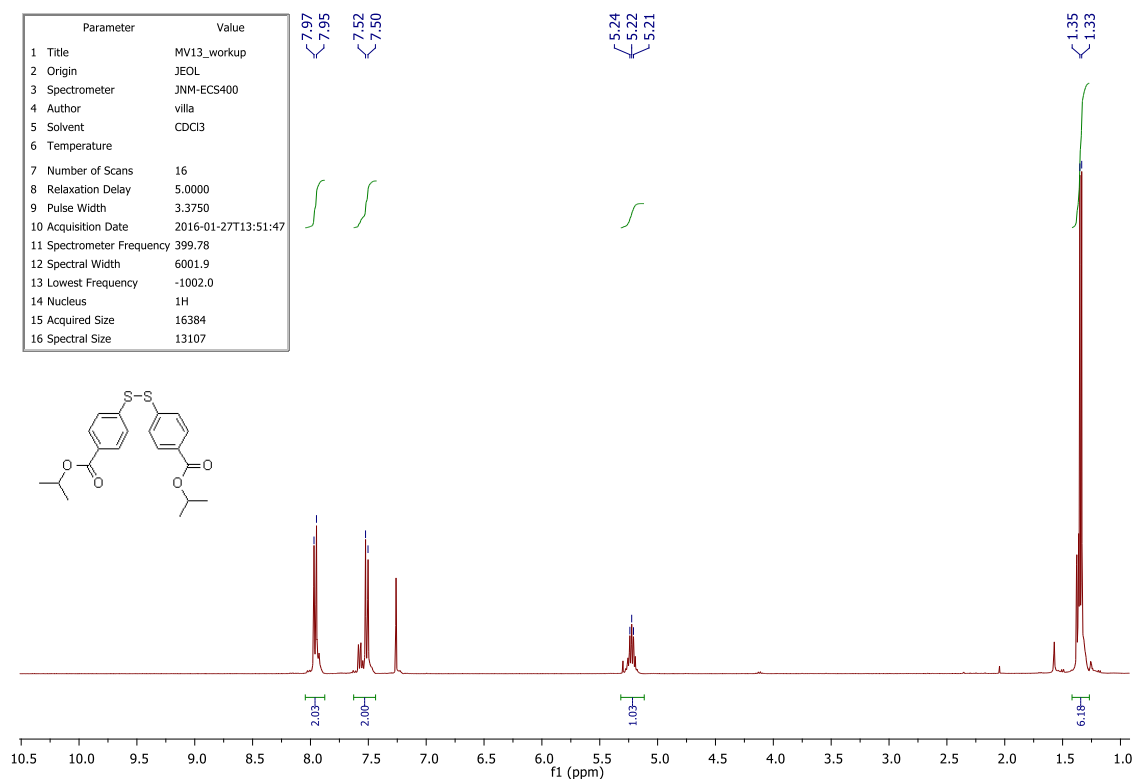
References:

- 1) M. Villa, M. Roy, G. Bergamini, P. Ceroni, M. Gingras *Chem Plus Chem* (2020), *85*, 1481-1486.

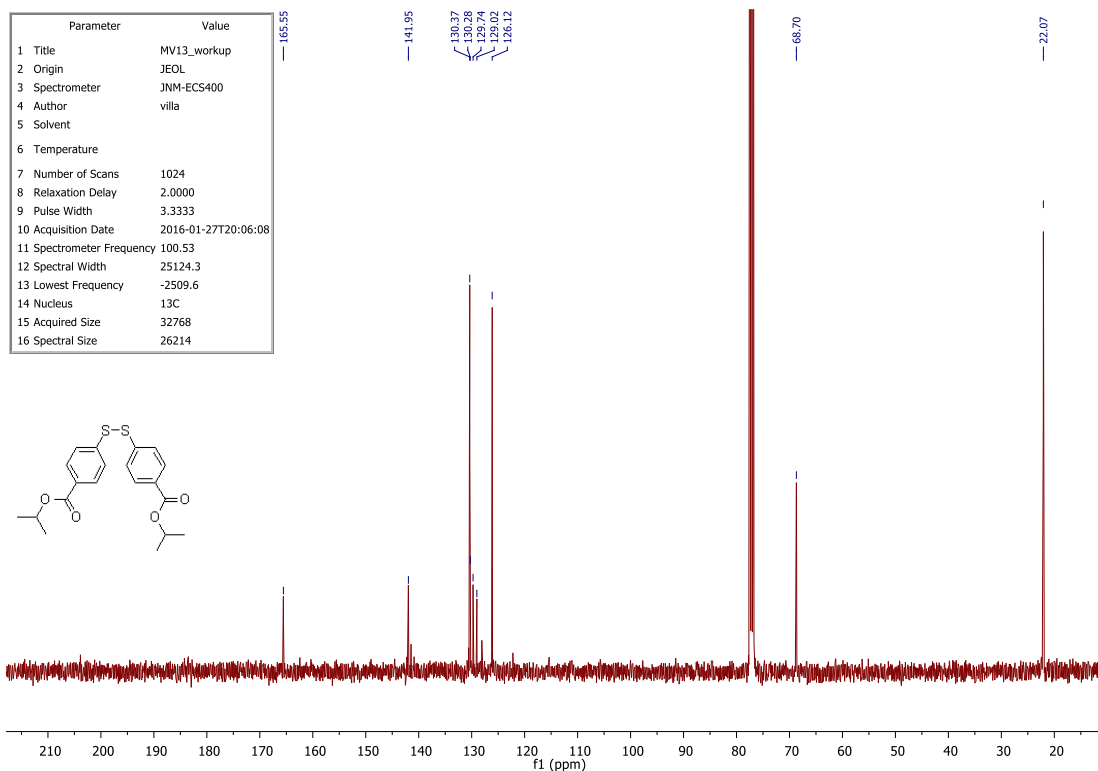
- 2) M. Villa; B. Del Secco; L. Ravotto; M. Roy; E. Rampazzo; N. Zaccheroni; L. Prodi; M. Gingras; S.A. Vinogradov; P. Ceroni *J. Phys. Chem. C* (2019), 123, 29884-29890.
- 3) X. Yan; C. Li; X. Xu; Q. He; X. Zhao; Y. Pan *Tetrahedron* (2019), 75, 3081-3087.
- 4) M. Villa; M. Roy; G. Bergamini; M. Gingras; P. Ceroni *Dalton Trans.* (2019), 48, 3815-3818.



FT-IR (ATR) spectrum of diisopropyl 4,4'-dithiobisbenzoate (**35**)



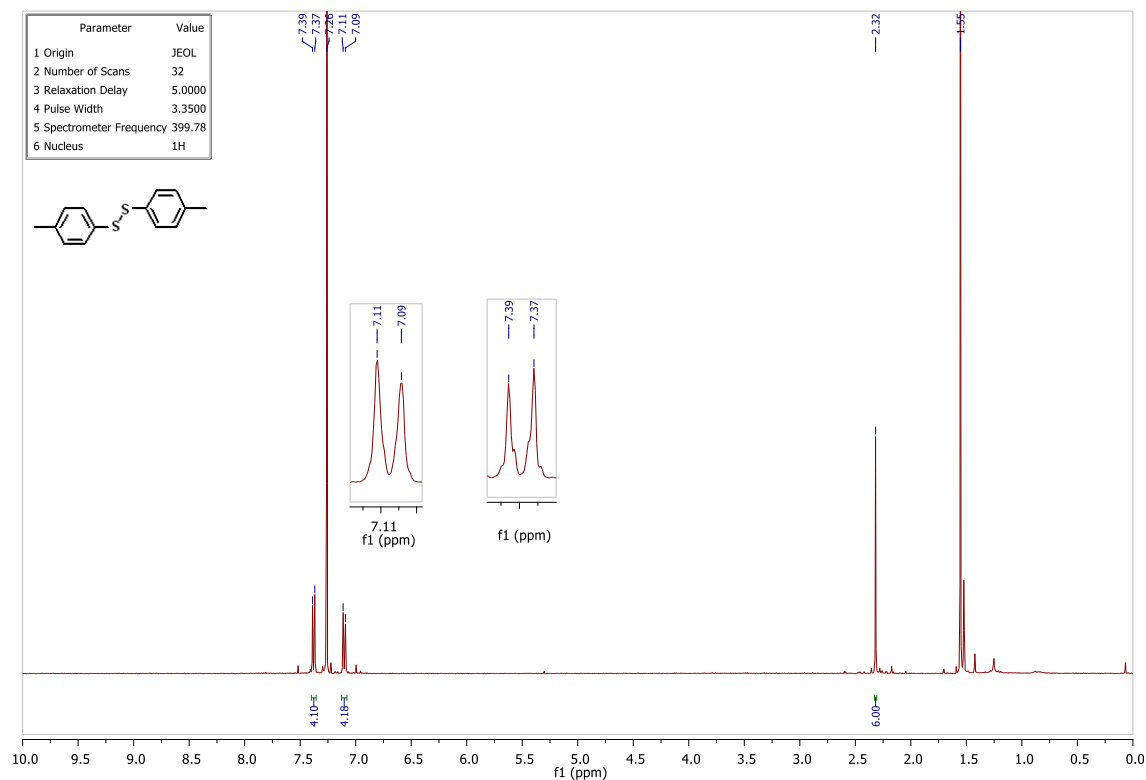
¹H-NMR spectrum of diisopropyl 4,4'-dithiobisbenzoate (**35**) (CDCl₃, 399.78 MHz)



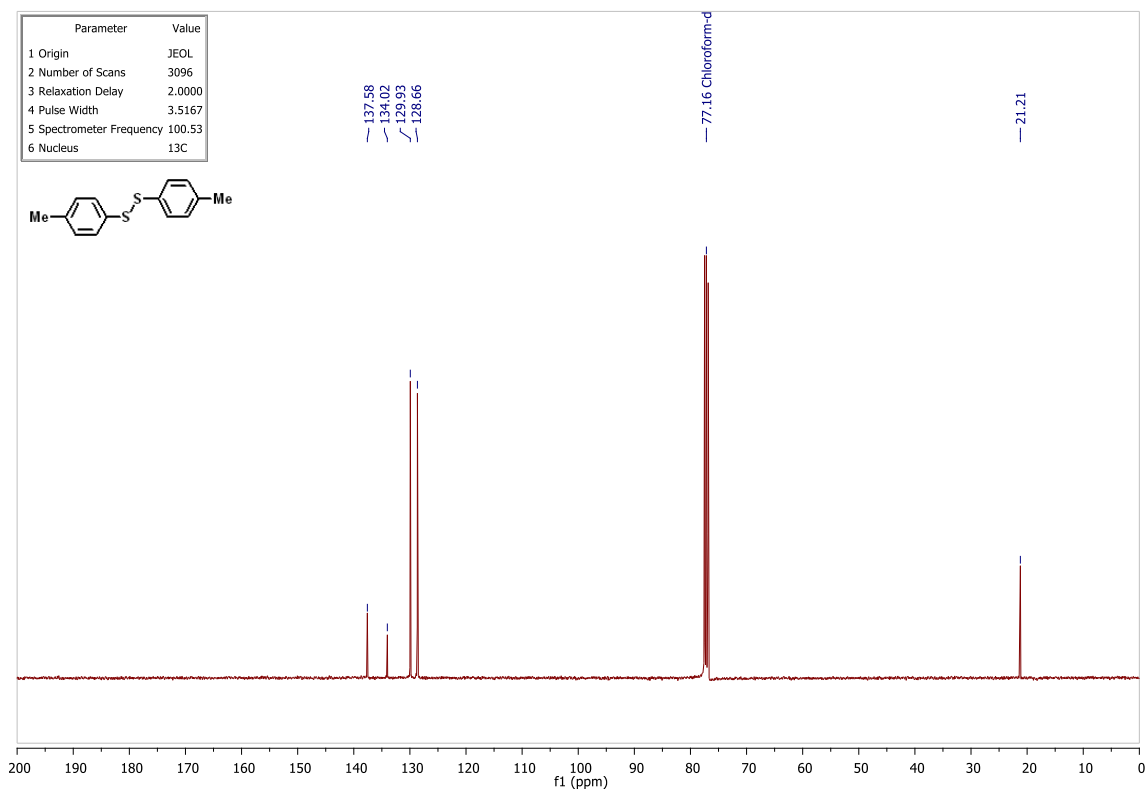
^{13}C -NMR spectrum of diisopropyl 4,4'-dithiobisbenzoate (**35**) (CDCl_3 , 100.53 MHz)

Bis(4-methylphenyl) disulfide (**33**) (commercial)

^1H NMR (399.78 MHz, CDCl_3 , ppm) δ = 7.38 (d_{app}, J = 8.1 Hz, 4H), 7.09 (d_{app}, J = 8.1 Hz, 4H), 2.32 (s, 6H); ^{13}C NMR (100.53 MHz, CDCl_3 , ppm) δ = 137.58, 134.02, 129.93, 128.66, 21.21.



^1H -NMR of bis(4-methylphenyl) disulfide (CDCl_3 , 399.78 MHz)



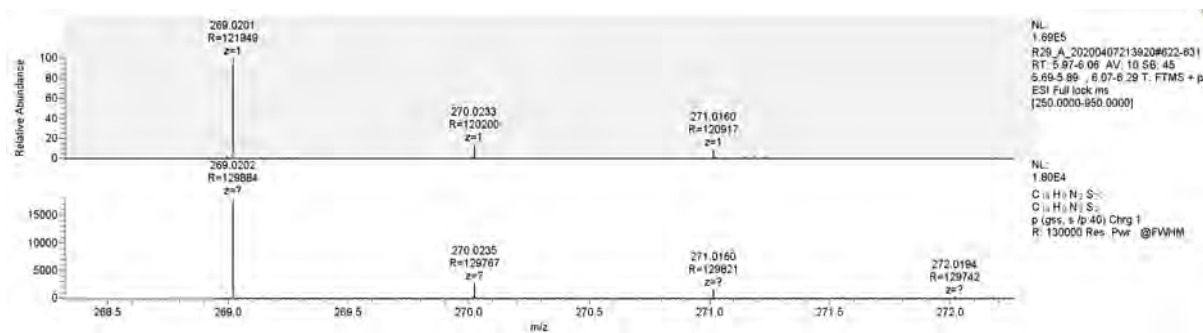
¹³C-NMR spectrum of bis(4-methylphenyl) disulfide (CDCl₃, 100.53 MHz)

Bis(4-cyanophenyl) disulfide (47)

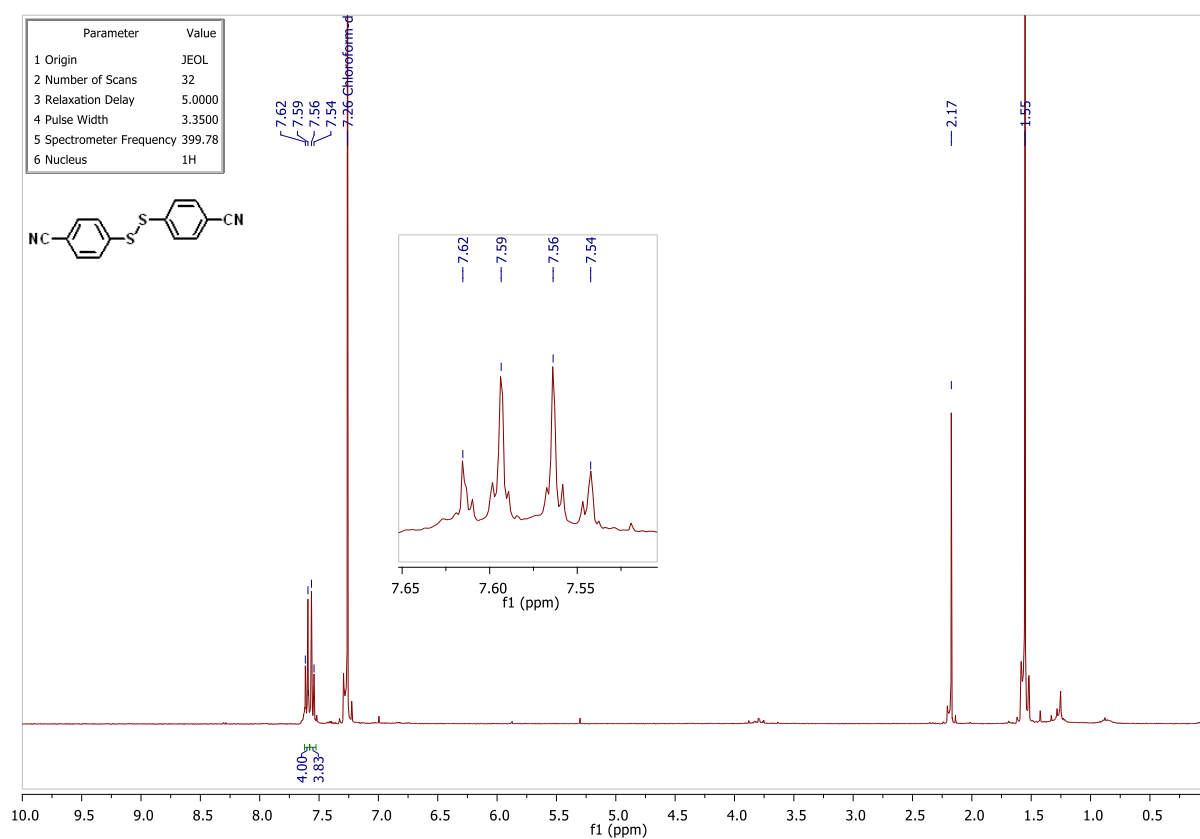
¹H NMR (399.78 MHz, CDCl₃, ppm) δ = 7.60 (d, *J* = 8.9 Hz, 4H), 7.55 (d, *J* = 8.8 Hz, 4H); ¹³C NMR (100.53 MHz, CDCl₃, ppm) δ = 139.33, 132.36, 128.52, 118.60, 108.43; HRMS (ESI+) calculated for [C₁₄H₈N₂S₂ +H⁺]: 269.0202 Da, found [M+H⁺] 269.0201 m/z;

References:

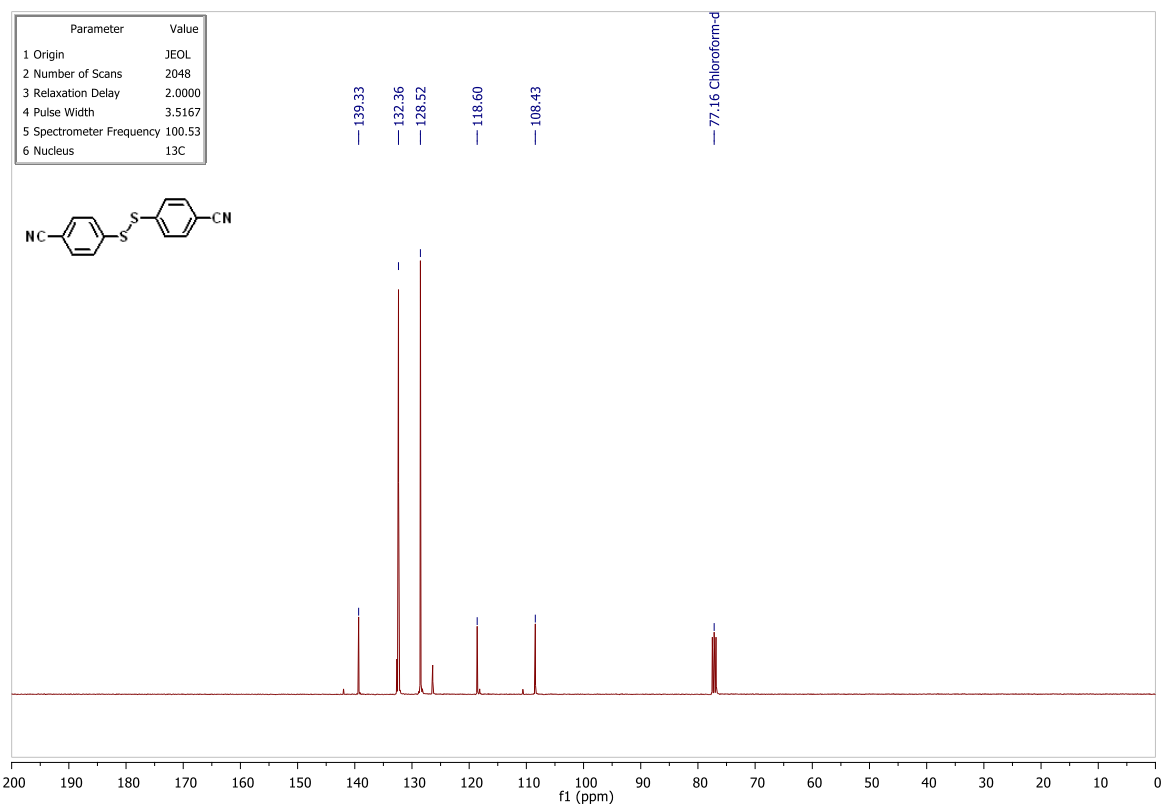
- 1) E. W. McClelland; L.A. Warren *J. Chem. Soc.* (1930), 1095-1102.
- 2) L. Bauer; J. Cymerman *J. Chem. Soc.* (1949), 3434.
- 3) L. Bauer; J. Cymerman *J. Chem. Soc.* (1950), 109-14.
- 4) J. Cymerman; J.B. Willis *J. Chem. Soc.* (1951), 1332-7.
- 5) R. Sato; S. Takizawa; S. Oae *Phosphorus, Sulfur Silicon Rel. Elem.* (1979), 7, 229-34.
- 6) S. Krishnamurthy; D. Aimino *J. Org. Chem.* (1989), 54, 4458-62.
- 7) C. Combellas; S. Dellerue; G. Mathey; A. Thiebault *Tetrahedron Lett.* (1997), 38, 539-542.
- 8) S. Antonello; K. Daasbjerg; H. Jensen; F. Taddei; F. Maran *J. Am. Chem. Soc.* (2003), 125, 14.
- 9) J. Tobias; P. Knochel *Synlett* (2005), 1185-1187.
- 10) H.-Y. Chen; W.-T. Peng; Y.-H. Lee; Y.-L. Chang; Y.-J. Chen; Y.-C. Lai; N.-Y. Jheng; H.-Y. Chen *Organometallics* (2013), 32, 5514-5522.
- 11) J.-T. Yu; H. Guo; Y. Yi; H. Fei; Y. Jiang *Adv. Synth. & Catal.* (2014), 356, 749-752.
- 12) M. Abbasi; N. Nowrouzi; H. Latifi *J. Organomet. Chem.* (2016), 822, 112-117.
- 13) Y. Zheng; F.-L. Qing; Y. Huang; X.-H. Xu *Adv. Synth. & Catal.* (2016), 358, 3477-3481.



HRMS (ESI, positive mode) of **(47)**



¹H-NMR of **(47)** (CDCl₃, 399.78 MHz)

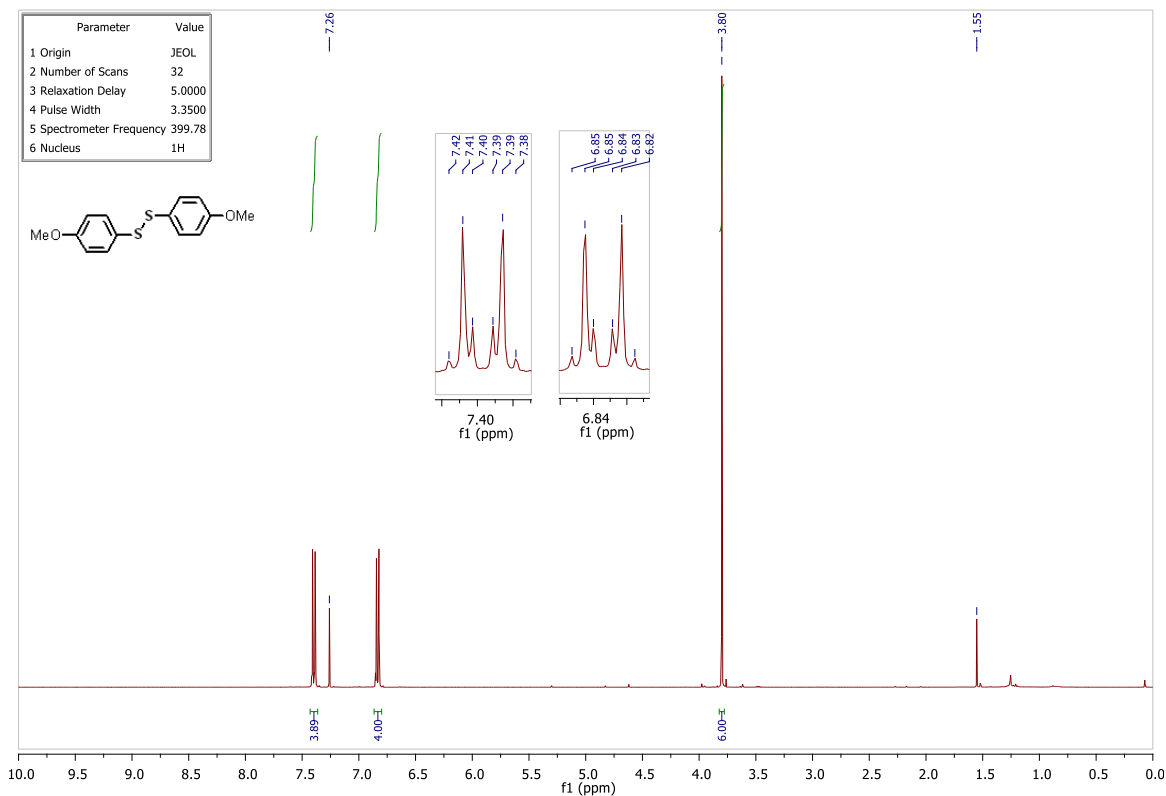


¹³C-NMR spectrum of **(47)** (CDCl₃, 100.53 MHz)

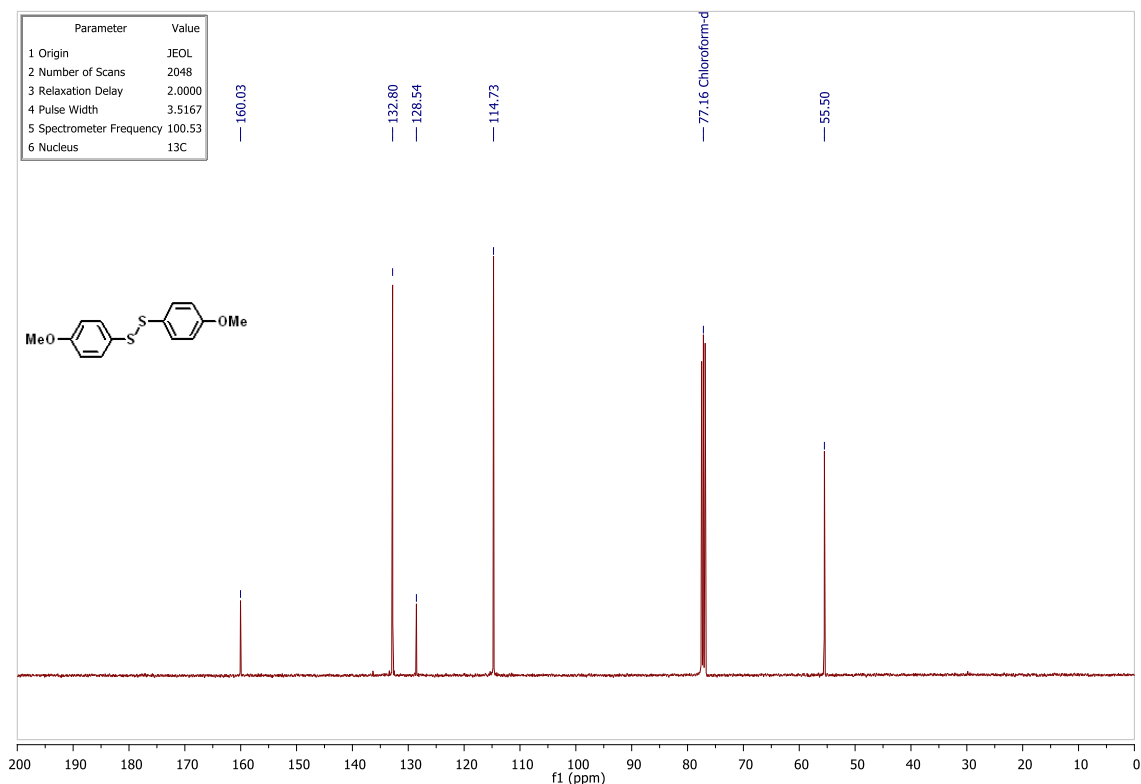
Bis(4-methoxyphenyl) disulfide (commercial)

¹H NMR (399.78 MHz, CDCl₃, ppm) δ = 7.40 (d, *J* = 9.0 Hz, 4H), 6.83 (d, *J* = 8.8 Hz, 4H), 3.80 (s, 6H);

¹³C NMR (100.53 MHz, CDCl₃, ppm) δ = 160.03, 132.80, 128.54, 114.73, 55.50; HRMS (ESI+) calculated for [C₁₄H₁₄O₂S₂ + H⁺]: 279.0508 Da, found [M+H⁺] 279.0509 m/z;



¹H-NMR of bis(4-methoxyphenyl) disulfide (CDCl₃, 399.78 MHz)

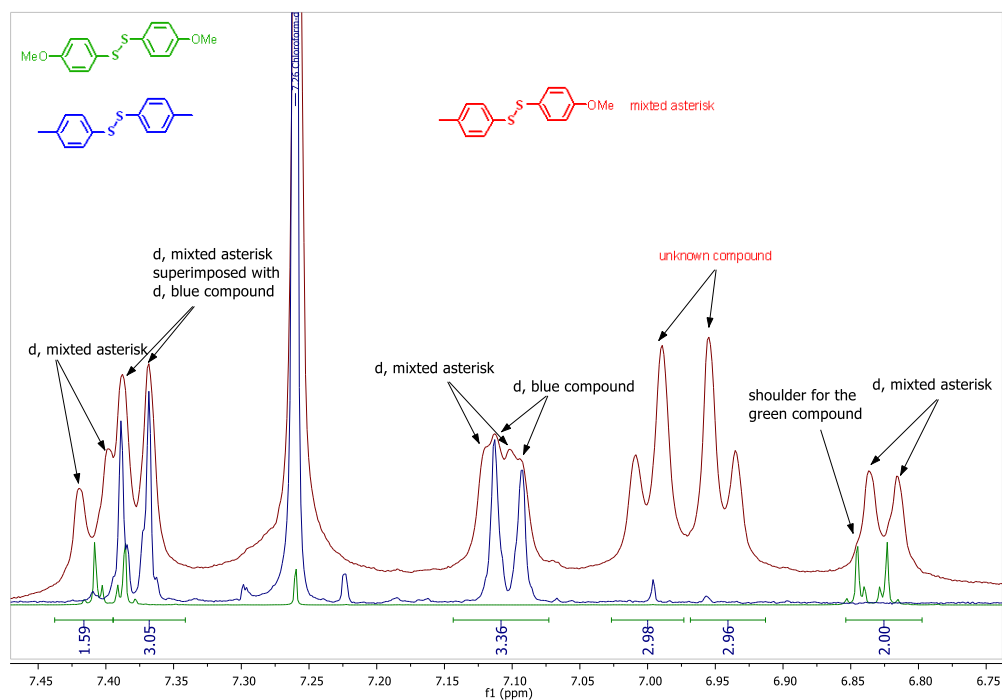


^{13}C -NMR spectrum of bis(4-methoxyphenyl) disulfide (CDCl_3 , 100.53 MHz)

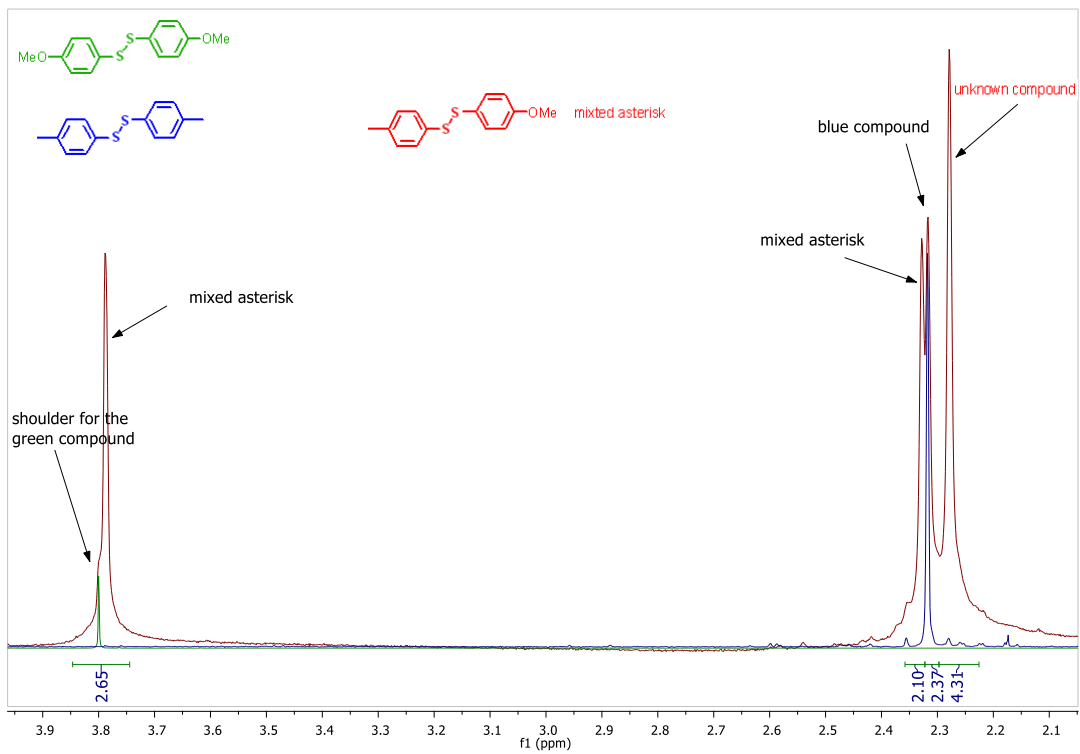
List of mixed disulfides

4-Methylphenyl-4-methoxyphenyl disulfide (58)

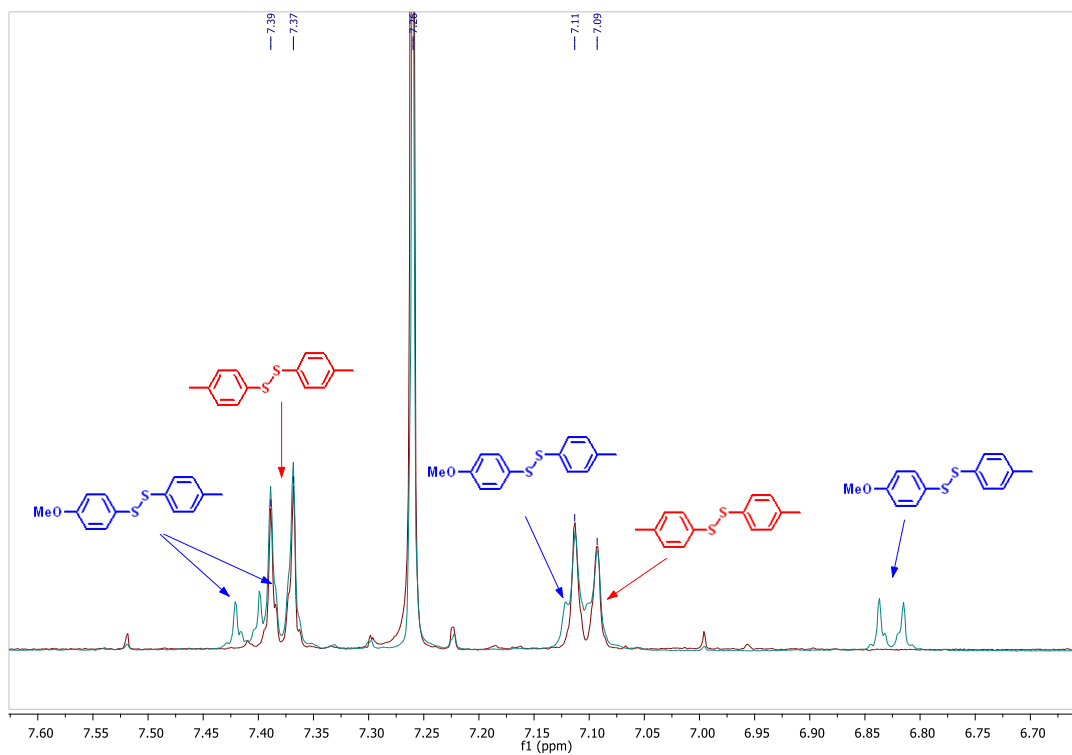
^1H NMR (399.78 MHz, CDCl_3 , ppm) δ = 7.41 (d, J = 8.2 Hz, 2H), 7.38 (d, J = 7.8 Hz, 2H), 7.11 (d, J = 7.4 Hz, 2H), 6.83 (d, J = 8.3 Hz, 2H), 3.79 (s, 3H), 2.33 (s, 3H).



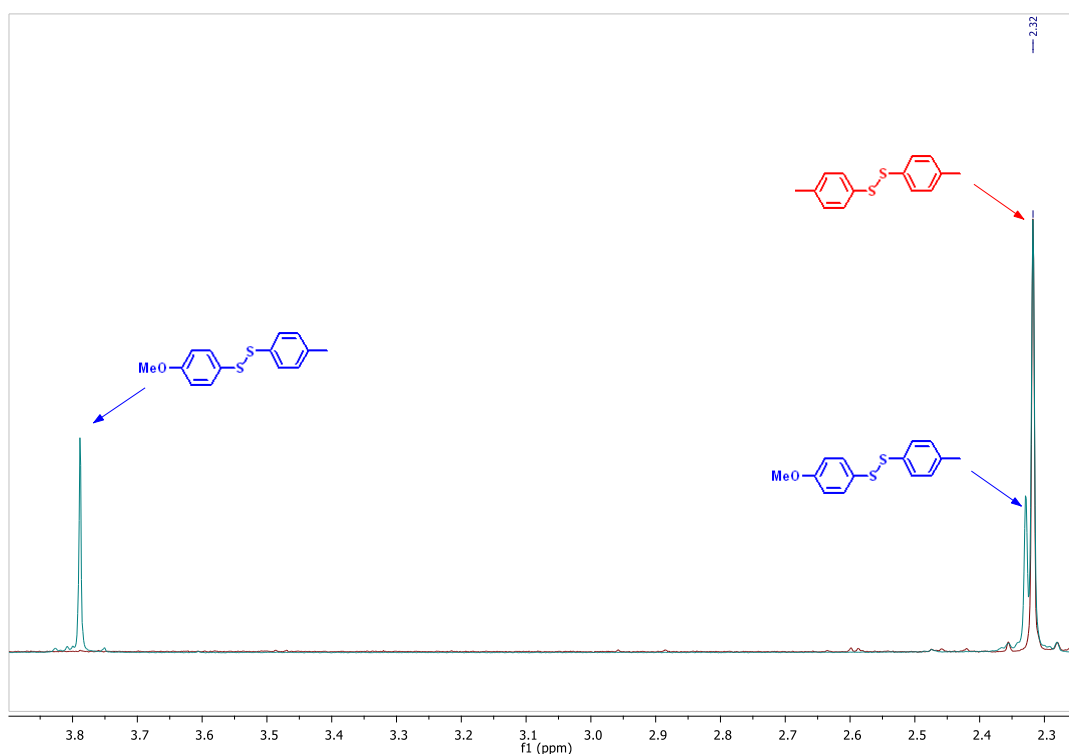
^1H -NMR (CDCl_3 , 399.78 MHz)



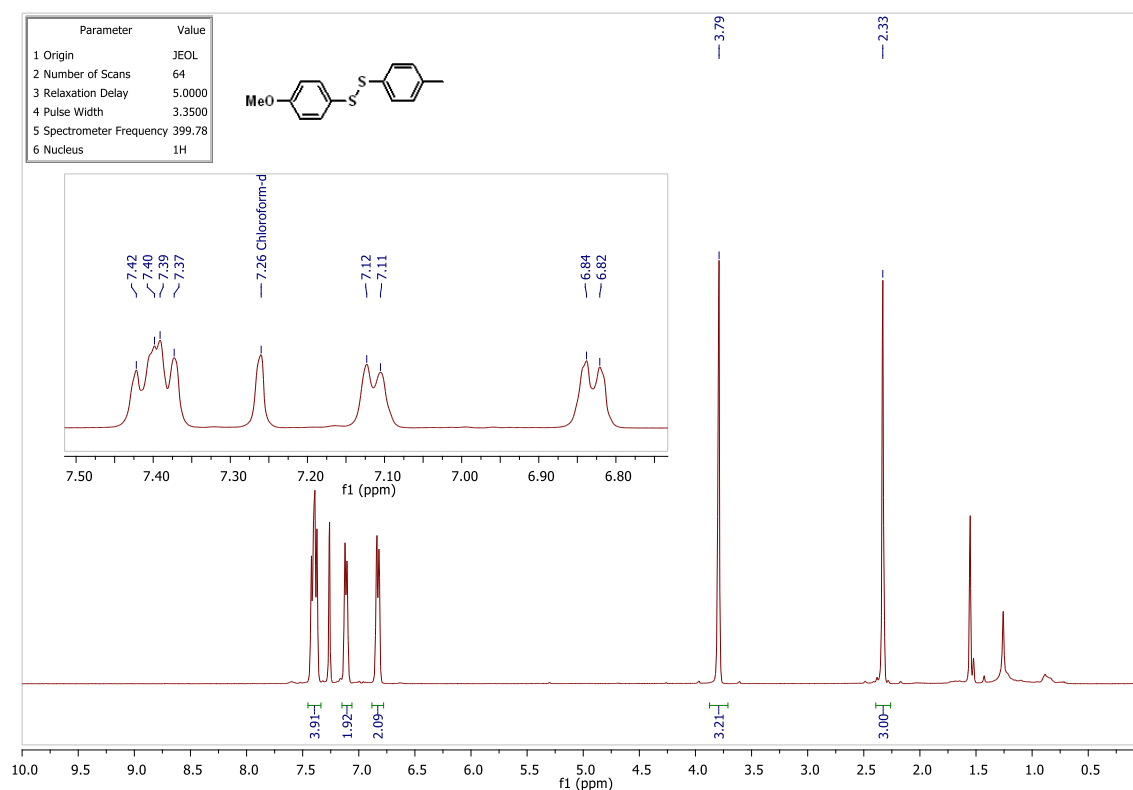
¹H-NMR (CDCl₃, 399.78 MHz)



¹H-NMR (CDCl₃, 399.78 MHz)



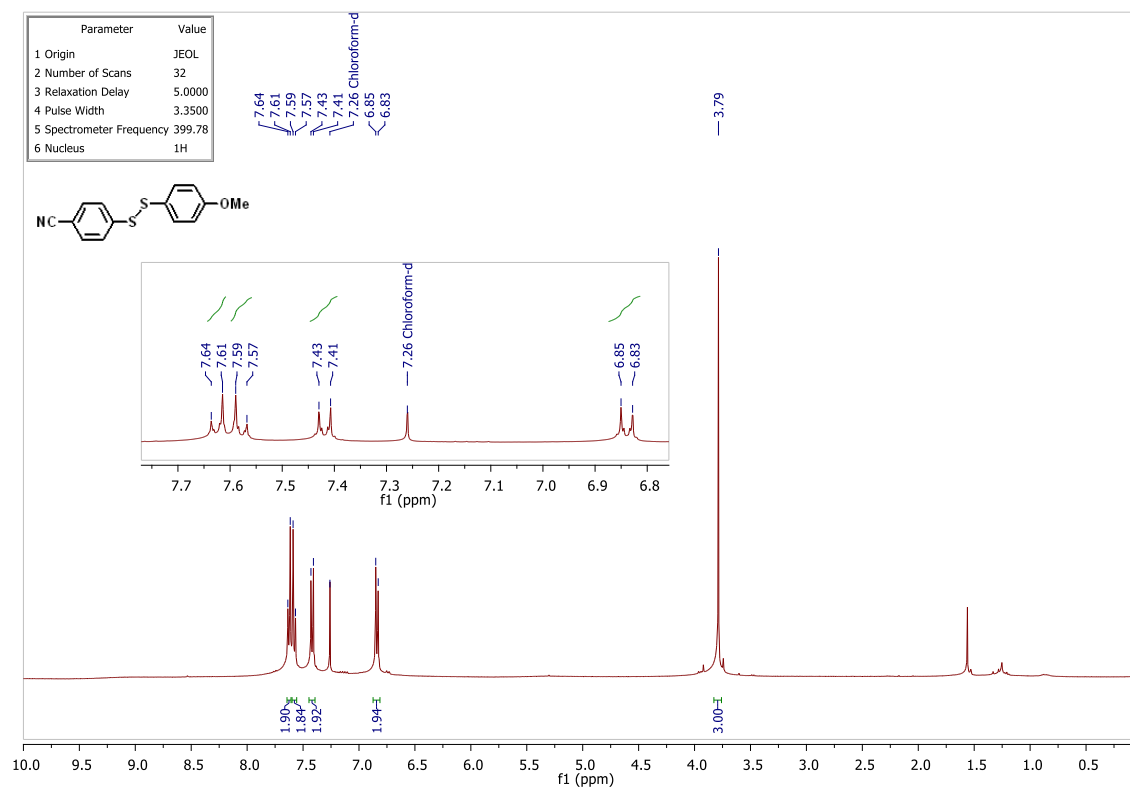
$^1\text{H-NMR}$ (CDCl_3 , 399.78 MHz)



$^1\text{H-NMR}$ of 4-methylphenyl-4-methoxyphenyl disulfide (**58**) (CDCl_3 , 399.78 MHz)

4-Methoxyphenyl-4-cyanophenyl disulfide (**59**)

$^1\text{H NMR}$ (399.78 MHz, CDCl_3 , ppm) δ = 7.63 (d, J = 8.6 Hz, 2H), 7.58 (d, J = 8.7 Hz, 2H), 7.42 (d, J = 8.8 Hz, 2H), 6.84 (d, J = 8.9 Hz, 2H), 3.79 (s, 3H).



¹H-NMR of 4-methoxyphenyl-4-cyanophenyl disulfide (**59**) (CDCl₃, 399.78 MHz)

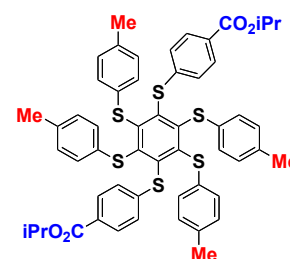
References:

- 1) D. Wang; X. Liang; M. Xiong; H. Zhu; Y. Zhou; Y. Pan, *Org. & Biomol. Chem.* (2020), 18, 4447-4451.
- 2) L. Delarue Bizzini; P. Zwick; M. Mayor *Eur. J. Org. Chem.* (2019), 6956-6960.
- 3) N. Taniguchi *Tetrahedron* (2017), 73, 2030-2035
- 4) H. Kutuk; N. Turkoz *Phosphorus, Sulfur Silicon Rel. Elem.* (2011), 186, 1515-1522.
- 5) N. Stellenboom; R. Hunter; M. R. Caira *Tetrahedron* (2010), 66, 3228-3241.
- 6) S. Demkowicz; J. Rachon; D. Witt *Synthesis* (2008), 2033-2038.
- 7) G. Palumbo; M. Parrilli; O. Neri; C. Ferreri; R. Caputo *Tetrahedron Lett.* (1982), 23, 2391-4.
- 8) E.R. Cole *Nature* (London, United Kingdom) (1963), 198(4885), 1083-4.

2.5 Mixed hexa(thio) benzene asterisks

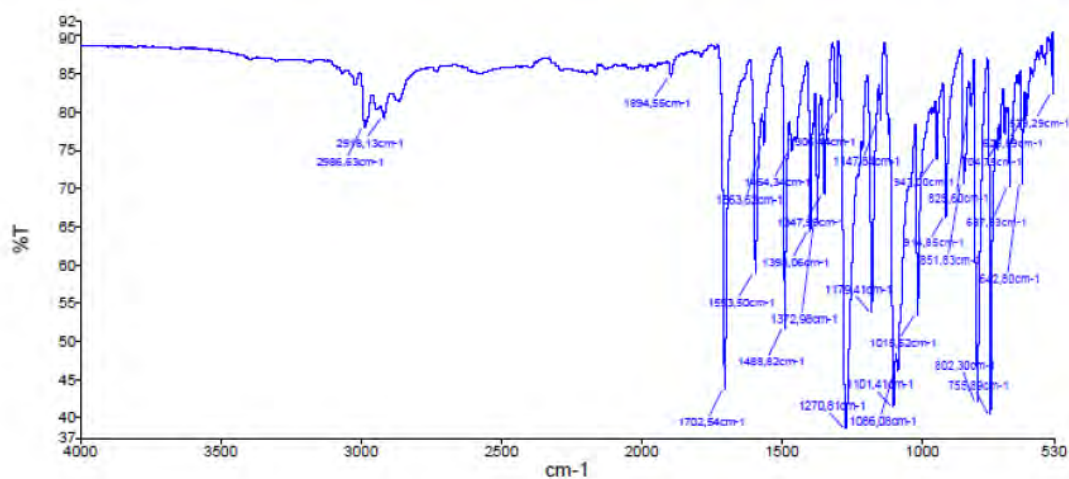
1,4-Bis(4-isopropoxycarbonyl-phenylthio)- 2,3,5,6-tetrakis(4-methylphenylthio)benzene (**32**, n= 2)

In an oven-dried glass tube were placed 2,3,5,6-tetrafluoro-1,2-bis(4-isopropoxycarbonyl-phenylthio) benzene (400 mg, 0.743 mmol, 1.00 mol-eq), *p*-methylbenzenethiol (372 mg, 3.00 mmol, 4.04 mol-eq) and dry potassium carbonate (614 mg, 4.44 mmol, 5.98 mol-eq) under an argon atmosphere. All reagents were freshly dried under vacuum for about 30 min prior to use them. Under argon, dry DMF (3.7 mL, kept over activated 3Å molecular sieves) was then injected, the tube was sealed and the mixture was vigorously stirred at 20°C for 45 min.. An aqueous HCl solution (1M, 100 mL) was added and a yellow-brown solution was extracted with toluene (3x25 mL). The

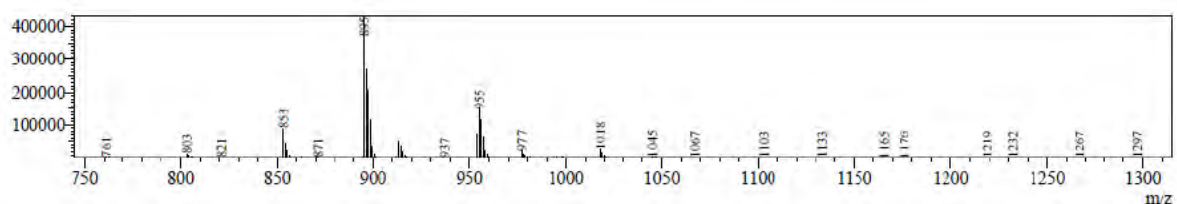
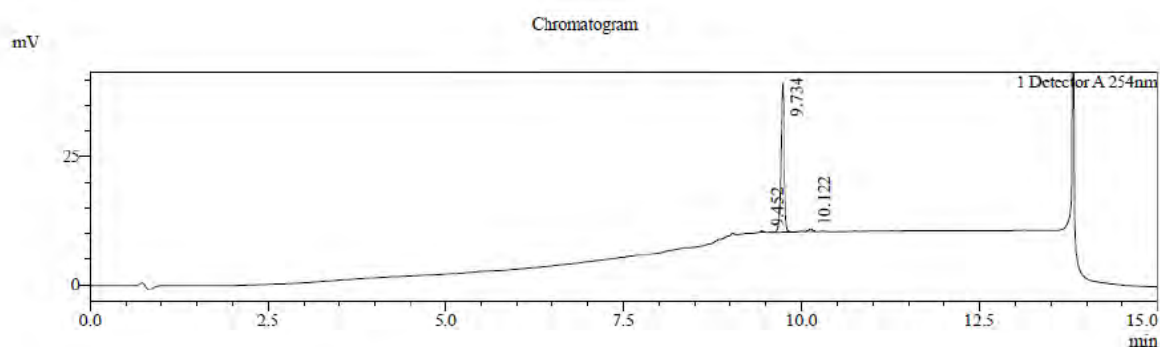


combined organic phases were washed with water (5x25 mL), and dried over anhydrous MgSO₄. After filtration, and evaporation of solvents, a yellow-brown solid was obtained and a purification by column chromatography on silica gel (eluent: toluene/DCM: 80/20) afforded a yellow solid (453 mg, 0.474 mmol, 64 % yield).

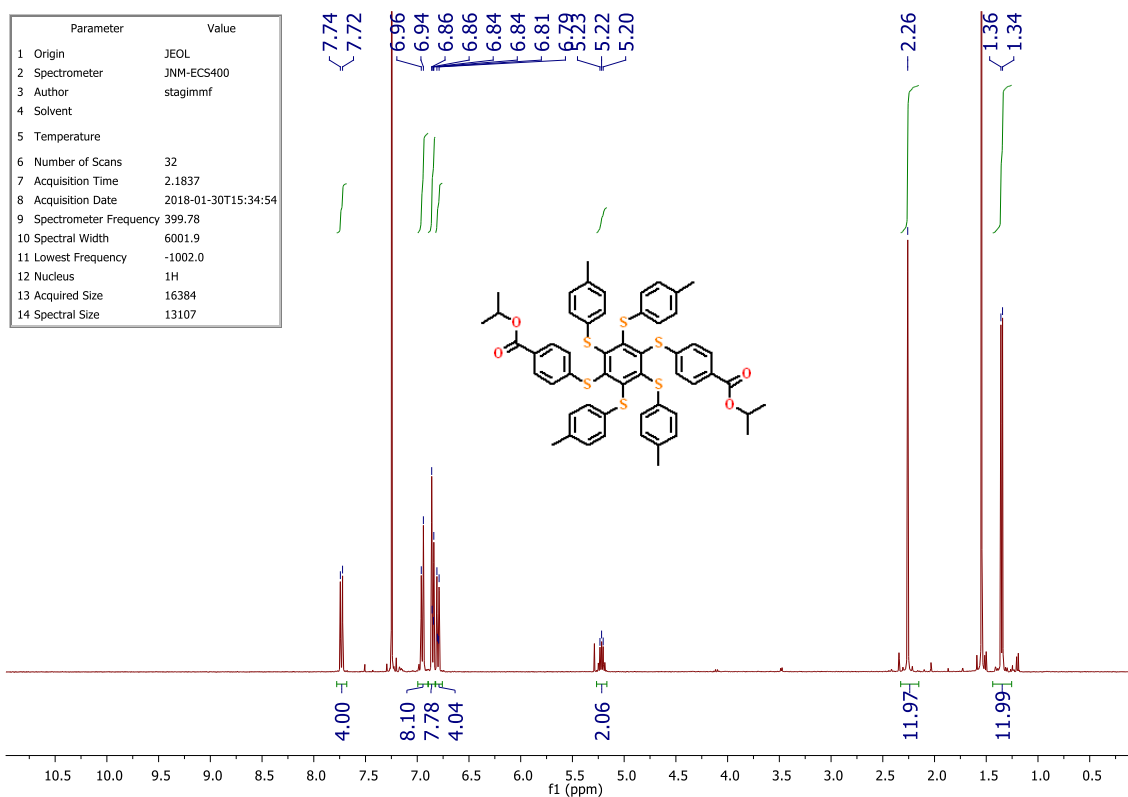
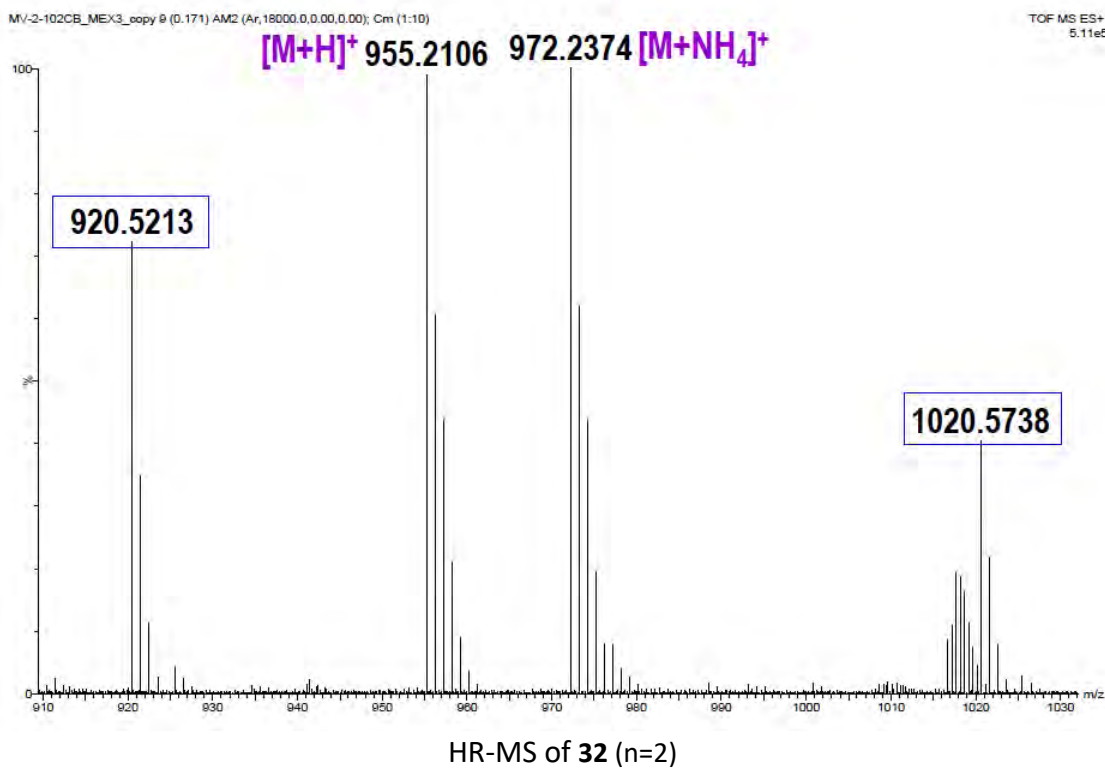
TLC (toluene/DCM : 80/20) R_f = 0.25; **FT-IR** (ATR, diamond contact, neat, cm⁻¹) ν = 2986, 2918, 1702, 1593, 1488, 1270, 1179, 1101, 1085, 914, 802, 755; **¹H NMR** (399.78 MHz, CDCl₃, ppm): δ = 7.74 (d, J = 8.5 Hz, 4H), 6.96 (d, J = 8.0 Hz, 8H), 6.86 (d, J = 8.0 Hz, 8H), 6.81 (d, J = 8.5 Hz, 4H), 5.23 (sept, J = 6.3 Hz, 2H), 2.27 (s, 12H) 1.36 (d, J = 6.3 Hz, 12H); **¹³C NMR** (100.53 MHz, CDCl₃, ppm): δ = 165.74, 148.78, 146.41, 143.89, 136.67, 133.90, 130.07, 129.92, 129.13, 128.01, 126.35, 68.46, 22.15, 21.22; **MS** (LC-MS acetonitrile/water, 0.1% formic acid; APCI) 955 m/z [M+H]⁺; **HRMS (ESI+)** calculated for [C₅₄H₅₀O₄S₆ + NH₄]⁺: 972.2377 Da, found 972.2374 m/z [M+NH₄]⁺; **HRMS (ESI+)** calculated for [C₅₄H₅₀O₄S₆ + H]⁺: 955.2106 Da, found [M+H]⁺ 955.2106 m/z.

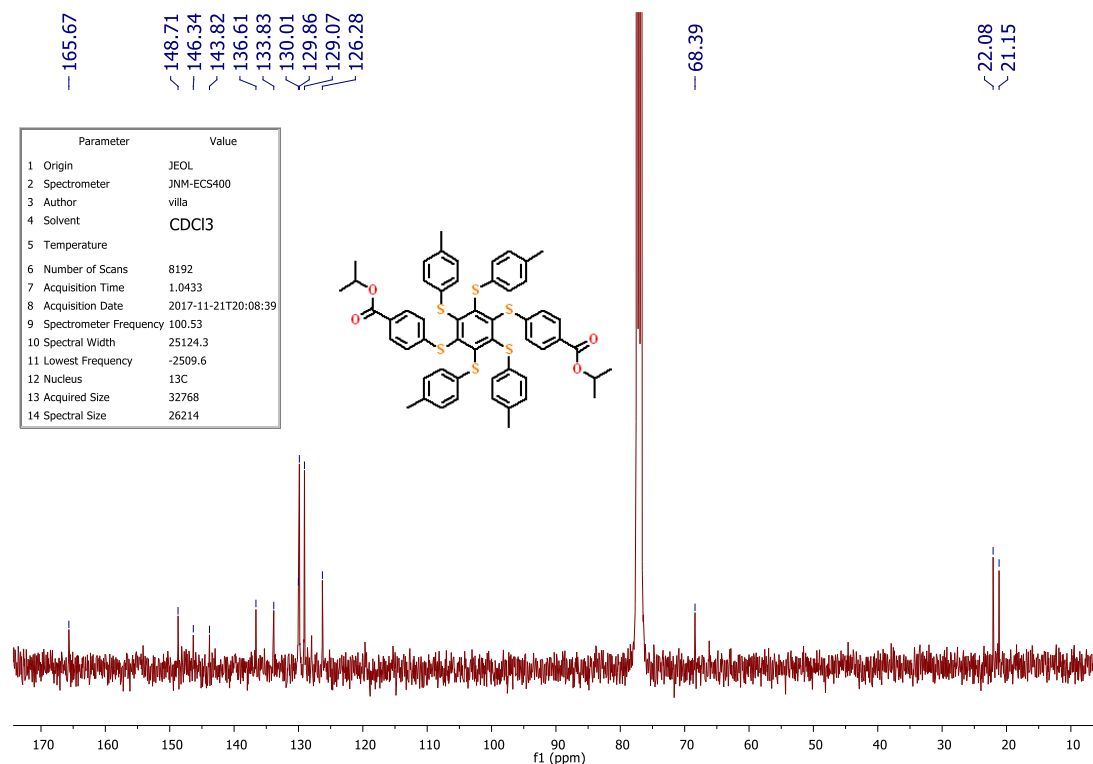


FT-IR spectrum of **32** (n=2)



Reverse phase HPLC chromatogram and MS-APCI of **32** (n=2)

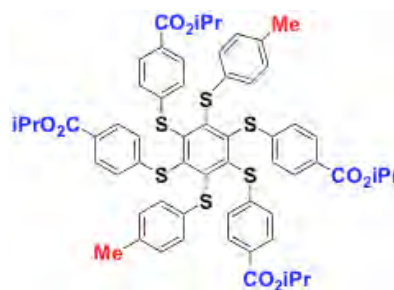




^{13}C -NMR of **32** (n=2) (CDCl_3 , 100.53 MHz)

2,3,5,6-Tetrakis(4-isopropoxyxycarbonyl-phenylthio)-1,4-bis(4-methylphenylthio)benzene (**60**)¹

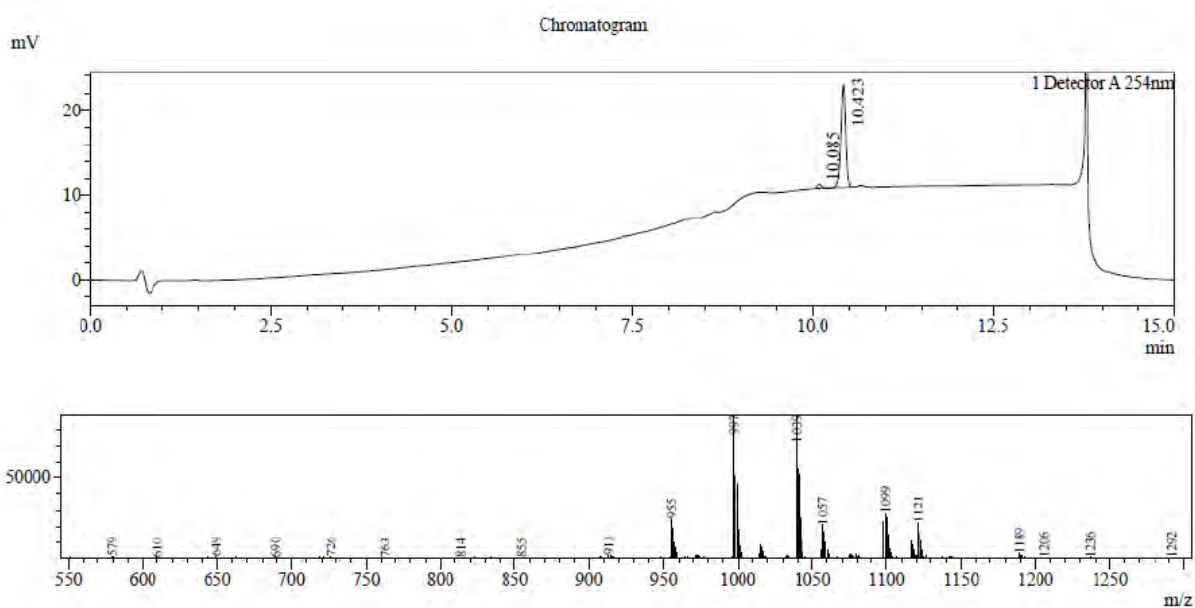
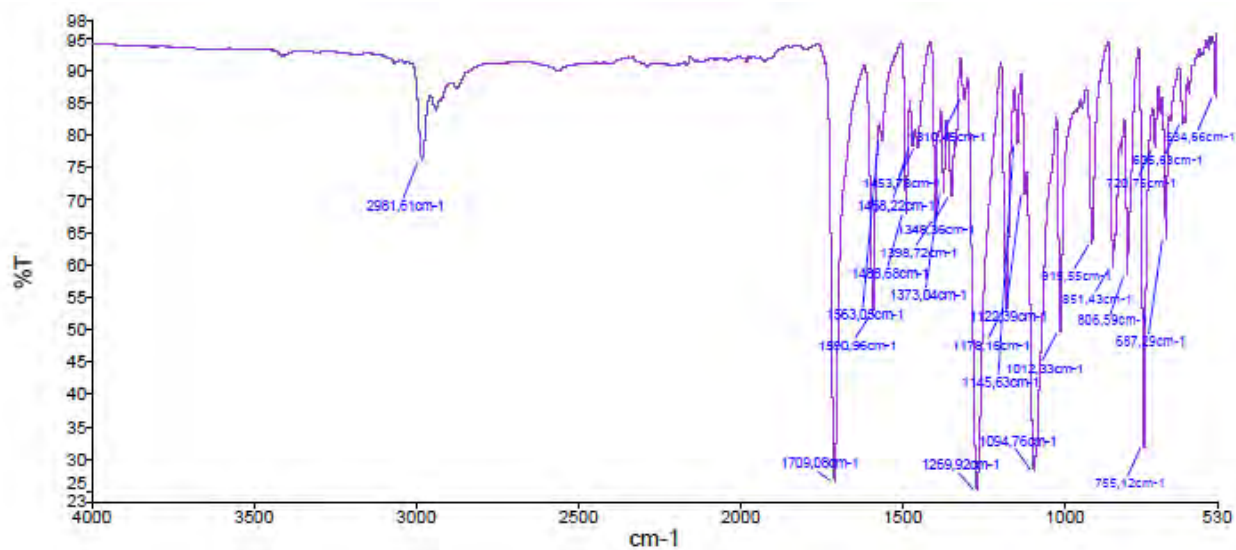
In an oven-dried tube were placed 1,4-difluoro-2,3,5,6-tetrakis(4-isopropoxyxycarbonyl-phenylthio)benzene (400 mg, 0.449 mmol, 1.00 mol-eq), *p*-methylbenzenethiol (114.1 mg, 0.919 mmol, 2.05 mol-eq) and dry potassium carbonate (198.2 mg, 1.44 mmol, 3.21 mol-eq) under an argon atmosphere. All reagents were freshly dried under vacuum for about 30 min prior to use them. Under argon, dry DMF (3.7 mL, kept over molecular sieves 3A) was injected, the tube was sealed, and the mixture was vigorously stirred at 80°C (oil bath temperature) for 4 days. After cooling down to room temperature, an aqueous HCl solution (1M, 100 mL) was added and it was extracted with toluene (3x25 mL). The combined organic phases were washed with water (5x25 mL), and dried over anhydrous MgSO_4 . After filtration, and evaporation of solvents, a yellow-brown solid was obtained. A purification by a chromatography column over silica gel (eluent: toluene/DCM: 80:20 v/v) afforded a yellow solid (370 mg, 0.337 mmol, 75 %).



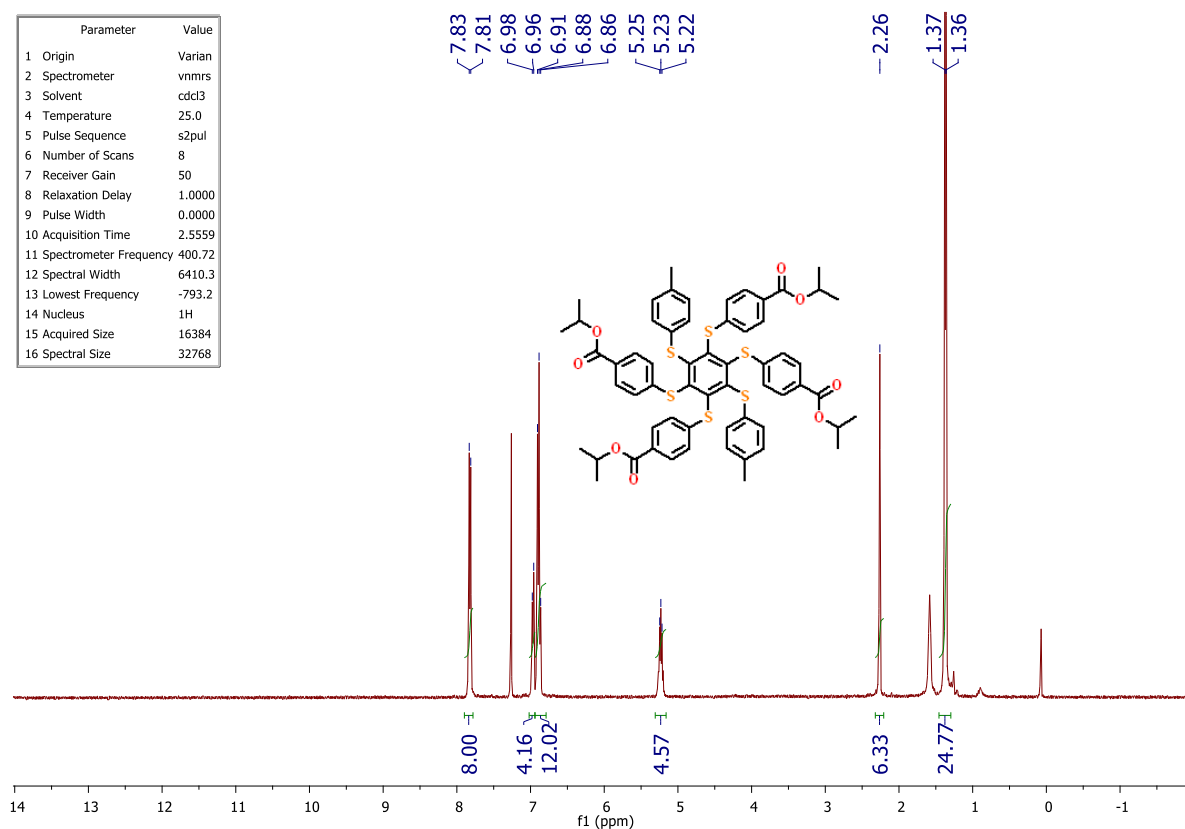
TLC (tol/DCM: 80/20 v/v) $R_f = 0.5$; **FT-IR** (ATR, diamond contact, neat, cm^{-1}) $\nu = 2981, 1709, 1590, 1488, 1269, 1178, 1094, 1012, 915, 851, 806, 755, 687$; **^1H NMR** (400.72 MHz, CDCl_3 , ppm): $\delta = 7.82$ (d, $J = 8.2$ Hz, 8H), 6.97 (d, $J = 8.0$ Hz, 4H), 6.90 (d, $J = 8.3$ Hz, 8H), 6.87 (d, $J = 8.2$ Hz, 4H), 5.23 (sept, $J = 6.3$ Hz, 4H), 2.26 (s, 6H), 1.37 (d, $J = 6.3$ Hz, 24H); **^{13}C NMR** (100.77 MHz, CDCl_3 , ppm): $\delta = 165.55, 149.83, 147.09, 143.30, 137.21, 133.31, 130.27, 130.09, 129.42, 128.64, 126.77, 68.60, 22.12, 21.18$; **MS** (LC-MS acetonitrile/water, 0.1% formic acid; APCI) 1099 $[\text{M}+\text{H}]^+$.

Reference

- 1) M. Villa; B. Del Secco; L. Ravotto; M. Roy; E. Rampazzo; N. Zaccheroni; L. Prodi; M. Gingras; S. Vinogradov; P. Ceroni *J. Phys. Chem. C* (2019), 123, 29884-29890.

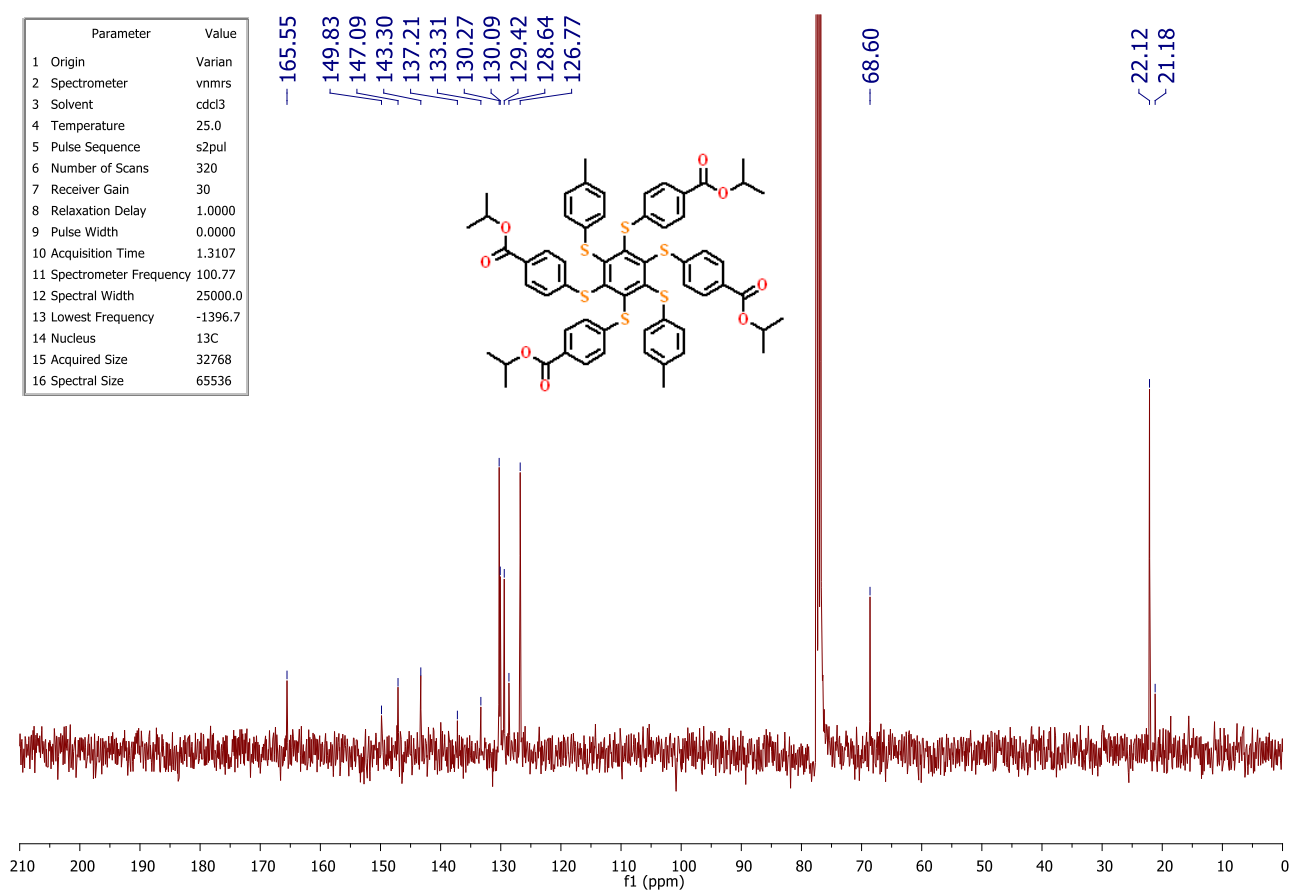


Parameter	Value
1 Origin	Varian
2 Spectrometer	nmrs
3 Solvent	cdcl3
4 Temperature	25.0
5 Pulse Sequence	s2pul
6 Number of Scans	8
7 Receiver Gain	50
8 Relaxation Delay	1.0000
9 Pulse Width	0.0000
10 Acquisition Time	2.5559
11 Spectrometer Frequency	400.72
12 Spectral Width	6410.3
13 Lowest Frequency	-793.2
14 Nucleus	¹ H
15 Acquired Size	16384
16 Spectral Size	32768



¹H-NMR of (60) (CDCl₃, 400.72 MHz, Varian)

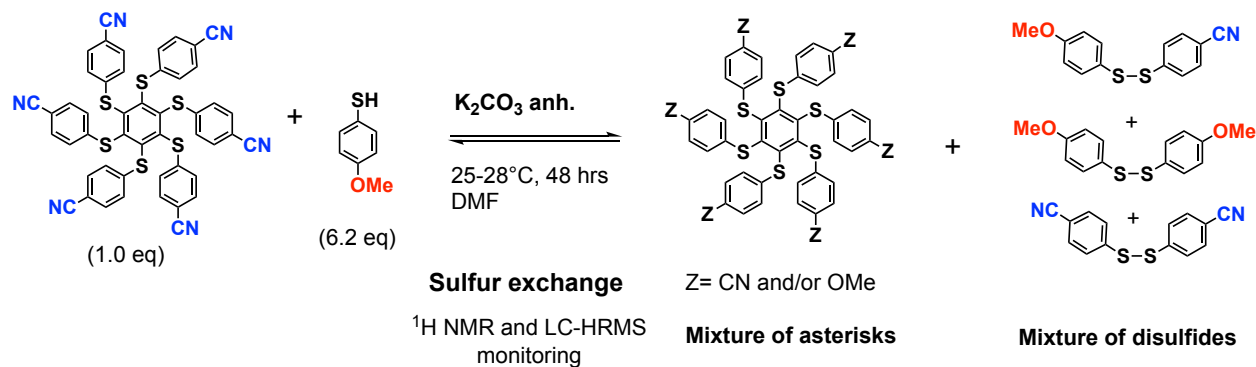
Parameter	Value
1 Origin	Varian
2 Spectrometer	nmrs
3 Solvent	cdcl3
4 Temperature	25.0
5 Pulse Sequence	s2pul
6 Number of Scans	320
7 Receiver Gain	30
8 Relaxation Delay	1.0000
9 Pulse Width	0.0000
10 Acquisition Time	1.3107
11 Spectrometer Frequency	100.77
12 Spectral Width	25000.0
13 Lowest Frequency	-1396.7
14 Nucleus	¹³ C
15 Acquired Size	32768
16 Spectral Size	65536



¹³C-NMR of (60) (CDCl₃, 100.77 MHz, Varian ARX Inova 400 NMR)

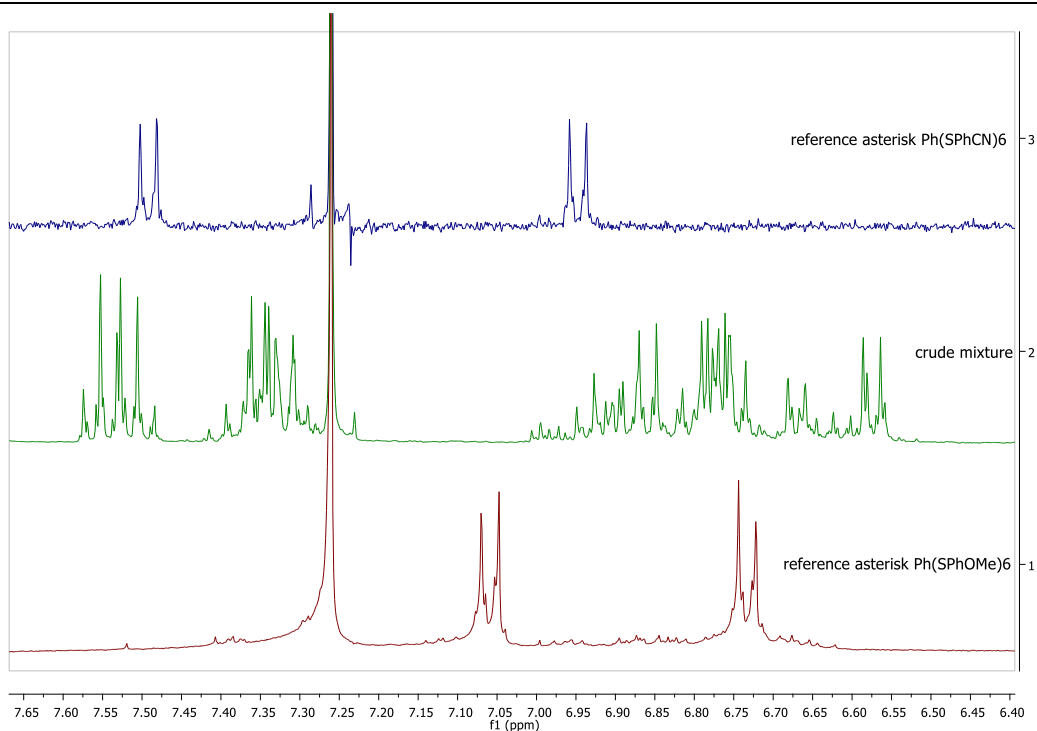
3.0 Sulfur exchange reactions on hexa(thio) benzene asterisks

SULFUR EXCHANGE REACTIONS WITH HEXAKIS(4-CYANOPHENYLTHIO)BENZENE.

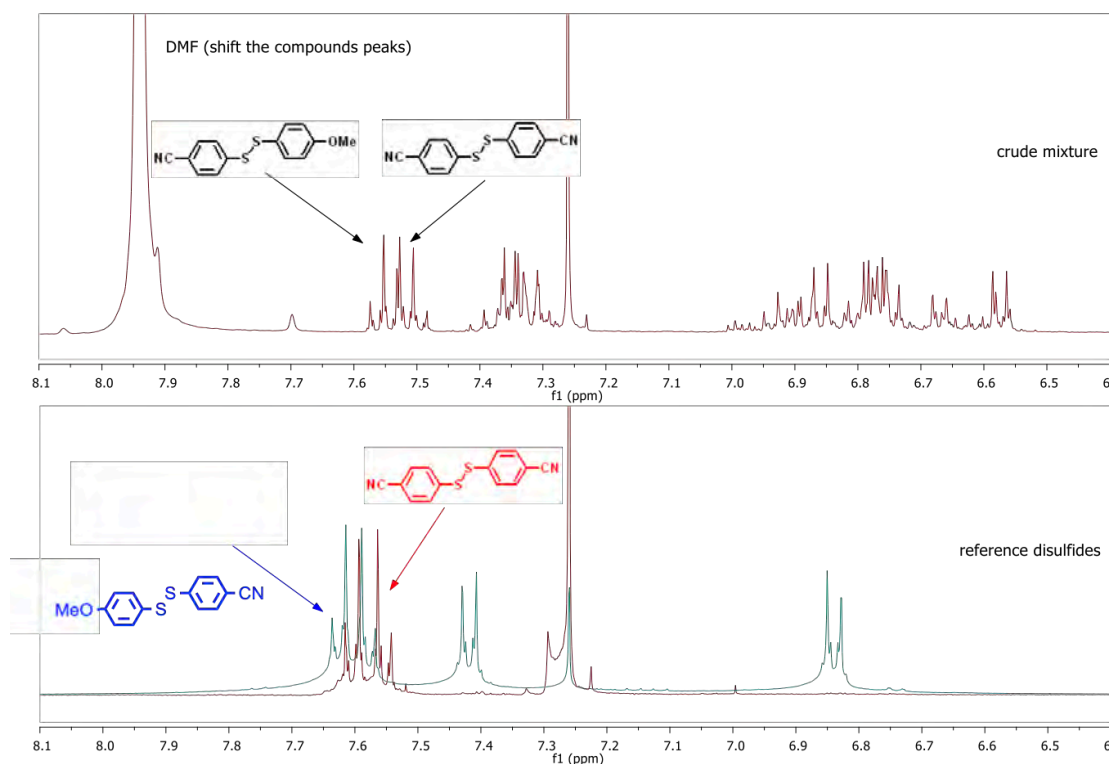


(R-29) Procedure. In an oven-dried glass tube were placed hexakis(4-cyanophenylthio)benzene (40 mg, 0.046 mmol, 1.00 mol-eq.) and dried potassium carbonate (39.7 mg, 0.287 mmol, 6.24 mol-eq.) under a flow of argon. 4-Methoxythiophenol (39.9 mg, 0.285 mmol, 35 μL , 6.2 mol-eq.) in dry DMF (0.5mL, kept over activated molecular sieves 3 \AA) was injected via a syringe. Argon was bubbled through the mixture for 5-10 min.. The tube was sealed, and the reaction was stirred at room temperature (25-28 $^\circ\text{C}$) for 2 days. It was monitored by TLC (SiO_2 , 10% to 30% EtOAc/*n*-hept or 80% tol/*n*-hept). After one day, TLC (30% EtOAc/*n*-hept) indicated under UV-vis lamp two less polar spots corresponding to some disulfides. The two more polar spots were yellow. One corresponded to hexakis (4-cyanophenylthio)benzene. After collecting a small aliquot, addition of H_2O and extraction with CHCl_3 , the reaction was monitored by $^1\text{H NMR}$ (**SG-I-152-A**). It indicated some ligand exchanges after 16 hrs. The reaction mixture reacted for two days and it was stopped by adding water (5 mL) and CHCl_3 (5 mL). The organic phase was separated and washed further with H_2O (2x5mL) for removing DMF. It was dried over anhydrous MgSO_4 , filtered and evaporated. The crude product was purified by column chromatography over SiO_2 while using an increasing polarity of eluent from 5% EtOAc to 30% EtOAc in cyclohexane. Some fractions and the crude were analyzed by LC-HRMS.

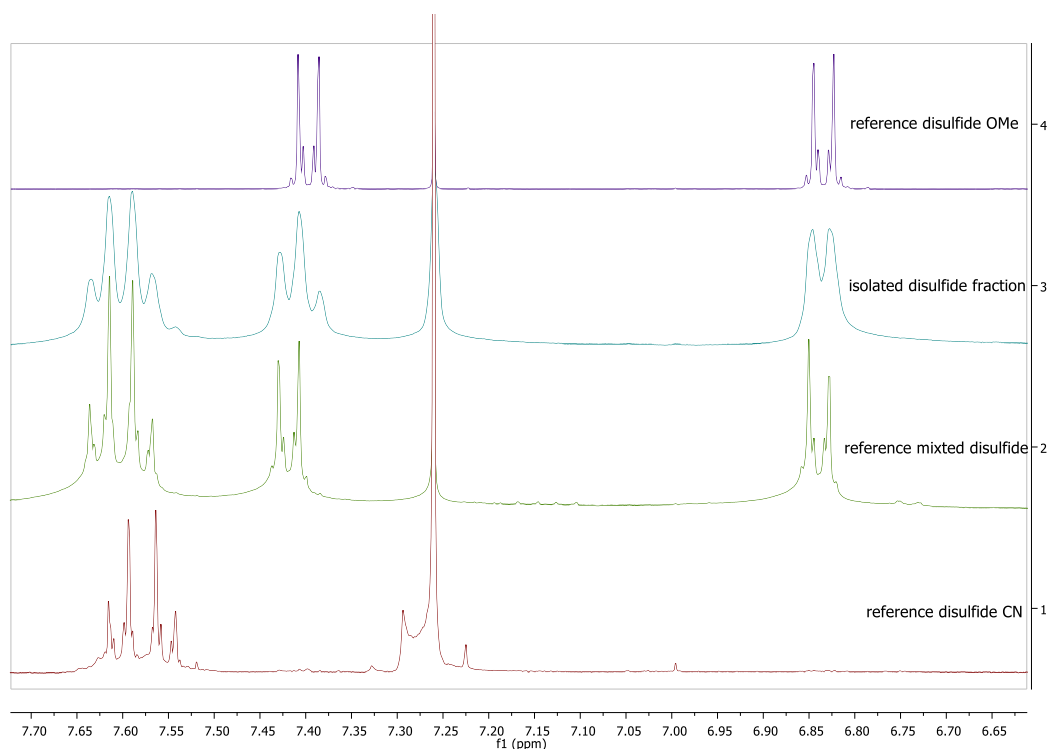
^1H NMR monitoring and analysis of the mixture



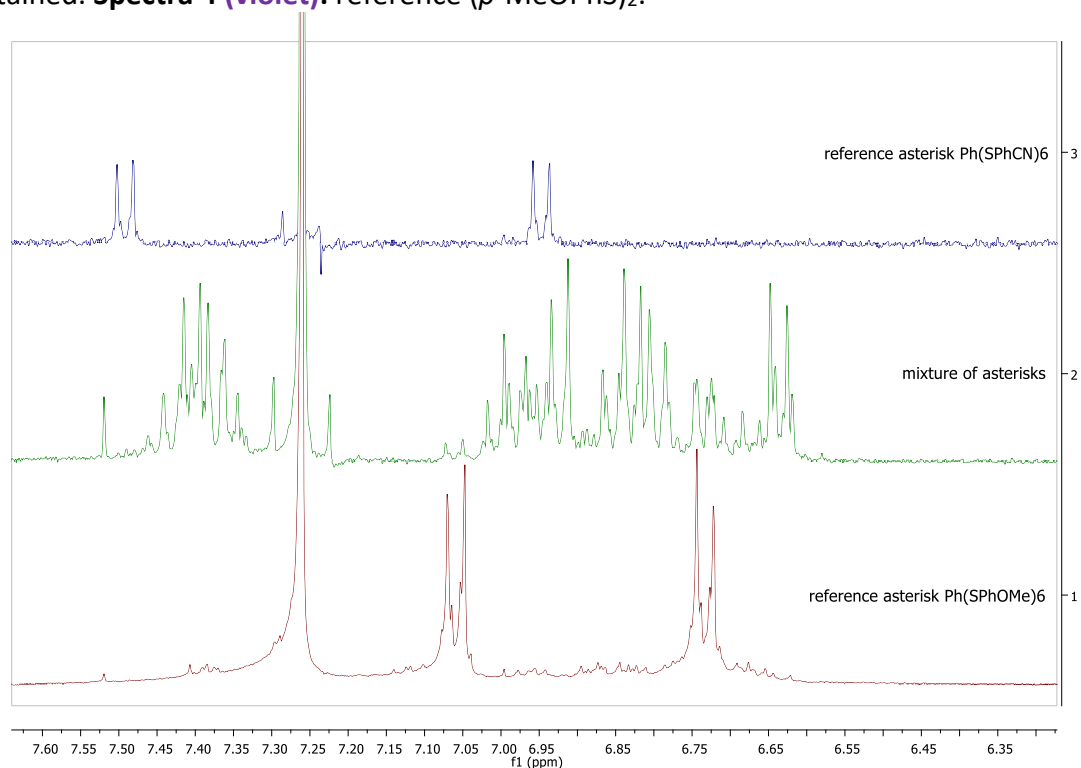
^1H NMR (CDCl_3 , 399.78 MHz) of the two reference hexathiobenzene asterisks (**blue**: $\text{Ph}(\text{SPhCN})_6$ and **red**: $\text{Ph}(\text{SPhOMe})_6$) and the crude mixture (**green**: middle spectrum) after 16 hrs at 25–28°C. **Conclusion:** the starting asterisk $\text{Ph}(\text{SPhCN})_6$ fully reacted after 16 hrs at 25–28°C.



^1H NMR (CDCl_3 , 399.78 MHz). Above: crude mixture after 16 hrs at room temperature. Below: two reference disulfides superimposed. The presence of the mixed disulfides proves that some thiol exchange reactions occurred.

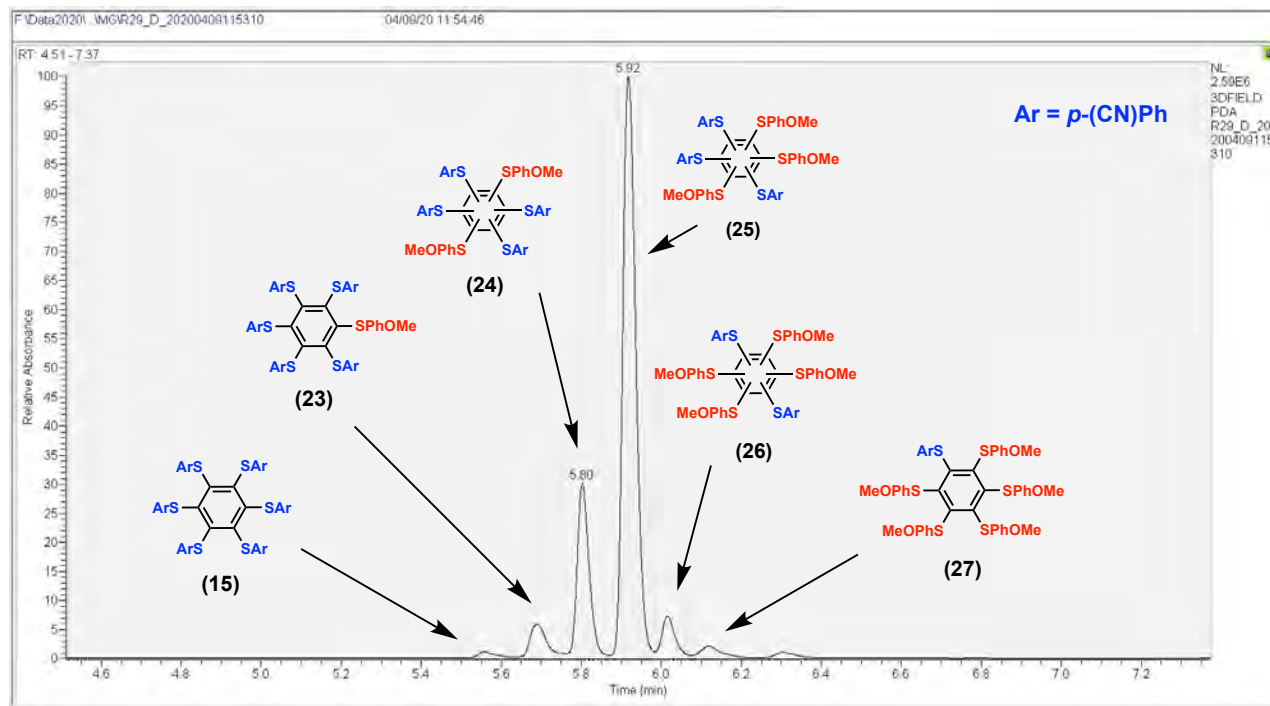


¹H NMR (CDCl₃, 399.78 MHz). **Spectra 1 (red):** reference (*p*-CNPhS)₂. **Spectra 2 (green):** reference mixed disulfide (*p*-CNPhS-*p*-MeOPh). **Spectra 3 (blue):** one of the column fraction containing a mixture of disulfides (less polar fractions) from a comparison to reference spectra of symmetrical and mixed disulfides. The presence of *p*-CNPhS-*p*-MeOPh and (*p*-MeOPhS)₂ can be clearly ascertained. **Spectra 4 (violet):** reference (*p*-MeOPhS)₂.



¹H NMR (CDCl₃, 399.78 MHz) **Spectrum 1 (red):** reference Ph(SPhOMe)₆. **Spectrum 2 (green):** one of the column fraction containing a mixture of mixed asterisks. The column fraction might contain a small amount of Ph(PhOMe)₆ and several mixed asterisks. No starting material could be found in any column fractions. **Spectrum 3 (blue):** reference Ph(SPhCN)₆.

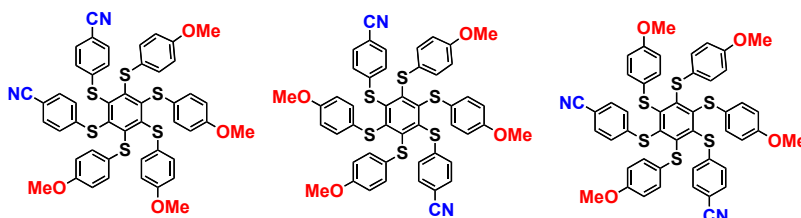
LC-HRMS analysis of the crude mixture



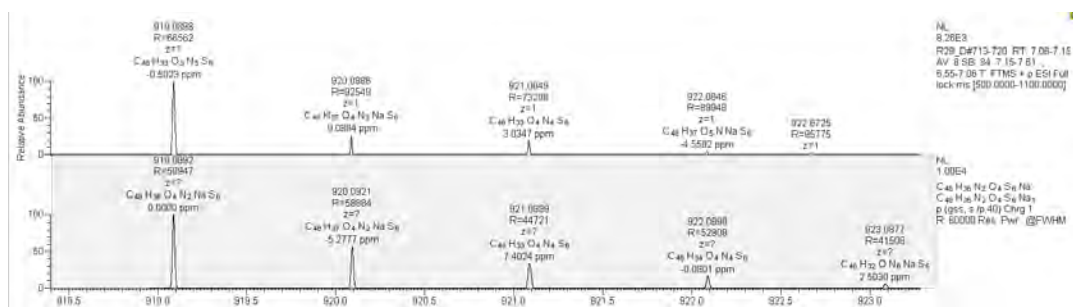
LC-Chromatogram (R-29)

4 Substitutions with *p*-MeOPhSH:

HRMS (ESI+) calculated for $[C_{48}H_{36}O_4N_2+Na^+]$: 919.0892 Da, found $[M+Na^+]$ 919.0898 m/z;
Possible isomers:



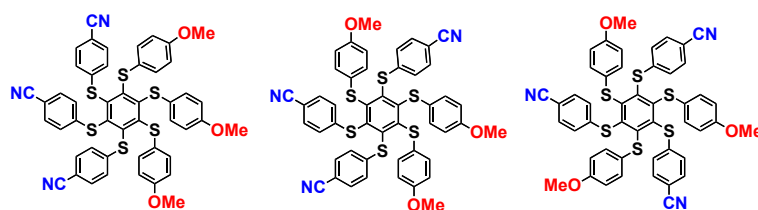
4 substitutions of *p*-MeOPhSH ($C_{48}H_{36}O_4N_2NaS_6$)



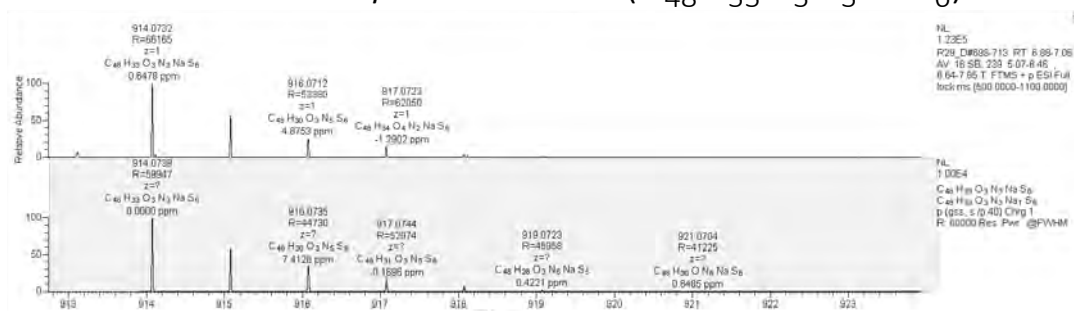
3 Substitutions with *p*-MeOPhSH:

HRMS (ESI+) calculated for $[C_{48}H_{33}O_3N_3+Na^+]$: 914.0738 Da, found $[M+Na^+]$ 914.0732 m/z

Possible isomers:



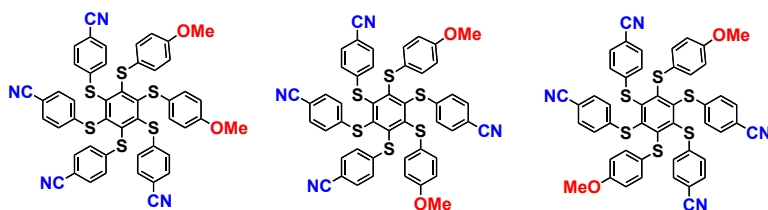
3 substitutions of *p*-MeOPhSH ($C_{48}H_{33}O_3N_3NaS_6$)



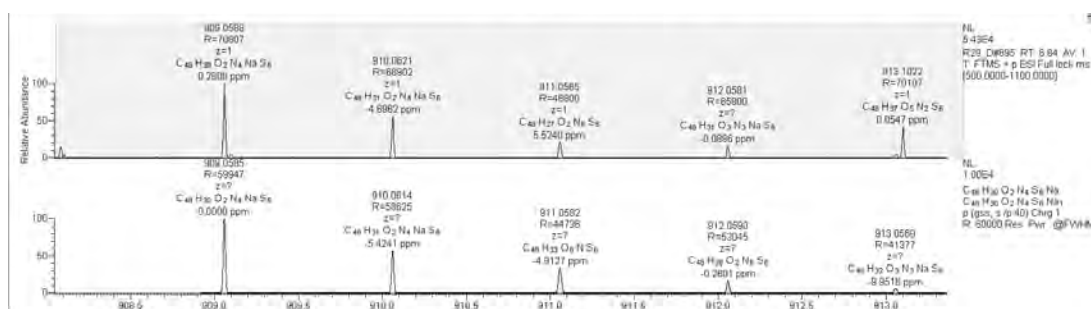
2 Substitutions with *p*-MeOPhSH:

HRMS (ESI+) calculated for $[C_{48}H_{33}O_2N_4+Na^+]$: 909.0585 Da, found $[M+Na^+]$ 909.0588 m/z.

Possible isomers:

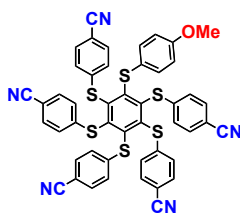


2 substitutions of *p*-MeOPhSH ($C_{48}H_{30}O_2N_4NaS_6$)

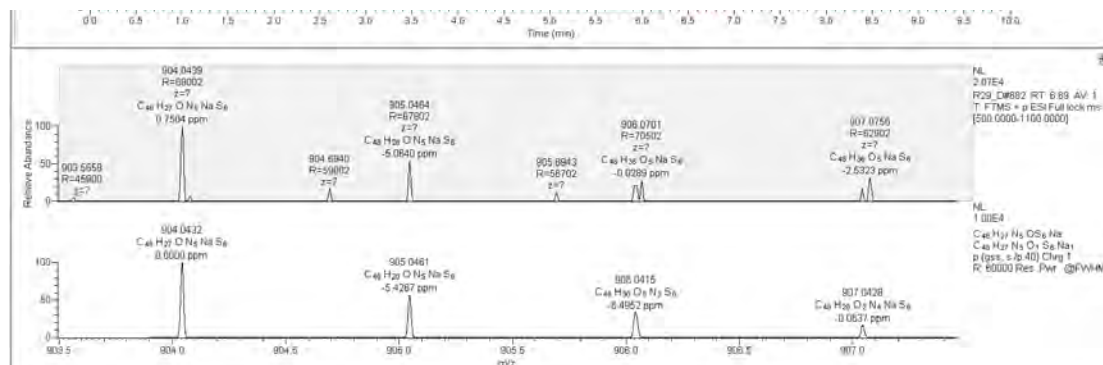


1 Substitution with *p*-MeOPhSH:

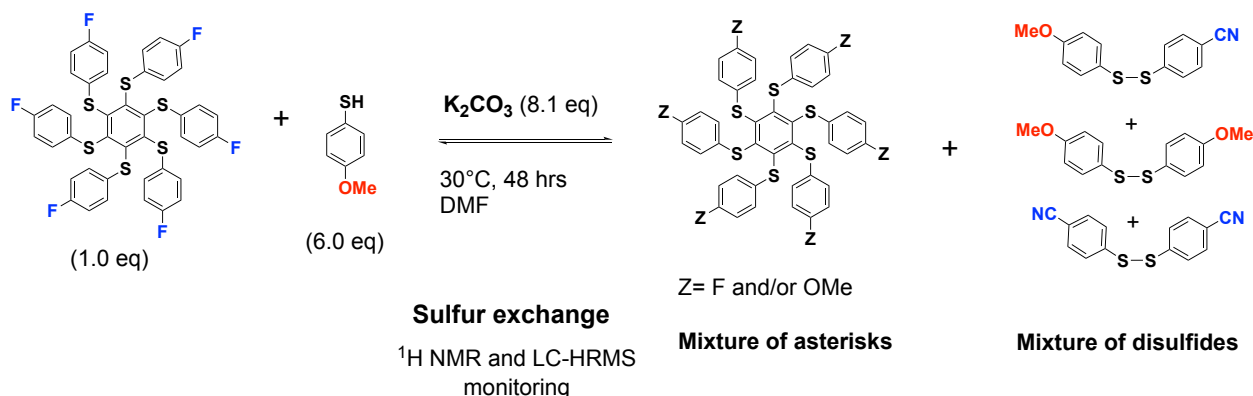
HRMS (ESI+) calculated for $[C_{48}H_{33}O_1N_5+Na^+]$: 904.0432 Da, found $[M+Na^+]$ 904.0439 m/z;



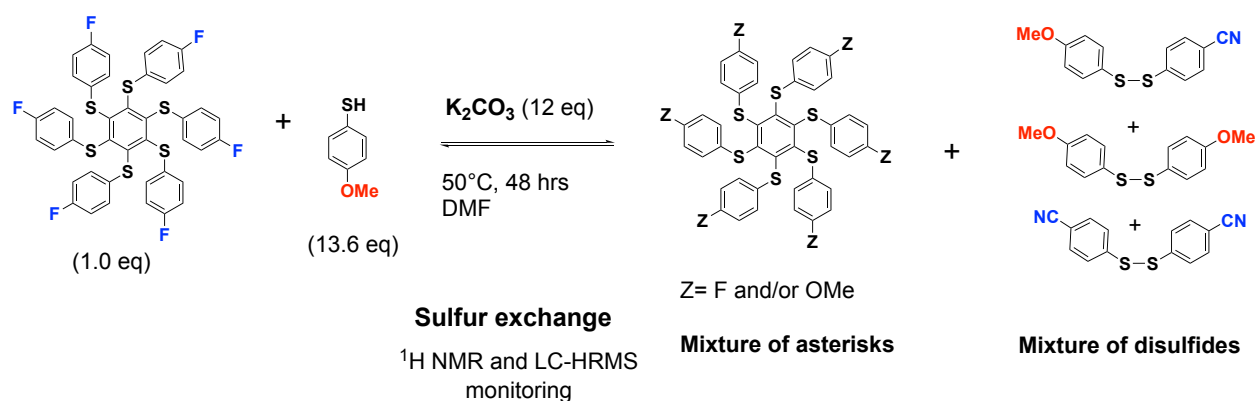
1 substitution of *p*-MeOPhSH ($C_{48}H_{27}ON_5NaS_6$)



SULFUR EXCHANGE REACTIONS WITH HEXAKIS(4-FLUOROPHENYLTHIO)BENZENE



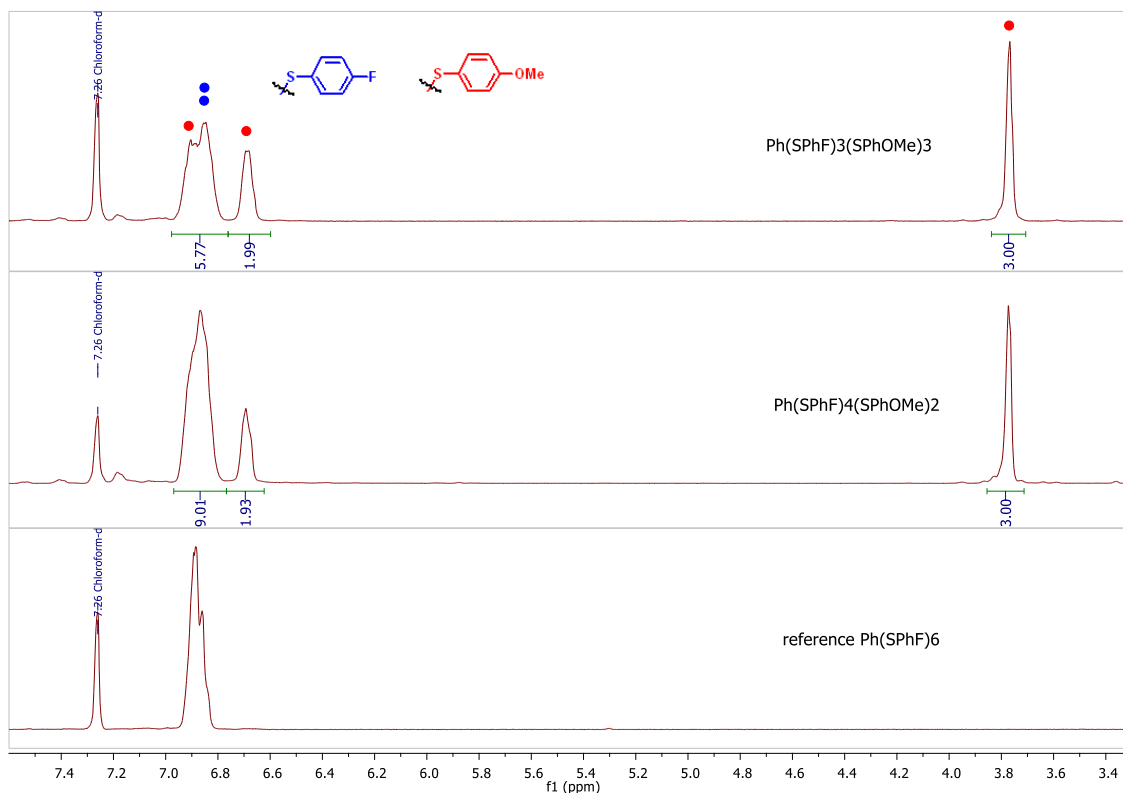
(R-66) Procedure. In an oven-dried tube, purged with argon, was added hexakis (4-fluorophenylthio)benzene (15.1 mg, 0.0181 mmol, 1.00 mol-eq.), dried potassium carbonate (20.3 mg, 0.0147 mmol, 8.12 mol-eq.) and 4-methoxythiophenol (15.1 mg, 0.108 mmol, 13.2 μ L, 5.97 mol-eq) in dry DMF (0.6 mL, dried and kept over 3Å molecular sieves). Argon was bubbled through the mixture for 5-10 min.. The tube was sealed and the reaction was vigorously stirred at 30°C (water bath temperature) for 43 hrs. The reaction was monitored by TLC (SiO_2 , 50% and 80% tol/cyclohex). After 43 hrs, 4 spots were observed under UV-vis lamp on TLC plates (eluent: 50% and 80% tol/cyclohex). To the reaction mixture was added toluene (20 mL) and water (20 mL). The organic phase was kept and further washed with H_2O (3×20 mL) for removing DMF. It was dried over anhydrous $MgSO_4$, filtered and evaporated. The crude product was analyzed. The components of the mixture were separated by column chromatography over SiO_2 by using an increasing polarity of eluent from 10% toluene in cyclohexane (v/v) to 100% toluene.



(R-74) Procedure. In an oven-dried tube, purged with argon, was added hexakis (4-fluorophenylthio)benzene (10.0 mg, 0.0119 mmol, 1.00 mol-eq.), dried potassium carbonate (20.0 mg, 0.0144 mmol, 12 mol-eq.) and 4-methoxythiophenol (22.8 mg, 0.163 mmol, 20 μ L, 13.6 mol-eq) in dry DMF (0.25 mL, dried and kept over 3 \AA molecular sieves). Argon was bubbled through the mixture for 5-10 min.. The tube was sealed and the reaction was vigorously stirred at 50°C for 48 hrs. The reaction was monitored by TLC (SiO₂, 50% and 80% tol/cyclohex). After 48 hrs 7 spots were observed under UV-vis lamp (eluent: 80% tol/cyclohex). To the reaction mixture was added toluene (20 mL) and water (20 mL). The organic phase was kept and further washed with H₂O (3 \times 20 mL) for removing DMF. It was dried over anhydrous MgSO₄, filtered and evaporated. The crude product was analyzed. Mass obtained: 8.6 mg. The components of the mixture were separated by column chromatography over SiO₂ by using an increasing polarity of eluent from 10% toluene in cyclohexane (v/v) to 100% toluene.

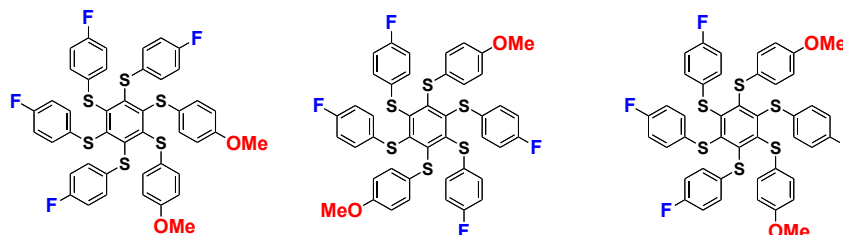
¹H NMR monitoring and analysis of the mixture

Although no mixed disulfide could be isolated from this reaction, the starting hexakis(4-fluorophenylthio)benzene was consumed and two mixed asterisks were isolated. A tentative structural assignment is proposed from the NMR integration area in the aromatic region as well as in the aliphatic region. The low resolution does not allow to ascertain the number of regioisomers per fraction nor the symmetry of the molecules. In short, we observed two and three substitutions with *p*-MeOPhSH:



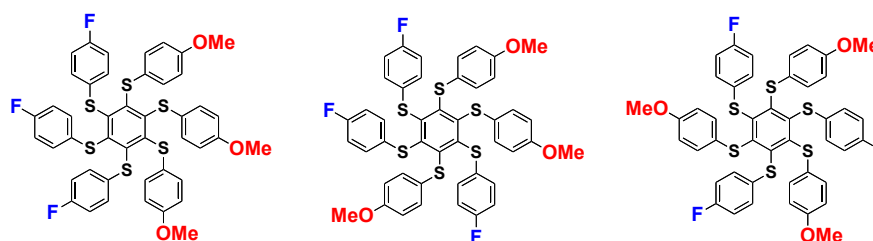
2 substitutions of *p*-MeOPhSH

Possible regioisomers:



3 substitutions of *p*-MeOPhSH

Possible regioisomers:

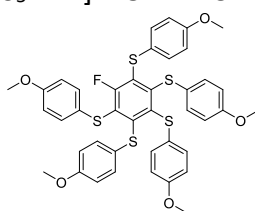


LC-HRMS analysis of the crude mixture

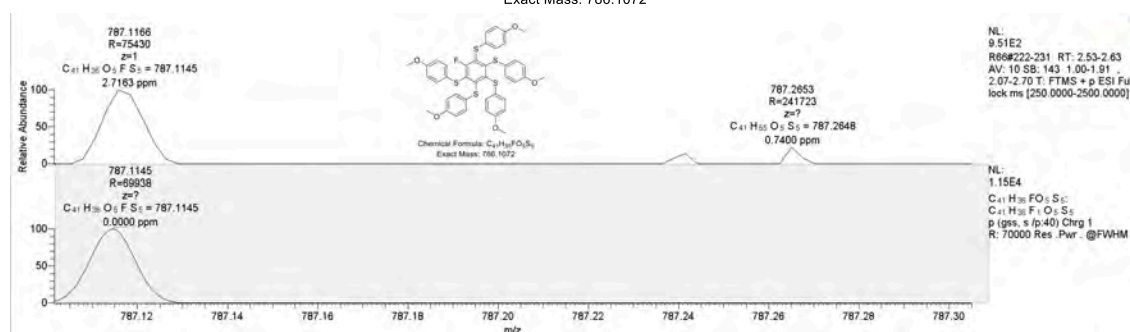
R-66 Sulfur exchanges at 30°C with *p*-OMePhSH:
LC-Chromatogram

5 Substitutions with *p*-MeOPhSH:

HRMS (ESI+) calculated for [C₄₁H₃₅O₅FS₅ + H⁺]: 787.1145 Da, found [M+H⁺] 787.1166 m/z;



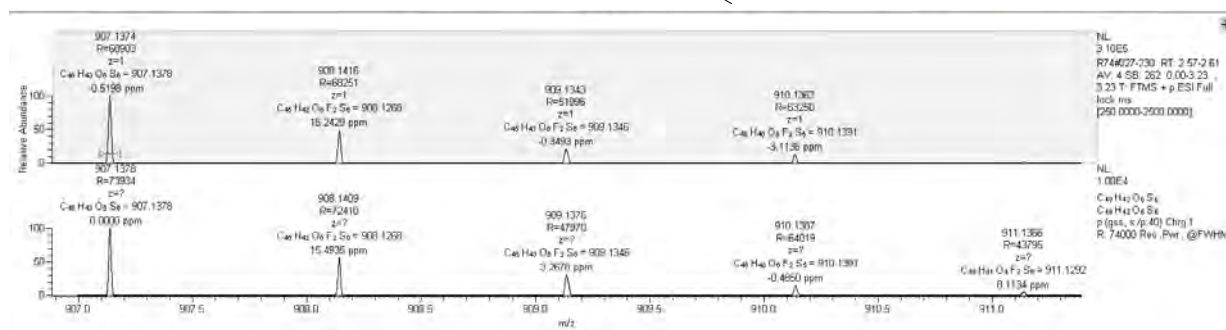
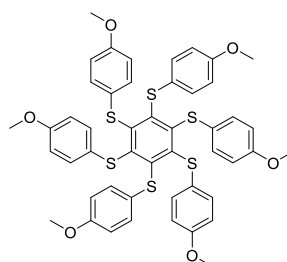
Chemical Formula: C₄₁H₃₅FO₅S₅
Exact Mass: 786.1072



R-74 Sulfur exchanges at 50°C :
LC-Chromatogram

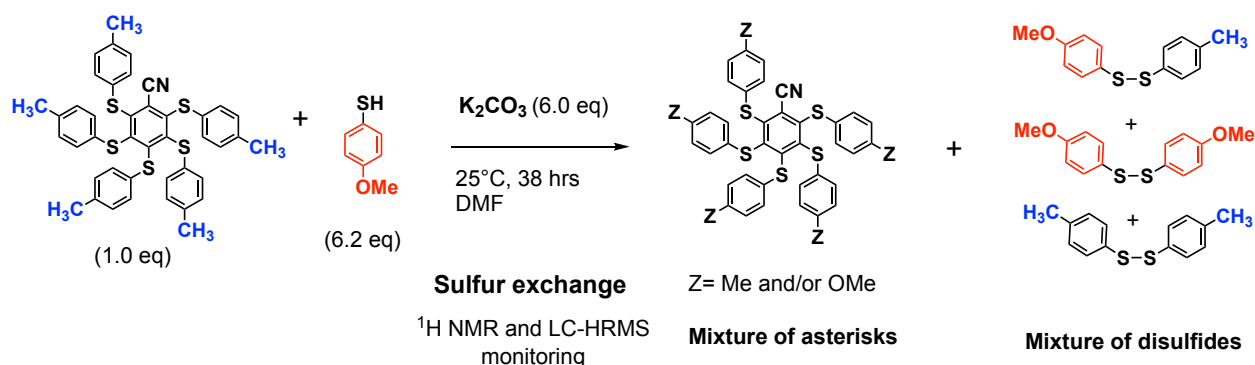
6 Substitutions with *p*-MeOPhSH:

HRMS (ESI+) calculated for [C₄₈H₄₂O₆S₆ + H⁺]: 907,1378 Da, found [M+H⁺] 907,1374 m/z;



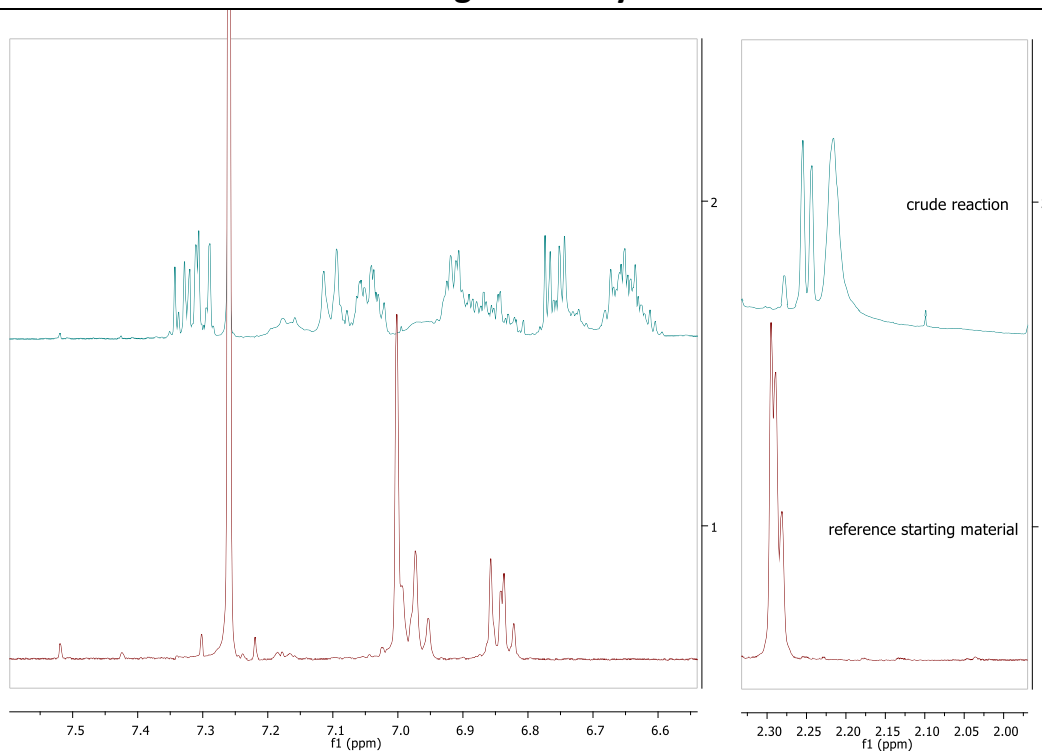
4.0 Sulfur exchange reactions on penta(thio) benzene asterisks

SULFUR EXCHANGE REACTIONS WITH 1-CYANO-2,3,4,5,6-PENTAKIS(4-PHENYLTHIO) BENZENE



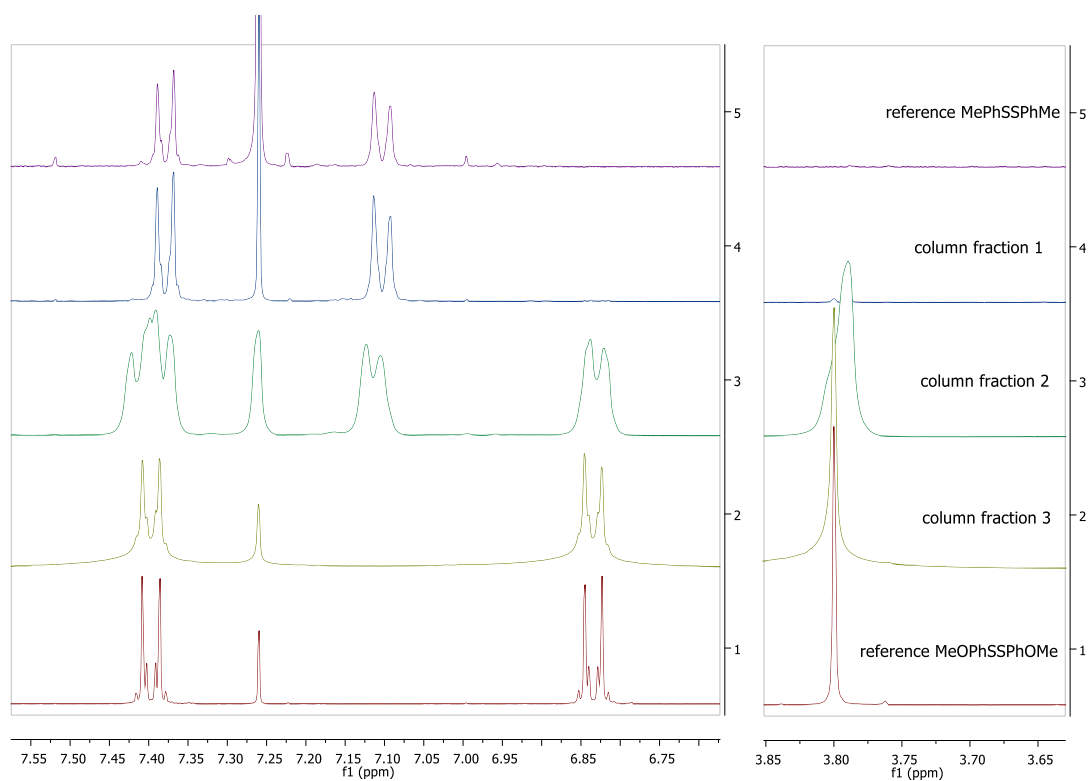
(R-37) Procedure. In an oven-dried tube, purged with argon, was added 1-cyano-2,3,4,5,6-pentakis(4-phenylthio)benzene (40.9 mg, 0.0573 mmol, 1.00 mol-eq.), dried potassium carbonate (47.9 mg, 0.346 mmol, 6.03 mol-eq.) and 4-methoxybenzenethiol (49 mg, 0.35mmol, 43 μ L, 6.2 mol-eq.) in dry DMF (0.5 mL dried with molecular sieves 3 Å). Argon was bubbled through the mixture for 5-10 min.. The tube was sealed and the reaction was vigorously stirred at 25°C for 38 hrs. Six TLC spots (SiO₂, eluent: tol/cyclohex. 80:20 v/v) were observed by UV-vis. The three less polar spots correspond to disulfides. The fourth yellow spot which was slightly more polar, and other polar spots, correspond to some asterisks. The mixture was taken up in toluene (10 mL) and water (10 mL). The organic phase was separated and further washed with water (4x10mL). The organic phase was dried over anhydrous MgSO₄, filtered and evaporated; mass of the crude mixture: 56.7 mg. Separation of the components in the crude mixture was achieved by column chromatography over silica gel, by using an increasing polarity of the eluent, starting from 30% toluene/70% cyclohexane to 100% toluene, and then to 5% EtOAc in toluene.

¹H NMR monitoring and analysis of the mixture



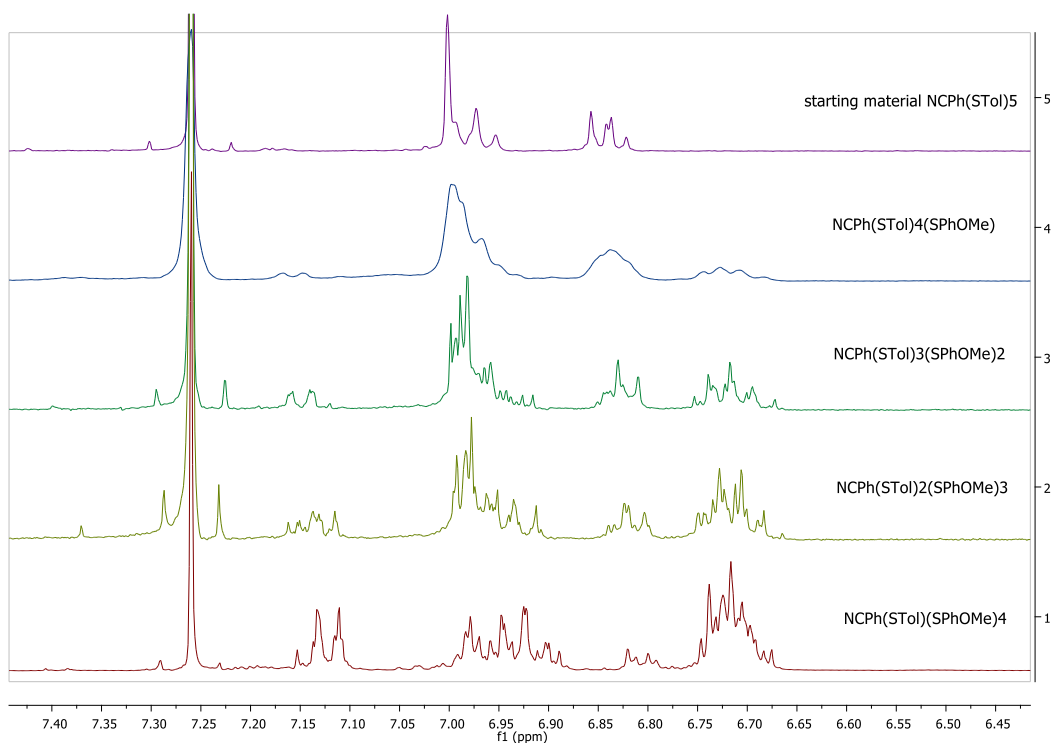
¹H-NMR (CDCl₃, 399.78 MHz). **Spectrum 1 (red):** reference 1-cyano-pentakis(4-phenylthio)benzene. **Spectrum 2 (blue):** crude reaction mixture; all the starting material was

consumed after 38 hrs at 25°C. However, the presence of DMF in the crude mixture might induce some chemical shifts.



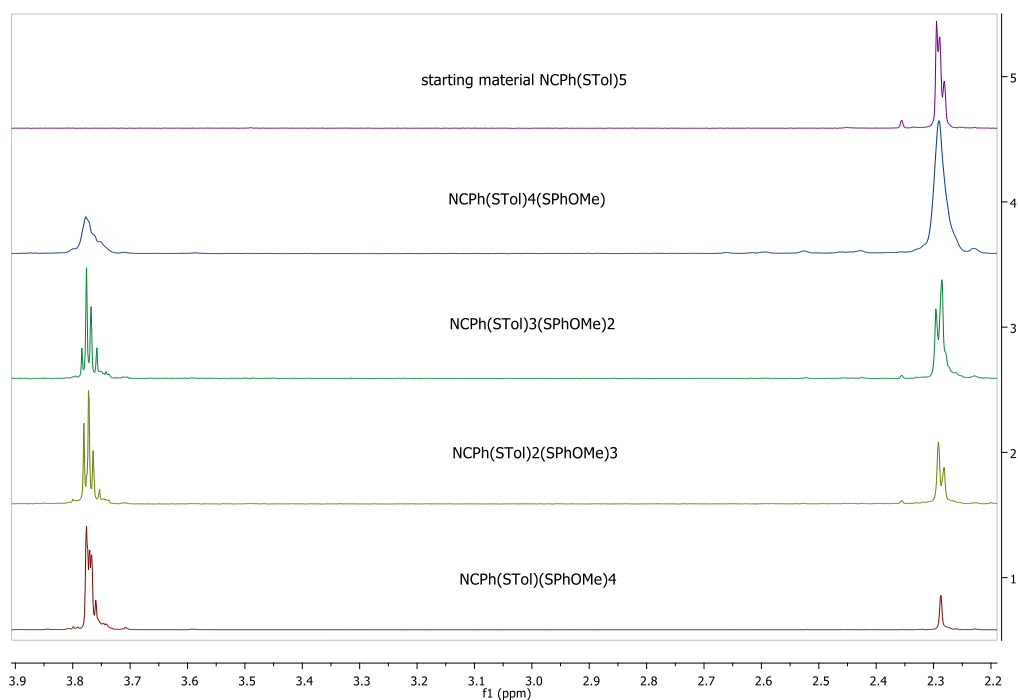
¹H NMR (CDCl₃, 399.78 MHz). **Spectrum 1 (red)**: reference disulfide (*p*-MeOPhS)₂. **Spectrum 2 (brown)**: column fraction 3 (more polar). **Spectrum 3 (green)**: column fraction 3 corresponds to the unsymmetrical disulfide (*p*-MePhS)-(S-*p*-MeOPh). **Spectrum 4 (blue)**: column fraction 4. **Spectrum 5 (violet)**: reference disulfide (*p*-MePhS)₂. The first three fractions correspond to the disulfides. The first fraction contains only symmetrical (*p*-MePhS)₂ while the third one contains only the symmetrical (*p*-MeOPhS)₂. The second fraction corresponds to the mixed disulfide (*p*-MePhS)-(S-*p*-MeOPh) with some symmetrical (*p*-MeOPhS)₂ as can be seen, thanks to the shoulder of the methoxy signal (CH₃O).

Conclusion: The presence of the mixed disulfide (*p*-MePhS)-(S-*p*-MeOPh) as well as the symmetrical (*p*-MePhS)₂ disulfide demonstrates the exchange of sulfur substituents on the starting material 1-cyano-pentakis(4-phenylthio)benzene at 25°C.



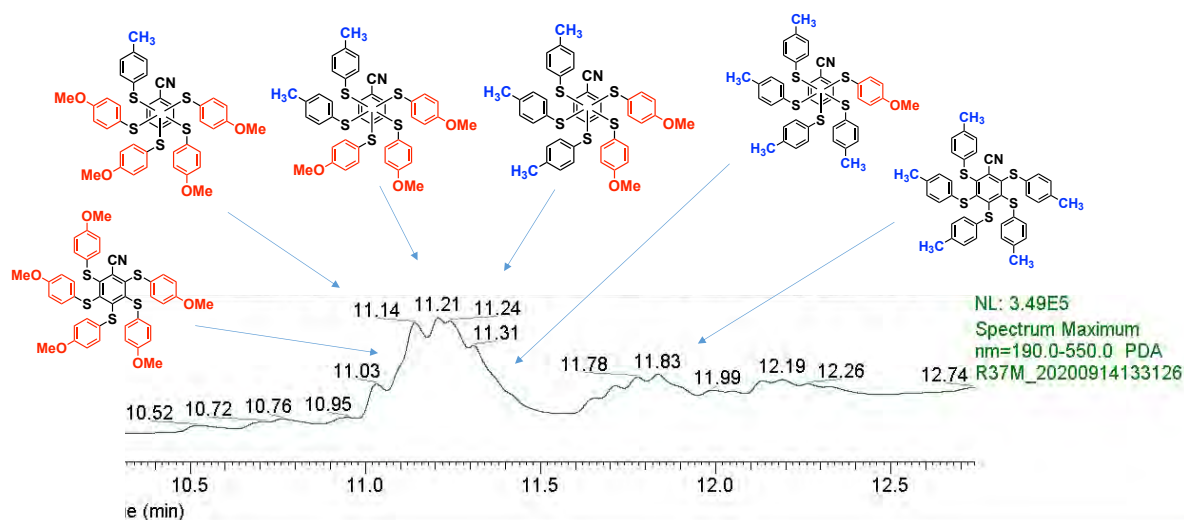
¹H-NMR (CDCl₃, 399.78 MHz). ¹H-NMR spectra of the aromatic region of many isolated fractions indicated a complex mixture of asterisks incorporating various number of SPhOMe substituents. **Spectrum 1 (red)**: four SPhOMe substituents. **Spectrum 2 (yellow-green)**: three SPhOMe substituents. **Spectrum 3 (green)**: two SPhOMe substituents. **Spectrum 4 (blue)**: one SPhOMe substituent. **Spectrum 5 (violet)**: starting 1-cyano-pentakis(4-phenylthio)benzene.

Conclusion: even though the exact isomeric structure of some asterisk compounds cannot be proposed with certainty, these spectra clearly and unambiguously demonstrate sulfur exchange reactions occurring with starting 1-cyano-pentakis(4-phenylthio)benzene at 25°C leading to a library of asterisks containing various ratio of SPhOMe substituents.



¹H-NMR (CDCl₃, 399.78 MHz). ¹H-NMR of the methyl and methoxy groups of different isolated fractions. The assignment is attempted thanks to the relative integration of these ¹H NMR signals. **Conclusion:** even though the exact isomeric structure of some asterisk compounds cannot be proposed with certainty, these spectra clearly and unambiguously demonstrate sulfur ligands exchange reactions occurring with starting 1-cyano-pentakis(4-phenylthio)benzene at 25°C as a penta(thio) benzene asterisk.

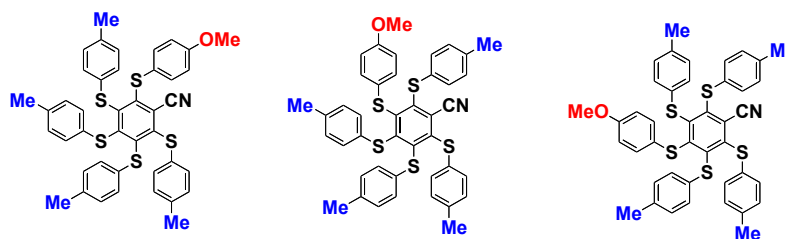
LC-HRMS analysis of the crude mixture



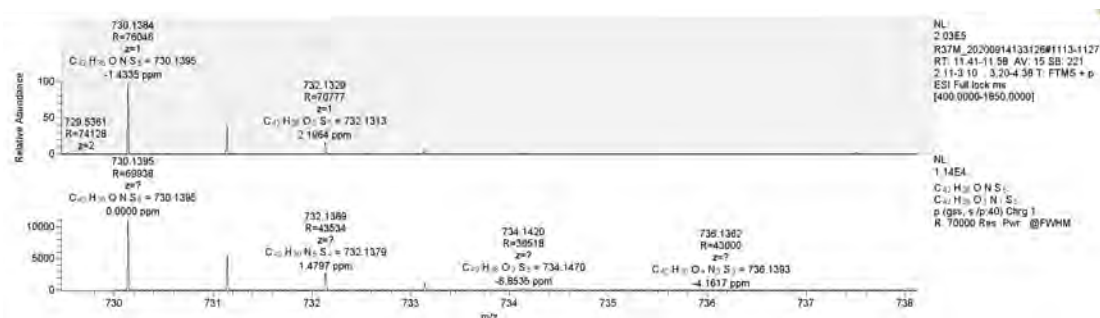
LC-Chromatogram of the crude (R-37)

1 Substitution with *p*-MeOPhSH:

HRMS (ESI+) calculated for [C₄₂H₃₅ONS₅ + H⁺]: 730.1395 Da, found [M+H⁺] 730.1384 m/z;
Possible isomers:



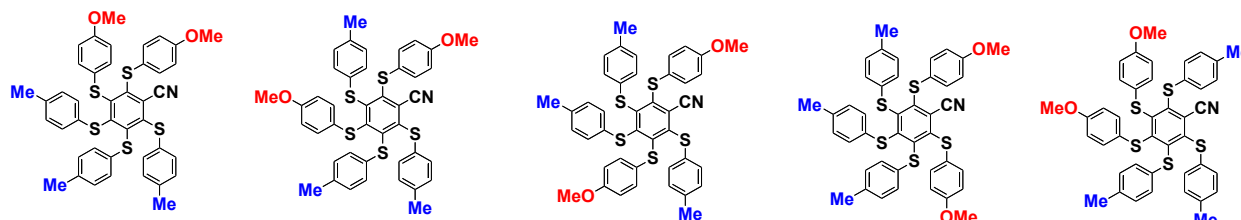
1 substitution by *p*-MeOPhSH (C₄₂H₃₆ONS₅)



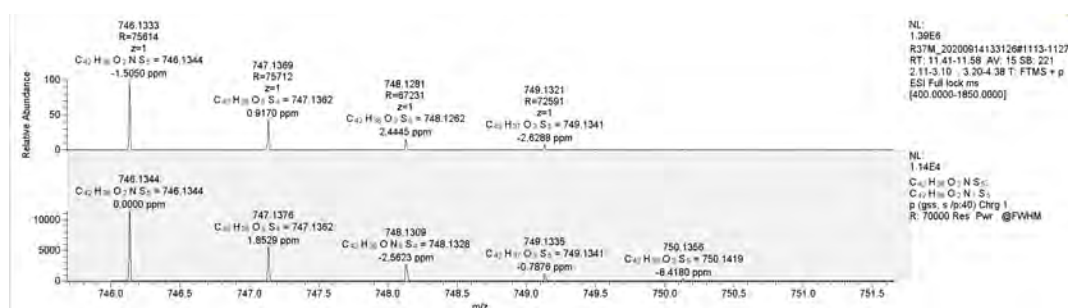
2 Substitutions with *p*-MeOPhSH:

HRMS (ESI+) calculated for $[C_{42}H_{35}O_2NS_5 + H^+]$: 746.1344 Da, found $[M+H^+]$ 746.1333 m/z;

Possible isomers:



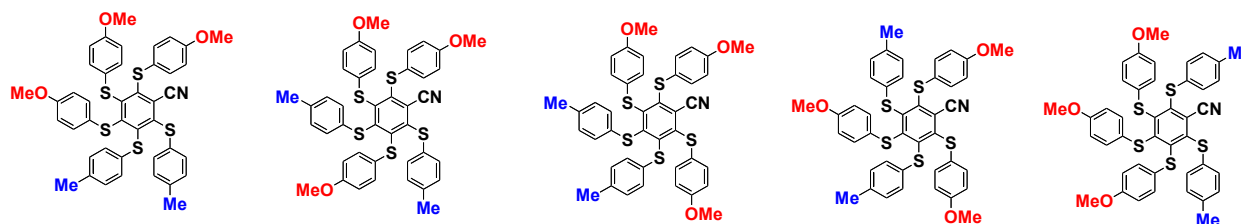
2 substitutions by *p*-MeOPhSH ($C_{42}H_{36}O_2NS_5$)



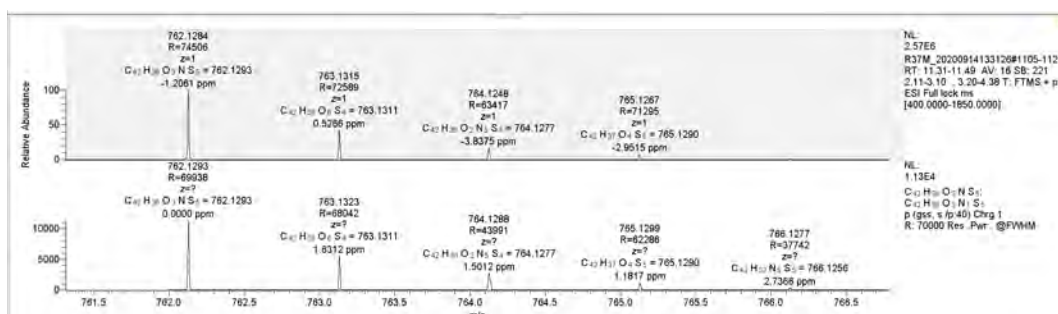
3 Substitutions with *p*-MeOPhSH:

HRMS (ESI+) calculated for $[C_{42}H_{35}O_3NS_5 + H^+]$: 762.1293 Da, found $[M+H^+]$ 762.1284 m/z;

Possible isomers:

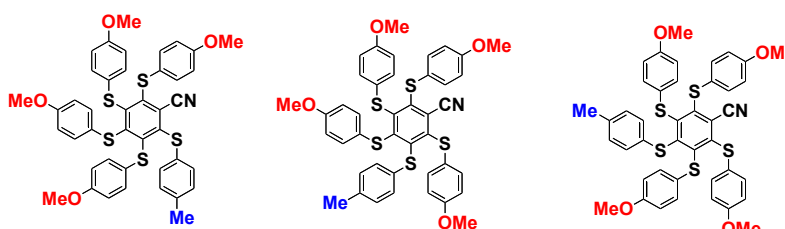


3 substitutions by *p*-MeOPhSH ($C_{42}H_{36}O_3NS_5$)

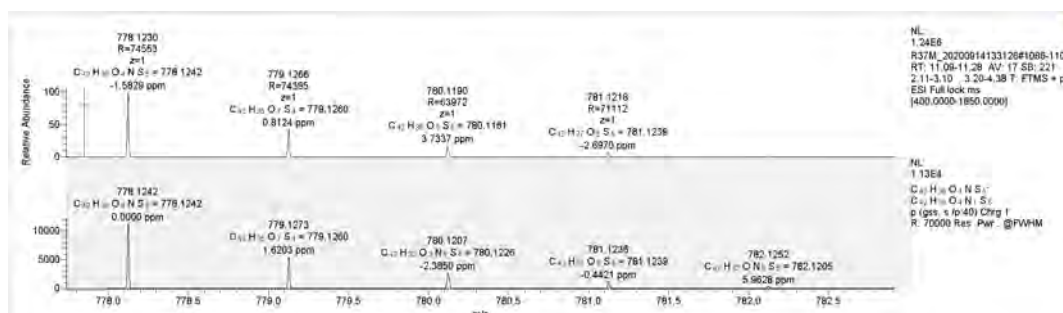


4 Substitutions with *p*-MeOPhSH:

HRMS (ESI+) calculated for $[C_{42}H_{35}O_4NS_5 + H^+]$: 778.1242 Da, found $[M+H^+]$ 778.1230 m/z;
Possible isomers:

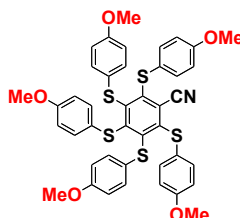


4 substitutions by *p*-MeOPhSH ($C_{42}H_{36}O_4NS_5$)

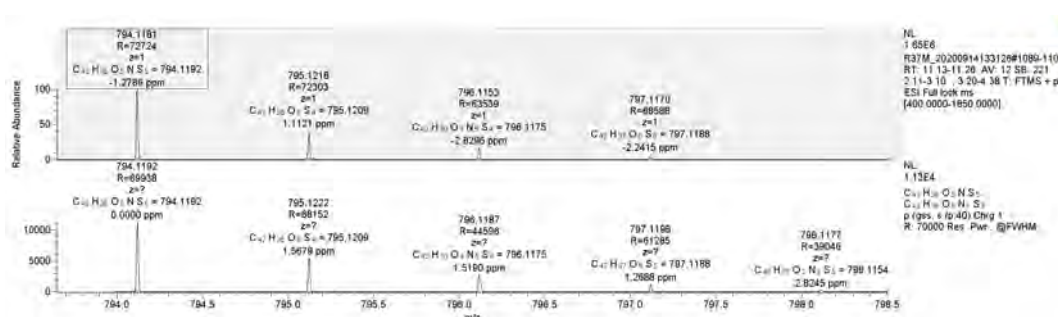


5 Substitutions with *p*-MeOPhSH:

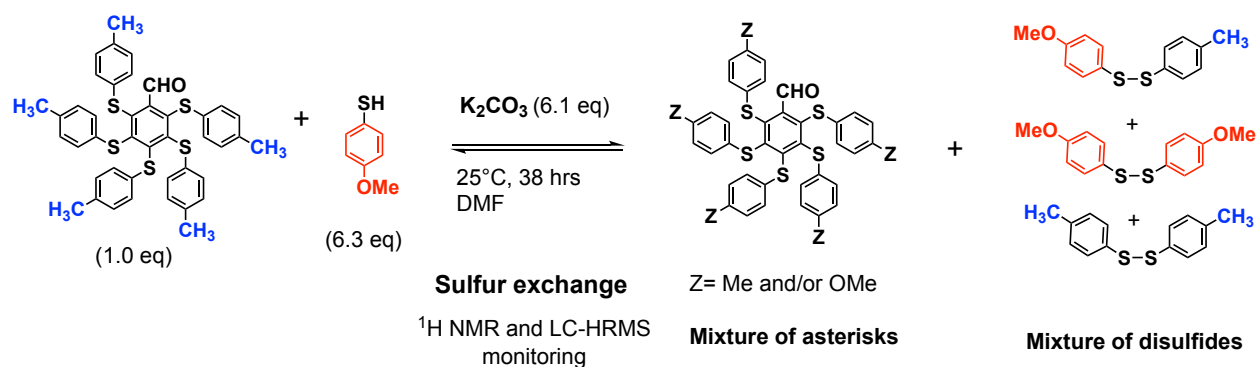
HRMS (ESI+) calculated for $[C_{42}H_{35}O_5NS_5 + H^+]$: 794.1192 Da, found $[M+H^+]$ 794.1181 m/z;
Possible isomers:



5 substitutions by *p*-MeOPhSH ($C_{42}H_{36}O_5NS_5$)



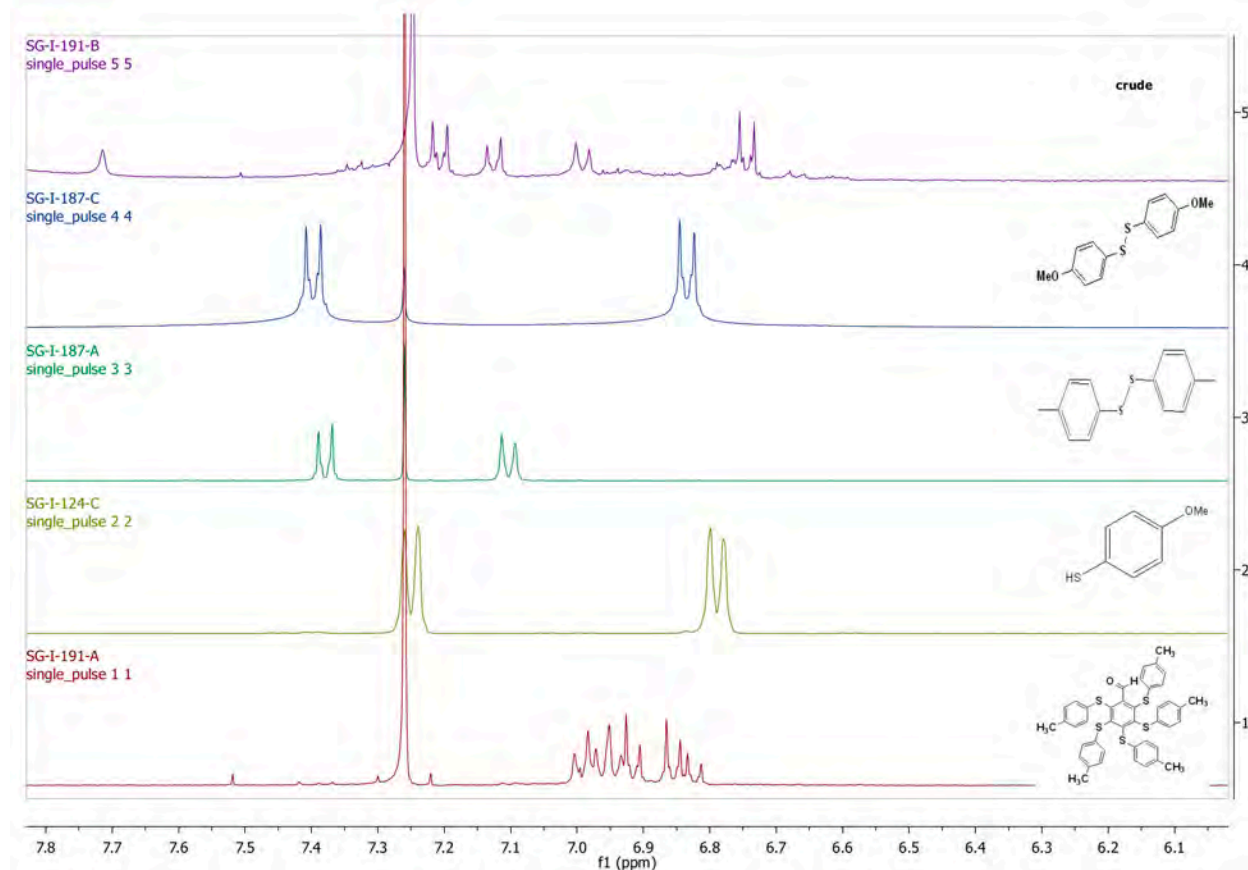
SULFUR EXCHANGE REACTIONS WITH PENTAKIS (4-METHYL-PHENYLTHIO) BENZALDEHYDE



(R-38) Procedure. In an oven-dried tube, purged with argon, was added pentakis(4-methylphenylthio)benzaldehyde (40.0 mg, 0.0558 mmol, 1.00 mol-eq.), dried potassium carbonate (46.9 mg, 0.340 mmol, 6.09 mol-eq.) and 4-methoxythiophenol (49.0 mg, 0.349 mmol, 43 μL , 6.3 mol-eq.) in dry DMF (0.5 mL, dried and kept over activated 3 \AA molecular sieves). Argon was bubbled through the mixture for 5-10 min.. The tube was sealed and the reaction was vigorously stirred at 25 $^\circ\text{C}$ for 38 hrs. The consistency of the original mixture changed quickly over time. The mixture was taken up in toluene (10 mL) and water (10 mL). The organic phase was separated and further washed with water (3 \times 10 mL). The organic phase was dried over anhydrous MgSO_4 , filtered and evaporated; mass of the crude product: 60.9 mg.

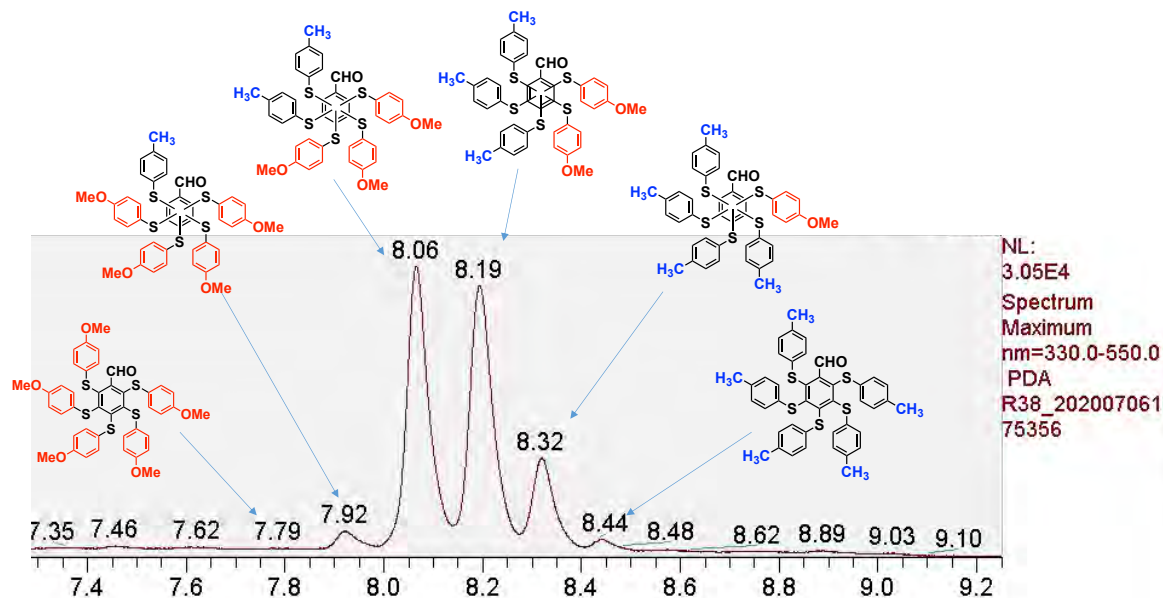
NMR results: ^1H NMR (399.78 MHz, CDCl_3 , **SG-I-191-B**) indicates many exchanges of ligands at 25 $^\circ\text{C}$ in DMF. A mixture of asterisks containing OMe and Me groups was formed.

Reference NMR: ^1H NMR (**SG-I-191-A**): ^{13}C NMR (**SG-I-191-C**)



$^1\text{H-NMR}$ (CDCl_3 , 399.78 MHz)

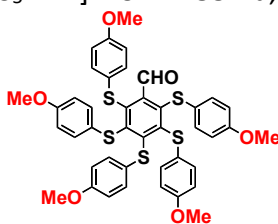
LC-HRMS analysis of the crude mixture



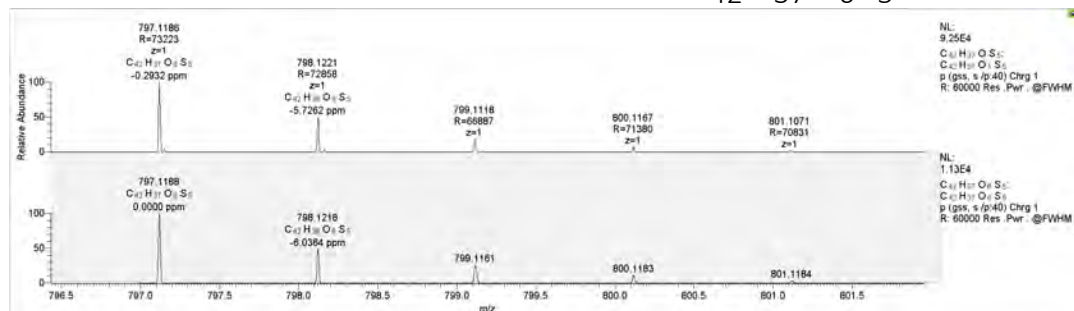
LC-Chromatogram (R-38)

5 Substitutions:

HRMS (ESI+) calculated for $[\text{C}_{42}\text{H}_{36}\text{O}_6\text{S}_5 + \text{H}^+]$: 797.1188 Da, found $[\text{M} + \text{H}^+]$ 797.1186 m/z;



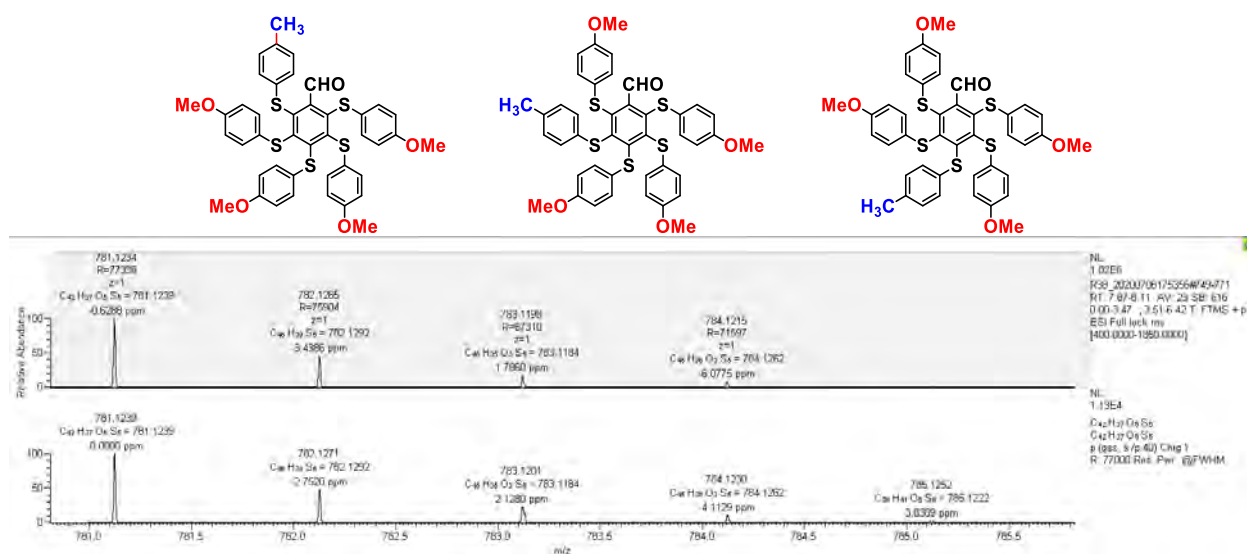
5 substitutions with *p*-MeOPhSH ($\text{C}_{42}\text{H}_{37}\text{O}_6\text{S}_5$)



4 substitutions :

HRMS (ESI+) calculated for $[\text{C}_{42}\text{H}_{36}\text{O}_5\text{S}_5 + \text{H}^+]$: 781.1239 Da, found $[\text{M} + \text{H}^+]$ 781.1234 m/z;

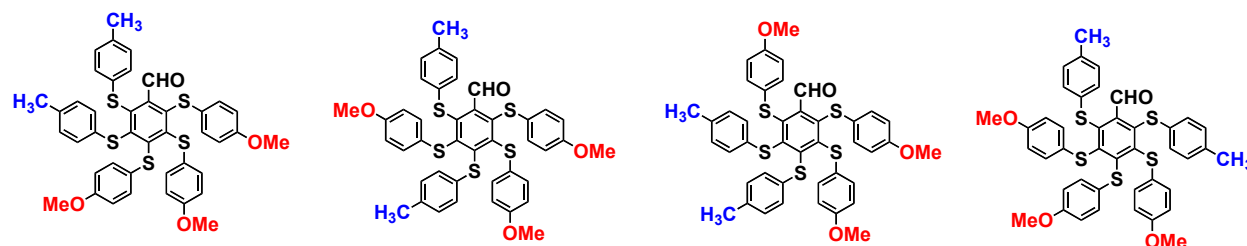
Possible isomers:



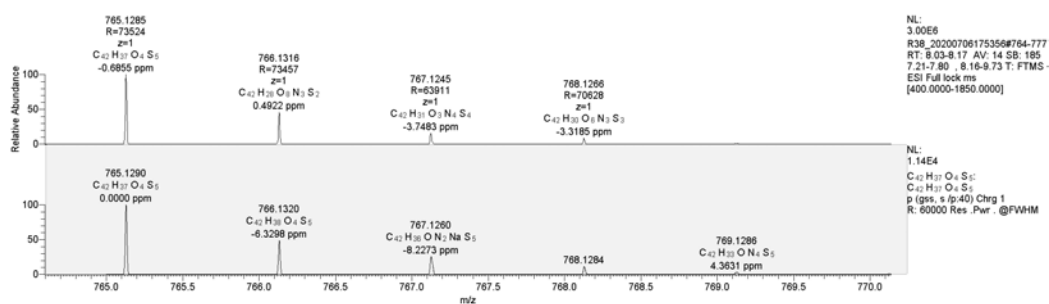
3 Substitutions:

HRMS (ESI+) calculated for $[C_{42}H_{36}O_4S_5 + H^+]$: 765.1290 Da, found $[M+H^+]$ 765.1285 m/z;

Possible isomers:



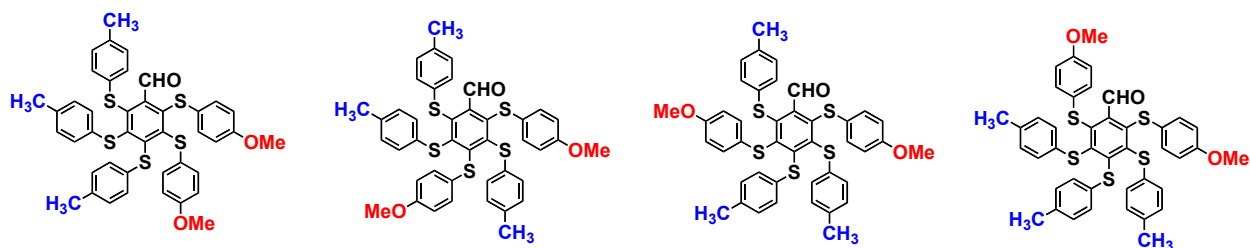
3 substitutions with *p*-MeOPhSH ($C_{42}H_{37}O_4S_5$)



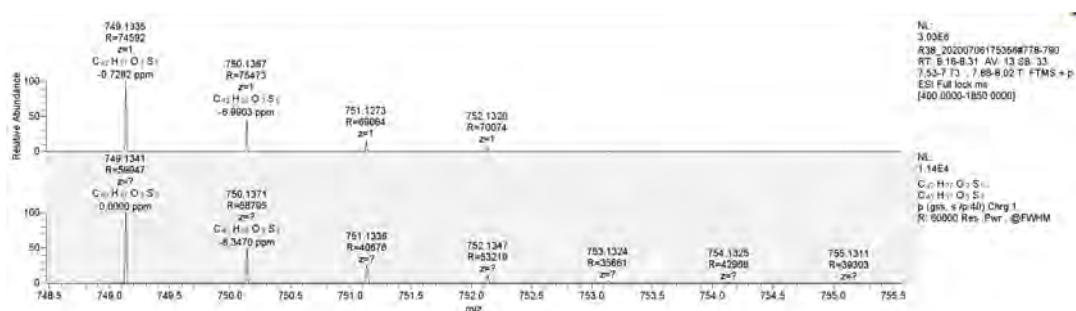
2 Substitutions:

HRMS (ESI+) calculated for $[C_{42}H_{36}O_3S_5 + H^+]$: 749.1341 Da, found $[M+H^+]$ 749.1335 m/z;

Possible isomers:

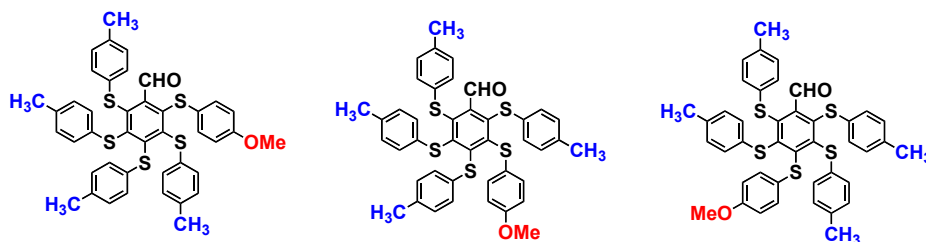


2 substitutions with *p*-MeOPhSH (C₄₂H₃₇O₃S₅)

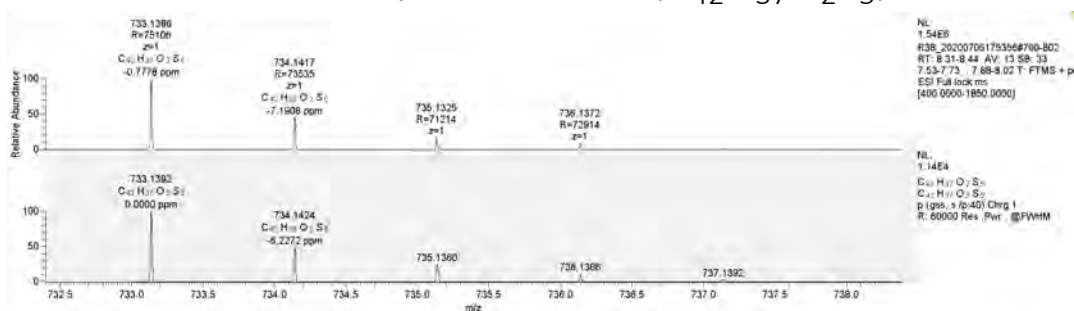


1 substitution:

HRMS (ESI+) calculated for [C₄₂H₃₆O₂S₅ + H⁺]: 733.1392 Da, found [M+H⁺] 733.1386 m/z;
Possible isomers:

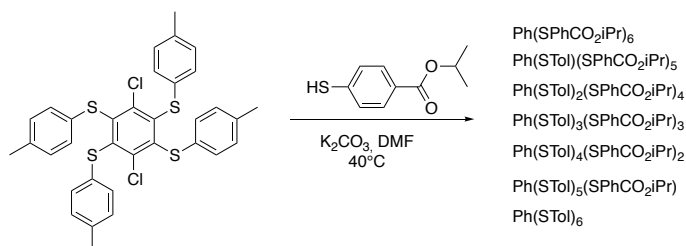


1 substitution with *p*-MeOPhSH (C₄₂H₃₇O₂S₅)



5.0 Sulfur exchange reactions on tetra(thio) benzene asterisks

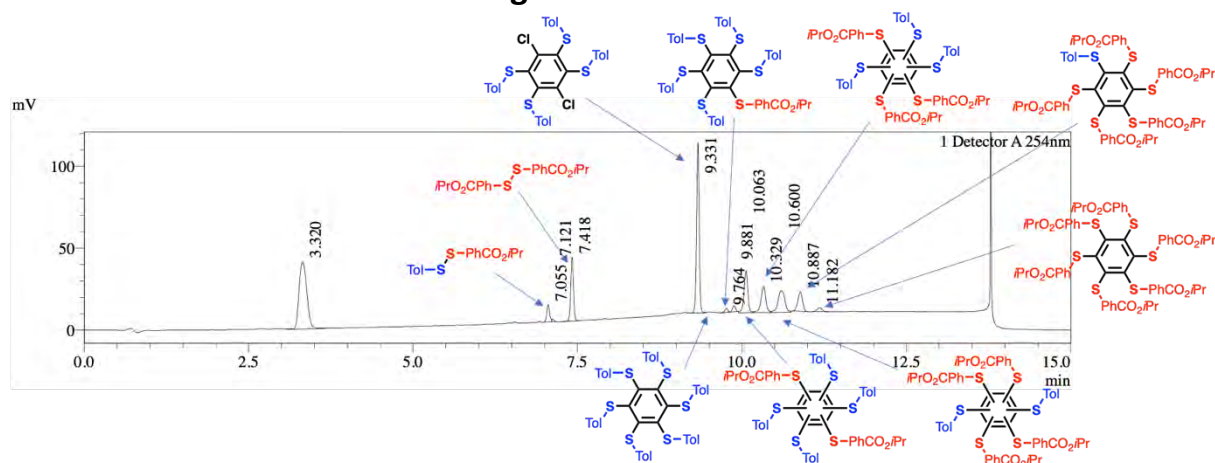
SULFUR EXCHANGE REACTIONS WITH 1,4-DICHOHO-2,3,5,6-TETRAKIS(4-METHYLPHENYLTHIO)BENZENE



MV-II-36 Procedure. In an oven-dried glass tube were placed 1,4-dichloro-2,3,5,6-tetrakis(4-methylphenylthio)benzene (112 mg, 0.176 mmol, 1.00 mol-eq.), isopropyl-4-mercaptobenzoate (73.0 mg, 0.372 mmol, 2.11 mol-eq.) and dry potassium carbonate (77.0 mg, 0.558 mmol, 3.17 mol-eq.) under an argon atmosphere. All reagents were freshly dried under vacuum for about 30 min prior to use them. Under argon, dry DMF (1.0 mL, kept over 3Å molecular sieves) was injected and argon was bubbled through the mixture for about 20 min.. The tube was sealed and the mixture was vigorously stirred at 40°C for 22 hrs. An aqueous HCl solution (1M, 100 mL) was added and it was extracted with toluene (3x25 mL). The combined organic phases were washed with water (5x25 mL), and dried over anhydrous MgSO_4 . After filtration and evaporation of solvents, a yellow-brown solid was obtained.

LC-MS analysis of the mixture

LC-Chromatogram of the crude mixture

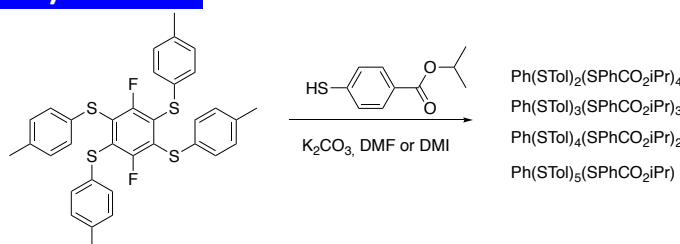


Retention Time	m/z	Formula	Structure	UV %
7.055	318	$[\text{M}]^+ = \text{C}_{17}\text{H}_{18}\text{O}_2\text{S}_2$	$\text{CH}_3\text{PhSSPhCO}_2i\text{Pr}$	N/A
7.418	390	$[\text{M}]^+ = \text{C}_{20}\text{H}_{22}\text{O}_4\text{S}_2$	$(\text{CO}_2i\text{PrPhS})_2$	N/A
9.331	635	$[\text{M}+\text{H}]^+ = \text{C}_{34}\text{H}_{28}\text{Cl}_2\text{S}_4$	$\text{PhCl}_2(\text{SPhCH}_3)_4$	44%
9.492	811	$[\text{M}+\text{H}]^+ = \text{C}_{48}\text{H}_{42}\text{S}_6$	$\text{Ph}(\text{SPhCH}_3)_6$	traces
9.764	883	$[\text{M}+\text{H}]^+ = \text{C}_{51}\text{H}_{46}\text{O}_2\text{S}_6$	$\text{Ph}(\text{SPhCH}_3)_5(\text{SPhCO}_2i\text{Pr})$	1%
10.063	955	$[\text{M}+\text{H}]^+ = \text{C}_{54}\text{H}_{50}\text{O}_4\text{S}_6$	$\text{Ph}(\text{SPhCH}_3)_4(\text{SPhCO}_2i\text{Pr})_2$	15%
10.329	1027	$[\text{M}+\text{H}]^+ = \text{C}_{57}\text{H}_{54}\text{O}_6\text{S}_6$	$\text{Ph}(\text{SPhCH}_3)_3(\text{SPhCO}_2i\text{Pr})_3$	12%
10.600	1099	$[\text{M}+\text{H}]^+ = \text{C}_{60}\text{H}_{58}\text{O}_8\text{S}_6$	$\text{Ph}(\text{SPhCH}_3)_2(\text{SPhCO}_2i\text{Pr})_4$	14%

10.887	1171	[M+H] ⁺ = C ₆₃ H ₆₂ O ₁₀ S ₆	Ph(SPhCH ₃) ₁ (SPhCO ₂ iPr) ₅	9%
11.182	1183	[M-OiPr] ⁺ = C ₆₃ H ₅₉ O ₁₁ S ₆	Ph(SPhCO ₂ iPr) ₆	2%

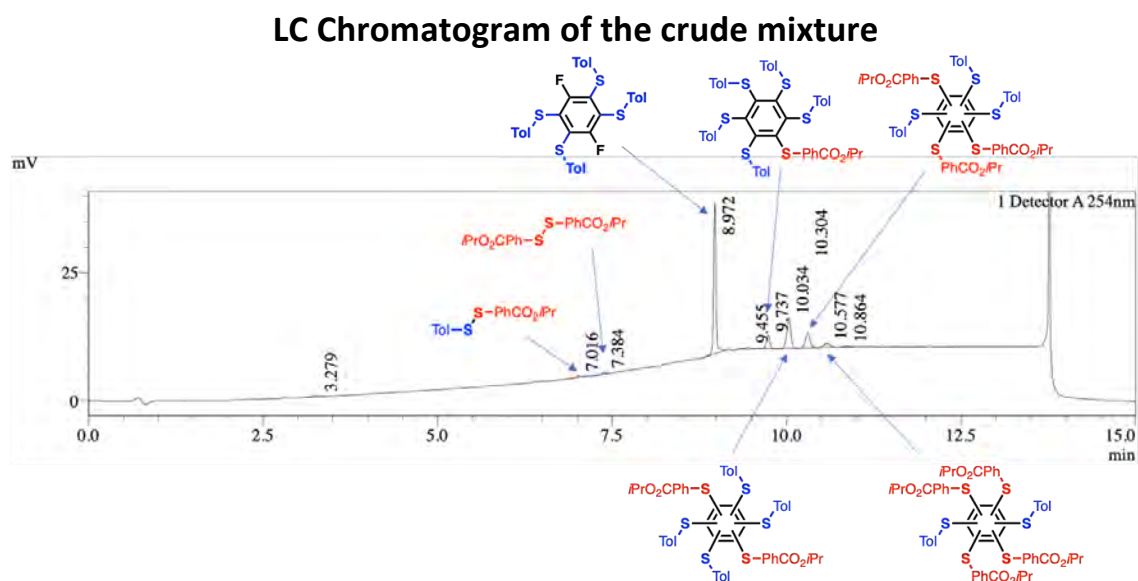
Conclusion: LC-MS data of the mixture indicated a series of mixed asterisks formed with one to six SPhCO₂iPr substituents (the remaining ones are SPhMe). Some ligand exchanges occur under mild conditions at 40°C. It should be noted that some *p*-MePhS ligands make some exchanges to provide asterisks with five and six *p*-MePhS substituents, clearly demonstrating a "sulfur dance" around the central benzene core.

SULFUR EXCHANGE REACTIONS WITH 1,4-DIFLUORO-2,3,5,6-TETRAKIS(4-METHYLPHENYLTHIO)BENZENE



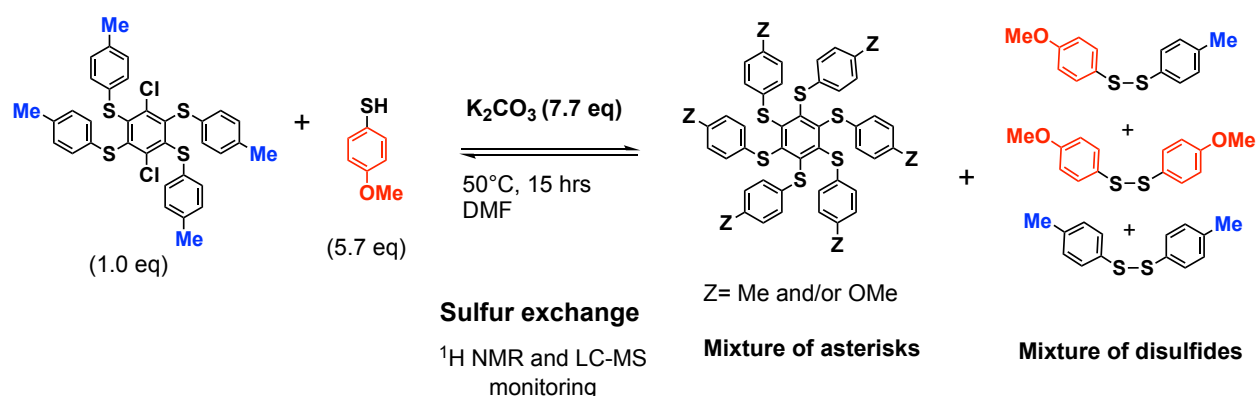
Procedure. In an oven-dried glass tube were placed 1,4-difluoro-2,3,5,6-tetrakis(4-methylphenylthio) benzene (400 mg, 0.66 mmol, 1.00 mol-eq), isopropyl-4-mercaptobenzoate (273 mg, 1.39 mmol, 2.09 mol-eq) and dry potassium carbonate (230 mg, 1.67 mmol, 2.51 mol-eq) under an argon atmosphere. All reagents were freshly dried under vacuum for about 30 min prior to use them. Under argon, dry DMF (5.5 mL, kept over 3Å molecular sieves) was then injected, the tube was sealed and the mixture was vigorously stirred at 40°C for 22 hours. An aqueous HCl solution (1M, 100 mL) was added and it was extracted with toluene (3 x 25 mL). The combined organic phases were washed with water (5 x 25 mL), and dried over anhydrous MgSO₄. After filtration and evaporation of solvents, a yellow-brown solid was obtained.

LC-MS analysis of the mixture



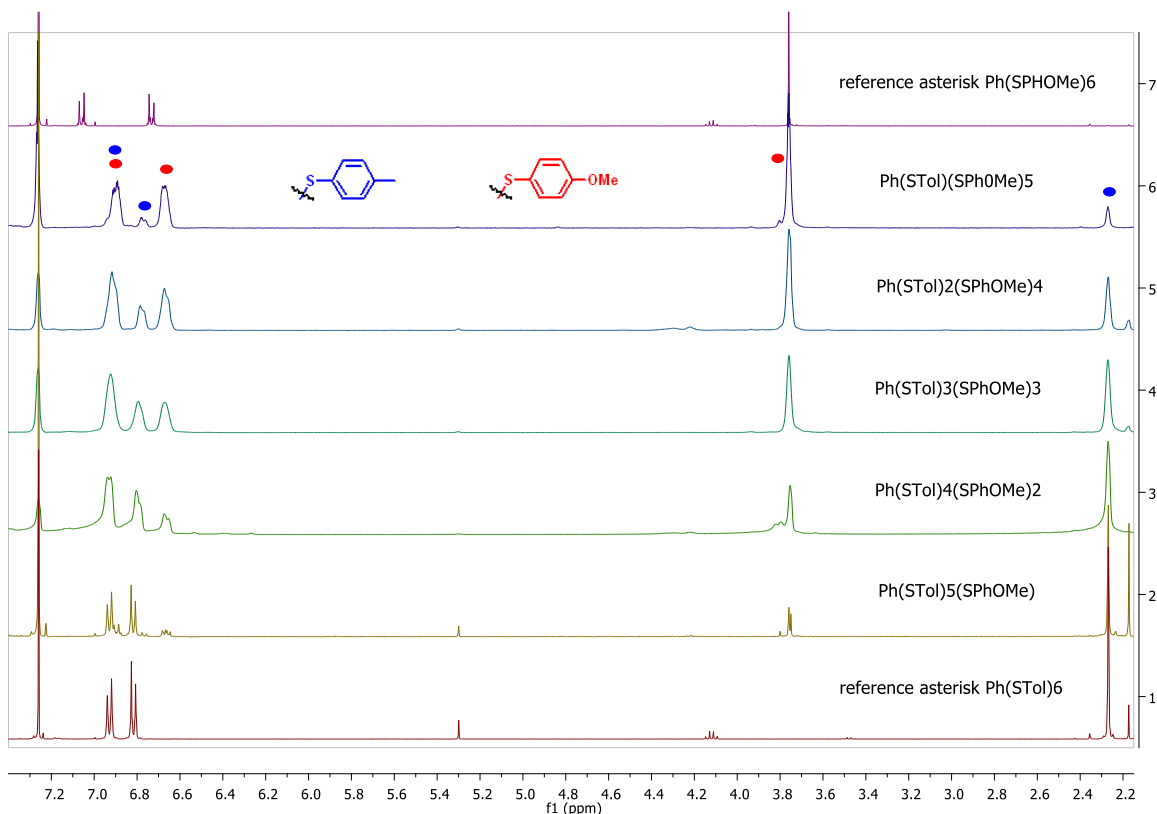
Retention Time	m/z	Formula	Structure	UV %
7.016	318	[M] ⁺ = C ₁₇ H ₁₈ O ₂ S ₂	CH ₃ PhSSPhCO ₂ <i>i</i> Pr	N/A
7.384	390	[M] ⁺ = C ₂₀ H ₂₂ O ₄ S ₂	(CO ₂ <i>i</i> PrPhS) ₂	N/A
8.972	603	[M+H] ⁺ = C ₃₄ H ₂₈ F ₂ S ₄	PhF ₂ (SPhCH ₃) ₄	54%
9.737	883	[M+H] ⁺ = C ₅₁ H ₄₆ O ₂ S ₆	Ph(SPhCH ₃) ₅ (SPhCO ₂ <i>i</i> Pr)	6%
10.034	955	[M+H] ⁺ = C ₅₄ H ₅₀ O ₄ S ₆	Ph(SPhCH ₃) ₄ (SPhCO ₂ <i>i</i> Pr) ₂	17%
10.304	1027	[M+H] ⁺ = C ₅₇ H ₅₄ O ₆ S ₆	Ph(SPhCH ₃) ₃ (SPhCO ₂ <i>i</i> Pr) ₃	10%
10.577	1099	[M+H] ⁺ = C ₆₀ H ₅₈ O ₈ S ₆	Ph(SPhCH ₃) ₂ (SPhCO ₂ <i>i</i> Pr) ₄	4%

SULFUR EXCHANGE REACTIONS WITH 1,4-DICHLORO-2,3,5,6-TETRAKIS(4-METHYLPHENYLTHIO)BENZENE



(R-62) Procedure. In an oven-dried tube, purged with argon, was added 1,4-dichloro-2,3,5,6-tetrakis(*p*-tolylthio) benzene (20.1 mg, 0.0330 mmol, 1.00 mol-eq.), dried potassium carbonate (35.1 mg, 0.254 mmol, 7.70 mol-eq.) and 4-methoxythiophenol (26.4 mg, 0.188 mmol, 23 μ L, 5.70 mol-eq.) in dry DMF (1.0 mL, dried with 3 \AA molecular sieves). Argon was bubbled through the mixture for 5-10 min.. The tube was sealed under argon and the reaction was vigorously stirred at 50°C for 15 hrs. To the reaction mixture was added H₂O (20 mL) and the mixture was extracted with toluene (5 \times 15 mL). The collected organic phases were dried over anhydrous MgSO₄, filtered and the solvent evaporated. The crude product was analyzed by ¹H NMR and LC-MS.

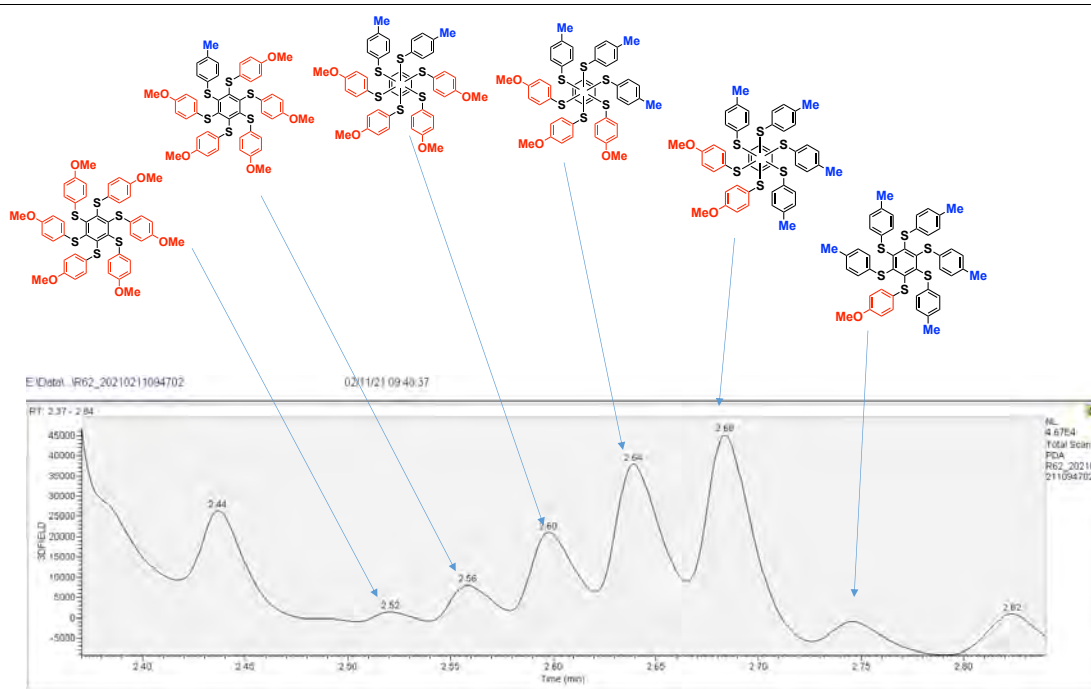
¹H NMR monitoring and analysis of the mixture



^1H NMR (CDCl_3 , 399.78 MHz)

Conclusion: 5 constitutional asterisk isomers with mixed ligands were isolated. The assignment was established by area integration in the aromatic region as well as in the aliphatic region. The low resolution does not allow ascertaining the number of regioisomers per fraction or the symmetry of the molecules.

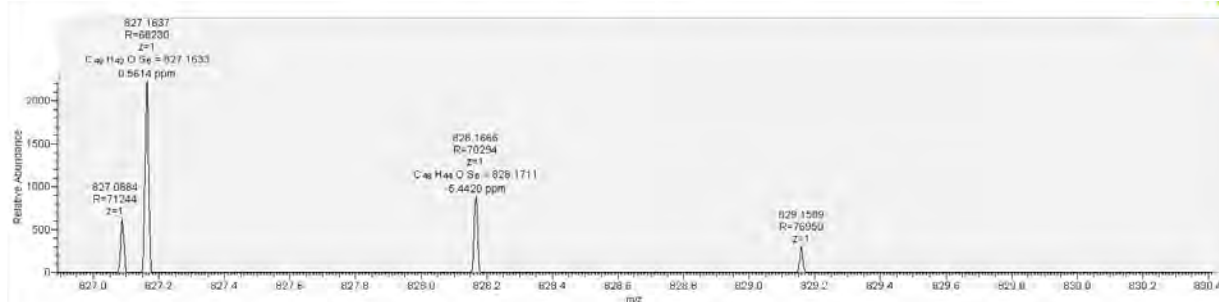
LC-HRMS analysis of the crude mixture



LC Chromatogram of the crude mixture (R-62)

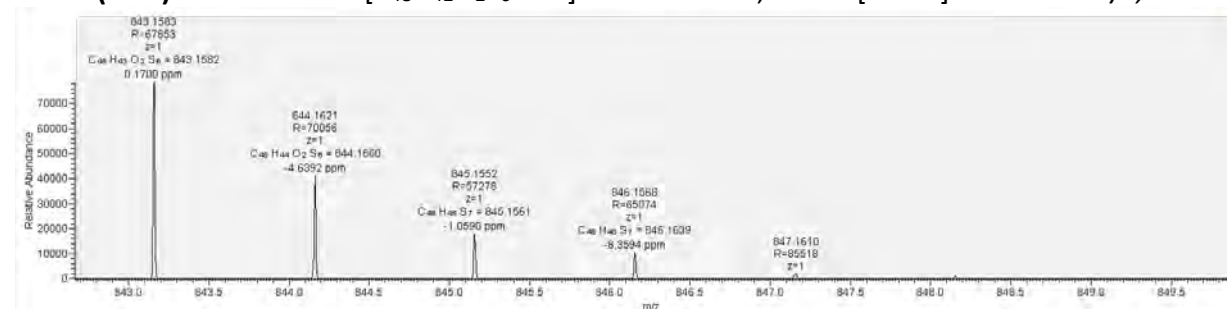
1 Substitution by MeOPhSH:

HRMS (ESI+) calculated for $[C_{48}H_{42}OS_6 + H^+]$: 827.1637 Da, found $[M+H^+]$ 827.1633 m/z;



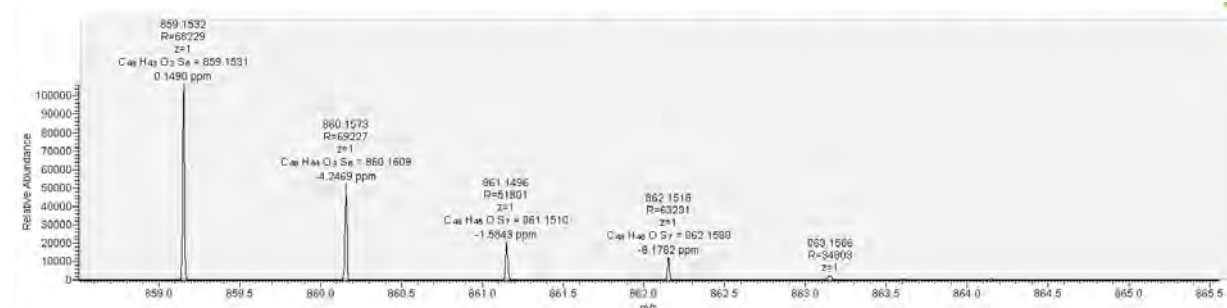
2 Substitutions by MeOPhSH:

HRMS (ESI+) calculated for $[C_{48}H_{42}O_2S_6 + H^+]$: 843.1583 Da, found $[M+H^+]$ 843.1582 m/z;



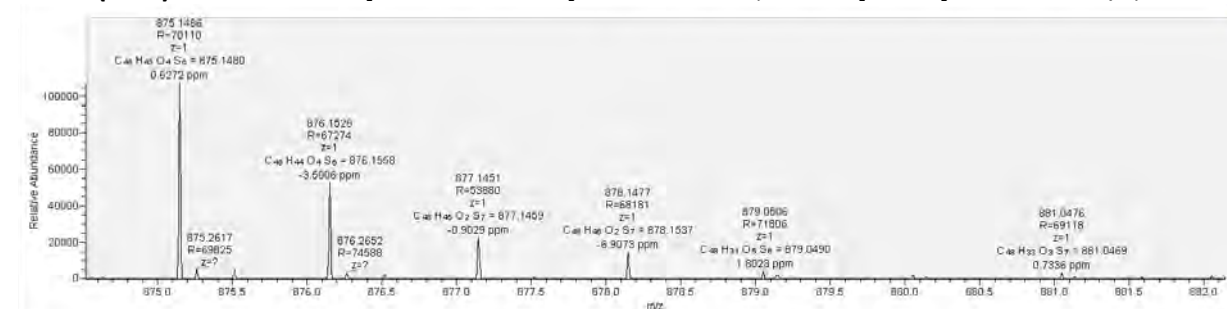
3 Substitutions by MeOPhSH:

HRMS (ESI+) calculated for $[C_{48}H_{42}O_3S_6 + H^+]$: 859.1532 Da, found $[M+H^+]$ 859.1531 m/z;



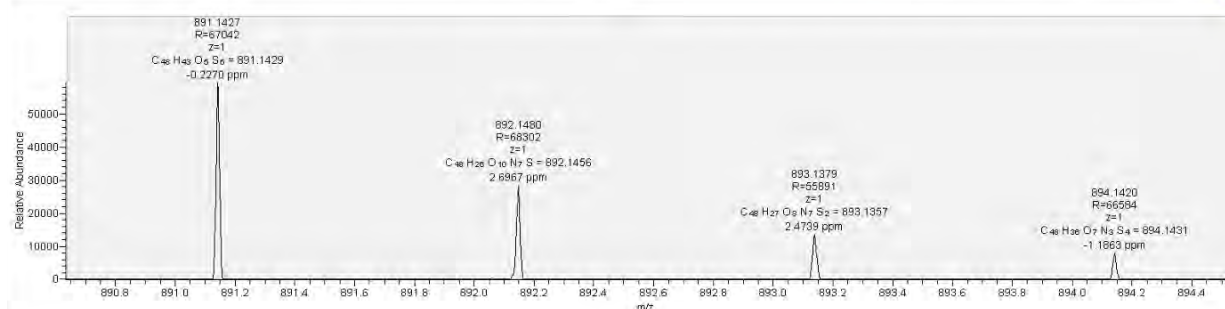
4 Substitutions by MeOPhSH:

HRMS (ESI+) calculated for $[C_{48}H_{42}O_4S_6 + H^+]$: 875.1486 Da, found $[M+H^+]$ 875.1480 m/z;

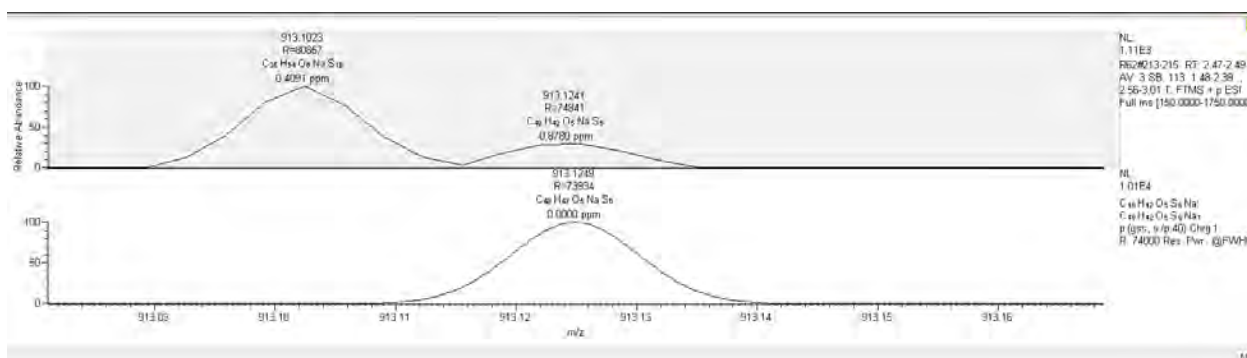


5 Substitutions by MeOPhSH:

HRMS (ESI+) calculated for $[C_{48}H_{42}O_5S_6 + H^+]$: 891.1429 Da, found $[M + H^+]$ 891.1427 m/z;

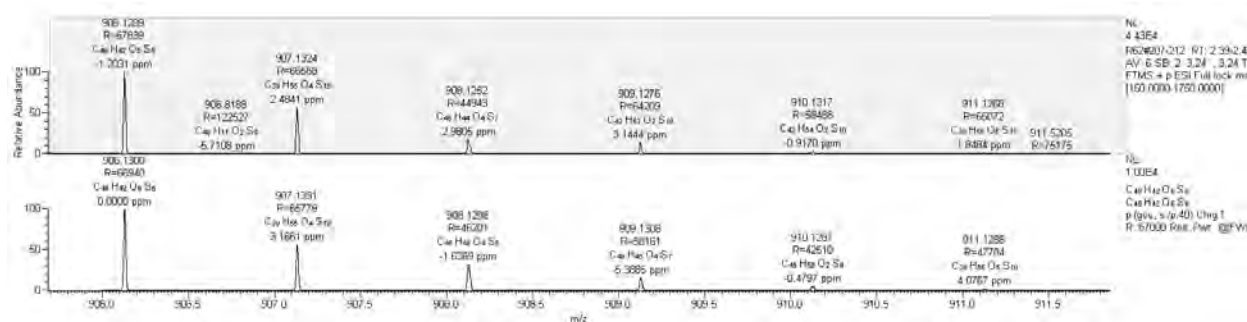


HRMS (ESI+) calculated for $[C_{48}H_{43}O_5S_6 + Na^+]$: 913.1249 Da, found $[M + Na^+]$ 913.1241 m/z;



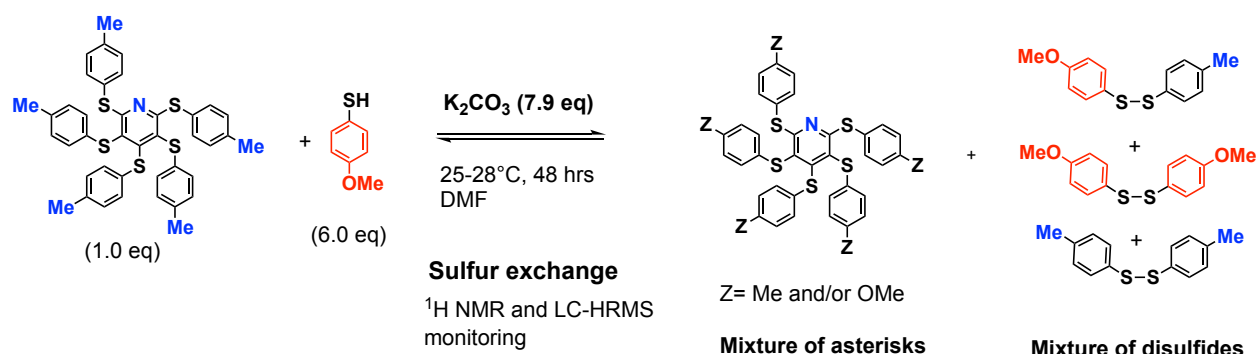
6 Substitutions by MeOPhSH:

HRMS (ESI+) calculated for $[C_{48}H_{42}O_6S_6]$: 906.1300 Da, found $[M^+]$ 891.1289 m/z;



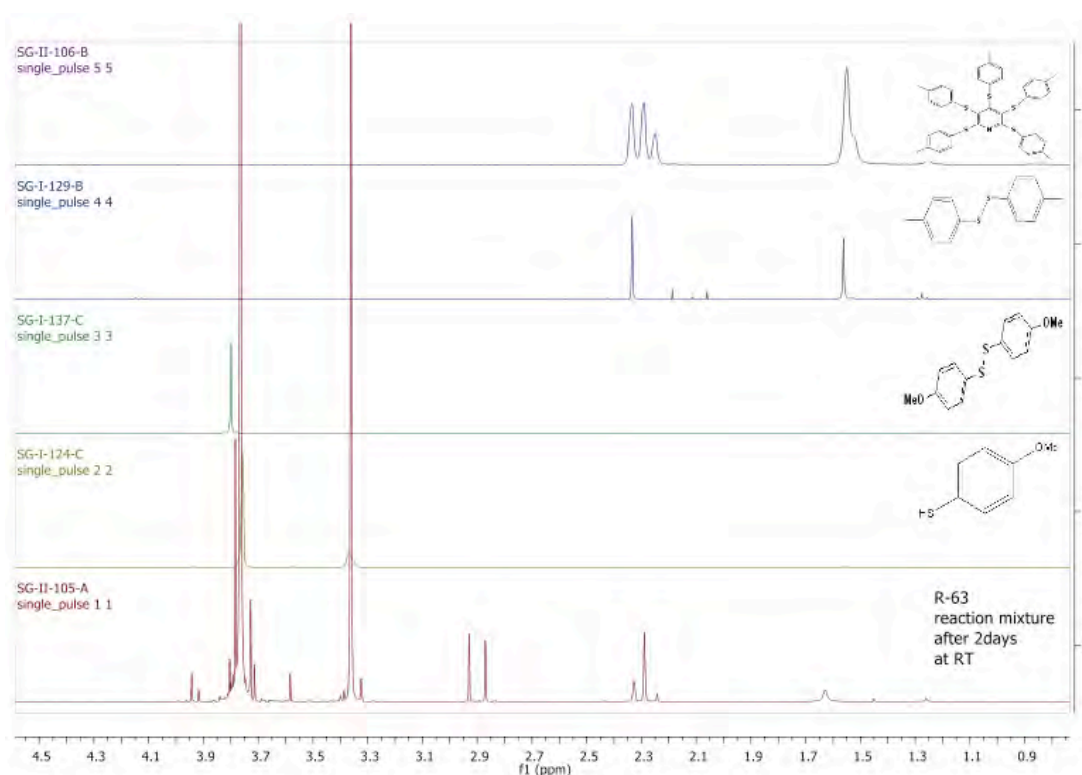
6.0 Sulfur exchange reactions on tetra(thio)pyridine asterisks

SULFUR EXCHANGE REACTIONS WITH 2,3,4,5,6-PENTAKIS(P-TOLYLTHIO)PYRIDINE AT 25-28°C



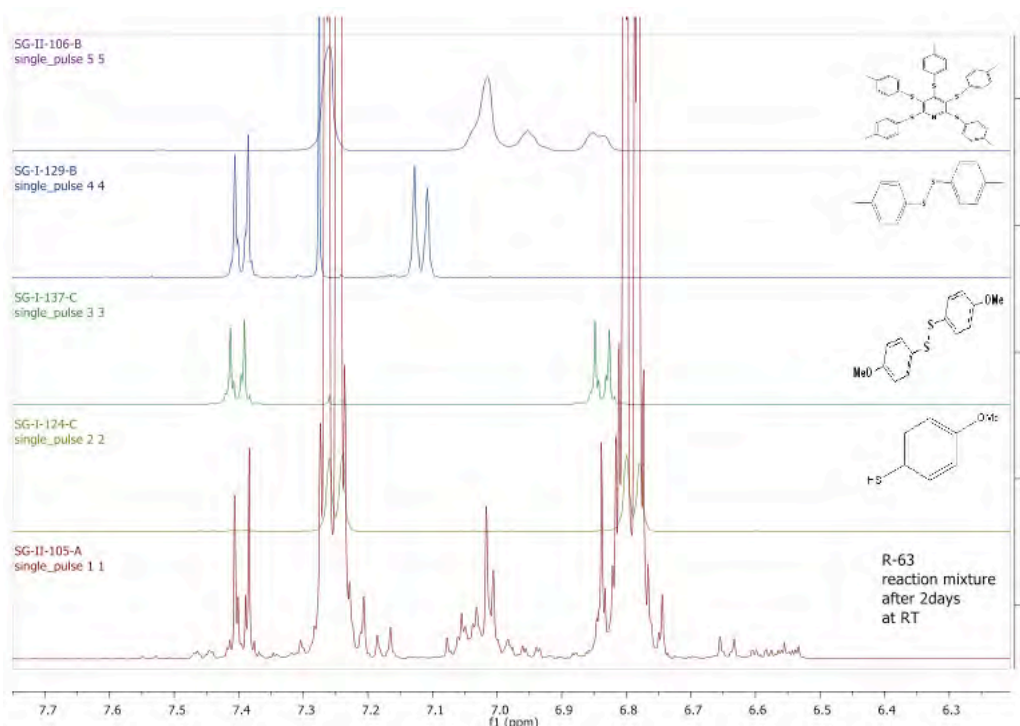
(R-63M) Procedure: In an oven-dried tube, purged with argon, was added 2,3,4,5,6-pentakis(*p*-tolylthio)pyridine (20.6 mg, 0.0299 mmol, 1.00 mol-eq.), dried potassium carbonate (32.8 mg, 0.237 mmol, 7.93 mol-eq.) and 4-methoxythiophenol (24.3 mg, 0.173 mmol, 21 μ L, 5.79 mol-eq.) in dry DMF (1.0 mL, dried and kept over 3Å molecular sieves). Argon was bubbled through the mixture for 5-10 min.. The tube was sealed and the reaction was vigorously stirred at 25-28°C for 48 hrs. The color turned from white to dark brown within a few seconds. After two days, the color turned to yellow. The reaction mixture was monitored by TLC (SiO₂, 10% and 80% tol/cyclohex). After 2 days, no starting material was detected by TLC, and mainly 3 spots were observed by UV-vis. To the reaction mixture was added H₂O (20 mL) and extracted with toluene (4× 20 mL). The collected organic phases were dried over anhydrous MgSO₄, filtered and the solvent evaporated; mass of crude: 396.2 mg.

¹H NMR monitoring and analysis of the mixture



¹H NMR (399.78 MHz, CDCl₃) spectra 1 (SG-II-105A): indicates that the pattern of CH₃ signals between 2.20 to 2.35 ppm for **spectra 1** changed relative to the composition of CH₃ signals of the pyridine asterisk reference in **spectra 5**. These signals do not correspond to a significant amount of *p*-methylphenyl disulfide (when looking at the aromatic CH region).

Conclusion: From the CH₃ signals, we can conclude that other asterisks were formed by ligand exchanges with *p*-MeOPhSH.

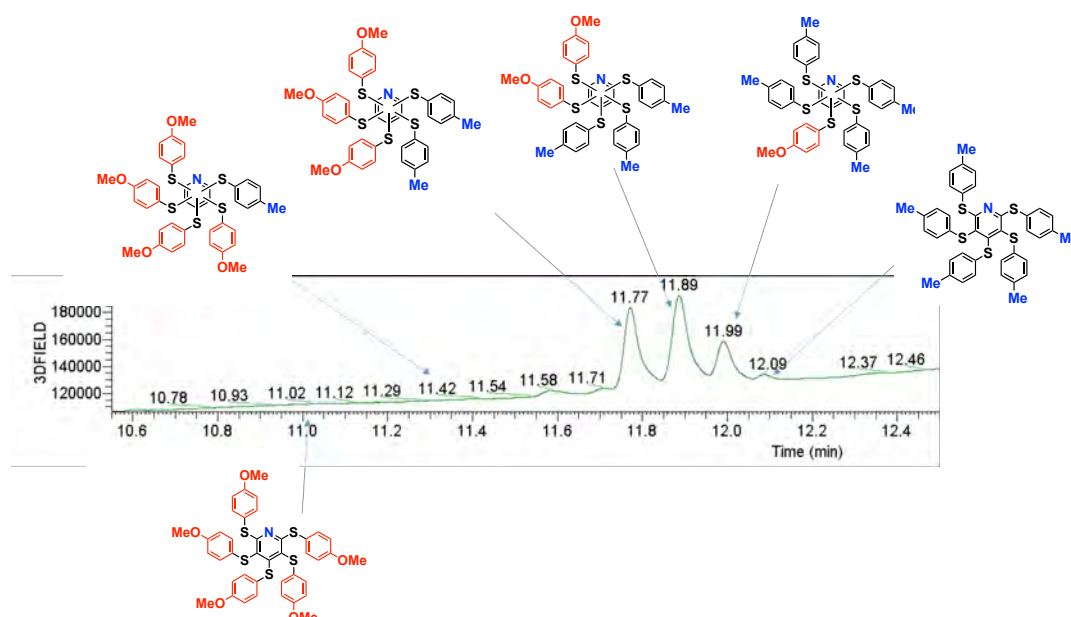


^1H NMR (399.78 MHz, CDCl_3) spectra 1 (SG-II-105A) of the reaction mixture indicates a drastic change of the pattern of aromatic C-H signals from 7.00 to 7.05 ppm relative to the C-H aromatic signals of the reference pyridine asterisk in spectra 5 (starting material).

Conclusion: From the C-H aromatic signals, we can conclude that other asterisks were formed by sulfur exchanges with *p*-MeOPhSH.

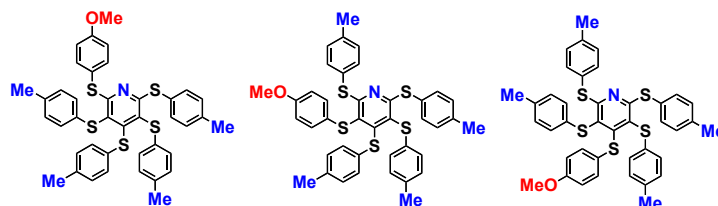
General conclusion: ^1H NMR (399.78 MHz, CDCl_3 , SG-II-105-A) monitoring after stirring for 48 hrs at 25-28°C indicated many sulfur exchange reactions at 25-28°C in DMF. A mixture of asterisks containing OMe and Me groups was formed.

LC-HRMS analysis of the crude mixture

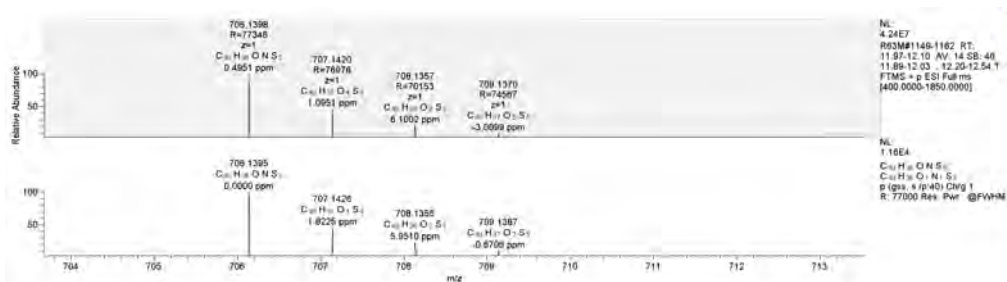


1 Substitution:

HRMS (ESI+) calculated for $[C_{40}H_{35}ONS_5 + H^+]$: 706.1395 Da, found $[M+H^+]$ 706.1398 m/z;
Possible isomers:

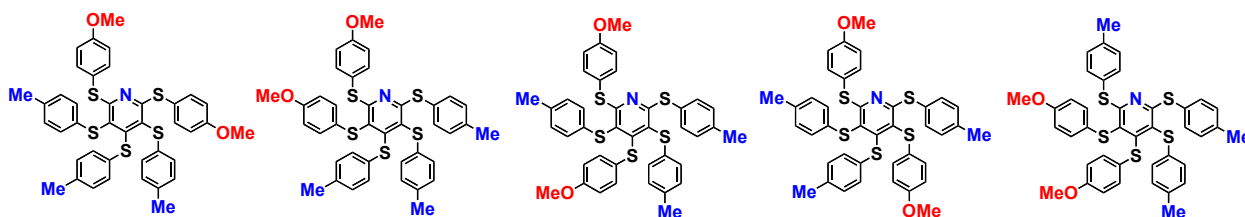


1 substitution by *p*-OMePhSH ($C_{40}H_{36}ONS_5$)

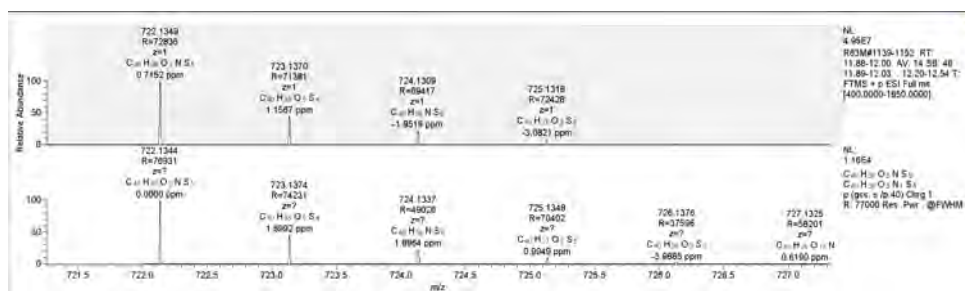


2 Substitutions:

HRMS (ESI+) calculated for $[C_{40}H_{35}O_2NS_5 + H^+]$: 722.1344 Da, found $[M+H^+]$ 722.1349 m/z;
Possible isomers:

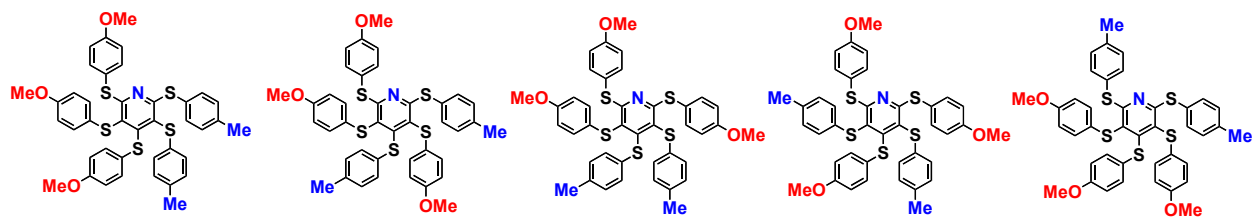


2 substitutions by *p*-OMePhSH ($C_{40}H_{36}O_2NS_5$)

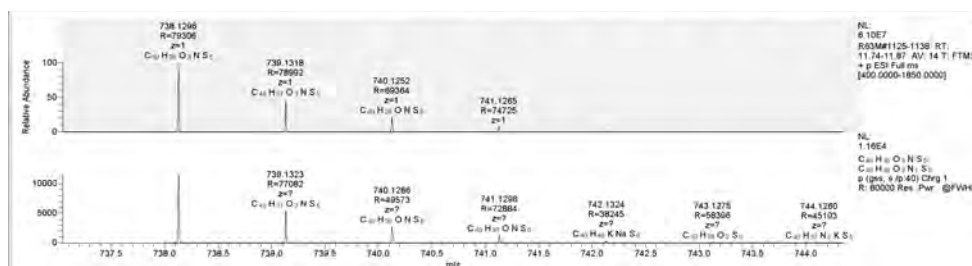


3 Substitutions:

HRMS (ESI+) calculated for $[C_{40}H_{35}O_3NS_5 + H^+]$: 738.1299 Da, found $[M+H^+]$ 738.1296 m/z;
Possible isomers:

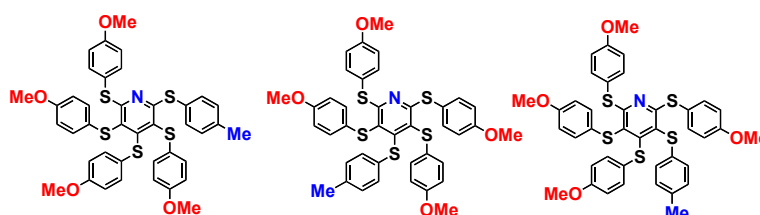


3 substitutions by *p*-OMePhSH ($C_{40}H_{36}O_3NS_5$)

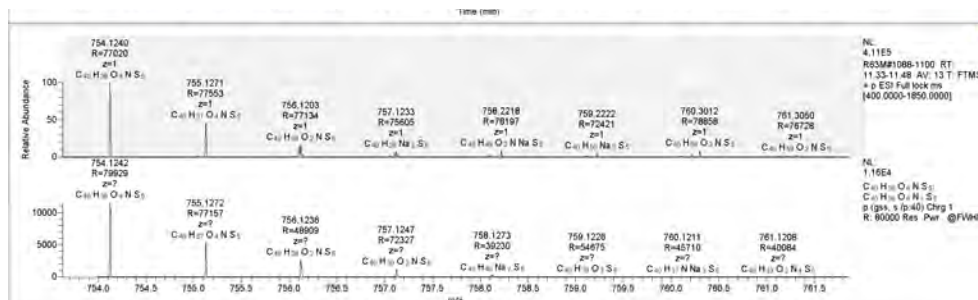


4 Substitutions:

HRMS (ESI+) calculated for $[C_{40}H_{35}O_4NS_5 + H^+]$: 754.1242 Da, found $[M+H^+]$ 754.1240 m/z;
Possible isomers:

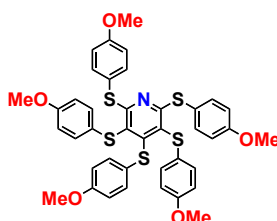


4 substitutions by *p*-OMePhSH ($C_{40}H_{36}O_4NS_5$)

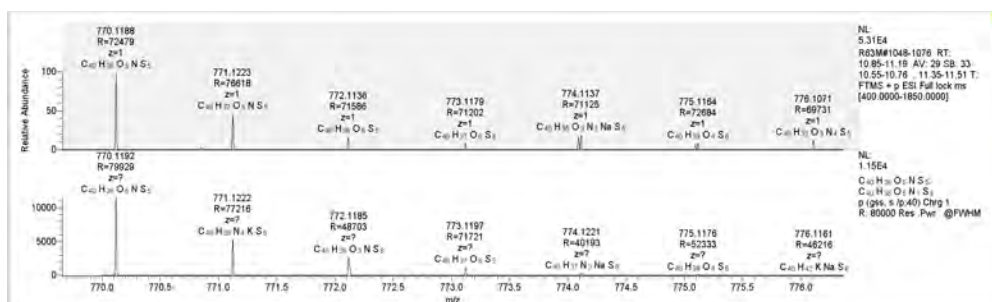


5 Substitutions:

HRMS (ESI+) calculated for $[C_{40}H_{35}O_5NS_5 + H^+]$: 770.1192 Da, found $[M+H^+]$ 770.1188 m/z;
Possible isomers:

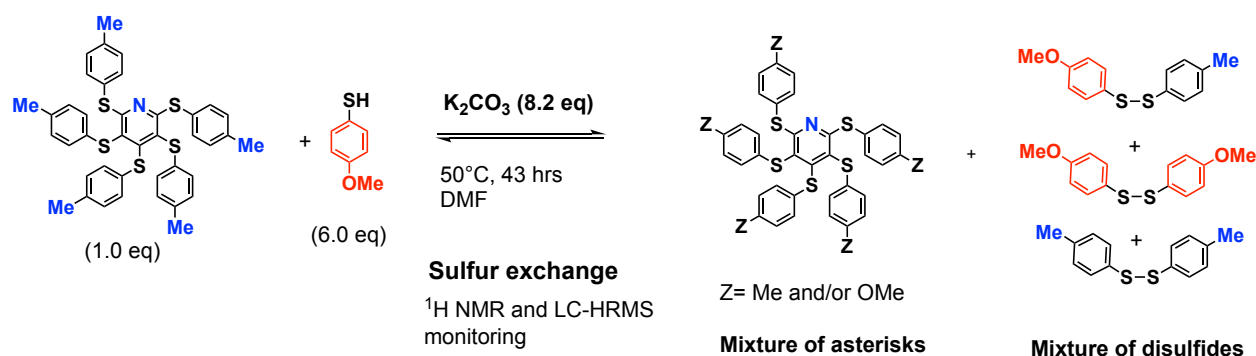


5 substitutions by *p*-OMePhSH (C₄₀H₃₆O₅NS₅)



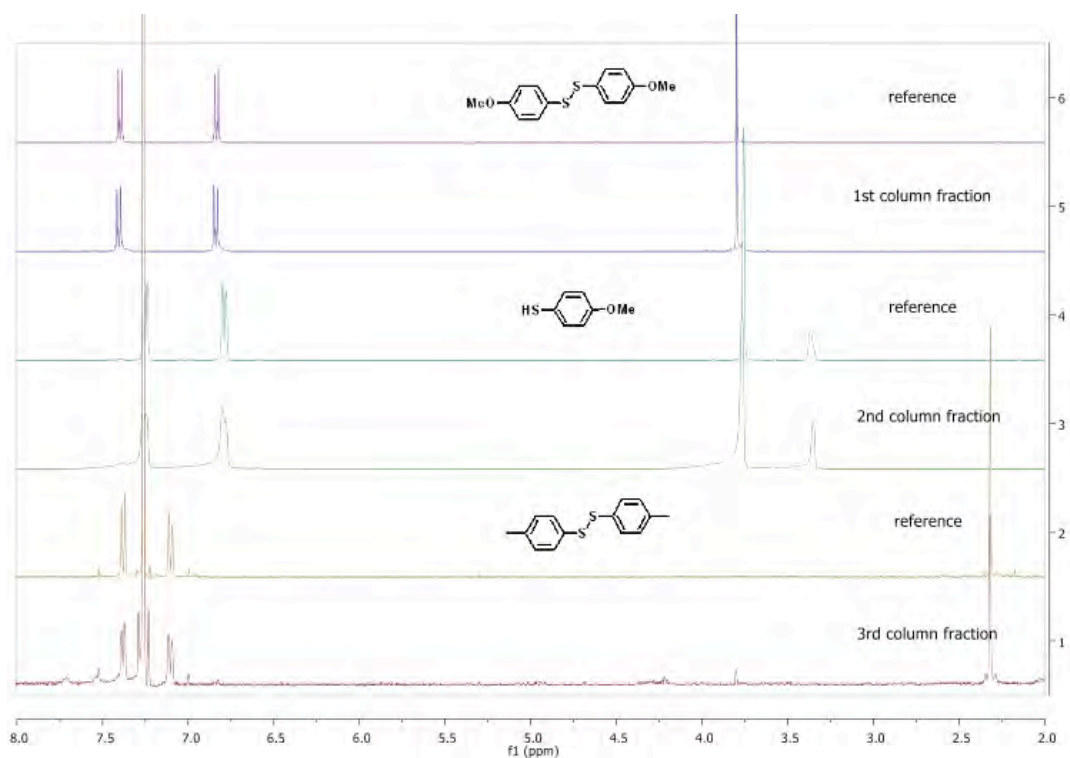
Conclusion: Some ligand exchanges occur in DCC under mild conditions at 25°C with 2,3,4,5,6-pentakis(*p*-tolylthio)pyridine. Up to five substitutions by *p*-MeOPhSH are noticed. Some selectivity is observed from the UV-vis integration of the signals in the chromatogram, for producing asterisks with disubstituted and trisubstituted *p*-MeOPhS groups, as the major products, even if 6 mol-eq. of *p*-MeOPhSH are used. Details of the exact structure of some possible regioisomers are not available at this stage.

SULFUR EXCHANGE REACTIONS WITH 2,3,4,5,6-PENTAKIS(*p*-METHYLPHENYLTHIO) PYRIDINE AT 50°C



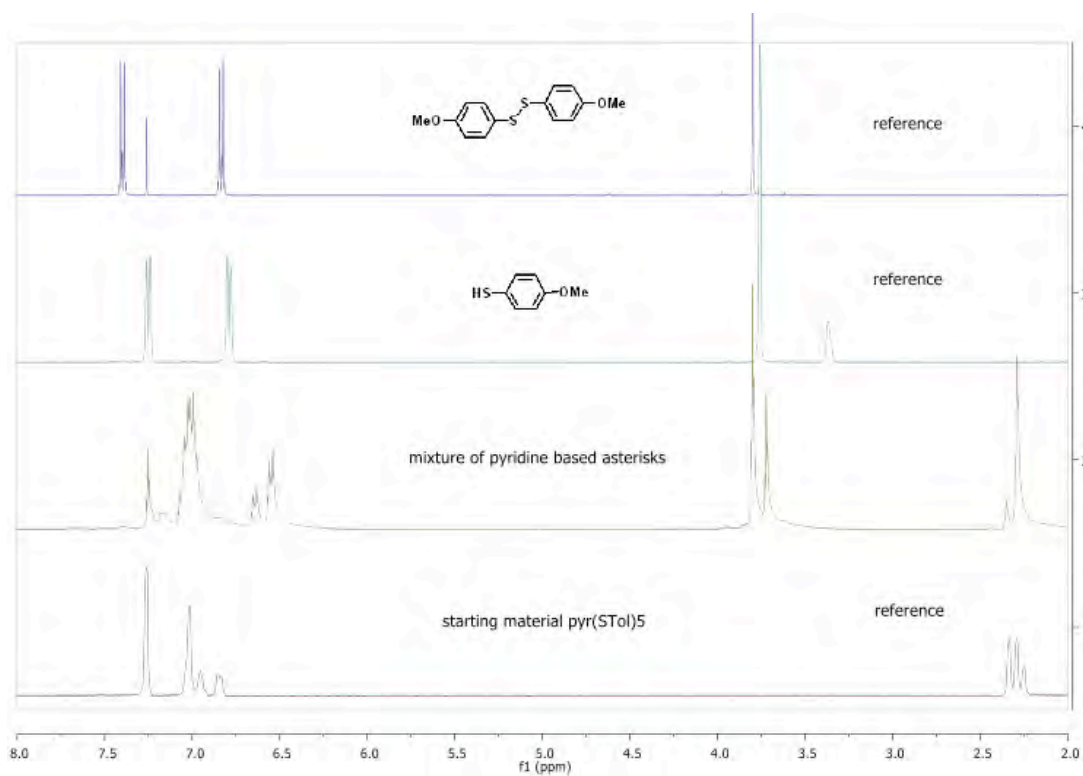
(R-64) Procedure: In an oven-dried tube, purged with argon, was added 2,3,4,5,6-pentakis(*p*-tolylthio)pyridine (20.1 mg, 0.0291 mmol, 1.00 mol-eq.), dried potassium carbonate (32.9 mg, 0.238 mmol, 8.18 mol-eq.) and 4-methoxythiophenol (24.3 mg, 0.173 mmol, 21 μL, 5.96 mol-eq) in dry DMF (0.6 mL, dried and kept over 3Å molecular sieves). Argon was bubbled through the mixture for 5-10 min.. The tube was sealed and the mixture was vigorously stirred at 50°C The reaction was monitored by TLC (SiO₂, eluent: tol/cyclohex. 80:20 v/v). After 43 hrs. no starting material was found by TLC (UV-vis) and four spots were detected (eluent: toluene/cyclohex. 80:20 v/v). The reaction mixture was taken-up in toluene (20 mL) and water (20 mL). The aqueous phase was discarded and the organic phase was further washed with water (3×20 mL). It was then dried over anhydrous MgSO₄, filtered and evaporated; mass of crude to be analyzed : 349.7 mg. The components of the crude were separated by chromatography over silica gel, by using an increasing polarity of the eluent from 10% toluene in cyclohexane to 100% toluene.

¹H NMR monitoring and analysis of the mixture



¹H NMR (399.78 MHz, CDCl₃, R-64)

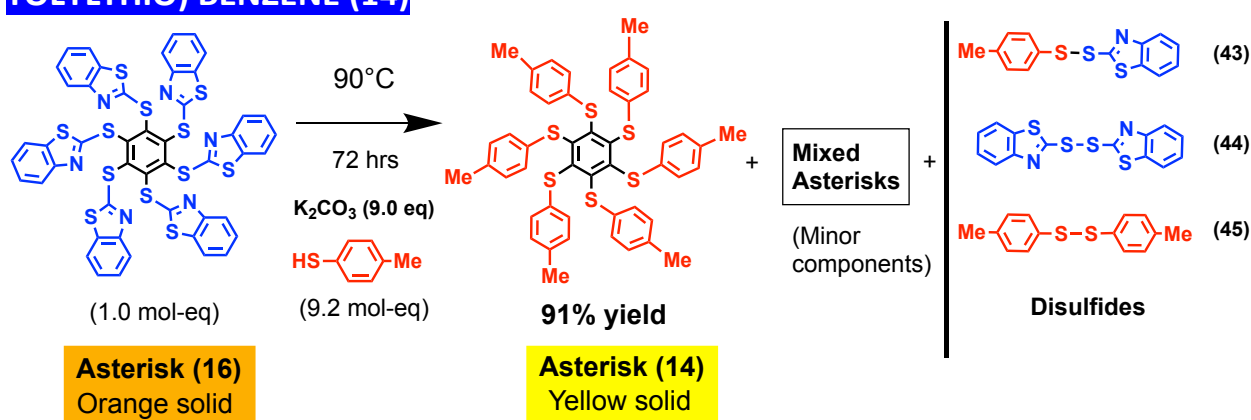
Conclusion. NMR signals between 2.0-4.0 ppm (CH₃Ph and MeOPh region): among thiols and disulfides isolated, a small amount of *p*-tolyl disulfide (3rd column fraction, *vide infra*) could be identified. This clearly demonstrates the displacement of *p*-tolylthio groups in pentakis(*p*-tolylthio)pyridine.



Conclusion: NMR signals between 6.0-7.0 ppm (aromatic region): the different pyridine-based methoxylated asterisks could not be separated. Methoxylated and methylated units can be easily identified by ^1H NMR of the mixture. The methoxy signals do not come from remaining *p*-methoxyphenyl disulfide or from *p*-methoxybenzenethiol as can be seen in the figure above. Thus, it confirms the sulfur exchange reactions on the pyridine ring.

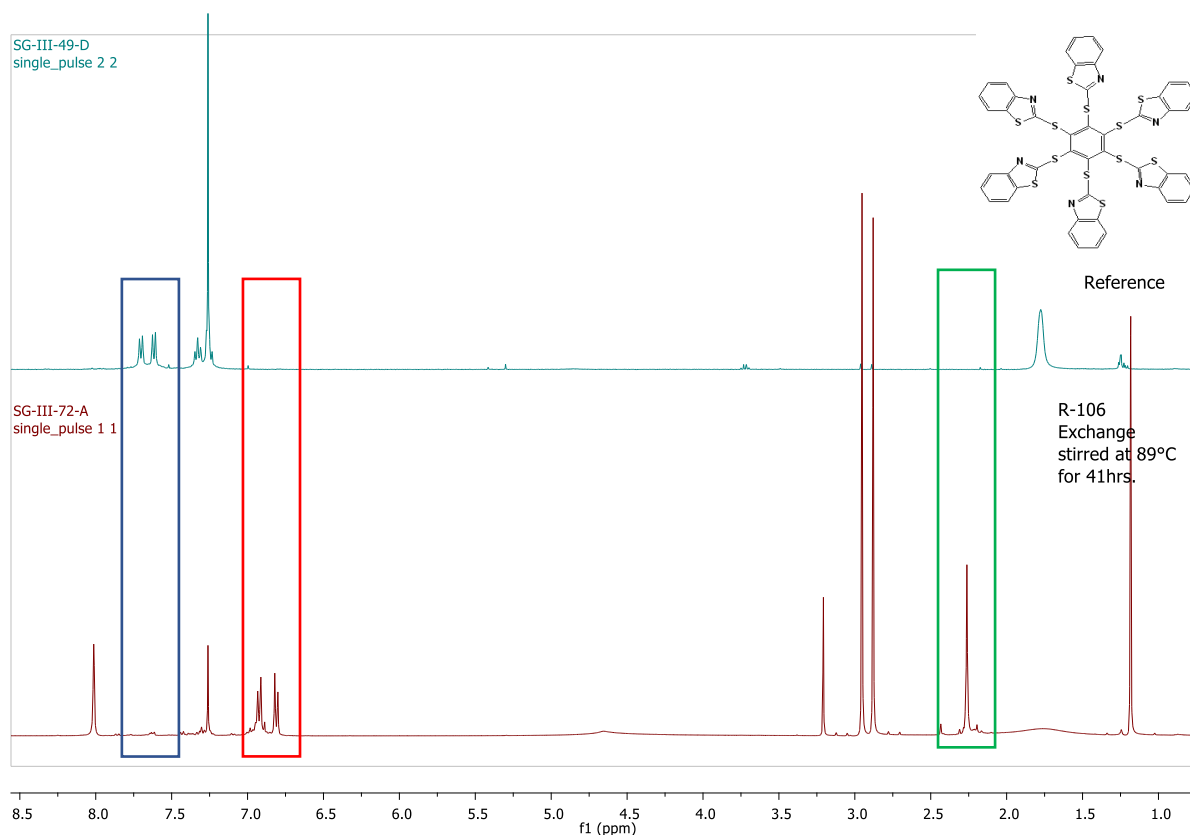
7.0 Conversion between two hexa(thio)benzene asterisks

CONVERSION OF HEXAKIS(BENZOTHIAZOLYLTHIO) BENZENE (16) TO HEXAKIS (*p*-TOLYLTHIO) BENZENE (14)



(R-106) Procedure: In an oven-dried tube, purged with argon, was added hexakis (benzothiazolyl-2-thio) benzene (16) (100.0 mg, 0.0935 mmol, 1.00 mol-eq.), dried potassium carbonate (116.3 mg, 0.841 mmol, 9.00 mol-eq.), 4-methylthiophenol (106.8 mg, 0.860 mmol, 9.20 mol-eq.) in dry DMF (1.0 mL, dried over activated 3Å molecular sieves). Argon was bubbled through the mixture for 5-10 min.. The tube was sealed under argon and the reaction was stirred at 90°C in an oil bath for 3 days. After cooling to 20°C, water (30 mL) was added to the mixture, and the product was extracted with toluene (5 x 30 mL). The combined organic phases were dried over anhydrous MgSO_4 , filtered and evaporated to dryness. TLC (SiO_2 , acetone/cyclohexane 10:90 v/v) indicated six spots under a UV-vis lamp, among which one intense luminescent yellow spot. The mixture of compounds was separated by column chromatography over silica gel (eluent: acetone/cyclohexane 10:90 v/v) as eluent. The luminescent yellow spot corresponded to hexakis (*p*-tolylthio)benzene (69.1 mg, 0.0852 mmol, 91% yield).

^1H NMR monitoring and analysis of the mixture



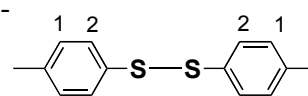
^1H -NMR (399.78 MHz, CDCl_3) monitoring after stirring for 41 hrs at 90°C.

a) **Green spectra:** hexakis(benzenethiazolyl-2-thio)benzene; b) **Red spectra:** reaction mixture after 41 hrs at 90°C.

Conclusion: Comparison of ^1H NMR spectra of hexakis(benzenethiazolyl-2-thio)benzene (green spectra) with ^1H NMR spectra of the reaction mixture (red spectra) after sulfur exchanges with 4-methylbenzenethiol indicates an excellent conversion of hexakis(benzenethiazolyl-2-thio)benzene (see blue rectangle) to hexakis(4-methylphenylthio)benzene (see red rectangle). It was observed over time some new signals at 6.93 ppm (doublet), 6.84 ppm (doublet) (red rectangle), and a singlet at 2.29 ppm (green rectangle). Thus, 4-methylbenzenethiol promoted the exchange of ligands to make hexakis(4-methylphenylthio)benzene in a 91% isolated yield.

After column chromatography (SiO_2 , eluent: acetone/cyclohexane 10:90 v/v) several components were separated, including disulfides. The release of benzenethiazolyl-2-thio groups for making mixed or symmetrical disulfides is also confirmed by ^1H NMR.

a) Fraction [12-17] (1st less polar spot on top of TLC): ^1H -NMR (SG-III-72-B) indicates *p*-tolyl disulfide as a major component; ^1H NMR (399.78 MHz, CDCl_3 , ppm) δ = 7.38 (d_{app} , J = 8.1 Hz, 4H), 7.10 (d_{app} , J = 8.1 Hz, 4H), 2.32 (s, 6H). Mass: 3.7 mg.



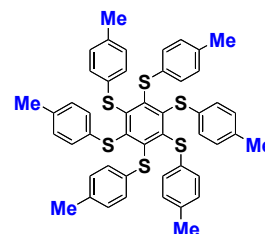
b) Fraction [40] (2nd spot from the top of TLC): ¹H-NMR (SG-III-72-C) indicates a methyl and a benzothiazole group corresponding to the mixed disulfide: *p*-tolyl-2-benzothiazolyl disulfide;. Mass: 0.4 mg.

c) Fraction [42] (mixture of 1st and 2nd spot on TLC). Mass: 1.8 mg

d) Fraction [43-47] (mixture of 1st, 2nd and 3rd spot on TLC). Mass: 10.5 mg

e) Fraction [48] (mixture of 2nd and 3rd spot on TLC)

f) Fraction [50-58] (3rd spot on TLC, asterisk (14)): ¹H NMR (SG-III-72-D) indicates an excellent sulfur exchange to hexakis(*p*-tolylthio) benzene; ¹H NMR (399.78 MHz, CDCl₃, ppm) δ = 6.93 (d_{app}, *J* = 8.1 Hz, 12H), 6.82 (d_{app}, *J* = 8.2 Hz, 12H), 2.29 (s, 18H); ¹³C NMR (100.53 MHz, CDCl₃, ppm) (SG-III-72-H) δ = 148.03, 135.97, 134.53, 129.73, 128.65, 21.22. Mass: 69.1 mg.



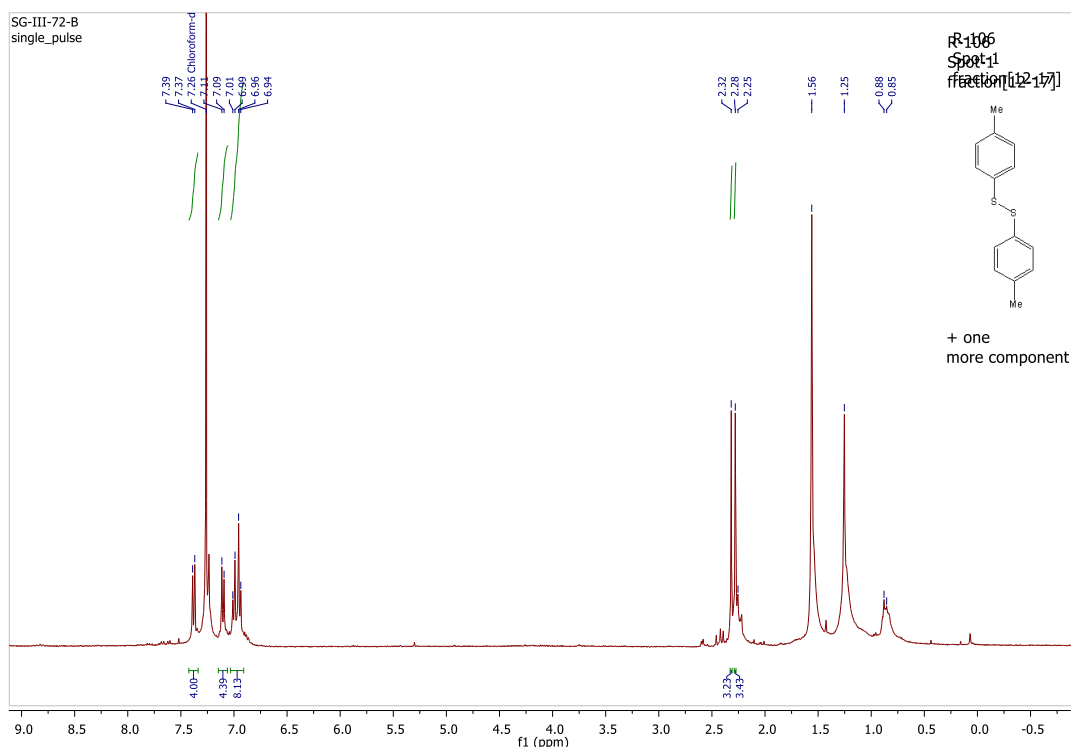
g) Fraction [59-60] (mixture of 3rd and 4th spot on TLC). Mass: 3.7 mg.

Fraction [61-63] (4th spot on TLC, yellow): ¹H NMR (SG-III-72-E) indicates a mixture of asterisks. Mass: 0.9 mg.

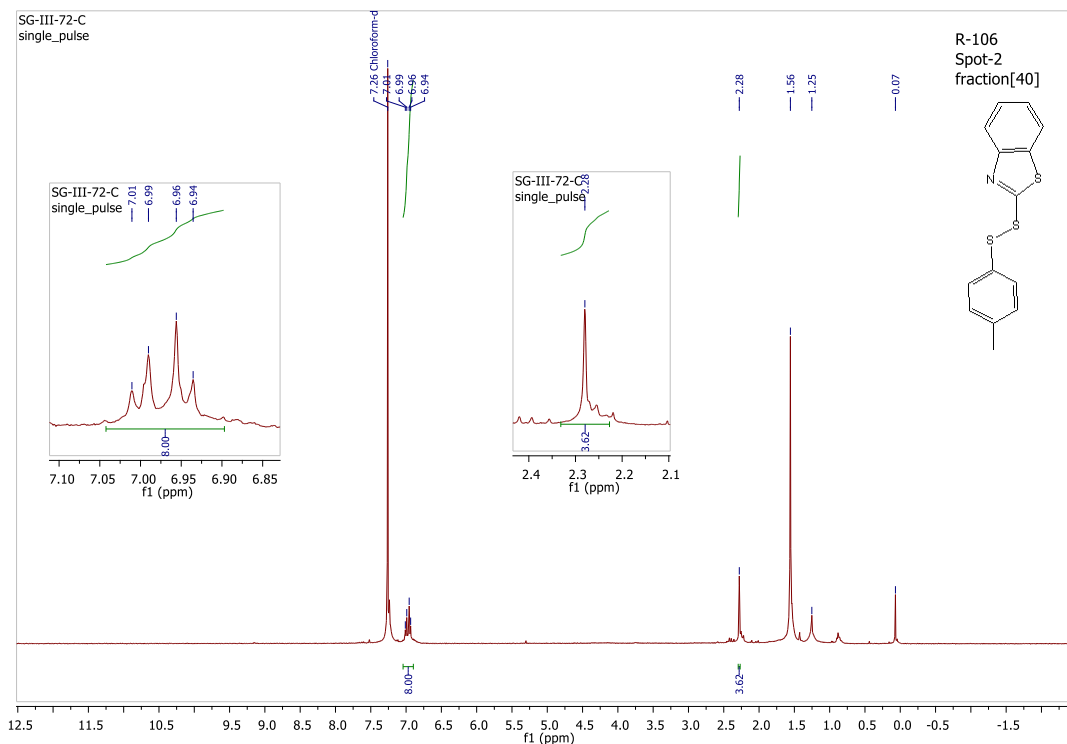
h) Fraction [72-80] (5th spot on TLC, yellow): ¹H NMR (SG-III-72-F) indicates a mixture of asterisks. Mass: 19.8 mg.

i) Fraction [95] (6th spot on TLC): ¹H NMR indicates a mixture of 2- mercaptobenzothiazole and asterisks. Mass: 14.3 mg.

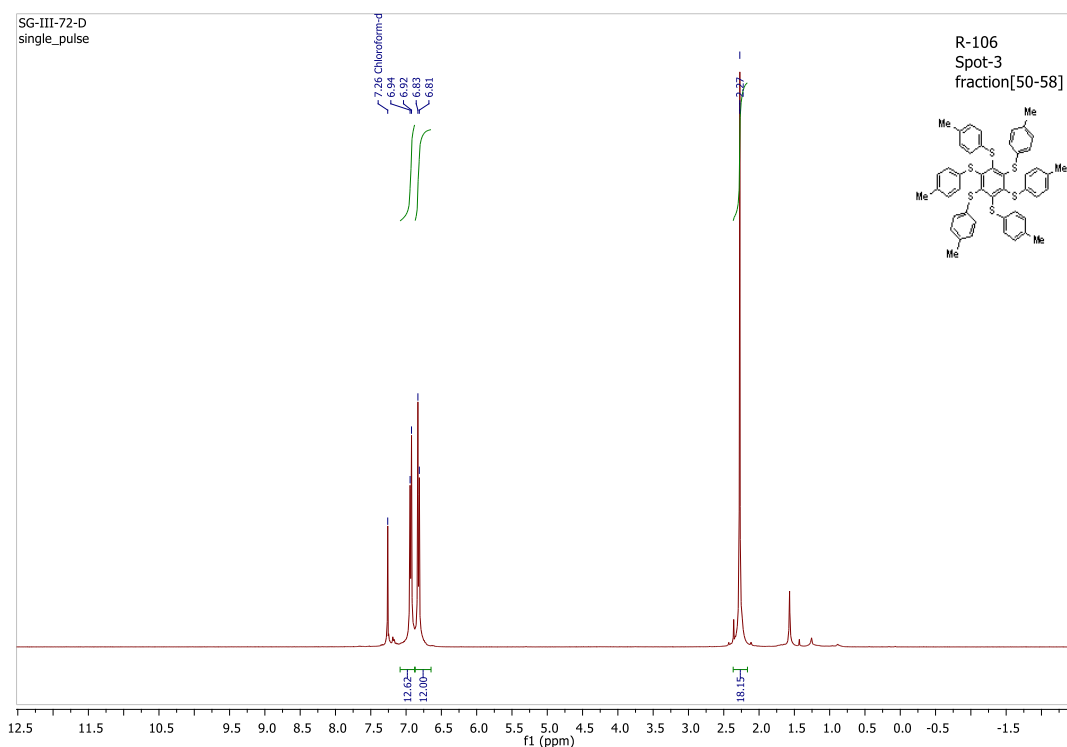
List of corresponding ¹H- and ¹³C-NMR spectra



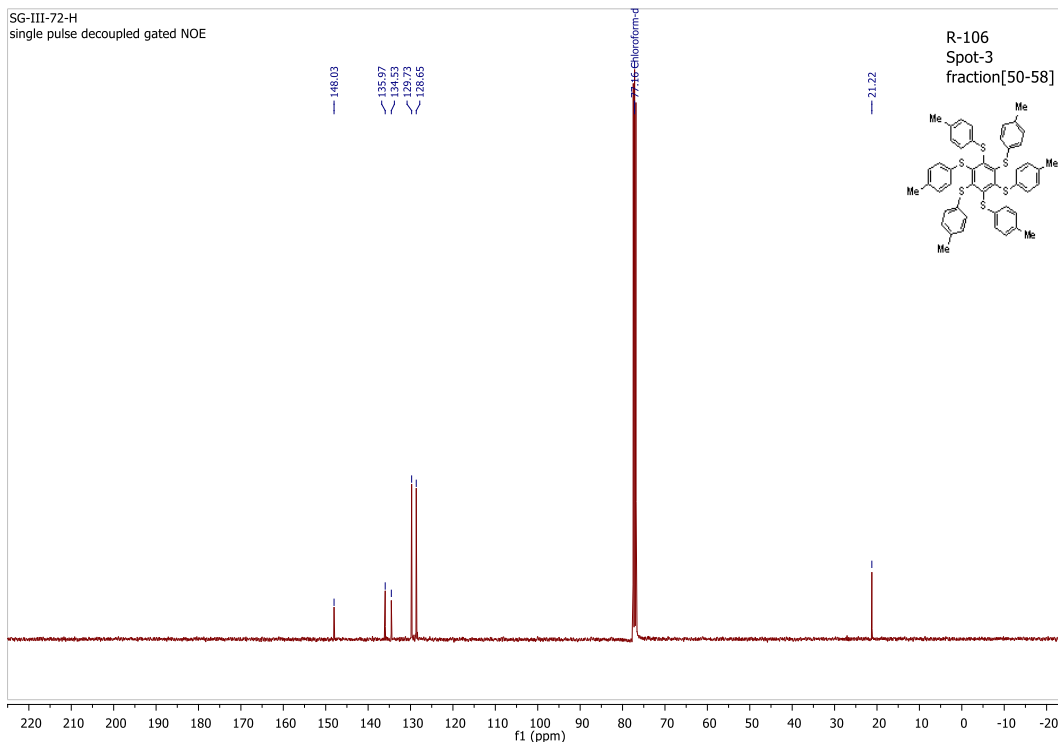
¹H-NMR (399.78 MHz, CDCl₃) - SG-III-72B (fractions 12-17)



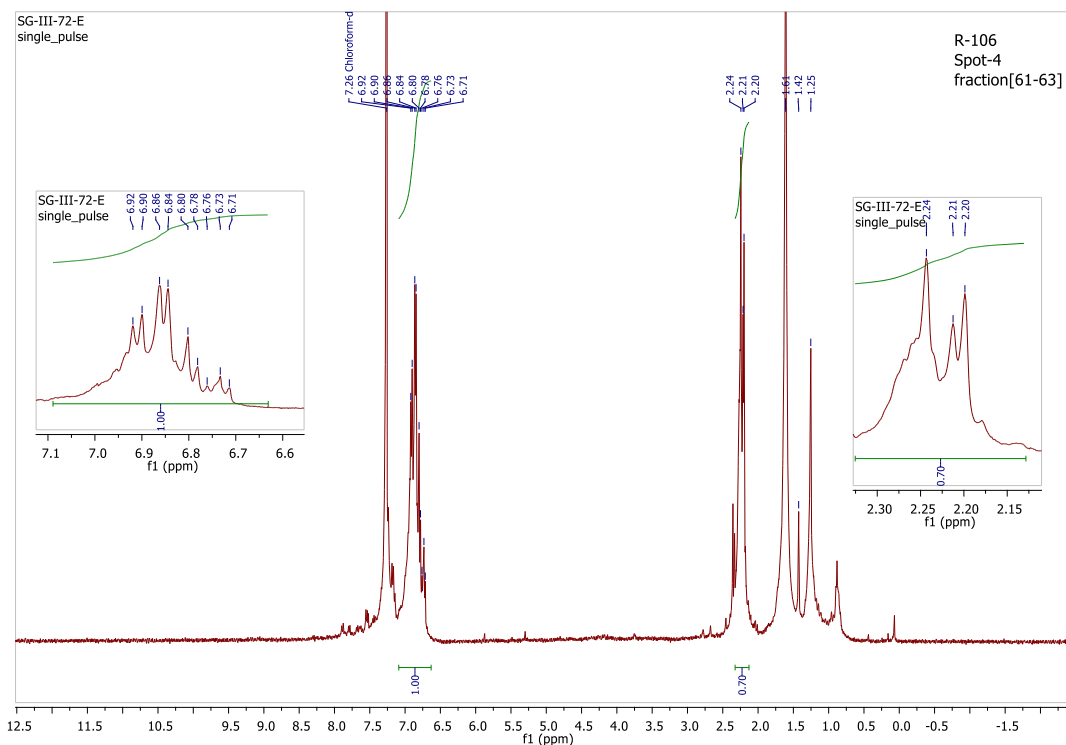
$^1\text{H-NMR}$ (399.78 MHz, CDCl_3) - SG-III-72C (fraction 40)



$^1\text{H-NMR}$ (399.78 MHz, CDCl_3) - SG-III-72D (fractions 50-58)



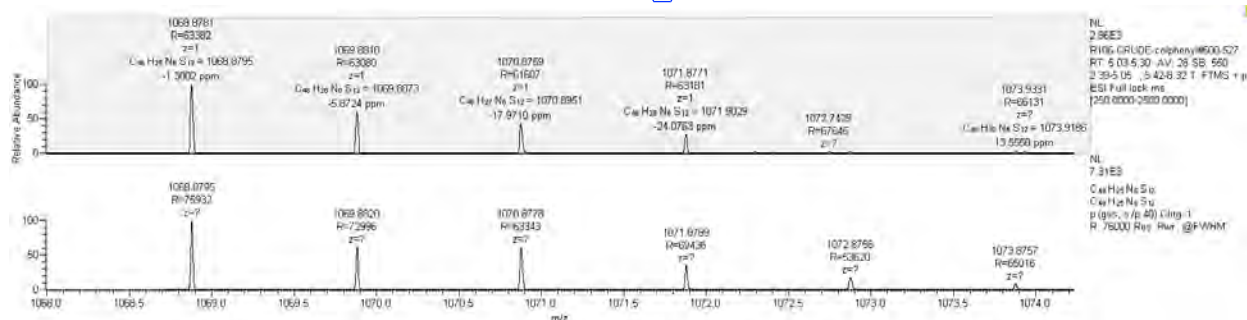
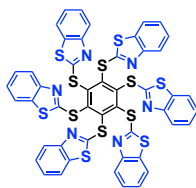
¹³C-NMR (399.78 MHz, CDCl₃) - SG-III-72H (fractions 50-58)



¹H-NMR (399.78 MHz, CDCl₃) - SG-III-72E (fractions 61-63)

0 Substitution: Asterisk (16) hexakis(benzenethiazolyl-2-thio) benzene

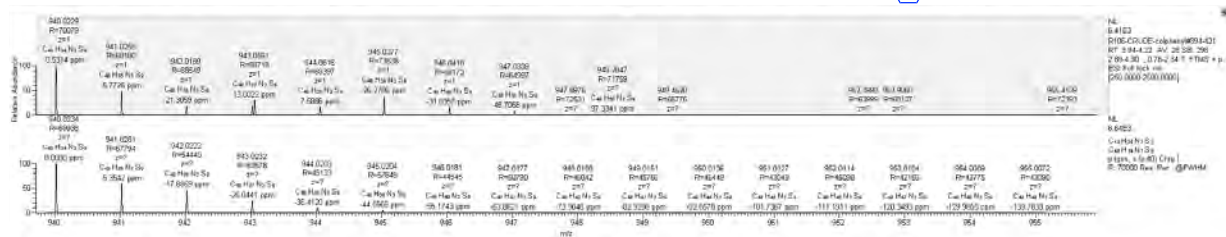
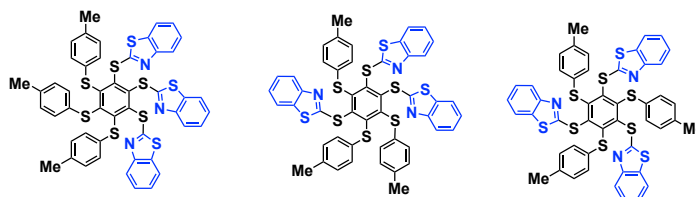
HRMS (ESI+) calculated for $[C_{48}H_{24}N_6S_{12} + H^+]$: 1068.8795 Da, found $[M+H^+]$ 1068.8781 m/z;



3 Substitutions by MePhSH (minor component):

HRMS (ESI+) calculated for $[C_{48}H_{33}N_3S_9 + H^+]$: 940.0234 Da, found $[M+H^+]$ 940.0229 m/z;

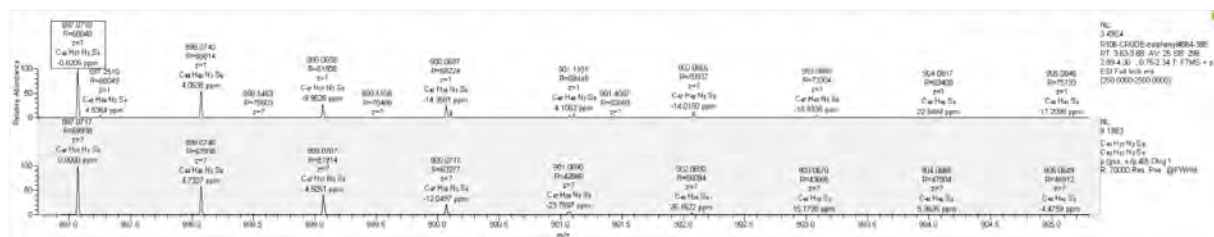
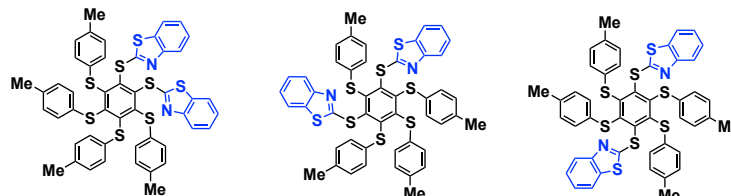
Possible isomers:



4 Substitutions by MePhSH (minor component):

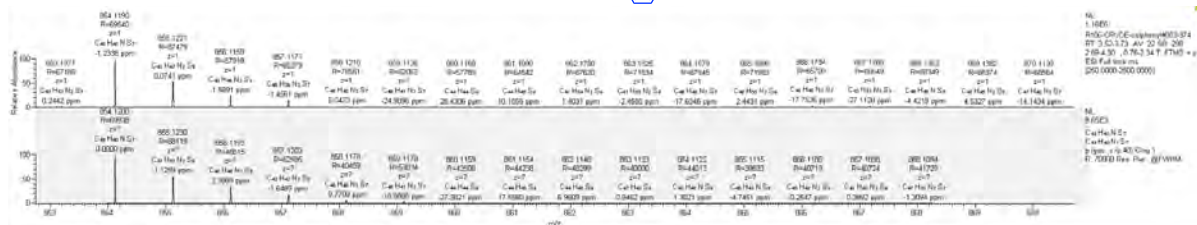
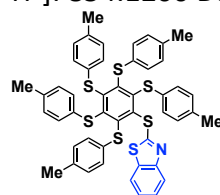
HRMS (ESI+) calculated for $[C_{48}H_{36}N_2S_8 + H^+]$: 897.0717 Da, found $[M+H^+]$ 897.0710 m/z;

Possible isomers:



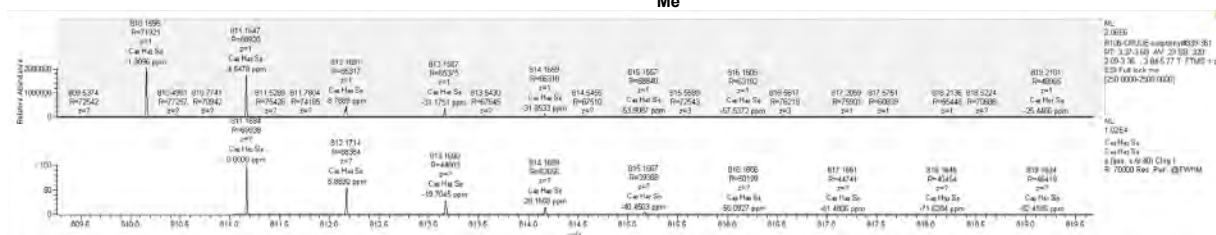
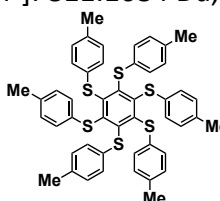
5 Substitutions by MePhSH (minor component):

HRMS (ESI+) calculated for $[C_{48}H_{39}NS_7 + H^+]$: 854.1200 Da, found $[M+H^+]$ 854.1190 m/z;

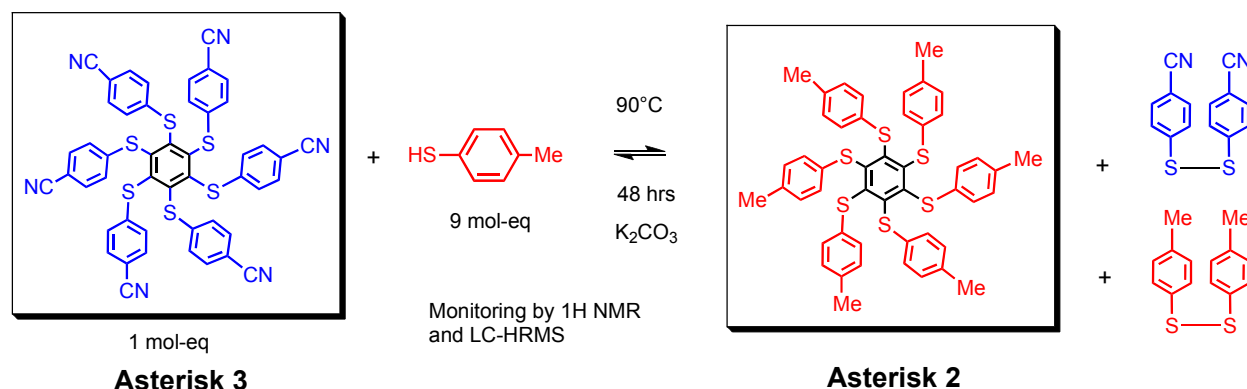


6 Substitutions by MePhSH. (Asterisk (14) is the major compound isolated):

HRMS (ESI+) calculated for $[C_{48}H_{42}S_6 + H^+]$: 811.1684 Da, found $[M+H^+]$ 811.1647 m/z;



(R109) CONVERSION OF HEXAKIS(4-CYANOPHENYLTHIO)BENZENE TO HEXAKIS(4-METHYLPHENYLTHIO) BENZENE

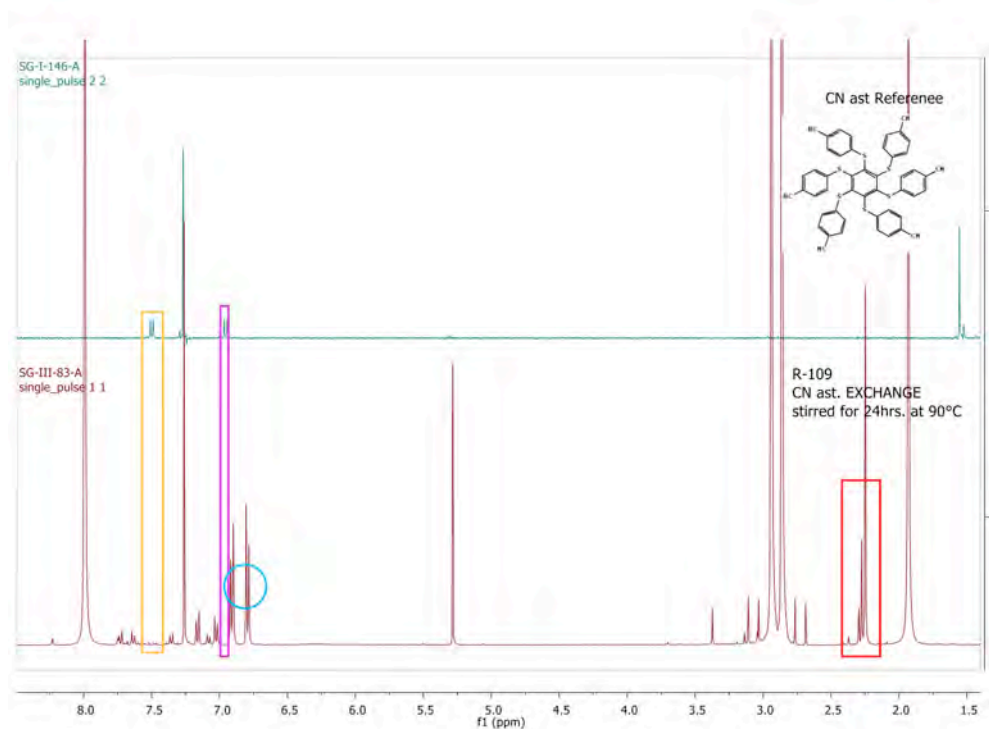


Procedure. In an oven-dried tube, purged with argon, was added hexakis(4-cyanophenylthio)benzene (30.2 mg, 0.034 mmol, 1.00 mol-eq.), dried potassium carbonate (42.6 mg, 0.308 mmol, 9.00 mol-eq.) and 4-methylthiophenol (39.7 mg, 0.319 mmol, 9.00 mol-eq.) in dry DMF (0.5mL, dried with activated 3Å molecular sieves). Argon was bubbled through the mixture for 5-10minutes in the tube. The tube was sealed under argon, and the reaction was

stirred in an oil bath at 90°C for 2 days. The reaction mixture was monitored by TLC (SiO₂, eluent: 100% cyclohex. and tol/cyclohex. 80:20 v/v). Mainly two spots were observed by UV-vis in 100% cyclohexane and only one spot in tol/cyclohex (80:20 v/v). DMF was removed from the reaction mixture under reduced pressure on a rotary evaporator. To the crude mixture was added water (30 mL) and it was extracted with toluene (4 × 25mL). The collected organic phases were dried over anhydrous MgSO₄, filtered, and the solvent evaporated. The products were separated by column chromatography over silica gel using toluene/cyclohex. (5:95 v/v) as eluent. Hexakis(*p*-tolylthio)benzene was isolated as a major product (25.1 mg, 90% yield).

¹H NMR monitoring and analysis of the mixture

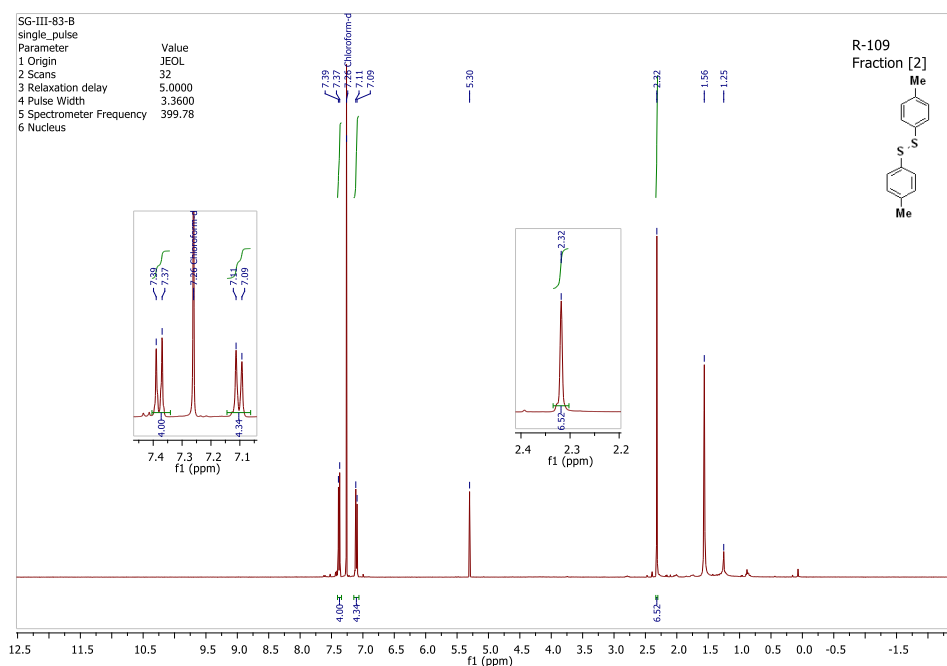
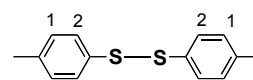
Comparison of ¹H NMR spectra of starting hexakis(4-cyanophenylthio)benzene with ¹H NMR spectra of the reaction mixture after sulfur ligand exchanges with 4-methylbenzenethiol indicated an excellent conversion to hexakis(4-methylphenylthio)benzene. It was observed over time some new signals at 6.93 ppm (doublet), 6.84 ppm (doublet), and 2.29 ppm. Finally, 4-methylbenzenethiol promoted the exchange of ligands to make hexakis (4-methylphenylthio) benzene in a 90% yield after 2 days at 90°C.



¹H-NMR (399.78 MHz, CDCl₃, SG-III-83A) monitoring after stirring for 24 hrs at 90°C. Comparison of ¹H-NMR spectra of starting hexakis (4-cyanophenylthio)benzene (spectra 2, blue) with its characteristic signals at 6.96 ppm (d_{app}), 7.50 ppm (d_{app}) and the spectra from reaction mixture (spectra 1, red) indicated that most starting asterisk was consumed (see orange and pink boxes for changes of signals), which is also confirmed by TLC. Some new methyl signals appear between 2.25-2.30 ppm (shown in red box), corresponding to hexakis(4-methylphenylthio)benzene.

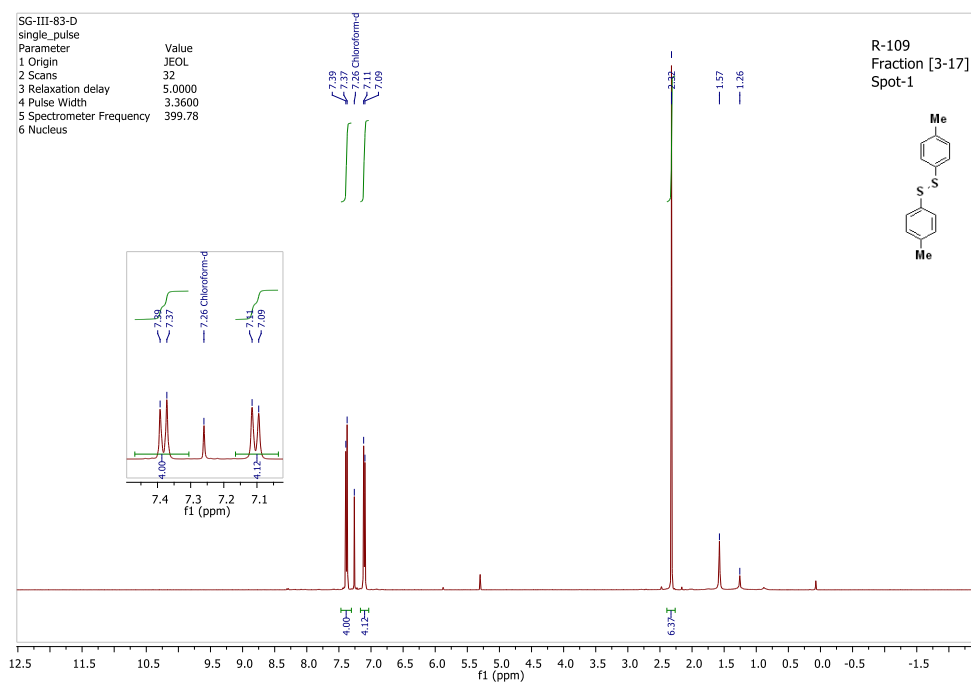
After column chromatography over silica gel, several compounds were separated.

Fraction [2] (1st less polar spot on TLC): ¹H NMR (SG-III-83-B) indicates the formation of *p*-tolyl disulfide: ¹H NMR (399.78 MHz, CDCl₃, ppm) δ = 7.38 (d_{app}, *J* = 8.1 Hz), 7.10 (d_{app}, *J* = 8.1 Hz), 2.32 (s, 6H), when compared to an authentic sample.

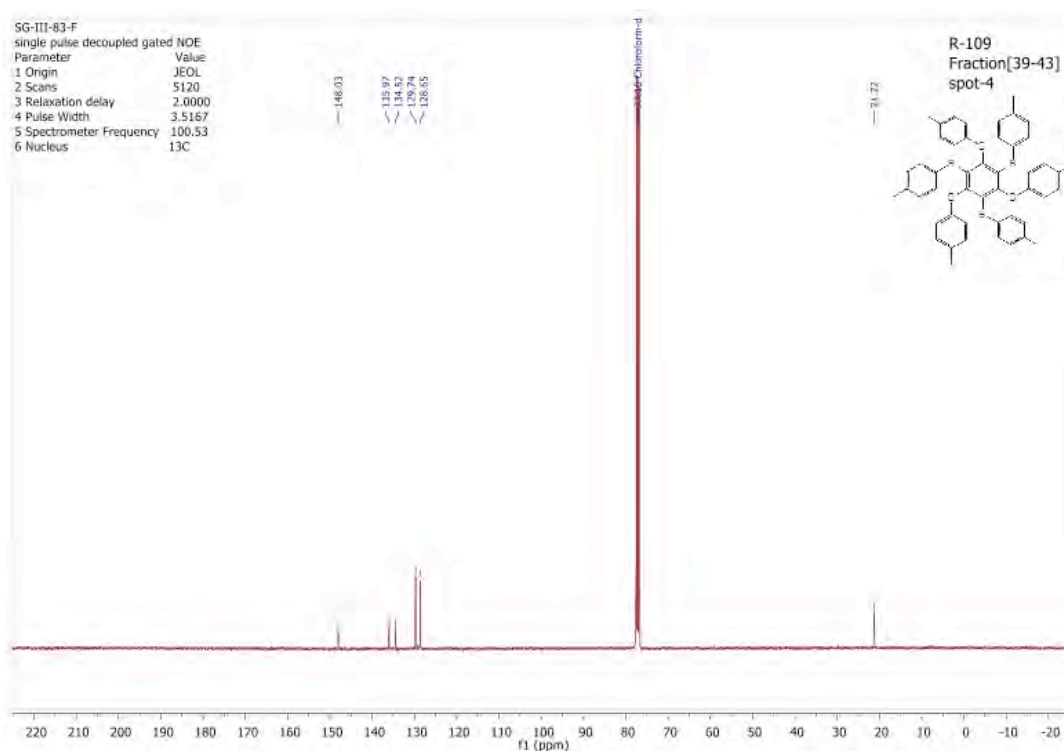


¹H-NMR (399.78 MHz, CDCl₃) SG-III-83B (fraction 2)

Fraction [3-17] (1st less polar spot on TLC): ¹H-NMR SG-III-83-D indicates disulfide containing Me groups (MePhSSPhMe). ¹H NMR (399.78 MHz, CDCl₃, ppm) δ = 7.38 (d_{app}, *J* = 8.1 Hz), 7.10 (d_{app}, *J* = 8.1 Hz), 2.32 (s, 6H). Mass: 0.7 mg.

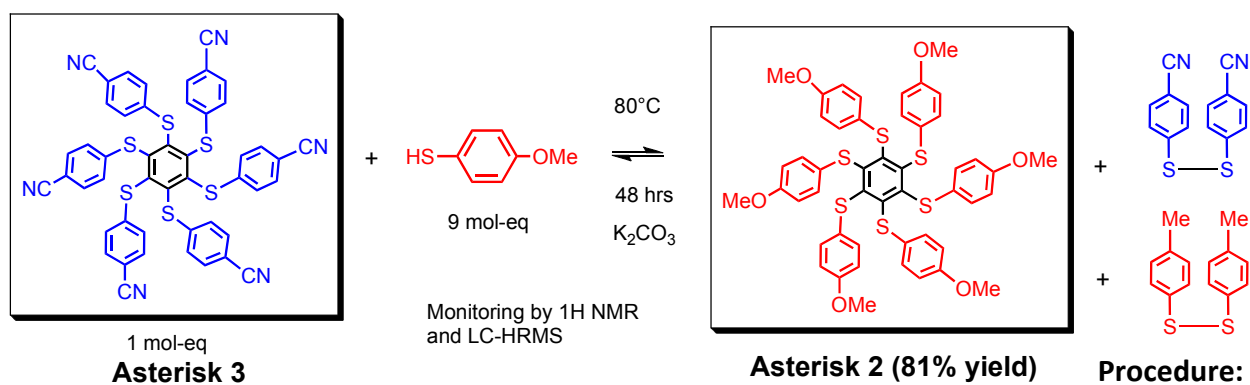


¹H-NMR (399.78 MHz, CDCl₃) SG-III-83D (fractions 3-17)



¹³C-NMR (399.78 MHz, CDCl₃) SG-III-83E (fraction 39-43)

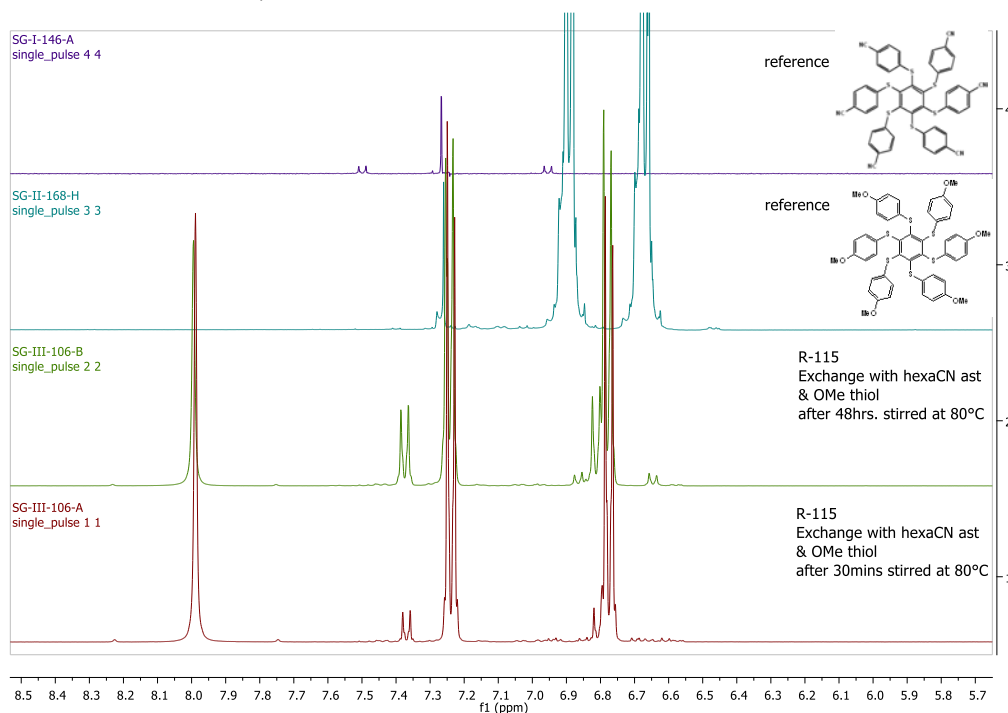
(R-115) CONVERSION OF HEXAKIS(4-CYANOPHENYLTHIO)BENZENE TO HEXAKIS(4-METHOXYPHENYLTHIO) BENZENE



Procedure. In an oven-dried tube, purged with argon, was added hexakis(4-cyanophenylthio) benzene (10.04 mg, 0.011 mmol, 1.00 mol-eq.), dried potassium carbonate (14.4 mg, 0.104 mmol, 9.45 mol-eq.) and 4-methoxybenzenethiol (14.8 mg, 0.105mmol, 13 μ L, 9.55 mol-eq.) in dry DMF (1.0 mL, dried and kept over activated 3 Å molecular sieves). Argon was bubbled through the mixture for 5-10 min.. The tube was sealed, and the reaction was stirred in an oil bath at 80°C for 2 days. DMF was removed from the reaction mixture on a rotary evaporator under reduced pressure. To the crude mixture was added water (30 mL) and it was extracted with toluene (4 \times 30 mL). The collected organic phases were dried over anhydrous MgSO₄, filtered, and the solvent evaporated. The products were separated by column chromatography over silica gel using acetone/cyclohex. (30:70 v/v) as eluent. Hexakis(*p*-tolylthio)benzene was isolated as a major product (8.1 mg, 81% yield).

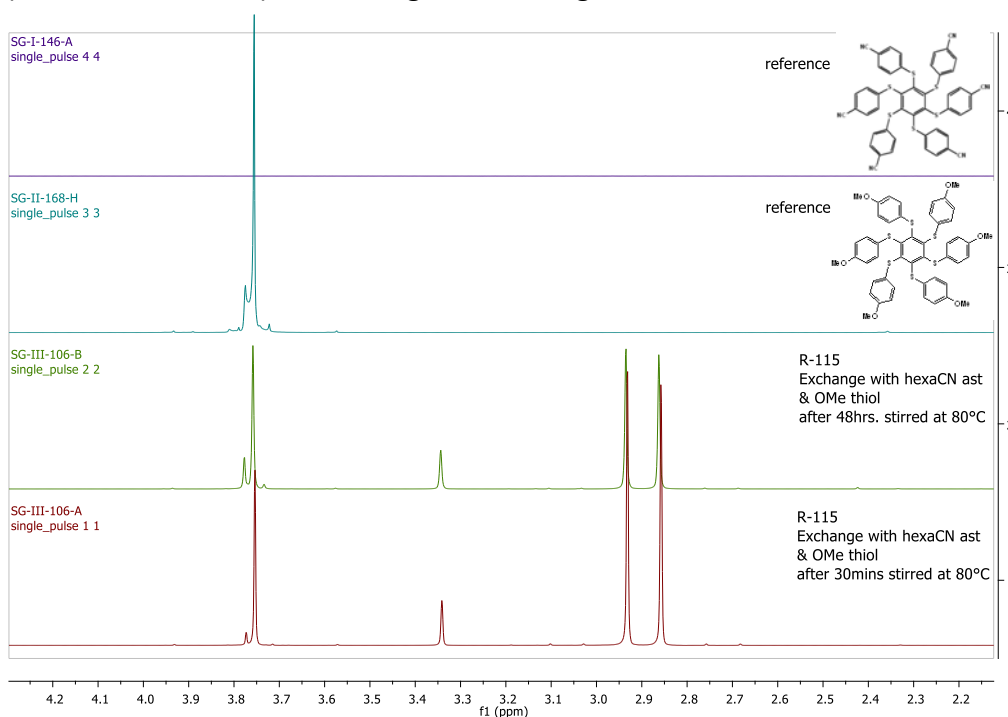
^1H NMR monitoring and analysis of the mixture

^1H NMR (399.78 MHz, CDCl_3 , SG-III-106-A) monitoring after stirring for 30 min. at 80°C below.



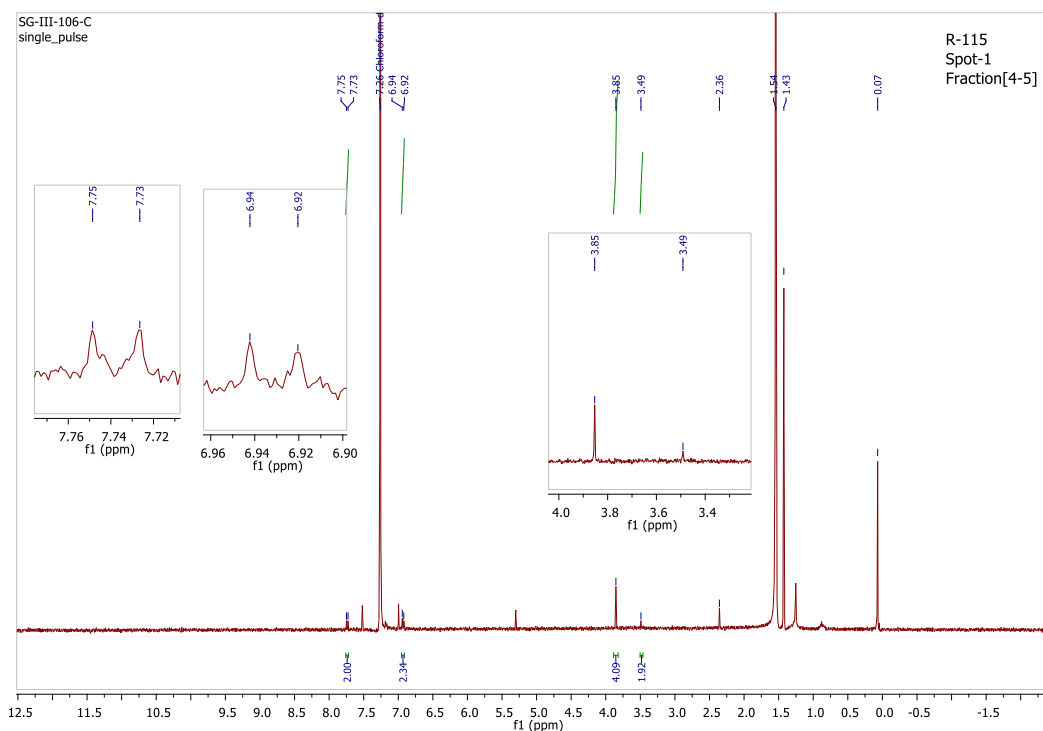
^1H NMR (399.78 MHz, CDCl_3 , SG-III-106-A)

^1H NMR (399.78 MHz, CDCl_3) monitoring after stirring for 48 hrs at 80°C below.



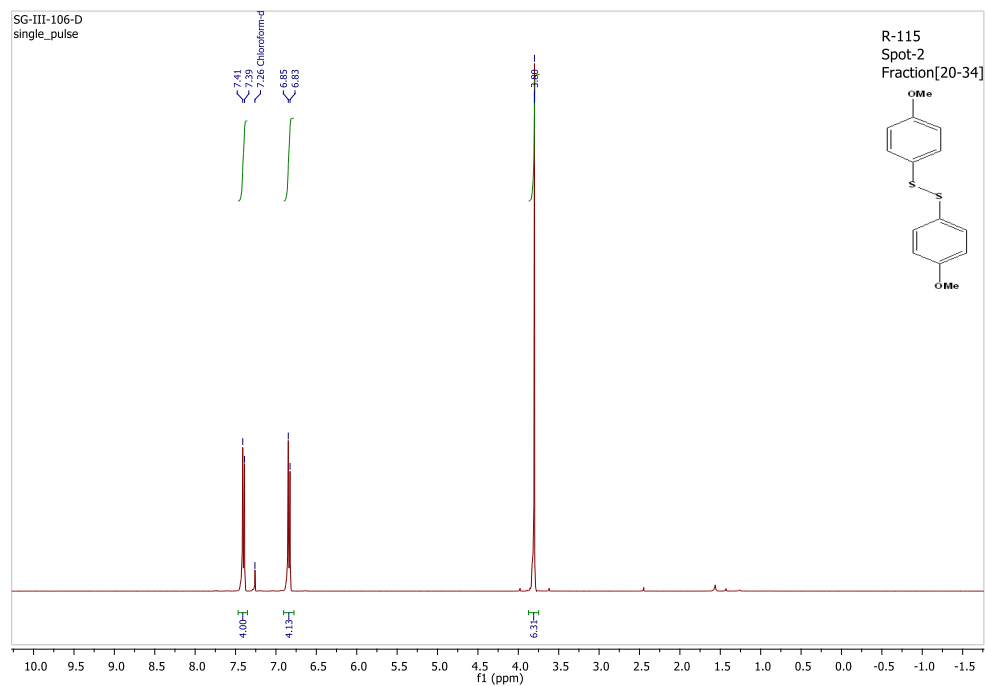
^1H NMR (399.78 MHz, CDCl_3 , SG-III-106-B)

Fraction [4-5] (1st spot on TLC, SG-III-106-C): Mass: 0.6 mg.

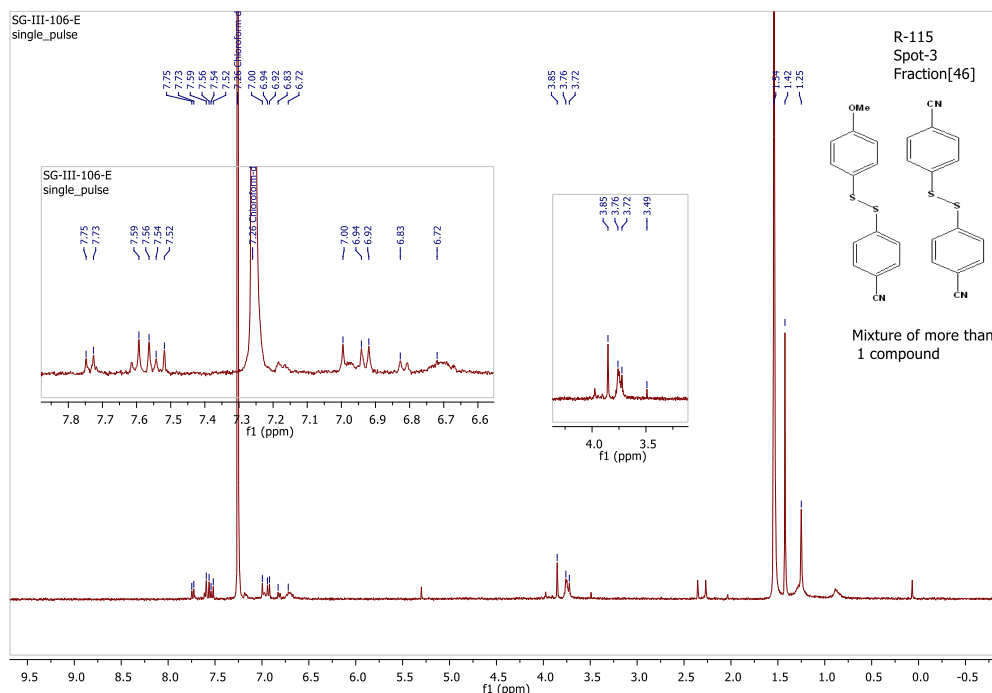


Fraction [6-19] (mixture of 1st and 2nd spot on TLC)

Fraction [20-34] (2nd spot on TLC): ¹H NMR (399.78 MHz, CDCl₃, SG-III-106-D) indicates disulfide containing OMe groups for **MeOPhSSPhOMe**, as compared to the reference disulfide. ¹H NMR (399.78 MHz, CDCl₃, ppm) δ = 7.40 (d, J = 9.0 Hz, 4H), 6.84 (d, J = 8.8 Hz, 4H), 3.78 (s, 6H). Mass: 87.7 mg.



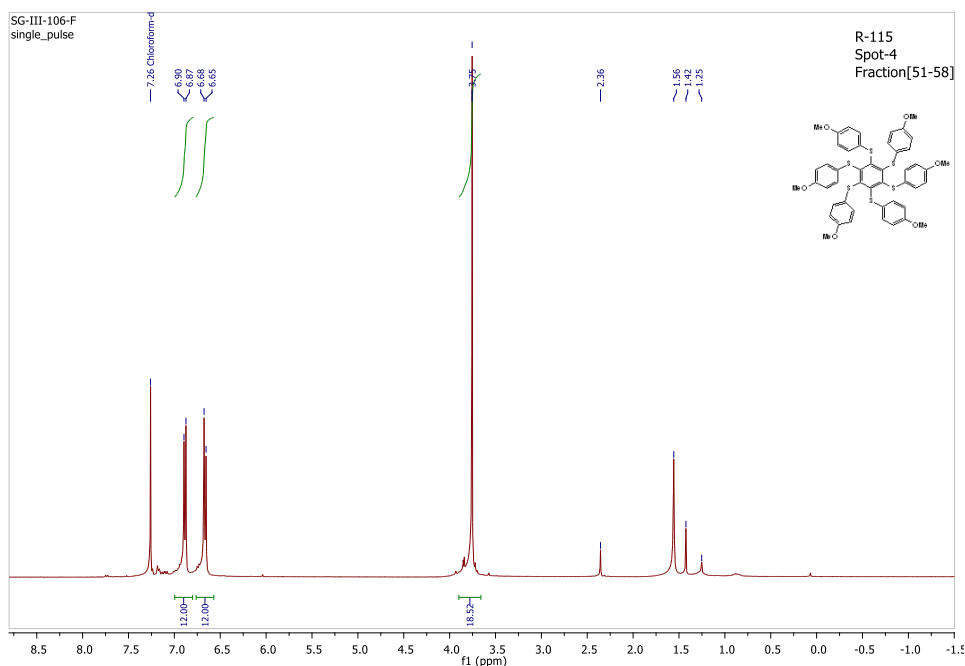
Fraction [46] (3rd spot on TLC): ¹H NMR (SG-III-106-E) indicates a mixture of disulfides containing OMe and CN groups (**MeOPhSSPhOMe**, **MeOPhSSPhCN**, **NCPHSSPhCN**). Mass: 0.1 mg.



¹H NMR (399.78 MHz, CDCl₃, SG-III-106-E)

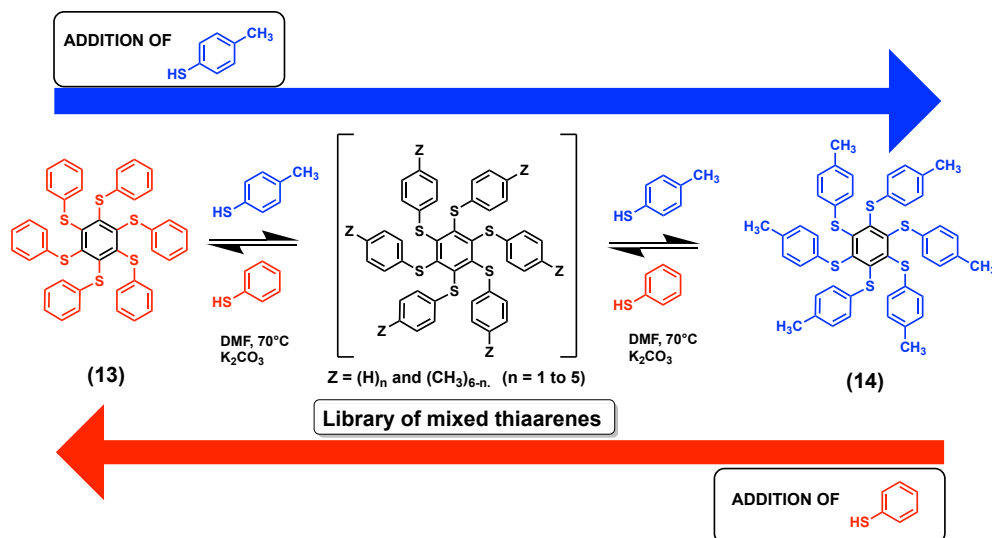
Fraction [47-50] (mixture of 3rd and 4th spot on TLC). Mass: 2.0 mg

Fraction [51-58] (4th spot on TLC): ¹H-NMR (SG-III-106-F) indicates **hexakis(p-methoxyphenylthio) benzene**, as compared to the reference asterisk. ¹H NMR (399.78 MHz, CDCl₃, ppm) δ = 6.89 (d_{app}, J = 8.7 Hz, 12H), 6.67 (d_{app}, J = 8.7 Hz, 12H), 3.76 (s, 18H). Mass: 8.1 mg.



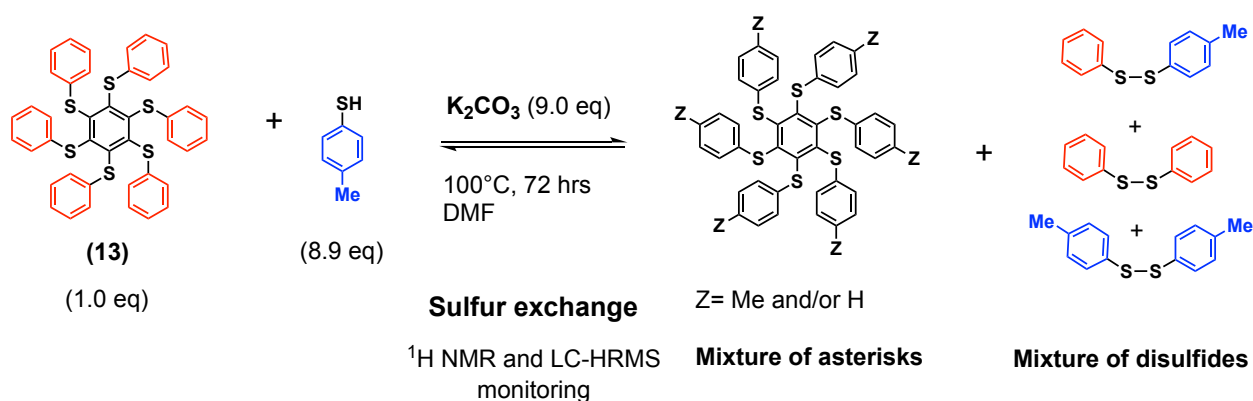
¹H NMR (399.78 MHz, CDCl₃, SG-III-106-F)

8.0 Demonstration of reversibility in S_NAr



Conclusion: Asterisk (**13**) reacted with *p*-thiocresol (8.9 mol-eq) to provide a library of mixed thiaarenes and (**14**) (Figure 4, reaction from left to right – **blue arrow**). When asterisk (**14**) reacted with thiophenol (9 mol-eq.), a similar library of mixed asterisks and (**13**) was produced (Figure 4 reaction from right to left – **red arrow**). The convergence of the product distribution in the two processes points to the reversible nature of the S_NAr process. It was monitored by ¹H NMR and LC-HRMS, as shown below.

SULFUR EXCHANGE REACTIONS WITH HEXAKIS(PHENYLTHIO)BENZENE AND 4-METHYLBENZENETHIOL



(R-124) Procedure: In an oven-dried sealed tube, purged with argon, was added hexakis(phenylthio)benzene (50.1 mg, 0.0689 mmol, 1.00 mol-eq), dried potassium carbonate (85.7 mg, 0.620 mmol, 9.00 mol-eq.) and 4-methylbenzenethiol (76.4 mg, 0.615 mmol, 8.93 mol-eq.) in dry DMF (0.9 mL, dried with molecular sieves 3 Å). Argon was bubbled through the mixture for 5-10 minutes in the tube. The tube was sealed under argon, and the reaction was stirred at 100°C in an oil bath for 3 days. DMF was removed from reaction mixture by evaporation under vacuum. To the crude mixture was added H₂O (20 mL), and the aqueous phase was extracted with toluene (4×20 mL). The collected organic phases were dried over anhydrous MgSO₄, filtered,

and evaporated. TLC (SiO₂; acetone/cyclohexane 3:7 V/V and 60% toluene/cyclohexane (60:40 V/V) indicated two spots, the more polar was yellow. The solid was triturated with EtOH (5 mL) and filtered. A yellow solid was obtained: mass: 43.9 mg

¹H NMR monitoring and analysis of the mixture

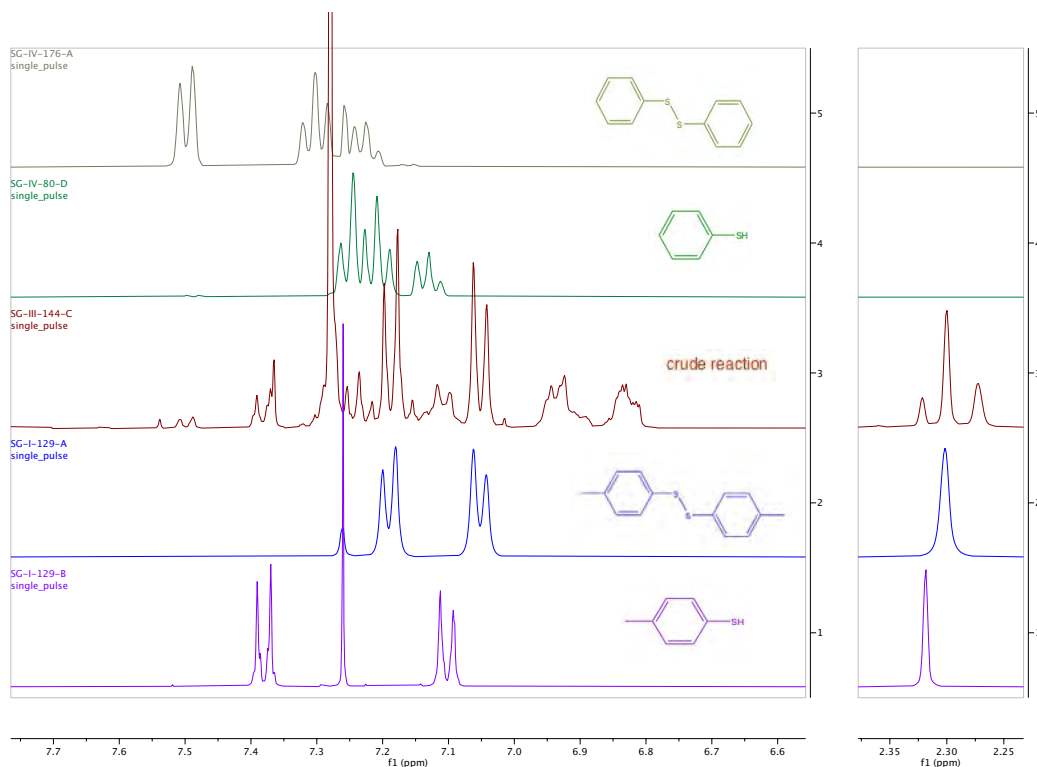
RESULTS

¹H NMR **SG-III-144-A** (CDCl₃, 400MHz): reference asterisk (**13**)

¹H NMR **SG-III-144-B** (CDCl₃, 400MHz): reference asterisk (**14**)

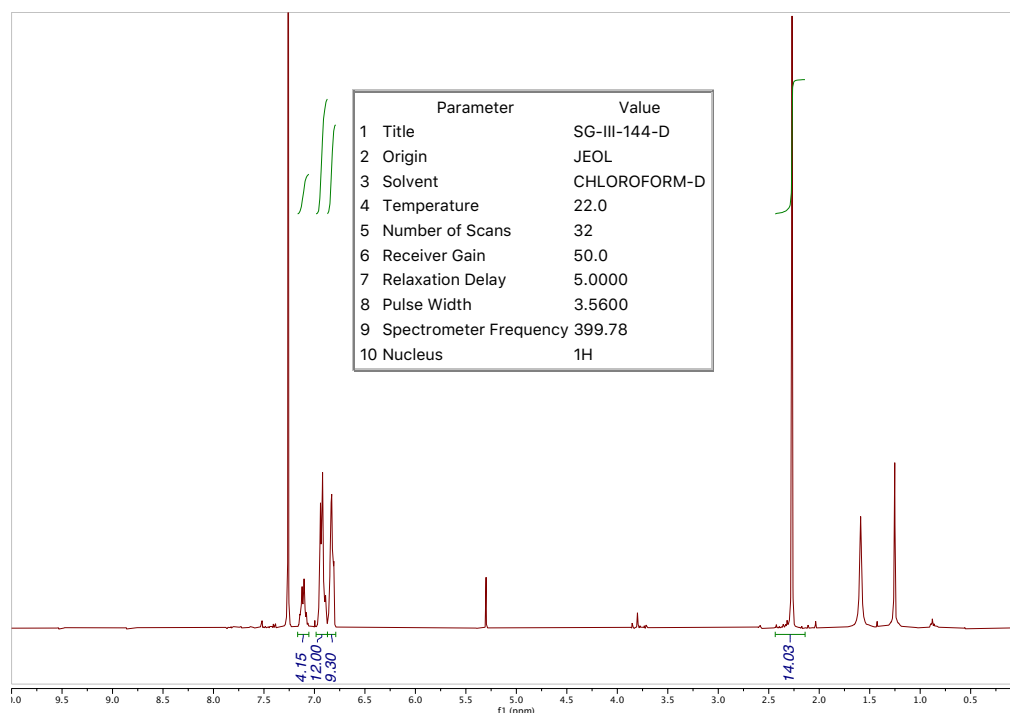
¹H NMR **SG-III-144-C** (CDCl₃, 400MHz): Small workup, after stirred for 48hrs. at 100°C

¹H NMR **SG-III-144-D** (CDCl₃, 400MHz): crude solid triturated with EtOH.

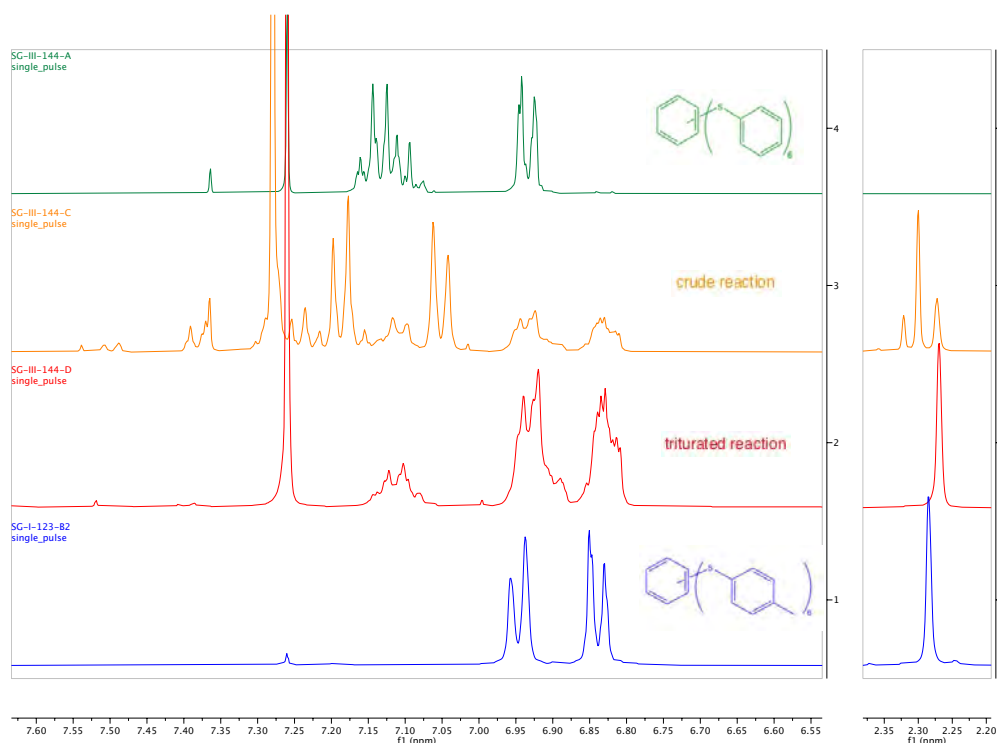


(R-124) ¹H NMR (399.78 MHz, CDCl₃): **Spectra 1 (violet)**: reference spectra of 4-methylbenzenethiol. **Spectra 2 (blue)**: reference spectra of *p*-tolyl disulfide. **Spectra 3 (red)**: spectra of the crude reaction. **Spectra 4 (green)**: reference spectra of benzenethiol. **Spectra 5 (yellow-green)**: reference spectra of phenyl disulfide.

Conclusion: ¹H NMR indicated the presence of *p*-tolyl disulfide and *p*-thiocresol, as expected. Traces of phenyl disulfide and benzenethiol can also be seen. These species can only come from the displacement of the phenylthio groups from starting hexakis(phenylthio)benzene (**13**).



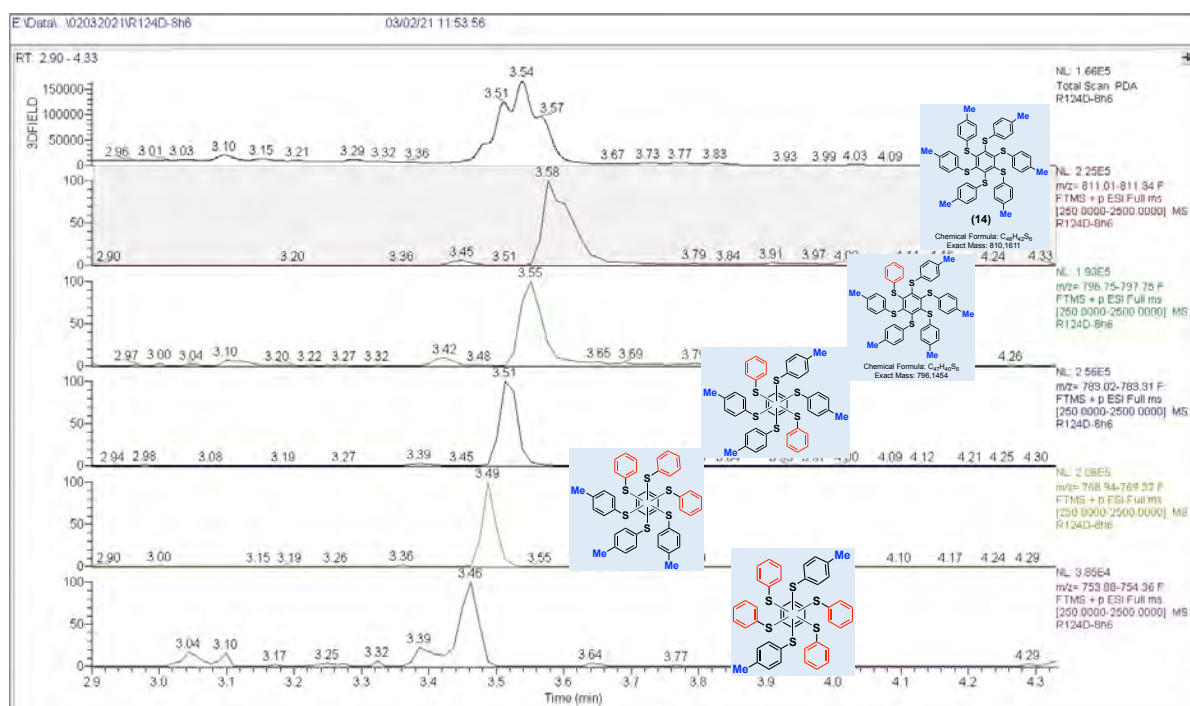
(R-124) ^1H NMR (399.78 MHz, CDCl_3): A trituration with EtOH removed most disulfides and thiols leaving mainly a mixture of asterisks. Most of the asterisks signals (6.8-7.0 ppm) of the crude and trituated reaction do not correspond to the reference spectra of asterisk (**13**) and (**14**), and additional signals are observed.



(R-124) ^1H NMR (399.78 MHz, CDCl_3): **Spectra 1 (blue)**: reference spectra of hexakis(*p*-tolylthio)benzene (**14**). **Spectra 2 (red)**: spectra after trituration with EtOH. **Spectra 3 (orange)**: spectra of the crude reaction. **Spectra 4 (green)**: reference spectra of hexakis(phenylthio)benzene (**13**).

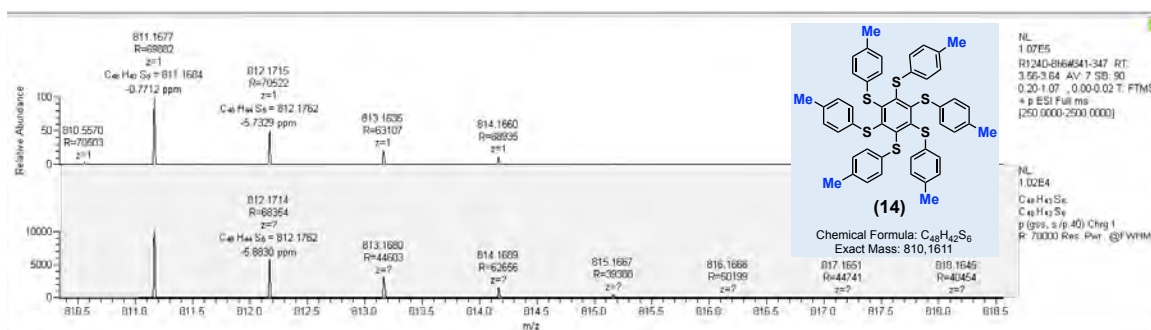
Conclusion: Sulfur components exchanges were clearly demonstrated by ^1H NMR in that direction of exchange. A mixture of asterisks incorporating phenyl and *p*-tolylthio groups was formed. The presence of benzenethiol and phenyl disulfide in the crude mixture confirmed the release of benzenethiol from (13). A relative integration in the aromatic region shows an average of 4.6 tolyl groups incorporated into the structures of the asterisks, as a mixture.

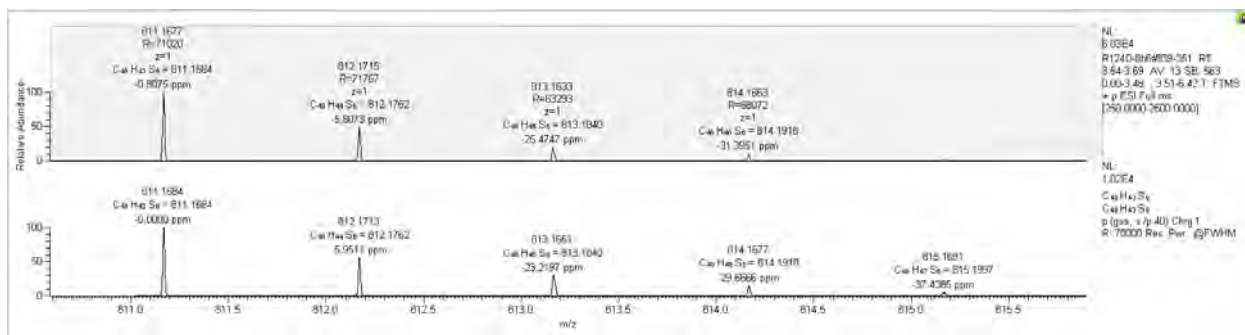
LC-HRMS analysis of the crude mixture



6 Substitutions by 4-MePhSH:

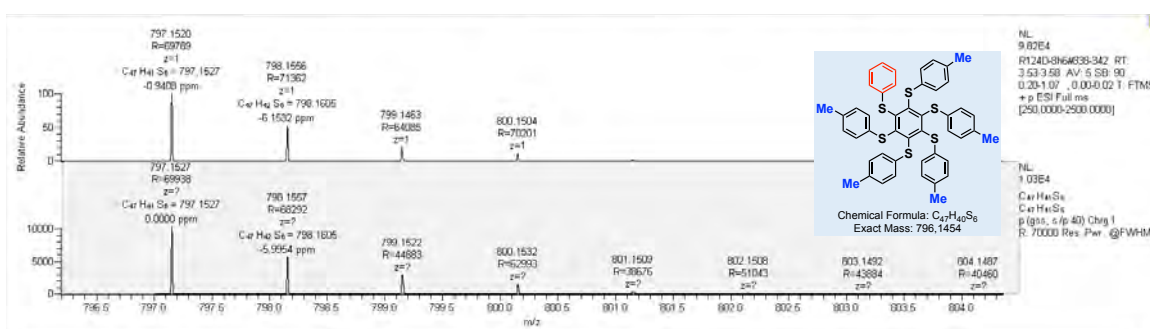
HRMS (ESI+) calculated for $[\text{C}_{48}\text{H}_{42}\text{S}_6 + \text{H}^+]$: 811.1684 Da, found $[\text{M} + \text{H}^+]$ 811.1677 m/z;





5 Substitutions by 4-MePhSH:

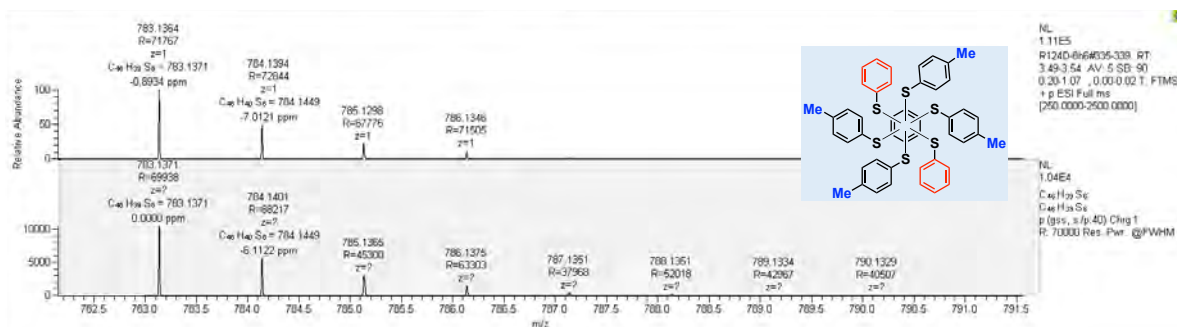
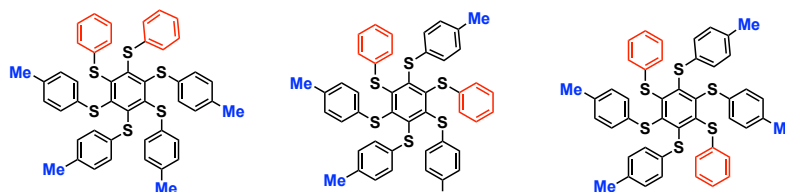
HRMS (ESI+) calculated for [C₄₇H₄₀S₆ + H⁺]: 797.1527 Da, found [M+H⁺] 797.1520 m/z;



4 Substitutions by 4-MePhSH:

HRMS (ESI+) calculated for [C₄₆H₃₈S₆ + H⁺]: 783.1371 Da, found [M+H⁺] 783.1364 m/z;

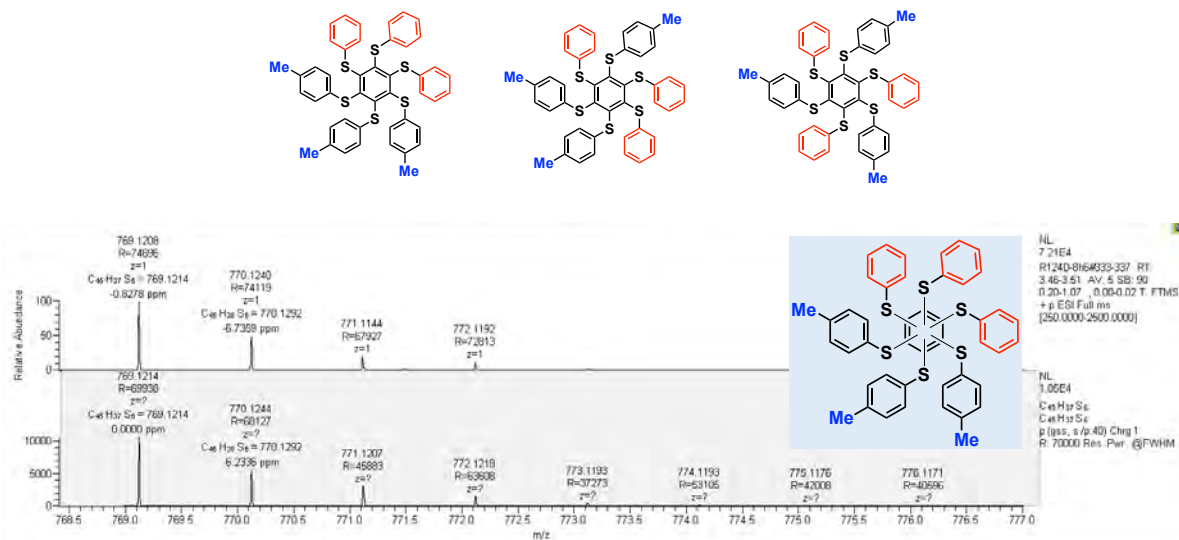
Possible isomers:



3 Substitutions by 4-MePhSH:

HRMS (ESI+) calculated for [C₄₅H₃₆S₆ + H⁺]: 769.1214 Da, found [M+H⁺] 769.1208 m/z;

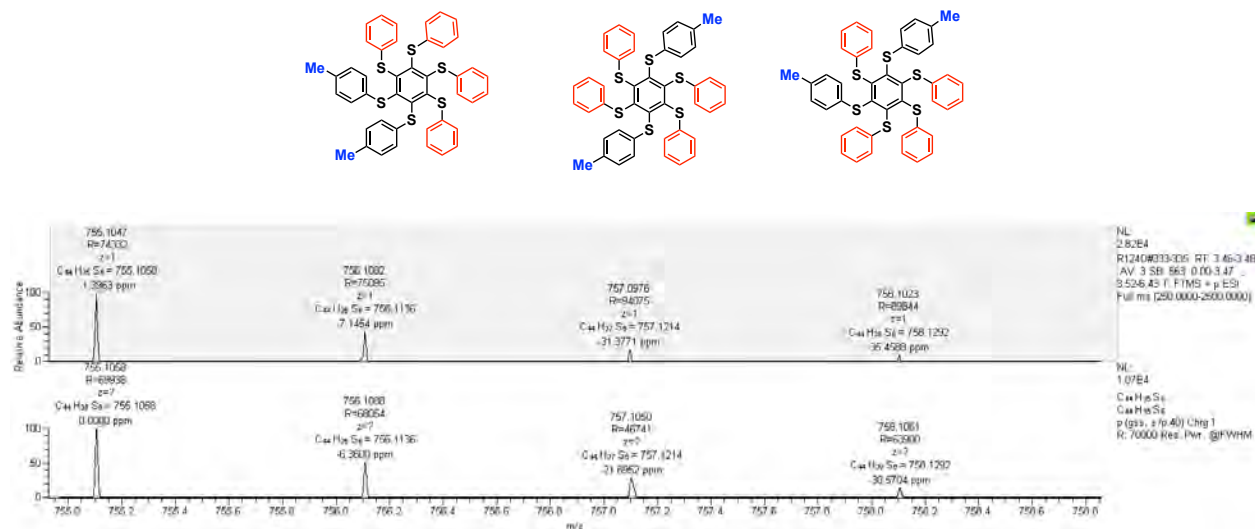
Possible isomers:



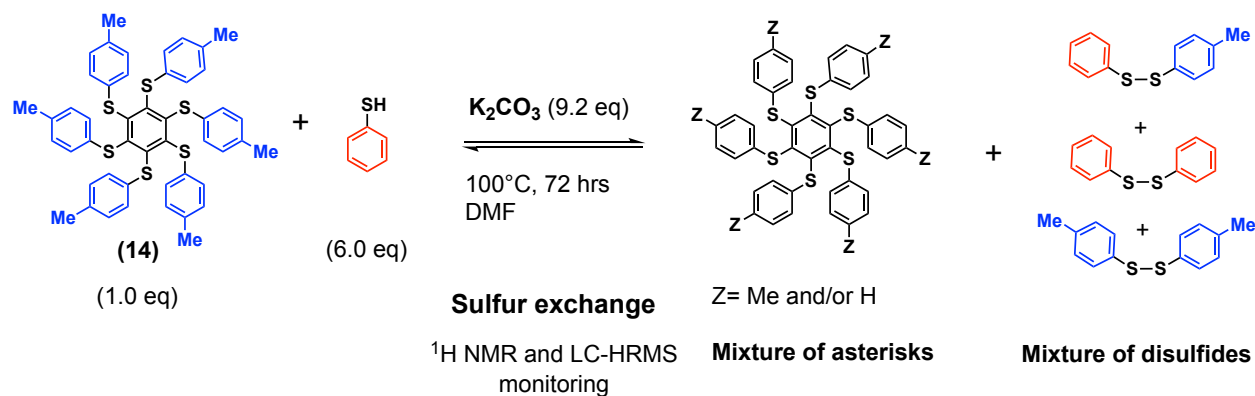
2 Substitutions by 4-MePhSH:

HRMS (ESI+) calculated for $[C_{44}H_{34}S_6 + H^+]$: 755.1058 Da, found $[M+H^+]$ 755.1407 m/z;

Possible isomers:



Sulfur exchange with hexakis(4-tolylthio)benzene and 4-methylbenzenethiol

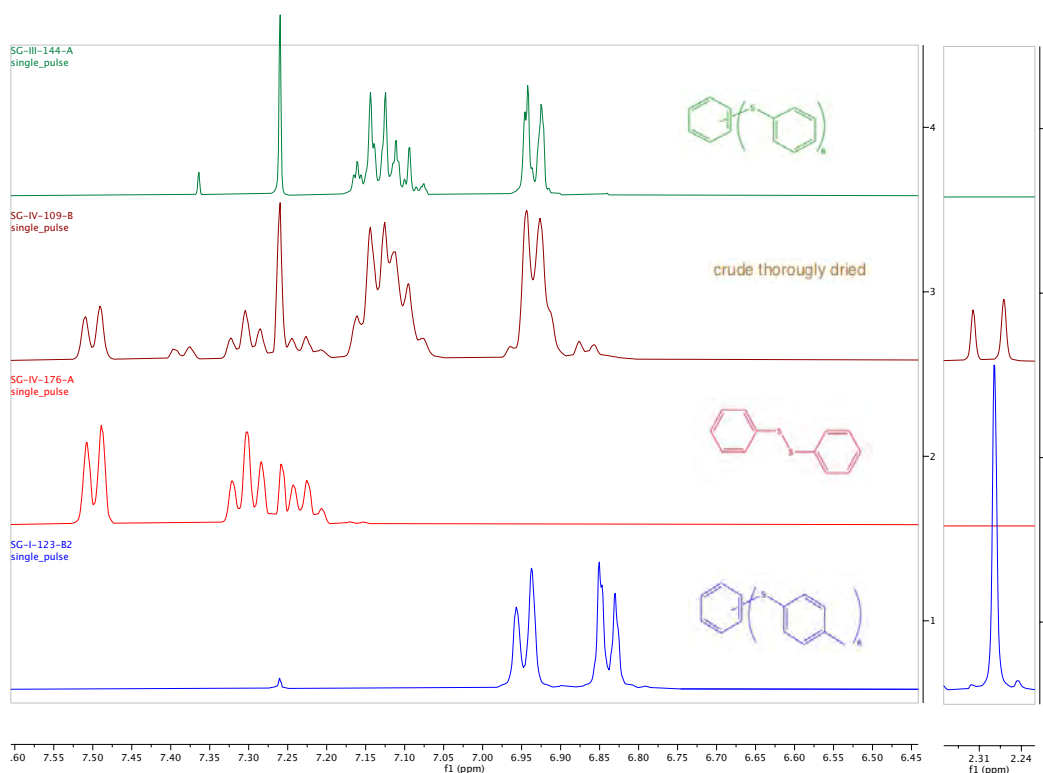


(R-177) Procedure: In an oven-dried sealed tube, purged with argon, was added hexakis(4-methylphenylthio) benzene (**14**) (50.4 mg, 0.0621 mmol, 1.00 mol-eq.), dried potassium carbonate (78.5 mg, 0.568 mmol, 9.15 mol-eq.) and thiophenol (41.0 mg, 0.372 mmol, 38 μ L, 6.0 mol-eq.) in dry DMF (1.0 mL, dried with molecular sieves 3 Å). Argon was bubbled through the mixture for 5-10 minutes in the tube. It was sealed under argon, and the reaction was stirred at 100 $^{\circ}$ C in an oil bath for 3 days. To the crude mixture was added H₂O (20 mL), and the aqueous phase was extracted with toluene (3 \times 20 mL). The collected organic phases were dried over anhydrous MgSO₄, filtered, and evaporated. Mass: 53.1 mg.

¹H NMR monitoring and analysis of the mixture

1H-NMR **SG-IV-109-A**: small workup, after 3 days at 100 $^{\circ}$ C

1H-NMR **SG-IV-109-B**: after final workup, 3 days at 100 $^{\circ}$ C



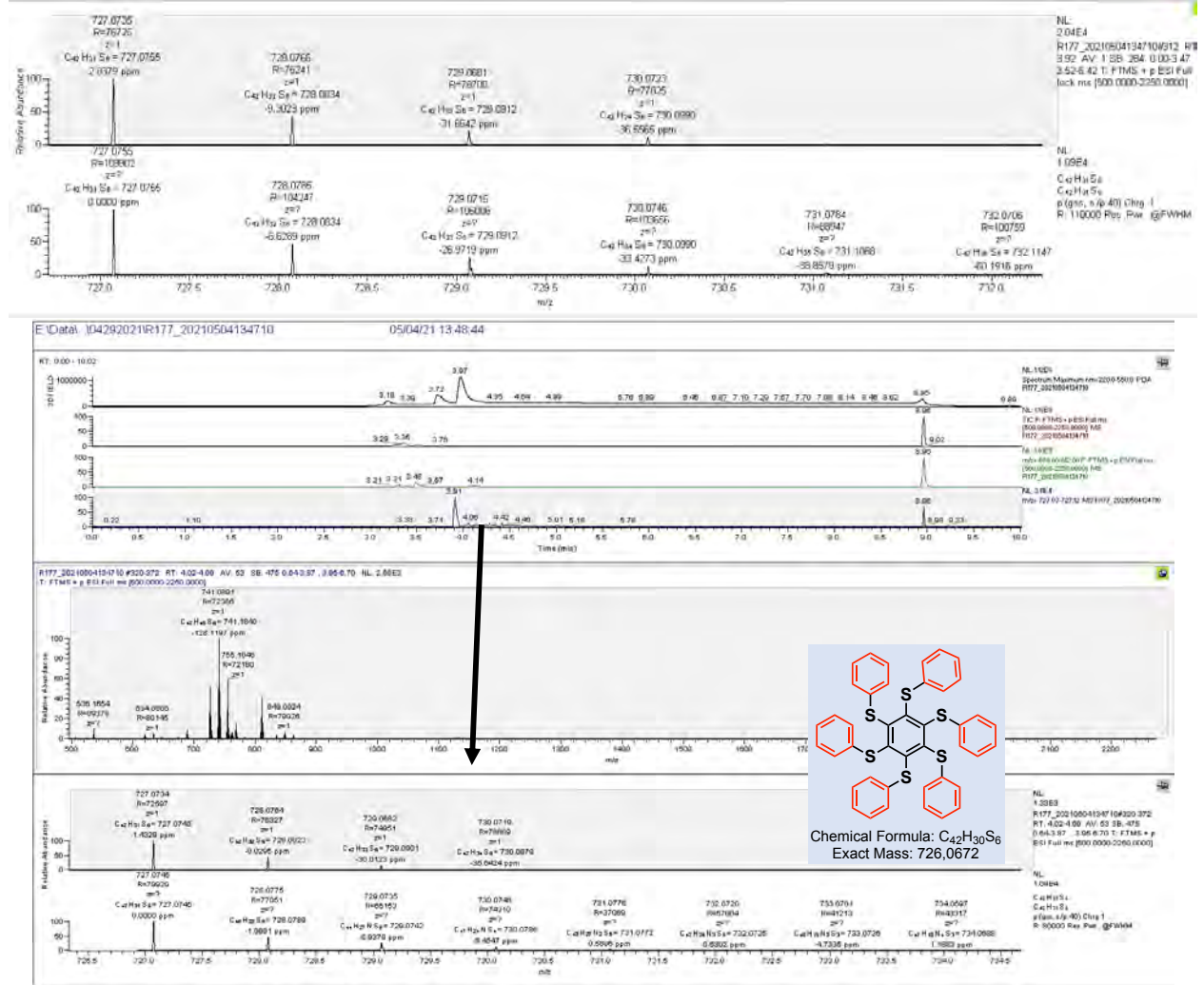
(R-177) ¹H NMR (399.78 MHz, CDCl₃): **Spectra 1 (blue)**: reference spectra of hexakis (*p*-tolylthio) benzene (**14**). **Spectra 2 (red)**: reference spectra of phenyl disulfide. **Spectra 3 (dark red)**: spectra of the crude reaction. **Spectra 4 (green)**: reference spectra of hexakis (phenylthio)benzene (**13**).

Conclusion: In the crude spectrum, as expected, phenyl disulfide can be clearly identified. The starting asterisk hexakis(*p*-tolylthio)benzene (**14**) had mostly reacted, and a mixture of new asterisks were generated, likely to be hexakis(phenylthio)benzene (**13**) as a major component, as well as mixed asterisks and/or a mixed disulfide.

LC-HRMS analysis of the crude mixture

6 Substitutions by PhSH:

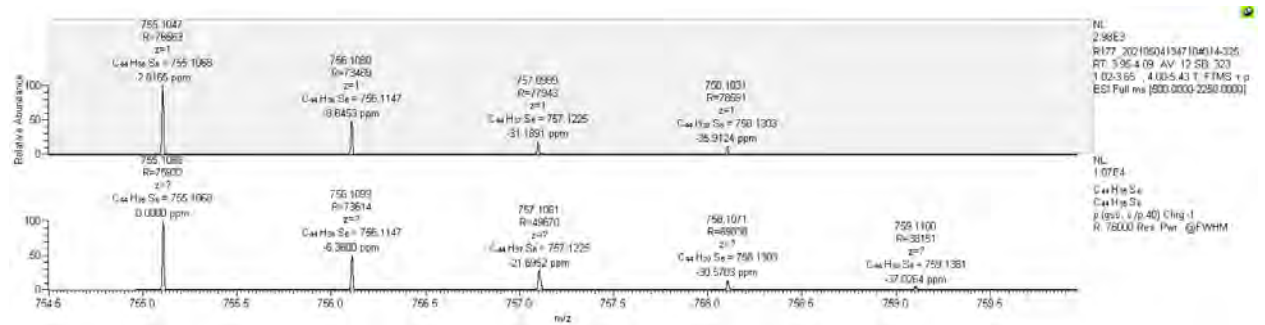
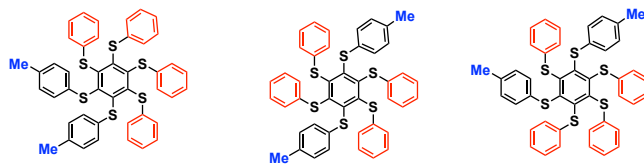
HRMS (ESI+) calculated for $[C_{42}H_{30}S_6 + H^+]$: 727.0755 Da, found $[M+H^+]$ 727.0735 m/z;



4 Substitutions by PhSH:

HRMS (ESI+) calculated for $[C_{44}H_{34}S_6 + H^+]$: 755.1068 Da, found $[M+H^+]$ 755.1047 m/z;

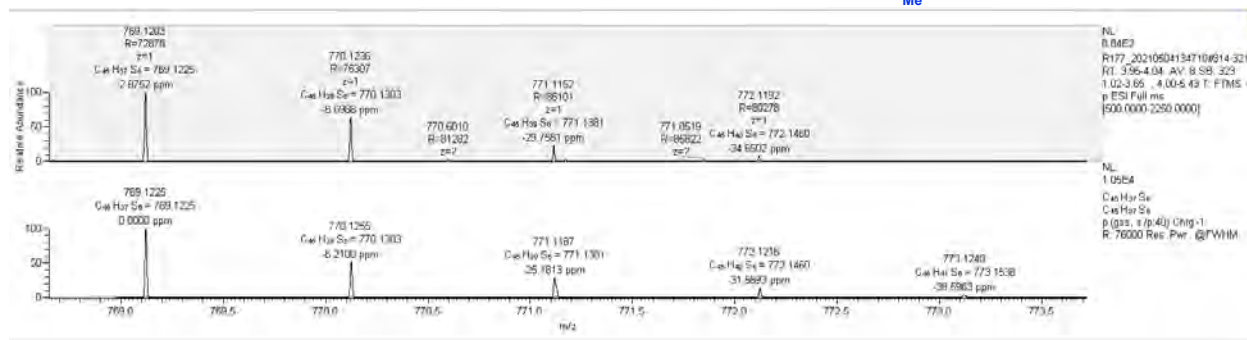
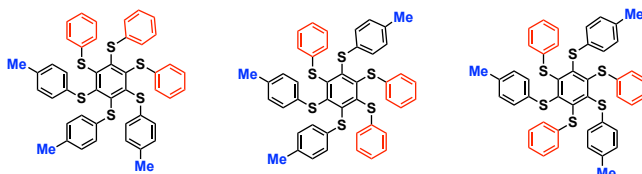
Possible isomers:



3 Substitutions by PhSH:

HRMS (ESI+) calculated for $[C_{45}H_{36}S_6 + H^+]$: 769.1225 Da, found $[M+H^+]$ 769.1203 m/z;

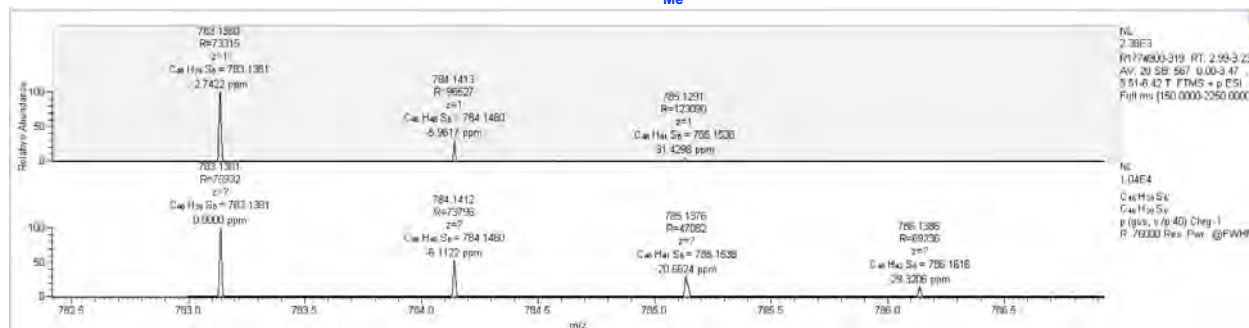
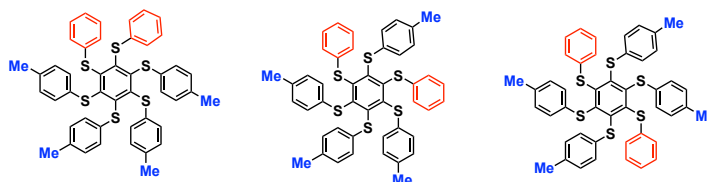
Possible isomers:



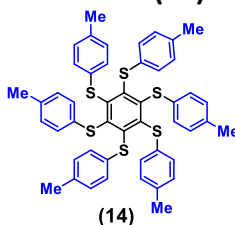
2 Substitutions by PhSH:

HRMS (ESI+) calculated for $[C_{46}H_{38}S_6 + H^+]$: 783.1381 Da, found $[M+H^+]$ 783.1360 m/z;

Possible isomers:

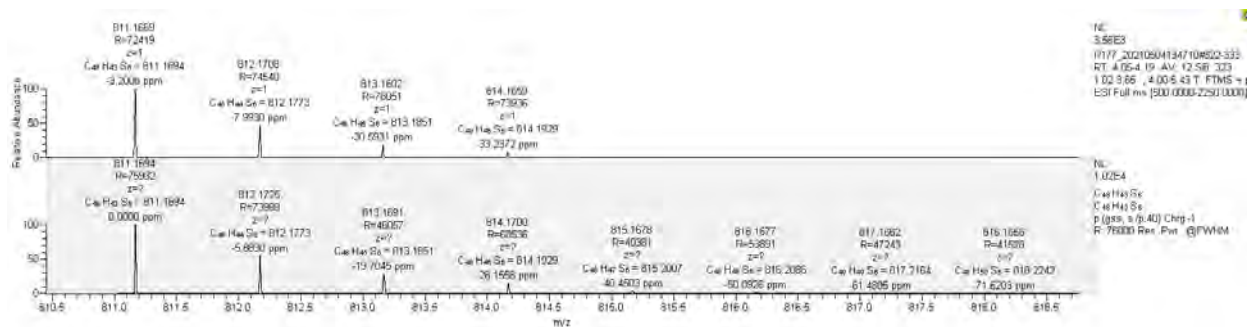


Asterisk (14)

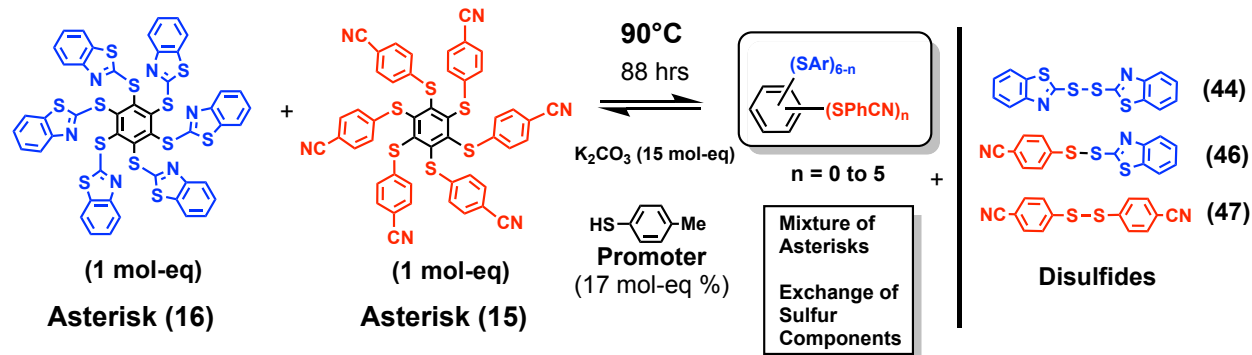


0 Substitution by PhSH:

HRMS (ESI+) calculated for $[C_{48}H_{42}S_6 + H^+]$: 811.1694 Da, found $[M+H^+]$ 811.1669 m/z;



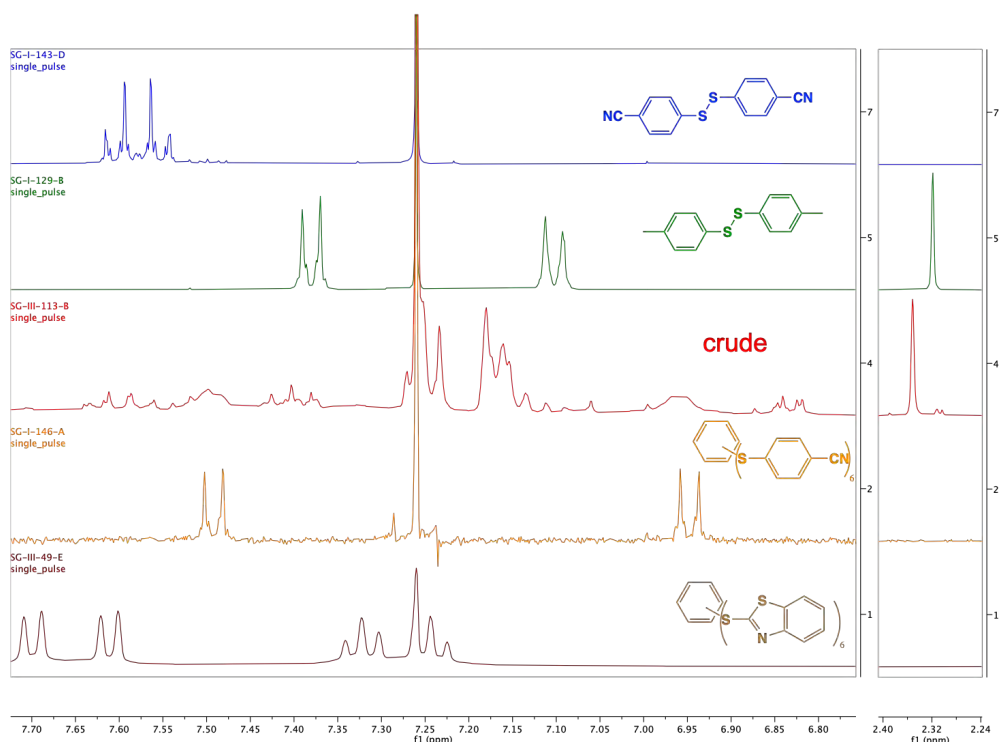
9.0 Exchange of sulfur components between two asterisks with a thiol as a promoter (demonstration of reversibility)



(R-114) Procedure: In an oven-dried sealed tube, purged with argon, was added hexakis(4-cyano-phenylthio)benzene asterisk **(15)** (8.23 mg, 0.0094 mmol, 1,00 mol-eq.), dried potassium carbonate (20.0 mg, 0.144 mmol, 20 mol%, 15,3 mol-eq.) and hexakis(benzenethiazolyl-2-thio)benzene **(16)** (10.0 mg, 0.0093 mmol, 1,00 mol-eq.), 4-methylbenzenethiol (0.2 mg, 0.0016 mmol, 17 mol% relative to **15** or **16**) in dry DMF (0.9 mL - dried with molecular sieves 3Å). Argon was bubbled through the mixture for 5-10 minutes in the tube. It was sealed, and the reaction was stirred at 90°C in an oil bath for 88 hrs. Most of DMF was removed from reaction mixture in vacuo. To the crude mixture was added H₂O (30 mL), and the aqueous phase was extracted with toluene (4×30 mL). The collected organic phases were dried over anhydrous MgSO₄, filtered, and evaporated. TLC (30% acetone/70% cyclohexane V/V) indicated several spots and the mass obtained was 2.4 mg.

¹H NMR monitoring and analysis of the mixture

Results: ¹H-NMR **SG-III-113-B** (CDCl₃, 400MHz): After workup and drying.



(R-114) ^1H NMR (399.78 MHz, CDCl_3): **Spectra 1 (brown)**: reference spectra hexakis(benzenethiazolyl-2-thio)benzene (**16**). **Spectra 2 (orange)**: reference spectra of hexakis(*p*-cyanophenylthio)benzene (**15**). **Spectra 3 (red)**: spectra of crude reaction mixture. **Spectra 4 (green)**: reference spectra of *p*-tolyl disulfide. **Spectra 5 (blue)**: reference spectra of *p*-cyanophenyl disulfide (**47**)

Conclusion: According to ^1H -NMR, there is no *p*-tolyl disulfide in the crude reaction (nor thiol). The signals of hexakis(benzenethiazolyl-2-thio)benzene (**16**) asterisk disappeared, but we cannot rule out the presence of hexakis(4-cyanophenylthio)benzene asterisk (**15**). From a comparison to the reference spectra of 4-cyanophenyl disulfide (spectra 5, blue), we can conclude to the presence in the crude of 4-cyanophenylthio groups, either from mixed disulfides (**46**), from some mixed cyano-containing asterisks or from 4-cyanophenyl disulfide (**47**). Overall, we can conclude for some sulfur component exchanges, as confirmed by LC-HRMS (next section).

LC-HRMS analysis of the crude mixture

Conclusion: Exchange of sulfur components between asterisks (**15**) and (**16**) through reversible $\text{S}_\text{N}\text{Ar}$ in the “sulfur dance” is promoted by *p*-thiocresol. Products resulting from reversible exchange of sulfur components from asterisks (**15**) and (**16**) are observed, as determined by LC-HRMS (below, Figure 5b and LC-HRMS chromatogram)

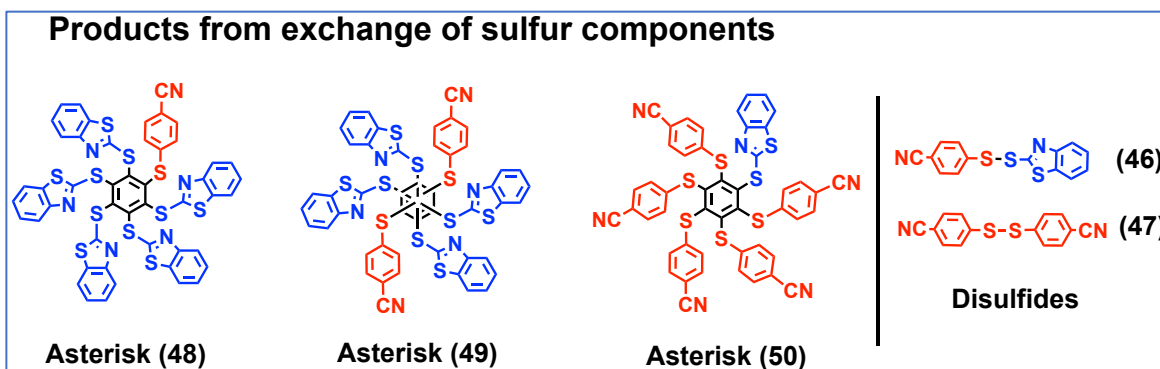
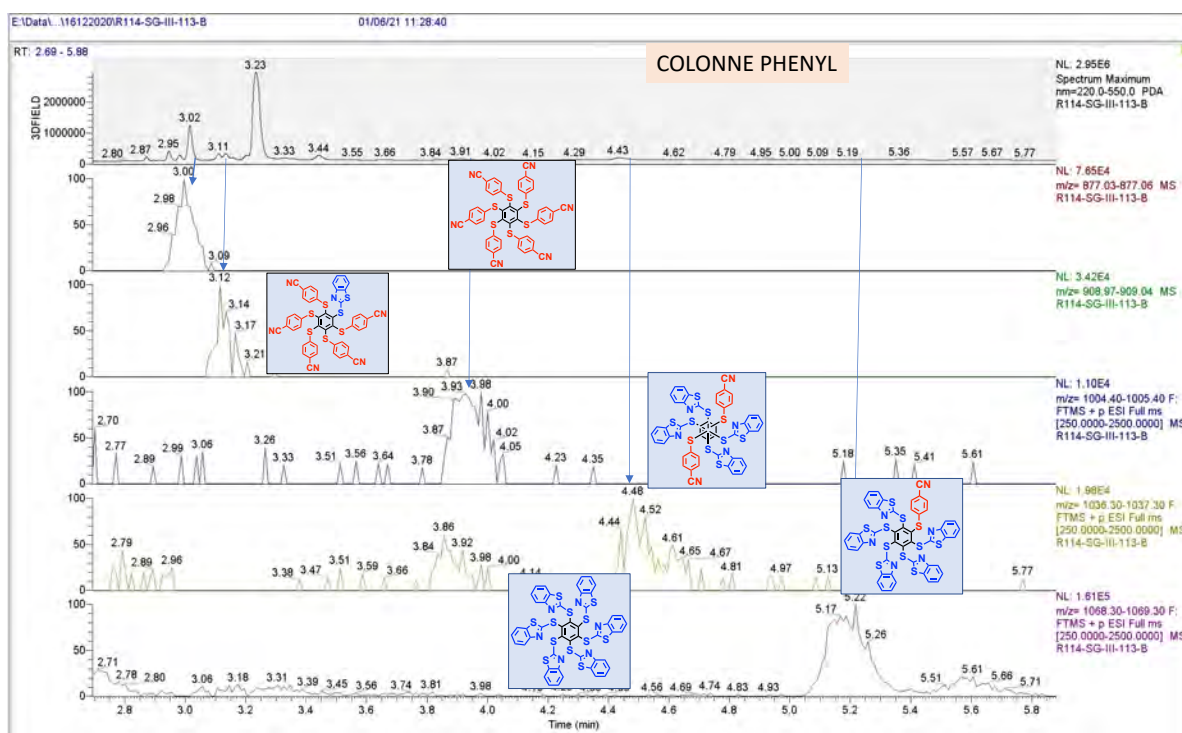


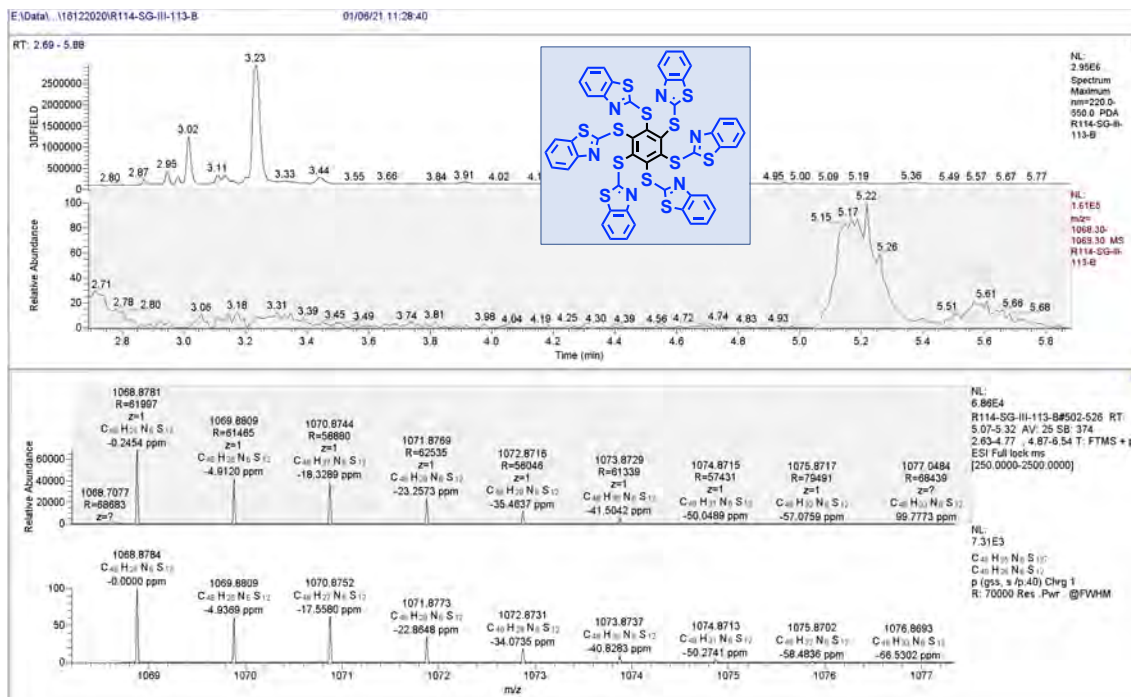
Figure 5b: products detected by LC-HRMS

**LC-HRMS Chromatogram of the mixture (R-113):
sulfur component exchanges**



Asterisk (16)

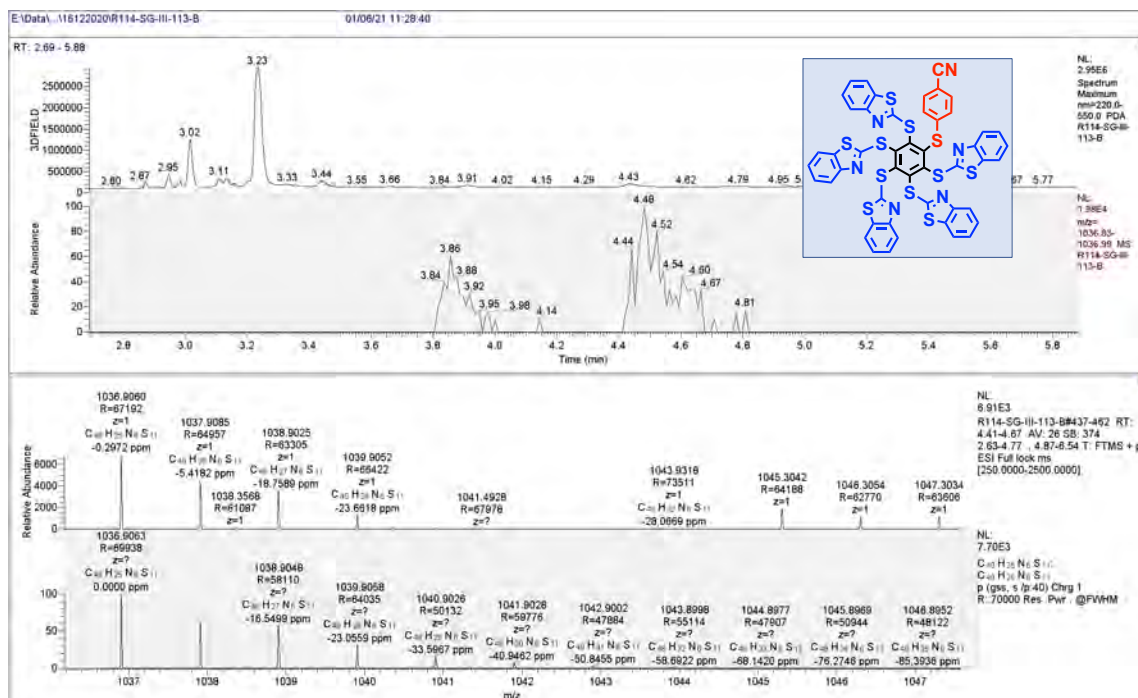
HRMS (ESI+) calculated for $[C_{48}H_{24}N_6S_{12} + H^+]$: 1068.8784 Da, found $[M+H^+]$ 1068.8781 m/z;



Asterisk (48):

1 Substitution by 4-CNPhSh:

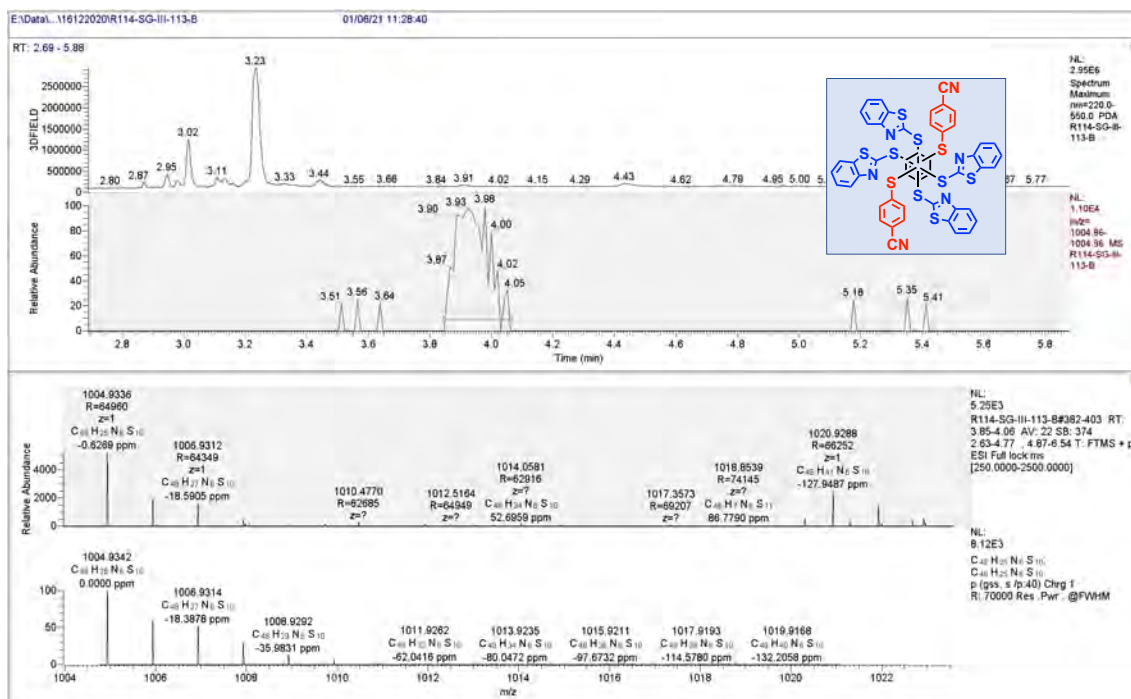
HRMS (ESI+) calculated for $[C_{48}H_{24}N_6S_{11} + H^+]$: 1036.9063 Da, found $[M+H^+]$ 1036.9060 m/z;



Asterisk (49)

2 Substitutions by 4-CNPhSH:

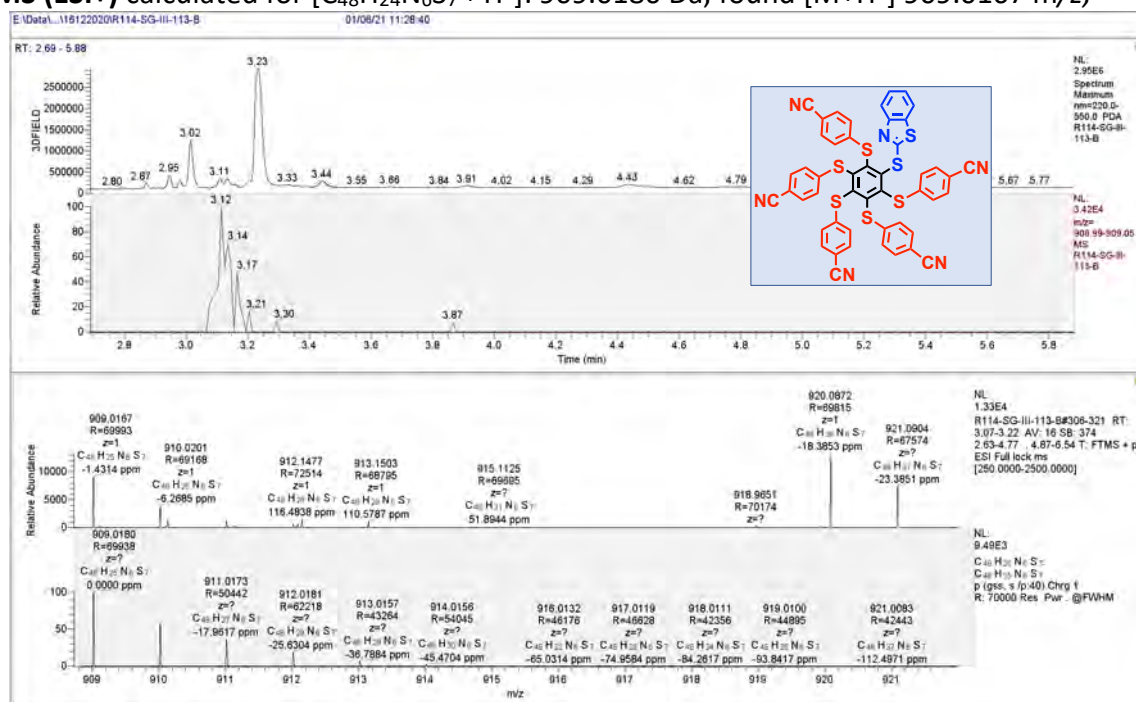
HRMS (ESI+) calculated for $[C_{48}H_{24}N_6S_{10} + H^+]$: 1004.9432 Da, found $[M+H^+]$ 1004.9336 m/z;



Asterisk (50)

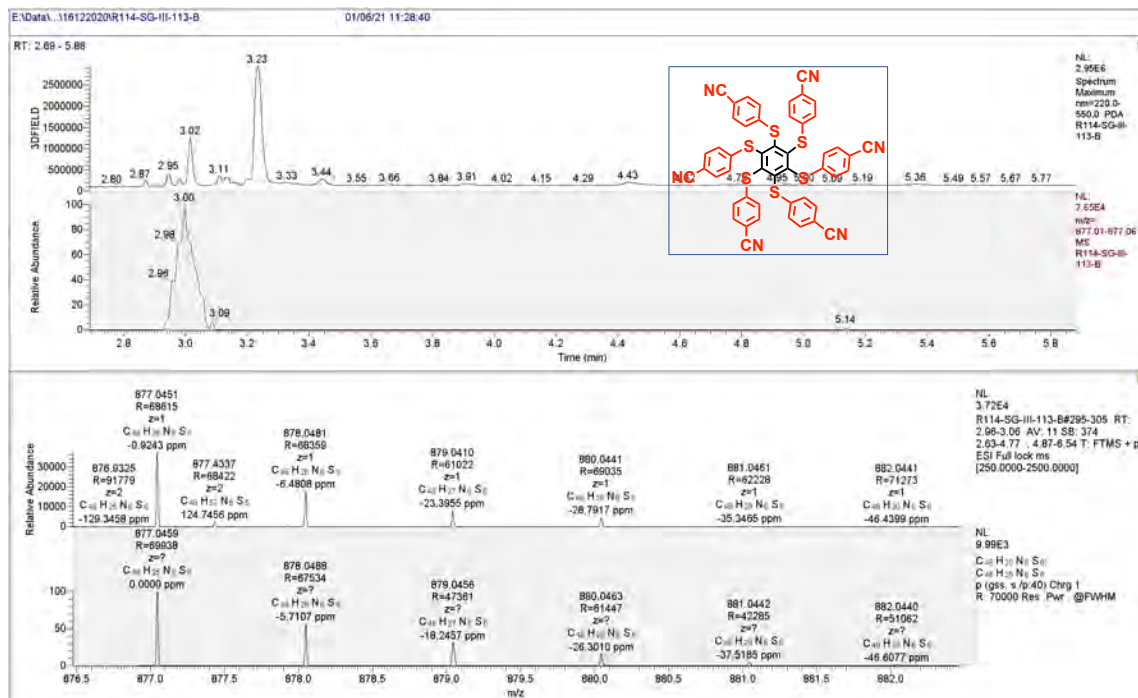
4 Substitutions by 4-CNPhSH:

HRMS (ESI+) calculated for $[C_{48}H_{24}N_6S_7 + H^+]$: 909.0180 Da, found $[M+H^+]$ 909.0167 m/z;

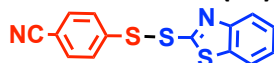


Asterisk (15)

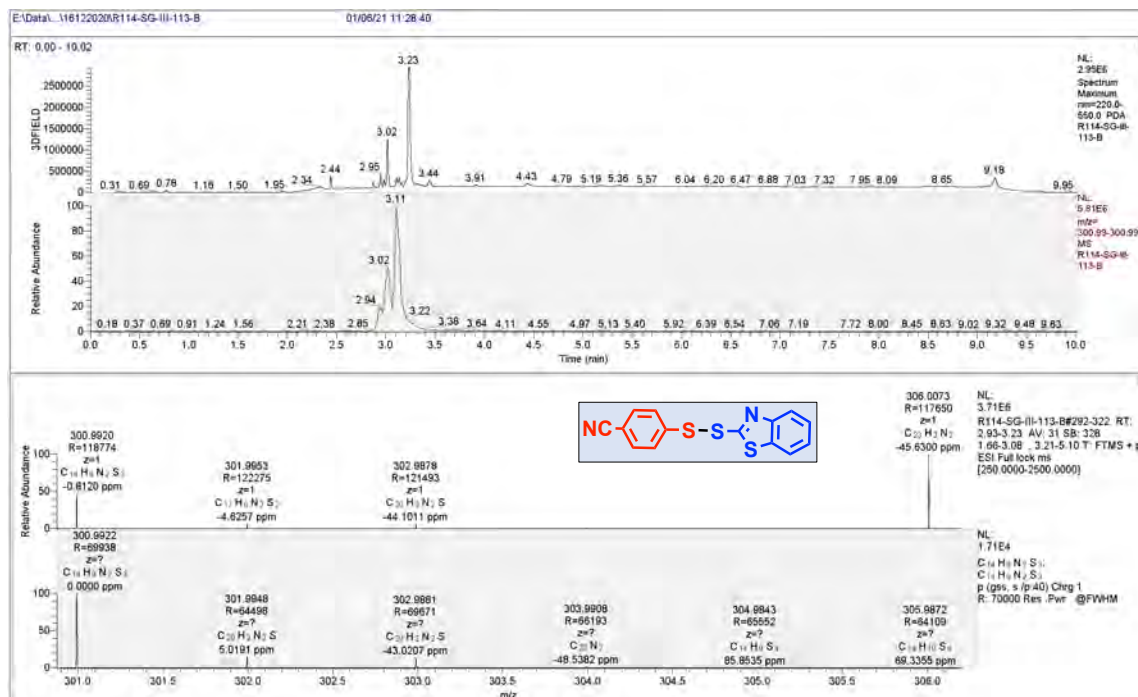
HRMS (ESI+) calculated for $[C_{48}H_{24}N_6S_6 + H^+]$: 877.0459 Da, found $[M+H^+]$ 877.0451 m/z;



Mixed Disulfide (46):



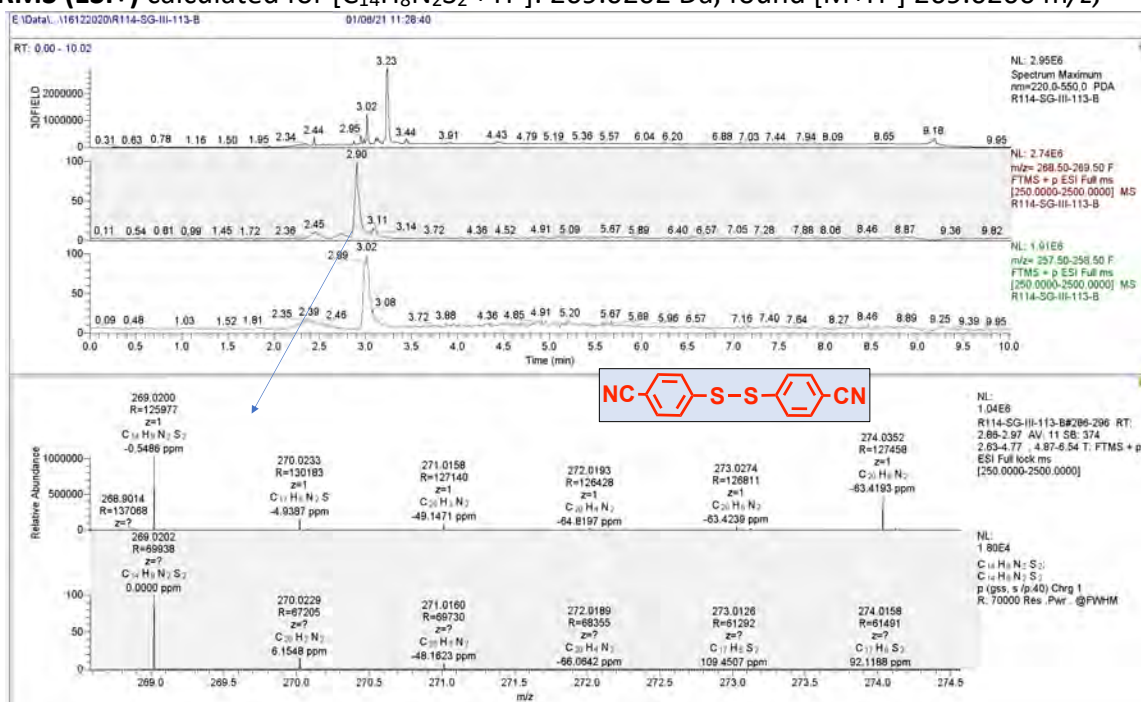
HRMS (ESI+) calculated for $[C_{14}H_8N_2S_3 + H^+]$: 300.9922 Da, found $[M+H^+]$ 300.9920 m/z;



Disulfide (47):



HRMS (ESI+) calculated for [C₁₄H₈N₂S₂ + H⁺]: 269.0202 Da, found [M+H⁺] 269.0200 m/z;



LC-HRMS Chromatogram of the mixture (R-114):
***p*-thiocresol promoter incorporated into asterisks (15) and (16)**

Products resulting from the **incorporation** of *p*-thiocresol as a promoter into asterisks (15) and (16), as determined by LC-HRMS. Compounds (44) to (55) were identified after work-up (below, Figure 5c).

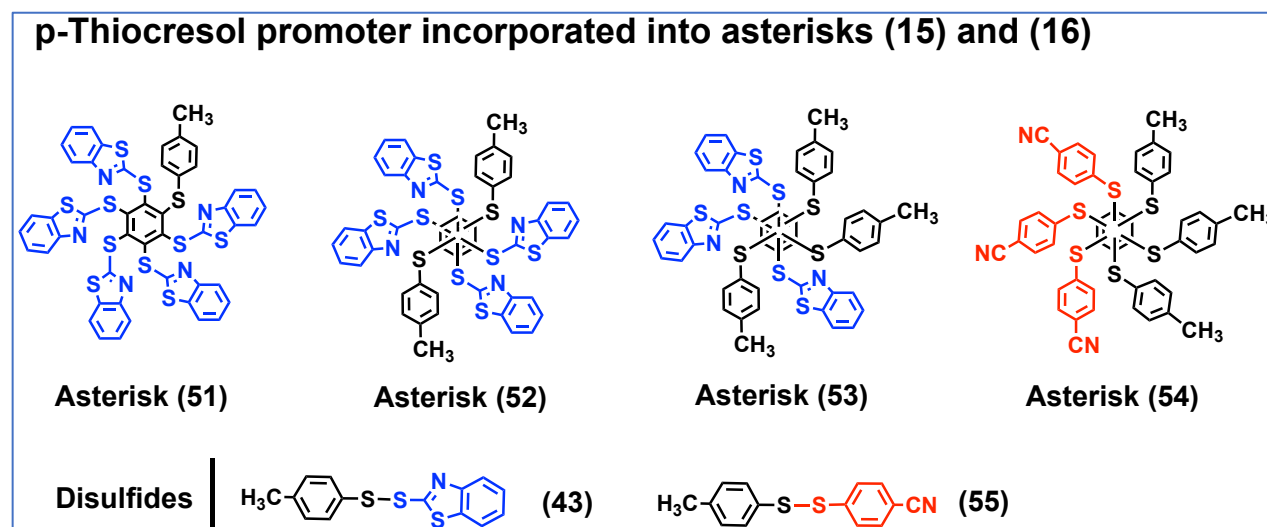
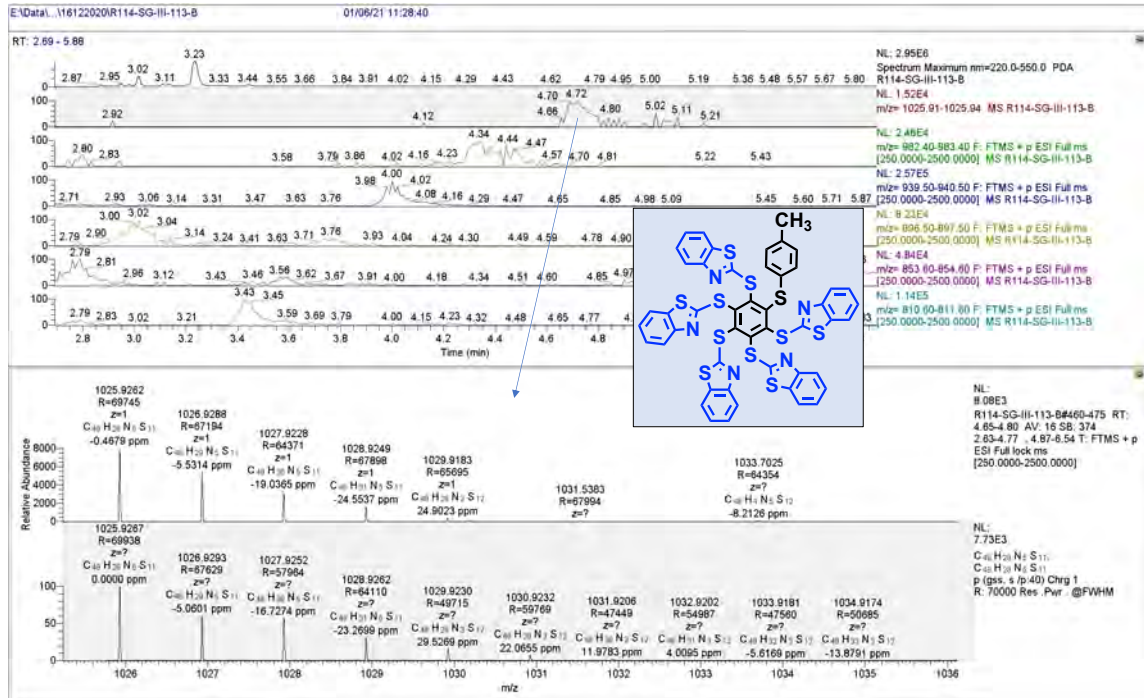


Figure 5c

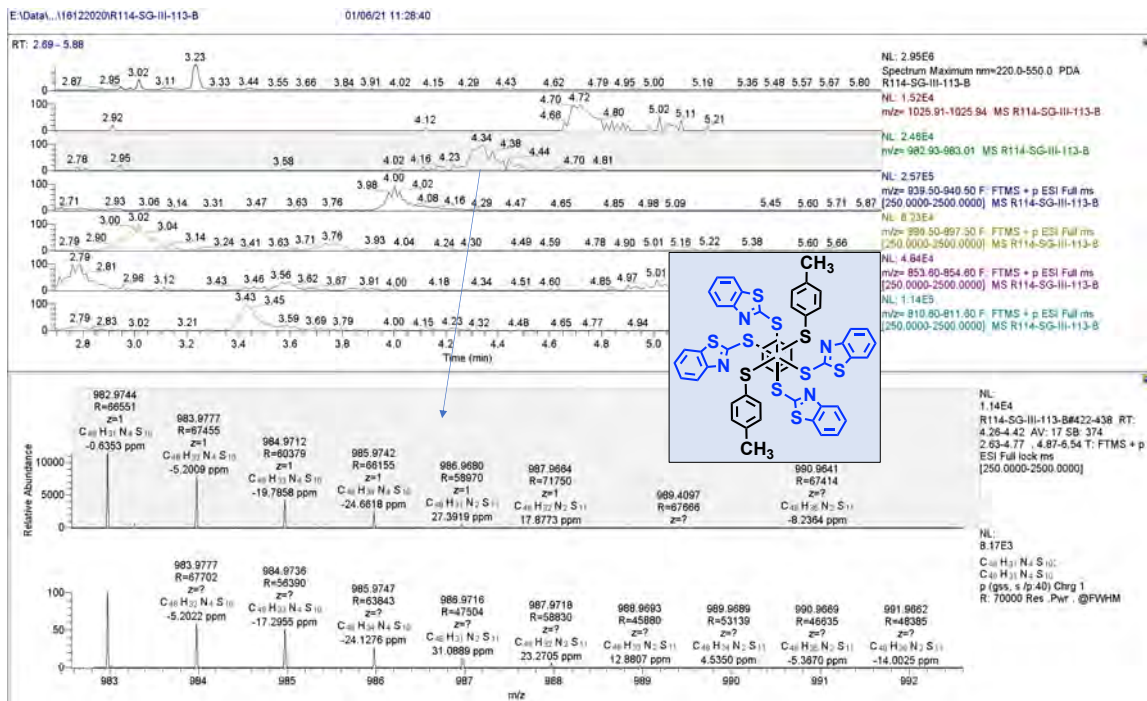
Asterisk (51)

HRMS (ESI+) calculated for $[C_{48}H_{27}N_5S_{11} + H^+]$: 1025.9267 Da, found $[M+H^+]$ 1025.9262 m/z;



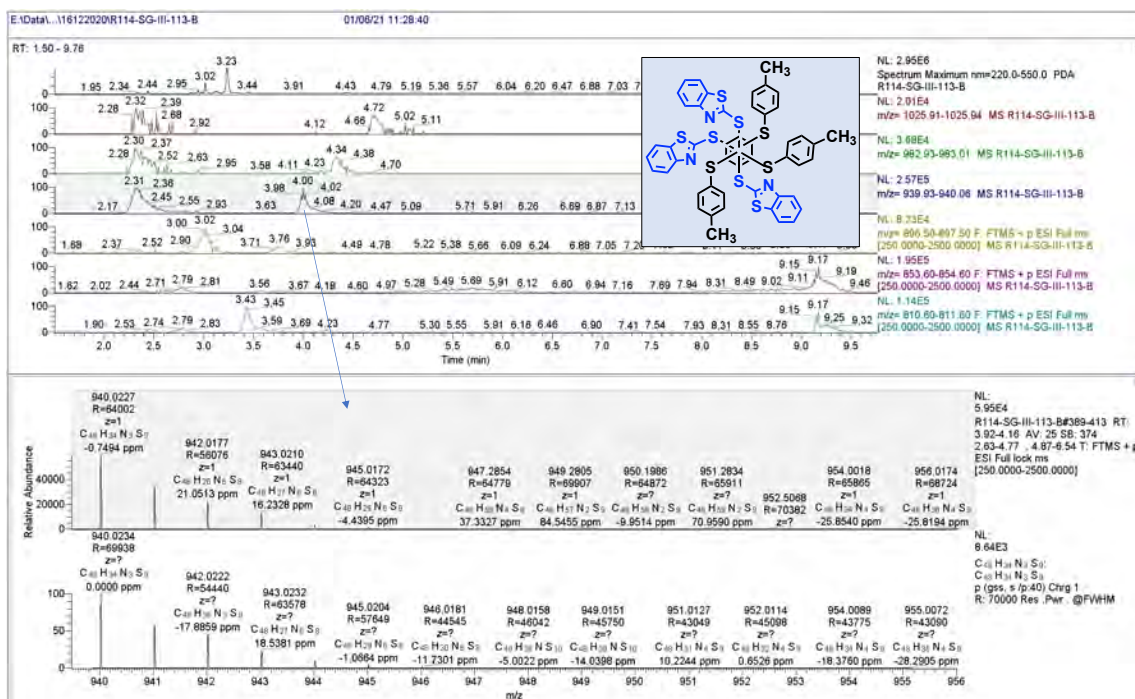
Asterisk (52)

HRMS (ESI+) calculated for $[C_{48}H_{30}N_4S_{10} + H^+]$: 982.9750 Da, found $[M+H^+]$ 982.9744 m/z;



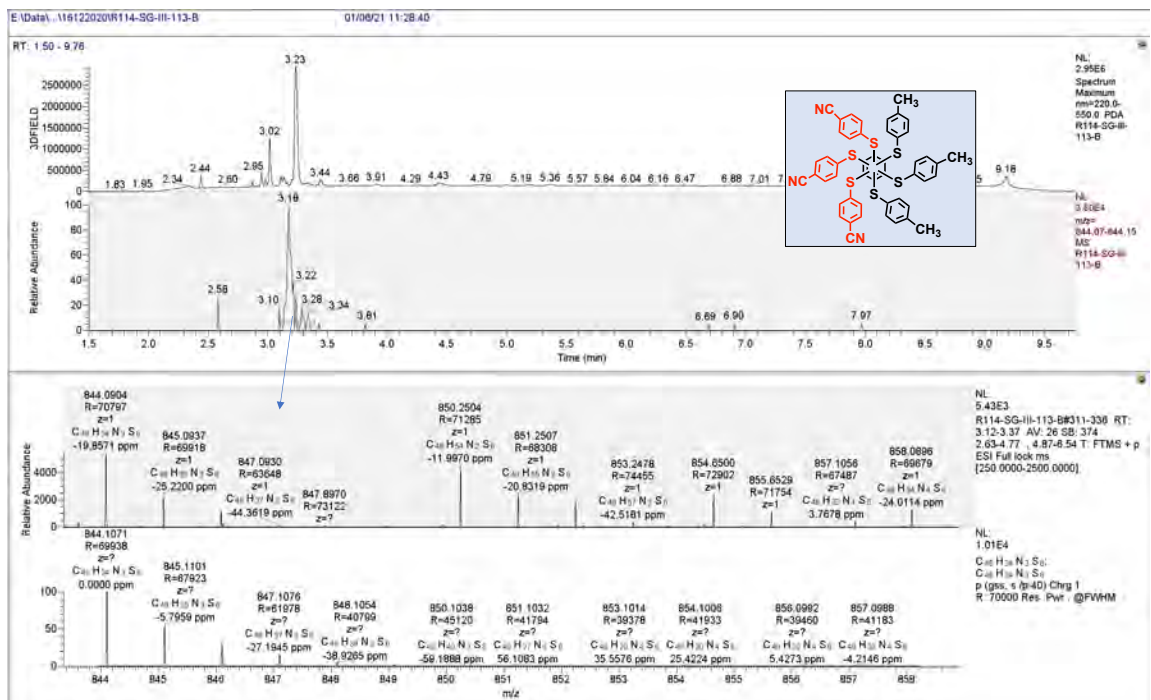
Asterisk (53)

HRMS (ESI+) calculated for $[C_{48}H_{33}N_3S_9 + H^+]$: 940.0234 Da, found $[M+H^+]$ 940.0227 m/z;

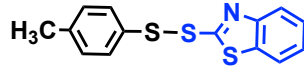


Asterisk (54)

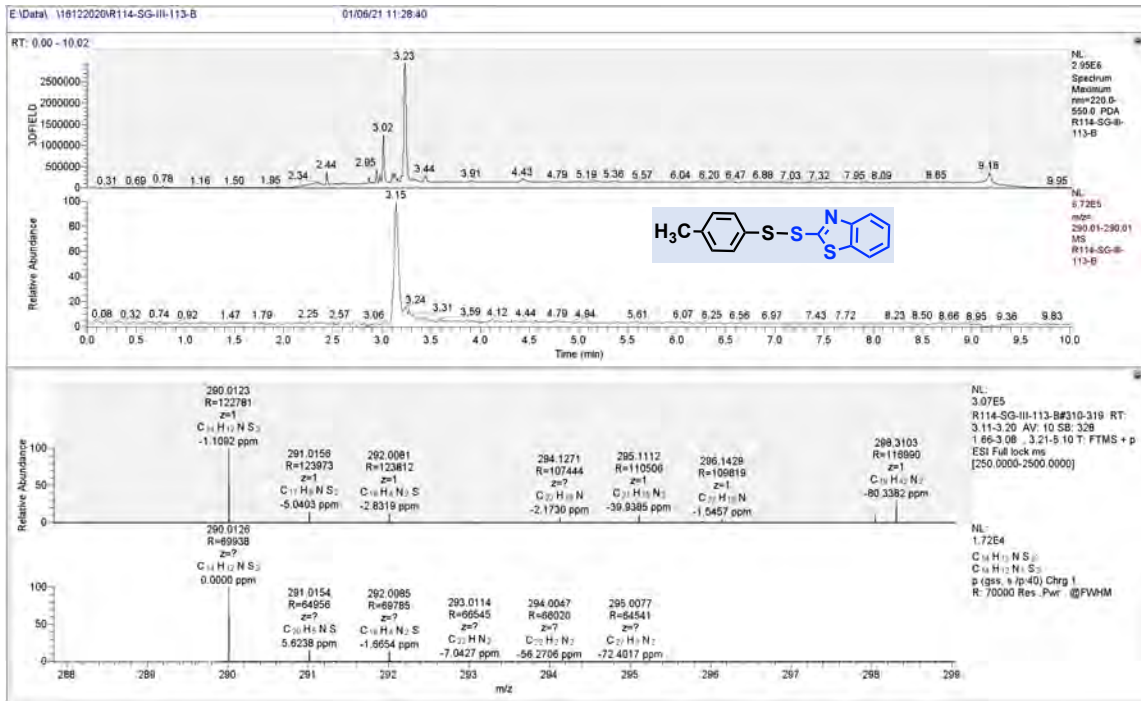
HRMS (ESI+) calculated for $[C_{48}H_{34}N_3S_6 + H^+]$: 844.1071 Da, found $[M+H^+]$ 844.0904 m/z;



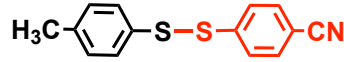
Mixed Disulfide (43)



HRMS (ESI+) calculated for [C₁₄H₁₁N₁S₃ + H⁺]: 290.126 Da, found [M+H⁺] 290.0123 m/z;



Mixed Disulfide (55)



HRMS (ESI+) calculated for [C₁₄H₁₁N₁S₂ + H⁺]: 258.0406 Da, found [M+H⁺] 258.0404 m/z;

